AD_____

Award Number: DAMD17-01-1-0765

TITLE: NTX00 Common Mechanisms of Neuronal Cell Death after Exposure to Diverse Environmental Insults: Implications for Treatment

PRINCIPAL INVESTIGATOR: Ronald L. Hayes, Ph.D.

CONTRACTING ORGANIZATION: University of Florida
Gainesville, FL 32610

REPORT DATE: October 2005

TYPE OF REPORT: Final

PREPARED FOR: U.S. Army Medical Research and Materiel Command
Fort Detrick, Maryland 21702-5012

REPORT DOCUMENTATION PAGE

Form Approved
OMB No. 0704-0188

1. REPORT DATE *(DD-MM-YYYY)*	**2. REPORT TYPE**	**3. DATES COVERED** *(From - To)*
01-10-2005	Final	27 SEP 2001 - 26 SEP 2005

4. TITLE AND SUBTITLE
NTX00 Common Mechanisms of Neuronal Cell Death after Exposure to Diverse Environmental Insults: Implications for Treatment

5a. CONTRACT NUMBER

5b. GRANT NUMBER
DAMD17-01-1-0765

5c. PROGRAM ELEMENT NUMBER

6. AUTHOR(S)
Ronald L. Hayes, Ph.D.

E-Mail: hayes@mbi.ufl.edu

5d. PROJECT NUMBER

5e. TASK NUMBER

5f. WORK UNIT NUMBER

7. PERFORMING ORGANIZATION NAME(S) AND ADDRESS(ES)
University of Florida
Gainesville, FL 32610

8. PERFORMING ORGANIZATION REPORT NUMBER

9. SPONSORING / MONITORING AGENCY NAME(S) AND ADDRESS(ES)
U.S. Army Medical Research and Materiel Command
Fort Detrick, Maryland 21702-5012

10. SPONSOR/MONITOR'S ACRONYM(S)

11. SPONSOR/MONITOR'S REPORT NUMBER(S)

12. DISTRIBUTION / AVAILABILITY STATEMENT
Approved for Public Release; Distribution Unlimited

13. SUPPLEMENTARY NOTES

14. ABSTRACT: Neuronal cell death after exposure to neurotoxins or after central nervous system (CNS) injury is the major cause of devastating neurological pathologies associated with military combat-related morbidity and mortality. An understanding of the cellular and molecular mechanisms contributing to neuronal cell death is critical to development of appropriate treatment strategies. Although the environmental causes of CNS injury are diverse (e.g., penetrating injuries, concussive injuries, neurotoxin exposure, etc), we hypothesize that regardless of the injury mechanisms, a relatively small subset of cellular and molecular events is responsible for the vast majority of cell death. The research results contained in this annual report summarize the findings of the second year of supported research on this grant. We have made great progress in implementing the proposed studies and have generated a wealth of data that supports both our broad and specific hypotheses. Importantly, our research indicates that the calcium activated family of cysteine proteases-the calpains- are rapidly activated in response to a variety of cellular insults while the cysteine protease caspase-3 is only activated in response to more specific cellular signals. These results suggest that inhibition of both calpain and caspase may provide greater neuroprotection than either inhibitor given alone.

15. SUBJECT TERMS
brain trauma, cell death, neurotoxins, proteases, calpains, caspases

16. SECURITY CLASSIFICATION OF:			**17. LIMITATION OF ABSTRACT**	**18. NUMBER OF PAGES**	**19a. NAME OF RESPONSIBLE PERSON**
a. REPORT	**b. ABSTRACT**	**c. THIS PAGE**			USAMRMC
U	U	U	UU	261	**19b. TELEPHONE NUMBER** *(include area code)*

Standard Form 298 (Rev. 8-98)
Prescribed by ANSI Std. Z39.18

Table of Contents

TITLE: Common Mechanisms of Neuronal Cell Death after Exposure to Diverse Environmental Insults: Implications for Treatment

INTRODUCTION AND BACKGROUND

This final report summarizes research to study pathobiological mechanisms of traumatic brain injury (TBI). TBI has historically been a major civilian health problem. However, our recent experience in Iraq indicates that TBI is a major challenge for military medicine. More than 60% of combat casualties probably experience attendant brain injuries. Many of these injuries go undiagnosed in the combat environment. Thus, it has become increasingly important to understand the basic pathobiology of TBI and to develop insights that would lead to non-invasive diagnostics useful in combat environments. Our laboratory and others have consistently demonstrated the important roles of two families of cysteine proteases, calpains and caspases, and the study of these proteases is the central theme of this proposal.

This proposal was originally submitted by Dr. Brian Pike who left academic research and turned the proposal over to Dr. Ronald L. Hayes shortly after the grant was awarded. Since Dr. Pike's departure, research emphases have evolved. This evolution has occurred in response to scientific advances made since original submission of the proposal as well as the desire of Dr. Hayes to provide important insights into pathobiological mechanisms of brain injury that would have the broadest application to studies of acute injury and neurodegeneration both in military and civilian contexts. However, this evolution has remained faithful to the original hypothesis of the proposal that "regardless of injury mechanism, a relatively small subset of cellular and molecular events is responsible for the vast majority of cell death" (p 5). In addition, Dr. Pike pointed out that "while calpain and caspases have been widely implicated as mediators of cell death, rapid progress in understanding mechanisms contributing to protease regulation and cell death is hindered in animal models of CNS injury (p 5)." The evolution of our studies has reflected both a continuing and productive elaboration of pathobiological mechanisms of calpain and caspase-3 activation. In addition, while Dr. Pike originally felt that *in vitro* studies would provide the major opportunity for examining proteolytic mechanisms of cell death, we and others have made rapid advances in the development of biomarkers allowing non-invasive study of proteolytic pathology in *in vivo* models and ultimately in humans. The body of the report summarizes data collected and is organized under revised SOWs reflecting the evolved research goals of the proposal.

SOWs 1 and 2 provide detailed summaries of data that are directly relevant to SOWs included in the original proposal. These studies were completed during the funding period of the original proposal and included major contributions by Dr. Pike, as reflected in the authorship. However, funding support for this work under the present proposal was inappropriately omitted. In any case, the data outlined in SOWs 1 and 2 provide documentation of significant progress directly relevant to the original proposal. It is also important to understand that the original proposal focused on comparing a variety of more clinically relevant insults (e.g. ischemia/stretch injury, glutamate) to neurotoxin-induced damage. The proposed neurotoxins were maitotoxin and staurosporine (p 18). Thus, data summarized in SOW 1 and 2 both support the fidelity of the research conducted to the major hypotheses of the original proposal as well as provide a background for other research supported by this initiative.

BODY

SOW 1

Hypothesis: Distinct cell death modalities are better defined by biochemical markers of proteolysis than by standard approaches of phenotypic descriptions of apoptosis and necrosis. Oxygen glucose

deprivation (OGD) produces differential activation of caspase-3 and calpain that can accurately characterize necrotic and apoptotic cell death mechanisms.

The original hypothesis of this proposal for SOW 1 was: "to test the hypothesis that various CNS-related insults produced differential activation of caspase-3 and calpain depending upon the pathological signal and/or neuronal cell type. Distinct cell death modalities are better defined by such biochemical markers than by standard approaches of phenotypic descriptions of apoptosis and necrosis" (p 4). The original SOW proposed to examine calpain and caspase-3 activation in primary mixed and neuronally enhanced septo-hippocampal cultures following CNS-related insults (mechanical stretch injury, glucose-oxygen deprivation, glutamate toxicity) or neurotoxin production of apoptotic (by staurosporine) or necrotic (by maitotoxin) cell death phenotypes. The SOW further proposed to examine relationships between archetypal apoptotic and necrotic cell death phenotypes and calpain and caspase-3 activation after CNS-related injury or after neurotoxin exposure (p 4).

The current SOW closely follows the major thrust of research proposed in SOW 1 of the original proposal and is based on uniquely comprehensive studies by our laboratory, including research conducted by Dr. Pike, systematically examining the relationship between biochemical markers of necrosis and apoptosis and phenotypic expression of necrotic and apoptotic cell death. These studies employed examination of processing of α-spectrin by calpain and caspase-3 as markers of protease activation potentially associated with necrosis (calpain activation) or apoptosis (caspase-3 activation) and generally employed primary-septo-hippocampal cultures, one of the more clinically relevant culture systems employed in CNS injury studies. This previous research had established that varying insults produced different patterns of protease activation and necrotic and apoptotic cell death. The neurotoxin, staurosporine, reliably induces apoptosis and was associated with robust activation of caspase-3, as well as classic phenotypic markers of apoptosis including membrane blebbing and nuclear chromatin condensation. Surprisingly, there was also reliable activation of calpain, suggesting that calpain could also play a role in some forms of expression of the apoptotic phenotype **(Pike et al., J Neurosci. Res., 1998)**. In contrast, maitotoxin, a neurotoxin that activates voltage and receptor-mediated calcium channels and produces necrosis, produced significant calpain but not caspase-3 activation. Thus, these data suggested that calpain activation was a major contributor to necrotic cell death **(Zhao et al., Neurochem. Res., 1999)**. These observations were extended to a novel *in vitro* model of stretch injury which approximates biomechanical forces seen in TBI *in vivo* **(Pike et al., J Neurotrauma, 2000)**. Stretch injury was associated with prominent and rapid calpain activation with delayed caspase-3 activity at much lower levels. Thus, as our *in vivo* data confirm (see SOW 5B below), mechanical injury is reliably associated with a predominance of calpain activation. Glutamate toxicity is thought to be a major component of acute CNS injury. We showed novel characteristics of glutamate-induced cell death in primary septo-hippocampal cultures and examined their relationship to calpain and caspase-3 protease activation **(Zhao et al., JCBFM, 2000)**. Importantly, glutamate toxicity was associated with a previously undescribed cell death phenotype that differed from necrotic or apoptotic changes observed after maitotoxin or staurosporine exposure, respectively. However, expression of this cell death phenotype was associated with increases in calpain and caspase-3 activation.

In summary, this line of research had lead us to conclude that exclusive reliance on phenotypic expression of cell death, the classic approach to descriptions of necrosis and apoptosis, was unsatisfactory. However, in the early phase of this proposal we wanted to expand this body of research to examine the relationship of cell death phenotype and protease activation in an *in vitro* model of ischemia, oxygen-glucose deprivation in primary septo-hippocampal cultures.

SOW 1-Plan

To examine calpain and caspase-3 activation in primary mixed and neuronally enhanced septo-hippocampal cultures following the clinically relevant, CNS-related insult, glucose-oxygen deprivation (OGD) and to compare this toxicity to assessments of toxicity produced by neurotoxins (staurosporine, maitotoxin).

In this SOW, we systematically examined the relationship between calpain and caspase-3 activity and necrotic and apoptotic cell death phenotypes in a widely used *in vitro* model of ischemia, oxygen-glucose deprivation **(Newcomb-Fernandez et al., 2001)**. Importantly, this was the first study to investigate the *concurrent* activation of calpain and caspase-3 in archetypal necrotic and apoptotic cell death phenotypes after any CNS insult. Experiments used a model of OGD in primary septo-hippocampal cultures and assessed cell viability, occurrence of apoptotic and necrotic cell death phenotypes, and protease activation. Experiments focused on 10 hrs of OGD combined with 24 hrs of reperfusion (normoxia after OGD). Immunoblots using an antibody detecting calpain and caspase-3 proteolysis of α-spectrin showed greater accumulation of calpain-mediated breakdown products (BDPs) compared with caspase-3 BDPs.

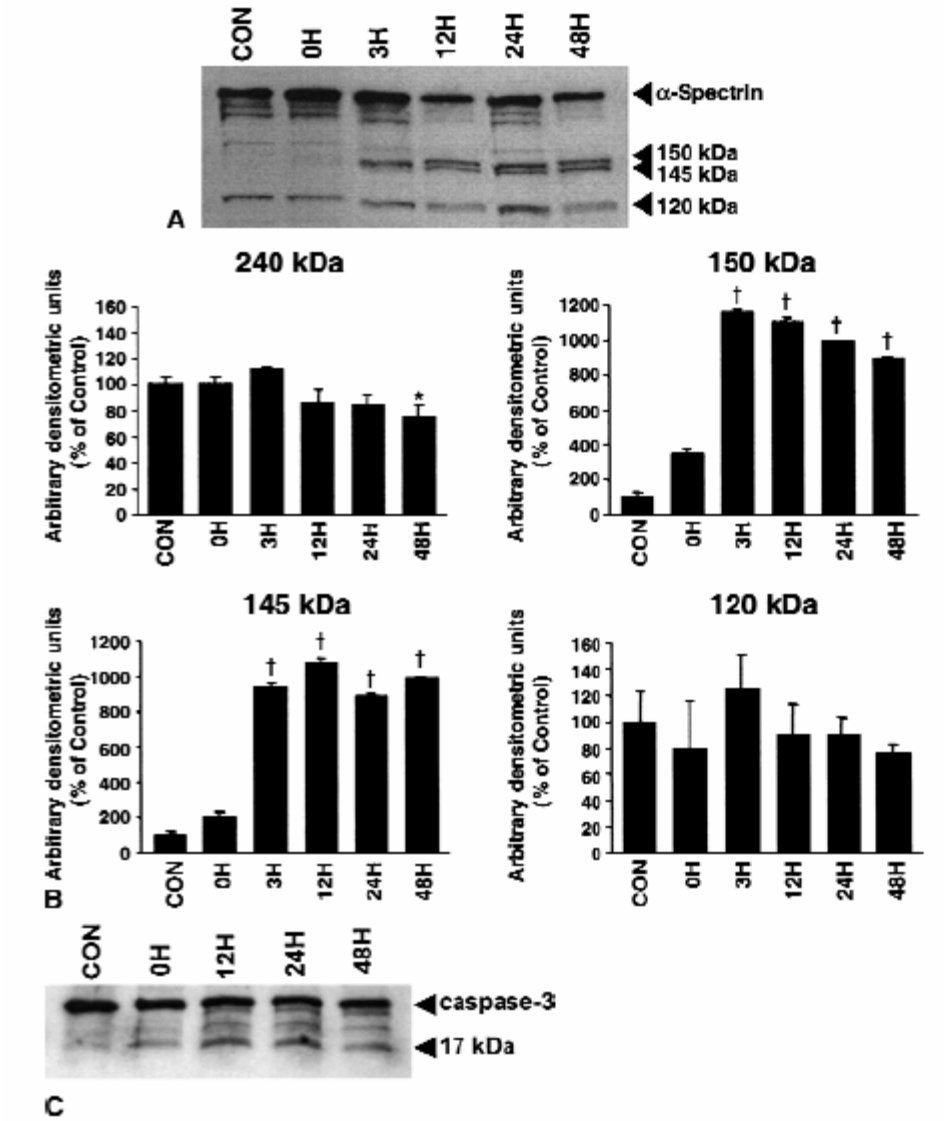

FIG. 4. Calpain- and caspase-3–mediated proteolysis of α-spectrin after oxygen–glucose deprivation (OGD). **(A)** Representative Western blot showing calpain- and caspase-3–mediated proteolysis of α-spectrin after OGD. Control samples and samples collected immediately (0 hour) after injury showed no evidence of calpain-mediated proteolysis of α-spectrin. Accumulation of the 150- and 145-kDa BDPs was detected 3, 12, 24, and 48 hours after OGD. Moderate increases in the caspase-3–mediated BDP were detected after injury, but formation of the 120-kDa BDP was variable. **(B)** Calpain- and caspase-3–mediated proteolysis of α-spectrin semiquantitative analysis. Data from multiple Western blots analyzing α-spectrin proteolysis were acquired as integrated densitometric values and transformed to percentages of the densitometric values obtained from control samples. Formation of the 150- and 145-kDa BDPs was increased after OGD with 3, 12, 24, and 48 hours of reperfusion, whereas modest degradation of native α-spectrin (240 kDa) was detected after 48 hours of reperfusion. Accumulation of the caspase-3–mediated 120-kDa BDP was variable. *$P <$ 0.01. †$P <$ 0.001. **(C)** Activation of caspase-3 after OGD. Proteolysis of caspase-3 (32 kDa) to the activated isoform (17 kDa) was examined after 10 hours of OGD and 0, 12, 24, or 48 hours of reperfusion. Degradation of the proenzyme (32 kDa) was evident 12, 24, and 48 hours after injury. Proteolysis of caspase-3 into the 17-kDa subunit was detected with all lengths of reperfusion examined.

As shown in Fig 4 from the original manuscript, robust accumulation of calpain mediated proteolysis was detected using α-spectrin for up to 48 hrs following OGD. Moderate increases in the caspase-3 mediated BDP were detected after injury, but formation of this BDP was variable (Fig 4A-4B). However, an

antibody specifically detecting the activated form of caspase-3 was able to detect evidence of caspase-3 activation (Fig 4C). Administration of calpain and caspase-3 inhibitors confirmed that activation of these proteases contributed to cell death, as inferred by lactate dehydrogenase (LDH)

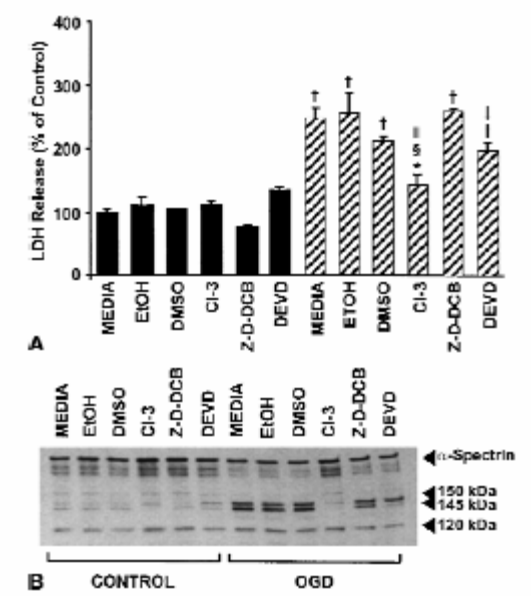

FIG. 6. (A) Effect of protease inhibition on lactate dehydrogenase (LDH) release following oxygen–glucose deprivation (OGD). Cultures were subjected to OGD (10 hours + 12 hours of reperfusion) alone, or combined with varying doses of protease inhibitors. Cell viability was assessed by measuring LDH release and expressed as percent of control. Significant decreases in LDH release were detected with administration of CI-3 (100 μmol/L) compared to vehicle-treated cultures. DEVD-fmk (100 μmol/L) also inhibited LDH release; however, decreases were not statistically significant compared to vehicle-treated cultures. Z-D-DCB (100 μmol/L) had no effect on cell viability. DMSO (2 μL/mL) also decreased LDH release, but its effect was not significantly different from the OGD/media cultures. *$P < 0.05$ and †$P < 0.001$ compared to control; ‡$P < 0.05$ and §$P < 0.001$ compared to OGD/media; ‖$P < 0.01$ compared to vehicle-treated OGD. (B) Effect of protease inhibition on α-spectrin proteolysis. Western blot analyses of α-spectrin proteolysis assessed inhibition of appropriate proteases. CI-3 (100 μmol/L) decreased proteolysis of native 240 kDa α-spectrin and the formation of the 150/145 kDa doublet. Z-D-DCB (100 μmol/L) had a small effect on the accumulation of the 145 kDa and 120 kDa BDPs. DEVD-fmk (100 μmol/L) substantially reduced the formation of the 145 kDa BDP, but had only a modest effect on the formation of the 120 kDa BDP.

release.

As shown in Figure 6A of the original manuscript, LDH showed significant decreases in release following treatment with a calpain inhibitor. The specific caspase-3 inhibitor also inhibited LDH release, although decreases were not statistically significant compared with vehicle treated cultures. The pan caspase inhibitor had no effect on LDH release. Consistent with LDH data Western blot analyses of these samples (Fig 6B) showed that calpain inhibition almost completely blocked the formation of calpain-specific breakdown products. The pan caspase inhibitor also inhibited formation of the calpain-specific breakdown product to small extent but had only a minor effect on the caspase-3 BDP. Surprisingly, the caspase-3 inhibitor dramatically reduced evidence of calpain activation but had only a modest effect on caspase activation. Future experiments need to examine the specificity of these drugs in more detail. OGD deprivation resulted in expression of apoptotic and necrotic cell death phenotypes, especially in neurons. Immunocytochemical studies of calpain and caspase-3 activation in apoptotic cells indicated that these proteases are almost always concurrently activated during apoptosis **(See Figure 5 in Newcomb-Fernandez, et al., 2001).** As shown in Figure 5 from the manuscript, cultures deprived of oxygen and glucose had significantly increased cellular co-localization of SBDP 150 (calpain activation) and SBDP 120 (caspase-3 activation), compared with control cultures. Although OGD cultures contain substantially

more immunoreactive cells than control cultures, immunocytochemistry showed a similar distribution of protease activation, regardless of treatment of condition (Fig 5A & 5C). Virtually all immunoreactive cells in control and OGD cultures showed concurrent calpain and caspase proteolysis of varying magnitudes (Fig 5A & 5C). This profile strongly suggests that co-activation of these proteases is a reliable feature of cell death expression and is especially prominent in apoptotic phenotypes. Importantly, these studies systematically examined and compared the effects of OGD to the effects of neurotoxins, maitotoxin and staurosporine (see Fig 5).

In summary, these data provided a novel and compelling demonstration that is inconsistent with the more widely held scientific understanding that caspase-3 is the principle, if not exclusive, mediator of the apoptotic cell death phenotype. These data demonstrated that co-activation of calpain and caspase-3 is a reliable characteristic of apoptotic cell death following ischemic injury *in vitro*. These observations strongly suggest that calpain activation, in combination with caspase-3 activation, could contribute to the expression of apoptotic cell death by assisting in the proteolytic degradation of important cellular proteins. In addition, interactions between these two cysteine proteases could be important determinants of cell death, including injury produced by neurotoxins.

SOW 2

Hypothesis: Tumor necrosis factor alpha (TNF-α) is a receptor coupled cell death mediator that primarily involves apoptotic rather than necrotic cell death pathways. Thus, TNF-α-mediated cell death is associated predominantly with caspase-3 rather than calpain activation.

SOW 3 of the original proposal focused on testing the hypothesis that in response to various CNS-related injuries or neurotoxin exposure, tumor necrosis factor (TNF-α) triggers proteolytic activation of caspase-8/10 that results in caspase-3 activation of apoptotic cell death. Caspase-8/10 proteolytic activation requires receptor mediated coupling of TNF-α, and the magnitude and duration of this cascade may vary depending on the initiating signal and neuronal cell type. Early in this funding period, Dr. Pike collaborated in studies showing that caspase-8 expression occurred in conjunction with caspase-3 activation and apoptosis in an *in vivo* model of TBI **(Beer, et al., 2001)**. This research also examined caspase-8 expression in different cell types. These data also provided an important confirmation of SOW 4 of the original proposal which proposed to examine the effects of TBI *in vivo* on caspase-3 activation mediated by two apoptotic cell death pathways including the TNF-α/caspase-8 pathway. In addition, SOW 3 of the original proposal sought to examine the effects of exogenous TNF-α on primary cell cultures for evidence of activation of caspase-8/10, activation of caspase-3 and their contribution to apoptotic cell death (SOW 3A, p 4). The data reviewed below directly addressed the role of the effects of exogenous TNF-α on caspase-3 activation.

SOW 2-Plan

To examine the effects of exogenous TNF-α on primary cultures for evidence of activation of calpain and caspase-3 and their contribution to apoptotic cell death.

Tumor necrosis factor-α (TNF-α) is a pleotrophic cytokine with both secreted and transmembrane forms which is known to mediate immune and inflammatory responses. A substantial body of evidence indicates that TNF-α has a pro-inflammatory role that is acutely upregulated in ischemic and traumatic brain injury. In order to examine the role of TNF-α on cell viability, this SOW investigated the effects of TNF-α stimulation on calpain and caspase-3 protease activation and on necrotic and apoptotic cell death phenotypes in primary septo-hippocampal cultures. This research provided the first systematic examination of the effects of TNF-α on activation of these two important proteases.

In this study **(Zhao et al., JNR, 2001)** primary septo-hippocampal cell cultures were incubated in varying concentrations of TNF-α to examine proteolysis of α-spectrin to a signature 145 kDa fragment by calpain and to the apoptotic-linked 120 kDa fragment by caspase-3. The effect of TNF-α incubation on morphology and cell viability were assayed by fluoroscene diacitate-propidium iodide (FDA-PI) staining, assays of lactate dehydrogenase (LDH) release, nuclear chromatin alterations (Hoechst 33258), and internucleosomal DNA fragmentation. Incubation with varying concentrations of TNF-α produced rapid increases in LDH release and nuclear PI uptake that were sustained over 48 hrs. As shown in Figure 5 from the original manuscript, incubation with 30ng/ml TNF-α, a does that yielded maximal, 3-fold, increase in LDH release, was associated with caspase-3 120 kDa fragments, but not calpain-specific 145 kDa fragments as early as 3.5 hrs after injury. **[See Fig 5 in Zhao et al., JNR, 2001, included with report].** Exposure to 30ng/ml of TNF-α caused a time dependent proteolysis of α-spectrin by caspase-3 but not calpain. There was a significant increase in caspase activation as early as 3.5 hrs following TNF-α administration that was sustained over 72 hrs. In contrast, there was no evidence of accumulation of calpain activation at any time point after TNF-α treatment. As shown in Figure 6 from the original manuscript, incubation with the pan-caspase inhibitor, Z-D-DCB significantly reduced LDH release produced by TNF-α as well as evidence of caspase-3 activation. **[See Fig 6 in Zhao et al., JNR, 2001, included with report]**. An LDH assay was used to assess cell viability following TNF-α and/or administration of a calpain inhibitor, a caspase-3 inhibitor or cycloheximide (Fig 6B). Administration of the caspase-3 inhibitor (Z-D-DCB) significantly reduced LDH release. Calpain inhibition had no protection against LDH release. Cycloheximide had the greatest effect against LDH release, consistent with an apoptotic profile following TNF-α treatment. Administration of a caspase-3 inhibitor or cycloheximide significantly decreased the accumulation of the 120 kDa caspase specific breakdown product of α-spectrin (Fig 6A). In contrast, calpain inhibition did not provide any protection against proteolysis of α-spectrin. These data confirm that caspase-3 but not calpain was activated after TNF-α stimulation in this primary culture system. As shown in Figure 4 of the original manuscript, apoptotic-associated oligonucleosomal-size DNA fragmentation on agorose gels was detected from 6-72 hrs after exposure to TNF-α. **[See Fig 4 in Zhao et al., JNR, 2001, included with report]**. TNF-α induced detectible DNA laddering on agerose gels that was most apparent 24 hrs following treatment. However, gels showed substantial smearing even at 24 hrs, indicating random DNA fragmentation characteristic of some necrosis. Histochemical changes included chromatin condensation, nuclear fragmentation and formation of apoptotic bodies.

In summary, although previous research had studied TNF-α activation of caspases in non-neuronal cells (e.g. neutrophils), this research provided the first demonstration that TNF-α induces activation of caspase-3 in neuronal cell systems. Importantly, these results indicate that TNF-α may play an important role as an effector of receptor mediated apoptotic cell death in the CNS and may have relevance to both acute CNS injury as well as neurodegeneration.

SOW 3

Hypothesis: Rat hippocampal slices can provide a useful *ex vivo* model for studying calcium mediated neurotoxicity potentially linked to excitotoxic and proteolytic mechanisms of cell death.

Our laboratory has recognized, as reflected in Dr. Pike's original proposal that the exclusive use of culture systems in *in vitro* models is limiting. Thus, we felt it important to develop intermediate *ex vivo* models to bridge data collected from *in vitro* and *in vivo* models. We focused on the effect of calcium-related changes since calcium dysregulation is a major component of CNS injury and is an important mediator of calpain activation. Since diffusion-weighted magnetic resonance imaging (MRI) is often an important component of diagnosing CNS injury and has been used as a surrogate marker of acute brain pathology,

we sought to clarify the utility of this approach as well as to characterize the use of rat hippocampal slices to study acute CNS injury.

SOW 3-Plan

To conduct diffusion magnetic resonance imaging studies of the effects of a calcium ionophore (A23187) on rat hippocampal slices and relate to histopathological evidence of cell death.

This SOW sought to characterize MRI-detected changes in water diffusion during the acute phase of injury using a 17.6-T wide-bore magnet to measure multi-component water diffusion at high *b*-values (7-8, 080 s/mm$_2$) for rat hippocampal slices at baseline and serially for 8 hrs after treatment with the calcium ionophore A23187 **(Shepherd et al., JCBFM, 2003)**. Hippocampal slices were removed and placed into ice-cold artificial cerebrospinal fluid and continuously perfused in a perfusion chamber that was lowered into the magnet. High-resolution diffusion-weighted images were obtained of rat hippocampal slices to determine achievable signal-to-noise ratio and spatial resolution per time unit.

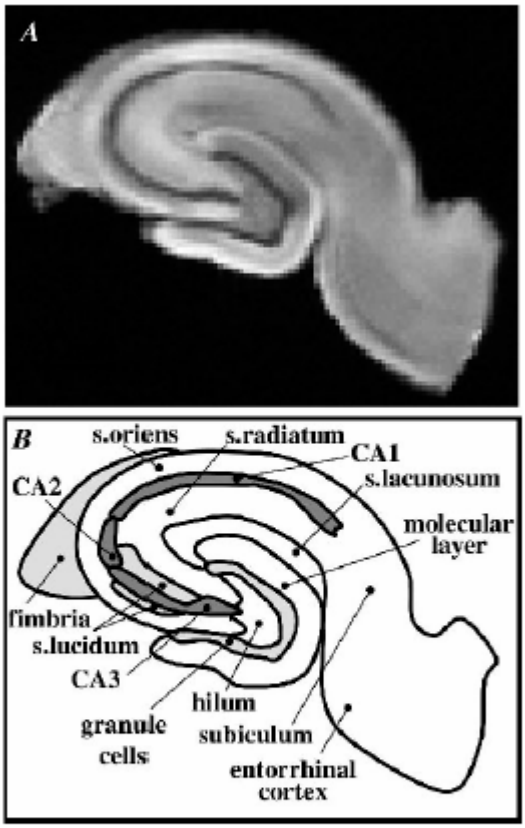

FIG. 1. A diffusion-weighted magnetic resonance image with 59-μm in-plane resolution (A) reveals the detailed lamellar anatomy of a 500-μm-thick rat hippocampal slice cut perpendicular to the septotemporal axis (MRI scan parameters: repetition time/echo time = 2,000/34 milliseconds, b = 3,630 s/mm^2, matrix = 256 × 256, field of view = 15 × 15 mm, slice thickness = 300 μm, averages = 32, time = 4.5 hours). As illustrated in panel B, many anatomical regions of the hippocampus and dentate gyrus can be distinguished in this sample based on differences in diffusion-weighted signal intensity (s, stratum).

As shown in Fig 1 of the original manuscript, these images exhibited the detailed laminar anatomy of the hippocampus, but required long acquisition times (4.5 hrs per b-value measurement). For this study, high spatial resolution was sacrificed for better temporal resolution of the water-diffusion changes that accompany slice perturbation with A23187 (4.2 min per *b*-value measurement).

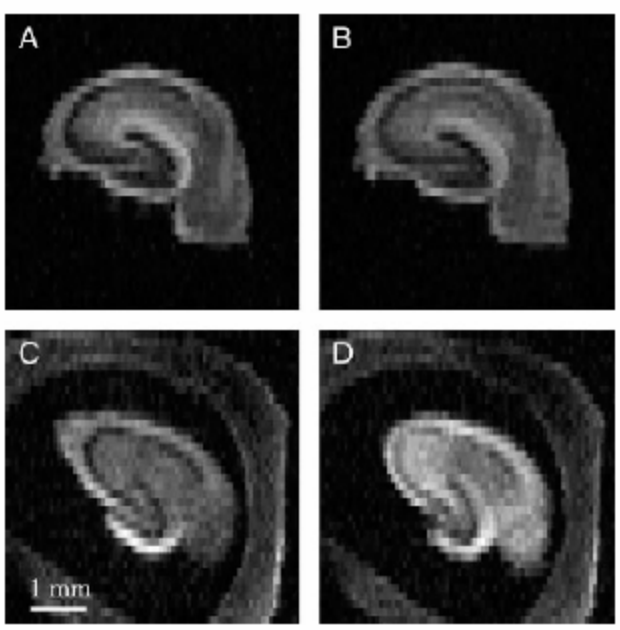

FIG. 2. Typical diffusion-weighted images (b = 7,977 s/mm^2) of rat hippocampal slices. Panels **A** and **B** show a control rat hippocampal slice before and after 8 hours of treatment with 0.1% DMSO vehicle, respectively. Panels **C** and **D** show a different slice before and 8 hours after treatment with 10-µmol/L A23187, respectively (the latex spacer of the perfusion chamber is visible in these two images). At this b-value, signal intensity in the A23187-treated slice increased 42% whereas the vehicle-treated slice signal intensity increased 6% over 8 hours.

Figure 2 from the original manuscript shows lower resolution images illustrating signal intensity changes that occur after treatment with A23187. The mean fast diffusion water fraction (F_{fast}) progressively decreased for slices treated with varying doses of A23187. Slices treated with a higher dose had significantly reduced F_{fast} 80 min earlier than slices treated with the lower dose, but otherwise, the two doses had equivalent effects on the diffusion properties of tissue water. As shown in Figure 5 from the original manuscript, correlative histologic analyses showed a dose-related selective vulnerability of hippocampal pyramidal neurons (CA1 > CA3) to pathological swelling induced by A23187, confirming that particular introvoxal cell populations may contribute disproportionately to water diffusion changes observed by MRI after acute brain injury.

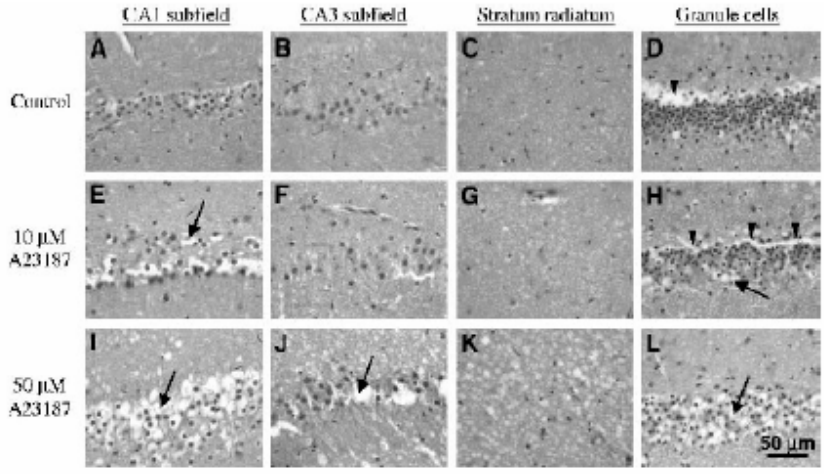

FIG. 5. Correlative histology of rat hippocampal slices 8 hours after treatment with DMSO vehicle (**A–D**), 10-µmol/L A23187 (**E– H**). and 50-µmol/L A23187 (**I–L**) A23187 had dose-related effects on the CA1 subfield, CA3 subfield, stratum radiatum, and internal blade of the dentate gyrus. Arrows illustrate cells ruptured from pathologic swelling and arrowheads denote artifact from paraffin wax embedding. Sections (8-µm thick) were stained with hematoxylin and eosin and are shown at 630× magnification with oil immersion.

This study confirmed that brain slices provide a stable and highly controllable nervous tissue model. This

research successfully used diffusion-weighted MRI of rat hippocampal slices to study the acute temporal evolution of multi component water-diffusion changes after treatment with the calcium ionophore A23187. Data obtained from this *ex-vivo* model of acute brain injury suggest that the biexpenential diffusion parameter F_{fast} may be a sensitive correlate of cellular swelling in nervous tissue in that diffusion changes after acute brain injury may be introvoxal volume-average summation of responses from anatomically or temporally distinct healthy and pathologically injured cell populations. This platform could be an important intermediate *ex vivo* model to link *in vitro* and *in vivo* studies of calpain and caspase mechanisms of necrotic and apoptotic cell death. These studies could also lead to refinement of non-invasive surrogate markers of brain injury.

SOW 4

Hypothesis: Cell-specific upregulation of a developmentally significant protein, survivin, occurs after TBI and attenuate caspase-3 mediated apoptosis.

This research was initiated following the unexpected and novel observation that survivin, a unique member of the inhibitor of apoptosis protein (IAP) family is upregulated after TBI. Survivin is also an evolutionarily conserved chromosomal passenger protein that is required for proper completion of mitosis. Survivin is present during normal tissue development but is absent in most adult tissues including the brain. Many cancer cell lines and cancer tumors which proliferate at high rates exhibit survivin overexpression. In addition, blocking survivin expression in these cell lines leads to cell death. Importantly, prior to our research, no investigations had studied changes in survivin following acute CNS injury. However, we noted that this protein could serve important anti-apoptotic and cell proliferation properties that could have important implications for both acute CNS injury and neurodegeneration. Thus, we felt it was extremely important to pursue this novel finding and explore the potential role of survivin in caspase-3 mediated apoptosis.

SOW 4-Plan

To examine the protein expression and cellular localization of survivin and proliferating cell nuclear antigen (PCNA) after controlled cortical impact injury in rats and characterize the relationship between co-expression of survivin and activated caspase-3 and DNA fragmentation in astrocytes and neurons.

In our first study **(Johnson et al., J Neurotrauma, 2004)**, we examined the expression and cellular localization of survivin and proliferating cell nuclear antigen (PCNA) after controlled cortical impact TBI in rats. PCNA is a cell cycle protein which we studied in order to look at potential relationships with mitosis. There was a remarkable and sustained induction of survivin mRNA and protein in the ipsilateral cortex in hippocampus of rats after TBI, peaking at 5 days post injury. In contrast, both survivin mRNA and protein were virtually undetectable in craniotomy control animals. Figure 2 from the original manuscript shows a representative Western blot of survivin in various brain regions from injured and control rats.

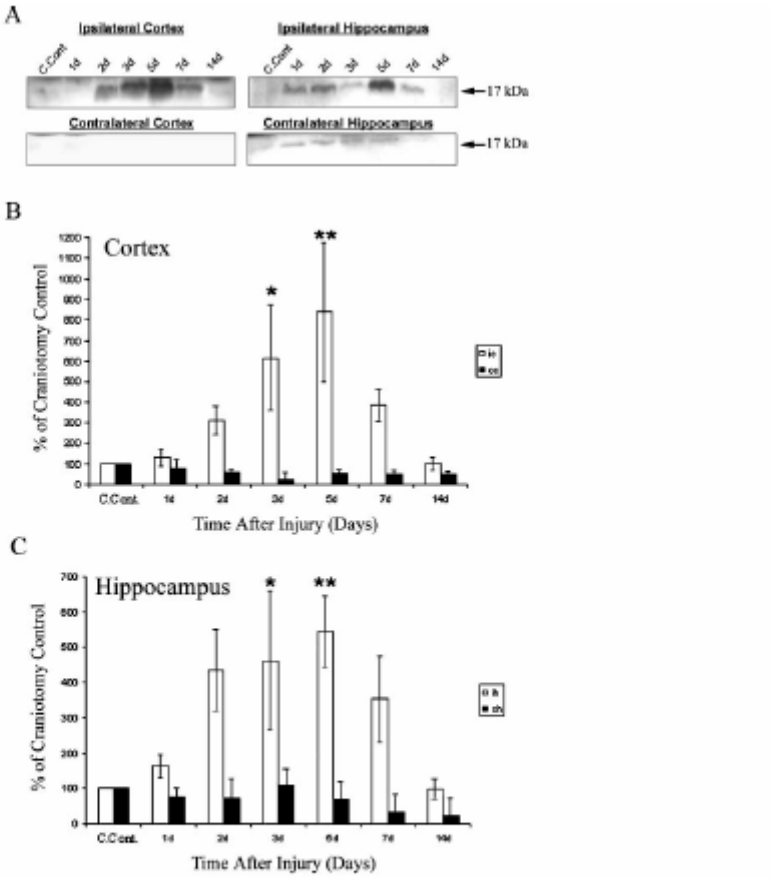

FIG. 2. Expression of survivin protein after TBI in rats. Brain tissue homogenate proteins (40 μg) were separated using SDS-PAGE, immunoblotted with survivin antibody, and visualized. (A) Representative Western blot of survivin (17-kDa protein) in ipsilateral cortex (ic) and hippocampus (ih), contralateral cortex (cc) and hippocampus (ch) obtained from injured rats, and from craniotomy control rats without cortical impact (C. Cont.). Densitometry analysis representation of survivin-positive bands in ipsilateral (ic) and contralateral (cc) cortex (B) and ipsilateral (ih) and contralateral (ch) hippocampus (C) after TBI is shown as percent of craniotomy control values. Each data point represents the mean ± SEM of four to six independent experiments. *$p <$ 0.05, **$p < 0.001$ versus craniotomy control (one-way ANOVA test with *post hoc* Bonferroni analysis).

Western blot analyses provided unequivocal evidence of increased levels of survivin protein after injury in the ipsilateral cortex and hippocampus. Densitometric analyses (Fig 2B) confirmed statistically 4-8 fold increases in survivin protein especially in the 3rd and 5th day after injury. Concurrently, expression of PCNA was also significantly enhanced in the ipsilateral cortex and hippocampus of these rats with similar temporal and spatial patterns. Immunohistochemistry revealed that survivin and PCNA were co-expressed in the same cells and had a focal distribution within the inured brain.

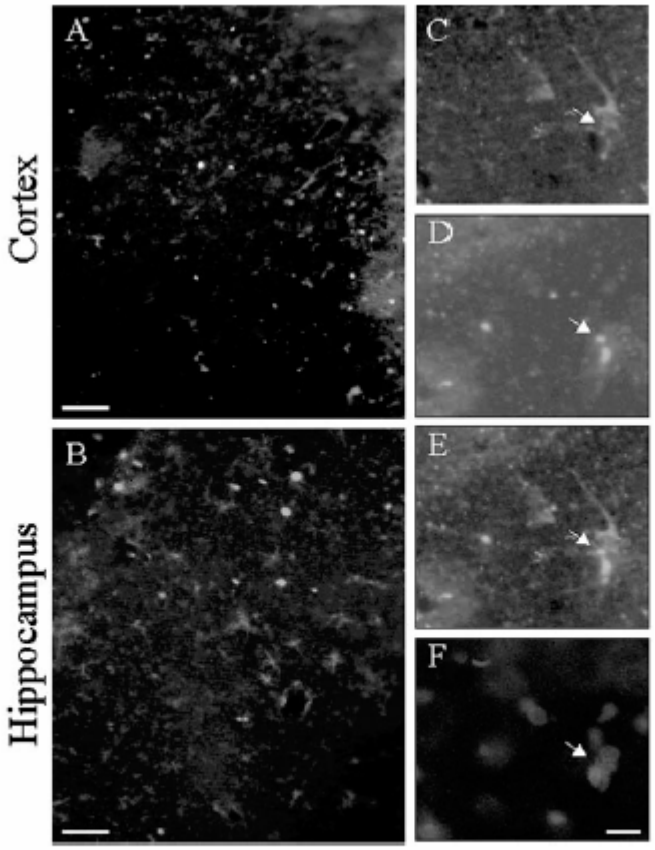

FIG. 4. Immunohistochemistry of survivin and PCNA. Double fluorescent immunostaining for survivin (red) and PCNA (green) was performed in the ipsilateral cortex (**A**) and hippocampus (**B**) at 5 day post-injury. Survivin is expressed in the cytoplasm (**C**, red), while PCNA is expressed in the nucleus (**D**, green). The white arrow indicates the typical focal co-expression of survivin and PCNA as shown in merged survivin and PCNA images (**E**). PCNA expression was co-incident with DAPI staining (**F**, blue, white arrow). Original magnification, ×200; bar = 50 μm (A,B); original magnification ×400, bar = 20 μm (C–F).

Figure 4 from the original manuscript shows the immunohistochemistry of survivin in PCNA in the cortex and hippocampus at 5 days post injury. Survivin was primarily expressed in the cytoplasm while PCNA was expressed in the nucleus. Further analyses revealed a frequent co-localization of survivin in GFAP, an astrocytic marker, in both the ipsilateral cortex and hippocampus, while a much smaller subset of cells showed co-localization of survivin and NeuN, a mature neuronal marker. Neuronal localization of survivin was observed predominantly in the ipsilateral cortex in contralateral hippocampus after TBI.

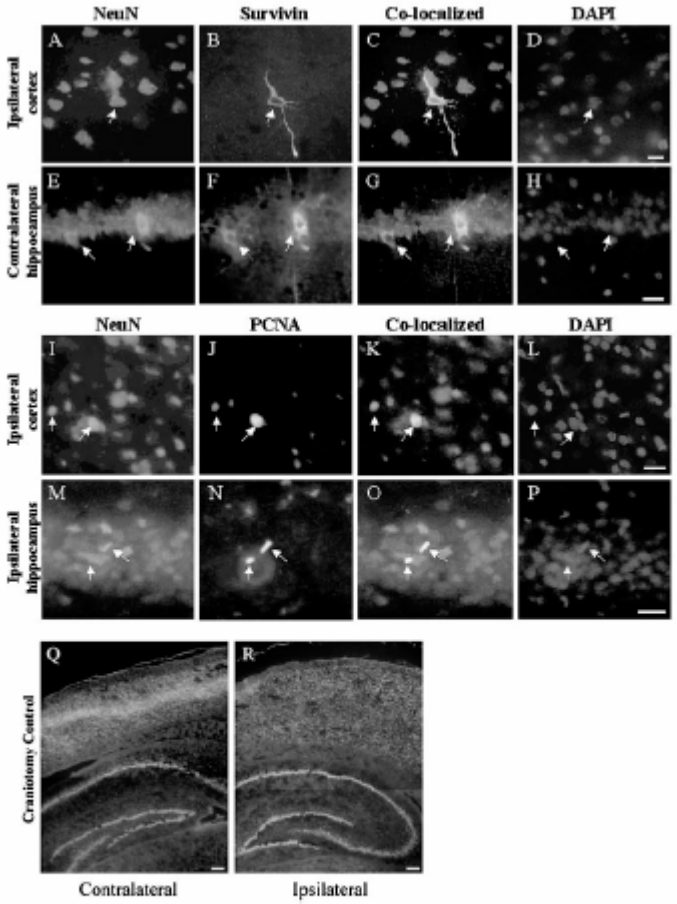

FIG. 7. A sub-set of NeuN-positive neurons express survivin and PCNA after TBI. Double fluorescent immunohistochemistry for survivin (green) and NeuN (red) in the ipsilateral cortex (A,B) and the CA1 pyramidal layer of the contralateral hippocampus (E,F) was performed. Survivin is expressed in the cytoplasm and, to a limited extent, in the processes of NeuN-positive neurons (merged images C/G). Dual staining for PCNA (green) and NeuN (red) is shown in the ipsilateral cortex (I,J) and the CA1 pyramidal layer of the ipsilateral hippocampus (M,N). The nuclei are shown using DAPI staining (D,H, blue). PCNA is expressed in the nucleus of NeuN-positive neurons (merged images K/O). PCNA expression was co-incident with DAPI staining in these examples (L,P, blue). White arrows indicate focal co-localization of survivin/NeuN and PCNA/NeuN. Survivin/NeuN co-localization of survivin (green) and NeuN (red) was seen only in TBI rats as opposed to either hemisphere of craniotomy control (Q,R). Original magnification, ×400, bar = 20 μm (A–P); original magnification, ×50, bar = 100,000 μm (Q,R).

As shown in Figure 7 from the original manuscript, a subset of NeuN-positive neurons expressed survivin in PCNA after TBI. These cells were usually located in the ipsilateral cortex and CA1 in the pyramidal layer of some hippocampal neurons. Survivin was expressed in a cytoplasm and, to a limited extent, in the processes of new NeuN positive neurons. PCNA was usually expressed in the nucleus of NeuN-positive neurons. Other analyses showed PCNA protein expression was detected in both astrocytes and neurons of the ipsilateral cortex and hippocampus after TBI.

In summary, our data demonstrated for the first time the induction of survivin in the rat brain following TBI. Expression of survivin occurred predominantly in astrocytes but also in a smaller subset of neurons and was accompanied by the expression of PCNA. The appearance of survivin and PCNA separately in neurons and astrocytes along with co-localization of survivin with PCNA in the same cells provide correlative data to suggest an activation of a cell cycle-like program in astrocytes and a smaller subset of neurons after TBI. In addition, these studies lay the foundation for the next series of studies more directly examining the potential anti-apoptotic role of survivin.

Since the previous paper provided the first evidence of survivin upregulation following TBI, we conducted subsequent research to look at the effect of survivin upregulation on phenotypic expression of apoptotic cell death associated with caspase-3 activation **(Johnson et al., Exp. Br. Res., 2005)**. Although

survivin does not prevent the activation of caspases from their inactive proforms, evidence has shown that survivin can bind and inhibit the activity of caspase-3. Thus, we sought to examine the relationships between survivin and apoptosis, specifically the accumulation of active-caspase-3 and downstream DNA fragmentation (TUNEL). As shown in Fig 1 of the original manuscript, Western blot analyses revealed significant increases in active caspase-3 in a time dependent manner between 5 and 14 days after injury **[see FIG 1 in Johnson paper, included in this report].** Active caspase-3 was readily detectible in the ipsilateral cortex and hippocampus of rats subjected to TBI (Fig 1A). In the ipsilateral cortex, significant increases in caspase-3 levels were most prominent at 5 & 7 days after injury, but were still significantly increased 14 days after injury. Increased caspase-3 activation was significant in the ipsilateral hippocampus at 14 days post injury (Fig 1B). No difference was observed between the percentage of survivin-positive and survivin-negative cells labeled with active caspase-3 at 5 or 7 days post-injury, as indicated by dual fluorescent immunostaining. However, as shown in Fig 3 of the original manuscript, survivin-negative cells exhibited significantly greater labeling with TUNEL compared with survivin-positive cells, suggesting that suppression of survivin may attenuate DNA cleavage and progression of apoptosis. **[see FIG 3 in Johnson paper, included in this report]** Thus, quantitative analysis of immunohistochemical data shown in Figure 3 revealed no significant difference in the accumulation of active caspase-3 in survivin-positive cells compared with survivin-negative cells at 5 days post-injury in either the cortex or hippocampus. However, a significantly higher percentage of TUNEL labeling was observed in survivin-negative cells, as compared with survivin-positive cells in both regions. A higher percentage of astrocytes accumulated active caspase-3 compared with neurons in contrast, neurons showed a higher co-localization with TUNEL than did with astrocytes. These data suggest that survivin expression may attenuate DNA cleavage and cell death and that this mechanism operates in a cell type-specific manner after TBI. Figure 7 of the original manuscript shows a putative mechanism for apoptosis inhibition by survivin. Following upstream caspase activation in cleavage of pro-caspase-3 to active caspase-3, survivin acts to attenuate the apoptotic cascade in DNA cleavage by inhibiting caspase-3 activity. **[See FIG 7 in Johnson paper, included in this report].**

In conclusion, our data provide the previously unreported demonstration that caspase-3 is activated in the rat brain after TBI in the same course region and cell type expression pattern as survivin (see summary of preceding manuscript). These data suggest that DNA cleavage may be attenuated by the expression of survivin protein following TBI in a cell specific fashion. Namely, astrocytes have significantly lower TUNEL and more frequent survivin labeling than neurons, suggesting a more robust anti-apoptotic role for survivin in astrocytes. Taken together, these results suggest that survivin may be part of counter-acting mechanisms to diminish expression of the apoptotic cell death phenotype following TBI in rats.

SOW 5

Hypothesis: Activation of calpain and/or caspase-3 is associated with generation of specific proteins or peptide fragments detectible in cerebrospinal fluid (CSF) that are biochemical markers of necrosis and/or apoptosis. In addition, proteomics-based platforms can provide powerful technologies to detect biomarkers ultimately providing capabilities for non-invasive assessments of pathological mechanisms of CNS injury and neurodegeneration in CSF and/or blood samples.

This grant originally proposed that biochemical markers could more reliably characterize necrosis and apoptosis than standard phenotypic approaches (SOW 1, p4). This insight, originally proposed by Dr. Pike, provided a theoretical framework for biomarker studies that led to exciting novel applications unanticipated in the original proposal. While SOW 1 had firmly established that biomarkers could provide accurate information on necrosis and apoptosis, additional *in vitro* data suggested the unprecedented hypothesis that biochemical events occurring within cells may ultimately be accessible non-invasively.

These *in vitro* studies examined the effects of a neurotoxin (NMDA) on the breakdown products (BDPs) of α-spectrin produced by calpain and caspase-3 activation, the same biochemical markers of necrosis and apoptosis employed in SOW 1.

FIGURE A

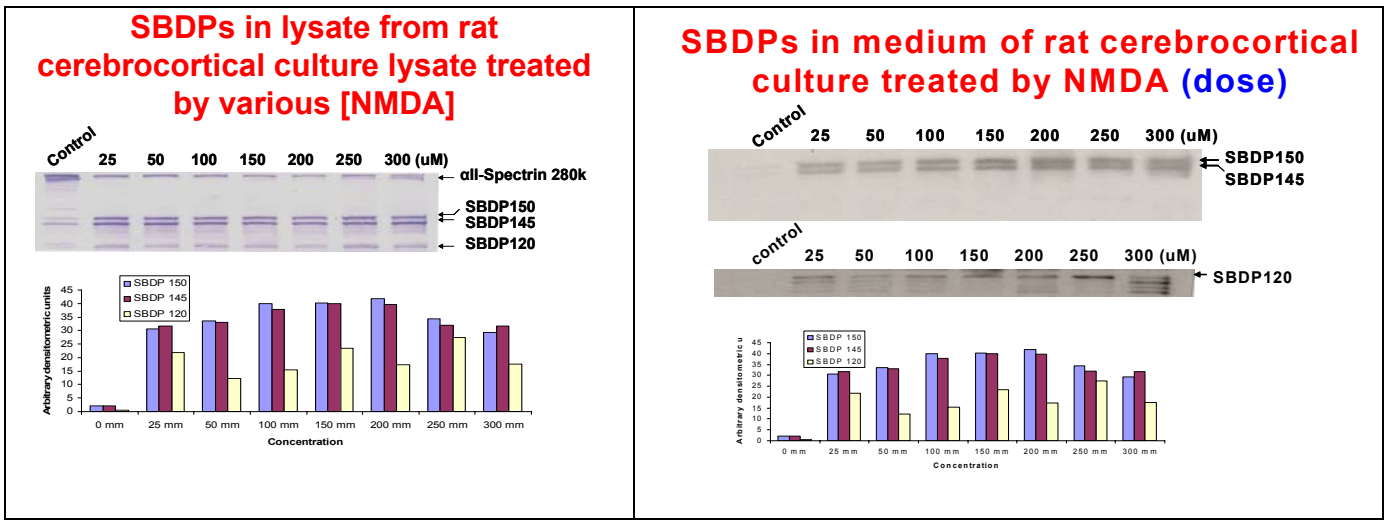

As shown in Figure A, cell lysates from rat cerebrocortical cultures treated by varying concentrations of NMDA showed characteristic profiles of calpain (SBDP 150, SBDP 145) and caspase-3 (SBDP 120) activation. Importantly, these SBDPs were also detected in the medium of rat cerebrocortical cultures treated by the same dose of NMDA. Time course analyses indicated that these BDPs were rapidly released from cells into the culture medium. This observation suggested the exciting possibility that injured cells in the intact brain could ultimately release biochemical markers of injury into the extracellular space and ultimately into the CSF. These observations provided the impetus for the research reviewed in SOW 4. This research includes the first systematic studies to provide initial assessments of the relevance of biochemical markers of necrosis and apoptosis to pathology expressed following acute CNS injury produced by trauma or ischemia. In addition, we initiated the first systematic studies, including proteomics-based approaches, to identify new biochemical markers of cell injury and death, including novel markers of necrosis and apoptosis.

SOW 5A-Plan

To examine the accumulation of biochemical markers of calpain and caspase-3 activation in CSF of rats following cerebral ischemia produced by middle cerebral artery occlusion (MCAO).

Prior to his departure, and during the funding period of the original proposal, Dr. Pike had recognized the important implications of the potential of developing capabilities of assessing non-invasively biochemical markers of CNS injury, including markers of necrosis and apoptosis. Thus, we initiated a study of the accumulation of α-spectrin and its associated BDPs in CSF after TBI in rats **(Pike et al., J Neurochem., 2001)**. This paper represented the first study of the accumulation of cellular BDPs of α-spectrin in CSF after TBI. This study demonstrated robust increases in calpain mediated BDPs in CSF following injury. Caspase-3 specific BDPs were observed to increase in CSF in some animals but generally to a lesser degree. These results indicated that αII-spectrin and its BDPs could be a powerful discriminator of outcome in protease activation after TBI.

Thus, we sought to expand these observations to the study of ischemia produced by MCAO in rats **(Pike et al., JCBFM, 2003)**. This investigation examined accumulation of calpain- and caspase-3-cleaved α-spectrin BDPs in CSF of rodents subjected to 2 hrs of transient MCAO followed by reperfusion. As shown in Figure 2 of the original manuscript, following MCAO injury, full length α-spectrin protein was

decreased in brain tissue and increased in CSF from 24 hrs to 72 hrs after injury. Calpain- and caspase-3-specific BDPs were also increased in brain CSF after injury. Levels of calpain-specific BDPs were greater at each post-injury time point than levels of caspase-3 specific BDPs. Levels of these proteins were undetectable in CSF of uninjured control rats .

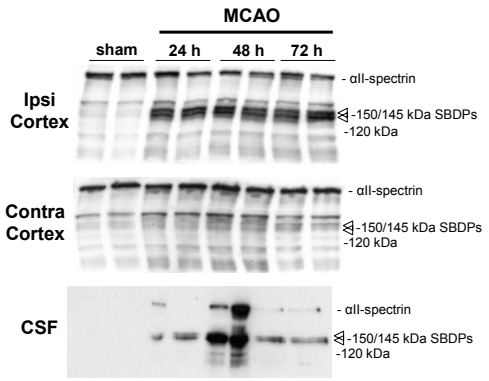

Figure 2. MCAO injury causes accumulation of full-length αII-spectrin (280 kDa) protein, and calpain-mediated 145 kDa and caspase-3 mediated 120 kDa αII-SBDPs in CSF. MCAO resulted in proteolysis of constitutively expressed brain αII-spectrin (280 kDa) in ipsilateral but not contralateral cortex. The caspase-3-mediated, apoptotic-specific 120 kDa αII-SBDP was also increased in ipsilateral cortex after ischemia compared to sham-injured controls. Marked increases in the calpain-specific 145 kDa αII-SBDP were detected in brain and CSF of MCAO animals, but not in sham-injured animals, at all time points. Interestingly, while increased levels of the caspase-3-specific 120 kDa αII-SBDP were detected at all post-injury time points in the ipsilateral cortex, CSF levels were only detected at 48 hours post-injury.

We also examined the relationship between expression of BDPs in brain tissue and CSF. Densitometric analyses were conducted on Western blots and least squares regression lines of levels of brain and CSF spectrin and its BDPs were plotted on the same graph.

Figure 4. Mean (± s.d.) cortical vs. CSF levels of αII-spectrin (280 kDa) and αII-SBDPs (150, 145, and 120 kDa) over days post-injury. Least squares regression lines of brain and CSF spectrin and SBDP levels were plotted on the same graph. Pearson correlation coefficients for each regression line are indicated. Results indicate that parenchymal decreases in levels of native αII-spectrin (280 kDa) are associated with increases in CSF accumulation while increased parenchymal levels of calpain-mediated αII-SBDPs (150 & 145 kDa) are associated with increased CSF accumulation. On average, there were no changes in parenchymal or CSF levels of the caspase-3-mediated 120 kDa αII-SBDP across days. However, individual rats at different time points (particularly 48 hours post-injury) showed some increase in CSF levels of the 120 kDa product.

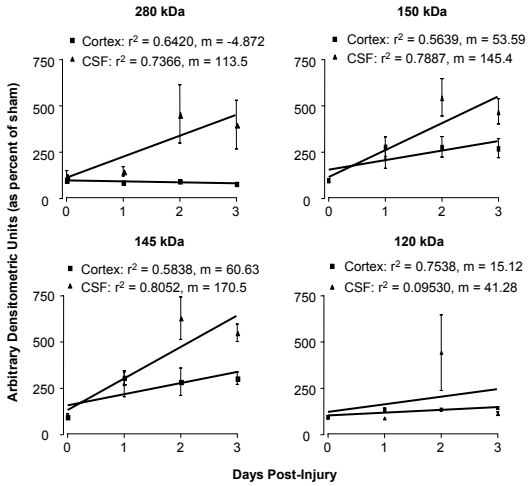

As shown in Fig 4 from the original manuscript, parenchymal decreases in levels of intact α-spectrin are associated with increases in CSF accumulation while increased parenchymal levels of calpain-mediated BDPs (150 and 145 kDa) are associated with increased levels of these markers of calpain activation. On average, there were no changes in pyrinchamal or CSF levels of caspase-3-mediated BDPs across days. However, individual rats at different time points (especially at later time points) showed some increases in CSF levels of the 120 kDa product related to caspase-3 activation.

In combination with our previously published data on TBI, this study provided a powerful proof of principle of the general utility of assessment of biochemical markers of necrosis and apoptosis in CSF. Since CSF is routinely accessible in many medical emergencies, including severe TBI, these data suggest the potential of minimally invasive assessments of these important biochemical markers. In addition, these data suggested the even more exciting possibility that these markers could ultimately be detected in blood. We further explored the general utility of biomarkers of proteolytic damage following TBI in a review paper **(Pineda, et al., Brain Path., 2004)**. This paper reviewed the current state of knowledge concerning caspase and calpain as specific markers of TBI, and discussed α-spectrin as a potential marker useful for such assessments.

SOW 5B-Plan
To examine the potential clinical utility of biochemical markers of calpain and caspase-3 activation in CSF of rats following TBI produced by closed cortical impact (CCI). Assessments of validity would include studies of relationship between injury magnitude, lesion size and outcome.

An optimal biomarker of acute brain injury should minimally provide information about the magnitude of injury, the extent of tissue damage and predict outcome. Thus, we examined the levels of α-spectrin breakdown products (SBDPs) in the ipsilateral cortex and CSF of rats at varying times after two levels of controlled CCI **(Ringger et al., J Neurotrauma, 2004)**. Densitometric analyses SBDPs incorporated a combined examination of the 145/150 kDa doublet detected on Western blots. SBDPs were measured by Western blot from the CSF and ipsilateral cortex at 2, 6, and 24 hrs after two magnitudes of TBI. Western blots were also subjected to densitometric analyses.

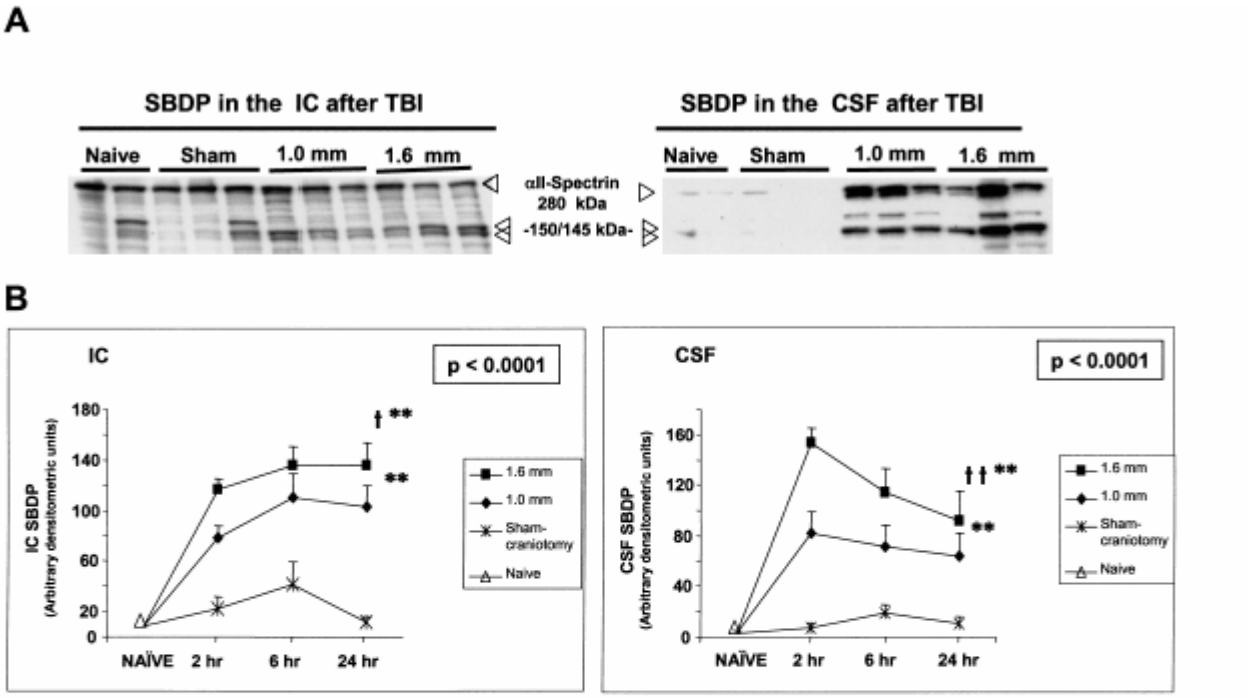

FIG. 1. Injury magnitude increases levels of SBDP in the ipsilateral cortex (IC) and CSF. (**A**) A representative Western blot of αII-spectrin and SBDP in the IC (left) and CSF (right) at 24 and 2 h, respectively, after TBI. Samples were collected after severe (1.6 mm) injury, mild (1.0 mm) injury, sham-craniotomy or from naive rats. Higher levels of SBDP are seen after severe (1.6 mm) injury than after mild (1.0) injury. Minimal SBDP is seen in the IC or CSF of naive rats or after sham-craniotomy in rats. (**B**) SBDP levels (145–150-kDa fragments) in the IC (left panel) and CSF (right panel) after sham-craniotomy, mild (1.0 mm) injury and severe (1.6 mm) injury at 2, 6, and 24 h were quantified using computer-assisted densitometric analysis (ImageJ, version 1.29×, NIH, USA). Values from naive animals were averaged as a separate time point. At each time point of 2, 6, and 24 h, 9 rats received severe (1.6 mm) injury, 9 rats received mild (1.0 mm) injury, 8 rats received a sham-cra-niotomy and 4 rats remained naive. An ANOVA was performed followed by contrast with pair-wise comparisons. Data is presented as the mean plus standard error. Standard error bars on the shams are present but not easily visable. Injury magnitude significantly increased mean levels of IC and CSF SBDP over time ($p < 0.0001$). Mean levels of SBDP after severe (1.6 mm) injury were significantly higher from the mean levels of SBDP after mild (1.0 mm) injury ($^{\dagger\dagger}p = 0.0001$ and $^{\dagger}p < 0.05$, respectively, for CSF and IC levels of SBDP). Mean levels of IC and CSF SBDP after both severe (1.6 mm) and mild (1.0 mm) injury were significantly greater than mean levels of SBDP after sham-craniotomy or in naive controls ($^{**}p < 0.0001$). Mean levels of CSF and IC SBDP did not differ between naive and sham.

As shown in Figure 1 of the original manuscript, statistical analyses indicated that injury magnitude significantly increased the level of cortical SBDPs (Fig 1B). Mean levels of cortical SBDPs after severe (1.6mm) injury were significantly higher than mean levels of SBDPs after mild (1.0mm) injury. Mean levels of SBDPs after both severe and mild injury were significantly greater than mean levels of SBDPs after craniotomy or naïve controls. Representative gels showed that levels of SBDPs increased with injury magnitude in the ipsilateral cortex in CSF (Fig 1A). Statistical analyses also indicated that injury magnitude significantly increased the level of CSF SBDPs (Fig 1B). Mean levels of CSF SBDPs after severe injury were significantly higher than mean levels of CSF SBDPs after mild injury. Mean levels of CSF SBDPs after both severe and mild injury were significantly greater than mean levels of CSF SBDPs after craniotomy (naïve controls). Lesion size on T2 weighted images increased with injury magnitude 24 hrs after TBI. Importantly, as shown in Figure 3 from the original manuscript, there was a significant relationship between the levels of CSF SBDPs with lesion size detected on MRI 24 hrs after injury.

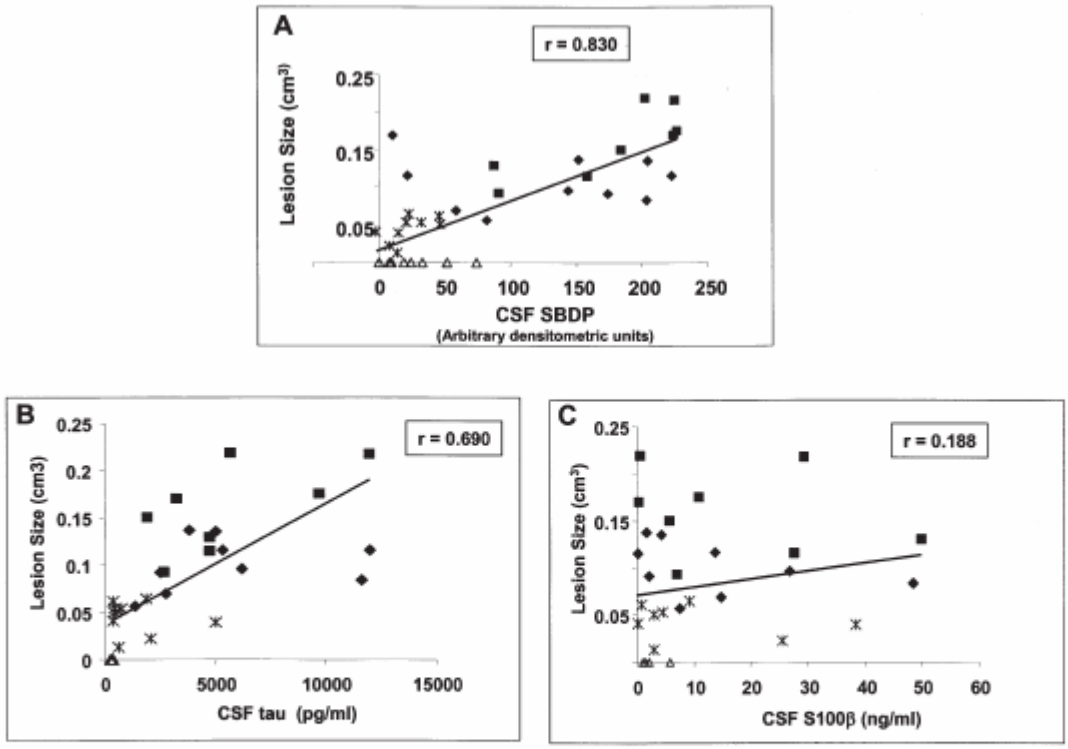

FIG. 3. The relationship of levels of CSF SBDP and tau with lesion size 24 h after TBI. Regression analysis was performed with lesion size as the out-come variable and levels of CSF markers (SBDP, tau, S100β) 24 h after TBI as the predictor variable. (**A**) Levels of CSF SBDP correlate with lesion size after TBI ($r = 0.83$, $p \leq 0.0001$). A linear regression equation showed that CSF SBDP significantly contributed to prediction of lesion size ($p \leq 0.0001$). (**B**) Levels of CSF tau correlate with lesion size after TBI ($r = 0.690$, $p < 0.001$). A linear regression equation showed that CSF tau significantly contributed to prediction of lesion size ($p \leq 0.0001$). The correlation with CSF SBDP and tau was not significant if craniotomy and sham rats were not considered in the analysis. (C) Levels of CSF S100β did not correlate with lesion size ($r = 0.188$). ■, rats after 1.6 mm injury; ◆, rats after 1.0 mm injury, ✳, rats after sham-craniotomy; △, naive rats.

Thus, CSF SBDP significantly contributed to the prediction of lesion size. This predictive value was greater than that for CSF tau or for S100β, other putative biomarkers of brain injury. Although the predictive value of the tau biomarker was statistically significant, levels of CSF S100β did not correlate with lesion size. Because CSF SBDP correlated with lesion size at 24 hrs, we looked at the relationship between lesion size and motor performance. Motor performance was assessed in the same rats that lesion size was measured. Importantly, larger lesion sizes were associated with decreased assessment of motor performance on the rotorrod.

In summary, this work provided the first systematic preclinical assessment of the potential clinical utility of SBDPs in CSF. These studies provided a critical confirmation that the magnitude of changes in SBDPs was reliably associated with the magnitude of injury and lesion size. In addition, the study provided data suggesting that biomarker analyses could ultimately be used to predict behavioral outcome.

SOW 5C-Plan

Proteomics-based technologies including SDS-PAGE-capillary liquid chromatography-tandem mass spectrometry and high throughput immunoblotting can provide powerful tools for discovery of novel biochemical markers of TBI, some of which could reflect calpain and/or caspase-3 activation.

Rapid advances in mass spectrometry methods capable of identifying thousands of proteins in a single sample by protease-specific peptide sequences provides the exciting possibility of rapid discovery of protein biomarkers in complex samples. However, this technique is challenged by several limitations. Poorly resolved proteins elude identification, while well resolved, multiply labeled, proteins produce

abundant identifications with mass spectrometry. Given our emphasis on rapid analysis, rather than more comprehensive initial characterization, we selected the limited resolving power of SDS-PAGE as an effective means to reduce redundant identifications and accelerate the discovery of putative protein biomarkers. Importantly, this initiative represented the first systematic approach to apply contemporary proteomics technologies to the discovery of novel biomarkers following acute CNS injury.

We employed SDS-PAGE-capillary liquid chromatography-tandem mass spectrometry (SDS-PAGE-capillary LC-MS^2) **(Haskins et al., 2005)**. Ipsilateral hippocampal samples were collected from naïve rats and rats subjected to control cortical impact in rats. Protein database searching with 15,558 uninterpreted MS^2 spectra, collected in 3 days via data-dependent capillary LC- MS^2 of pooled cyanine dye-labeled samples separated by SDS-PAGE, identified more than 305 unique proteins. Differential proteomic analysis revealed differences in protein sequence coverage for 170 mammalian proteins (57 in naïve only; 74 in injured only; and 39 of 64 in both), suggesting these are putative biomarkers of TBI (See Table 1 in original manuscript). Inspection of the proteins falling into each of these 3 categories of protein markers showed that several well studied proteins involved in TBI were observed in both naïve and injured samples, including brain creatine kinase (CKB), α-spectrin, neuron-specific enolase (NSE), α-synuclein (α-Syn), microtubule associated protein 2a and 2b (MAP2), neurofilament (NF), proteolipid protein (PLP), and myelin basic protein (MBP). The injured-to-naïve ratio of protein sequence coverage suggested putative biomarkers that may exhibit significant differences in protein concentration between naïve and injured samples. However, protein sequence coverage is only a semi-quantitative measure of protein concentration. This is particularly true for protein identifications based on single tryptic peptide sequences, and is even more pronounced for degraded proteins. However, proteins observed only in naïve samples, or proteins observed with greater sequence coverage in naïve samples than in injured samples, suggests a subset of putative biomarkers that are down-regulated, released, or degraded during TBI-for example αII-spectrin **(Pike et al., 2001, 2003)**. Likewise, proteins observed in only injured samples, or proteins observed with greater sequence coverage in injured samples than in naïve samples, suggests a subset of putative biomarkers that are upregulated or aggregated during TBI-for example, NSE. The presence of known biomarkers of TBI such as α-spectrin and NSE in our data set increased confidence in our results. As shown in Figure 3 of the original manuscript, approximately 10% of our putative biomarkers were neuronal, suggesting a number of potentially useful markers of neuronal damage

following TBI.

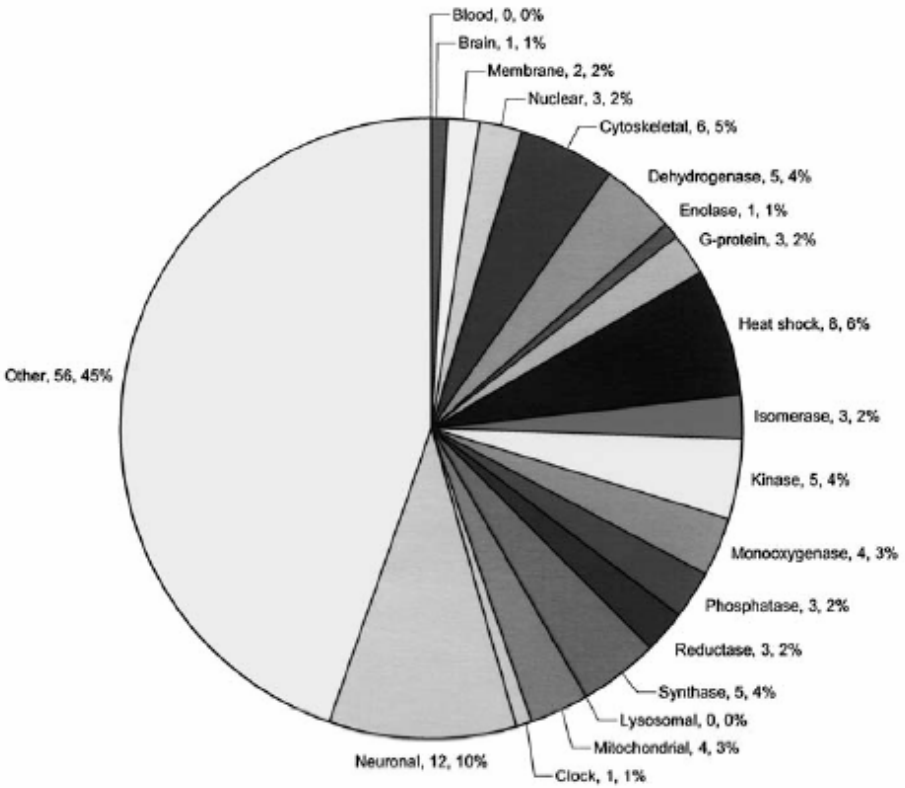

FIG. 3. Stratification of the putative protein biomarkers discovered in injured hippocampus only. Protein class, number of proteins, fraction of protein biomarkers. Proteins were sorted into classes based on function and localization with increasingly stringent specificity: blood, brain < membrane < nuclear < cytoskeletal < dehydrogenase, enolase, clock, G-protein, heat shock, isomerase, kinase, monooxygenase, phosphatase, reductase < synthase < lysosomal, mitochondrial < neuronal.

In summary, this study was the first of its kind to employ advanced MS proteomic techniques to biomarkers discovery following acute CNS injury. These data provide important proof-of-principle for more rapid and comprehensive sequence-specific biomarker discovery strategies incorporating protein separation prior to capillary LC- $MS^{2.}$ Thus, this work established a critical platform for productive future biomarker discovery.

Prior to the completion of the funding period for this proposal, we also initiated the first studies using a novel high throughput immunoblotting (HTPI) approach employing 1,000 monoclonal antibodies (PowerBlot) to more specifically compare calpain and caspase-3 degradation of a large number of substrates following experimental TBI in rats. This research was published subsequent to the end of the funding period and is included in this report **(Liu et al., 2006)**. HTPI is a proteomic method targeting human or rat/mouse proteins. A total of 5 large SDS-PAGE gel/blots were done. Then each of these blots was separated into 40 lanes and each lane was than subjected to multiple monoclonal antibodies that target protein antigens with good data separation. Since HTPI is still essentially a Western blot, it is excellent for separating intact proteins and their potential BDPs. We further hypothesized that HTPI could assist us in identifying the complete set of brain protein substrates (degradome) that undergo proteolic degradation during and after brain injury. We termed this "the TBI degradome" in light of the widely recognized effort to patrician the proteome into subsets of post-translational modification events including proteolytic degradation. To further identify the degradome, we in parallel contrasted the TBI differential proteome with caspase-2 and caspase-3 degradomes, as generated by *in vitro* digestion of naïve hippocampal lysate with these two proteases, respectively. In addition, this was the first effort to use the HTPI approach to explore proteolytic systems in both *in vitro* and *in vivo* systems. We compared pooled rat hippocampal lysate samples from 4 treatment groups: 1) naïve, 2) TBI (48 hrs after controlled cortical impact), 3) *in vitro* calpain II digestion and 4) *in vitro* caspase-3 digestion. As shown in Table 1 of the

original manuscript, we identified 54 and 38 proteins vulnerable to calpain II and caspase-3 proteolysis, respectively. In addition, 48 proteins were down-regulated following TBI while only 9 were upregulated.

A

Degradome	Template A	Template B	Template C	Template D	Template E	TOTAL Hits
Calpain-2	23	13	8	3	7	54
Caspase-3	11	12	6	2	7	38
TBI	18	14	10	7	8	57

B

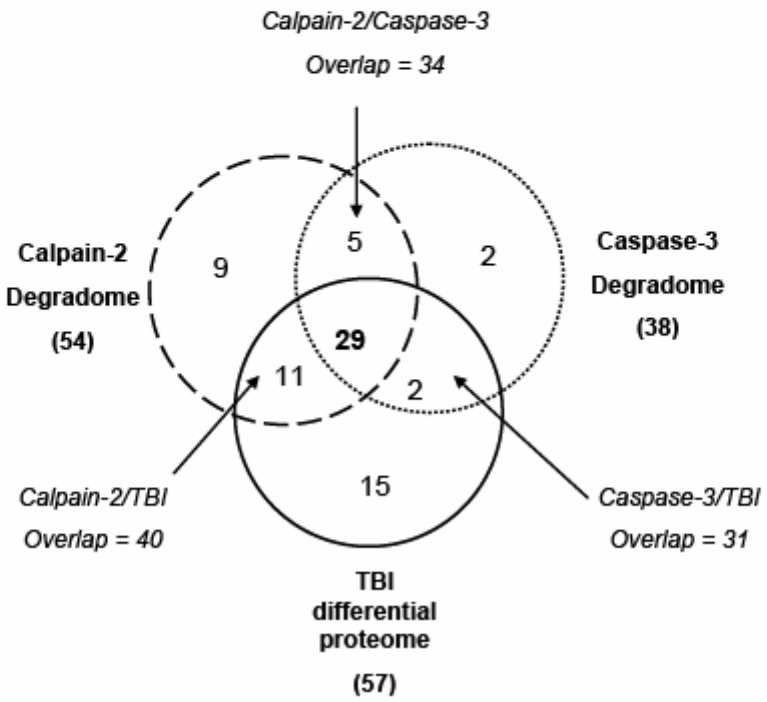

Figure 7 from the original manuscript summarizes characterization of the 3 degradomes studied: caspase-2 degradome, caspase-3 degradome and TBI degradome. Figure 7B employs a VIN diagram to show overlap of protein targets in the 3 degradomes. Thus, among proteins down regulated in TBI, 42 of them overlapped with calpain-2 and/or caspase-3 degradomes, suggesting that these also might be proteolytic targets in TBI. We further confirmed several novel TBI-linked proteolytic substrates by traditional immunoblotting, including βII-spectrin, striatin, synaptotagmen-1, synaptojanin-1 and NSF.

In summary, these studies represent the first effort to apply HTPI to biomarker identification following acute CNS injury. Importantly, we have begun critical studies subdividing the CNS injury proteome into meaningful degradome subcomponents.

KEY RESEARCH ACCOMPLISHMENTS

- Provided the first systematic evidence that distinct cell death modalities are better defined by biochemical markers of proteolysis (e.g. calpain, caspase-3 activation) than by previously employed approaches of phenotypic descriptions of apoptosis and necrosis.

- Provided systematic confirmation that TNF-α is a potent mediator of caspase-3 activation. Associated *in vivo* studies, provided the first evidence that caspase-8 mediated pathways (activated by TNF-α receptor coupled mechanisms) could be the predominant pathway regulating caspase-3 activation and apoptotic cell death following TBI.
- Characterized a rat hippocampal slice model as a useful *ex vivo* model for studying calcium mediated neurotoxicity potentially linked to excitotoxic and proteolytic mechanisms of cell death, especially calpain proteolysis.
- Provided the first observation that apoptosis produced by caspase-3 activation may be regulated by a novel anti-apoptotic protein, survivin.
- Developed the first biochemical markers useful to assess necrotic and apoptotic cell death following acute CNS injury *in vivo* and conducted preclinical studies rigorously examining their potential clinical utility.
- Pioneered the application of proteomics including MS and high throughput protein immunoblots, to the study of the pathobiology of TBI. Studies laid foundation for development of novel biochemical markers of calpain and caspase proteolysis.

REPORTABLE OUTCOMES

Abstracts

T.M. Shepherd, B.R. Pike, P.E. Thelwall, **R.L. Hayes**, E.D. Wirth III. Diffusion-weighted magnetic resonance imaging of cell death in rat hippocampal slices. 19th Annual National Neurotrauma Society Symposium, November, 2001.

Pike, BR, Flint, J, Dutta, S, Wang, DS, Wang, KKW, **Hayes, RL**. Accumulation of spectrin and calpain-cleaved spectrin breakdown products in CSF after TBI in rats.ASN, June 2002.

J Flint, BR Pike, **RL Hayes**, JR Moffett, JR Dave, X-CM Lu, FC Tortella. Accumulation of calpain and caspase-3 cleaved αII-spectrin breakdown products in CSF after middle cerebral artery occlusion in rats. NINTS, 2002.

Jose A Pineda, Jada M Aikman, Erik A Johnson, Barbara E. O'Steen, Tao Fan & **Ronald L Hayes**. Temporal profile of αII-spectrin breakdown products after TBI in immature rats. NINTS, Oct. 2002.

N.C. Ringger, X. Silver, B. O'Steen, J.G. Brabham, S.M. DeFord, B.R. Pike, J. Pineda & **R.L. Hayes**. CSF Accumulation of calpain-specific αII-spectrin breakdown products are associated with injury magnitude and lesion volume after TBI in rats. NINTS, Oct., 2002.

R.L. Hayes, N.C. Ringger, X. Silver, B. O'Steen, J.G. Brabham, S.M. DeFord, B.R.Pike, J. Pineda. CSF accumulation of calpain-specific αII-spectrin breakdown products correlate with injury magnitude and lesion volume after traumatic brain injury in rats. Winter Conference on Brain Research, Jan., 2003.

William E. Haskins, Kevin K.W. Wang, Ming Chen Liu, Scott H. McClung, Alexi G. Lundberg, Barbara E. O'Steen, Marjorie M. Chow, Jose A. Pineda, Nancy D. Denslow and **Ronald L. Hayes.** Discovering novel protein biomarkers of traumatic brain injury in hippocampus and CSF by 1D-DIGE/CLC/MS. American Society for Mass Spectrometry, June, 2003.

Ronald L. Hayes. Comparison of biomarkers alpha-II spectrin breakdown products, S100B, and tau after traumatic brain injury. Advanced Technology Application for Combat Casualty Care (ATACCC) meeting in St. Petersburg, FL, Aug. 2003.

Will Haskins, Firas Kobeissy, Ming Chen Liu, Barbara O'Steen, Scott McClung, Marjorie Chow, Nancy Denslow Jitendra Dave, X-C May Lu, Frank Tortella**, Ronald L. Hayes**, & Kevin K.W. Wang. Differential in gel electrophoresis-capillary liquid chromatography-tandem mass spectrometry-based discovery of biomarkers for traumatic and ischemic brain injuries in rats. ATACCC, St. Petersburg, FL, Aug. 2003.

Ronald L. Hayes. Systematic comparisons of biomarkers after TBI: Alpha II-spectrin breakdown products, S100B and tau. 3rd International Conference on Biochemical Markers for Brain Damage, Lund, Sweden. Sept. 2003.

William E. Haskins, Ming Cheng Liu, Firas H. Kobeissy, Scott H. McClung, Alexia G. Lundberg, Barbara E. O'Steen, Marjorie M. Chow, Jose A. Pineda, Nancy D. Denslow, **Ronald L. Hayes**, Kevin K.W. Wang. Discovering novel protein biomarkers of TBI by differential gel electrophoresis-capillary liquid chromatography-tandem mass spectrometry. National Neurotrauma Society (NNT) Nov. 2003.

Ming Cheng Liu, **Ronald L. Hayes**, Kevin K. W. Wang. Extensive myelin basic protein degradation in rat brain after TBI. NNT, Nov. 2003.

Ronald L. Hayes & Andrew K. Ottens. Developing proteomics-based platforms to study brain injury: Challenges in data analysis and interpretation. Applied Math Seminar, UF Department of Mathematics, Apr. 2004.

Andrew K Ottens, Firas H Kobeissy, Zhiqun Zhang, Erin Golden, Regina Wolper, Su-Shing Chen, Ming Chen Liu, **Ronald L Hayes**, Kevin KW Wang. The bioinformatic challenge in brain injury neuroproteomics. Bioinformatics Workshop, 2004.

S Sadasivan, RC Ellis, W O'Steen, MC Liu, **RL Hayes,** D Anderson, KKW Wang. Concurrent proteolysis of axonal αII-spectrin and myelin basic protein following spinal cord injury. 10th Annual Kentucky Spinal Cord & Head Injury Research Symposium, June 2004.

Kevin KW Wang, Nancy D Denslow & **Ronald L Hayes**. Applying proteomics in brain injury studies. International Neurotrauma Symposium (INTS), September 2004.

AK Ottens, EC Golden, MC Liu, R Wolper, ND Denslow, **RL Hayes,** KKW Wang. Quantitative degradomic mass spectrometry approach to monitoring myelin basic protein proteolysis resulting from TBI. SFN, Oct. 2004.

Wenrong Zheng, Ming Cheng Liu, **Ronald L Hayes**, Kevin KW Wang. Simultaneous breakdown of αII- and βII-spectrin by calpain and caspase-3 in rat cerebrocortical culture under oncotic, apoptotic and excitotoxic challenges. NNS, Oct. 2004.

Ming Cheng Liu, Wenrong Zheng, B O'Steen, **Ronald L Hayes** and Kevin KW Wang. Degradation of βII-spectrin in rat brain after traumatic brain injury. NNS, Oct. 2004.

Ronald L. Hayes. An integrated platform for discovery and preclinical/clinical validation of biomarkers of brain injury. CHI Biomarker Validation meeting, San Francisco, Feb. 2005.

Published Papers

* W.E. Haskins, F.H. Kobeissy, R.A. Wolper, A.K. Ottens, J.W. Kitlen, S.H. McClung, B.E. O'Steen, M.M. Chow, J.A. Pineda, N.D. Denslow, **R. L. Hayes**, K.KW Wang. Rapid discovery of putative protein biomarkers of traumatic brain injury by SDS-PAGE-capillary liquid chromatography-tandem mass spectrometry. J Neurotrauma 22(6): 629-644, 2005.

* Erik A Johnson, Stanislav I Svetlov, Kevin KW Wang, **Ronald L Hayes** and Jose A Pineda. Cell-specific DNA fragmentation may be attenuated by a survivin-dependent mechanism after traumatic brain injury in rats. Exp Brain Res, 167(1): 17-26, 2005.

*** M C Liu, V Akle, W Zheng, J R Dave, F C Tortella, **R L Hayes**, K K W Wang. Comparing calpain- and caspase-3 mediated degradation patterns in traumatic brain injury by differential proteome analysis. Biochem. Journal, 394:715-25, 2006.

** Jennifer K. Newcomb-Fernandez, Xiurong Zhao, Brian R. Pike, Kevin K.W. Wang, Andreas Kampfl, Ronald Beer, S. Michelle DeFord and **Ronald L. Hayes**. Concurrent assessment of calpain and caspase-3 activation after oxygen-glucose deprivation in primary septo-hippocampal cultures. JCBFM 21:1281-1294, 2001.

* Jose A. Pineda, Kevin K.W. Wang, **Ronald L. Hayes**. Biomarkers of proteolytic damage following traumatic brain injury. Brain Pathology 14(2), 202-209, 2004.

* Pike BR, Flint J, Dave JR, Lu XC, Wang KK, Tortella FC, **Hayes RL**. Accumulation of calpain and caspase-3 proteolytic fragments of brain-derived αII-spectrin in CSF after middle cerebral artery occlusion in rats. JCBFM, 24(1): 98-106, 2003.

* NC Ringger, BE O'Steen, JG Brabham, X Siler, J Pineda, KKW Wang, **RL Hayes**. A novel marker for traumatic brain injury: CSF αII-spectrin breakdown product levels. J Neurotrauma, 21(10) 1443-1456, 2004.

* Timothy M. Shepherd, Peter E. Thelwall, Stephen J. Blackband, Brian R. Pike, **Ronald L. Hayes** and Edward D. Wirth, III. Diffusion MRI study of a rat hippocampal slice model for acute brain injury. JCBFM, 23: 1461-1470, 2003.

** Xiurong Zhao, Brian Bausano, Brian R. Pike, Jennifer K. Newcomb-Fernandez, Kevin K.W. Wang, Esther Shohami, N.C. Ringger, S.M. DeFord, Douglas K. Anderson and **Ronald L. Hayes**. TNF-α stimulates caspase-3 activation and apoptotic cell death in primary septo-hippocampal cultures. JNR 64: 121-131, 2001.

*Supported by DAMD17-01-1-0765

** DAMD17-01-1-0765 erroneously not cited. Relevant to SOWs of original proposal and contributed to by Dr. Pike.

***Work conducted during funding period – published after funding period ended.

Presentations

Invited Lecturer (2 lectures), UCLA Division of Neurosurgery, Los Angeles, CA (Jan, 2002)

Invited Attendee, Advanced Technology Applications for Combat Casualty Care, sponsored by the DoD, St. Petersburg, FL (Sept, 2002)

Invited Discussant, 1st NINDS/NIH "Proteomics in the Neurosciences" Workshop Washington, DC (Dec, 2002)

Invited Speaker, Santa Lucia Hospital, Rome, Italy (Feb, 2003)

Invited Speaker, NIH/NINDS (Apr, 2003)

Invited Speaker, Uniformed Services University of the Health Sciences And NBIRTT sponsored conference, Bethesda, MD (June, 2003)

Invited Speaker, Post Traumatic Brain Contusions and Lacerations International meeting, Rimini, Italy (Sept, 2003)

Invited Speaker, 3rd International Conference on Biochemical Markers for Brain Damage Lund, Sweden (Sept, 2003)

Invited Participant, NIH Bullock DSMB, Richmond, VA (Nov, 2003)

Invited Speaker, Grand Rounds, Univ of Mississippi Dept Neurosurgery, Jackson MS (Apr, 2004)

Invited Speaker & Poster Presentation, DoD Peer Review Medical Research Program Meeting, San Juan, Puerto Rico (Apr, 2004)

Invited Speaker, Combine ATACCC & NATO Meetings, St. Petersburg, FL (Aug, 2004)

Invited Speaker, ACRM-ASNR Joint Conference, Ponte Vedra, FL (Sept, 2004)

Invited Speaker, CHI's 2nd Annual Biomarker Validation conference, San Francisco CA (Feb, 2005)

Invited Speaker, VA Sponsored TBI Workshop, WRAMC, Silver Spring, MD (Apr, 2005)

Invited Speaker, 3rd Pannonian Symposium on CNS Injury, Pecs, Hungary (Apr, 2005)

Invited Lecturer, Fondazione Santa Lucia, Rome, Italy (May, 2005)

Invited Speaker, National Chinese Academy Workshop on Cranial Cerebral Trauma Shanghai, China (May, 2005)

Invited Speaker, Beijing Neurosurgical Practice Group, Beijing, China (May, 2005)

Invited Speaker, Shanghai Neurosurgical Practice Group, Shanghai, China (May, 2005)

Invited Speaker, Xian Neurosurgical Practice Group, Xian, China (May, 2005)

Invited Attendee, ATACCC, St. Petersburg, FL (Aug, 2005)

CONCLUSIONS

Our laboratory made significant contributions to testing the general hypotheses outlined in Dr. Pike's original proposal. Consistent with SOW 1 of the original proposal, we examined the contribution of calpain and caspase-3 activation to expression of necrotic and apoptotic phenotypes following the clinically relevant manipulation of oxygen glucose deprivation. This work extended the systematic examination of the role of these proteases in phenotypic expression of necrosis and apoptosis conducted by Dr. Pike and other in our laboratory and outlined in SOW 1. Consistent with SOW 3 and 4, we confirmed the role of receptor coupled, TNF-α mediated activation of caspase-3 and resulting apoptosis *in vitro* (SOW 3). We also provided the first demonstration that caspase-8 (activated by TNF-α coupled receptors) results in caspase-3 activation in apoptosis following TBI *in vivo* (SOW 4).

This research has also led to important novel and unanticipated findings. These findings included the development of a *ex vivo* model (rat hippocampal slice) useful for studying calcium mediated neurotoxicity typically closely linked to proteolytic mechanisms of cell death, especially calpain proteolysis. We have also provided exciting and entirely unique observations that apoptosis following TBI produced by caspase-3 activation may be reduced by the anti-apoptotic protein, survivin. Finally, we have built on Dr. Pike's original assertion that biochemical markers could be accurate and reliable indices of cell death mechanisms. Thus, we have focused on developing the first program to systematically identify and preclinically validate biochemical markers of acute CNS injury. We have provided strong evidence that breakdown products of α-spectrin identical to those used by Dr. Pike in his *in vitro* studies will be useful biomarkers of acute CNS injury produced by a variety of insults including neurotoxins. In addition, we have developed the first proteomics-based platform to discover novel biochemical markers of acute insults, including novel markers of calpain and caspase-3 proteolysis.

REFERENCES

Ronny Beer, Gerhard Franz, Stanislaw Krajewski, Brian R. Pike, **Ronald L. Hayes**, John C. Reed, Kevin K. Wang, Christian Klimmer, Erich Schmutzhard, Werner Poewe, and Andreas Kampfl. Temporal and spatial profile of caspase 8 expression and proteolysis after experimental traumatic brain injury. J Neurochem. 78, 862-873, 2001.

* W.E. Haskins, F.H. Kobeissy, R.A. Wolper, A.K. Ottens, J.W. Kitlen, S.H. McClung, B.E. O'Steen, M.M. Chow, J.A. Pineda, N.D. Denslow, **R. L. Hayes**, K.KW Wang. Rapid discovery of putative protein biomarkers of traumatic brain injury by SDS-PAGE-capillary liquid chromatography-tandem mass spectrometry. J Neurotrauma 22(6): 629-644, 2005.

Erik A Johnson, Stanislav I Svetlov, Brian R Pike, Paul J Tolentino, Gerald Shaw, Kevin KW Wang, **Ronald L. Hayes** and Jose A Pineda. Cell-specific upregulation of survivn after experimental traumatic brain injury in rats. JNT 21(9): 1183-1195, 2004.

* Erik A Johnson, Stanislav I Svetlov, Kevin KW Wang, **Ronald L Hayes** and Jose A Pineda. Cell-specific DNA fragmentation may be attenuated by a survivin-dependent mechanism after traumatic brain injury in rats. Exp Brain Res, 167(1): 17-26, 2005.

*** M C Liu, V Akle, W Zheng, J R Dave, F C Tortella, **R L Hayes**, K K W Wang. Comparing calpain- and caspase-3 mediated degradation patterns in traumatic brain injury by differential proteome analysis. Biochem. Journal, 394:715-25, 2006.

** Jennifer K. Newcomb-Fernandez, Xiurong Zhao, Brian R. Pike, Kevin K.W. Wang, Andreas Kampfl, Ronald Beer, S. Michelle DeFord and **Ronald L. Hayes**. Concurrent assessment of calpain and caspase-3 activation after oxygen-glucose deprivation in primary septo-hippocampal cultures. JCBFM 21:1281-1294, 2001.

* Jose A. Pineda, Kevin K.W. Wang, **Ronald L. Hayes**. Biomarkers of proteolytic damage following traumatic brain injury. Brain Pathology 14(2), 202-209, 2004.

Brian R. Pike, Xiurong Zhao, Jennifer K. Newcomb, Kevin K.W. Wang, Rand M. Posmantur and **Ronald L. Hayes.** Temporal relationships between *de novo* protein synthesis, calpain and caspase 3-like protease activation, and DNA fragmentation during apoptosis in septo-hippocampal cultures. J. Neurosci. Res. 52: 505-520, 1998.

Brian R. Pike, Xiurong Zhao, Jennifer K. Newcomb, Christopher C. Glenn, Douglas K. Anderson and **Ronald L. Hayes**. Stretch injury causes calpain and caspase-3 activation and necrotic and apoptotic cell death in septo-hippocampal cell cultures. J. Neurotrauma. 17(4): 283-298, 2000.

Brian R Pike, Jeremy Flint, Satavisha Dutta, Erik Johnson, Kevin K.W. Wang and **Ronald L. Hayes.** Accumulation of non-erythroid αII-spectrin and calpain-cleaved αII-spectrin breakdown products in cerebrospinal fluid after TBI in rats. J. Neurochem. 78: 1297-1306, 2001.

* Pike BR, Flint J, Dave JR, Lu XC, Wang KK, Tortella FC, **Hayes RL**. Accumulation of calpain and caspase-3 proteolytic fragments of brain-derived αII-spectrin in CSF after middle cerebral artery occlusion in rats. JCBFM, 24(1): 98-106, 2003.

* NC Ringger, BE O'Steen, JG Brabham, X Siler, J Pineda, KKW Wang, **RL Hayes**. A novel marker for traumatic brain injury: CSF αII-spectrin breakdown product levels. J Neurotrauma, 21(10) 1443-1456, 2004.

* Timothy M. Shepherd, Peter E. Thelwall, Stephen J. Blackband, Brian R. Pike, **Ronald L. Hayes** and Edward D. Wirth, III. Diffusion MRI study of a rat hippocampal slice model for acute brain injury. JCBFM, 23: 1461-1470, 2003.

Zhao, X., Pike, B.R., Newcomb, J.K., Wang K.K.W., Posmantur, R.M. and **Hayes, R.L.** Maitotoxin induces calpain but not caspase-3 activation and necrotic cell death in primary septo-hippocampal cultures. Neurochem. Res. 24(3): 371-382, 1999.

Xiurong Zhao, Jennifer K. Newcomb, Brian R. Pike, Kevin K.W. Wang, Domenico d'Avella, and **Ronald L. Hayes.** Novel characteristics of glutamate-induced cell death in primary septo-hippocampal cultures: Relationship to calpain and caspase-3 protease activation. J. Cereb. Blood Flow Metab. 20(3): 550-562, 2000.

** Xiurong Zhao, Brian Bausano, Brian R. Pike, Jennifer K. Newcomb-Fernandez, Kevin K.W. Wang, Esther Shohami, N.C. Ringger, S.M. DeFord, Douglas K. Anderson and **Ronald L. Hayes**. TNF-α stimulates caspase-3 activation and apoptotic cell death in primary septo-hippocampal cultures. JNR 64: 121-131, 2001.

*Supported by DAMD17-01-1-0765

** DAMD17-01-1-0765 erroneously not cited. Relevant to SOWs of original proposal and contributed to by Dr. Pike.

***Work conducted during funding period – published after funding period ended.

Liu et al. (2005) Biochem. J. (revised) # **BJ2005/0905**

Biochem Journal 394 : 715-725, 2006

Comparing calpain- and caspase-3-degradomes to traumatic brain injury differential proteome: A high throughput immunoblotting approach

Ming Cheng LIU[1,2], Veronica AKLE[1,2], Wenrong ZHENG[1,2], Jitendra R. DAVE[4], Frank C. TORTELLA[4] and Ronald L. HAYES[1,2,3] and Kevin K.W. WANG[1,2,3]

Center for Neuroproteomics and Biomarkers Research, Department of Psychiatry[1], Center for Traumatic Brain Injury Studies, Department of Neuroscience[2], McKnight Brain Institute, University of Florida, PO Box 100256, Gainesville, FL 32610, USA, Banyan Biomarkers, Inc[3]. 12085 Research Drive; Suite 180, Alachua, FL 32615, USA
Department of Neuropharmacology and Molecular Biology[4], Division of Neurosciences, Walter Reed Army Institute of Research, Silver Spring, Maryland, USA

*Correspondence: All correspondence should be addressed to: Dr Kevin Wang, McKnight Brain Institute, L4-100, P.O. Box 100256, University of Florida, Gainesville, FL 32610, USA. kwang1@ ufl.edu, Fax: 352-392-2579

Key words: Proteases, degradation, cell death, proteomics

Short title: Calpain and caspase degradomes versus traumatic brain injury proteome

Abbreviations:

BDP: breakdown products

HTPI: high throughput immunoblotting

TBI: traumatic brain injury

NSF: N-ethylmaleimide sensitive fusion protein

SNARE: soluble N -ethylmaleimide-sensitive fusion protein attachment protein receptor

SNAP-25: Synaptosome-Associated Protein of 25 kDa

SNAP-23: Synaptosome-Associated Protein of 23 kDa

CaMPK-II: Calcium/Calmodulin-Dependent Protein Kinase II

CaMPK-IV: Calcium/Calmodulin-Dependent Protein Kinase IV

Psme3; proteasome activator subunit 3

NES1; serine protease inhibitor kallikrein

PEX19; peroxisome assembly factor 19

Scamp1; secretary carrier-associated membrane protein 1

RIP; receptor-interacting protein kinase

Synopsis

A major theme of traumatic brain injury (TBI) pathology is the over-activation of multiple proteases. For example, we have previously shown that calpain-1 and 2 and caspase-3 simultaneously produced αII-spectrin breakdown products following TBI. In this study, we attempted to further identify a comprehensive set of protease substrates (degradomes) for calpains and caspase-3. We further hypothesize that the TBI differential proteome is likely to overlap significantly with calpain- and caspase-3-degradomes. Using a novel high throughput immunoblotting (HTPI) approach with 1,000 monoclonal antibodies (PowerBlot), we compared pooled rat hippocampal lysate samples from four treatment groups: (i) naïve, (ii) TBI (48 h after controlled cortical impact), (iii) *in vitro* calpain-2 digestion and (iv) caspase-3 digestion. In total, we identified 54 and 38 proteins were respectively vulnerable to calpain-2 and caspase-3 proteolysis. In addition, 48 proteins were down-regulated following TBI, while only 9 were upregulated. Among those down-regulated in TBI, 42 of them overlapped with calpain-2 and/or caspase-3 degradomes, suggesting that these might also be proteolytic targets in TBI. We further confirmed several novel TBI-linked proteolytic substrates by traditional immunoblotting, including βII-spectrin, striatin, synaptotagmin-1, synaptojanin-1 and NSF (N-ethylmaleimide sensitive fusion protein). In summary, we demonstrated that HTPI is a novel and powerful method for studying proteolytic pathways *in vivo* and *in vitro*.

Introduction

Traumatic brain injury (TBI) represents a major CNS disorder without any clinically proven therapy. However, significant progress has been made in understanding the biochemical mechanism of injury. Indeed, protease over-activation is a major theme in traumatic and ischemic brain injury. These include cysteine proteases (calpain-1 and -2 and caspase-3, cathepsin-B and –L [1], metalloproteases (e.g., MMP-2 and -9) [2-3] and threonine protease proteasome [4]. Of particular interest are calpains and caspase-3 [5]. Calpain is activated during both oncotic (necrotic) and apoptotic cell death in neurons, while caspase-3 is strictly activated in neuronal apoptosis. Evidence demonstrates that both necrotic and apoptotic cell death are present in traumatic and ischemic brain injury. Our laboratory has shown that calpain-produced and caspase-3-produced αII-spectrin breakdown products (SBDPs) are present following both traumatic and ischemic brain injury. We further showed that the same SBDPs could be found in the cerebrospinal fluid following TBI in rats [6]. In fact, many other brain proteins have previously and independently been identified as vulnerable to proteolytic attack after neural toxic insults or by calpain and/or caspase-3 action. These include βII-spectrin, CaMPK-IV and CaMPK-II [5, 7-8].

Novel high throughput immunoblotting (HTPI) technology (BD PowerBlot^{TM}) [9-16] has recently been developed. This proteomic method employs a panel of 1,000 monoclonal antibodies targeting human or rat/mouse proteins. A total of 5 large SDS-PAGE gel / blots were done. Then each of these blots was separated into 40 lanes using a manifold system. Each lane was then subjected to multiple monoclonal antibodies that target protein antigens with good data separation (molecular mass difference), thus achieving a high throughput status. Since HTPI is still Western blot in principle, it is excellent for separating intact proteins and their potential breakdown products. We argue that it is an excellent system to study proteolysis. We further hypothesize that HTPI can assist us identifying the complete set of brain protein substrates (degradome) that undergo proteolytic degradation during and after traumatic brain injury. We termed this the "TBI degradome," fashioned after the term "degradomes" coined by Lopez-Otin and

Overall ([17]. It is likely that following TBI, some proteins will be up- or down-regulated, rather than just being proteolytically modified. Thus, to further identify those that are degradomic, we in parallel contrasted the TBI differential proteome with calpain-2- and caspase-3- degradomes, as generated by *in vitro* digestion of naïve hippocampal lysate with these two proteases, respectively. To our knowledge, this is the first report of using HTPI approach to explore proteolytic systems in both *in vitro* and *in vivo* systems. Our method might also find utilities in identifying protein substrates for novel proteases with unknown functions.

Experimental

In vivo model of traumatic brain injury model

A controlled cortical impact (CCI) device was used to model TBI in rats as previously described (Pike 1998). Briefly, adult male (280-300 g) Sprague-Dawley rats (Harlan: Indianapolis, IN) were anesthetized with 4% isoflurane in a carrier gas of 1:1 O_2/N_2O (4 min) followed by maintenance anesthesia of 2.5% isoflurane in the same carrier gas. Core body temperature was monitored continuously by a rectal thermistor probe and maintained at 37±1°C by placing an adjustable temperature controlled heating pad beneath the rats. Animals were mounted in a stereotactic frame in a prone position and secured by ear and incisor bars. A midline cranial incision was made, the soft tissues reflected, and a unilateral (ipsilateral to site of impact) craniotomy (7 mm diameter) was performed adjacent to the central suture, midway between bregma and lambda. The dura mater was kept intact over the cortex. Brain trauma was produced by impacting the right cortex (ipsilateral cortex) with a 5 mm diameter aluminum impactor tip (housed in a pneumatic cylinder) at a velocity of 3.5 m/s with a 1.6 mm (severe) compression and 150 ms dwell time (compression duration). These injuries were associated with local cortical contusion and more diffuse axonal damage. Velocity was controlled by adjusting the pressure (compressed N_2) supplied to the pneumatic cylinder. Velocity and dwell time were measured by a linear velocity displacement transducer (Lucas Shaevitz™ model 500 HR, Detroit, MI) that produced an analogue signal that was recorded by a storage-trace oscilloscope (BK Precision, model 2522B, Placentia, CA). Sham-injured control animals underwent identical surgical procedures but did not receive an impact injury. Pre- and post-injury management were in compliance with guidelines set forth by the University of Florida Institutional Animal Care and Use Committee and the National Institutes of Health guidelines detailed in the Guide for the Care and Use of Laboratory Animals.

Hippocampus tissue collection and protein extraction

Forty-eight hours after CCI, animals were anesthetized and immediately sacrificed by decapitation. Brains were immediately removed, rinsed with ice-cold PBS and halved. For the left injured hemispheres, hippocampus was rapidly dissected, rinsed in ice cold PBS, snap-frozen in liquid nitrogen, and frozen at –80°C until used. For Western blot analysis, the brain samples were pulverized with a small mortar-pestle set over dry ice to a fine powder. The pulverized hippocampal tissue powder was then lysed for 90 min at 4°C with 50 mM Tris (pH 7.4), 5 mM EDTA, 1% (v/v) Triton X-100, 1 mM DTT. Due to the need for *in vitro* protease digestion, protease inhibitor cocktail was not used. Instead, extreme care was taken to keep samples as cold as possible and to work rapidly to reduce post-mortem artefact. The brain lysate was then centrifuged at 8000 g for 5 min at 4°C to clear and remove insoluble debris, snap-frozen and stored at -85°C until used.

Calpain-2 and caspase-3 digestion of naïve brain lysate and purified proteins

Hippocampus tissue lysate was prepared as above. For purified protein digestion, βII-spectrin and synaptotagmin were used. βII-spectrin (as a subunit of αII- and βII-spectrin heterotetramer) was purified from rat brain as described previously [27]. Recombinant synaptotagmin (as a GST fusion protein) was obtained from Abnova Corp (Taiwan).

In vitro protease digestion of naïve rat hippocampus lysate (5 mg) or purified protein with purified proteases, human calpain-2 (Calbiochem, Cat# 208715 calpain-2, 1μg/μl) and recombinant human caspase-3 (Chemicon Cat# cc119, caspase-3, 1 Unit/μl) (at a protein/protease ratio of 1/200 and 1/50, respectively) was performed in a buffer containing 100 mM Tris-HCl (pH 7.4) and 20 mM dithiothreitol. For calpain-2, 10 mM $CaCl_2$ was also added, and then incubated at room temperature for 30 minutes. For caspase-3, 2 mM EDTA was added in stead of $CaCl_2$ and was incubated at 37°C for 4 hours. The protease reaction was stopped by the addition of SDS-PAGE sample buffer containing 1% (w/v) SDS.

High throughput Immunoblotting

Four sets of pooled samples (n=6; naïve rat hippocampus, TBI, calpain-digestion, and caspase-3 digestion) were prepared and subjected to sets of 5 gel/blots (templates A-E). The electrophoresis and blots were performed at BD Bioscience facility (Bringamham, KY). Briefly, the gels were 13 X 10 cm, 4-15% gradient SDS-polyacrylamide, 0.5 mm thick (Bio-Rad Criterion IPG well comb). A gradient system was used so a wide size range of proteins can be detected on one gel. Protein extract (200 µg) was loaded in one big well across the entire width of the gel. This translates into ~10 µg per lane on a standard 10 well mini-gel. The gel was run for 1.5 hours at 150 volts. Proteins in the gel were transferred to Immobilon-P membrane (0.2 um, Millipore) for 2 hours at 200 mAmp. We used a wet electrophoretic transfer apparatus TE Series from Hoefer. After transfer, the membrane is dried and re-wet in methanol. The membrane was blocked for one hour with blocking buffer (LI-COR). Next, the membrane was clamped with a Western blotting manifold that isolates 40 channels across the membrane. In each channel, a complex antibody cocktail (4-6 antibodies) was added and allowed to hybridize for one hour at 37°C. Each blot has 39 usable lanes and one lane probed with antibodies against molecular weight markers (MW) on the far right lane: MW Standards – Lane 40 of Templates A, B, C, and D blots were loaded with a cocktail composed of MW standards: p190 (190 kDa), Adaptin beta (106 kDa), STAT-3 (92 kDa), PTP1D (72 kDa), Mek-2 (46 kDa), RACK-1 (36 kDa), GRB-2 (24 kDa) and Rap2 (21 kDa). Lanes 20 and 40 of Template E blots wereloaded with two standardization cocktails (#1, 112 kDa, 83 kDa, 62 kDa, 55 kDa, 42 kDa, 28 kDa and 15 kDa; #2, 190 kDa, 120 kDa, 101 kDa, 60 kDa, 50 kDa, 27 kDa and 21 kDa). The blot was removed from the manifold, washed and hybridized for 30 minutes at 37°C with secondary goat anti-mouse conjugated to Alexa680 fluorescent dye (Molecular Probes). The membrane was washed, dried and scanned at 700 nm for monoclonal antibody target detection using the Odyssey Infrared Imaging System (LI-COR). Samples were run in triplicate and analyzed using a 3X3 matrix comparison method.

Traditional immunoblotting

Tissue samples (20 µg) were subjected to electrophoresis, equal volume of samples for SDS-PAGE was prepared within a two-fold loading buffer (0.25 M Tris (pH 6.8), 0.2 M DTT, 8% SDS, 0.02% Bromophenol Blue, and 20% glycerol in distilled H_2O), gels were run at 120 V for 2 hours in a mini-gel unit (Invitrogen). Protein bands were transferred to PDVF membrane on a semi-dry Transblot unit (BioRad) at 20V for 2 h. After electrotransfer, blotting membranes were blocked for 1 h at ambient temperature in 5% non-fat milk in TBST (20 mM Tris-HCl, pH 7.4, 150 mM NaCl and 0.05% (w/v) Tween-20), then incubated in primary monoclonal antibody in TBST with 5% milk. Primary antibodies used were Anti-αII-spectrin from Affiniti (FG6090), Anti-βII-spectrin, CaMPK-II (C89220), CaMPK-IV (C28420), striatin (S66020), synaptojanin-1 (S12520), synaptotagmin (S39520), and NSF (N14920) from BD Bioscience. The blot was then washed three times for 15 minutes with TBST and exposed to biotinylated secondary antibody (Amersham) followed by a 30 min incubation with strepavidin-conjugated alkaline phosphatase (colorimetric method). Colorimetric development was performed with a one-step BCIP-reagent (Sigma). Molecular weight of intact proteins and their potential breakdown products (BDPs) were assessed by running along side rainbow colored molecular weight standards (Amersham). Semi-quantitative evaluations of protein and BDP levels were performed via computer-assisted densitometric scanning (Epson XL3500 high resolution flatbed scanner) and image analysis with Image-J software (NIH).

Results

αII-spectrin immunoblot as positive control before HTPI.

Our experimental design calls for four groups: Naïve hippocampal lysate (naïve), TBI (traumatic brain injury in the form of controlled cortical impact with 1.6 mm deformation distance), *in vitro* calpain-2 and caspase-3 digestion of naïve hippocampal lysate. We initially considered using unpooled individual samples

for the HTPI analysis, but by running n=6 for the four conditions (naïve, calpain, caspase and TBI), it would mean a total of 24 samples. The cost for running such expansive analyses would be formidable and extremely time consuming. We have, therefore, decided on an alternative strategy of pooling 6 samples from each group to enhance signal-to-noise ratio and to identify "putative" hits. Subsequent to that, our strategy was to rely on follow-up "hit" confirmation with individual brain lysate samples and purified protein digestion analysis with traditional immunoblots. Naïve hippocampus lysate was separately prepared from 6 individual rats and 1 mg protein was pooled from each sample. Similarly, TBI samples were prepared from 6 injured individual rats and 1 mg samples were pooled. As for calpain-2 and caspase-3 digestion, 3 mg pooled naïve samples were separately digested with calpain-2 or caspase-3 at protease:substrate protein ratio (1/200 and 1/50, respectively). This process was repeated twice to build up to 6 mg of protein digest.

To ensure the quality of the pooled samples was sound before subjecting them to the rigorous high throughput immunoblotting (HTPI) process, we subjected these pooled samples to traditional immunoblotting against αII-spectrin, a well established target for both calpains and caspases [5]. Naïve brains present only intact αII-spectrin of molecular weight 280 kDa. Calpain-2 digestion reduced the levels of intact αII-spectrin and produced breakdown products of 150 kDa and 145 kDa (SBDP150 and SBDP145) while caspase-3 digestion also reduced the levels of intact αII-spectrin and yielded breakdown products of 149 kDa (SBDP149; also known as SBDP150i) and 120 kDa (SBDP120), as expected, based on our previous experience [5, 18] (**Fig. 1**). In the pooled TBI hippocampal samples, the reduction of αII-spectrin was not as notable, but a mixture of SBDP150/149, SBDP145 and SBDP120 were observed (**Fig. 1**), as previously identified [19]. This confirmed that the four samples we prepared for this proteomic study have preserved the expected characteristic features.

HTPI has high run-to-run reproducibility

Each pooled sample was run in triplicate on each of the five HTPI templates (A-E). Of the 1,000 antibodies probed, 550 of them gave a recognized and quantifiable signal after development. Figure 2 illustrated triplicate naïve samples developed as template A blots, showing relatively high-reproducibility in overall banding profile (**Fig. 2**). However, some variations in protein bands intensity of selected protein bands were observed, as expected from this type of analysis. Thus, it is important that samples are always run and compared in triplicate. Other templates (B-D) also showed similar levels of same-sample-consistency (results not shown).

Calpain-2, caspase-3 degradomes and TBI differential proteome identified by HTPI

Since samples were run in triplicate, for each pair-wise comparison (e.g., calpain-2 vs naïve), a 3 X 3 matrix of comparison was made to cover all 9 combinations. Based on vigorous densitometer-computer-assisted and manual comparisons, we focused on parent protein bands with significantly reduced intensity while also looking for appearance of potential breakdown product (BDP) bands after calpain-2/caspase-3 digestion (**Fig. 3 & 4**) or after TBI (**Fig. 5**). For example, Figure 3 contrasts representative template A blots for naïve and that for calpain-2 digestion. We noted that 23 parent proteins had average intensity reduced more than two-fold after calpain digestion while 9 potential BDP bands (lanes 2, 10, 11, 13, and 36) were observed after calpain-2 digestion (**Fig. 3**, lower panel). Similarly, 12 parent proteins in template A were significantly reduced after caspase-3 as a result of proteolysis, with at least three identifiable BDPs observed in lanes 8 and 13 (**Fig. 4**). Again, when template A for naïve hippocampus was compared to that of the TBI counterpart, 16 parent proteins were reduced in intensity, and therefore were either expression-down-regulated proteins or were potential proteolytic substrates (**Fig. 5**). In addition, two potential BDPs can be readily observed (lane 13, 18 and 29). In parallel, two proteins were found regulated in levels after TBI (CASK; A3 and Psme3; A29) (**Fig. 5**).

Template B comparisons also identified 13, 12 potential proteolysis targets for calpain-2, caspase-3, respectively and 14 differentially regulated proteins in TBI, (**Fig. 6**). In addition, templates C-E showed very similar proteomic patterns (results not shown). **Table 1** summarized the number of hits from each template when naïve was compared to calpain-2, caspase-3, and TBI, respectively. In all, 54 and 38 proteins were putatively sensitive to calpain-2 and caspase-3 proteolysis, respectively, while 48 proteins appeared down regulated or degraded following TBI, while only 9 proteins were up-regulated (CASK, Psme3, α-actinin, ceruloplasmin, cdk2, NES1, TBP, GS27 and Smg) (**Fig. 7A**). Parent protein signal reduction was from 2-fold to more than 10-fold. Based on 1,000 antibodies used, the "hit" rate for calpain vs. naïve, and caspase-3 digestion vs. naïve, and TBI vs. naïve were 5.4%, 3.8%, and 5.7%, respectively. Furthermore, 40 of these proteins were common between calpain-2 degradome and TBI differential proteome, while 31 proteins were common between caspase-3 degradome and TBI differential proteome, as illustrated by the Venn diagram (**Fig. 7B**). There were also significant overlaps (34 proteins) between the calpain-2 and caspase-3 degradomes. Lastly, there were 29 proteins identified to be putative degradomic targets under all three treatment conditions. However, it is important to note that the TBI differential proteome is not necessarily all degradative, but, in part, a result of changes in protein expression. Besides the 42 proteins in TBI that overlapped with calpain/caspase-3 degradomes, we also found 6 additional proteins with decreased signal but with no calpain/caspase degradation counterparts (RIP2/RICK; C26, syntaxin-6; C7, Rona; D27, PEX19; D29, SCAMP1; D38, and SLK; E13).(**Fig. 7A,Table 1)**

Table 1 further details the identity of putative calpain-2, caspase-3 substrates, and TBI differential target proteins. As expected, some previously known calpain substrates were identified by HTPI, including calcium/calmodulin-dependent protein kinase II (CaMPK-II; A36) [7], dynamin (B26) [19] protein kinase C (PKC)-alpha (B25), -beta (A18) and -gamma isoforms (A30) [5, 18]; SNAP-25 (A7) was described as a calpain substrate, although it was not well studied [20]. Previously reported dual calpain/caspase-3 substrates identified by HTPI included the

plasma membrane calcium pump isoform 2 (PMCA2; A17) ([20-21], βII-spectrin (E8) [18] and calcium/calmodulin dependent protein kinase IV (CaMPK-IV; C12) [8] (**Table 1**). Of 48 TBI-down-regulated proteins, (**Table 1**), nine proteins are associated with synaptic vesicle formation of their docking and trafficking: Synaptojanin-1 (synaptic IP3-kinase), synaptotagmin-1 (synaptic vesicle–exocytosis calcium sensor) and NSF (N-ethylmaleimide sensitive fusion protein) and synapsin-Ia and -II, SNAP-25, Munc-18, a/b-SNAP, amphiphysin and rabphilin 3A. These data suggest that proteolysis might play a significant role in the synaptic dysfunctions following TBI.

Cytoskeleton-associated protein dynamin and dynactin, as well as actin-binding protein profiling, were also identified as TBI-proteolytic substrates. Adhesion molecules (M-calherin and integrin-alpha3) and adaptor proteins beta-catenin and adaptin were also identified. Again, proteolysis of these proteins can lead to cytoskeletal degradation and cell shape compromise. Two neurotransmitter receptor, metabotropic glutamate receptor 1 (mGluR1) and GABE-B receptor 2 (GABA-B-R2), also appeared to be sensitive to proteolysis (**Table 1**).

Two cell cycle proteins (Ki67 and p55 Cdc) were also identified in TBI differential proteome. The TBI differential proteome also includes two apoptosis proteins, previously not identified to be sensitive to proteases-Bad protein (B36) that translocates to mitochondria as well as the mitochondria-released Smac/Daiblo (B6) that binds apoptosis inhibitor proteins IAP1/2, thus facilitating the induction of apoptosis. How proteolysis influences the functions of some of these proteins remains to be elucidated.

Degradomic and TBI differential proteomic target validation

In order to assess the confidence of the degradomic target assignment based on HTPI, we first asked how the HTPI results compared to traditional immunoblotting for a specific protein. From Template E (lane E8), we observed that out of all triplicate runs, βII-spectrin (240 kDa) consistently diminished upon protease treatments, while putative breakdown products (BDPs) of 110 KDa was

identified upon calpain digestion, while BDP of 108 kDa and 85 kDa were observed upon caspase-3 digestion. TBI also produced loss of intact βII-spectrin and fainter BDP bands of 110/108 kDa and 85 kDa (**Fig. 8A**). In parallel to HTPI, we applied pooled naïve hippocampal lysate and those subjected to calpain-2 and capase-3 digestion to traditional SDS-polyacrylamide gel electrophoresis (SDS-PAGE) followed by immunoblotting with a monoclonal anti-βII-spectrin antibody (BD Bioscience) that was identical to that used in the HTPI. As illustrated by Figure 6B, while naïve brains contained no BDPs, calpain-2 and capase-3 digestions produced BDPs of 110 kDa and BDP-108kDa and 85kDa, respectively, virtually identical to the patterns generated by HTPI (**Fig. 8A**). In addition, we also assessed the integrity of βII-spectrin in four individual naïve and four individual TBI hippocampal samples. Consistent with the HTPI data shown in figure 7A, we again observed, in traditional immunoblots, the presence of BDP of 110 kDa, 108 kDa and 85 kDa in all three TBI samples, but not in the naïve samples (**Fig. 8B**).

In this study, we identified over 30 novel protease substrates (see **Table 1**). To ascertain that these are truly proteolytic substrates, traditional immunoblots were again performed to four selected "novel" degradomic targets: striatin (C22) and NSF (E13) as calpain-2/caspase-3/TBI triple target; synaptojanin-1 (A23) and synaptotagmin-1 (A11) as calpain/TBI double targets (see **Table 1**). Traditional immunoblotting results showed that striatin (110 kDa) was indeed sensitive to calpain-2 digestion, producing BDPs of 40K and 35K as predicted from HTPI. Caspase-3 digestion also produced a high MW fragment of 100K (**Fig 9A**), which was not readily observed in HTPI. TBI samples also showed both caspase-produced BDP of 100K and calpain-produced BDPs of 40K and 35K. Next, we confirmed that synaptojanin-1 (140 kDa) was highly sensitive to calpain, producing BDP of 70K. Caspase-3 digestion, also partially degraded synaptojanin-1 to a faint 70K fragment, which was not observed in HTPI, probably due to sensitivity differences. Importantly, following TBI intact synaptojanin-1 protein was almost completely degraded to the 70K BDP (**Fig 9B**). Synaptotagmin-1 (65 kDa; A11) was degraded by calpain-2 to BDP of 33K

but not by caspase-3 (**Fig 9C**). The BDP-33K was also readily observed in all four TBI hippocampal samples (**Fig 9C**). Lastly, NSF was degraded by calpain and caspase-3 (to a lesser extent) to BDPs of 30K and 25K (**Fig 9D**). We also established that both of these BDPs were readily observed in TBI samples but not in naïve samples (**Fig 9D**).

Finally, to directly prove that purified HTPI-identified target proteins are indeed vulnerable to calpain and/or caspase-3, we tested two proteins. We obtained purified βII-spectrin (as a subunit of rat brain αII/βII-spectrin hetero-tetramer) and recombinant synaptotagmin-1 (as a GST-fusion protein) and subjected them to calpain/caspase-3 digestion. Coomassie blue staining of PAGE gel revealed that both αII- and βII-spectrin subunits (280 kDa and 260 kDa, respectively) were degraded by calpain and caspase-3, producing multiple fragments (**Figure 10A**). To ascertain that βII-spectrin was indeed a substrate for calpain and caspase-3, immunoblotting of the same samples probed with anti- βII-spectrin antibody was performed. We observed βII-spectrin breakdown patterns (BDP-110K for calpain, BDP-108K and -85K for caspase-3) (**Figure 10A**), virtually identical to those observed in HTPI of hippocampal lysate digest (**Figure 8**). Similarly, recombinant synaptotagmin-1 (as N-terminal GST fusion protein, about 90 kDa) was vulnerable to calpain-2 proteolysis, producing three major fragments (65K, 33K and 21K) (**Figure 10B**). Again, to ensure that the fragments were derived from the intact synaptotagmin portion of the fusion protein, we performed immunoblotting with anti-synaptotagmin antibody and identified two immunoreactive polypeptides (65K and 33K) (**Figure 10B**). While the 65K represents the full length synaptotagmin truncated from the GST portion (appeared as a 21K fragment) at the artificial linker region, the 33 kDa synaptotagmin BDP was identical in size to that produced when hippocampal lysate was digested with calpain (**Figure 9**).

Discussion

In this study, we combined two powerful and emerging areas in proteomics: degradomics [22] and high throughput monoclonal antibody panel-based immunoblotting (HTPI) for protein identification [9, 11]. Based on others' and our previous evidence showing dual attacks of neural proteins by calpains and caspase-3 under neural injury situations [5], we hypothesize that there will be significant overlap between the neuronal proteins vulnerable to proteolysis by direct calpain and caspase-3 digestion and following traumatic brain injury (i.e., calpain, caspase-3, and TBI-degradomes).

For our specific study, we compared and contrasted naïve versus traumatically injured hippocampal lysate. Craniotomy (sham) controls were performed, but not included in this study as this procedure also produced a mild form of brain trauma. As for the classical and ubiquitously distributed calpain-1 and –2, our evidence and others have concluded that they share identical substrate sets [23]. Thus for simplicity, only calpain-2 was used in the *in vitro* digestion of hippocampal lysate. Similarly, various caspases are activated in brain-injury induced neuronal apoptosis (caspase-3, -8, -9 and –12) [23-26]. Among the execution caspases, the most relevant and well studied is caspase-3. Therefore, it was selected for this comparative degradomic study. The calpain-2 and caspase-3 degradomic data generated were then compared to TBI degradomic data (**Table 1, Fig. 6**).

Using HTPI, we identified 43 proteins in the rat hippocampal proteome that were putatively degraded following TBI, while 54 and 38 proteins were respectively vulnerable to calpain-2 and cspase-3 proteolysis (**Table 1**). We further found that there were significant overlaps among the calpain-2, caspase-3 degradomes, and TBI differential proteome, with 29 of these proteins common among the three degradomes (**Fig. 6**). Within the calpain-2 and caspase-3 degradomes are previously identified calpain and capsase-3 substrates such as βII-spectrin, CaMPK-II and –IV (**Fig. 7-8**). We identified and confirmed a number of previously unknown protease-sensitive target proteins in TBI, such as striatin, synaptotagmin-1, synaptojanin-1 and NSF using traditional immunoblotting analysis of treated and untreated hippocampal lysate (**Fig. 9**). We further

confirmed that purified βII-spectrin and synaptotagmin-1 were *in vitro* substrates of calpain and/or caspase-3 (**Figure 10**).

Based on the significant overlaps among the calpain degradome, caspase-3 degradome and TBI differential proteome, it appears that these two proteases are operating in concert in TBI attacking a subset of cellular proteins that are important to neural functions. For example, many novel TBI proteolysis targets are synaptic vesicle proteins (**Table 1**; **Figure 9**). It is tempting to suggest that proteolysis play a significant role in the synaptic dysfunction following TBI. Many cytoskeleton proteins (dynamin, dynactin, and profilin and βII-spectrin) and cell adhesion proteins (adaptin and β-catenin) also appear to be at risk for proteolysis following TBI (**Table 1**). It should be noted that there are difference between TBI differential proteome versus the combined calpain/caspase-2 degradomes: while 42 TBI-down regulated proteins overlapped with calpain/caspase-3 degradomes, 6 other TBI-down-regulated-proteins have no calpain/caspase counterparts. In addition, there are also 9 prominently up-regulated proteins in TBI that could not be accounted for with calpain/capase-3 degradomes (**Table 1**, **Figure 7**).

To date, there are only a handful of published studies using HTPI/PowerBlot to address a biological problem [9-14]. Interestingly, only one previous paper used HTPI to study posttranslational modification–protein conjugation to ISG15, a ubiquitin-like protein [12]. Thus, to our knowledge, the current work is the first report to use HTPI to study protein proteolysis. While there are now several emerging proteomic technologies including tryptic peptide analysis by tandem mass spectrometry, antibody microarray) [27], the HTPI is the most ideally suited proteomic method to rapidly identify potential targets for a protease system. Most proteomic methods (MS/MS, antibody array) cannot readily distinguish intact proteins from their fragmented forms. However, HTPI, in contrast, is built on traditional immunoblotting technology. In this case, intact proteins and their potential fragments were first resolved by 1D-SDS-PAGE before progression to electrotransfer and antibody probing. This method has been proven to be extremely powerful in identifying the occurrence of proteolysis, as well as distinct protein fragments (**Fig. 7B**). We determined that to be the case for HTPI as well

(**Fig. 7A**). Another powerful aspect of HTPI is the relative ease for protein identification and "hits" confirmation. Since all the protein bands in the 5 templates were also identified and annotated based on the applied monoclonal antibodies, putative protein identification is very rapid. Furthermore, since the exact antibodies used in the HTPI analysis are individually available, hit confirmation is very rapid and robust (**Fig. 7-9**). One potential drawback of using antibody array approach is that antibody recognition of antigen might be species-specific. However, the 1,000 antibody sets (from BD Bioscience) we employed were tested for species cross-reactivity (human/rat/mouse) and over 90% cross-react with protein antigen in human rat and mouse. Of the 74 total hits we have in Table 1, all but 3 have confirmed rat-reactivity (thus 95%). The three exceptions are DRBP76, cathepsin L and p55-Cdc.

One of the potential limitations of the HTPI method is that it is not exhaustive. Currently the expansion of HTPI is limited by the availability of antibody to specific protein antigens. However, in only a few years, the HTPI panel had already grown from 700 [9] to over 1,000 monoclonal antibodies (present study). Another caution of using HTPI to identify proteolytic substrates *in vivo* is that this method will also detect protein with significantly reduced expression levels rather than degraded. However, we contrast *in vivo* TBI differential proteome to *in vitro* protease degradomes (**Fig. 3-5**), followed by traditional immunoblots confirmation and detection of BDPs (**Fig. 9**). Therefore, our approach adds another level of confidence in our degradomic data interpretation. Finally, any degradomic targets identified by HTPI (**Fig. 3-5**) should be confirmed independently with follow-up studies, including cell-based studies where proteases of interest can be activated.

In summary, we demonstrated that HTPI is a powerful and novel method for studying proteolytic pathways. In this case, we have used hippocampal proteome as an example to demonstrate the feasibility of using HTPI to study proteolysis targets *in vivo* and *in vitro*. This platform technology is applicable in identifying potential targets for novel proteases with unknown functions. It is also possible to

identify specific protein hydrolysis/processing in a unique organ or cell system under physiologic or pathologic conditions.

References

[1] Yamashima, T. (2000) Implication of cysteine proteases calpain, cathepsin and caspase in ischemic neuronal death of primates. Prog. Neurobiol. **62**, 273-295.

[2] Asahi M., Asahi K., Jung J.C., del Zoppo G.J., Fini M.E., Lo E.H. (2000) Role for matrix metalloproteinase 9 after focal cerebral ischemia, effects of gene knockout and enzyme inhibition with BB-94. J. Cereb. Blood Flow Metab. **20**, 1681-1689.

[3] Clark A.W., Krekoski C.A., Bou S.S., Chapman K.R., Edwards D.R. (1997) Increased gelatinase A (MMP-2) and gelatinase B (MMP-9) activities in human brain after focal ischemia. Neurosci. Lett. **238**, 53-56.

[4] Phillips J.B., Williams A.J., Adams J., Elliott P.J., Tortella F.C. (2000) Proteasome inhibitor PS519 reduces infarction and attenuates leukocyte infiltration in a rat model of focal cerebral ischemia. Stroke **31**, 1686-1693.

[5] Wang, K.K.W. (2000) Calpain and Caspase, Can You Tell the Difference. Trends Neurosci. **23**, 20-26.

[6] Pike, B.R., Flint, J, Johnson, E., Glenn, C.C., Dutta, S., Wang, KKW and Hayes, R.L. (2001) Accumulation of Calpain-Cleaved Non-Erythroid (II-Spectrin in Cerebrospinal Fluid after Traumatic Brain Injury in Rats. J. Neurochem. **78**, 1297-1306.

[7] Hajimohammadreza, I., Nath, R., Raser, K.J., Nadimpalli, R. and Wang, K.K.W. (1997) Proteolysis of Neuronal nitric oxide synthase and calmodulin-dependent protein kinase IIalpha undergo neurotoxin-induced proteolysis. J. Neurochem. **69**, 1006-1013.

[8] McGinnis, K.M., Whitton, M., Gnegy, M.E., Wang, K.K.W. (1998) Calmodulin-dependent protein kinase IV differentially cleaved by caspase-3 and calpain in SH-SY5Y human neuroblastoma cells. J. Biol. Chem. **273**, 1999-20000.

[9] Pasinetti G.M., Ho L. (2001) From cDNA microarrays to high-throughput proteomics. Implications in the search for preventive initiatives to slow the

clinical progression of Alzheimer's disease dementia. Restor. Neurol. Neurosci. **18**, 137-142.

[10] Castedo M., Ferri K.F., Blanco J., Roumier T., Larochette N., Barretina J., Amendola A, Nardacci R, Metivier D, Este JA, Piacentini M, Kroemer G. (2001) Human Immunodeficiency Virus 1 Envelope Glycoprotein Complex-induced Apoptosis Involves Mammalian Target of Rapamycin/ FKBP12-Rapamycin-associated Protein-mediated p53 Phosphorylation. J. Exp. Med. **194**, 1097-1110.

[11] Melnick M, Chen H, Min Zhou Y, Jaskoll T. (2001) The functional genomic response of developing embryonic submandibular glands to NF-kappaB inhibition. BMC Dev. Biol. **1**, 15.

[12] Yoo G.H., Piechocki M.P., Ensley J.F., Nguyen T., Oliver J., Meng H., Kewson D., Shibuya TY, Lonardo F, Tainsky MA. (2002) High-throughput immunoblotting. Ubiquitiin-like protein ISG15 modifies key regulators of signal transduction. J. Biol. Chem. **278**, 16608-16613.

[13] Malakhov MP, Kim KI, Malakhova OA, Jacobs BS, Borden EC, Zhang DE. 2002 Docetaxel induced gene expression patterns in head and neck squamous cell carcinoma using cDNA microarray and PowerBlot. Clin. Cancer Res. **8**, 3910-3921.

[14] Gifford S.M., Cale J.M., Tsoi S., Magness R.R., Bird IM. (2003) Pregnancy-specific changes in uterine artery endothelial cell signaling in vivo are both programmed and retained in primary culture. Endocrinology **144**, 3639-3650.

[15] Lorenz P, Ruschpler P, Koczan D, Stiehl P, Thiesen HJ. (2003) From transcriptome to proteome, differentially expressed proteins identified in synovial tissue of patients suffering from rheumatoid arthritis and osteoarthritis by an initial screen with a panel of 791 antibodies. Proteomics **3**, 991-1002.

[16] Cicala C., Arthos J., Selig S.M., Dennis G. Jr., Hosack D.A., Van Ryk D., Spangler M.L., Steenbeke T.D., Khazanie P., Gupta N., Yang J., Daucher

M., Lempicki RA, Fauci AS. (2002) HIV Envelop Induces a Cascade of Cell Signals in Non-Proliferating Target Cells that Favors Virus Replication. Proc. Natl. Acad. Sci. **99**, 9380-9385.

[17] Overall C.M., McQuibban G.A., Clark-Lewis I.. (2002) Discovery of chemokine substrates for matrix metalloproteinases by exosite scanning, a new tool for degradomics. Biol. Chem. **383**, 1059-1066.

[18] Wang, K.K.W., Posmantur, R., Nath, R., McGinnis, K., Whitton, M., Talanian, R.V., Glantz, S., Morrow, J. (1998) Simultaneous Degradation of alphaII- and BetaII-Spectrin by Caspase 3 (CPP32) in Apoptotic Cells. J. Biol. Chem. **273**, 22490-22497.

[19] Santella L., Kyozuka K., Hoving S., Munchbach M., Quadroni M. Dainese P., Zamparelli C., James P,. Carafoli E. (2000) Breakdown of cytoskeletal proteins during meiosis of starfish oocytes and proteolysis induced by calpain. Exp. Cell Res. **259**, 117-126.

[20] Wang, K.K.W., Villalobo, A. and Roufogalis, B.D. (1989) Calmodulin-binding proteins as calpain substrates. Biochem. J. **262**, 693-706.

[21] Schwab B.L., Guerini D, Didszun C, Bano D, Ferrando-May E, Fava E, Tam J, Xu D, Xanthoudakis S, Nicholson DW, Carafoli E, Nicotera P. (2002) Cleavage of plasma membrane calcium pumps by caspases, a link between apoptosis and necrosis. Cell Death Differ. **9**, 818-831.

[20] Zimmerman U.J., Malek S.K., Liu L., Li H.L. (1999) Proteolysis of synaptobrevin, syntaxin, and SNAP-25 in alveolar epithelial type II cells. IUBMB Life. **48**, 453-458.

[21] Pike, B.R., Zhao, X., Newcomb, J.K., Posmantur, R.M., Wang, K.K.W., Hayes, R.L. (1998) Regional calpain and caspase-3 proteolysis of alpha-spectrin after traumatic brain injury. NeuroReport **9**, 2437-2442.

[22] Lopez-Otin C, Overall CM. (2002) Protease degradomics, a new challenge for proteomics. Nat. Rev. Mol. Cell Biol. **3**, 509-519.

[23] Wang, K.K.W. and Yuen, P.w. (1994) Calpain inhibition: an overview of its therapeutic potentials. Trends Pharmacol. Sci. **15**, 412-419.

[24] Ni B, Wu X, Du Y., Su Y., Hamilton-Byrd E., Rockey P.K., Rosteck P. Jr., Poirier G.G., Paul S.M. (1997) Cloning and expression of a rat brain interleukin-1beta-converting enzyme (ICE)-related protease (IRP) and its possible role in apoptosis of cultured cerebellar granule neurons. J. Neurosci. **17**, 1561-1569.

[24] Posmantur, R., McGinnis, K. Nadimpalli, R., Gilbertsen, R. and Wang, K.K.W. (1997) Characterization of CPP32-like protease activity following apoptotic challenge in SH-SY5Y neuroblastoma cells. J. Neurochem. **68**, 2328-2337.

[25] Larner, S.F., McKinsey, D.M., Torres, M., Pike, M. Hayes, R.L. and Wang, KKW. (2004) Upregulation of caspase-12 after traumatic brain injury in rats. J. Neurochem. **88**, 78-90.

[27] Wang, K.K.W., Ottens, A., Haskins, W.E., Liu, M.C., Denslow, N., Chen, S.S., Hayes, R.L. (2004) Neuroproteomic studies of traumatic brain injury. Int. Rev. Neurobiol. **61**, 215-240.

[26] Beer, R., Franz, G., Krajewski, S., Pike, B.R., Hayes, R.L., Reed, J.C., Wang, K.K., Klimmer, C., Schmutzhard, E., Poewe, W., Kampfl, A. (2001) Temporal and spatial profile of caspase 8 expression and proteolysis after experimental traumatic brain injury. J. Neurochem. **78**, 862-873.

[27] Levilliers, N., Peron-Renner, M., Coffe, G., Pudies, J. (1986). Gelation and fodrin purification from rat brain extracts. Biochem Biophys Acta **3**: 113-126.

Acknowledgments and Declaration of interest

The authors would like to acknowledge support of Department of Defense grants DAMD17-03-1-0066 and DAMD17-01-1-0765; NIH grants R01 NS39091 and R01 NS40182. Research was conducted in compliance with the Animal Welfare Act and other federal statutes and regulations relating to animals and experiments involving animals and adheres to principles stated in the Guide for the Care and Use of Laboratory Animals, NCR Publication, 1996 Edition. Opinions, interpretations, conclusions, and recommendations are those of the author and are not necessarily endorsed by the US Army. Drs. Wang and Hayes hold equity in Banyan Biomarkers, a company commercializing the brain injury

biomarker technology. However, none of the authors have financial interests in BD Bioscience that assists with the PowerBlot analysis.

Legends to figures

Figure 1. αII-spectrin immunoblot as positive control before HTPI. Pooled naïve rat hippocampus lysate, lysate digested in calpain-2 or caspase-3 *in vitro* and traumatically injured rat hippocampus (TBI). Naïve and TBI were pooled from 6 individual animals, respectively. To confirm the extent of proteolysis of the last three samples are comparable, we analyzed 20 μg of these samples by traditional SDS-PAGE (6% polyacrylamide) and immunoblotting, probed with monoclonal anti-αII-spectrin antibody (Affiniti anti-fodrin #FG6090). Intact protein (280 kDa) was observed in all conditions. Calpain-2 digestion produced major fragments SBDP150 (150 kDa) and SBDP145 (145 kDa) (solid arrows) while caspase-3 digestion produced SBP149 (SBDP150i, 149 kDa) and SBDP120 (120 kDa) (open arrow heads) [5]. In TBI, a mixture of SBDP150, 149, 145 and SBDP120 were observed.

Figure 2. HTPI has low run-to-run variability. Pooled naïve hippocampus samples were run in triplicate (1 mg protein loaded per blot). Images of developed blots (Template A) were shown from top to bottom. Each template has 39 usable lanes for antibody probing and the last lane (40) was probed with "molecular weight markers-antibodies" (their MW is illustrated on the right margins). Lane numbers were indicated over the top margin. Each lane is separated and probed with 4-7 monoclonal antibodies. With the use of the manifold partition system, there is no lane-to lane primary antibody cross-contamination. The results confirm the low variability in banding patent with same sample analysis.

Figure 3. Example of Calpain-2 Degradome (Template A). Template A's from naïve hippocampus (**upper panel**) and calpain-2 digested hippocampal lysate (**lower panel)** were compared in triplicate (9 comparisons in total). One set of representative blots was shown. Molecular weight markers (lane 40) are as indicated on the right. Protein bands with sufficient intensity were subsequently

decoded and quantified by computer software (BD-Bioscience). We noted that in a number of proteins (indicated in solid box; upper panel), their average intensity reduced more than 2-fold after calpain digestion and several BDPs were also observed (BDP; in dotted box; lower panel).

Figure 4. Example of Caspase-3 Degradome (Template A). Template A's from naïve hippocampus (**upper panel**) and caspase-3 digested hippocampal lysate (**lower panel)** were compared in triplicate. One set of representative blots was shown. Molecular weight markers (lane 40) are as indicated on the right. Similar to figure 3, 9 parent proteins in template A (in solid box, upper panel) were significantly reduced after caspase-3 digestion as a result of proteolysis, and several BDPs were observed (in dotted box; lower panel).

Figure 5. Example of TBI differential proteome (Template A). Template A for naïve hippocampus (**upper panel**) was compared to that of a TBI (1.6 mm deformation distance, 48 h) counterpart (**lower panel).** Comparisons were made in triplicate. One set of representative blots was shown. Molecular weight markers (lane 40) are indicated on the right. Thirteen proteins in template A had reduced in average intensity (down-regulated) after TBI, (in solid box; upper panel). In addition, several BDPs can be readily observed (in dotted box; lower panel). Two proteins found to be up-regulated in TBI were CASK (A3) and Psme3 (A29) (in dotted box).

Figure 6. Comparison of Template B from Naïve, TBI, calpain-2 and caspase-3 digestion. Template B for naïve hippocampus (upper left) was compared to that of calpain-2 (upper right) and caspase-3 digestion (lower left) and TBI (lower right). Molecular weight markers (lane 40) are as indicated on the right. Proteins reduced in average intensity are potentially proteolytic targets for calpain and caspase-3 or down-regulated in the case of TBI (in solid box).Two proteins found to be up-regulated in TBI were cerulplasmin (B37) and alpha-actinin (B9) (in dotted box). In addition, several BDPs produced by calpain-2 or caspase-3 can be readily observed (in dotted box).

Figure 7. Summary of Calpain-2, caspase-3 and TBI differential proteome results from HTPI. (A) The number of putative degradomic hits for each template based on calpain-2 vs. naïve, caspase-3 vs. naïve and TBI vs. naïve comparisons were tabulated. The total number of degradome hits was listed on the far right. (B) Venn Diagram shows overlap of protein targets in the three degradomes (calpain: dashed line; caspase-3: dotted line; TBI: solid line). Total number of protein targets is in brackets. Overlaps and triple overlap numbers are as indicated.

Figure 8. HTPI approach allows rapid target confirmation. (A) Extracted lanes (E7) from template E of the HTPI analysis were shown: intact βII-spectrin (240 kDa) was identified to be significantly reduced in level by calpain-2 digestion, caspase-3 digestion and in TBI. One calpain-mediated breakdown product (BDP) of 110 kDa (black label) and two caspase-mediated BDPs of 108 kDa and 85 kDa, respectively (grey labels) were tentatively identified. These three BDP's were also tentatively identified in the TBI. (**B**) Traditional SDS-PAGE and Western blot were also performed with identical monoclonal Anti-βII-spectrin antibody (BD Bioscience product # S31120). Samples analyzed were naïve (pooled) vs. calpain-2 and capase-3 digestion (left three lanes) as well as four separate naïve and TBI samples, respectively. Again, BDPs of 110 kDa (solid arrow) and of 108 kDa and 85 kDa (open arrow heads) were observed. The asterisks indicate rat IgG heavy chain and fragments from contaminating blood that cross-react with the secondary anti-mouse IgG detection system used.

Figure 9. Examples of four proteins identified by HTPI as novel proteolytic targets. Four proteins were identified as proteolytic targets for either calpain-2, capase-3 and/or in TBI: striatin (A), synaptojanin-1 (B), synaptotagmin-1 (C) and NSF (D). Traditional SDS-PAGE and Western blot were also performed with monoclonal antibodies against striatin, synaptojanin-1, synaptotagmin (isoform I) and NSF. Samples analyzed were calpain-2 and capase-3 digestions (left two

lanes) as well as four separate naïve and TBI samples, respectively. In (A)-(D), intact proteins are shown with bold arrows (with M.W. in brackets). Calpain-2-mediated BDPs are shown with solid arrows. Caspase-3 mediated BDPs are shown with open arrow head. Molecular weights are as indicated. The asterisk in (A) indicates rat IgG light chain from contaminating blood that cross-react with the secondary anti--mouse IgG detection system used.

Figure 10. Examples of two purified proteins confirmed to be protelytic targets for calpain /caspase-3: bII-spectrin and synaptotagmin-1. Purified βII -spectrin (as subunit of rat brain spectrin) (A) and recombinant GST-fused synaptotagmin-1 (B) were subjected to calpain-2 /caspase-3 digestion and calpain-2 only digestion, respectively. Both Coomassie blue stained blotting membrane (left panels) and immunoblotting analysis with βII-spectrin and synaptotagmin-1 antibodies (right panels) were performed. Intact proteins and major BDPs were labeled with arrows. Several major αII-spectrin BDPs were also identified (open triangles).

Table 1. Identity of degradomic protein targets for calpain-2 and capase-3, and differentially regulated proteins after TBI. Protein names or abbreviations are listed on the far left column. Their template and lane location are listed on the second column. Swiss Pro ID and predicted molecular weight are also listed. Whenever a protein is altered in levels in one of the three conditions (Calpain-2, Capase-3, or TBI), the fold-change of the parent protein is indicated in the three columns on the far right. Since the majority of proteins showed decreased levels in the treatment group vs. control (naive), the fold change always indicates decrease as the default. When protein level is increased (for some proteins in TBI), the fold increase is indicated with a (+) sign and the fold change is in brackets. Also, we used high stringency inclusion criteria. Only proteins with band decrease or increase with at least 1.5-fold in all 9 possible comparisons between 3 treatment replica vs. 3 control replica are shown.

Protein name	Template + Lane	Swiss Pro ID	M.W. (kDa)	Calpain-2 vs. Naïve [fold-decrease]	Caspase-3 vs. Naïve [fold-decrease]	TBI vs. Naïve [fold-decrease (increase)]
AKAP220	A 1	Q62924	220	> 10	> 10	> 10
Amphiphysin	A 1	O95163	125	> 10		
ASAP1	A 39	Q9QWY8	130	> 10		
BRMP2	A 15	O08539	96/89	> 10	7.31	
CaMPK-II	A 36	P11275	52	5.23		5.67
CASK	A 3	Q62915	120			(+5.8)
Dynactin	A 19	Q13561	50	> 10	> 10	> 10
Endopeptidase	A 29	P42676	80	> 10		
GABA-B-R2	A 36	O088871	130	> 10	> 10	> 10
GSPT2	A 33	O88180	88	4.77		
Integrin-a3	A 22	Q62470	135	> 10	> 10	> 10
M-Calherin	A 34	P10287	130	> 10		
mGluR1	A 19	P23385	133	> 10		3.20
Munc-18	A 3	Q99PV2	68	> 10		> 10
MYPT1	A 29	Q9DBR7	130	3.38	3.93	5.00
nNOS	A7	P29475	155		> 10	
PkC-b	A 18	P05771	80	> 10		7.31
PKC-e	A 10	Q02156	90	6.50		
PKC-g	A 30	P05129	80	> 10	3.30	> 10
PMCA2	A 17	P11506	133	> 10	> 10	> 10
Psme3	A 29	Q12920	36			(+4.7)
Rabphilin-3A	A 23	P47709	75	> 10		> 10
SNAP-25	A 7	P13795	25	> 10	> 10	> 10
Synapsin-IIa	A 13	Q63537	74	> 10	1.70	10.10
Synaptojanin-1	A 23	Q62910	140	> 10		> 10
Synaptotagmin	A 11	P21579	65	2.91		1.50
a-actinin	B 9	AAA51582	104			(+8.41)
Adaptin	B 29	P17426	112	> 10		6.12
Bad	B 30	Q61337	23	10.80	3.23	3.00
b-Catenin	B 5	Q02248	92	> 10	> 10	> 10
Cathepsin L	B 22	P07711	43	7.18	> 10	7.71
Ceruloplasmin	B 37	Q61147	150			(> +10)
Dynamin	B 26	P21575	>100	10.69	> 10	4.41
Ki-67	B 8	P46013	395		> 10	> 10
MEF2D	B 3	Q63943	70	> 10	> 10	
NCK	B 2	P16333	47		> 10	
NSP1	B 24	Q9Y2X4	72	> 10	> 10	> 10
P150Glued	B 26	P28023	150	> 10	> 10	> 10
P190	B 3	Q13017	190	> 10	> 10	> 10
PKC-a	B 25	P17252	82	3.67		> 10
SII/TFIIS	B 32	P23193	38	> 10	> 10	> 10
Smac/Diablo	B 6	Q9NR28	22	> 10	> 10	> 10
DRBP76	B 7	Q12906	90	> 10		
Arp-3	C 18	P32391	50		> 10	> 10
CaMPK-IV	C 12	Q16566	60	3.11	2.63	4.26
c-Cbl	C 9	P22681	120	>100		
cdk2	C 9	P24941				(>+10)
hPrp-17	C 15	O60508	66	> 10	3.33	2.36
Nek2	C 5	P51955	46	> 10		
NES1	C 38	O43240	30			(>+10)
P55 Cdc	C 8	Q9BW56	55	> 10		
Profilin	C 28	P07737	15	> 10	> 10	
RIP2/RICK	C 26	AAH04553	61			2.59
a-/b-SNAP	C 21	P54920	35/36	> 10		13.79
Syntaxin 6	C 7	Q63635	31			3.81
Striatin	C 22	P70483	110	9.31	3.01	6.51
TBP	C 26	P20226	37			(+7.31)
TNIK	C 38	Q9UKE5	150		2.59	
Catenin/pp120	D 32	P30999	120	> 10	> 10	> 10
GS27	D10	O14653	27			(>+10)
P190-B	D 28	Q13017	195	> 10	> 10	> 10
PEX19	D 29	P40855	38			6.31
RONa	D 27	Q04912	40			> 10
SCAMP1	D 38	O15126	36			7.40
Synapsin-Ia	D 38	P09951	80	> 10		9.90
ATP Synthase a	E 21	P15999	55	> 10	5.84	> 10
BII-Spectrin	E 8	Q01082	240	> 10	> 10	6.30
B-Raf	E 25	P15056	95/72	> 10	> 10	2.71
Clathrin Heavy Chain	E 39	P11442	120	> 10	> 10	7.43
CtBP1	E 26	Q91W16	48	> 10	> 10	
NSF	E 13	P46459	82	> 10	3.30	2.59
SCAR-1	E 4	Q92588	80	> 10	7.50	3.23
SLK	E 13	NP_055535	125			4.00
Smg/GDS	E13	CAA45067	57			(>+10)

Liu et al. Figure 1

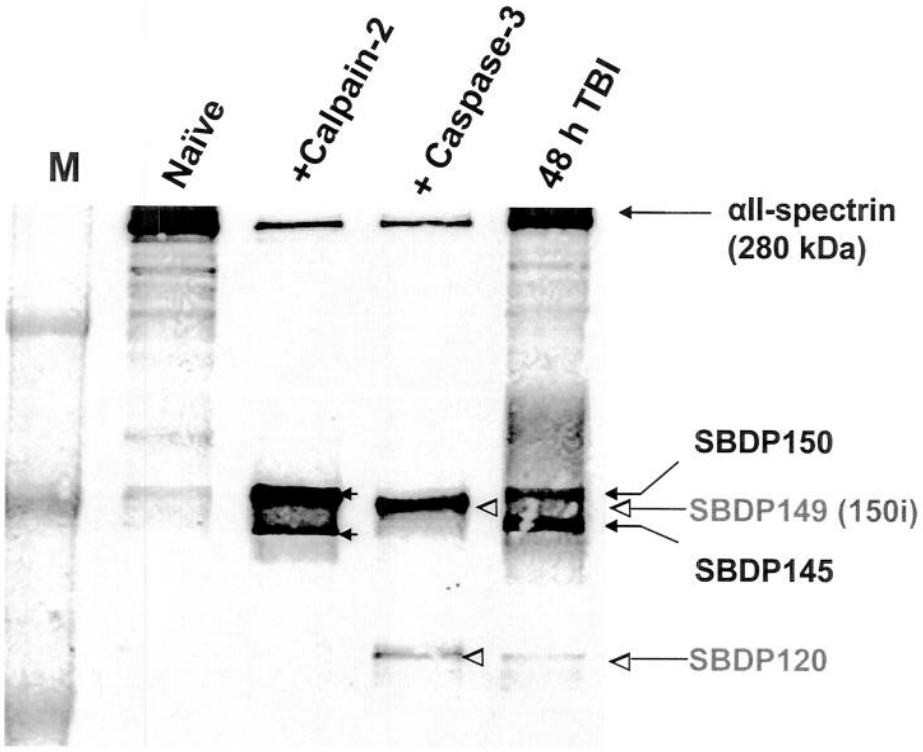

Liu et al. Figure 2

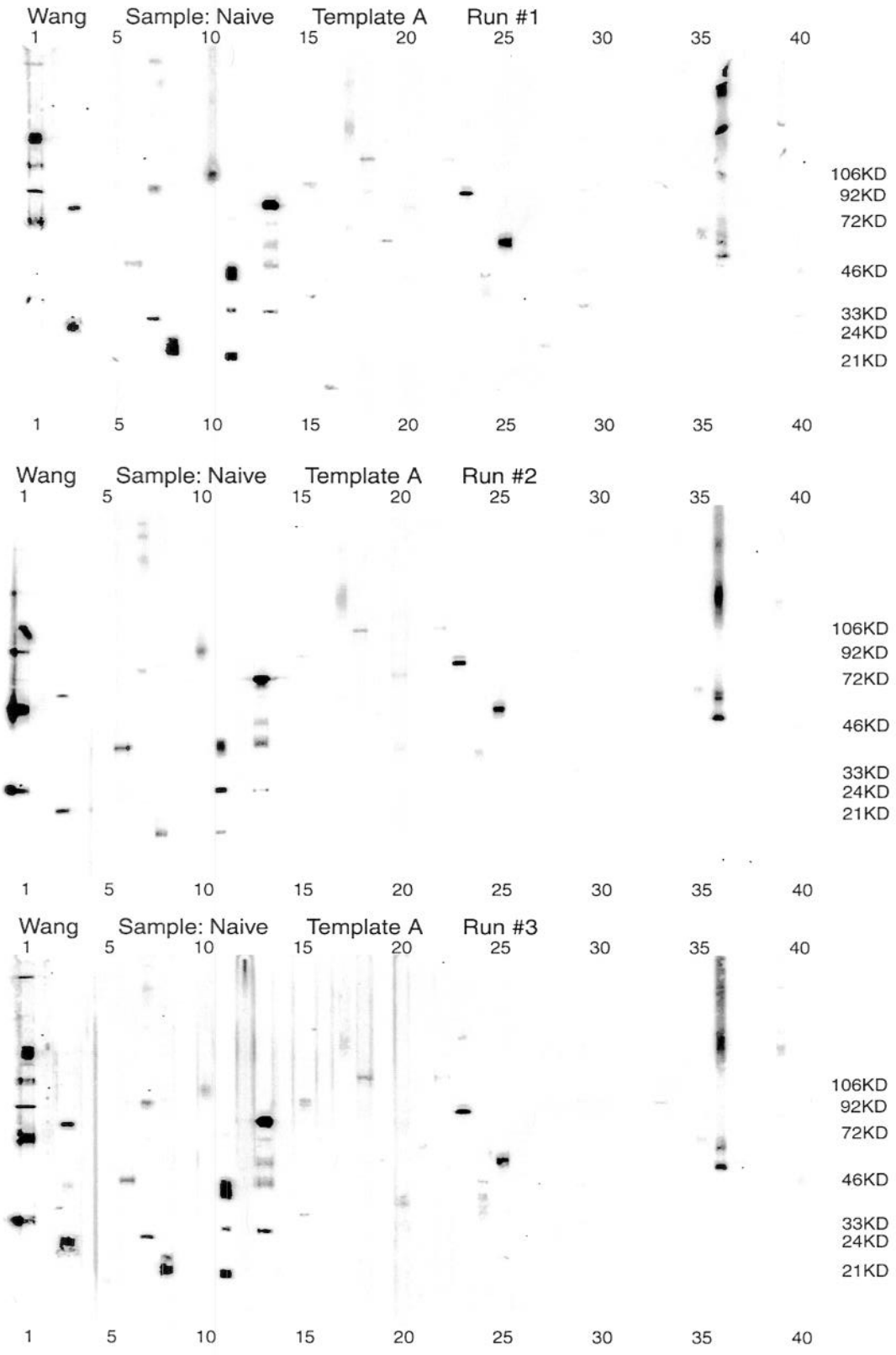

Liu et al. Figure 3

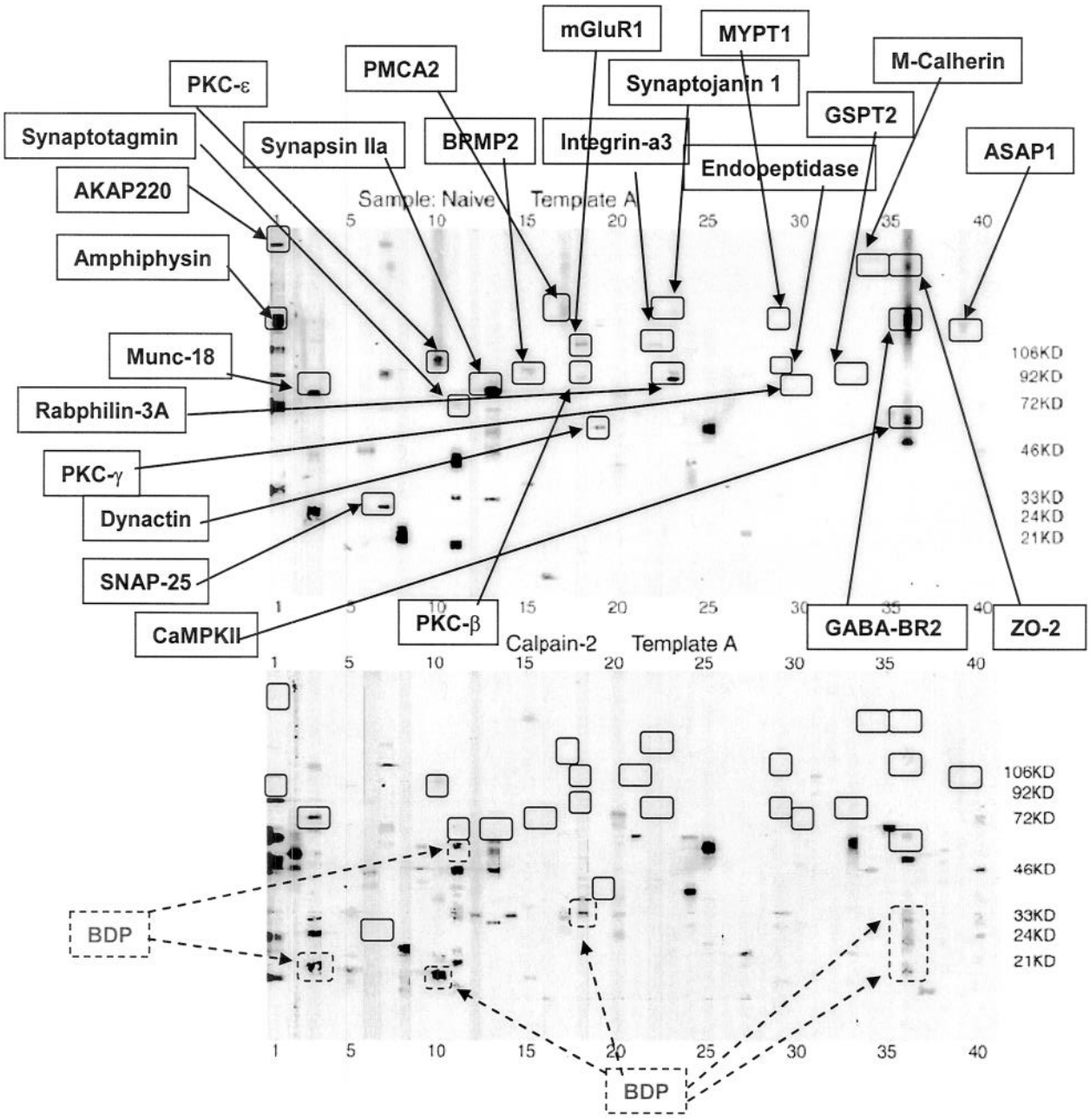

Liu et al. Figure 4

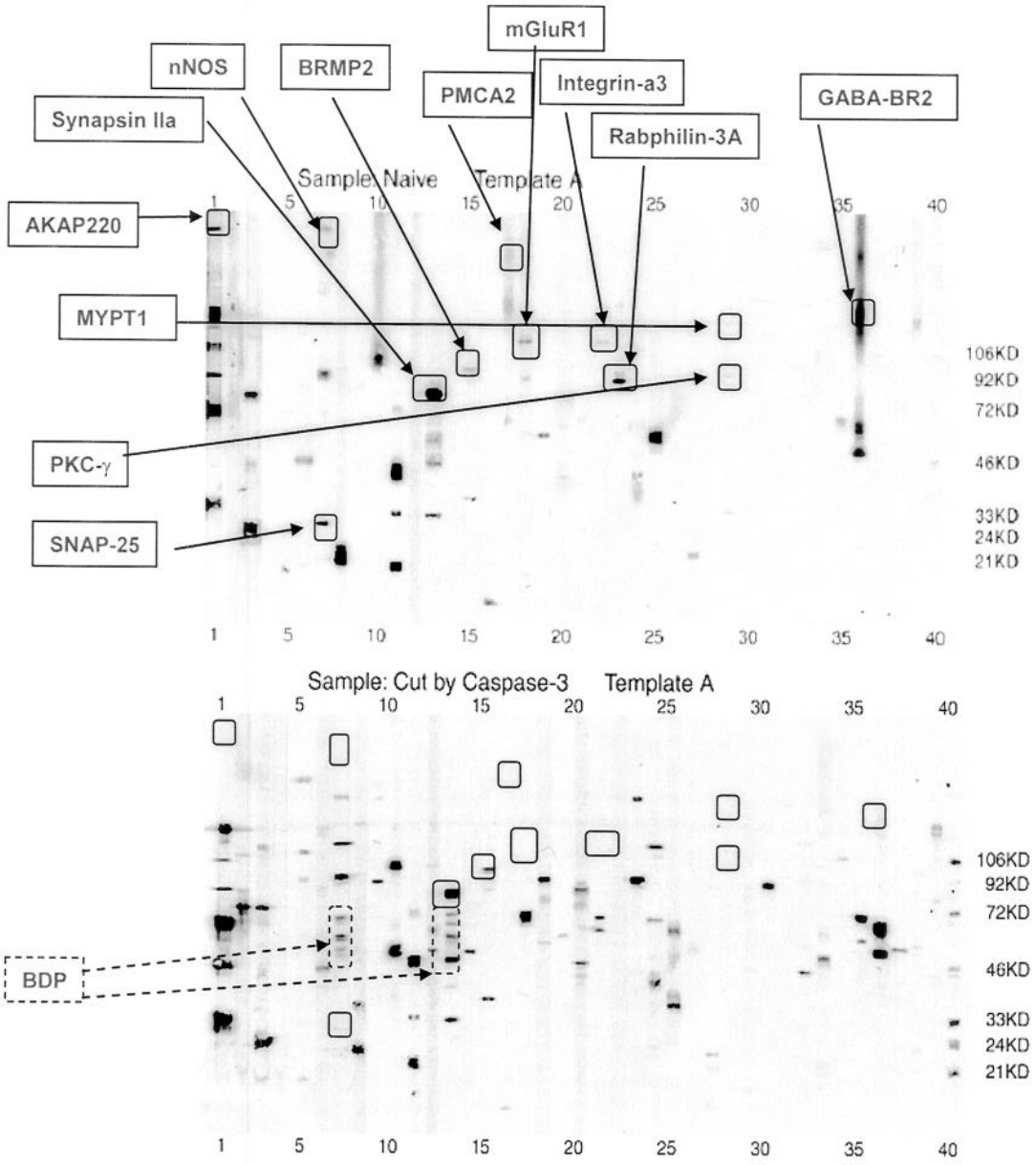

Liu et al. Figure 5

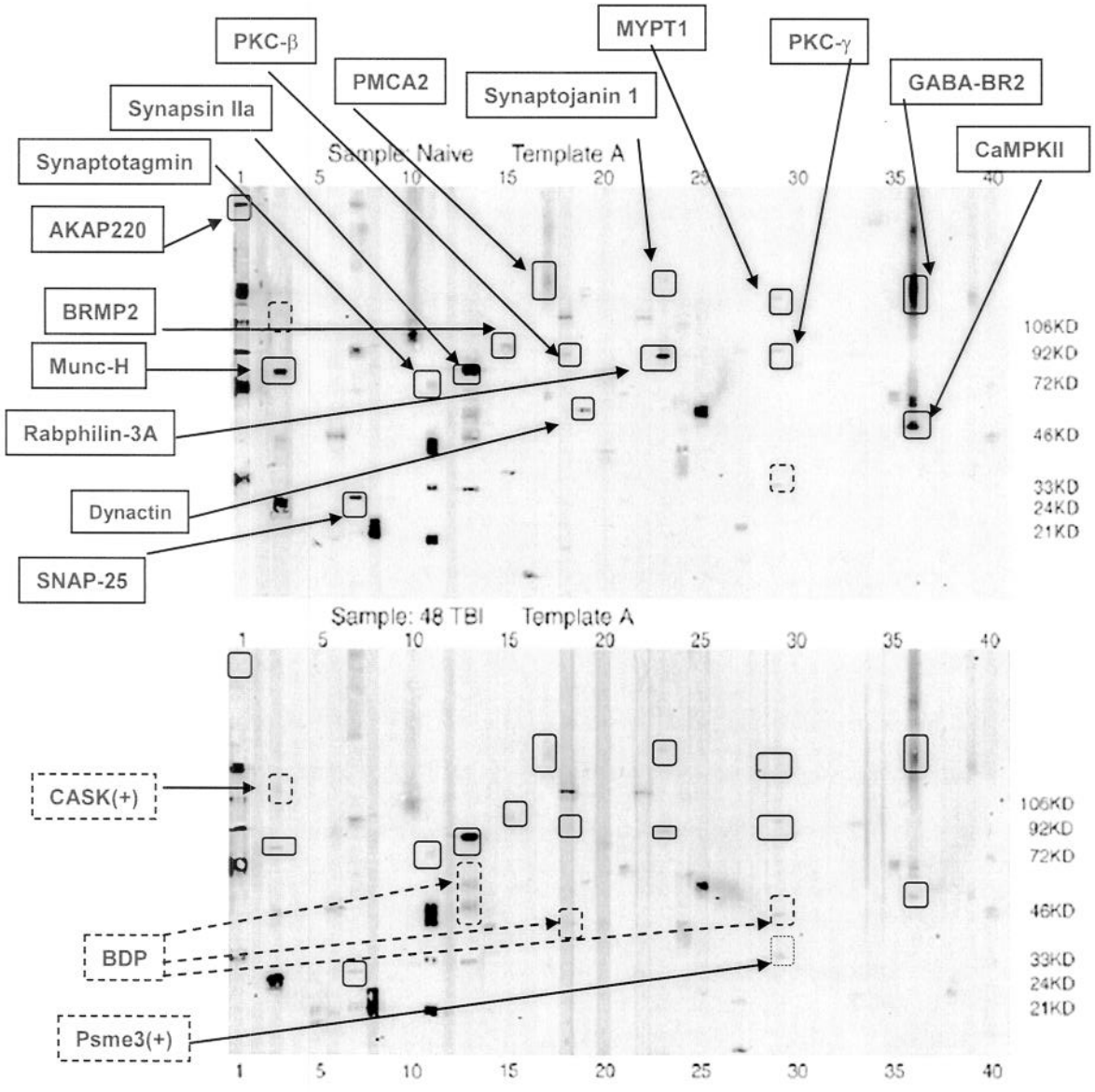

Liu et al. Figure 6

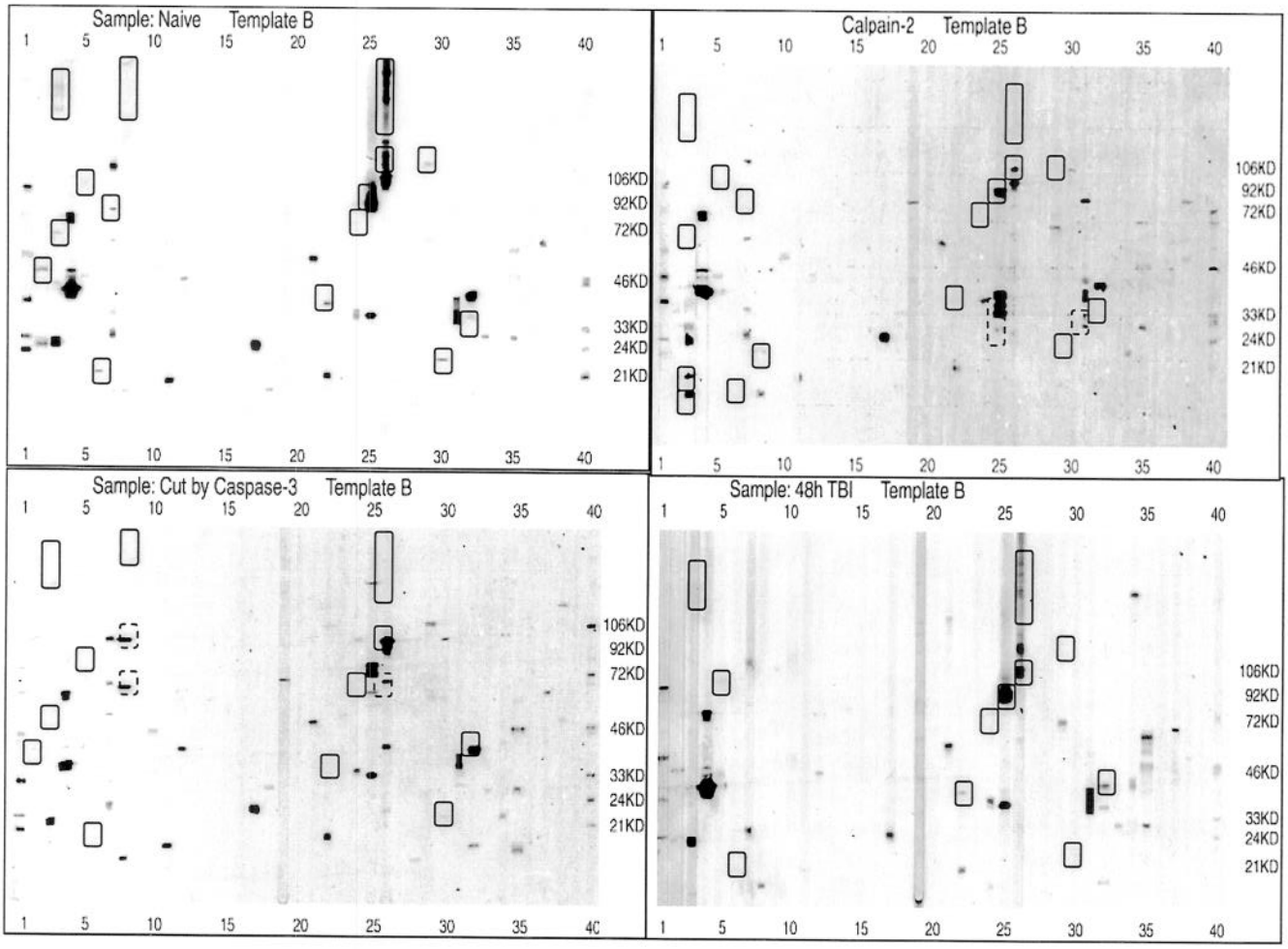

Liu et al. Figure 7

A

Degradome	Template A	Template B	Template C	Template D	Template E	TOTAL Hits
Calpain-2	23	13	8	3	7	54
Caspase-3	11	12	6	2	7	38
TBI	18	14	10	7	8	57

B

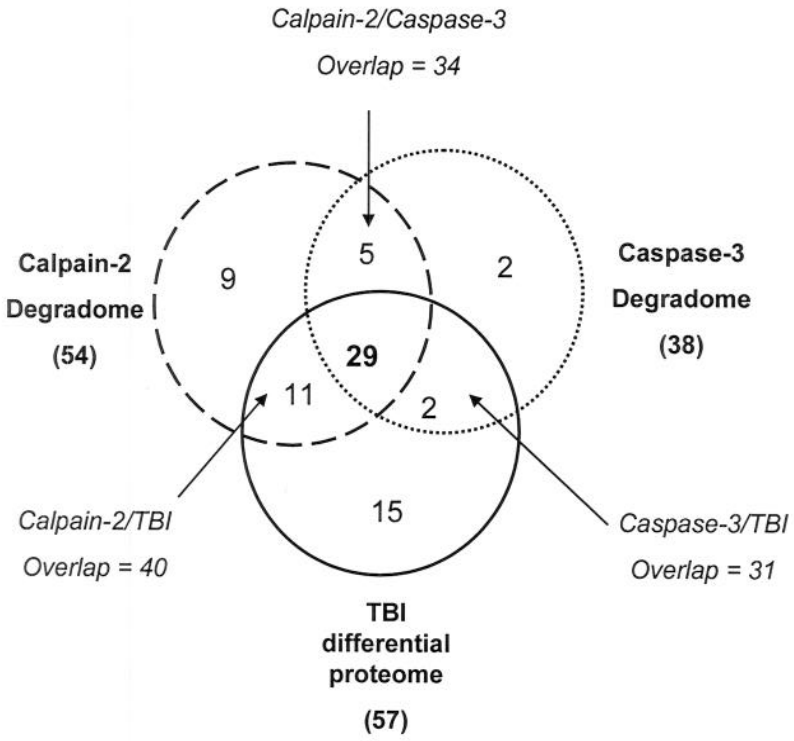

Liu et al. Figure 8

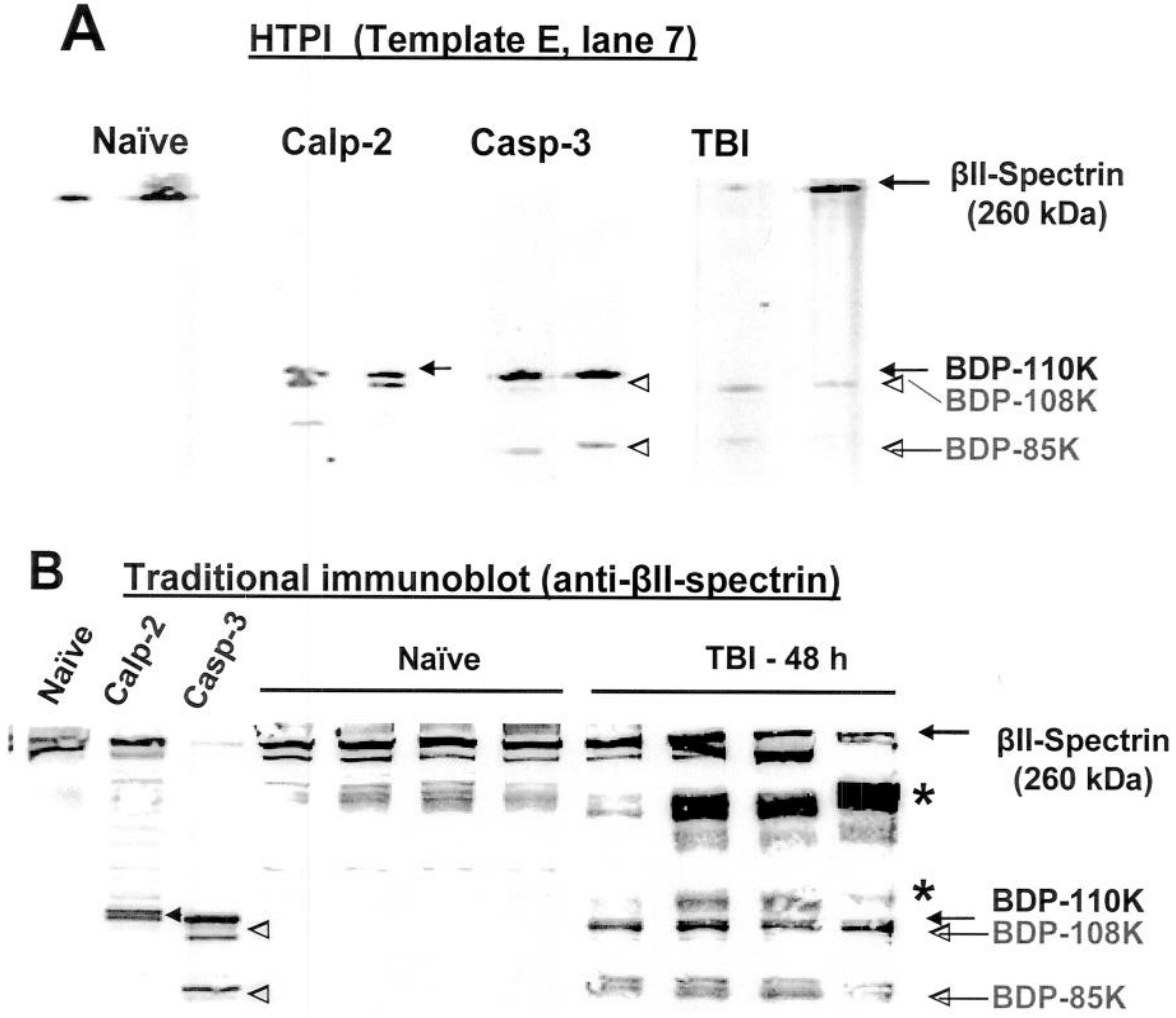

Liu et al. Figure 9

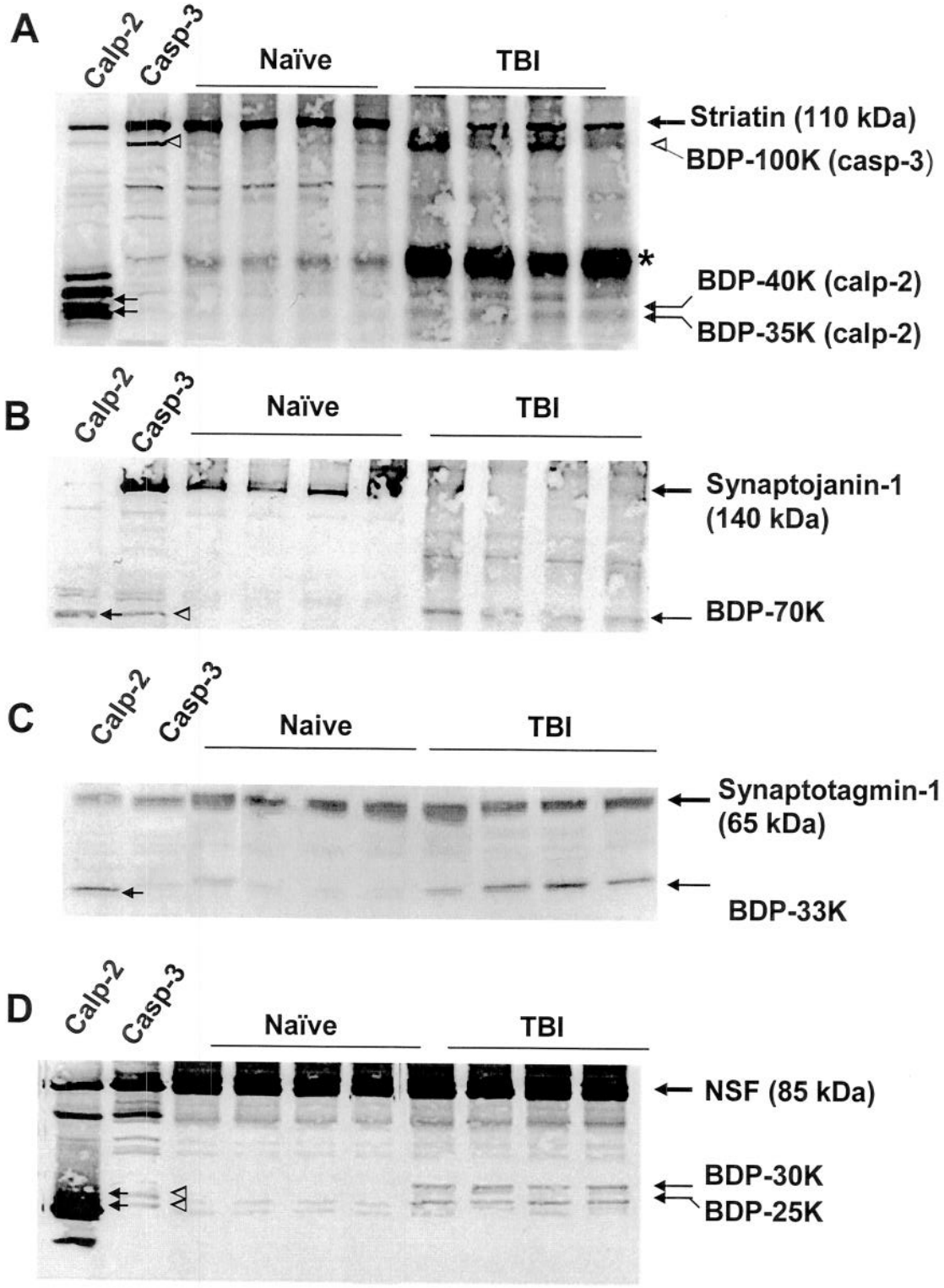

Liu et al., Figure 10

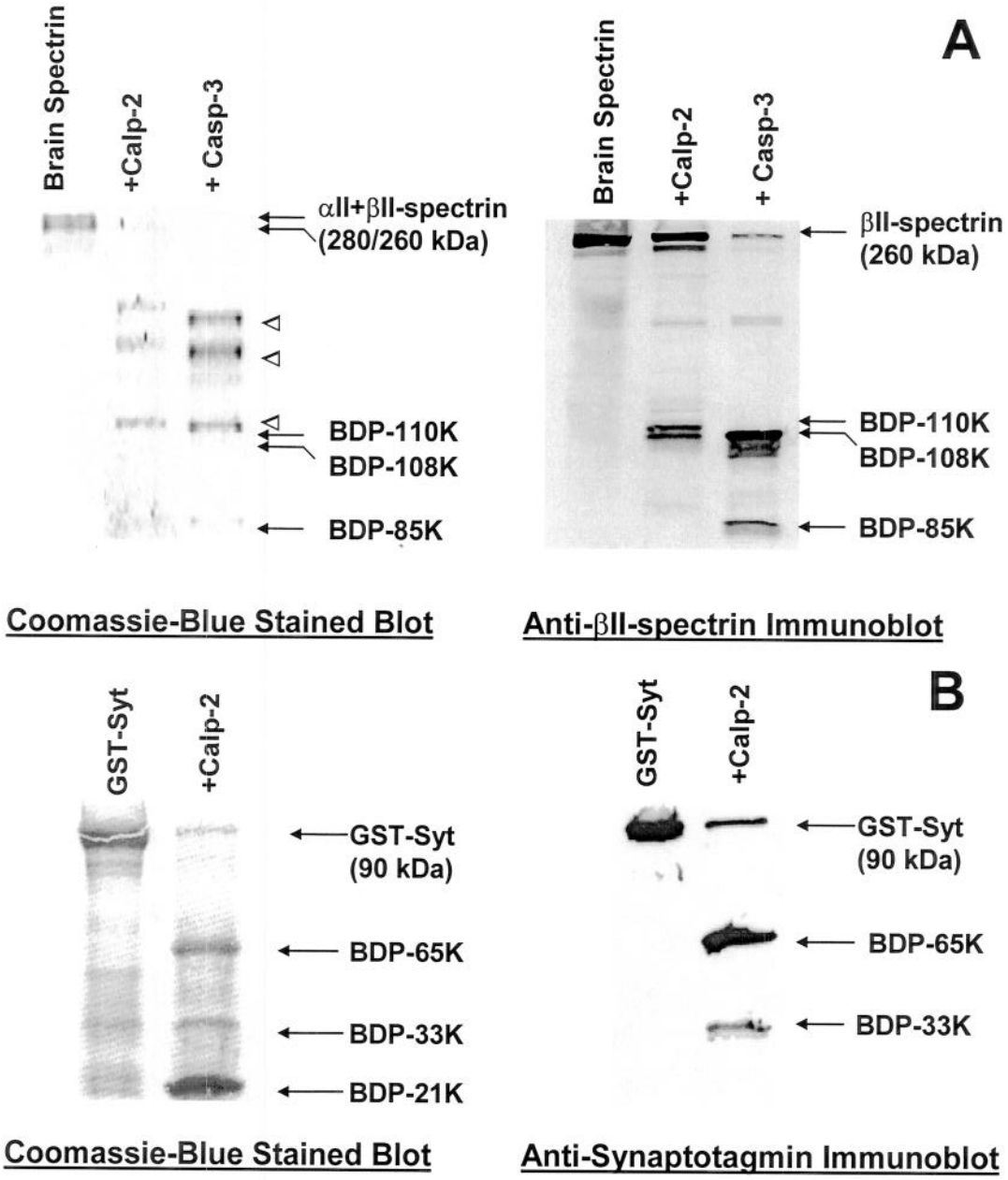

Neurochemical Research, Vol. 24, No. 3, 1999, pp. 371–382

Maitotoxin Induces Calpain But Not Caspase-3 Activation and Necrotic Cell Death in Primary Septo-Hippocampal Cultures

X. Zhao,[1] B.R. Pike,[1] J.K. Newcomb,[1] K.K.W. Wang,[2] R.M. Posmantur,[3] and R.L. Hayes[1,4]

(Accepted August 11, 1998)

Maitotoxin is a potent toxin that activates voltage and receptor-mediated Ca^{2+} channels, resulting in Ca^{2+} overload and rapid cell death. We report that maitotoxin-induced cell death is associated with activation of calpain but not caspase-3 proteases in septo-hippocampal cell cultures. Calpain and caspase-3 activation were examined by accumulation of protease-specific breakdown products to α-spectrin. Cell death manifested exclusively necrotic-like characteristics including round, shrunken nuclei, even distribution of chromatin, absence of DNA fragmentation and failure of protein synthesis inhibition to reduce cell death. Necrotic cell death was observed in neurons and astroglia. Calpain inhibitor II inhibited calpain-specific processing of α-spectrin and significantly reduced cell death. The pan-caspase inhibitor, Z-D-DCB, nominally attenuated cell death. Results suggest that: (1) calpain, but not caspase-3, is activated as a result of maitotoxin-induced Ca^{2+} influx; (2) necrotic cell death caused by maitotoxin exposure is partially mediated by calpain activation; (3) maitotoxin is a useful tool to investigate pathological mechanisms of necrosis.

KEY WORDS: Calpain; caspases; maitotoxin; necrosis; apoptosis.

INTRODUCTION

Calpains are calcium activated, neutral, cytosolic cysteine proteases. Currently, two major isoenzymes of calpain are known to exist in the central nervous system, μ-calpain and m-calpain (1–5). μ-Calpain has micromolar sensitivity to calcium and is located primarily in neuronal soma and dendrites and less abundantly in axons and glia (6, 7). m-Calpain has millimolar sensitivity to calcium activation and is primarily glial, with low levels also found in axons (6) as well as being a possible constituent of myelin (8). Calpain has relative selectivity for proteolysis of a subset of cellular proteins including cytoskeletal proteins, calmodulin binding proteins, enzymes involved in signal transduction (e.g. kinases, phosphotases, phospholipases), membrane proteins (e.g. receptors) and transcription factors (e.g. Fos, Jun), (3, 4, 9). Recent interest in calpain is attributable to growing recognition that pathological cascades following central nervous system insults including traumatic brain injury, cerebral ischemia and spinal cord injury are at least partially mediated by increased intracellular calcium and activation of calpains. Many investigators hypothesize that activated calpain breaks down cytoskeletal proteins resulting in loss of cell integrity and subsequent cell death (10–12).

[1] Vivian L. Smith Center for Neurologic Research, The University of Texas-Houston, Medical School, 6431 Fannin, Suite 7.154, Houston, TX 77030.
[2] Parke-Davis Pharmaceutical Research, Warner Lambert Company, 2800 Plymouth Road, Department of Immunopathology/Department of Neuroscience Therapeutics, Ann Arbor, MI 48105.
[3] Bristol-Myers Squibb Co., Pharmaceutical Research Institute, 5 Research Parkway, Wallingford, CT 06492.
[4] Address reprint requests to: Ronald L. Hayes, Ph.D., Vivian L. Smith Center for Neurologic Research, University of Texas-Houston, Medical School, 6431 Fannin, Suite 7.154, Houston, TX 77030. Phone: 713-500-6132 Fax: 713-500-7787

0364-3190/99/0300-0371$15.00/0

blocked calpain and caspase activation as well as apoptotic cell death in this system (17). Following each experiment, cells were fixed for staining, or protein or DNA extraction was performed.

Morphological Assessments of Cell Damage

1. Fluorescein Diacetate and Propidium Iodide Assay of Cell Viability. Fluorescein diacetate (FDA) and propidium iodide (PI) dyes were used to assess cell viability after maitotoxin incubation. FDA enters normal cells and emits a green fluorescence when it is cleaved by esterases. Once cleaved, FDA can no longer permeate cell membranes. PI is an intravital dye that is normally excluded from cells. After injury, PI penetrates cells and binds to DNA in the nucleus and emits a red fluorescence. This technique is commonly used to quantitate cell injury (41). As per Jones and Senft (41), a stock solution of FDA (20 mg/mL) was dissolved in acetone. A PI stock solution was prepared by dissolving 5 mg/mL in PBS. The FDA and PI working solutions were freshly prepared by adding 10 µl of the FDA and 3 µl of PI stock to 10 ml of phosphate buffered saline (PBS). Two-hundred microliters per well of FDA/PI working solution were added directly to the cells. Cells were stained for 3 min. at room temperature and put on ice. Stained cells were examined with a fluorescence microscope equipped with epi-illumination, band pass 450–490 nM exciter filter, 510 nm chromatic beam splitter, and a long pass 520 nm barrier filter. This filter combination permitted both green and red fluorescing cells to be seen simultaneously. The percent of viable cells in control cultures and following maitotoxin insult (with or without protease and protein synthesis inhibitors) at different time points was determined from three separate experiments using FDA/PI. Cell viability can be determined since this procedure results in the nuclei of dead cells fluorescing red while the cytoplasm of living cells fluoresces green. Cell loss was calculated in 100X fields (five sequential 100X fields were counted and averaged per well) for three wells in each experiment as a percent of total cell number.

2. Hoechst Staining of Apoptotic Nuclei. The A-T base-pair-specific dye, Hoechst 33258 (bis-benzimide; Sigma) was used to stain cell nuclei. Following overnight fixation in 4% paraformaldyhide at 4 °C, cells grown on German Glass were washed three times with PBS and labeled with 1 µg/ml of the DNA dye Hoechst 33258 in PBS for 5–10 min. at room temperature, using enough solution to cover the cells completely. Cells were rinsed twice with PBS and mounted with crystal-mount medium (Biomeda). Cells were observed and photographed on a phase contrast and fluorescence microscope with a UV2A filter.

DNA Fragmentation Assay. DNA gel electrophoresis was done as described in Gong *et al.* (42). Briefly, cells were collected in the same manner as for immunoblotting. Cells in each treatment condition were collected by centrifugation and fixed in suspension in 70% cold ethanol and stored in fixative at −20 °C for 24–72 hours. Cells were then centrifuged at 800g for 5 min. and ethanol was thoroughly removed. Cell pellets were resuspended in 40 µl of phosphate-citrate (PC) buffer consisting of 192 parts of 0.2 M Na_2HPO_4 and 8 parts of 0.1 M citric acid (pH 7.8) at room temperature for 1 hour. After centrifugation at 1000g for 5 min., the supernatant was transferred to new tubes and concentrated by vacuum in a SpeedVac concentrator for 15–30 min. Three µl of 0.25% Nonidet NP-40 in distilled water was then added, followed by 3 µl of a solution of DNase-free RNase (1 mg/mL). After 30 min. incubation at 37 °C, 3 µl of a solution of proteinase K (1 mg/mL) was added and the extract was incubated for additional 30 min. at 37 °C. After the incubation, 1 µl of 6X loading buffer (0.25% bromophenol blue, 0.25% xylene cyanol FF, 30% glycerol in water) was added and the entire content of the tube was transferred to a 1.5% agarose gel and electrophoresis was performed in 1X TBE (0.1 M Tris, 0.09 M Boric Acid, 1 mM EDTA, pH 8.4) at 40V for 2 hours. The DNA in the gels was visualized and photographed under UV light after staining with 5 µg/mL of ethidium bromide.

Assessment of α-Spectrin Degradation by Calpains and Caspase-3

SDS-Polyacrylamide Gel Electrophoresis and Immunoblotting. Because α-spectrin contains sequence motifs preferred by both calpains and caspase-3 proteases, activation of these two families of cysteine proteases can be assessed concurrently by immunoblot identification of calpain and/or caspase-3 signature cleavage products. Calpain has a high affinity for two sites on the native 240 kDa α-spectrin protein. Following calpain activation, intact α-spectrin (280 kDa) is proteolyzed into distinct 150 kDa and 145 kDa fragments detected on immunoblots. The first site is rapidly attacked following calpain activation resulting in a 150 kDa spectrin breakdown product (BDP). Further calpain processing of 150 kDa BDPs at the N-terminal yields a calpain-specific 145 kDa BDP (13, 14, 37). Caspase-3 proteases are aspartic acid-specific cysteine proteases that recognize a different cleavage motif in target substrates. One or more members of the caspase 3-like protease family cleave intact α-spectrin to produce 150 kDa BDPs, and further processing of 150 kDa fragments results in a unique caspase-3 specific 120 kDa BDP (25). Moreover, the 120 kDa fragment has been shown to be associated with caspase-3 activation in various in vitro systems of apoptosis (13, 14, 17, 25).

At the end of an experiment, cells were harvested from 5 identical culture wells and collected in 15 ml centrifuge tubes and centrifuged at 3000 g for 5 min. The medium was removed and the pellet cells were rinsed with 1X PBS. Cells were lysed in ice cold homogenization buffer [20 mM PIPES (pH 7.6), 1 mM EDTA, 2 mM EGTA, 1mM DTT, 0.5 mM PMSF, 50 µg/ml Leupeptin, and 10 µg/ml each of AEBSF, apotinin, pepstatin, TLCK and TPCK] for 30 min., and sheared through a 1.0 ml syringe with a 25 gauge needle 15 times. Protein content in the samples was assayed by the Micro BCA method (Pierce, Rockford, IL, USA). For protein electrophoresis, equal amounts of total protein (30 µg) were prepared in (two fold loading buffer containing 0.25 M Tris (pH 6.8), 0.2 M DTT, 8% SDS, 0.02% Bromophenol Blue, and 20% glycerol, and heated at 95 °C for 10 min. Samples were resolved in a vertical electrophoresis chamber using a 4% stacking gel over a 7% acrylamide resolving gel for 1 hour at 200V. For immunoblotting, separated proteins were laterally transferred to nitrocellulose membranes (0.45 µM) using a transfer buffer consisting of 0.192 M glycine and 0.025 M Tris (pH 8.3) with 10% methanol at a constant voltage (100 V) for 1 hour at 4 °C. Blots were blocked overnight in 5% non-fat milk in 20 mM Tris, 0.15 M NaCl, and 0.005% Tween-20 at 4 °C. Coomassie blue and Ponceau red (Sigma, St. Louis, MO) were used to stain gels and nitrocellulose membranes (respectively) to confirm that equal amounts of protein were loaded in each lane.

Immunoblots were probed with an anti-α-spectrin monoclonal antibody (Affiniti Research Products, UK; catalogue #: FG 6090, clone AA6) that detects intact α-spectrin (280 kDa) and 150, 145, and 120 kDa βBDPs. The 150 kDa βBDP has been reported to be a spectrin cleavage product produced by either calpain or caspase proteases (13, 25). However, the 145 kDa βBDP is a specific proteolytic fragment of calpain (14, 25). In addition, the 120 kDa βBDP is reported to be a specific proteolytic fragment of caspase-3 activation (25–27). Following incubation with the primary antibody (1:4000) for 2 hours at room temperature, the blots were incubated in peroxidase-conjugated sheep anti-mouse IgG for 1 hour (1:10,000). Enhanced chemilumines-

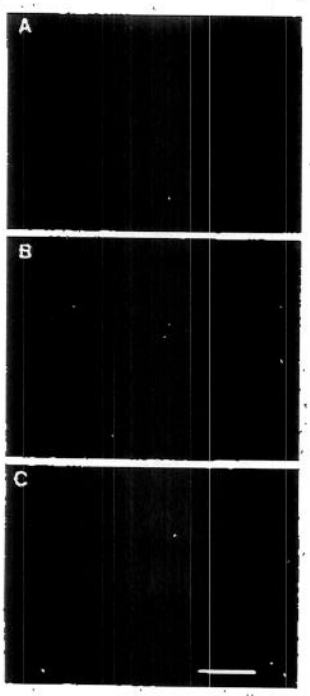

Fig. 2. Fluorescein diacetate (FDA) and propidium iodide (PI) staining of septo-hippocampal cultures undergoing necrosis.
(A) Control cultures: Note normal somal structure in the cells that take up FDA (green fluorescence) and the lack of PI uptake. Within 30 min. after incubation with 0.1 nM of maitotoxin, PI was taken up by cells (B). PI uptake was even more apparent 2 hours after injury. In addition, nuclei stained with PI appeared smaller and more uniformly round (C). Cells stained with FDA were swollen by 30 min. after maitotoxin treatment, and fewer living cells were observed 2 hours after treatment. (Scale Bar = 10μm).

or formation of apoptotic bodies characteristic of apoptotic nuclear phenotypes.

3. DNA Fragmentation. Condensation and aggregation of chromatin at the nuclear membrane may occur independently of endonuclease activation (44). Thus, a DNA fragmentation assay was used to assess whether the absence of an apoptotic response to maitotoxin in septo-hippocampal cultures, indicated by Hoechst 33258 staining, could have still been associated with endonuclease activity. Fig. 4 shows the characteristic pattern of nucleosomal sized (~180 bp) DNA laddering following exposure of septo-hippocampal cells to 0.5 μM staurosporine, a classic index of apoptosis (17). In contrast, there was no evidence of DNA ladders from 15 min. to 5 hours following maitotoxin treatment (Fig. 4).

4. Maitotoxin Induces Necrosis in Both Neurons and Astroglia. To dissociate the type of cell (i.e., astroglial vs. neuronal) committed to death, cultures were stained with Hoechst 33258 and GFAP (for astrocytes) or MAP-2 and NeuN (for neurons). One hour following maitotoxin treatment, there was a substantial reduction in neurons identified by MAP-2 and NeuN immunoreactivity (Fig. 5A vs. C). In contrast to normal appearing Hoechst staining in control neurons (Fig. 5B), neurons with residual MAP-2 and NeuN immunoreactivity showed Hoechst staining profiles characteristic of necrotic cell death (Fig. 5D). Maitotoxin treatment also produced astroglial cell death in injury (Fig. 6A vs. C). Compared to normal Hoechst staining in untreated cultures (Fig. 6B), astroglia treated with maitotoxin also showed Hoechst staining profiles characteristic of necrosis (Fig. 6D).

II. Calpain But Not Caspase-3 Proteolysis of α-Spectrin

In addition to causing necrosis, exposure to 0.1 nM maitotoxin caused a time dependent proteolysis of neuronal α-spectrin by calpain but not caspase-3 proteases (Fig. 7). By 30 min. following maitotoxin administration, there was an increase in both 150 kDa and calpain specific 145 kDa breakdown products to α-spectrin. By 1 hour after maitotoxin treatment, there was a further increase in the accumulation of calpain specific 145 kDa breakdown products to α-spectrin. In contrast, there was no evidence of accumulation of caspase-3-specific 120 kDa breakdown product at 30 min. or 1 hour after maitotoxin treatment.

III. Effects of CalpInh-II, Z-D-DCB or Cycloheximide on Cell Death and α-Spectrin Proteolysis

To investigate the relative contributory effects of calpain and/or caspase-like proteases to maitotoxin-induced cell death and α-spectrin proteolysis, the effect of a calpain inhibitor (CalpInh-II) or a pan caspase inhibitor (Z-D-DCB) was examined. The co-administration of CalpInh-II and Z-D-DCB was also investigated. Since de novo protein synthesis is required for at least some forms of apoptosis and specifically for staurosporine-induced apoptosis in septo-hippocampal cultures, the ef-

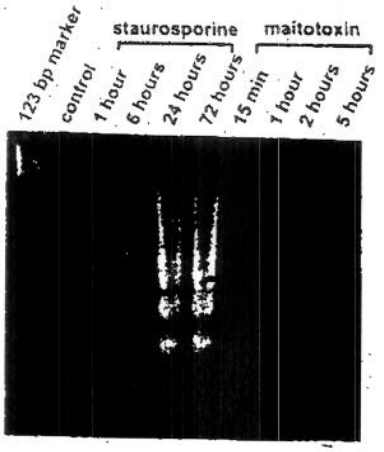

Fig. 4. Oligonucleosomal size fragmentation of DNA produced by staurosporine but not maitotoxin in septo-hippocampal cell cultures. 0.1 nM maitotoxin did not produce DNA laddering on agarose gels at 15 min., 1 hour, 2 hours or 5 hours following treatment. However, DNA laddering is reliably produced by 0.5 μM staurosporine from 6 to 72 hours following treatment.

staurosporine-induced apoptosis in septo-hippocampal cell cultures (17) and other cultures systems, cycloheximide had no effect on PI uptake 30 min. following maitotoxin treatment (Fig. 8).

One hour following maitotoxin administration, the percentage of cells stained for PI increased to 60.7%. Administration of CalpInh-II, Z-D-DCB or CalpInh-II+Z-D-DCB significantly reduced the percentage of cell staining for PI to 23.0%, 49.3% and 20.0%, respectively (Fig. 8). Again, Z-D-DCB produced significantly less protection against PI uptake than CalpInh-II ($p \leq 0.001$, and CalpInh-II+Z-D-DCB produced protection of a magnitude similar to that observed with administration of CalpInh-II alone. Cycloheximide had no effect on PI uptake 1 hour following maitotoxin treatment.

2. α-Spectrin Proteolysis. Administration of CalpInh-II during 30 min. of maitotoxin treatment completely abolished the accumulation of 150 kDa and calpain-specific 145 kDa breakdown products to α-spectrin (Fig. 7). In contrast, neither Z-D-DCB nor cycloheximide provided any protection against proteolysis of α-spectrin 30 min. following maitotoxin treatment. In fact, there was a tendency, most pronounced in cultures treated with Z-D-DCB, to show increased accumulation of breakdown products compared with maitotoxin cultures treated with no inhibitor. Similarly, 1 hour following maitotoxin treatment, CalpInh-II completely blocked the formation of 150 kDa and calpain-specific 145 kDa breakdown products to α-spectrin (Fig. 7). Z-D-DCB and cycloheximide had no effect on accumulation of these breakdown products, suggesting that the 150 kDa fragment was indeed derived from calpain. The results of these experiments confirm that the administration of CalpInh-II employed in these studies blocked calpain but not caspase proteolysis following maitotoxin treatment in primary septo-hippocampal cultures, further confirming that maitotoxin-induced necrotic cell death is related to calpain but not caspase activation

DISCUSSION

This study is the first demonstration that maitotoxin induces activation of calpain but not caspase-3 proteases associated exclusively with necrotic cell death in neurons and astroglia. The absence of any evidence of apoptotic cell death is notable since maitotoxin can evoke a number of calcium-dependent cellular processes such as phospholipase C activation (31, 46, 47) and arachidonic acid release (47) which could contribute to membrane lipid peroxidation (48) and potentially promote a cascade of events that culminates an apoptotic cell death. Moreover, our failure to detect caspase-3 activation following maitotoxin treatment is in accord with studies suggesting that caspases are activated only in apoptosis but not in necrosis (25, 29).

Maitotoxin Induces Calpain but not Caspase-3 Proteolysis of α-Spectrin During Necrotic Cell Death

Recent research on proteolytic mechanisms of necrotic and apoptotic cell death has focused on identification of key substrates cleaved during different cell death programs. Although calpain mediated cleavage of α-spectrin has been well documented in previous studies of necrotic cell death (36, 49, 50), it has only recently been recognized that cleavage of α-spectrin occurs during apoptosis induced by numerous stimuli (13–17, 25, 51). Cleavage of cytoskeletal proteins such as α-spectrin may contribute to non-specific cellular disintegration characteristic of necrosis. During apoptosis, cleavage of cytoskeletal protein, such as α-spectrin may contribute to characteristic changes including cell shrinkage, membrane blebbing and could alter cell signaling systems. (24).

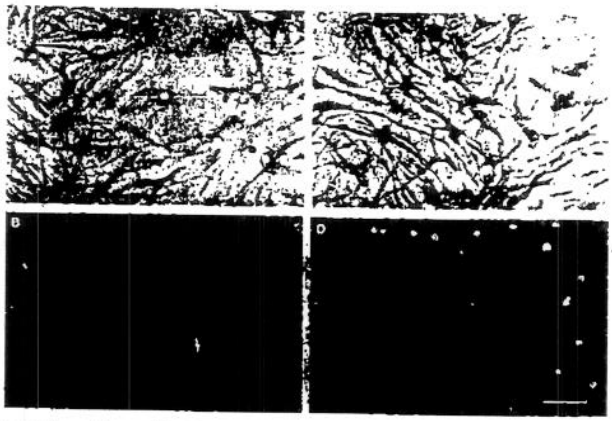

Fig. 6. Necrosis in astroglial cell types in mixed septo-hippocampal cultures.
Phase contrast light microscopy of double labeled astroglia stained with GFAP (A, C) and Hoechst 33258 (B, D). Control cultures (A, B) were compared to cultures 1 hour following maitotoxin challenge (C, D). Maitotoxin treatment produced significant detachment of astroglia that often occurred in discreet, necrotic patches (C, open curved arrow). In addition, astroglia showed typical injury profiles including increased GFAP immunoreactivity and swelling of glial appendages (C, closed curved arrow). Injured GFAP positive cells frequently showed staining characteristic of necrosis, including evenly distributed DNA and shrunken rounded nuclei (D, closed curved arrow) in contrast to normal appearing Hoechst staining in control cultures (straight arrow; A, B). (Scale Bar = 10 μm).

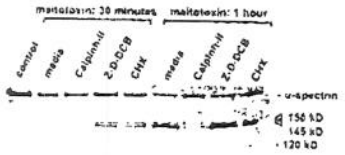

Fig. 7. Calpain but not caspase-3 protease activation following maitotoxin treatment.
Western blots were employed to examine proteolysis of α-spectrin into 150 kDa, calpain-specific 145 kDa and caspase 3-specific 120 kDa breakdown products. Increased accumulation of 150 kDa and 145 kDa breakdown products to α-spectrin was seen 30 minutes following maitotoxin treatment, as compared to untreated controls. By 1 hour following maitotoxin treatment, increased processing of the 150 kDa band to calpain-specific 145 kDa breakdown products was observed. Administration of calpInh-II (37.5 μM) but not Z-D-DCB (30 μM) or cycloheximide (1 μg/ml), completely blocked calpain-mediated proteolysis of α-spectrin. There was no evidence of caspase 3 mediated proteolysis of α-spectrin to 120 kDa breakdown products.

Hoechst 33258, absence of DNA fragmentation produced by endonuclease activation and the failure of inhibition of protein synthesis to reduce cell death

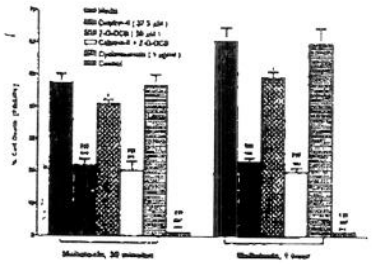

Fig. 8. Inhibition of propidium iodide uptake by CalpInh-II and Z-D-DCB but not by cycloheximide.
Maitotoxin-induced uptake of propidium iodide was attenuated by CalpInh-II and Z-D-DCB, but not cycloheximide, at 30 min. and 1 hour following maitotoxin treatment. CalpInh-II administration did not provide complete protection against uptake of propidium iodide, and significantly less protection was provided by administration of Z-D-DCB. Administration of CalpInh-II+Z-D-DCB, provided no better protection than administration of CalpInh-II alone.
*Compared to media controls (0.1 nM Maitotoxin). *$p \leq 0.05$; ***$p \leq 0.001$
#Compared to CalpInh-II. #$p \leq 0.05$; ###$p \leq 0.001$
▼Compared to Z-D-DCB. ▼$p \leq 0.05$; ▼▼▼$p \leq 0.001$

10. Kampfl, A., Posmantur, R.M., Zhao, X., Schmutzhard, E., Clifton, G.L., and Hayes, R.L. 1997. Mechanisms of calpain proteolysis following traumatic brain injury: implications for pathology and therapy: implications for pathology and therapy: a review and update. J. Neurotrauma 14:121–134.
11. Yuen, P., Gilbertsen, R.B., and Wang, K.K.W. 1996. Non-erythroid α-spectrin breakdown by calpain and interleukin 1β-converting-enzyme-like protease(s) in apoptotic cells: contributory roles of both protease families in neuronal apoptosis. Biochem. J. 319:683–690.
12. Bartus, R.T. 1997. The calpain hypothesis of neurodegeneration: Evidence for a common cytotoxic pathway. Neuroscientist 3:314–327.
13. Nath, R., McGinnis, K.J., Nadimpalli, R., Stafford, D., and Wang, K.K.W. 1996. Effects of ICE-like proteases and calpain inhibitors on neuronal apoptosis. Neuroreport 8:249–255.
14. Nath, R., Raser, K.J., Stafford, D., Hajimohammadreza, I., Posner, A., Allen, H., Talanian, R.V., Yuttori, T., Sato, N., Waguri, S., Karasawa, Y., Araki, H., Shibanai, K., Kominami, E., and Uchiyama, Y. 1995. Delayed neuronal death in the CA1 pyramidal cell layer of the gerbil hippocampus following transient ischemia is apoptosis. J. Neurosci. 15:1001–1011.
15. Martin, S.J., O'Brien, G.A., Nishioka, W.K., McGahon, A.J., Mahboubi, A., Saido, T.C., and Green, D.R. 1995. Proteolysis of fodrin (non-erythroid spectrin) during apoptosis. J. Biol. Chem. 270:6425–6428.
16. Squier, M.K.T., Miller, A.C.K., Malkinson, A.M., and Cohen, J.J. 1994. Calpain activation in apoptosis. J. Cell. Physiol. 159:229–237.
17. Pike, B.R., Zhao, X., Newcomb, J.K., Wang, K.K.W., Posmantur, R.M., and Hayes, R.L. 1998. Temporal relationships between De Novo protein synthesis, calpain and caspase-3 (CPP32) protease activation, and DNA fragmentation during apoptosis in septo-hippocampal cultures. J. Neurosci. Res., In press.
18. Behrens, M.M., Martinez, J.L., Morattlla, C., and Renart, J. 1995. Apoptosis induced by protein kinase-C inhibition in a neuroblastoma cell line. Cell Growth Diff. 6:1375–1380.
19. Jordan, J., Galindo, M.F., and Miller, R.J. 1997. Role of calpain- and interleukin-1β converting enzyme-like proteases in the β-amyloid-induced death of rat hippocampal neurons in culture. J. Neurochem. 68:1612–1621.
20. Eldadah, B.A., Yakovlev, A.G., and Faden, A.I. 1997. The role of CED-3-related cysteine proteases in apoptosis of cerebellar granule. J. Neurosci. 17(16):6105–6113.
21. Fraser, A., and Evan, G. 1996. A license to kill. Cell 85(6):781–4.
22. Miura, M., Zhu, H., Rotello, R., Hartwieg, E.A., and Yuan, J. 1993. Induction of apoptosis in fibroblasts by IL-1 beta-converting enzyme, a mammalian homolog of the C. elegans cell death gene ced-3. Cell 75(4):653–60.
23. Zhivotovsky, B., Burgess, D.H., Vanags, D.M., and Orrenius, S. 1997. Involvement of cellular proteolytic machinery in apoptosis. Biochem. Biophys. Res. Comm. 230:481–488.
24. Cohen, G.M. 1997. Caspases: the executioners of apoptosis. Biochem. J. 326:1–16.
25. Wang, K.K.W., Posmantur, R.M., M., Nath, R., McGinnis, K., Whitton, M., Talanian, R.V., Glantz, S.B., and Morrow, J.S. 1998. Simultaneous degradation of α II and β-II spectrin by caspase 3 (CPP32) in apoptotic cells. J. Biol. Chem., In press.
26. Nath, R., Raser, K.J., Stafford, D., Hajimohammadreza, I., Posner, A., Allen, H., Talanian, R.V., Yuen, P., Gilbertsen, R.B., and Wang, K.K. 1996. Non-erythroid alpha-spectrin breakdown by calpain and interleukin 1 beta-converting-enzyme-like protease(s) in apoptotic cells: contributory roles of both protease families in neuronal apoptosis. Biochemical J. 319 (Pt 3):683–90.
27. Nath, R., Robert, A., McGinnis, K.M., and Wang, K.K.W. 1998. Evidence for activation of caspase-3-like protease in excitotoxins and hipoxia/hypoglycemia-injured cerebrocortical neurons. J. Neurochem., In press.
28. Falcieri, E., Martelli, A.M., Bareggi, R., Cataldi, A., and Cocco, L. 1993. The protein kinase inhibitor staurosporine induces morphological changes typical of apoptosis in MOLT-4 cells without concomitant DNA fragmentation. Biochem. Biophys. Res. Comm. 193:19–25.
29. Armstrong, R.C., Aja, T., Xiang, J., Gaur, S., Krebs, J.F., Hoang, K., Bai, X., Korsmeyer, S.J. Karanewsky, D.S., Fritz, L.C., and Tomaselli, K.J. 1996. Fas-induced activation of the cell death-related protease CPP32 is inhibited by Bcl-2 and by ICE family protease inhibitors. J. Biol. Chem. 271(28):16850–5.
30. Wang, K.K.W., Nath, R., and Raser, K.J. 1996. Hajimohammadreza I. Maitotoxin induces calpain activation in SH-SY5Y neuroblastoma cells and cerebrocortical cultures. Arch. Biochem. Biophys. 331(2):208–14.
31. Gusovsky, F., and Daly, J.W. 1990. Maitotoxin: a unique pharmacological tool for research on calcium-dependent mechanisms. Biochem. Pharmacol. 39(11):1633–9.
32. Soergel, D.G., Yasumoto, T., Daly, J.W., and Gusovsky, F. 1992. Maitotoxin effects are blocked by SK&F 96365, an inhibitor of receptor-mediated calcium entry. Mol. Pharmacol. 41:487–493.
33. Meucci, O., Grimaldi, M., Scorziello, A., Govoni, S., Bergamaschi, S., Yasumoto, T., and Schettini, G. 1992. Maitotoxin-induced intracellular calcium rise in PC12 cells: involvement of dihydropyridine-sensitive and omega-conotoxin-sensitive calcium channels and phosphoinositide breakdown. J. Neurochem. 59:679–688.
34. Musgrave, I.F., Seifert, R., and Schultz, G. 1994. Maitotoxin activates cation channels distinct from the receptor-activated non-selective cation channels of HL-60 cells. Biochem. J. 301:437–441.
35. Regan, R.F., Panter, S.S., Witz, A., Tilly, J.L., and Giffard, R.G. 1995. Ultrastructure of excitotoxic neuronal death in murine cortical culture. Brain Res. 705(1–2):188–98.
36. Roberts-Lewis, J.M., Savage, M.J., Marcy, V.R., Pinsker, L.R., and Siman, R. 1994. Immunolocalization of calpain I-mediated spectrin degradation to vulnerable neurons in the ischemic gerbil brain. J. Neurosci. 14(6):3934–44.
37. Wang, K.K.W. 1998. An overview of calpain. Bio-reguladores, In press.
38. Kampfl, A., Zhao, X., Whitson, J.S., Posmantur, R., Dixon, C.E., Yang, K., Clifton, G.L., and Hayes, R.L. 1996. Calpain inhibitors protect against depolarization induced neurofilament protein loss of septo-hippocampal neurons in culture. Eur. J. Neurosci. 8:344–352.
39. Koh, J., Wie, M.B., Gwag, B.J., Sensi, S.L., Canzoniero, M.T., Demaro, J., Csernansky, C., and Choi, D.W. 1995. Staurosporine-induced neuronal apoptosis. Exp. Neurol. 135:153–159.
40. Martin, D.P., Schmidt, R.E., DiStefano, P.S., Lowry, O.H., Carter, J.G., and Johnson, E.M. 1988. Inhibitors of protein synthesis and RNA synthesis prevent neuronal death caused by nerve growth factor deprivation. J. Cell. Biol. 106:829–844.
41. Jones, K.H., and Senft, A.J. 1985. An improved method to determine cell viability by simultaneous staining with fluorescein diacetate-propidium iodide. J. Histochem. Cytochem 33:77–79.
42. Gong, J., Traganos, F., and Darzynkiewicz, Z. 1994. A selective procedure for DNA extraction from apoptotic cells applicable for gel electrophoresis and flow cytometry. Analyt. Biochem. 218(2): 314–319.
43. Terao, K., Ito, E., Sakamaki, Y., Igarashi, K., Yokoyama, A., and Yasumoto, T. 1998. Histopathological studies of experimental marine toxin poisoning. II. The acute effects of maitotoxin on the stomach, heart and lymphoid tissues in mice and rats. Toxicon 26(4):395–402, 1988.
44. Oberhammer, F., Fritsch, G., Schmied, M., Pavelka, M., Printz, D., Purchio, T., Lassmann, H., and Schulte-Hermann, R. 1993. Condensation of the chromatin at the membrane of an apoptotic nucleus is not associated with activation of an endonuclease. J. Cell. Science 104:317–326.

Journal of Cerebral Blood Flow & Metabolism
23:1461–1470 © 2003 The International Society for Cerebral Blood Flow and Metabolism
Published by Lippincott Williams & Wilkins, Inc., Baltimore

Diffusion Magnetic Resonance Imaging Study of a Rat Hippocampal Slice Model for Acute Brain Injury

*Timothy M. Shepherd, *Peter E. Thelwall, *†Stephen J. Blackband, *Brian R. Pike, §Ronald L. Hayes, and *Edward D. Wirth, III

**Department of Neuroscience, Evelyn F. & William McKnight Brain Institute, University of Florida, Gainesville, Florida, U.S.A.; †National High Magnetic Field Laboratory, Tallahassee, Florida, U.S.A.; and §Center for Traumatic Brain Injury Studies, Department of Neuroscience, Evelyn F. & William McKnight Brain Institute, University of Florida, Gainesville, Florida, U.S.A.*

Summary: Diffusion magnetic resonance imaging (MRI) provides a surrogate marker of acute brain pathology, yet few studies have resolved the evolution of water diffusion changes during the first 8 hours after acute injury, a critical period for therapeutic intervention. To characterize this early period, this study used a 17.6-T wide-bore magnet to measure multicomponent water diffusion at high *b*-values (7 to 8,080 s/mm^2) for rat hippocampal slices at baseline and serially for 8 hours after treatment with the calcium ionophore A23187. The mean fast diffusing water fraction (F_{fast}) progressively decreased for slices treated with 10-μmol/L A23187 (−20.9 ± 6.3% at 8 hours). Slices treated with 50-μmol/L A23187 had significantly reduced F_{fast} 80 minutes earlier than slices treated with 10-μmol/L A23187 ($P < 0.05$), but otherwise, the two doses had equivalent effects on the diffusion properties of tissue water. Correlative histologic analysis showed dose-related selective vulnerability of hippocampal pyramidal neurons (CA1 > CA3) to pathologic swelling induced by A23187, confirming that particular intravoxel cell populations may contribute disproportionately to water diffusion changes observed by MRI after acute brain injury. These data suggest diffusion-weighted images at high *b*-values and the diffusion parameter F_{fast} may be highly sensitive correlates of cell swelling in nervous issue after acute injury. **Key Words:** Calcium—Neurotoxicity—Cell death—A23187—Multicomponent diffusion.

Many neuroprotective strategies have proven successful for treating animal models of ischemic stroke and traumatic brain injury, yet have failed to improve clinical outcome in human patients during clinical trials (Faden, 2001). The frequent disappointments in these studies have often been attributed, in part, to defects in clinical trial design wherein studies fail to rapidly assess and stratify potential subjects based on the severity, location, and complexity of their acute brain injuries (Faden, 2001). Appropriate subject selection is particularly important because brain injury patients represent a far more heterogeneous population compared to their corresponding animal models of disease (Statler et al., 2001). To address this problem, it has recently proven beneficial to incorporate diffusion-weighted magnetic resonance imaging (MRI) into clinical trials (Warach, 2001) because of its sensitivity to changes in nervous-tissue water diffusion that occur immediately after injury (Moseley et al., 1990). Diffusion-weighted MRI of stroke patients, for example, aids recognition of the "perfusion-diffusion mismatch," which identifies penumbral volumes of nervous tissue that may be rescued from subsequent injury by prompt infusion of tissue plasminogen activator (Warach, 2002).

An improved understanding of water diffusion in nervous tissue and the acute water-diffusion changes that follow injury may further increase the sensitivity and specificity of diffusion-weighted MRI as a surrogate marker of acute brain injury. Unfortunately, previous clinical diffusion MRI studies have provided limited data from the first 24 hours after ischemic or traumatic brain

Received May 9, 2003; final version received September 16, 2003; accepted September 23, 2003.

Dr. Pike is currently affiliated with the Office of Scientific Review, NIH/NIGMS, Bethesda, Maryland, U.S.A. Dr. Wirth is currently affiliated with the Section of Neurosurgery, University of Chicago, Chicago, Illinois, U.S.A.

Supported by grants from the Florida Brain and Spinal Cord Injury Research Trust Fund, NIH RO1 NS3–6992, NIH RO1 NS39091, NIH RO1 NS40182, and DAMD17-01-1-0765.

Address correspondence and reprint requests to Dr. Shepherd, Department of Neuroscience, PO Box 100244, McKnight Brain Institute, University of Florida, Gainesville, FL 32610, U.S.A.; e-mail: tms@mbi.ufl.edu

DOI: 10.1097/01.WCB.0000100852.67976.C2

183

injury (for example, Beaulieu et al., 1999). Although this information has proven useful for understanding the chronic progression of diffusion changes after brain injury, it is well beyond the optimal therapeutic windows when experimental interventions are most likely to succeed (Marler et al., 2000). Thus, studies that better resolve the acute temporal progression of diffusion changes after brain injury are needed to provide improved patient stratification based on injury severity and to monitor the effects of therapeutic interventions early after brain injury.

Unlike previous clinical studies of acute brain injury, recent studies have demonstrated that diffusion-weighted signal attenuation is nonmonoexponential in rat (Niendorf et al., 1996) and human brains (Mulkern et al., 1999) when measured with very strong diffusion-sensitizing gradients (high *b*-values). As a first approximation, a biexponential function may be used to describe water diffusion in nervous tissue by separating the MRI signal into contributions from fast and slow diffusing components. Shifts between these two components may correlate with changes in the relative size of the intracellular compartment (Niendorf et al., 1996; Thelwall et al., 2002). Although the biexponential model is an incomplete description of tissue water diffusion, it is more appropriate than the monoexponential fits currently employed clinically.

Continuous acquisition of water diffusion data for multicomponent analysis throughout the first 8 hours after an acute brain injury would prove extremely difficult in human or animal subjects because of their limited tolerance for long imaging times, and because high *b*-value diffusion weighting is difficult to obtain on relatively large subjects owing to current hardware limitations. Thus, to further investigate the value of diffusion MRI as a surrogate marker of acute brain injury, we measured water diffusion in perfused rat hippocampal slices using a 17.6-T magnet with strong diffusion-sensitizing gradients (1,000 mT/m). Unlike human and animal subjects, rat hippocampal slices tolerate long periods of investigation yet maintain the heterogeneous neuronal and glial cell populations (Aitken et al., 1995) that determine *in vivo* MRI contrast. Furthermore, studies of hippocampal slices are not confounded by anesthesia or movement and perfusion artifacts (Aitken et al., 1995). Previous studies have used diffusion-weighted MRI of rat hippocampal slices (Blackband et al., 1997) and have shown that slices perturbed by ouabain and *N*-methyl-D-aspartate respond similarly (Buckley et al., 1999; Bui et al., 1999) to the same perturbations of *in vivo* rat brain (Benveniste et al., 1992). Also, human brain slices have water diffusion properties comparable to those reported for human patients and rat brain slices, improving the confidence that the rat hippocampal slices are a valid model of human brain tissue (Shepherd et al., 2003).

In the present study, water diffusion was monitored in rat hippocampal slices before and after treatment with different doses of the neurotoxin A23187. This carboxylic acid calcium ionophore rapidly diminishes calcium gradients across cell membranes (Pressman, 1976) as is known to occur *in vivo* after ischemic or traumatic injury (Choi 1988). Previous studies have shown that neuronal cultures treated with high doses of calcium ionophores, such as A23187, experienced rapid loss of calcium homeostasis and pathologic cell swelling (Chan et al., 1998; Gwag et al., 1999; Takadera and Ohyashiki, 1997). We hypothesized that this cellular response would be detectable in rat hippocampal slices using diffusion-weighted MRI and correlative histology. Unlike previous diffusion studies of nervous tissue injury, using A23187 allows this study to uniquely evaluate water-diffusion changes after calcium overload (Petersen et al., 2000), a downstream integrating event in many forms of acute brain injury (e.g., ischemic stroke or traumatic brain injury) (Choi, 1988; McIntosh et al., 1998). Results of this investigation indicated that the biexponential diffusion parameter F_{fast} and diffusion-weighted MRI at high *b*-values provide rapid and sensitive measures of A23187-induced tissue injury that are correlated with neuronal cell swelling and overt histopathology in selectively vulnerable regions of the rat hippocampal slice.

MATERIALS AND METHODS

Brain slice procurement

The University of Florida Institutional Animal Care and Use Committee approved the use of laboratory animals for this study. Rat hippocampal slice procurement has been described previously (Aitken et al., 1995). Briefly, male Long-Evans rats (250 to 350 g) were anesthetized with isoflurane and decapitated. The brain was removed and placed into ice-cold artificial cerebrospinal fluid (aCSF) (120-mmol/L NaCl, 3-mmol/L KCl, 10-mmol/L glucose, 26-mmol/L $NaHCO_3$, 2-mmol/L $CaCl_2$, 1.5-mmol/L KH_2PO_4, and 1.4-mmol/L $MgSO_4$) gassed with 95% O_2 and 5% CO_2 to maintain a pH of 7.4. The aCSF osmolality was 300 ± 1 mOsm/kg as determined by Osmette A freezing point depression osmometer (Precision System, Natick, MA,, U.S.A.). Both hippocampi were dissected and cut orthogonal to the septohippocampal axis into 500-μm-thick sections with a McIlwain tissue chopper within 10 minutes of decapitation. Hippocampal slices remained immersed in ice-cold aCSF for 1 hour after decapitation to minimize procurement-induced ischemic damage (Newman et al., 1992). Slices then were warmed gradually to room temperature (20°C) for the MRI experiment and placed into a multislice perfusion chamber (Shepherd et al., 2002).

Slices were perfused continuously with aCSF (2 mL/min) while the perfusion chamber was lowered into the magnet and during pilot image acquisition. Although perfusion was discontinued during all diffusion measurements (described below), calculations based on the published metabolic rates of nervous tissue (Magistretti, 1999) indicate that the typical 6-mg hippocampal slice consumes less than 0.2% of the glucose available

in the perfusion chamber (containing 3.0 mL aCSF) during a 35-minute MRI acquisition. Further, it has been shown previously that intermittent cessation of aCSF flow does not affect slice viability for at least 8 hours after slice procurement (Shepherd et al., 2002).

Diffusion MRI of rat hippocampal slices

All MRI data were obtained at room temperature using a 15-mm birdcage coil interfaced to a Bruker 17.6-T vertical wide-bore magnet and console. Pilot multislice axial, sagittal, and coronal T_1 and diffusion-weighted imaging sequences were used to locate the perfusion chamber, then to optimize the positions of axial magnetic resonance-defined slices through the center of the 500-μm-thick rat hippocampal slices. Diffusion-weighted images were acquired using a pulsed gradient spin-echo multislice sequence with a diffusion time of 14 milliseconds and an echo time of 30 milliseconds. This diffusion measurement consisted of a series of 8 diffusion-weighted images (128 × 64 matrix, 1.5-cm field of view, 2-second repetition, 30-millisecond echo time, 2 averages, $\delta = 3$ milliseconds, $\Delta = 15$ milliseconds) using diffusion gradients aligned perpendicular to the plane of the MRI images in linear strength increments from 0 to 940 mT/m. This resulted in 8 diffusion-weighted images with *b*-values between 7 and 8080 s/mm^2 (including imaging terms). Image slice thickness was 300 μm with 117 × 234-μm in-plane resolution and the protocol required 34 minutes for completion. Additional pilot images were acquired between diffusion measurements to monitor for slice movement due to aCSF perfusion; data from hippocampal slices that moved during the experiment were rejected ($n = 1$).

Slice perturbation with A23187

Before slice procurement, rat hippocampal slices were randomly assigned to treatment by control aCSF, or aCSF containing 10–μmol/L A23187 or 50-μmol/L A23187. Hippocampal slices were exposed to higher doses of A23187 than previous studies in neuronal cultures (Mattson et al., 1991; Petersen et al., 2000) because the slice model was composed of high-density, heterogeneous cell populations studied at lower temperatures. Dimethyl sulfoxide (DMSO) was required to solubilize A23187 in aCSF, so control aCSF contained 0.1% DMSO. The additions of 0.1% DMSO with or without A23187 did not affect the pH or osmolality of the aCSF solution. Previous studies in our laboratories suggest that 0.1% DMSO does not affect calcium movement in slices as indicated by the absence of calcium-mediated calpain activation (Zhao et al., 1999). Each of the aCSF treatment solutions were gassed with 95% O_2 and 5% CO_2 throughout the experiment. All slices were perfused with standard aCSF during pilot scans and before initial baseline diffusion measurements were acquired. Slices then were perfused with the assigned treatment aCSF for 20 minutes, then perfusion was stopped and a post-treatment diffusion protocol obtained. Preliminary studies demonstrated that an initial perfusion duration of 20 minutes with treatment aCSF was sufficient for perfusate exchange. A cycle consisting of 6 minutes of perfusion with the assigned treatment aCSF followed by an additional diffusion measurement (34 minutes) was repeated serially until 12 hours after initial brain slice procurement (each complete cycle required 40 minutes).

The initial treatment period for slices occurred at slightly different times after brain slice procurement because of variations in the time required for hippocampal slice placement and pilot MRI scans (mean time delay from procurement to baseline diffusion measurement was 3.1 ± 0.4 hours). Therefore diffusion data from rat brain slices required assignment to time-bins for statistical comparisons. The baseline diffusion measurement for each slice was assigned to 0 minutes and subsequent data were assigned to time points increasing in 40-minute increments. Although data were reassigned to time points relative to the initial MRI measurement, diffusion data acquired more than 12 hours after slice procurement were excluded from the analysis.

Analysis of diffusion data

To analyze changes in the diffusion-weighted signal intensity in rat hippocampal slices after treatment with the various aCSF solutions, a region of interest (ROI) was drawn on the images to enclose the entire hippocampal slice. Previous studies demonstrated that diffusion-weighted water signal attenuation in rat hippocampal slices is nonmonoexponential at high *b*-values (Buckley et al., 1999). A biexponential equation (Eq. 1) was fitted to the diffusion-weighted signal attenuation in the rat hippocampal slice ROIs using the Levenberg-Marquandt nonlinear least-squares fitting routine:

$$S(b) = S_0 \cdot [F_{fast} \cdot \exp(-bD_{fast}) + (1 - F_{fast}) \cdot \exp(-bD_{slow})]$$

where S_0 is signal intensity without diffusion weighting, F_{fast} is the fraction of water with fast apparent diffusion coefficient (ADC), and D_{fast} and D_{slow} represent the ADCs of the fast and slow diffusing water components, respectively. Observed changes over time from baseline in the biexponential parameters of the three treatment groups (control, 10-μmol/L A23187, and 50-μmol/L A23187) were compared statistically using a two-way repeated-measures analysis of variance (ANOVA) with one factor repeated (Sigma Stat 2.03). If the ANOVA test detected a statistically significant difference among treatment groups at a particular time point, a Tukey multiple comparisons test was used to isolate treatments that differed significantly from one another. Statistical significance for all tests was defined as $P < 0.05$.

Histology of rat hippocampal slices

Because it proved difficult to consistently recover rat hippocampal slices used in the diffusion MRI experiments for subsequent study, three additional rats were required to provide slices for histologic correlation. These slices experienced the same experimental procedure as slices used in the diffusion MRI measurements and at 12 hours after procurement, the slices were gently removed from the perfusion chambers and immersion-fixed with 4% paraformaldehyde in phosphate-buffered saline. Some slices were fixed either immediately after procurement or before perfusion with treatment aCSF (4 hours after procurement) to serve as additional controls. In addition, a few slices that were recovered after the MRI experiments were fixed for histologic analyses to assess whether differences existed for slices treated in the magnet versus slices treated in the correlative protocol.

The fixed slices were embedded in paraffin wax, cut into 8-μm-thick sections, mounted onto slides and stained with hematoxylin and eosin (H&E). Most slices were sectioned parallel to the plane of the slice (orthogonal to the septotemporal axis of the rat hippocampus), but in some slices, sections were cut perpendicular to the plane of the tissue (cross section). These sections were used to determine whether cells at different depths from the tissue surface were affected differently by the various aCSF treatment solutions. Superficial and central planar sections, stained with H&E, also were compared to assess the potential variable effects of tissue depth on tissue response to A23187 treatment.

In all H&E-stained sections, morphologic characteristics of granule and pyramidal neurons from the dentate gyrus, CA1,

CA2, and CA3 fields were noted. Nuclear changes such as pyknotic and eosinophilic nuclei, karyorrhexis, or karyolysis were noted. The cytoplasm of cells was observed for evidence of eosinophilia, microvacuolation, and loss of structure or fragmentation. The surrounding neuropil, in such regions as the stratum radiatum, were also inspected for vacuolization and other pathologic changes. These features were compared between the slices treated with control, 10-μmol/L A23187, or 50-μmol/L A23187 aCSF solutions for differences in injury-induced cellular morphology and pathology.

RESULTS

Diffusion-weighted MRI of rat hippocampal slices

Twenty-nine of the 35 rat hippocampal slices procured from 17 rats were included for the diffusion MRI aspects of this investigation. The other six slices were rejected because of perfusion chamber flooding (n = 3), susceptibility artifacts due to air bubbles in the perfusion chamber (n = 2), and slice movement (n = 1). In comparing the three treatment groups, there were no significant differences for the post-procurement time when the first baseline diffusion measurements were obtained (ANOVA, $P = 0.265$) or for the time when slices were subsequently treated (ANOVA, $P = 0.393$). Mean time to treatment for all slices (3.8 ± 0.5 hours) closely matched the time when correlative rat hippocampal slices were treated outside the magnet for histology studies (4 hours). Diffusion measurements were obtained on all 29 slices up to 6 hours after treatment, on 28 of 29 slices up to 7.3 hours after treatment, and on 20 of 29 slices 8 hours after treatment.

Preliminary high-resolution diffusion-weighted images were obtained of rat hippocampal slices to determine achievable signal-to-noise ratio (SNR) and spatial resolution per unit time. Such images (Fig. 1) exhibited the detailed laminar anatomy of the hippocampus, but required long acquisition times (4.5 hours per *b*-value measurement) without sufficient perfusion to maintain slice viability (Shepherd et al., 2002). For this study, such high spatial resolution was sacrificed for better temporal resolution of the water-diffusion changes that accompany slice perturbation with A23187 (4.2 minutes per *b*-value measurement). In Fig. 2, the lower-resolution images show the signal intensity changes that occur after treatment with 10-μmol/L A23187. Plotting the signal intensity of the hippocampal slice ROI versus *b*-value gave nonmonoexponential diffusion-weighted signal attenuation curves. Figure 3 shows that treatment with 10-μmol/L A23187 caused a progressive decrease in the rate of diffusion-weighted signal attenuation over the 8 hours. This change was most evident at *b*-values above 4000 s/mm^2 (see box B). Similar results to those shown in Figs. 2 and 3 were also observed for slices treated with 50-μmol/L A23187.

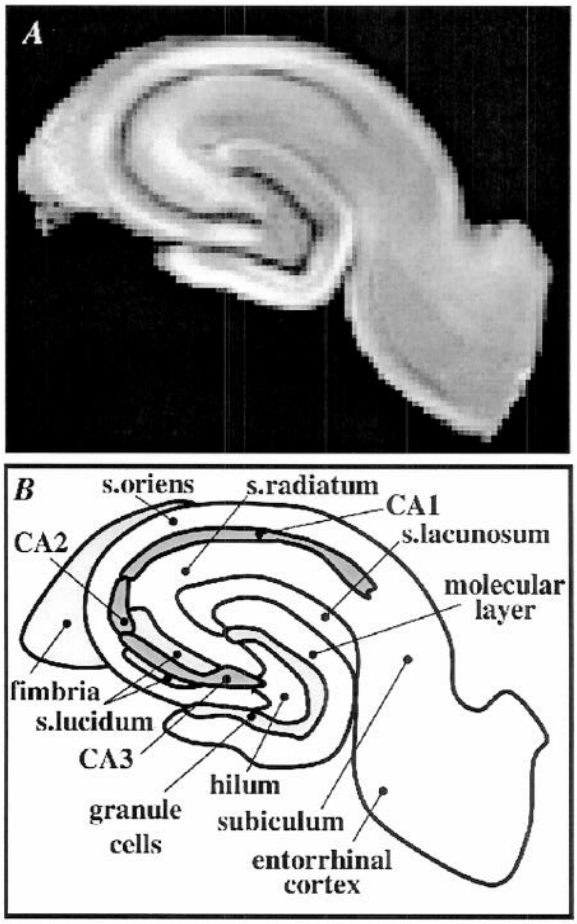

FIG. 1. A diffusion-weighted magnetic resonance image with 59-μm in-plane resolution (**A**) reveals the detailed lamellar anatomy of a 500-μm-thick rat hippocampal slice cut perpendicular to the septotemporal axis (MRI scan parameters: repetition time/echo time = 2,000/34 milliseconds, b = 3,630 s/mm^2, matrix = 256 × 256, field of view = 15 × 15 mm, slice thickness = 300 μm, averages = 32, time = 4.5 hours). As illustrated in panel **B**, many anatomical regions of the hippocampus and dentate gyrus can be distinguished in this sample based on differences in diffusion-weighted signal intensity (s, stratum).

Biexponential analysis of diffusion in hippocampal slices treated with A23187

The diffusion-weighted signal attenuation curves of rat hippocampal slices (Fig. 3) were well described by the biexponential function (Eq. 1) ($R^2 > 0.99$). The biexponential-derived diffusion parameters for all 29 rat hippocampal slices before treatment (mean ± SD) were 0.601 ± 0.057 for F_{fast}, $1.14 \pm 0.14 \times 10^{-3}$ mm^2/s for D_{fast} and $0.067 \pm 0.010 \times 10^{-3}$ mm^2/s for D_{slow}. These values were comparable to previous reports of water diffusion in rat hippocampal slices (Buckley et al., 1999; Bui et al., 1999; Shepherd et al., 2002) and were qualitatively similar to biexponential diffusion parameters reported for *in vivo* human brain (Mulkern et al., 1999). There were small yet statistically significant differences in the baseline biexponential parameters F_{fast} and D_{slow} for slices

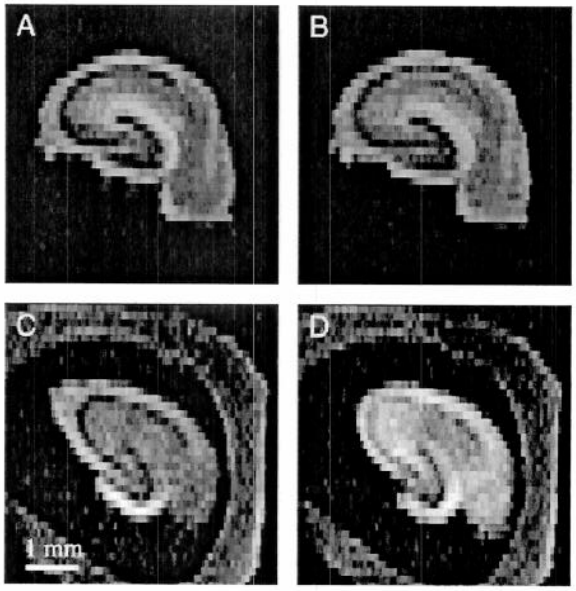

FIG. 2. Typical diffusion-weighted images (b = 7,977 s/mm^2) of rat hippocampal slices. Panels **A** and **B** show a control rat hippocampal slice before and after 8 hours of treatment with 0.1% DMSO vehicle, respectively. Panels **C** and **D** show a different slice before and 8 hours after treatment with 10-μmol/L A23187, respectively (the latex spacer of the perfusion chamber is visible in these two images). At this b-value, signal intensity in the A23187-treated slice increased 42% whereas the vehicle-treated slice signal intensity increased 6% over 8 hours.

assigned to the three different aCSF treatment groups (Table 1). Possible explanations for these differences are addressed in the Discussion.

The biexponential water diffusion parameters for control slices before and immediately after treatment with aCSF containing 0.1% DMSO were not statistically different (ANOVA, $P > 0.05$). The mean F_{fast} of DMSO-treated slices decreased stepwise by approximately 5% only 9 hours after procurement. This change, although not statistically significant, represented a trend present in the data from most individual slices. For the three treatment groups, there were statistically significant interactions between time and treatment in the change from baseline for the diffusion parameter F_{fast} (ANOVA, P <0.001), but not for D_{fast} (P = 0.945) or D_{slow} (P = 0.870). Figure 4 depicts the mean percentage change from baseline in the biexponential parameters F_{fast} for slices treated with aCSF containing 0.1% DMSO, 10–μmol/L A23187, and 50-μmol/L A23187. Compared to vehicle-treated slices, the percentage change in the fraction of fast diffusing water (F_{fast}) for slices treated with 50-μmol/L A23187 was significantly different for all time points after baseline (Tukey, P <0.05). Changes from baseline for slices treated with 10-μmol/L A23187 were significantly different than vehicle-treated slices for all time points after 80 minutes (Tukey, $P < 0.05$). Although the dose of A23187 (10 or 50 μmol/L) predicted when the F_{fast} diffusion parameter of A23187-treated slices would first differ statistically from vehicle-treated slices, at no time point were data from the 10-μmol/L or 50-μmol/L A23187-treated slices statistically distinct from each other.

Histology of A23187-induced pathologic cell swelling

Correlative H&E histology of the rat hippocampal slices exhibited clear dose-related differences in particular hippocampal regions (Fig. 5). In rat hippocampal slices treated with A23187, susceptible neurons typically manifested pathologic change by intense microvacuolation of the neuronal perikaryon and stranded, slightly

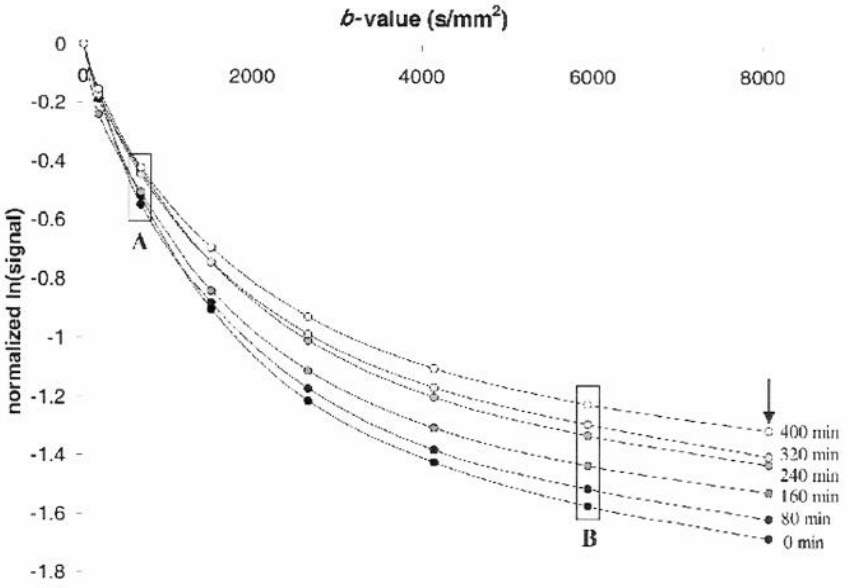

FIG. 3. Typical semilog plot showing temporal changes in the diffusion-weighted signal attenuation curves for a rat hippocampal slice treated with 10-μmol/L A23187. Each point represents the log signal intensity for the slice ROI in a diffusion-weighted image normalized to the signal intensity of the first image (b = 7 s/mm^2). Although diffusion data were collected every 40 minutes, only alternating data from baseline (0 minutes), 80, 160, 240, 320, and 400 minutes are shown for clarity. Comparison of boxes labeled *A* and *B* illustrates that the signal intensity changes after A23187 treatment are better resolved at higher b-values given sufficient signal-to-noise. The arrow indicates approximately where data from Fig. 2 (b = 7,977 s/mm^2) would be plotted in the signal-attenuation curve.

TABLE 1. *Baseline diffusion characteristics for rat hippocampal slices in each of the three treatment groups*

Group	0.1% DMSO	10-μmol/L A23187	50-μmol/L A23187	*P* (ANOVA)	Total/mean
F_{fast}	0.560 ± 0.040*	0.617 ± 0.070	0.623 ± 0.037*	0.025	0.601 ± 0.057
D_{fast} ($\times 10^{-3}$ mm^2/s)	1.08 ± 0.11	1.19 ± 0.17	1.16 ± 0.12	0.216	1.14 ± 0.14
D_{slow} ($\times 10^{-3}$ mm^2/s)	0.060 ± 0.006*	0.071 ± 0.012*	0.067 ± 0.008	0.045	0.067 ± 0.010

Data are mean ± SD.

* Groups that were statistically different from one another as determined post-ANOVA by a Tukey multiple comparisons test ($P < 0.05$).

DMSO, dimethyl sulfoxide, ANOVA, analysis of variance, F_{fast}, fast diffusing water fraction, D_{fast}, fast apparent diffusion coefficient, D_{slow}, slow apparent diffusion coefficient.

pyknotic nuclei. These features are typical oncotic changes that frequently lead to the appearance of necrotic cells at later time points than observable for this study (Majno and Joris, 1995). The described cellular changes were most prominent in aspects of the CA1 cell band (CA1a), but also present in the ends of the CA3 cell band (CA3a and CA3c) and the granule cell layer in the internal blade of the dentate gyrus. The changes were more severe in slices treated with aCSF containing 50-μmol/L A23187 than slices treated with 10-μmol/L A23187. Other regions of the hippocampus, such as CA2, appeared relatively unaffected by A23187, although the neuropil surrounding the affected pyramidal and granule cells did exhibit some staining pallor and vacuolation as well (Fig. 5).

Similar to previous studies (Newman et al., 1992), comparison of H&E-stained cross sections and planar sections from different depths in the hippocampal slices did not suggest different reactions to A23187-treatment based on tissue depth. Additional control slices taken shortly after slice procurement (at 30 minutes after rat decapitation) and before perfusion with aCSF treatment solutions (at 4 hours after procurement) did not show differences from hippocampal specimens obtained by intracardiac perfusion of normal rats with 4% paraformaldehyde except for some minor pathology of the internal blade of the dentate gyrus (see Discussion). The histologic appearance of the few slices recovered from the diffusion MRI studies also did not differ from correlative slices with the same aCSF treatment assignment (data not shown).

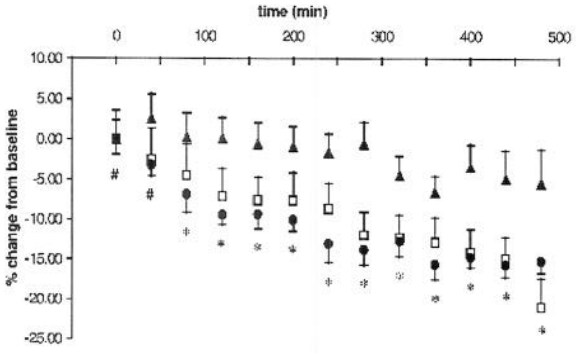

FIG. 4. Mean percentage change from baseline over time for the fraction of fast diffusing water in rat hippocampal slices treated with aCSF containing 0.1% DMSO vehicle (▲; n = 9), 10-μmol/L A23187 (□; n = 10) or 50-μmol/L A23187 (●; n = 10) (mean ± SEM). At early time points, slices treated with 50-μmol/L A23187 statistically differed from vehicle-treated slices (#) whereas at later time points slices treated with either 10–μmol/L or 50-μmol/L A23187 differed from vehicle-treated slices (*) ($P < 0.05$).

DISCUSSION

Pyramidal neurons and granule cells in rat hippocampal slices treated with A23187 showed substantial cytoplasmic microvacuolation indicative of pathologic cell swelling. The neuropil apposed to such damaged neurons also appeared vacuolated. The neuronal pathology after A23187 treatment resembles early ischemic cell changes (Brierley et al., 1973) and electron microscopy studies have correlated such microvacuolation with mitochondrial swelling (Auer and Benveniste, 1997). Although pathologic oncotic swelling is clearly evident, it is difficult to determine whether some neurons ruptured during the experiment because cellular membranes rendered unstable by A23187 treatment might also rupture on fixation (Auer et al., 1985). These findings concur with previous descriptions of pathologic swelling in cultured neurons treated with the calcium ionophores ionomycin or A23187 (Takadera and Ohyashiki, 1997; Chan et al., 1998; Gwag et al., 1999) and are appropriate to the mechanisms of A23187 toxicity. A23187 initiates a rapid intracellular calcium overload in the neuropil that spreads to the neuronal perikaryon at higher doses (Gwag et al., 1999). This calcium overload then provokes mitochondrial permeability transition pore formation and pathologic cell swelling (Petersen et al., 2000).

Unlike previous neuronal cell culture studies (Chan et al., 1998; Petersen et al., 2000), A23187 treatment did not affect all neurons in the hippocampal slices equally. This anatomically selective pattern of pathology in slices after A23187 treatment reproduces the selective vulnerability of the CA1 and CA3 hippocampal regions to ischemic and traumatic injuries (Kotapka et al., 1994). Selective vulnerability of the hippocampus has been attributed to differences in *N*-methyl-D-aspartate receptor distributions (Monaghan and Cotman, 1985), yet A23187 initially bypasses neurotransmitter–receptor interactions by increasing calcium concentrations inside the cell. This

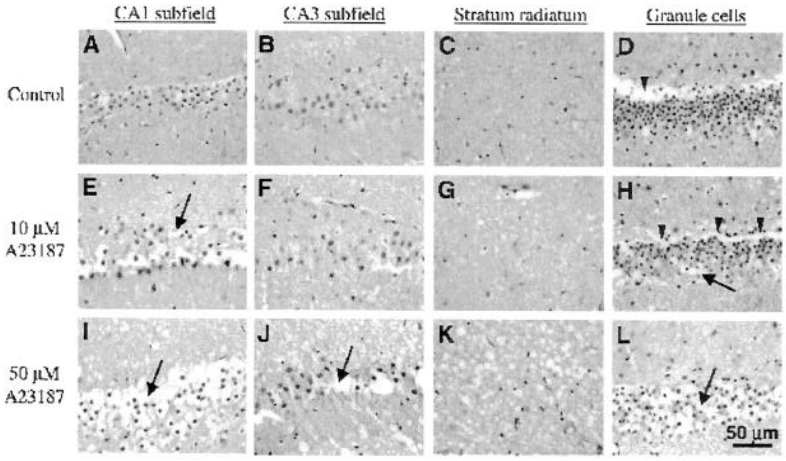

FIG. 5. Correlative histology of rat hippocampal slices 8 hours after treatment with DMSO vehicle (**A–D**), 10-μmol/L A23187 (**E– H**). and 50-μmol/L A23187 (**I–L**) A23187 had dose-related effects on the CA1 subfield, CA3 subfield, stratum radiatum, and internal blade of the dentate gyrus. Arrows illustrate cells ruptured from pathologic swelling and arrowheads denote artifact from paraffin wax embedding. Sections (8-μm thick) were stained with hematoxylin and eosin and are shown at 630× magnification with oil immersion.

suggests there may be differences in intracellular calcium-dependent enzyme cascades that contribute to selective vulnerability in the rat hippocampal slice. Pathology in the granule cell layer differed from previous reports of perturbation-induced granule cell injury (Auer et al., 1985) and suggests metabolic injury occurring during procurement may increase the vulnerability of this particular hippocampal region to A23187 (Newman et al., 1992).

Vulnerable regions of the rat hippocampal slices also showed dose-related differences in the magnitude of pathological cell swelling induced by A23187 (see Fig. 5). These dose-related histopathologic differences were difficult to distinguish with the diffusion MRI measurements using the whole-slice ROI method because regions affected by A23187 in a dose-related fashion were volume-averaged with relatively unaffected regions. However, dose-related differences were noted after A23187 treatment when the F_{fast} of slices became statistically distinct from control slices. With either A23187 dose, the F_{fast} for slices was reduced 7% to 10% from baseline during the first 2 hours after treatment, but it then took an additional 6 hours of A23187 treatment to double this reduction.

The biophysical interpretation of F_{fast} reductions observed in rat hippocampal slices treated with A23187 is not trivial because the biexponential model of water diffusion in nervous tissue is too simplistic. Although the fast and slow diffusing components of water diffusion can not be directly attributed to the extracellular and intracellular compartments respectively, studies have shown that changes in the F_{fast} do correlate with perturbation-induced changes in the relative size of the intracellular compartment (Niendorf et al., 1996; Thelwall et al., 2002). There are several additional biophysical properties of nervous tissue that affect water diffusion and are unaccounted for by the biexponential model; for example, transmembrane water exchange rates, intracellular restriction, and extracellular tortuosity also influence the biexponential diffusion parameters obtained (including F_{fast}) (Thelwall et al., 2002). When neurons are pathologically injured by A23187 treatment, these additional biophysical features are also likely to be altered and influence the biexponential parameters obtained. Given sufficient time and SNR, future studies could use more complex analytical models, such as the one developed by Stanisz et al. (1998), to better describe the biophysical tissue properties of hippocampal slices altered by A23187-induced pathologic cell swelling.

Despite these limitations, the biexponential model does provide a more complete description of nervous-tissue water diffusion than the monoexponential ADC fits currently in clinical use, and it is reasonable to cautiously interpret changes in F_{fast} to correlate with changes in the relative size of the intracellular compartment. Previous clinical studies have shown decreased ADC in acute ischemic brain followed by an increase in ADC beyond normal values several days later (Beaulieu et al., 1999). These diffusion changes, noted in animal models of both ischemic and traumatic injury, may be due to cellular swelling followed by lysis (Assaf et al., 1997; Knight et al., 1994;). Because high doses of A23187 caused a similar yet accelerated pattern of cell swelling and lysis in neuronal cultures (Chan et al., 1998; Takadera and Ohyashiki, 1997), a biphasic pattern of F_{fast} changes was hypothesized to be observable for F_{fast} within the time span of this experiment on rat hippocampal slices treated with A23187. Thus, as cells swell, F_{fast} would decrease, but then as cells rupture, F_{fast} would be predicted to increase.

Because potential dose-related differences in F_{fast} were only observable during the first 80 minutes after A23187 treatment, the results of this study might suggest that there were a limited number of A23187-sensitive cell populations within the rat hippocampal slices. At high doses of A23187, these cells swell more quickly

(reducing F_{fast}), but the A23187-sensitive populations become saturated such that the high and low doses of A23187 become indistinguishable at later time points. However, the correlative histology suggests that more neurons were recruited to pathologic swelling by the higher A23187 dose. Thus, a better explanation may be that in slices treated with 50-μmol/L A23187, 2 hours after treatment the F_{fast} increases due to lysis in the initially injured cell population may have been obscured by F_{fast} decreases due to neurons subsequently recruited to pathologic cell swelling. Thus, dose-related differences in A23187 injury may be obscured at later time points by volume averaging of not only healthy and injured neurons, but also by volume averaging of neurons at different stages of cellular injury (swelling and lysis).

Nonetheless, this study shows that the F_{fast} diffusion parameter may be used as a sensitive correlate of cellular swelling after acute brain injury in future clinical evaluations. However, compared to correlative histology, the diffusion MRI measurements failed to observe the appearance of substantial dose-related, region-specific pathologic changes in the rat hippocampal slices because the present MRI analysis did not examine individual anatomical regions. This also may explain the failure to observe a biphasic F_{fast} response in hippocampal slices treated with the higher dose of A23187. Because the SNR advantages of a 17.6-T magnet were used to make water diffusion measurements suitable for the biexponential model with high temporal resolution, the ROI volume chosen for this study (2 mm^3) was comparable to typical MRI voxel volumes in clinical diffusion studies (Beaulieu et al., 1999). As such, this study highlights how potential variations in regional, cell subtype, and dose-related responses to acute injury may pass unobserved in diffusion measurements that sacrifice spatial resolution to obtain adequate signal-to-noise ratios in practical scan times, particularly when correlative techniques are not used. Clearly, this will continue to be a challenging problem clinically. Previous studies in human patients also have suggested that ADC changes in ischemic stroke may be heterogeneous and might reflect "different temporal rates of tissue evolution toward infarction" (Nagesh et al., 1998).

The time and hardware limitations in present clinical imaging protocols make it difficult to collect data sufficient even for biexponential analysis of water diffusion. Alternatively the diffusion data can be examined without biexponential analysis by simply comparing images of slices at particular diffusion weightings before and after A23187 exposure. A23187 treatment increased diffusion-weighted signal intensity for all rat hippocampal slices treated with either 10-μmol/L or 50-μmol/L A23187, and these changes were noted at all nonzero *b*-values. In Fig. 2, for example, diffusion-weighted slice signal intensity at $b = 7{,}977$ s/mm^2 increased 42% after 8 hours treatment with 10-μmol/L A23187. Although the SNR is decreased at higher *b*-values, the increases in diffusion-weighted signal intensity between slice MRI images at baseline and at different time points after A23187 treatment were better resolved with increasing *b*-value (for example, see Fig. 3 boxes A and B). These results support previous reports that suggested stronger diffusion-weighting (higher *b*-values) may increase the tissue characterization capabilities of diffusion-weighted MRI in human patients when there is sufficient contrast-to-noise (Meyer et al., 2000; Sze and Anderson, 2000). This may be because high *b*-value diffusion-weighted signal intensity emphasizes water diffusion in the intracellular compartment where most of the initial pathologic injury to tissue occurs. Future studies will be required to further investigate the clinical merits of high *b*-value diffusion-weighted MRI.

There are some caveats to the interpretation of the diffusion MRI data presented. The comparison of baseline diffusion parameters for slices based on treatment group assignment (Table 1) revealed some significant pretreatment differences in the diffusion parameters F_{fast} and D_{slow}. Procurement conditions were unlikely to contribute significantly to these baseline differences because slices were procured under neuroprotective hypothermic conditions (see below). Instead, the initial diffusion differences may be attributed to differences in positioning the MR image location within the hippocampal tissue (see Materials and Methods). The undesired inclusion of aCSF within the MRI-defined slice can increase the amount of freely diffusing water present in the slice ROI, which then alters the biexponential diffusion parameters obtained. The study design controlled for such pretreatment differences by examining change in water diffusion in individual slices from baseline after treatment.

Brain slices have some limitations as models of *in vivo* nervous tissue. Rat hippocampal slices were procured at low temperatures to minimize procurement-induced injury before A23187 treatment (Newman et al., 1992; Aitken et al., 1995). In addition, water diffusion changes were measured in rat hippocampal slices treated with A23187 at room temperature instead of 37°C because this simplifies slice perfusion-chamber design and permits hippocampal slices sufficiently thick (500 μm) for MRI study (Aitken et al., 1995). The neuroprotective effects of hypothermia suggest that the measured diffusion responses in this tissue injury model may underestimate the responses of *in vivo* nervous tissue. In addition, the diffusion coefficient of unrestricted water will increase approximately 50% when heated from room temperature to 37°C (Harris and Woolf, 1980). This may limit direct extrapolation of the data presented; however, the study focused on relative changes that should be comparable between the slice model and *in vivo* subjects.

Despite the neuroprotective effects of hypothermia, some histopathology was notable in control slices 12 hours after slice procurement (e.g., CA1 and the internal blade of the granule cell layer). Although not statistically significant, there also was a 5% decrease in mean F_{fast} for control slices at the conclusion of the experiment. Further, the conditions under which brain slice experiments occur (e.g., slice procurement and intermittent aCSF perfusion) might enhance A23187-induced tissue injury (Newman et al., 1992). These findings indicate that brain slices can not perfectly model healthy and pathologic *in vivo* nervous tissue, yet over the duration of the present experiment, changes to control slices were of limited magnitude compared to the histopathology and water diffusion changes due to pathologic swelling induced by A23187 treatment. Thus, hippocampal slices provided a workable tissue model for comparing water diffusion in injured and viable nervous tissue. Brain slices tolerate long imaging periods in very-high-field magnets that enable data collection not possible in current clinical scanners. Thus, brain slice methodology will remain highly relevant in the future to developing a better understanding of the biophysical basis for water diffusion changes after acute brain injury.

CONCLUSION

This study successfully used diffusion-weighted MRI of rat hippocampal slices to study the acute temporal evolution of multicomponent water-diffusion changes after A23187 treatment. Brain slices provided a stable and highly controllable nervous tissue model. Data obtained from this model of acute brain injury suggest that the biexponential diffusion parameter F_{fast} may be a sensitive correlate of cellular swelling in nervous tissue and that diffusion changes after acute brain injury may be intravoxel volume-averaged summations of responses from anatomically or temporally distinct healthy and pathologically injured cell populations. These results suggest that regional analysis of A23187-treated hippocampal slices may improve our understanding of the unique and heterogeneous morphologic processes that follow acute cellular injury and contribute to improved clinical measurements of diffusion in human stroke and traumatic brain injury patients. In addition, data from this study concur with findings of previous clinical studies that diffusion-weighted images at high *b*-values may offer improved characterization of normal and pathologic nervous tissue. Future perturbation studies of rat hippocampal slices may be capable of reconciling complex, data-intensive mathematical models of nervous-tissue water diffusion with diffusion MRI data obtained from human patients with acute brain injuries.

Acknowledgments: The authors thank Dr. Michael King for reviewing the manuscript and acknowledge the valuable technical assistance of Deborah Dalziel, Daniel Plant, and Barbara O'Steen.

REFERENCES

Aitken PG, Breese GR, Dudek FF, Edwards F, Espanol MT, Larkman PM, Lipton P, Newman GC, Nowak TS Jr, Panizzon KL, Raley-susman KM, Reid KH, Rice ME, Sarvey JM, Schoepp DD, Segal M, Taylor CP, Teyler TJ, Voulalas PJ (1995) Preparative methods for brain slices: a discussion. *J Neurosci Methods* 59:139–149

Assaf Y, Beit-Yannai E, Shohami E, Berman E, Cohen Y (1997) Diffusion- and T2-weighted MRI of closed-head injury in rats: a time course study and correlation with histology. *Magn Reson Imaging* 15:77–85

Auer R, Kalimo H, Olsson Y, Wieloch T (1985) The dentate gyrus in hypoglycemia: pathology implicating excitotoxin- mediated neuronal necrosis. *Acta Neuro Pathol (Berl)* 67:279–288

Auer RN, Benveniste H (1997) Hypoxia and related conditions. In: *Greenfield's neuropathology, Vol. 1* (Graham DI, Lantos PL, eds), London: Oxford University Press, pp 315–396

Beaulieu C, de Crespigny A, Tong DC, Moseley ME, Albers GW, Marks MP (1999) Longitudinal magnetic resonance imaging study of perfusion and diffusion in stroke: evolution of lesion volume and correlation with clinical outcome. *Ann Neurol* 46:568–578

Benveniste H, Hedlund LW, Johnson GA (1992) Mechanism of detection of acute cerebral ischemia in rats by diffusion-weighted magnetic resonance microscopy. *Stroke* 23:746–754

Blackband SJ, Bui JD, Buckley DL, Zelles T, Plant HD, Inglis BA, Phillips MI (1997) MR microscopy of perfused brain slices. *Magn Reson Med* 38:1012–1015

Brierley JB, Meldrum BS, Brown AW (1973) The threshold and neuropathology of cerebral "anoxic-ischemic" cell change. *Arch Neurol* 29:367–374

Buckley DL, Bui JD, Phillips MI, Zelles T, Inglis BA, Plant HD, Blackband SJ (1999) The effect of ouabain on water diffusion in the rat hippocampal slice measured by high resolution NMR imaging. *Magn Reson Med* 41:137–142

Bui JD, Buckley DL, Phillips MI, Blackband SJ (1999) Nuclear magnetic resonance imaging measurements of water diffusion in the perfused hippocampal slice during N-methyl-D-aspartate-induced excitotoxicity. *J Neurosci* 93:487–490

Chan SO, Runko E, Anyane-Yeboa K, Ko L, Chiu FC (1998) Calcium ionophore-induced degradation of neurofilament and cell death in MSN neuroblastoma cells. *Neurochem Res* 23:393–400

Choi DW (1988) Calcium-mediated neurotoxicity: relationship to specific channel types and role in ischemic damage. *Trends Neurosci* 11:465–469

Faden AI (2001) Neuroprotection and traumatic brain injury: the search continues. *Arch Neurol* 58:1553–1555

Gwag BJ, Canzoniero LM, Sensi SL, Demaro JA, Koh JY, Goldberg MP, Jacquin M, Choi DW (1999) Calcium ionophores can induce either apoptosis or necrosis in cultured cortical neurons. *Neuroscience* 90:1339–1348

Harris, KR, Woolf, LA (1980) Pressure and temperature-dependence of the self-diffusion coefficient of water and O-18 water. *J Chem Soc Faraday Trans I* 76:377–385

Knight RA, Dereski MO, Helpern JA, Ordidge RJ, Chopp M (1994) Magnetic resonance imaging assessment of evolving focal cerebral ischemia. Comparison with histopathology in rats. *Stroke* 25:1252–1261

Kotapka MJ, Graham DI, Adams JH, Gennarelli TA (1994) Hippocampal pathology in fatal human head injury without high intracranial pressure. *J Neurotrauma* 11:317–324

Magistretti P (1999) Brain energy metabolism. In: *Fundamental neuroscience* (Zigmond, Bloom, Landis, Roberts, Squire, eds), London: Academic Press, p 389

Majino G, Joris I (1995) Apoptosis, oncosis, and necrosis. An overview of cell death [see comments]. *Am J Pathol* 146:3–15

Marler JR, Tilley BC, Lu M, Brott TG, Lyden PC, Grotta JC, Broderick

JP, Levine SR, Frankel MP, Horowitz SH, Haley EC Jr, Lewandowski CA, Kwiatkowski TP (2000) Early stroke treatment associated with better outcome: the NINDS rt-PA stroke study. *Neurology* 55:1649–1655

Mattson MP, Rychlik B, Chu C, Christakos S (1991) Evidence for calcium-reducing and excito-protective roles for the calcium-binding protein calbindin-D28k in cultured hippocampal neurons. *Neuron* 6:41–51

McIntosh TK, Saatman KE, Raghupathi R, Graham DI, Smith DH, Lee VM, Trojanowski JQ (1998) The Dorothy Russell Memorial Lecture. The molecular and cellular sequelae of experimental traumatic brain injury: pathogenetic mechanisms. *Neuropathol Appl Neurobiol* 24:251–267

Meyer JR, Gutierrez A, Mock B, Hebron D, Prager JM, Gorey MT, Homer D (2000) High-b-value diffusion-weighted MR imaging of suspected brain infarction. *AJNR Am J Neuroradiol* 21:1821–1829

Monaghan DT, Cotman CW (1985) Distribution of N-methyl-D-aspartate-sensitive L-[3H]glutamate-binding sites in rat brain. *J Neurosci* 5:2909–2919

Moseley ME, Cohen Y, Mintorovitch J, Chileuitt L, Shimizu H, Kucharczyk J, Wendland MF, Weinstein PR (1990) Early detection of regional cerebral ischemia in cats: comparison of diffusion- and T2-Weighted MRI and Spectroscopy. *Magn Reson Med* 14:330–346

Mulkern RV, Gudbjartsson H, Westin CF, Zengingonul HP, Gartner W, Guttmann CR, Robertson RL, Kyriakos W, Schwartz R, Holtzman D, Jolesz FA, Maier SE (1999) Multi-component apparent diffusion coefficients in human brain. *NMR Biomed* 12:51–6

Nagesh V, Welch KM, Windham JP, Patel S, Levine SR, Hearshen D, Peck D, Robbins K, D'Olhaberriague L, Soltanian-Zadeh H, Boska MD (1998) Time course of ADCw changes in ischemic stroke: beyond the human eye! *Stroke* 29:1778–1782

Newman GC, Qi H, Hospod FE, Grundmann K (1992) Preservation of hippocampal brain slices with *in vivo* or *in vitro* hypothermia. *Brain Res* 575:159–163

Niendorf T, Dijkhuizen RM, Norris DG, van Lookeren CM, Nicolay K (1996) Biexponential diffusion attenuation in various states of brain tissue: implications for diffusion-weighted imaging. *Magn Reson Med* 36:847–857

Petersen A, Castilho RF, Hansson O, Wieloch T, Brundin P (2000) Oxidative stress, mitochondrial permeability transition and activation of caspases in calcium ionophore A23187-induced death of cultured striatal neurons. *Brain Res* 857:20–29

Pressman BC (1976) Biological applications of ionophores. *Annu Rev Biochem* 45:501–530

Shepherd TM, Blackband SJ, Wirth ED III (2002) Simultaneous diffusion MRI measurements from multiple perfused rat hippocampal slices. *Magn Reson Med* 48:565–569

Shepherd TM, Wirth ED III, Thelwall PE, Chen HX, Roper SN, Blackband SJ (2003) Water diffusion measurements in perfused human hippocampal slices undergoing tonicity changes. *Magn Reson Med* 49:856–863

Stanisz GJ, Li JG, Wright GA, Henkelman RM (1998) Water dynamics in human blood via combined measurements of T2 relaxation and diffusion in the presence of gadolinium. *Magn Reson Med* 39:223–233

Statler KD, Jenkins LW, Dixon CE, Clark RS, Marion DW, Kochanek PM (2001) The simple model versus the super model: translating experimental traumatic brain injury research to the bedside. *J Neurotrauma* 18:1195–1206

Sze G, Anderson A (2000) Diffusing into the future. *AJNR Am J Neuroradiol* 21:1780–1782

Takadera T, Ohyashiki T (1997) Apoptotic cell death and caspase 3 (CPP32) activation induced by calcium ionophore at low concentrations and their prevention by nerve growth factor in PC12 cells. *Eur J Biochem* 249:8–12

Thelwall PE, Grant SC, Stanisz GJ, Blackband SJ (2002) Human erythrocyte ghosts: exploring the origins of multiexponential water diffusion in a model biological tissue with magnetic resonance. *Magn Reson Med* 48:649–657

Warach S (2001) New imaging strategies for patient selection for thrombolytic and neuroprotective therapies. *Neurology* 57:S48–S52

Warach S (2002) Thrombolysis in stroke beyond three hours: Targeting patients with diffusion and perfusion MRI. *Ann Neurol* 51:11–13

Zhao X, Pike BR, Newcomb JK, Wang KKW, Posmantur RM, Hayes RL (1999) Maitotoxin induces calpain but not caspase-3 activation and necrotic cell death in primary septo-hippocampal cultures. *Neurochem Res* 24(3):371–382

JOURNAL OF NEUROTRAUMA
Volume 21, Number 10, 2004

Pp. 1443–1456

A Novel Marker for Traumatic Brain Injury: CSF αII-Spectrin Breakdown Product Levels

N.C. RINGGER,[1,4] B.E. O'STEEN,[1,4] J.G. BRABHAM,[1] X. SILVER,[5] J. PINEDA,[3,4] K.K.W. WANG,[1,2,4] and R.L. HAYES[1,2,4]

ABSTRACT

Currently, there is no definitive diagnostic test for traumatic brain injury (TBI) to help physicians determine the seriousness of injury or the extent of cellular pathology. Calpain cleaves αII-spectrin into breakdown products (SBDP) after TBI and ischemia. Mean levels of both ipsilateral cortex (IC) and cerebral spinal fluid (CSF) SBDP at 2, 6, and 24 h after two levels of controlled cortical impact (1.0 mm and 1.6 mm of cortical deformation) in rats were significantly elevated by injury. CSF and IC SBDP levels were significantly higher after severe (1.6 mm) injury than mild (1.0 mm) injury over time. The correlation between CSF SBDP levels and lesion size from T2-weighted magnetic resonance images 24 hours after TBI as well as correlation of tau and S100β was assessed. Mean levels of CSF SBDP ($r = 0.833$) and tau ($r = 0.693$) significantly correlated with lesion size while levels of CSF S100β did not ($r = 0.188$). Although levels of CSF and IC SBDP and lesion size are all significantly higher after 1.6 mm than 1.0 mm injury, the correlation between CSF SBDP and lesion size was not significant following the removal of controls from the analysis. This indicates CSF SBDP is a reliable marker of the presence or absence of injury. Furthermore, larger lesion sizes 24 h after TBI were negatively correlated with motor performance on days 1–5 after TBI ($r = -0.708$). Based on these data, evaluation of CSF SBDP levels as a biomarker of TBI is warranted in clinical studies.

Key words: biomarker; CSF; injury magnitude; lesion size; spectrin; S100β; tau

AU1

INTRODUCTION

THE DIFFICULTY of diagnosis and prediction of outcome after acute traumatic brain injury (TBI) is associated with the limitations of clinical assessment and neuroimaging (Zink, 2001). Sedatives may be used to treat patients with TBI that exhibit confusion, agitation, or non-compliance with accompanying increased brain metabolism (Mirski et al., 1995). Treatment with anticonvulsant or sedative drugs may confound information obtained from a clinical neuropsychological examination (Mirski et al., 1995). Many mild head trauma patients with a Glasgow Coma Scale (GCS) between 13 and 15 may have coincidental intoxication with drugs and alcohol that may also confound clinical neuropsychological examinations (Kelly, 1995). Head injuries may also be overlooked

[1]Department of Neuroscience, [2]Department of Psychiatry, [3]Department of Pediatrics, [4]Center for Traumatic Brain Injuries, and [5]Advanced Magnetic Resonance Imaging and Spectroscopy (AMRIS) Facility, Evelyn F. and William L. McKnight Brain Institute, University of Florida, Gainesville, Florida.

192

in multi-trauma patients (Buduhan and McRitchie, 2000). Clinical indicators may not predict significant intracranial trauma (Harad and Kerstein, 1992). Neurologic damage from TBI, stroke or perinatal asphyxia may precede changes seen by modern neuroimagining techniques. Although mild traumatic injury may cause long term disabilities, mild trauma may not be seen acutely with radiologic or magnetic resonance imaging (MRI). Computed tomography (CT) scanning is the quickest and most available neuroimaging, yet has low sensitivity for diffuse brain damage. In a critical care patient, cost, availability, and the time to acquire images limits use of the more sensitive measures of MRI and single photon emission CT scans. Single photon emission CT scans detect regional changes of blood flow but not necessarily structural damage. Furthermore, MRI and CT often do not predict outcome (Kido et al., 1992; Kurth et al., 1994; Wilson et al., 1995; Hanlon et al., 1999). Thus there is a need for a biochemical marker of neuronal injury to improve diagnosis and prediction of outcome after TBI.

An ideal biomarker would incorporate several properties. A good biomarker would diagnose neurologic damage before neuro-radiographic signs are evident. A biomarker of acute neuronal injury would provide a measure of injury magnitude and predict neuropsychological outcome. The biomarker would also serve as an indicator of the pathogenesis of cell death including secondary cell death and indicate a target for treatment. With earlier recognition, the window for therapeutic intervention could be extended. Furthermore, a good biomarker would allow for longitudinal monitoring of the effectiveness of therapy. A biomarker with these characteristics could be used as a surrogate marker and lower the cost of clinical trials. An ideal biomarker should also be specific to the central nervous system and provide a sensitive and specific test of neuronal injury.

Earlier biomarkers such as neuron-specific enolase, lactate dehydrogenase, or creatine kinase are not been specific to the CNS and failed to reflect pathophysiology, lesion size and outcome of the injury further reinforcing the need for research into better CNS trauma indicators (Ingebrigtsen and Romner, 2002). S100β, a low molecular weight calcium-binding protein released from astrocytes, has been examined in numerous TBI studies. Serum levels of S100β have been correlated with contusion volume (Raabe et al., 1998; Herrmann et al., 2000); injury severity (Herrmann et al., 2000); neuropsychological dysfunction (Herrmann et al., 2001); GCS on admission (Elting et al., 2000); and outcome measures such as the Glasgow Outcome Score (GOS) (McKeating et al., 1998; Elting et al., 2000; Jackson et al., 2000; Raabe and Seifert, 2000; Rothoerl et al., 2000). S100β appears to be a valuable indicator of brain lesion but it is not specific to the CNS. Importantly in multitrauma patients without head injuries, S100β reached high serum levels after bone fractures and thoracic contusion (Anderson et al., 2001). Another biomarker that is being examined as an indicator of brain injury is tau (Zemlan et al., 1999). Tau is a microtubule associated protein that is expressed predominantly in axon of neurons and implicated in microtubule stability, axon elongation and axon transport (Garcia and Cleveland, 2001). In severe TBI patients, increased CSF levels of cleaved tau were found to be significant predictors of intracranial pressure and GOS at discharge (Zemlan et al., 2002), but in recent studies, CSF total tau levels did not correlate with GOS in patients with severe TBI (Franz et al., 2003) nor did serum cleaved tau levels correlate with outcome measures (Chatfield et al., 2002).

αII-spectin in the CNS is primarily localized to axons and to the presynaptic terminal of neurons (Riederer et al., 1986). In acute neuronal injury, αII-spectin, a cytoskeletal protein, is a substrate for the calcium activated cysteine proteases, calpain (calpain-1 and -2) and caspase-3. After acute neuronal injury, calcium influx initiates a cytotoxic cascade of proteases, phospholipases, kinases and phosphatases including activation of calpain and caspases which results in necrotic and apoptotic cell death respectively. Calpain and caspase-3 both cleave the 280-kDa parent band of αII-spectrin into a 150-kDa breakdown product (SBDP150). Calpain and caspase-3 cleave signature breakdown products of 145 (SBDP145) and 120 kDa (SBDP120), respectively, *in vivo* and *in vitro* (Nath et al., 1996; Wang et al., 1998; Wang, 2000). Both the calpain-mediated SBDP 145 and SBDP 150 increased acutely in the injured cortex whereas the caspase-3 mediated SBDP 120 was absent in an unilateral controlled cortical impact (CCI) model of TBI (Pike et al., 1998). This may reflect a more prominent role of oncosis than apoptosis in the cortex in our CCI model.

αII-spectrin breakdown products (SBDP) have been used as an indicator of calpain activity in models of TBI (Newcomb et al., 1997) and ischemia (Saido et al., 1993; Roberts-Lewis et al., 1994; Bartus et al., 1998) In our laboratory, levels of SBDP have recently been found to increase in rat CSF after experimental controlled cortical impact TBI (Pike et al., 2001) and middle cerebral artery occlusion (Pike et al., 2004). In this study we extend this work by systematically comparing CSF SBDP to their counterpart in injured cortex, to injury magnitude, to CSF tau and S100â and to lesion volume (accessed by MRI). This study subjects a marker of CNS injury to rigorous preclinical examination. Based on the data we have obtained, we propose that CSF SBDP levels are a promising biomarker of injury and further study is warranted in clinical TBI.

MATERIALS AND METHODS

Animals

Three groups of adult male (280–300 g) Sprague-Dawley rats (Harlan; Indianapolis, IN) were used. For study 1, CSF was withdrawn from one group of 90 rats that were sacrificed 2, 6, and 24 h after TBI. At each time point of 2, 6, and 24 h, 9 rats received mild (1.0 mm of cortical deformation) injury, 9 rats received severe (1.6 mm of cortical deformation) injury, 8 rats received a craniotomy but no cortical deformation and 4 rats remained naive (no craniotomy or cortical deformation). For study 2, a second group of rats were sequentially scanned by MRI, subjected to CSF withdrawal, and were sacrificed at 24 h following TBI. Of the second group, 9 rats each received severe (1.6 mm) injury, mild (1.0 mm) injury or craniotomy surgery and 8 rats remained naive. One rat with severe injury was removed from the study because the CSF sample contained blood that could potentially dilute out the concentration of the marker in the CSF and introduce blood-born markers. For study 3, 35 rats were administered a rotarod test on days 1–5 after TBI and scanned by MRI at 24 h and 28 days after TBI. Of the third group of rats, 10 rats each received severe (1.6 mm) injury, mild (1.0 mm) injury or a craniotomy, and 5 rats remained naive.

Surgical Preparation and Controlled Cortical Impact Traumatic Brain Injury

As previously described (Dixon et al., 1991; Pike et al., 2001), a cortical impact injury device was used to produce TBI. Adult male rats were initially anesthetized with 4% isoflurane in a carrier gas of 1:1 O_2/N_2 (4 min) followed by maintenance anesthesia of 2.5% isoflurane in the same carrier gas. Core body temperature was maintained at 37 ± 1°C by placing an adjustable temperature controlled heating pad beneath the rats. Animals were mounted in a stereotactic frame in a prone position and secured by ear and incisor bars. A midline cranial incision was made, the soft tissues were reflected and a unilateral (ipsilateral to site of impact) craniotomy (7 mm diameter) was performed adjacent to the central suture, midway between bregma and lambda. The dura mater was kept intact over the cortex. Brain trauma in rats was produced by impacting the right cortex (ipsilateral cortex) with a 5 mm diameter aluminum impactor tip (housed in a pneumatic cylinder) at a velocity of 3.5 m/sec with a 150-msec dwell time (compression duration). Compression depth was set at 1.0 mm (mild), or 1.6 mm (severe). Velocity was controlled by adjusting the pressure (compressed N_2) supplied to the pneumatic cylinder. Velocity and dwell time were measured by a linear velocity displacement transducer (Lucas Shaevitz™ model 500 HR; Detroit, MI) that produces an analogue signal by a storage-trace oscilloscope (BK Precision, model 2522B; Placentia, CA). Animals underwent identical craniotomy procedures but did not receive cortical compression. Naive rats did not undergo surgery or injury. Appropriate pre- and post-injury management was maintained to insure that all guidelines set forth by the University of Florida Institutional Animal Care and Use Committee and the National Institutes of Health guidelines detailed in the *Guide for the Care and Use of Laboratory Animals* were complied with.

CSF Withdrawal

Under anesthesia, the rat was secured in the same stereotactic frame as used in surgery. The neck was flexed to optimize exposure of the atlanto-occipital space. A mid-line incision was made over the superficial cervical muscles. A 25-gauge needle attached to polyethylene tubing was inserted into the atlanto-occipital space and CSF was gently withdrawn. CSF was immediately spun at 9,000*g* for 5 min at 4°C to remove any red blood cells from the cortical impact or from the tap. CSF was frozen at −80°C until examined.

Tissue Lysis

Cortical tissues were collected from naive animals or at 2, 6, and 24 h after craniotomy or TBI. At the appropriate post-injury time-points, the animals were anesthetized with 4% isoflurane in a carrier gas of 1:1 O_2/N_2O (4 min) and subsequently sacrificed by decapitation. Ipsilateral (to the impact site) cortex samples were rapidly dissected and snap-frozen in liquid nitrogen. Tissue samples were stored at −80°C until further processing. Frozen samples were thawed and homogenized in a glass tube with a Teflon dounce pestle in 15 volumes of ice-cold detergent-free buffer (50 mM Tris-HCl, pH 7.4, 1 mM EDTA, 2 mM EGTA, 0.33 M sucrose, 1 mM DTT) containing a broad-range protease inhibitor cocktail (Roche Molecular Biochemicals, no. 1-836-145) and sonicated. Homogenized samples were then centrifuged at 9000*g* for 5 min at 4°C. The supernatant was stored at −80°C until immunoblot analysis.

Immunoblotting

Prior to sodium dodecyl sulfate–polyacrylamide gel electrophoresis (SDS-PAGE), protein content was assayed by the Micro BCA method (Pierce, Rockford, IL) using albumin standards. For each sample, 40 μg of protein from cortical tissue or 40 μg of protein from CSF samples were added to 2 × loading buffer containing 0.2 M Tris (pH 6.8), 400 mM 2-mercapto-ethanol, 8% SDS,

0.04% Bromophenol Blue, and 40% glycerol. The amount of protein for CSF samples was optimized to identify SBDP after both mild (1.0 mm) and severe (1.6 mm) injury. The optimal amount of protein to see the 145/150 band after mild injury resulted in an amount of protein after severe (1.6 mm) injury that sometimes would make the 145 and 150 bands indistinguishable. Semi-quantitation by densitometry was used to evaluate the 145–150-kDa band together thus the blurring of the 145/150 band was not a problem. The 145–150-kDa spectrin breakdown product represents primarily calpain initiated cleavage of spectrin in our model. Consistent with a previous report that CCI in our laboratory does not produce prominent caspase-3 levels (Pike et al., 1998), caspase-3–mediated SBDP 120 was inconsistent after severe (1.6 mm) injury and absent after mild (1.0 mm) injury and was not analyzed in this set of experiments. Semi-quantitation by densitometry evaluated both the 145–150-kDa band together thus the blurring was not a problem. Samples were heated at 96°C for 10 min and then centrifuged for 1 min at 10,000*g*. Samples were resolved in a vertical electrophoresis chamber for 70 min at 150 V. A 6.5% percent stacking acrylamide gel or a 4–20% Tris-Glycine gel (Invitrogen Life Technologies, Carlsbad, CA) were used. Separated proteins were either laterally transferred as a wet transfer to a nitrocellulose membrane (0.45 μM) using a transfer buffer consisting of glycine (192 mM) and tris (25 mM), (pH 8.3) with 10% methanol at a constant voltage of 100V for 70 min at 4°C or were horizontally transferred as a semi-dry transfer to an Immobilon-P polyvinylidene fluoride (PVDF) membrane (Millipore, Bedford, MA) using 39 mM glycine, 48 mM Tris, and 5% methanol at 20 V for 2 h at room temperature. All gels were stained with coomassie blue to confirm equal loading of protein on the gel. Selected blots were also stained with Panceau red (Sigma, St. Louis, MO) to confirm transfer and that equal amounts of protein were loaded in each lane. Blots were blocked for one hour in 5% non-fat milk in TBST (20 mM Tris, 0.15 M NaCl, and 0.005% Tween-20). Following overnight incubation with the primary antibody, anti-α-spectrin monoclonal antibody (1:10,000 dilution for cortex and 1:5,000 dilution for CSF; Affiniti Research Products, UK) and 1% non-fat milk/TBST at 4°C temperature, the blots were incubated with goat anti-mouse secondary antibody (1:1000 for cortex and 1:5000 for CSF; Biorad) and 3% non-fat milk/TBST for 1 h. Blots were then washed for 1 h in TBST. Enhanced chemiluminescence reagents (ECL and ECL-Plus, Amersham) were used to visualize immunolabeling of cortical tissue and CSF, respectively, and developed on Kodak BioMax Light Film (Kodak). Semi-quantitative evaluation of protein levels was conducting using computer-assisted one-dimensional densitometric scanning (ImageJ, version 1.29, NIH). Data were acquired as integrated densitometric values from similarly exposed films.

ELISA

CSF S100β levels were measured using a rat specific ELISA kit, Nexus D_x™ Rat S100 Test Kit from SynX (Toronto, Ontario, Canada) and CSF tau was measured using a kit,Innotest™ hTau Antigen from Innogenetics, Inc. (Alpharetta, GA). The sensitivities of the S100β and tau ELISA kits were 0.02 ng/mL and 75 pg/mL, respectively.

T2-Weighted Magnetic Resonance Imaging

Animals were scanned in the Advanced Magnetic Resonance Imaging and Spectroscopy (AMRIS) facility located in the McKnight Brain Institute of the University of Florida. Animals undergoing these imaging sessions were anesthetized using isoflurane (maintenance anesthesia of 1.5–2.5% isoflurane in 1 L/min 100% O_2 continuously delivered via a nose cone). Ophthalmic lubricant was used to prevent drying of the eyes during anesthesia. Anesthetized rats were placed on a custom Plexiglas cradle constructed to support the rat comfortably in the supine position. Oxygen saturation was monitored using a pulse oxymeter positioned on the left hind limb. Body temperature was monitored using a rectal flouroptic probe and maintained using warm air. A 4.7-Tesla magnet (Oxford Instruments) and Bruker Avance Console (Bruker, Germany) and a custom built 3.3-cm (inner diameter) quadrature birdcage coil were used for all image acquisitions. T2-weighted images were acquired at 24 h and 28 days after TBI. Twelve contiguous 1.25-mm coronal slices were acquired with the following parameters: a field of view = 3.6 × 3.6 cm^2, repetition time (TR) = 2.1 seconds, echo time (TE) = 81 msec, matrix = 256 × 256 points per dimension (140 μm in plane). Areas of hypo-intensity on MRI were associated with hemorrhage or mechanical disruption and areas of hyper-intensity were associated with edema (Albensi et al., 2000). Lesion size was drawn using ParaVision Image Analysis tools (Bruker, Germany) similar to the methodology in (Neumann-Haefelin et al., 2000). The area of each lesion in each coronal slice was multiplied by the slice thickness and then added to calculate the total lesion size.

Neurological Functional Evaluation

Motor behavior was assessed in the sub-acute period after TBI by a blinded observer using a Rota-rod (Ugo Basile, Comerio, Italy; Hamm et al., 1994). Rats were placed on a Rota-rod, a rotating rod, which was set to

slowly accelerate from 4 to 40 rpm within 5 min. The Rota-rod requires the rat to walk as the revolving rod accelerates and maintain balance. The trial lasted until the rat fell off and tripped a plate that recorded the time or until the rat had stayed on the rod for 300 sec was reached. Rats underwent conditioning of two trials a day for three days prior to TBI. After TBI, the rats were tested for two trials a day on days 1–5. The average of the latency in seconds of the two trials was recorded.

Statistical Analysis

Means and standard errors of the means were calculated from individual rat densitometric values of the 145–150-kDa SBDP combined as one value. Two-way ANOVA was used to examine main effects and interaction effects of time and injury magnitude. One-way ANOVA with contrast to do pair-wise comparisons was used to determine significance between levels of SBDP and between lesion sizes of the corresponding experimental groups. Regression analysis was performed with lesion size as the outcome variable and CSF markers (SBDP, tau, S100â) as the predictor variable. Pearson correlations were calculated and tested using the asymptotic Z-test. Correlations were calculated in the individual animal between CSF SBDP levels and lesion size. The analysis of the correlations included animals in all groups (naive, craniotomy, 1.0 mm and 1.6 mm injury) unless stated otherwise. Repeated measures ANOVA (4 groups $\times$ 5 time points) were performed to determine individual group differences over the five time points on the Rota-rod test.

RESULTS

Injury Magnitude Is Associated with Increased Levels of SBDP in the Cortex and CSF after TBI

SBDP were measured by Western blot from the CSF and ipsilateral cortex (IC) at 2, 6, and 24 h after two magnitudes of TBI. Naive rats and rats that had undergone a craniotomy served as controls for this study. The two response variables, SBDP in the CSF and SBDP in the IC were analyzed via ANOVA with terms for injury magnitude, time, and the interaction of time and injury magnitude.

The results indicated there was no interaction effect ($p = 0.88$) or time effect ($p = 0.12$) on IC SBDP levels. The analysis also indicated that injury magnitude significantly increased the level of cortical SBDP ($p \leq 0.0001$). Mean levels of IC SBDP after severe (1.6 mm) injury were significantly higher than the mean levels of IC SBDP after mild (1.0 mm) injury ($p < 0.05$). Mean levels of IC SBDP after both severe (1.6 mm) and mild (1.0 mm) injury were significantly greater than mean levels of SBDP after craniotomy or in naive controls ($p < 0.0001$). Mean levels of IC SBDP did not differ between naive and after craniotomy. Representative gels show that levels of SBDP increased with injury magnitude in the ipsilateral cortex and the CSF (Fig. 1A). Levels of SBDP (both 145 and 150 kDa are densitometrically quantified together) were highest after 1.6-mm injury in the IC and CSF at all time points (Fig. 1B). F1

After severe (1.6 mm) injury, the mean levels of IC SBDP were 116.4 ± 8.9, 135.9 ± 14.1, and 135.6 ± 17.7 and after mild (1.0 mm) injury, the mean levels of IC SBDP reached 78.1 ± 9.9, 110.1 ± 19.4, and 102.8 ± 17.2 at 2, 6, and 24 h, respectively. After craniotomy, the mean levels of IC SBDP reached 22.6 ± 9.1, 40.9 ± 18.2, and 11.8 ± 4.6 at 2, 6, and 24 h, respectively. In naive rats, the mean levels of IC SBDP were 4.4 ± 1.6, 15.4 7.0, and 4.4 ± 6.5 at 2, 6, and 24 h, respectively.

There was no interaction effect ($p = 0.39$) or time effect ($p = 0.13$) on CSF SBDP levels. The analysis also indicated that injury magnitude significantly increased the levels of CSF SBDP ($p \leq 0.0001$). Mean levels of CSF SBDP after severe (1.6 mm) injury were significantly higher than the mean levels of CSF SBDP after mild (1.0 mm) injury ($p = 0.0001$). Mean levels of CSF SBDP after both severe (1.6 mm) and mild (1.0 mm) injury were significantly greater than mean levels of CSF SBDP after craniotomy or in naive controls ($p < 0.0001$). Mean levels of CSF SBDP did not differ between naive and after craniotomy.

After 1.6 mm injury, the mean levels of CSF SBDP were 153.4 ± 11.3, 114.4 ± 19.1, and 91.2 ± 23.8 and after 1.0 mm injury, the mean CSF SBDP were 82.2 ± 17.3, 71.4 ± 17.3, and 64.3 ± 17.2 at 2, 6, and 24 h, respectively. After craniotomy, the mean levels of CSF SBDP reached 7.8 ± 2.7, 19.1 ± 6.0, and 10.3 ± 5.3 at 2, 6, and 24 h, respectively. In naive rats, the mean levels of CSF SBDP were 1.0 ± 0.7, 5.7 ± 3.4, and 3.0 ± 1.4 at 2, 6, and 24 h, respectively.

The Relationship of CSF SBDP Levels with Lesion Size at 24 h Post-Injury

CSF extraction to measure SBDP and T2-weighted imaging to measure lesion size was performed in the same groups of rats at 24 h after TBI. Representative T2-weighted images of a naive rat and a rat 24 h after craniotomy, mild (1.0 mm) injury and severe (1.6 mm) injury are shown in Figure 2A. Severe (1.6 mm) injury resulted in disruption of normal architecture and swelling of the ipsilateral cortex (arrow in Fig. 2A). Less disrup- F2

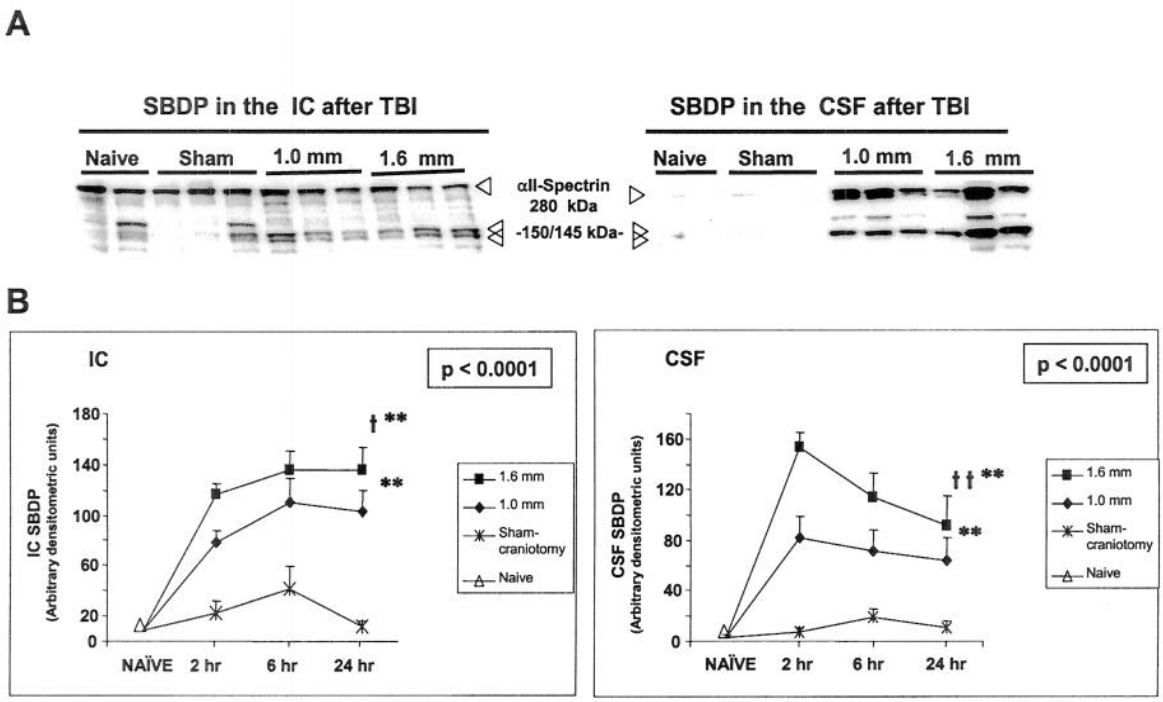

FIG. 1. Injury magnitude increases levels of SBDP in the ipsilateral cortex (IC) and CSF. (**A**) A representative Western blot of αII-spectrin and SBDP in the IC (left) and CSF (right) at 24 and 2 h, respectively, after TBI. Samples were collected after severe (1.6 mm) injury, mild (1.0 mm) injury, sham-craniotomy or from naive rats. Higher levels of SBDP are seen after severe (1.6 mm) injury than after mild (1.0) injury. Minimal SBDP is seen in the IC or CSF of naive rats or after sham-craniotomy in rats. (**B**) SBDP levels (145–150-kDa fragments) in the IC (left panel) and CSF (right panel) after sham-craniotomy, mild (1.0 mm) injury and severe (1.6 mm) injury at 2, 6, and 24 h were quantified using computer-assisted densitometric analysis (ImageJ, version 1.29×, NIH, USA). Values from naive animals were averaged as a separate time point. At each time point of 2, 6, and 24 h, 9 rats received severe (1.6 mm) injury, 9 rats received mild (1.0 mm) injury, 8 rats received a sham-cra-niotomy and 4 rats remained naive. An ANOVA was performed followed by contrast with pair-wise comparisons. Data is presented as the mean plus standard error. Standard error bars on the shams are present but not easily visable. Injury magnitude significantly increased mean levels of IC and CSF SBDP over time ($p < 0.0001$). Mean levels of SBDP after severe (1.6 mm) injury were significantly higher from the mean levels of SBDP after mild (1.0 mm) injury ($^{\dagger\dagger}p = 0.0001$ and $^{\dagger}p < 0.05$, respectively, for CSF and IC levels of SBDP). Mean levels of IC and CSF SBDP after both severe (1.6 mm) and mild (1.0 mm) injury were significantly greater than mean levels of SBDP after sham-craniotomy or in naive controls ($^{**}p < 0.0001$). Mean levels of CSF and IC SBDP did not differ between naive and sham.

FIG. 2. Lesion size on T2 weighted images increases with injury magnitude 24 h after TBI. (**A**) Representative serial T2-weighted magnetic resonance images of a naive rat and a rat 24 h after sham-craniotomy, mild (1.0 mm) and severe (1.6 mm) injury are shown. Twelve contiguous coronal 1.25 mm slices were acquired with the following parameters: a field of view = 3.6×3.6 cm^2, repetition time (TR) = 2100 sec, echo time (TE) = 81 msec, matrix = 256×256 points per dimension (140 μm in plane). Four of the 12 coronal slices for each rat are shown. Severe (1.6 mm) injury resulted in disruption of normal architecture and swelling of the ipsilateral cortex (arrow). Less disruption of normal architecture is noted after mild (1.0 mm) injury (arrowhead). Sham-craniotomy resulted in varying amounts of hyper-intensity in the ipsilateral cortex (arrowhead). (**B**) Lesion size was drawn using ParaVision Image Analysis tools (Bruker, Germany) similar to the methodology in (Neumann-Haefelin et al., 2000). The area of each lesion in each coronal slice was multiplied by the slice thickness and then added to calculate the total lesion size. One-way ANOVA with contrast to do pair-wise comparisons was used to determine difference between lesion sizes of the treatment groups. Nine rats each received severe (1.6 mm) injury, mild (1.0 mm) injury or sham surgery and 8 rats remained naive. The lesion after severe (1.6 mm) injury is significantly greater than the lesion size after mild (1.0 mm) injury ($^{\#\#}p \leq 0.001$) and both are significantly greater than after sham-craniotomy ($^{\dagger\dagger}p \leq 0.001$) or naive animals ($^{**}p \leq 0.001$) Sham injury is greater than the absense of a lesion in naive animals ($^{*}p < 0.05$).

tion of normal architecture is noted after mild (1.0 mm) injury (arrowhead in Fig. 2A). Craniotomy resulted in varying amounts of hyper-intensity in the ipsilateral cortex (arrowhead in Fig. 2A). Average lesion size was 0.044 $cm^3 \pm 0.00058$ after craniotomy, 0.100 $cm^3 \pm 0.010$ after 1.0 mm injury, and 0.166 $cm^3 \pm 0.016$ after 1.6 mm injury (Fig. 2B). Mean lesion size was significantly different between 1.6 mm and 1.0 mm injury groups and

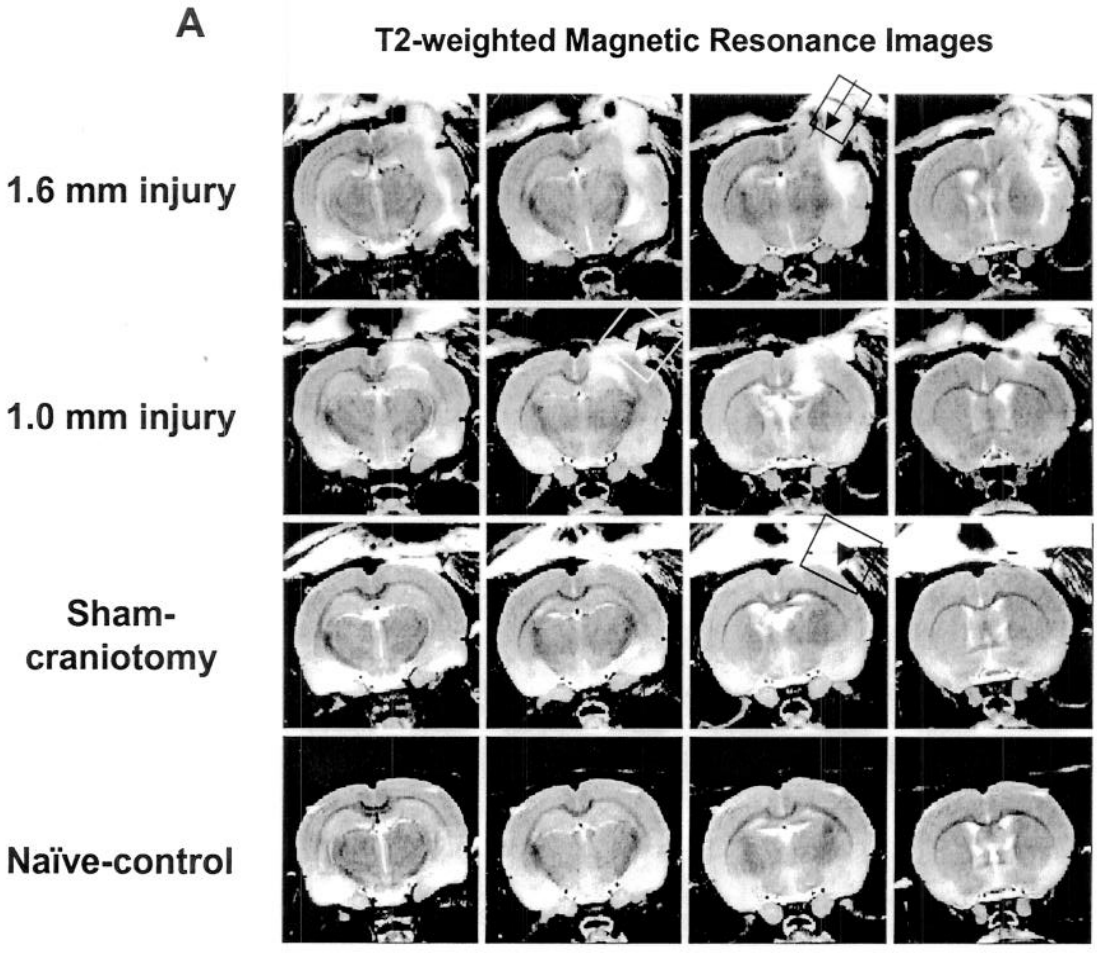

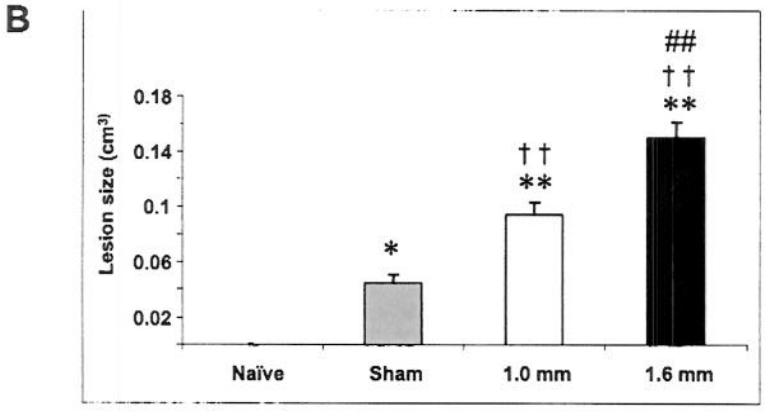

between both injury groups and after craniotomy ($p \leq 0.001$; Fig. 2B). Mean levels of CSF SBDP significantly correlated with lesion size ($r = 0.833$, $p < 0.0001$) when including all 4 groups (1.6 mm and 1.0 mm injury, craniotomy, and naive rats) (Fig. 3A). This correlation was not significant if craniotomy and sham rats were not considered in the analysis. To explore the ability of SBDP to predict lesion size, a regression analysis was run with lesion size as the outcome variable and CSF SBDP as the predictor variable from individual rats from all 4 groups. The regression weight for CSF SBDP was estimated to be 1059.86, and the parameter estimate of the intercept was 10.707. The regression analysis revealed CSF SBDP contributed significantly to predicting lesion volume ($p < 0.0001$).

Levels of CSF tau significantly correlated with lesion size ($r = 0.693$, $p < 0.0001$) (Fig. 3B) as levels of CSF S100β did not ($r = 0.188$) (Fig. 3C). The regression weight for CSF tau was estimated to be 0.00001258, and the parameter estimate of the intercept was 0.03485. CSF levels of tau significantly contributed to the prediction of lesion volume ($p < 0.0001$). Neither CSF tau or CSF S100β were correlated if just the 1.6-mm and 1.0-mm injured rats were used for analysis.

A regression analysis was performed to determine which marker or combination of markers (SBDP, tau and S100β) best predicted lesion size. A full regression model indicated the only significant variable was SBDP ($p < 0.0001$). S100β was eliminated from the model and the regression re-run looking at SBDP and tau as predictors of lesion size. CSF SBDP was again the only significant predictor of lesion size ($p < 0.0001$). CSF SBDP and CSF tau are significantly correlated ($r = 0.750$, $p < 0.0001$) and CSF SBDP has a higher correlation with CSF tau than CSF tau's correlation with lesion size.

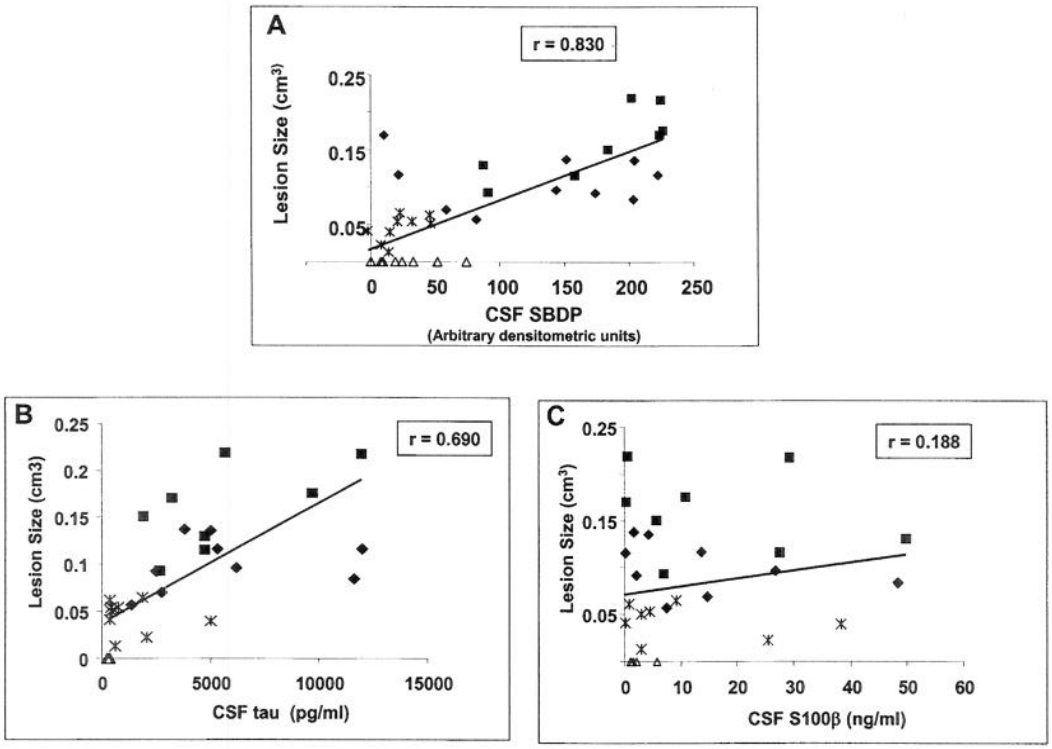

FIG. 3. The relationship of levels of CSF SBDP and tau with lesion size 24 h after TBI. Regression analysis was performed with lesion size as the out-come variable and levels of CSF markers (SBDP, tau, S100β) 24 h after TBI as the predictor variable. (**A**) Levels of CSF SBDP correlate with lesion size after TBI ($r = 0.83$, $p \leq 0.0001$). A linear regression equation showed that CSF SBDP significantly contributed to prediction of lesion size ($p \leq 0.0001$). (**B**) Levels of CSF tau correlate with lesion size after TBI ($r = 0.690$, $p < 0.001$). A linear regression equation showed that CSF tau significantly contributed to prediction of lesion size ($p \leq 0.0001$). The correlation with CSF SBDP and tau was not significant if craniotomy and sham rats were not considered in the analysis. (**C**) Levels of CSF S100β did not correlate with lesion size ($r = 0.188$). ■, rats after 1.6 mm injury; ◆, rats after 1.0 mm injury, ✳, rats after sham-craniotomy; △, naive rats.

Injury Magnitude Is Associated with Decreased Performance on the Rota-Rod Test and Increased Lesion Size

Because CSF SBDP correlated with lesion size at 24 hours, we looked at the relationship between lesion size and motor performance. Motor performance was assessed in the same (study 3) rats that lesion size was measured at 24 h and 28 days (Fig. 4A). Similar to 24 h, at 28 days lesion size varied with injury magnitude. Lesion size at 24 h in the individual animal was significantly correlated with lesion size at 28 days ($r = 0.881$, $p < 0.0001$). Assessment of Rota-rod performance prior to treatment revealed no significant differences between groups. Injury magnitude had a significant effect on Rota-rod performance ($p < 0.0001$). Mean Rota-rod scores were significantly lower after 1.6-mm injury at all time points (1–5 days after TBI) compared to mild (1.0 mm) injury, craniotomy, or naive rats ($p \leq 0.05$). After 1.0-mm injury, mean Rota-rod scores were significantly lower than in naive rats ($p < 0.01$) and showed a trend toward being lower than after craniotomy (Fig. 4A). Naive rats averaged close to a perfect score of 300 sec at all time points. Naive rats had significantly higher scores than rats after craniotomy ($p < 0.05$). Furthermore, larger lesion sizes were associated with decreased performance on the Rota-rod (Fig. 4B). In the individual rat, the average of the 5 days of Rota-rod scores correlated negatively with lesion size at 24 h ($r = -0.708$; $p < 0.0001$).

DISCUSSION

This paper examined the relationship between IC and CSF levels of SBDP and injury magnitude and outcome measures. The results show that SBDP levels in both CSF and IC SBDP increase with injury magnitude. Although both IC and CSF levels of SBDP increased, they did not parallel each other. Levels of CSF SBDP peaked at 2 h and decreased over time, while IC levels of SBDP slowly increased over the first 6 h after TBI. The correlation between lesion size and CSF levels of SBDP supported CSF SBDP as an indicator of injury. Correlational analysis of relationships between lesion size and CSF levels of SBDP indicated that CSF SBDP is a reliable marker of the presence or absence of injury but failed to be a reliable marker of injury magnitude. Although both CSF and IC SBDP levels and lesion size were significantly higher after 1.6-mm injury than after 1.0-mm injury, the correlation between CSF SBDP and lesion size was not significant following the removal of the control groups (naive and craniotomy) from the analysis. Further study is needed to show if CSF SBDP levels are a useful predictor of outcome such as lesion size.

Factors that affect brain derived protein levels in the CSF after injury have not been extensively explored and are likely to affect the variability of CSF SBDP levels and correlations with CSF SBDP. Petzold et al. (2003) suggest the main determinants of brain tissue proteins in the CSF are the extent of the primary lesion, the total pathological severity causing imbalance of brain home-

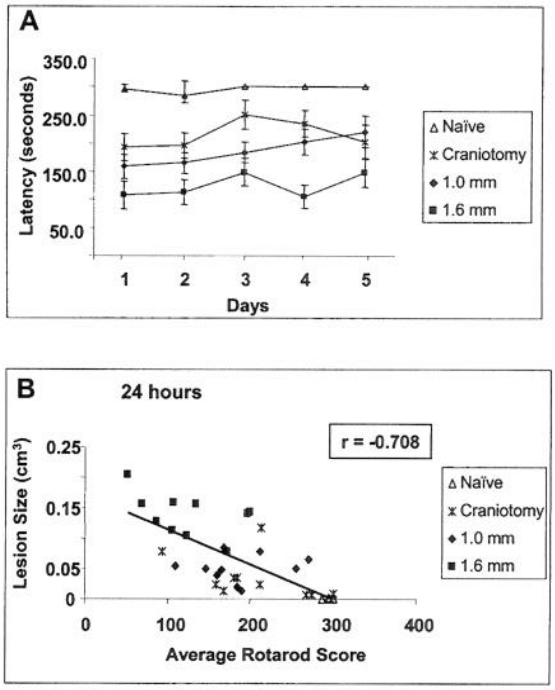

FIG. 4. Performance on the Rota-rod test decreases with increased injury magnitude and lesion size. (**A**) Rats were placed on a rotating rod, which slowly accelerated from 4 to 40 rpm within 5 min on days 1–5 after TBI. The rats were tested for two trials a day and the average of the latency in seconds of the two trials was recorded. Repeated measures ANOVA (4 groups × 5 time points) were performed to determine individual group differences over the five time points on the Rota-rod test. Of the third group of rats, 10 rats each received severe (1.6 mm) injury, mild (1.0 mm) injury or sham surgery and 5 rats remained naive. Data is presented as the mean ± SE. Injury magnitude significantly effected rotarod performance ($p < 0.0001$). Severely (1.6 mm) injured rats performed significantly worse on days 1–5 after TBI on the Rota-rod test than mildly (1.0 mm) injured rats or the sham-craniotomy group ($p < 0.05$ and $p < 0.01$, respectively). Both severe and mild injured groups performed significantly worse than the naive rats ($p < 0.01$). (**B**) Rotarod scores were averaged for the 5 days of testing for each individual rat. The average performance on the Rota-rod test was negatively correlated with lesion size at 24 h after TBI in the individual rat ($r = -0.708$; $p < 0.0001$). ■, rats after 1.6 mm injury; ◆, rats after 1.0 mm injury, ✳, rats after sham-craniotomy; △, naive rats.

ostasis, and the onset and duration of the brain injury. The CCI model that we have used in these studies has some inherent variability in impact force that affects lesion size, lesion severity and the location of pathology. Injured cells in the subarachnoid space can directly release protein into the CSF while protein from cells in the parenchyma must be transported to the CSF by flow of interstitial fluid or edema (Hans et al., 1999). The molecular flux/CSF flow theory suggests that changes in diffusion across the blood-brain and brain-CSF barriers are primarily predicated on CSF flow (Reiber and Peter, 2001; Reiber, 2003). If CSF flow rate is decreased after injury, then ventricular concentration of brain derived proteins is increased (Reiber, 2003). Variation of lesion impact might also cause variation in CSF flow rate and in the distance of brain-derived proteins from the CSF. As more is learned about factors effecting CSF levels of brain-derived proteins, the ability of CSF SBDP and other biomarkers to predict outcome may improve.

Hans et al. (1999) conducted one of the first studies to rigorously analyze a potential biomarker examining distribution and upregulation of mRNA and protein levels of IL-6 in tissue, and bioactivity of IL-6 in CSF and serum in a model of TBI. Similar to previous work in our lab examining mRNA of calpain-1 and calpain-2 (Ringger et al., 2004), IL-6 mRNA was upregulated after injury. Similar to our study, CSF levels of IL-6 peaked within 2–4 h after injury (Hans et al., 1999). IL-6 protein as seen on immunohistochemistry increased by 1 hour and persisted for 24 h, similar to the increase in IC SBDP on western blots at 2, 6, and 24 h after TBI. Hans et al. (1999) suggested that the increased tissue protein immunoreactivity reflected the increased IL-6 activity in the CSF. CSF levels of IL-6 were higher than serum levels between 2 and 8 h after injury. The CSF levels of IL-6 appear higher within 8 h of injury than in the CSF of sham animals, however the paper did not address this important question statistically.

Increased levels of calcium after TBI have been observed in several models (Fineman et al., 1993; Nadler et al., 1995; Verweij et al., 1997; Xiong et al., 1997). After TBI, calcium initiates a cytotoxic cascade of proteases including calpain which breaks down the cytoskeletal protein, spectrin. Higher levels of injury magnitude increased mRNA levels of calpain-1 and calpain-2 in the injured cortex and hippocampus (Ringger et al., 2004). Similar to our study, varying injury magnitude by depth or by velocity of impact, significantly effected lesion size (Goodman et al., 1994). Injury magnitude also significantly increased peak intracranial pressure and hippocampal neuron loss in similar models of TBI (Cherian et al., 1994; Goodman et al., 1994). Temporal increases in intracellular calcium were correlated with injury magnitude after lateral fluid percussion model of TBI in rats (Fineman et al., 1993). The corresponding increase in calcium after more severe TBI in the Fineman study may explain the association between injury magnitude and SBDP levels in the IC and CSF in our study.

In the acute time period following TBI, both CSF and IC SBDP significantly increased with injury magnitude. Calpain-mediated SBDP have been extensively examined and shown to increase in *in vivo* and *in vitro* models of neuronal injury (Bartus et al., 1995; Nath et al., 1996; Saatman et al., 1996a; Newcomb et al., 1997). Recently, it has been shown that CSF SBDP increased in models of TBI (Pike et al., 2001) and ischemia (Pike et al., 2004). The increased levels of SBDP150/145 are primarily associated with calpain activation in our CCI model. Although caspase-3 may also cleave spectrin to SBPD150, similar to prior work in our laboratory (Pike et al., 1998), the caspase-3 signature SBDP120 was not significant in our CCI model, suggesting a much less relevant role of caspase-3 in the production of SBDP in this model. Calpain inhibitors have been neuroprotective in models of TBI (Saatman et al., 1996a,b; Buki et al., 2003), ischemia (Bartus et al., 1994; Hong et al., 1994; Markgraf et al., 1998), and spinal cord injury (Banik et al., 1998). The ability of CSF levels of SBDP to reflect increased IC SBDP levels after acute neuronal injury may provide a therapeutic target for treatment of TBI and an effective way to monitor treatment of TBI if CSF is available.

CSF cleaved tau levels were significant predictors of outcome measures (intracranial pressure and GOS at discharge; Zemlan et al., 2002) supporting the finding of a significant correlation between CSF tau and lesion size in our study. On the other hand, Franz et al. (2003) showed that CSF levels of total tau did not correlate with injury severity (initial GCS) nor with outcome (GOS). The wide range of tau levels in that study was thought to be due to distance of the white matter lesion from the ventricles. Lesion variability is less in a model of CCI than in a clinical study of TBI.

An advantage of a serum biomarker is that it can be measured by less invasive methods than CSF biomarkers. The disadvantage of serum markers is that measurable serum levels of brain tissue proteins must cross the blood–brain and the CSF–blood barriers. Use of serum tau as a biomarker has produced conflicting results. Initial examination of serum cleaved tau indicated that the presence of serum cleaved tau increased the odds of the presence of an intracranial injury and a greater chance of a poor out-come (Shaw et al., 2002). Later work indicated serum cleaved tau levels did not correlate with outcome measures (Chatfield et al., 2002). After acute stroke, total tau increased in the CSF (Hesse

et al., 2001) and serum (Bitsch et al., 2002), and serum tau levels correlated to lesion size and severity. Serum tau levels, however, increased in less than 50% of stroke patients during the first 5 days after stroke (Bitsch et al., 2002).

Analysis of S100β has primarily been from the serum in clinical studies. Two clinical studies of serum levels of S100β revealed a correlation with contusion volume (Raabe et al., 1998; Herrmann et al., 2000), while in a study of mild TBI, serum S100β levels did not correlate with MRI or CT scans (Herrmann et al., 1999). S100β may be released from damaged glial cells, and this variable may not change consistently with lesion volume.

Importantly in multi-trauma patients without head injuries, S100β reached high serum levels after bone fractures and thoracic contusion and also increased after burns and minor bruising (Anderson et al., 2001). Numerous studies examined the use of S100β to mark cerebral damage after cardio-pulmonary bypass surgery (Ali et al., 2000), but S100β was found to be released from the mediastinum of cardiopulmonary bypass patients (Anderson et al., 2001). After stroke, higher serum S100β levels were associated with larger infarcts and more severe neuropsychological deficits (Aurell et al., 1991; Abraha et al., 1997; Buttner et al., 1997). Yet despite these promising correlations, Hill et al. (2000) found only 32% of stroke patients had elevated serum S100β on admission similar to serum tau levels (Bitsch et al., 2002). Early identification of stroke is necessary for optimal treatment within three hours.

The utility of SBDP as a serum marker has not been examined in clinical cases or models of stroke or TBI to the author's knowledge. Our study did not examine serum SBDP levels but further work will be important to establish if SBDP crosses the blood–brain and blood–CSF barrier and reflects SBDP levels in the CSF and brain. áII-spectrin is not found in red blood cells (Pike et al., 2001) although it is found in very low levels in other organs systems (Pike, Flint, Wang, and Hayes, unpublished data). The utility of SBDP as a marker would also benefit from knowledge of serum levels of SBDP in multi-trauma patients without head injuries and acutely after stroke.

Changes in high resolution MRI have been shown to correlate well with histology in a lateral fluid percussion model (Albensi et al., 2000) and a closed head injury model (Assaf et al., 1997) of TBI. Areas of hypo-intensity on MRI were associated with hemorrhage or mechanical disruption and areas of hyper-intensity were associated with edema (Albensi et al., 2000). At 24 h after rats underwent craniotomy, varying amounts of hyper-intensity were noted, most likely due to edema associated with the changes in cranial pressures. In the closed head injury model, areas of hyper-intensity decreased between 2 and 7 days after TBI likely representing resolution of edema (Assaf et al., 1997). Similarly in our study, the overall size of the lesion decreased between 24 h and 28 days, although a significant correlation was maintained between lesion size in individual rats at the two time points.

This study examined *in vivo* lesion size and the correlation to neuromotor function. Higher levels of injury magnitude significantly increased lesion size and decreased motor performance. In a stroke model, lesion size from T2-weighted images at 2 and 7 days after ischemia was significantly correlated with an average of individual neurological score (Palmer et al., 2001). Similarly in our study, the larger the lesion size, the worse the performance on the motor function test. Because lesion size at 24 h was highly correlated with lesion size at 28 days and significantly negatively correlated with motor performance, it is suggestive that acute levels of SBDP might correlate with both acute motor performance and chronic lesion size. Because withdrawal of CSF is a terminal procedure in our laboratory at this time, the correlation is only speculative.

In conclusion, the results of this study show that levels of SBDP in the IC and CSF are significantly higher after 1.6-mm injury than after 1.0-mm injury paralleling the significant difference in lesion size. We further showed that 24 hours after TBI, increased levels of CSF SBDP indicate the presence of a lesion. These studies strongly support the further study of CSF SBDP as a marker of CNS injury, and warrant evaluation of SBDP as a serum marker. Further examination may elucidate whether CSF or serum SBDP levels are predictors of outcome such as lesion size, GOS or neurological dysfunction. The contribution of this work is a foundation for future studies assessing the utility of this marker in human brain injury.

ACKNOWLEDGMENTS

We would like to acknowledge support of DAMD17-03-1-0066, DAMD17-01-1-0765, DAMD17-99-1-9565; NIH grants R01 NS39091, R01 NS40182. The authors would also like to thank Dr. Gary Stevens for his statistical contribution to this work. Drs. Kevin Wang and Ronald L. Hayes are inventors of technology to use alpha-spectrin as a brain injury biomarker discussed in this publication, Journal of Neurotrauma and hold equity in Banyan Biomarkers, a company commercializing the technology. Drs. Wang and Hayes may benefit from this technology by receiving royalties and equity growth.

REFERENCES

ABRAHA, H.D., BUTTERWORTH, R.J., BATH, P.M., WASSIF, W.S., GARTHWAITE, J., and SHERWOOD, R.A. (1997). Serum S-100 protein, relationship to clinical outcome in acute stroke. Ann. Clin. Biochem. **34,** 546–550.

ALBENSI, B.C., KNOBLACH, S.M., CHEW, B.G., O'REILLY, M.P., FADEN, A.I., and PEKAR, J.J. (2000). Diffusion and high resolution MRI of traumatic brain injury in rats: time course and correlation with histology. Exp. Neurol. **162,** 61–72.

ALI, M.S., HARMER, M., and VAUGHAN, R. (2000). Serum S100 protein as a marker of cerebral damage during cardiac surgery. Br. J. Anaesth. **85,** 287–298.

ANDERSON, R.E., HANSSON, L.O., NILSSON, O., DIJLAI-MERZOUG, R., and SETTERGREN, G. (2001). High serum S100B levels for trauma patients without head injuries. Neurosurgery **48,** 1255–1260.

ASSAF, Y., BEIT-YANNAI, E., SHOHAMI, E., BERMAN, E., and COHEN, Y. (1997). Diffusion- and T2-weighted MRI of closed-head injury in rats: a time course study and correlation with histology. Magn. Reson. Imaging **15,** 77–85.

AURELL, A., ROSENGREN, L.E., KARLSSON, B., OLSSON, J.E., ZBORNIKOVA, V., and HAGLID, K.G. (1991). Determination of S-100 and glial fibrillary acidic protein concentrations in cerebrospinal fluid after brain infarction. Stroke **22,** 1254–1258.

BANIK, N.L., SHIELDS, D.C., RAY, S., et al. (1998). Role of calpain in spinal cord injury: effects of calpain and free radical inhibitors. Ann. NY Acad. Sci. **844,** 131–137.

BARTUS, R.T., DEAN, R.L., MENNERICK, S., EVELETH, D., and LYNCH, G. (1998). Temporal ordering of pathogenic events following transient global ischemia. Brain Res. **790,** 1–13.

BARTUS, R.T., ELLIOTT, P.J., HAYWARD, N.J., et al. (1995). Calpain as a novel target for treating acute neurodegenerative disorders. Neurol. Res. **17,** 249–258.

BARTUS, R.T., HAYWARD, N.J., ELLIOTT, P.J., et al. (1994). Calpain inhibitor AK295 protects neurons from focal brain ischemia. Effects of postocclusion intra-arterial administration. Stroke **25,** 2265–2270.

BITSCH, A., HORN, C., KEMMLING, Y., et al. (2002). Serum tau protein level as a marker of axonal damage in acute ischemic stroke. Eur. Neurol. **47,** 45–51.

BUDUHAN, G., and McRITCHIE, D.I. (2000). Missed injuries in patients with multiple trauma. J. Trauma **49,** 600–605.

BUKI, A., FARKAS, O., DOCZI, T., and POVLISHOCK, J.T. (2003). Preinjury administration of the calpain inhibitor MDL-28170 attenuates traumatically induced axonal injury. J. Neurotrauma **20,** 261–268.

BUTTNER, T., WEYERS, S., POSTERT, T., SPRENGELMEYER, R., and KUHN, W. (1997). S-100 protein: serum marker of focal brain damage after ischemic territorial MCA infarction. Stroke **28,** 1961–1965.

CHATFIELD, D.A., ZEMLAN, F.P., DAY, D.J., and MENON, D.K. (2002). Discordant temporal patterns of S100beta and cleaved tau protein elevation after head injury: a pilot study. Br. J. Neurosurg. **16,** 471–476.

CHERIAN, L., ROBERTSON, C.S., CONTANT, C.F., JR., and BRYAN, R.M., JR. (1994). Lateral cortical impact injury in rats: cerebrovascular effects of varying depth of cortical deformation and impact velocity. J. Neurotrauma **11,** 573–585.

DIXON, C.E., CLIFTON, G.L., LIGHTHALL, J.W., YAGHMAI, A.A., and HAYES, R.L. (1991). A controlled cortical impact model of traumatic brain injury in the rat. J. Neurosci. Methods **39,** 253–262.

ELTING, J.W., DE JAGER, A.E., TEELKEN, A.W., et al. (2000). Comparison of serum S-100 protein levels following stroke and traumatic brain injury. J. Neurol. Sci. **181,** 104–110.

FINEMAN, I., HOVDA, D.A., SMITH, M., YOSHINO, A., and BECKER, D.P. (1993). Concussive brain injury is associated with a prolonged accumulation of calcium: a ^{45}Ca autoradiographic study. Brain Res. **624,** 94–102.

FRANZ, G., BEER, R., KAMPFL, A., et al. (2003). Amyloid beta 1–42 and tau in cerebrospinal fluid after severe traumatic brain injury. Neurology **60,** 1457–1461.

GARCIA, M.L., and CLEVELAND, D.W. (2001). Going new places using an old MAP: tau, microtubules and human neurodegenerative disease. Curr. Opin. Cell Biol. **13,** 41–48.

GOODMAN, J.C., CHERIAN, L., BRYAN, R.M., JR., and ROBERTSON, C.S. (1994). Lateral cortical impact injury in rats: pathologic effects of varying cortical compression and impact velocity. J. Neurotrauma **11,** 587–597.

HAMM, R.J., PIKE, B.R., O'DELL, D.M., LYETH, B.G., and JENKINS, L.W. (1994). The rotarod test: an evaluation of its effectiveness in assessing motor deficits following traumatic brain injury. J. Neurotrauma **11,** 187–196.

HANLON, R.E., DEMERY, J.A., MARTINOVICH, Z., and KELLY, J.P. (1999). Effects of acute injury characteristics on neurophysical status and vocational outcome following mild traumatic brain injury. Brain Inj. **13,** 873–887.

HANS, V.H., KOSSMANN, T., LENZLINGER, P.M., et al. (1999). Experimental axonal injury triggers interleukin-6 mRNA, protein synthesis and release into cerebrospinal fluid. J. Cereb. Blood Flow Metab. **19,** 184–194.

HARAD, F.T., and KERSTEIN, M.D. (1992). Inadequacy of bedside clinical indicators in identifying significant intracranial injury in trauma patients. J. Trauma **32,** 359–363.

HERRMANN, M., CURIO, N., JOST, S., et al. (2001). Release of biochemical markers of damage to neuronal and glial brain tissue is associated with short- and long-term neuropsychological outcome after traumatic brain injury. J. Neurol. Neurosurg. Psychiatry **70,** 95–100.

HERRMANN, M., EBERT, A.D., TOBER, D., HANN, J., and HUTH, C. (1999). A contrastive analysis of release patterns of biochemical markers of brain damage after coronary artery bypass grafting and valve replacement and their association with the neurobehavioral outcome after cardiac surgery. Eur. J. Cardiothorac Surg. **16,** 513–518.

HERRMANN, M., JOST, S., KUTZ, S., et al. (2000). Temporal profile of release of neurobiochemical markers of brain damage after traumatic brain injury is associated with intracranial pathology as demonstrated in cranial computerized tomography. J. Neurotrauma **17,** 113–122.

HESSE, C., ROSENGREN, L., ANDREASEN, N., et al. (2001). Transient increase in total tau but not phospho-tau in human cerebrospinal fluid after acute stroke. Neurosci. Lett. **297,** 187–190.

HILL, M.D., JACKOWSKI, G., BAYER, N., LAWRENCE, M., and JAESCHKE, R. (2000). Biochemical markers in acute ischemic stroke. CMAJ **162,** 1139–1140.

HONG, S.C., GOTO, Y., LANZINO, G., SOLEAU, S., KASSELL, N.F., and LEE, K.S. (1994). Neuroprotection with a calpain inhibitor in a model of focal cerebral ischemia. Stroke **25,** 663–669.

INGEBRIGTSEN, T., and ROMNER, B. (2002). Biochemical serum markers of traumatic brain injury. J. Trauma **52,** 798–808.

JACKSON, R.G., SAMRA, G.S., RADCLIFFE, J., CLARK, G.H., and PRICE, C.P. (2000). The early fall in levels of S-100 beta in traumatic brain injury. Clin. Chem. Lab. Med. **38,** 1165–1167.

KELLY, D.F. (1995). Alcohol and head injury: an issue revisited. J. Neurotrauma **12,** 883–890.

KIDO, D.K., COX, C., HAMILL, R.W., ROTHENBERG, B.M., and WOOLF, P.D. (1992). Traumatic brain injuries: predictive usefulness of CT. Radiology **182,** 777–781.

KURTH, S.M., BIGLER, E.D., and BLATTER, D.D. (1994). Neuropsychological outcome and quantitative image analysis of acute haemorrhage in traumatic brain injury: preliminary findings. Brain Inj. **8,** 489–500.

MARKGRAF, C.G., VELAYO, N.L., JOHNSON, M.P., et al. (1998). Six-hour window of opportunity for calpain inhibition in focal cerebral ischemia in rats. Stroke **29,** 152–158.

MCKEATING, E.G., ANDREWS, P.J., and MASCIA, L. (1998). Relationship of neuron specific enolase and protein S-100 concentrations in systemic and jugular venous serum to injury severity and outcome after traumatic brain injury. Acta Neurochir. Suppl. (Wien) **71,** 117–119.

MIRSKI, M.A., MUFFELMAN, B., ULATOWSKI, J.A., and HANLEY, D.F. (1995). Sedation for the critically ill neurologic patient. Crit. Care Med. **23,** 2038–2053.

NADLER, V., BIEGON, A., BEIT-YANNAI, E., ADAMCHIK, J., and SHOHAMI, E. (1995). ^{45}Ca accumulation in rat brain after closed head injury; attenuation by the novel neuroprotective agent HU-211. Brain Res. **685,** 1–11.

NATH, R., RASER, K.J., STAFFORD, D., et al. (1996). Non-erythroid alpha-spectrin breakdown by calpain and interleukin 1 beta-converting-enzyme-like protease(s) in apoptotic cells: contributory roles of both protease families in neuronal apoptosis. Biochem J. **319,** Pt 3, 683–690.

NEUMANN-HAEFELIN, T., KASTRUP, A., DE CRESPIGNY, A., et al. (2000). Serial MRI after transient focal cerebral ischemia in rats: dynamics of tissue injury, blood–brain barrier damage, and edema formation. Stroke **31,** 1965–1973.

NEWCOMB, J.K., KAMPFL, A., POSMANTUR, R.M., et al. (1997). Immunohistochemical study of calpain-mediated breakdown products to alpha-spectrin following controlled cortical impact injury in the rat. J. Neurotrauma **14,** 369–383.

PALMER, G.C., PEELING, J., CORBETT, D., DEL BIGIO, M.R., and HUDZIK, T.J. (2001). T2-weighted MRI correlates with long-term histopathology, neurology scores, and skilled motor behavior in a rat stroke model. Ann. NY Acad. Sci. **939,** 283–296.

PETZOLD, A., KEIR, G., LIM, D., SMITH., M, and THOMPSON, E.J., (2003). Cerebrospinal fluid (CSF) and serum S100B: release and washout pattern. Brain Res. Bull. **61,** 281–285.

PIKE, B.R., FLINT, J., DAVE, J.R., et al. (2004). Accumulation of calpain and caspase-3 proteolytic fragments of brain-derived alphaII-spectrin in cerebral spinal fluid after middle cerebral artery occlusion in rats. J. Cereb. Blood Flow Metab. **24,** 98–106.

PIKE, B.R., FLINT, J., DUTTA, S., JOHNSON, E., WANG, K.K., and HAYES, R.L. (2001). Accumulation of non-erythroid alpha II–spectrin and calpain-cleaved alpha II–spectrin breakdown products in cerebrospinal fluid after traumatic brain injury in rats. J. Neurochem. **78,** 1297–1306.

PIKE, B.R., ZHAO, X., NEWCOMB, J.K., POSMANTUR, R.M., WANG, K.K., and HAYES, R.L. (1998). Regional calpain and caspase-3 proteolysis of alpha-spectrin after traumatic brain injury. Neuroreport **9,** 2437–2442.

RAABE, A., GROLMS, C., KELLER, M., DOHNERT, J., SORGE, O., and SEIFERT, V. (1998). Correlation of computed tomography findings and serum brain damage markers following severe head injury. Acta Neurochir. (Wien) **140,** 787–792.

RAABE, A., and SEIFERT, V. (2000). Protein S-100B as a serum marker of brain damage in severe head injury: preliminary results. Neurosurg. Rev. **23,** 136–138.

REIBER, H. (2003). Proteins in cerebrospinal fluid and blood: barriers, CSF flow rate and source-related dynamics. Restor. Neurol. Neurosci. **21,** 79–96.

REIBER, H., and PETER, J.B. (2001). Cerebrospinal fluid analysis: disease-related data patterns and evaluation programs. J. Neurol. Sci. **184,** 101–122.

ROBERTS-LEWIS, J.M., SAVAGE, M.J., MARCY, V.R., PINSKER, L.R., and SIMAN, R. (1994). Immunolocaliza-

tion of calpain I–mediated spectrin degradation to vulnerable neurons in the ischemic gerbil brain. J. Neurosci. **14,** 3934–3944.

AU2 RINGGER, N.C., TOLENTINO, P.J., McKINSEY, D.M., PIKE, B.R., WANG, K.K.W., and HAYES, R.L. (2004). Effects of injury severity on regional and temporal mRNA expression levels of calpains and caspases after traumatic brain injury in rats. J. Neurotrauma. (in press).

ROTHOERL, R.D., WOERTGEN, C., and BRAWANSKI, A. (2000). S-100 serum levels and outcome after severe head injury. Acta Neurochir. Suppl. **76,** 97–100.

SAATMAN, K.E., BOZYCZKO-COYNE, D., MARCY, V., SIMAN, R., and McINTOSH, T.K. (1996a). Prolonged calpain-mediated spectrin breakdown occurs regionally following experimental brain injury in the rat. J. Neuropathol. Exp. Neurol. **55,** 850–860.

SAATMAN, K.E., MURAI, H., BARTUS, R.T., et al. (1996b). Calpain inhibitor AK295 attenuates motor and cognitive deficits following experimental brain injury in the rat. Proc. Natl. Acad. Sci. USA **93,** 3428–3433.

SAIDO, T.C., YOKOTA, M., NAGAO, S., et al. (1993). Spatial resolution of fodrin proteolysis in postischemic brain. J. Biol. Chem. **268,** 25239–25243.

SHAW, G.J., JAUCH, E.C., and ZEMLAN, F.P. (2002). Serum cleaved tau protein levels and clinical outcome in adult patients with closed head injury. Ann. Emerg. Med. **39,** 254–257.

VERWEIJ, B.H., MUIZELAAR, J.P., VINAS, F.C., PETERSON, P.L., XIONG, Y., and LEE, C.P. (1997). Mitochondrial dysfunction after experimental and human brain injury and its possible reversal with a selective N-type calcium channel antagonist (SNX-111). Neurol. Res. **19,** 334–339.

WANG, K.K. (2000). Calpain and caspase: can you tell the difference? Trends Neurosci. **23,** 59.

WANG, K.K., POSMANTUR, R., NATH, R., et al. (1998). Simultaneous degradation of alpha-II– and beta-II–spectrin by caspase 3 (CPP32) in apoptotic cells. J. Biol. Chem. **273,** 22490–22497.

WILSON, J.T., HADLEY, D.M., WIEDMANN, K.D., and TEASDALE, G.M. (1995). Neuropsychological consequences of two patterns of brain damage shown by MRI in survivors of severe head injury. J. Neurol. Neurosurg. Psychiatry **59,** 328–331.

XIONG, Y., GU, Q., PETERSON, P.L., MUIZELAAR, J.P., and LEE, C.P. (1997). Mitochondrial dysfunction and calcium perturbation induced by traumatic brain injury. J. Neurotrauma **14,** 23–34.

ZEMLAN, F.P., JAUCH, E.C., MULCHAHEY, J.J., et al. (2002). C-tau biomarker of neuronal damage in severe brain injured patients: association with elevated intracranial pressure and clinical outcome. Brain Res. **947,** 131–139.

ZEMLAN, F.P., ROSENBERG, W.S., LUEBBE, P.A., et al. (1999). Quantification of axonal damage in traumatic brain injury: affinity purification and characterization of cerebrospinal fluid tau proteins. J. Neurochem. **72,** 741–750.

ZINK, B.J. (2001). Traumatic brain injury outcome: concepts for emergency care. Ann. Emerg. Med. **37,** 318–332.

Address reprint requests to:
N.C. Ringger, D.V.M.
Department of Neuroscience
McKnight Brain Institute
University of Florida
100 S. Newell Dr.
L1-100 (P.O. Box 100244)
Gainesville, FL 32610

E-mail: ringger@ufbi.ufl.edu

JCBFM 24: 98-106, 2003
(1)

ACCUMULATION OF CALPAIN AND CASPASE-3 PROTEOLYTIC FRAGMENTS OF BRAIN-DERIVED αII-SPECTRIN IN CSF AFTER MIDDLE CEREBRAL ARTERY OCCLUSION IN RATS

Brian R. Pike[1]*, Jeremy Flint[1], Jitendra R. Dave[3], X.-C. May Lu[3], Kevin K.K. Wang[1,2], Frank C. Tortella[3], and Ronald L. Hayes[1]

[1]Department of Neuroscience and [2]Department of Psychiatry, Center for Traumatic Brain Injury Studies, E.F. & W.L. McKnight Brain Institute of the University of Florida, Gainesville, FL, USA

[3]Department of Neuropharmacology and Molecular Biology, Division of Neurosciences, Walter Reed Army Institute of Research, Silver Spring, MD, USA

*Current Address: Office of Scientific Review, NIH/NIGMS
Bethesda, MD 20892-6200

Contact Information:
Brian R. Pike, Ph.D.
Office of Scientific Review
National Institute of General Medical Sciences
Building 45, Room 3An.18
45 Center Dr., MSC 6200
Bethesda, MD 20892-6200

Tel: 301-594-3907
Fax: 301-480-8506
Email: pikbr@mail.nih.gov

Abstract

Preclinical studies have identified numerous neuroprotective drugs that attenuate brain damage and functional outcome after cerebral ischemia. Despite this success in animal models, neuroprotective therapies in the clinical setting have been unsuccessful. Identification of biochemical markers common to preclinical and clinical cerebral ischemia will provide a more sensitive and objective measure of injury severity and outcome to facilitate clinical management and treatment. However, there are currently no effective biomarkers available for assessment of stroke. Non-erythroid αII-spectrin is a cytoskeletal protein that is cleaved by calpain and caspase-3 proteases to signature αII-spectrin breakdown products (αII-SBDPs) after cerebral ischemia in rodents. This investigation examined accumulation of calpain- and caspase-3-cleaved αII-SBDPs in CSF of rodents subjected to 2 hours of transient focal cerebral ischemia produced by middle cerebral artery occlusion (MCAO) followed by reperfusion. Following MCAO injury, full-length αII-spectrin protein was decreased in brain tissue and increased in CSF from 24 hours to 72 hours after injury. Calpain- and caspase-3-specific αII-SBDPs were also increased in brain and CSF after injury. Levels of calpain-specific αII-SBDPs were greater at each post-injury time point than levels of caspase-3-specific αII-SBDPs. Levels of these proteins were undetectable in CSF of uninjured control rats. These results indicate that calpain- and caspase-3-cleaved αII-SBDPs in CSF may be useful diagnostic indicators of cerebral infarction that can provide important information about specific neurochemical events that have occurred in the brain after acute stroke.

Keywords: calpain, caspase-3, ischemia, stroke, biomarker, fodrin, α-spectrin, cerebrospinal fluid

Running title: Biomarkers of Stroke

Introduction

Acute ischemic stroke is a significant international health concern representing a potentially catastrophic debilitating medical emergency with poor prognosis for long-term disability. With the exception of diuretics, supportive measures, and when appropriate, thrombolytic therapy with recombinant tissue plasminogen activator (tPA), there are currently no approved drug treatments for ischemic brain injury (Grotta, 2002; Lees, 2002; Broderick and Hacke, 2002). Although a number of neuroprotective drugs have proven effective in reducing infarct size or improving functional outcome in preclinical testing, none have proven successful in clinical trials (Gladstone et al., 2002; Kidwell et al., 2001). Differences between preclinical and clinical trial outcome with neuroprotective drugs in acute ischemic stroke may be due to a variety of pitfalls that arise when attempting to extrapolate from animal to human investigations. These pitfalls may include differences in drug concentration and duration, differences in the window for therapeutic efficacy, differences in preclinical vs. clinical trial design, and the lack of standardized and sensitive outcome measures (Gladstone, et al., 2002; STAIR, 1999). For example, preclinical studies (typically in rodents) have traditionally utilized reduction of acute infarct volume as the primary measure of treatment efficacy, while clinical trials typically gauge treatment efficacy based on neurological and/or functional outcome (Gladstone et al., 2002). One approach to address these discrepancies in outcome measures is for preclinical and clinical trial designs to use outcome measures that are common to both human acute ischemic stroke and to preclinical animal models of ischemia. The use of common biochemical markers may provide such an approach.

Unlike other organ-based diseases where rapid diagnosis employing biomarkers (usually involving blood tests) prove invaluable to guide treatment of the disease, no such rapid and definitive diagnostic tests exist for acute ischemic brain injury. Biomarkers would have important applications in diagnosis, prognosis, and clinical research of ischemic brain injuries.

Simple and rapid diagnostic tools will immensely facilitate allocation of the major medical resources required to treat acute ischemic brain injuries. Accurate diagnosis in acute care environments can significantly enhance decisions about patient management, including decisions whether to admit or discharge patients or to administer other time consuming and expensive tests, including computed tomography (CT) and magnetic resonance imaging (MRI) scans. Biomarkers could provide major opportunities for the conduct of clinical research including confirmation of injury mechanism(s) and drug target identification. The temporal profile of changes in biomarkers could guide timing of treatment. Finally, biomarkers could provide a robust and sensitive clinical trial outcome measure that is obtainable more readily and with less expense than conventional neurological assessments, thereby significantly reducing the risks and costs of human clinical trials.

Previously reported biomarkers of cerebral ischemia include neuron-specific enolase (NSE), brain specific creatine kinase enzyme (CPK-BB), S-100β, and inflammatory cytokines such as IL-6 (Laskowitz et al., 1998). Of these, NSE and S-100β have been the most studied. After cardiac arrest, NSE elevations in serum and CSF have been correlated with neurological recovery (Roine et al., 1989; Martens, 1996; Dauberschmidt et al., 1991). Serum and CSF NSE values are reported to be elevated in rodent models of focal ischemia in proportion to the eventual infarct volume (Cunningham et al., 1991, 1996; Horn et al., 1995). In clinical trials, peak serum NSE values also predicted infarct volumes as shown by CT. However, correlating serum NSE values with functional outcome was less successful (Cunningham et al., 1991, 1996; Missler et al., 1997). S-100β protein has been studied most extensively for characterization of ischemic injuries after cardiac surgery and several reports have documented post-operative serum elevations (Sellman et al., 1992; Westaby et al., 1996). However, many of these reports do not include careful studies of neurological outcome and several investigators have recently criticized the diagnostic utility of S-100β during cardiac surgery (Anderson et al.,

2001). Thus, there is clearly a need for development of better biochemical markers for use in evaluating ischemic brain injury.

Our research efforts to develop biomarkers for traumatic brain injury (TBI) and acute ischemic brain injury have focused on αII-spectrin metabolic products as prototypical biochemical markers (Pike et al., 2001; Ringger et al., 2002). αII-spectrin is the major structural component of the cortical membrane cytoskeleton and is particularly abundant in axons and presynaptic terminals (Goodman et al., 1995; Riederer et al., 1986). Importantly, αII-spectrin is a major substrate for both and calpain and caspase-3 cysteine proteases (see **Fig. 1**), and the major calpain and caspase-3 cleavage sites of αII-spectrin have been well documented (Harris et al., 1988; Wang et al., 1998). Our laboratory has provided considerable evidence that αII-spectrin is processed by calpains and/or caspase-3 to signature cleavage products *in vivo* after TBI (Beer et al., 2000; Newcomb et al., 1997; Pike et al., 1998a, 2001) and in *in vitro* models of mechanical stretch injury (Pike et al., 2000), necrotic cell death (Zhao et al., 1999), apoptotic cell death (Pike et al., 1998b), and oxygen-glucose deprivation (Newcomb-Fernandez et al., 2001). Calpain and caspase-3 proteases also cleave αII-spectrin to signature proteolytic fragments in the brain in a rodent model of transient forebrain ischemia (Zhang et al., 2002). Although we have generated considerable laboratory data on the utility of αII-spectrin degradation as a biomarker for TBI in rodents (Pike et al., 2001), and more recently with preliminary data in human TBI patients (d'Avella et al., 2002), the present investigation is the first to provide evidence that calpain- and caspase-3-mediated αII-spectrin breakdown products (αII-SBDPs) can be detected in CSF after ischemic-reperfusion brain injury, and can used as biochemical markers in a rodent model of transient focal stroke in rats.

Methods

Surgical Procedures and Middle Cerebral Artery Occlusion: A "noninvasive" filament method of MCAO occlusion used extensively by our laboratories (Berti et al., 2002; Williams et

al., 2003) was used to produce cerebral ischemia in rats. The method described by Longa et al. (1989) and later modified in our laboratory by Britton et al. (1997) consists of blocking blood flow into the MCA with an intraluminal 3-0 monofilament nylon sterile suture with rounded tip introduced through an incision in the external carotid artery (ECA).

Under halothane anesthesia (5% halothane via induction chamber followed by 2% halothane via nose cone), the common carotid artery (CCA) was exposed at the level of external and internal carotid artery bifurcation with a midline neck incision. The internal carotid artery (ICA) was followed rostrally to the pterygopalatine branch and the ECA was ligated and cut at its lingual and maxillary branches. To prevent bleeding during suture insertion, the CCA and ICA were temporarily clamped with micro-aneurysm clips. The nylon suture was then introduced into the ICA via an incision on the ECA stump (the path of the suture can be monitored visually through the vessel wall) and advanced through the carotid canal approximately 20 mm from the carotid bifurcation until it becomes lodged in the narrowing of the anterior cerebral artery blocking the origin of the MCA. The skin incision was then closed using sterile autoclips. The endovascular suture remained in place for 2 hr at which time the rat was briefly re-anesthetized and the suture filament was retracted to allow reperfusion. For sham MCAO surgeries, the same procedure was followed but the filament was advanced only 10 mm beyond the internal-external carotid bifurcation and was left in place until sacrifice. During all surgical procedures, animals were maintained at 37.0°C by a homeothermic heating blanket (Harvard Apparatus, Holliston, MA).

Following surgery animals were placed in recovery cages with air temperature maintained at 22°C. During the 2 hr ischemia period and the initial 4 hr post-reperfusion period, 75-watt warming lamps were positioned directly over the top of each cage in order assist in maintaining normothermic body temperature throughout the experiment. Importantly, at the conclusion of each experiment, rat brains showing pathological evidence of subarachnoid hemorrhage upon

necropsy were excluded from the study. Also, all rats exhibiting convulsant behaviors at any time post MCAO were excluded from the experiment, as well as those animals not showing maximal neurologic impairment (NS=10, see description below) immediately prior to the 2 hr reperfusion.

Brain Tissue and CSF Collection: Brain (cortex and hippocampus) and CSF was collected from animals at various intervals after sham-injury or MCAO as previously described by our laboratory (Pike et al., 2001). At the appropriate time-points, MCAO or sham-injured animals were anesthetized as described above and secured in a stereotactic frame with the head allowed to move freely along the longitudinal axis. The head was flexed so that the external occipital protuberance in the neck was prominent and a dorsal midline incision was made over the cervical vertebrae and occiput. The atlanto-occipital membrane was exposed by blunt dissection and a 25G needle attached to polyethylene tubing was carefully lowered into the cisterna magna. Approximately 0.1 to 0.15 ml of CSF was collected from each rat. Following CSF collection, animals were removed from the stereotactic frame and immediately killed by decapitation. Ipsilateral and contralateral (to the site of infarct) cortices were then rapidly dissected, rinsed in ice cold PBS, and snap frozen in liquid nitrogen. Cortices were excised to the level of the white matter and extended ~4 mm laterally and ~7 mm rostrocaudally. CSF samples were centrifuged at 4000 g for 4 min. at 4°C to clear any contaminating erythrocytes. Cleared CSF and frozen tissue samples were stored at -80°C until ready for use. Cortices were homogenized in a glass tube with a Teflon dounce pestle in 15 volumes of an ice-cold triple detergent lysis buffer (20 mM Hepes, 1 mM EDTA, 2 mM EGTA, 150 mM NaCl, 0.1% SDS, 1.0% IGEPAL 40, 0.5% deoxycholic acid, pH 7.5) containing a broad range protease inhibitor cocktail (Roche Molecular Biochemicals, cat. #1-836-145).

Immunoblot Analyses of CSF and Cortical Tissues: Protein concentrations of tissue homogenates and CSF were determined by bicinchoninic acid microprotein assays (Pierce Inc.,

Rockford, IL) with albumin standards. Protein balanced samples were prepared for sodium dodecyl sulfate–polyacrylamide gel electrophoresis (SDS-PAGE) in twofold loading buffer containing 0.25 M Tris (pH 6.8), 0.2 M DTT, 8% SDS, 0.02% bromophenol blue, and 20% glycerol in distilled H_2O. Samples were heated for 10 min. at 100°C and centrifuged for 1 min. at 10,000 rpm in a microcentrifuge at ambient temperature. Twenty micrograms of protein per lane was routinely resolved by SDS-PAGE on 6.5% Tris/glycine gels for 1 hour at 200 V. Following electrophoresis, separated proteins were laterally transferred to polyvinylidene fluoride (PVDF) membranes in a transfer buffer containing 0.192 M glycine and 0.025 M Tris (pH 8.3) with 10% methanol at a constant voltage of 100 V for 1 hour at 4°C. Blots were blocked for 1 hour at ambient temperature in 5% nonfat milk in TBS and 0.05% Tween-20. Panceau Red (Sigma, St. Louis, MO) was used to stain membranes to confirm successful transfer of protein and to insure that an equal amount of protein was loaded in each lane.

Antibodies and Immunolabeling of PVDF Membranes: Immunoblots containing brain or CSF protein were probed with an anti-αII-spectrin (fodrin) monoclonal antibody (FG 6090 Ab; clone AA6; cat. # FG 6090; Affiniti Research Products Limited, UK) that detects intact non erythroid αII-spectrin (280 kDa) and 150, 145, and 120 kDa cleavage fragments to αII-spectrin. A cleavage product of 150 kDa is initially produced by calpains or caspase-3 proteases (each proteolytic cleavage yields a unique amino-terminal region; Nath et al., 1996; Wang et al., 1998; **Fig. 1**). The calpain-generated 150 kDa product is further cleaved by calpain to yield a specific calpain signature product of 145 kDa (Harris et al., 1988; Nath et al., 1996) whereas the caspase-3 generated 150 kDa product is further cleaved by caspase-3 to yield an apoptotic-specific caspase-3 signature product of 120 kDa (Nath et al., 1998; Wang et al., 1998; Wang, 2000). Following an overnight incubation at 4°C with the primary antibody (FG 6090 Ab, 1:4000 for brain tissue and 1:2000 for CSF), blots were incubated for 1 hr at ambient temperature in 3% nonfat milk that contained a horseradish peroxidase-conjugated goat anti-mouse IgG (1:10,000

dilution). Enhanced chemiluminescence (ECL, Amersham) reagents were used to visualize immunolabeling on Kodak Biomax ML chemiluminescent film.

Statistical Analyses: Semi-quantitative evaluation of protein levels detected by immunoblotting was performed by computer-assisted densitometric scanning (AlphaImager 2000 Digital Imaging System, San Leandro, CA). Data were acquired as integrated densitometric values and transformed to percentages of the densitometric levels obtained on scans from sham-injured animals visualized on the same blot. Data was evaluated by least squares linear regression followed by ANOVA. All values are given as mean ± SEM. Differences were considered significant if $p < 0.05$.

Results

Proteolysis of αII-Spectrin in the Ipsilateral Cortex by Calpains and Caspase-3 After MCAO Injury. In the ipsilateral cortex, MCAO injury caused significant ($p < 0.05$) accumulation of the non-specific 150 kDa αII-SBDP (generated by calpain and/or caspase-3), and of the calpain-specific 145 kDa αII-SBDP at all post-injury time points as compared to sham-injured control rats (**Fig. 2**). Levels of the calpain-specific 145 kDa αII-SBDP were 304%, 282%, and 301% of sham-injured control values at 24, 48, and 72 hours post-injury, respectively (**Fig. 3**). Levels of the non-specific 150 kDa αII-SBDP closely matched levels of the 145 kDa fragment, and were 276%, 275%, 268% of sham-injured control valules at 24, 48, and 72 hours, respectively (**Fig. 3**). MCAO injury also resulted in more modest, but significant ($p < 0.05$ to $p < 0.001$) levels of caspase-3-specific 120 kDa αII-SBDPs at all post-injury time points (**Fig. 2**). Levels of the caspase-3-specific 120 kDa fragment were 131%, 132%, and 140% of sham-injured control values at 24, 48, and 72 hours post-injury, respectively (**Fig. 3**). Although levels of the caspase-3-specific 120 kDa αII-SBDP were smaller than those produced by calpains,

between animal variability was much lower for levels of caspse-3 αII-SBDPs compared to the variability for levels of calpain αII-SBDPs.

In the contralateral cortex, MCAO injury caused no significant accumulation of calpain- or caspase-3-specific αII-SBDPs at any post-injury time point as compared to sham-injured control rats (**Fig. 2**).

Accumulation of Calpain and Caspase-3 Mediated αII-SBDPs in CSF after MCAO Injury. Cerebrospinal fluid levels of αII-spectrin and αII-SBDPs were undetectable in sham-injured control animals (**Fig. 2**). However, after MCAO injury accumulation of full length αII-spectrin (280 kDa) and the 150 kDa, 145 kDa, and 120 kDa αII-SBDPs were overtly apparent on immunoblots at various post-injury time points (**Fig. 2**). Levels of the full length αII-spectrin protein were increased in CSF of MCAO injured animals and were 144%, 453%, and 395% of sham-injured control levels at 24, 48, and 72 hours post-injury. However, there was considerable between animal variability in levels of the full length protein; thus, quantitative analysis failed to reach statistical significance (**Fig. 3**). Levels of the non-specific 150 kDa αII-SBDP, and of the calpain-specific 145 kDa αII-SBDP, were apparent on immunoblot at all post-injury time points, but only levels at 48 hours and 72 hours post-injury reached statistical significance ($p < 0.001$). Levels of the non-specific 150 kDa αII-SBDP were 216%, 523%, and 467% of sham-injured control animals, and levels of the calpain-specific 145 kDa αII-SBDP were 268%, 626%, and 546% of sham-injured control values at 24, 48, and 72 hours post-injury, respectively (**Fig. 3**). Levels of the caspase-3-specific 120 kDa αII-SBDP were 84%, 439%, and 110% of sham-injured control levels at 24, 48, and 72 hours post-injury, respectively (**Fig. 3**). Although levels of caspase-3-specific 120 kDa αII-SBDPs were 439% of sham-injured control values at 48 hours post-injury, large between animal variability precluded statistical significance.

Linear Regression Analyses of Cortical versus CSF Levels of αII-Spectrin and αII-SBDPs. Least squares linear regression was calculated to examine the relationship between cortical and CSF levels of αII-spectrin and αII-SBDPs over days post-injury in sham-control and MCAO-injured animals. The slopes of the regression lines for brain and CSF protein levels were analyzed by ANOVA.

The slope of the regression line for protein levels of the full-length 280 kDa αII-spectrin in the cortex across days post-injury was only slightly negative (m = -4.872), indicating modest decreases in total αII-spectrin protein (**Fig. 4**). The slope of the regression line for CSF levels of the full-length αII-spectrin protein across days post-injury was positive (m = 113.5), indicating increased accumulation of αII-spectrin in CSF from 24 h to 72 h after MCAO injury.

Slopes of the regression lines for the 150 kDa αII-SBDP in cortex and CSF across days post-injury were both positive (m = 53.59 and m = 145.4, respectively; **Fig. 4**). This result is consistent with the immunoblot data demonstrating increased accumulation of the 150 kDa αII-SBDP in cortex and CSF after MCAO injury. ANOVA indicated no significant difference (F = 2.14, p = 0.2172) between cortical and CSF slopes. This result indicates that rate of accumulation of the non-specific 150 kDa αII-SBDP in brain and CSF over days post-injury was approximately equivalent.

Slopes of the regression line for the 145 kDa αII-SBDP in cortex and CSF across days post-injury were both positive (m = 60.63 and m = 170.5, respectively; **Fig. 4**). This result is also consistent with the immunoblot data demonstrating increased accumulation of the 145 kDa αII-SBDP in cortex and CSF after MCAO injury. ANOVA indicated no significant difference (F = 2.50, p = 0.1889) between cortical and CSF slopes. This result indicates that rate of

accumulation of the calpain-specific 145 kDa αII-SBDP in brain and CSF over days post-injury was approximately equivalent.

Slopes of the regression line for the 120 kDa αII-SBDP in cortex and CSF across days post-injury were both slightly positive (m = 15.12 and m = 41.28, respectively; **Fig. 4**). This result is consistent with the immunoblot data demonstrating relatively small increases in accumulation of the 120 kDa αII-SBDP in cortex and CSF after MCAO injury. Again, ANOVA indicated no significant difference (F =0.08, p = 0.7861) between cortical and CSF slopes, indicating that rate of accumulation of the caspase-3 specific 120 kDa αII-SBDP in brain and CSF over days post-injury was approximately equivalent.

Discussion

This paper provides further evidence supporting the use of calpain and caspsase-3 specific αII-SBDPs as surrogate neurochemical markers of CNS injury. Previous data from our laboratory demonstrate that TBI causes robust and detectable accumulation of calpain-mediated αII-SBDPs (and to a lesser extent, caspase-3-mediated αII-SBDPs) in CSF of brain injured rodents (Pike et al., 2001). We now demonstrate that a rodent stroke model of focal ischemic injury also results in increased levels of calpain and caspase-3 αII-SBDPs in post-injury CSF. The results of these two studies are important in that they provide the first evidence that extra-parenchymal detection of specific protein metabolic products can be used as unequivocal biochemical markers for specific neurochemical events (i.e., calpain and caspase-3 activation) that have occurred in the injured brain in at least two preclinical models of brain injury (traumatic and ischemic). Importantly, recent preliminary clinical studies in patients with severe TBI also indicate robust levels of calpain and caspase-3 mediated αII-SBDPs in CSF (d'Avella et al., 2002).

Analysis of specific biochemical markers is a mandatory component of diagnosing dysfunction in a number of organs, including the use of troponin assays in patients with acute coronary syndromes (Newby et al., 2003). Indeed, troponin testing has rapidly evolved from its initial role in aiding diagnosis of myocardial infarction to a more complex role for risk stratification and guidance of treatment strategies (Newby et al., 2003). However, there are no such biomarkers of proven clinical utility for TBI and cerebral ischemia. In the case of TBI, this may be due, in part, to the fact that TBI is difficult to assess and clinical examinations are of restricted value during the first hours and days after injury. For instance, conventional diagnoses of TBI are based on neuroimaging techniques such as CT scanning, MRI, and single-photon emission CT scanning (Jacobs et al., 1996; Kant et al., 1997; Mitchener et al., 1997). CT scanning has low sensitivity to diffuse brain damage and the availability of MRI is limited (Kesler et al., 2000; Levi et al., 1900). In addition, single-photon emission CT scanning detects regional blood-flow abnormalities not necessarily related to structural damage. In the case of stroke, investigators have also generally recognized the need for more objective assessments of outcome, including the use of biochemical markers (Dirnagl et al., 1999; Zaremba et al., 2001). The approval of tPA as a treatment for acute stroke has additionally highlighted the potential utility of biochemical markers. For example, diagnosis of stroke is relatively straightforward when patients present with typical symptoms; however, often symptoms of stroke are more subtle and can delay diagnosis by hours or days (Elkind, 2003). Additionally, other causes of neurological symptoms, such as seizure, migraine, vasospasm, syncope, and peripheral vestibulopathy, can be indistinguishable from symptoms of thromboembolic transient ischemic attacks (Johnston et al., 2003). Thus, a rapid and reliable biochemical marker of stroke will facilitate diagnosis and might give assurance to physicians considering administering thrombolytic agents for treatment of acute ischemic stroke.

Our laboratories' assessment of αII-SBDPs as biochemical markers in models of TBI and focal cerebral ischemia may result in considerable improvement over currently existing biochemical markers of CNS injury. For instance, other putative biomarkers of CNS injury (e.g., CPK-BB, NSE, S-100β, lactate dehydrogenase, etc.) are of limited value due to a lack of specificity to CNS tissues, unreliability in predicting outcome, and because they provide no specific information regarding neurochemical pathology of injured CNS tissue. Recent studies have also examined the utility of cleaved tau protein (cTP) as a predictor of outcome. However, while cTP is axonal specific, it also provides no information about specific neurochemical events that have occurred in the injured CNS. Furthermore, recent studies have presented conflicting evidence as to the utility of cTP as a predictor of outcome after TBI in humans (Chatfield et al., 2002; Zemlan et al., 1999). In contrast, αII-SBDPs offer several advantages as compared to the putative biomarkers just described. For instance, αII-SBDPs provide concurrent information on post-injury activity of two important proteolytic enzymes (calpain and caspase-3). Low basal levels of these proteases further optimizes their utility as markers of cell injury. Another important characteristic is that αII-spectrin protein is not localized in erythrocytes (Goodman et al., 1995; Riederer, et al., 1986). Blood is a major source of CSF contamination after TBI and hemorrhagic ischemia. Results from our previously published studies in TBI clearly demonstrate that αII-spectrin and αII-SBDPs are not detectable in whole blood samples. In contrast, the erythroid isoform of spectrin, αI-spectrin, is detectable in both blood and brain tissues (Pike et al., 2001).

However, one disadvantage is that while αII-spectrin is highly enriched in brain, it is not specific to brain tissue. While this is not a concern for CSF detection of αII-SBDPs, it could be problematic for detection of αII-SBDPs in serum as human head-injured patients often present with multi-organ trauma. Additional studies in preclinical models and in human patients are needed to clarify this issue.

An ideal biomarker for a particular neurological disease is one that is 100% specific and sensitive for that particular disease. However, with TBI or stroke, it is not critical that a biomarker be specific to one or the other disorder, rather, the biomarker need only indicate, with as much sensitivity as possible, the severity of brain damage that has occurred as a result of brain trauma or cerebral infarction (although a biomarker that can rapidly and accurately discriminate between hemorrhagic and thrombolytic stroke would certainly be useful). The use of calpain- and caspase-3-mediated αII-SBDPs could provide a powerful approach for determining the severity of brain damage caused by a TBI or stroke, and could also provide a clinical tool for monitoring the duration of the acute injury response and the effects of emergency or therapeutic interventions. For instance, calpain and caspase-3 are potent mediators of cell death that can be rapidly activated in response to traumatic (Beer et al., 2000; Pike et al., 1998a; Sullivan et al., 2002) or ischemic brain injury (Davoli et al., 2002; Zhang et al., 2002), and brain regions with the highest accumulation of αII-SBDPs have the highest level of neuronal cell death (Roberts-Lewis et al., 1994; Newcomb et al., 1997). Importantly, calpain and caspsase-3 can be concurrently or independently activated after TBI (Pike et al., 1998a) or cerebral ischemia (Zhang et al., 2002), and the temporal duration of activity can vary for each protease. Thus, the ability to monitor both calpain and caspase-3 activation during the acute period of CNS injury is a major advantage of αII-SBDPs over other biomarkers. Indeed, recent preliminary data obtained from CSF of severely injured TBI patients indicate that temporal accumulation of calpain- and caspase-3-mediated αII-SBDPs show different patterns of temporal expression that vary in each patient (d'Avella et al., 2002). This result is similar to our preclinical TBI and ischemic injury models in which accumulation of calpain and/or caspase-3 αII-SBDPs also varies between individual animals. This variability emphasizes the heterogeneous nature of TBI and ischemic pathology, and points to important implications for

individualized treatment of human brain injured patients that is tailored to specific neurochemical cascades operative in the injured brain.

In summary, this paper provides further evidence supporting the use of calpain- and caspase-3-mediated αII-SBDPs as neurochemical markers of CNS injury. Although numerous other proteins, peptides, amino acids, etc., have been identified in CSF after TBI and acute cerebral ischemia, no such surrogate marker of CNS injury has yet provided a window of insight into specific neurochemical events that have occurred as a result of traumatic or ischemic brain injury. The use of protease-specific αII-SBDPs as biomarkers offers several advantages over existing biomarkers of traumatic or ischemic brain injury, including the ability to provide concurrent information about the activity of two major proteolytic effectors of cell death. Additional studies to further characterize the sensitivity of αII-SBDPs (e.g., in serum and across injury magnitudes) are ongoing. In addition, it is thought that the development of other CNS-specific biomarkers used in conjunction with αII-SBDPs will provide researchers and clinicians with powerful tools for diagnosing and assessing CNS injury, for monitoring recovery, and for guiding appropriate administration of therapeutic compounds. Finally, it is thought that recent advancements in antibody-based specific identification technologies will facilitate development of rapid, sensitive, and easy-to-use kits for research and clinical environments.

Acknowledgements

This work was supported by DAMD17-99-1-9565, NIH R01 NS39091, and NIH R01 NS40182 to R.L.H.; by DAMD17-01-1-0765 to B.R.P.; the State of Florida Brain and Spinal Cord Injury Rehabilitation Trust Fund (BSCIRTF); and by the United States Army Medical Research and Materiel Command (USAMRMC).

References

Anderson RE, Hansson LO, Nilsson O, Dijlai-Merzoug R, Settergren G (2001) High serum S100B levels for trauma patients without head injuries. *Neurosurgery* 48(6):1255-1258

Beer R, Franz G, Srinivasan A, Hayes RL, Pike BR, Zhao X, Schmutzhard E, Poewe W, Kampfl A (2000) Temporal profile and cell subtype distribution of activated caspase-3 following experimental traumatic brain injury. *J Neurochem* 75(3):1264-1273

Berti R, Williams AJ, Moffett JR, Hale SL, Velarde LC, Elliott PJ, Yao C, Dave JR, Tortella FC (2002) Quantitative real-time RT-PCR analysis of inflammatory gene expression associated with ischemia-reperfusion brain injury. *J Cereb Blood Flow Metab* 22(9):1068-1079

Britton P, Lu XC, Laskosky M, Tortella FC (1997) Dextromethorphan protects against cerebral injury following transient, but not permanent, focal ischemia in rats. *Life Sci* 60:1729-1740

Broderick JP, Hacke W (2002) Treatment of acute ischemic stroke: Part II: neuroprotection and medical management. *Circulation* 106(13):1736-1740

Chatfield DA, Zemlan FP, Day DJ, Menon DK (2002) Discordant temporal patterns of S100beta and cleaved tau protein elevation after head injury: a pilot study. *Br J Neurosurg* 16(5):471-476

Cunningham RT, Young IS, Winder J, O'Kane MJ, McKinstry S, Johnston CF, Dolan OM, Hawkins SA, Buchanan KD (1991) Serum neurone specific enolase (NSE) levels as an indicator of neuronal damage in patients with cerebral infarction. *Eur J Clin Invest* 21(5):497-500

Cunningham RT, Watt M, Winder J, McKinstry S, Lawson JT, Johnston CF, Hawkins SA, Buchanan, KD (1996) Serum neurone-specific enolase as an indicator of stroke volume. *Eur J Clin Invest* 26(4):298-303

Dauberschmidt R, Zinsmeyer J, Mrochen H, Meyer M (1991) Changes of neuron-specific enolase concentration in plasma after cardiac arrest and resuscitation. *Mol Chem Neuropathol* 14(3):237-245

d'Avella D, Aguennouz M, Angileri FF, de Divitiis O, Germanò A, Toscano A, Tomasello F, Vita G, Pike BR, Wang KKW, Hayes RL (2002) Accumulation of calpain and caspase-3 cleaved αII-spectrin breakdown products in CSF of patients with severe traumatic brain injury. [abstract] *J Neurotrauma* 19(10):1292

Davoli MA, Fourtounis J, Tam J, Xanthoudakis S, Nicholson D, Robertson GS, Ng GY, Xu D (2002) Immunohistochemical and biochemical assessment of caspase-3 activation and DNA fragmentation following transient focal ischemia in the rat. *Neuroscience* 115(1):125-136

Dirnagl U, Iadecola C, Moskowitz MA (1999) Pathobiology of ischaemic stroke: an integrated view. *Trends Neurosci* 22(9):391-397

Elkind MS (2003) Stroke in the elderly. *Mt Sinai J Med* 70(1):27-37

Gladstone DJ, Black SE, Hakim AM (2002) Toward wisdom from failure: lessons from neuroprotective stroke trials and new therapeutic directions. *Stroke* 33(8):2123-2136

Goodman SR, Zimmer WE, Clark MB, Zagon IS, Barker JE, Bloom ML (1995) Brain spectrin: of mice and men. *Brain Res Bull* 36(6):593-606

Grotta J (2002) Neuroprotection is unlikely to be effective in humans using current trial designs. *Stroke* 33(1):306-307

Harris AS, Croall DE, Morrow JS (1988) The calmodulin-binding site in alpha-fodrin is near the calcium-dependent protease-I cleavage site. *J Biol Chem* 263(30):15754-15761

Horn M, Seger F, Schlote W (1995) Neuron-specific enolase in gerbil brain and serum after transient cerebral ischemia. *Stroke* 26(2):290-296

Jacobs A, Put E, Ingels M, Put T, Bossuyt A (1996) One-year follow-up of technetium-99m-HMPAO SPECT in mild head injury. *J Nucl Med* 37(10):1605-1609

Johnston SC, Sidney S, Bernstein AL, Gress DR (2003) A comparison of risk factors for recurrent TIA and stroke in patients diagnosed with TIA. *Neurology* 60(2):280-285

Kant R, Smith-Seemiller L, Isaac G, Duffy J (1997) Tc-HMPAO SPECT in persistent post-concussion syndrome after mild head injury: comparison with MRI/CT. *Brain Inj* 11(2):115-124

Kesler SR, Adams HF, Bigler ED (2000) SPECT, MR and quantitative MR imaging: correlates with neuropsychological and psychological outcome in traumatic brain injury. *Brain Inj* 14(10):851-857

Kidwell CS, Liebeskind DS, Starkman S, Saver JL (2001) Trends in acute ischemic stroke trials through the 20th century. *Stroke* 32(6):1349-1359

Laskowitz DT, Grocott H, Hsia A, Copeland KR (1998) Serum Markers of Cerebral Ischemia. *J Stroke Cerebrovasc Dis* 7(4):234-241

Lees KR (2002) Neuroprotection is unlikely to be effective in humans using current trial designs: an opposing view. *Stroke* 33(1):308-309.

Levi L, Guilburd JN, Lemberger A, Soustiel JF, Feinsod M (1990) Diffuse axonal injury: analysis of 100 patients with radiological signs. *Neurosurgery* 27(3):429-432

Longa EL, Weinstein PR, Carlson S, Cummins R (1989) Reversible middle cerebral artery occlusion without craniectomy in rats. *Stroke* 20:84-91

Martens P (1996) Serum neuron-specific enolase as a prognostic marker for irreversible brain damage in comatose cardiac arrest surviviors. *Acad Emerg Med* 3(2):126-131

Missler U, Wiesmann M, Friedrich C, Kaps M (1997) S-100 protein and neuron-specific enolase concentrations in blood as indicators of infarction volume and prognosis in acute ischemic stroke. *Stroke* 28(10):1956-1960

Mitchener A, Wyper DJ, Patterson J, Hadley DM, Wilson JT, Scott LC, Jones M, Teasdale GM (1997) SPECT, CT, and MRI in head injury: acute abnormalities followed up at six months. *J Neurol Neurosurg Psychiatry* 62(6):633-636

Nath R, Raser KJ, Stafford D, Hajimohammadreza I, Posner A, Allen H, Talanian RV, Yuen P, Gilbertson RB, Wang KK (1996) Non-erythroid α-spectrin breakdown by calpain and interleukin 1β-converting-enzyme-like protease(s) in apoptotic cells: contributory roles of both protease families in neuronal apoptosis. *Biochem J* 319:683-690

Nath R, Probert A, McGinnis KM, Wang KKW (1998) Evidence for activation of caspase-3-like protease in excitotoxin- and hypoxia/hypoglycemia-injured neurons *J Neurochem* 71:186-195

Newby LK, Goldmann BU, Ohman EM (2003) Troponin: an important prognostic marker and risk-stratification tool in non-ST-segment elevation acute coronary syndromes. *J Am Coll Cardiol* 41(4 Suppl S):S31-S36

Newcomb-Fernandez JK, Zhao X, Pike BR, Wang KKW, Kampfl A, Beer R, DeFord SM, Hayes RL (2001) Concurrent assessment of calpain and caspase-3 activation after oxygen-glucose deprivation in primary septo-hippocampal cultures. *J Cereb Blood Flow Metab* 21(11):1281-1294

Newcomb JK, Kampfl A, Posmantur RM, Zhao X, Pike BR, Liu SJ, Clifton GL, Hayes RL (1997) Immunohistochemical study of calpain-mediated breakdown products to alpha-spectrin following controlled cortical impact injury in the rat. *J Neurotrauma* 14:369-383

Pike BR, Zhao X, Newcomb JK, Posmantur RM, Wang KKW, Hayes RL (1998a) Regional calpain and caspase-3 proteolysis of α-spectrin after traumatic brain injury. *Neuroreport* 9:2437-2442

Pike BR, Zhao X, Newcomb JK, Wang KKW, Posmantur RM, Hayes RL (1998b) Temporal relationships between *de novo* protein synthesis, calpain and caspase 3-like protease activation, and DNA fragmentation during apoptosis in septo-hippocampal cultures. *J Neurosci Res* 52: 505-520

Pike BR, Zhao X, Newcomb JK, Glenn CC, Anderson DK, Hayes RL (2000) Stretch injury causes calpain and caspase-3 activation and necrotic and apoptotic cell death in septo-hippocampal cell cultures. *J Neurotrauma* 17(4):283-298

Pike BR, Flint J, Dutta S, Johnson E, Wang KKW, Hayes RL (2001) Accumulation of calpain-cleaved non-erythroid αII-spectrin in cerebrospinal fluid after traumatic brain injury in rats. *J Neurochem* 78:297-1306

Riederer BM, Zagon IS, Goodman SR (1986) Brain spectrin(240/235) and brain spectrin(240/235E): two distinct spectrin subtypes with different locations within mammalian neural cells. *J Cell Biol* 102(6):2088-2097

Ringger NC, Silver X, O'Steen B, Brabham JG, Deford SM, Pike BR, Pineda J, Hayes RL (2002) CSF accumulation of calpain-specific αII-spectrin breakdown products are associated with injury magnitude and lesion volume after traumatic brain injury in rats. [abstract] *J Neurotrauma* 19(10):1302

Roberts-Lewis JM, Savage MJ, Marcy VR, Pinsker LR, Siman R (1994) Immunolocalization of calpain I-mediated spectrin degradation to vulnerable neurons in the ischemic gerbil brain. *J Neurosci* 14(6):3934-3944

Roine RO, Somer H, Kaste M, Viinikka L, Karonen SL (1989) Neurological outcome after out-of-hospital cardiac arrest. Prediction by cerebrospinal fluid enzyme analysis. *Arch Neurol* 46(7):753-756

Sellman M, Ivert T, Ronquist G, Caesarini K, Persson L, Semb BK (1992) Central nervous system damage during cardiac surgery assessed by 3 different biochemical markers in cerebrospinal fluid. *Scand J Thorac Cardiovasc Surg* 26(1):39-45

Stroke Therapy Academic Indurstry Roundtable (STAIR) (1999) Recommendations for standards regarding preclinical neuroprotective and restorative drug development. *Stroke* 30:2752-2758

Sullivan PG, Keller JN, Bussen WL, Scheff SW (2002) Cytochrome c release and caspase activation after traumatic brain injury. *Brain Res* 949(1-2):88-96

Wang KK, Posmantur R, Nath R, McGinnis K, Whitton M, Talanian RV, Glantz SB, Morrow JS (1998) Simultaneous degradation of alphaII- and betaII-spectrin by caspase 3 (CPP32) in apoptotic cells. *J Biol Chem* 273(35):22490-22497

Wang, KKW (2000) Calpain and caspase: can you tell the difference? *Trends Neurosci* 23(1):20-26

Westaby S, Johnsson P, Parry AJ, Blomqvist S, Solem JO, Alling C, Pillai R, Taggart DP, Grebenik C, Stahl E (1996) Serum S100 protein: a potential marker for cerebral events during cardiopulmonary bypass. *Ann Thorac Surg* 61(1):88-92

Williams AJ, Hale SL, Moffett JR, Dave JR, Elliott PJ, Adams J, Tortella FC (2003) Delayed treatment with MLN519 reduces infarction and associated neurologic deficit caused by focal ischemic brain injury in rats via antiinflammatory mechanisms involving nuclear factor-kappaB activation, gliosis, and leukocyte infiltration. *J Cereb Blood Flow Metab* 23(1):75-87

Zaremba J Losy J (2001) Early TNF-alpha levels correlate with ischaemic stroke severity. *Acta Neurol Scand* 104(5):288-295

Zemlan FP, Rosenberg WS, Luebbe PA, Campbell TA, Dean GE, Weiner NE, Cohen JA, Rudick RA, Woo D (1999) Quantification of axonal damage in traumatic brain injury: affinity purification and characterization of cerebrospinal fluid tau proteins. *J Neurochem* 72(2):741-750

Zhang C, Siman R, Xu YA, Mills AM, Frederick JR, Neumar RW (2002) Comparison of calpain and caspase activities in the adult rat brain after transient forebrain ischemia. *Neurobiol Dis* 10(3):289-305

Zhao X, Pike BR, Newcomb JK, Wang KKW, Posmantur RM, Hayes RL (1999) Maitotoxin induces calpain but not caspase-3 activation and necrotic cell death in primary septo-hippocampal cultures. *Neurochem Res* 24(3): 371-382

Figure Legends

Figure 1. Calpain and caspase-3 cleavage of non-erythroid αII-spectrin to protease-specific αII-spectrin breakdown products (SBDPs) . Illustrated are the calpain cleavages (left) in αII-spectrin that result in calpain-specific SBDPs (150 and 145 kDa) and the caspase-3 cleavages (right) in αII-spectrin that result in caspase-3-specific αII-SBDPS (150 and 120 kDa). Both proteases cleave αII-spectrin in repeat 11 near the calmodulin binding domain (CaM) to produce 150 kDa αII-SBDPs with unique N-terminal regions. A second cleavage by calpain in repeat 11 results in a calpain-specific 145 kDa αII-SBDP, while caspase-3 cleaves the protein in repeat 13 to produce a unique, apoptotic-specific 120 kDa fragment. For definitively identified cleavages, the flanking amino acids and initial N-terminal amino acid sequence is given.

Figure 2. MCAO injury causes accumulation of full-length αII-spectrin (280 kDa) protein, and calpain-mediated 145 kDa and caspase-3 mediated 120 kDa αII-SBDPs in CSF. MCAO resulted in proteolysis of constitutively expressed brain αII-spectrin (280 kDa) in ipsilateral but not contralateral cortex. The caspase-3-mediated, apoptotic-specific 120 kDa αII-SBDP was also increased in ipsilateral cortex after ischemia compared to sham-injured controls. Marked increases in the calpain-specific 145 kDa αII-SBDP were detected in brain and CSF of MCAO animals, but not in sham-injured animals, at all time points. Interestingly, while increased levels of the caspase-3-specific 120 kDa αII-SBDP were detected at all post-injury time points in the ipsilateral cortex, CSF levels were only detected at 48 hours post-injury.

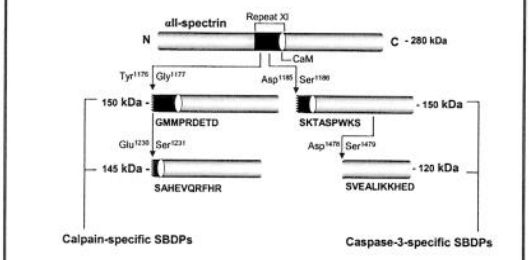
αII-spectrin
Repeat XI
N
C - 280 kDa
CaM
Tyr1176 Gly1177
Asp1185 Ser1186
150 kDa -
- 150 kDa
GMMPRDETD
SKTASPWKS
Glu1230 Ser1231
Asp1478 Ser1479
145 kDa -
- 120 kDa
SAHEVQRFHR
SVEALIKKHED
Calpain-specific SBDPs
Caspase-3-specific SBDPs

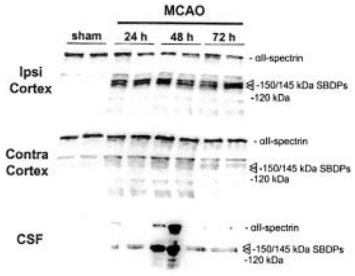
MCAO
sham
24 h
48 h
72 h
Ipsi Cortex
- αII-spectrin
-150/145 kDa SBDPs
-120 kDa
Contra Cortex
- αII-spectrin
-150/145 kDa SBDPs
-120 kDa
CSF
- αII-spectrin
-150/145 kDa SBDPs
-120 kDa

Figure 3. Mean (± s.d.) arbitrary densitometric units obtained from full-length 280 kDa αII-spectrin protein and the 150 kDa, 145 kDa, and 120 kDa αII-SBDPs. Densitometric units were converted to percent of sham-injured values. Decreases in 280 kDa αII-spectrin and increases in 150 kDa, 145 kDa, and 120 kDa αII-SBDPs (ipsilateral cortex) were associated with concomitant increases of these proteins in the CSF. Note that while 150 kDa and 145 kDa SBDPs were visibly detectable in CSF on western blot at 24 hours post-injury, densitometric levels were not statistically significant due to greater variability at this time point. Similarly, although the full-length 280 kDa spectrin protein and the 120 kDa αII-SBDPs were visibly detectable in CSF, large variability in protein levels between animals resulted in inability to detect statistical significance. *$p<0.05$ and ***$p<0.001$.

Figure 4. Mean (± s.d.) cortical vs. CSF levels of αII-spectrin (280 kDa) and αII-SBDPs (150, 145, and 120 kDa) over days post-injury. Least squares regression lines of brain and CSF spectrin and SBDP levels were plotted on the same graph. Pearson correlation coefficients for each regression line are indicated. Results indicate that parenchymal decreases in levels of native αII-spectrin (280 kDa) are associated with increases in CSF accumulation while increased parenchymal levels of calpain-mediated αII-SBDPs (150 & 145 kDa) are associated with increased CSF accumulation. On average, there were no changes in parenchymal or CSF levels of the caspase-3-mediated 120 kDa αII-SBDP across days. However, individual rats at different time points (particularly 48 hours post-injury) showed some increase in CSF levels of the 120 kDa product.

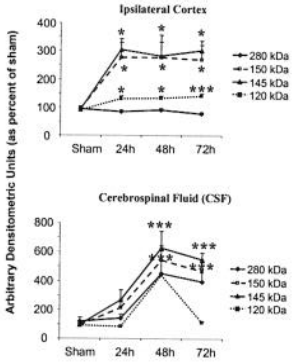
Ipsilateral Cortex
Arbitrary Densitometric Units (as percent of sham)
400
300
200
100
0
Sham
24h
48h
72h
280 kDa
150 kDa
145 kDa
120 kDa
Cerebrospinal Fluid (CSF)
800
600
400
200
0
Sham
24h
48h
72h
280 kDa
150 kDa
145 kDa
120 kDa

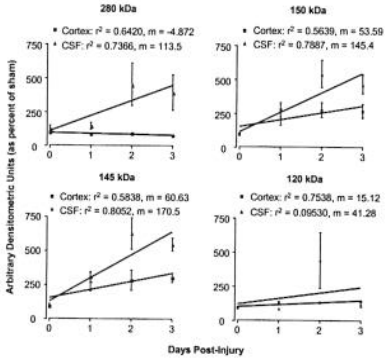
280 kDa
Cortex: r² = 0.6420, m = -4.872
CSF: r² = 0.7366, m = 113.5
150 kDa
Cortex: r² = 0.5639, m = 53.59
CSF: r² = 0.7887, m = 145.4
145 kDa
Cortex: r² = 0.5838, m = 60.63
CSF: r² = 0.8052, m = 170.5
120 kDa
Cortex: r² = 0.7538, m = 15.12
CSF: r² = 0.09530, m = 41.28
Arbitrary Densitometric Units (as percent of sham)
750
500
250
0
0
1
2
3
Days Post-Injury

Journal of Neurochemistry, 2001, **78**, 1–11

Accumulation of non-erythroid αII-spectrin and calpain-cleaved αII-spectrin breakdown products in cerebrospinal fluid after traumatic brain injury in rats

Brian R. Pike,* Jeremy Flint,* Satavisha Dutta,† Erik Johnson*, Kevin K. W. Wang* and Ronald L. Hayes*

*Department of Neuroscience, Evelyn F. and William L. McKnight Brain Institute of the University of Florida, Gainesville, Florida, USA

†Department of Neuroscience Therapeutics, Pfizer Inc, Ann Arbor, Michigan, USA

Abstract

Although a number of increased CSF proteins have been correlated with brain damage and outcome after traumatic brain injury (TBI), a major limitation of currently tested biomarkers is a lack of specificity for defining neuropathological cascades. Identification of surrogate biomarkers that are elevated in CSF in response to brain injury and that offer insight into one or more pathological neurochemical events will provide critical information for appropriate administration of therapeutic compounds for treatment of TBI patients. Non-erythroid αII-spectrin is a cytoskeletal protein that is a substrate of both calpain and caspase-3 cysteine proteases. As we have previously demonstrated, cleavage of αII-spectrin by calpain and caspase-3 results in accumulation of protease-specific spectrin breakdown products (SBDPs) that can be used to monitor the magnitude and temporal duration of protease activation. However, accumulation of αII-spectrin and αII-SBDPs in CSF after TBI has never been examined. Following a moderate level (2.0 mm) of controlled cortical impact TBI in rodents, native αII-spectrin protein was decreased in brain tissue and increased in CSF from 24 h to 72 h after injury. In addition, calpain-specific SBDPs were observed to increase in both brain and CSF after injury. Increases in the calpain-specific 145 kDa SBDP were 237%, 203% and 198% of sham-injured control animals at 24 h, 48 h and 72 h after TBI, respectively. The caspase-3-specific SBDP was observed to increase in CSF in some animals and to a lesser degree. Importantly, levels of these proteins were undetectable in CSF of uninjured control rats. These results indicate that detection of αII-spectrin and αII-SBDPs is a powerful discriminator of outcome and protease activation after TBI. In accord with our previous studies, results also indicate that calpain may be a more important effector of cell death after moderate TBI than caspase-3.

Keywords: calpain, caspase-3, cell death, cerebrospinal fluid, spectrin, traumatic brain injury.

J. Neurochem. (2001) **78**, 1–11.

The incidence of traumatic brain injury (TBI) in the United States of America is conservatively estimated to be more than 2 million persons annually with approximately 500 000 hospitalizations (Goldstein 1990). Of these, about 70 000–90 000 head injury survivors are permanently disabled. The annual economic cost to society for care of head-injured patients is estimated at $25 billion (Goldstein 1990). Thus, accurate and reliable measurement of outcome following head injury is of great interest to both head injury survivors and clinicians. Assessment of pathology and neurological impairment immediately after TBI is crucial for determination of appropriate clinical management and for predicting long-term outcome. The outcome measures most often used in head-injured patients are the Glasgow Coma Scale (GCS), the Glasgow Outcome Scale (GOS), and computed tomography (CT) scans to detect intracranial pathology.

Received March 26, 2001; revised manuscript received June 26, 2001; accepted June 27, 2001.

Address Reprint Requests to Dr Brian R. Pike, Department of Neuroscience, University of Florida, 100 S. Newell Dr, Box 100244, Gainesville, FL 32611 USA. E-mail: pike@ufbi.ufl.edu

Abbreviations used: CT, computed tomography; GCS, Glasgow Coma Scale, GOS, Glasgow Outcome Scale, PVDF, polyvinylidene fluoride; SBDPs, spectrin breakdown products; TBI, traumatic brain injury.

However, despite dramatically improved emergency triage systems based on these outcome measures, most TBI survivors suffer long-term (for a number of years) impairment, and a large number of TBI survivors are severely affected by TBI despite predictions of 'good recovery' on the GOS (Marion 1996). Because of the limitations of current clinical assessments of TBI severity, there has been an increased interest in the development of neurochemical markers for determining injury severity and for clinical evaluation of pathophysiological mechanisms operative in traumatized brain.

For example, TBI results in neuronal tissue death that can cause a variety of neurochemicals such as amino acids, ions and lactate, as well as a number of cellular proteins and enzymes, to be released into the blood and CSF (Goodman and Simpson 1996). Although assessment of cardiac and liver protein levels in the blood has routinely been used in medical practice for years (e.g. creatine kinase MB or troponin-T), assessment of CNS proteins in blood or CSF is far less developed. Thus, recent studies have measured a variety of neurochemical substances in the CSF or blood in attempt to identify specific surrogate markers of cellular damage and outcome after TBI and other CNS disorders (Haber and Grossman 1980; Inao *et al.* 1988; Robinson *et al.* 1990; Lyeth *et al.* 1993; Raabe and Seifert 1999; Raabe *et al.* 1999; Zemlan *et al.* 1999; Clark *et al.* 2000a; Tapiola *et al.* 2000). For example, creatine kinase BB, lactate dehydrogenase, myelin basic protein, and neuron-specific enolase have been measured in blood or CSF in various CNS disorders including TBI. However, these proteins are non-specific to the brain, offer no insight as to mechanism of injury, and/or prediction of outcome utilizing these proteins has not proven reliable (Goodman and Simpson 1996). Other proteins detected in CSF after brain injury such as S-100B are highly specific to the CNS and have been more robustly correlated with the outcome (Raabe and Seifert 1999; Raabe *et al.* 1999). Although brain-specific surrogate biomarkers like S-100B may be useful indicators of outcome after brain injury, detection of these proteins in blood or CSF offers no insight into neurochemical alterations that mediate brain damage after TBI. Thus, identification of neurochemical markers that are specific to the CNS and that provide information about specific ongoing neurochemical events would prove immensely beneficial for both prediction of outcome and for guidance of targeted therapeutic delivery.

Non-erythroid αII-spectrin is the major structural component of the cortical membrane cytoskeleton, is particularly abundant in axons and presynaptic terminals (Riederer *et al.* 1986; Goodman *et al.* 1995), and is a major substrate for both calpain and caspase-3 cysteine proteases (Wang *et al.* 1998). The calpain-mediated cleavage of αII-spectrin occurs between Tyr^{1176} and Gly^{1177} resulting in the formation of calpain-signature spectrin breakdown products (SBDPs) of 150 and 145 kDa (Harris *et al.* 1988). The caspase-3-mediated cleavages of αII-spectrin occur at Asp^{1185}, Ser^{1186}, Asp^{1478} and Ser^{1479} resulting in the formation of caspase-3-signature SBDPs of 150 and 120 kDa, respectively (Wang *et al.* 1998). Importantly, numerous investigations have documented increased pathological activation of calpain and/or caspase-3 proteases after TBI (Saatman *et al.* 1996a, 2000; Kampfl *et al.* 1997; Newcomb *et al.* 1997; Posmantur *et al.* 1997; Yakovlev *et al.* 1997; Pike *et al.* 1998a; Clark *et al.* 1999, 2000b; LaPlaca *et al.* 1999; Okonkwo *et al.* 1999; Zhang *et al.* 1999; Beer *et al.* 2000; Buki *et al.* 2000). In addition, our laboratory and others have provided extensive evidence the αII-spectrin is processed by calpains and/or caspase-3 to signature cleavage products *in vivo* after TBI (Beer *et al.* 2000; Newcomb *et al.* 1997; Pike *et al.* 1998a; Buki *et al.* 2000) and in *in vitro* models of mechanical stretch injury (Pike *et al.* 2000b), necrosis (Zhao *et al.* 1999), apoptosis (Nath *et al.* 1996a, 1996b; Pike *et al.* 1998b), glutamate or NMDA excitotoxicity (Nath *et al.* 2000; Zhao *et al.* 2000), and oxygen-glucose deprivation (Nath *et al.* 1998; Newcomb *et al.* 1998). Moreover, use of selective αII-SBDP antibodies has been used to demonstrate that brain regions with the highest accumulation of SBDPs also have the highest levels of neuronal cell death (Roberts-Lewis *et al.* 1994; Newcomb *et al.* 1997). Thus, the ubiquitous distribution of αII-spectrin in the brain coupled with the ability to utilize signature αII-spectrin proteolytic fragments generated by pathological activation of calpain and/or caspase-3 after TBI makes αII-spectrin a potentially important biomarker of brain damage. To test this hypothesis, the present investigation examined alterations in brain levels of αII-spectrin and αII-SBDPs after controlled cortical impact TBI in rodents, and compared these changes to accumulation of αII-spectrin and αII-SBDPs in CSF in the same animals.

Materials and methods

Surgical Preparation and controlled cortical impact traumatic brain injury

As previously described (Dixon *et al.* 1991; Pike *et al.* 1998a), a cortical impact injury device was used to produce TBI in rodents. Cortical impact TBI results in cortical deformation within the vicinity of the impactor tip associated with contusion, and neuronal and axonal damage that is constrained in the hemisphere ipsilateral to the site of injury (Gennarelli 1994; Meaney *et al.* 1994). Adult male (280–300 *g*) Sprague-Dawley rats (Harlan; Indianapolis, IN, USA) were initially anesthetized with 4% isoflurane in a carrier gas of 1 : 1 O_2/N_2O (4 min) followed by maintenance anesthesia of 2.5% isoflurane in the same carrier gas. Core body temperature was monitored continuously by a rectal thermistor probe and maintained at 37 ± 1°C by placing an adjustable temperature controlled heating pad beneath the rats. Animals were mounted in a stereotactic frame in a prone position and secured by ear and

incisor bars. A midline cranial incision was made, the soft tissues were reflected, and a unilateral (ipsilateral to site of impact) craniotomy (7 mm diameter) was performed adjacent to the central suture, midway between bregma and lambda. The dura mater was kept intact over the cortex. Brain trauma in rats ($n = 9$) was produced by impacting the right cortex (ipsilateral cortex) with a 5-mm diameter aluminum impactor tip (housed in a pneumatic cylinder) at a velocity of 3.5 m/s with a 2.0-mm compression and 150 ms dwell time (compression duration). Velocity was controlled by adjusting the pressure (compressed N_2) supplied to the pneumatic cylinder. Velocity and dwell time were measured by a linear velocity displacment transducer (Lucas Shaevitz™ model 500 HR; Detroit, MI, USA) that produces an analogue signal that was recorded by a storage-trace oscilloscope (BK Precision, model 2522B; Placentia, CA, USA). Sham-injured animals ($n = 4$) underwent identical surgical procedures but did not receive an impact injury. Appropriate pre- and post-injury management was maintained to insure that all guidelines set forth by the University of Florida Institutional Animal Care and Use Committee and the National Institutes of Health guidelines detailed in the Guide for the Care and use of Laboratory Animals was complied with.

CSF and cortical tissue preparation

The CSF and brain cortices were collected from animals at various intervals after sham-injury or TBI. At the appropriate time-points, TBI or sham-injured animals were anesthetized as described above and secured in a stereotactic frame with the head allowed to move freely along the longitudinal axis. The head was flexed so that the external occipital protuberance in the neck was prominent and a dorsal midline incision was made over the cervical vertebrae and occiput. The atlanto-occipital membrane was exposed by blunt dissection and a 25G needle attached to polyethylene tubing was carefully lowered into the cisterna magna. Approximately 0.1–0.15 mL of CSF was collected from each rat. Following CSF collection, animals were removed from the stereotactic frame and immediately killed by decapitation. Ipsilateral and contralateral (to the impact site) cortices were then rapidly dissected, rinsed in ice cold PBS, and snap frozen in liquid nitrogen. Cortices beneath the craniotomies were excised to the level of the white matter and extended ~4 mm laterally and ~7 mm rostrocaudally. The CSF samples were centrifuged at 4000 *g* for 4 min at 4°C to clear any contaminating erythrocytes. Cleared CSF and frozen tissue samples were stored at −80°C until ready for use. Cortices were homogenized in a glass tube with a Teflon dounce pestle in 15 volumes of an ice-cold triple detergent lysis buffer (20 mM HEPES, 1 mM EDTA, 2 mM EGTA, 150 mM NaCl, 0.1% SDS, 1.0% IGEPAL 40, 0.5% deoxycholic acid, pH 7.5) containing a broad range protease inhibitor cocktail (cat. #1-836-145Roche Molecular Biochemicals, Indianapolis, IN, USA).

Immunoblot analyses of CSF and cortical tissues

Protein concentrations of tissue homogenates and CSF were determined by bicinchoninic acid microprotein assays (Pierce Inc., Rockford, IL, USA) with albumin standards. Protein balanced samples were prepared for sodium dodecyl sulfate–polyacrylamide gel electrophoresis (SDS–PAGE) in twofold loading buffer containing 0.25 M Tris (pH 6.8), 0.2 M DTT, 8% SDS, 0.02% bromophenol blue, and 20% glycerol in distilled H_2O. Samples were heated for 10 min at 100°C and centrifuged for 1 min at 10 000 r.p.m. in a microcentrifuge at ambient temperature. Forty micrograms of protein per lane was routinely resolved by SDS–PAGE on 6.5% Tris/glycine gels for 1 h at 200 V. Following electrophoresis, separated proteins were laterally transferred to polyvinylidene fluoride (PVDF) membranes in a transfer buffer containing 0.192 M glycine and 0.025 M Tris (pH 8.3) with 10% methanol at a constant voltage of 100 V for 1 h at 4°C. Blots were blocked for 1 h at ambient temperature in 5% non-fat milk in TBS and 0.05% Tween-20. Panceau Red (Sigma, St Louis, MO, USA) was used to stain membranes to confirm successful transfer of protein and to insure that an equal amount of protein was loaded in each lane.

Antibodies and immunolabeling of PVDF membranes

Immunoblots containing brain or CSF protein were probed with an anti-α-spectrin (fodrin) monoclonal antibody (FG 6090 Ab; clone AA6; cat. # FG 6090; Affiniti Research Products Limited, UK) that detects intact non-erythroid αII-spectrin (280 kDa) and 150, 145 and 120 kDa cleavage fragments to αII-spectrin. A cleavage product of 150 kDa is initially produced by calpains or caspase-3 proteases (each proteolytic cleavage yields a unique amino-terminal region; Nath *et al.* 1996a; Wang *et al.* 1998). The calpain-generated 150 kDa product is further cleaved by calpain to yield a specific calpain signature product of 145 kDa (Harris *et al.* 1988; Nath *et al.* 1996a,b) whereas the caspase-3 generated 150 kDa product is further cleaved by caspase-3 to yield a specific caspase-3 signature product of 120 kDa (Nath *et al.* 1998; Wang *et al.* 1998). To further confirm the specificity of calpain-cleaved spectrin in CSF after TBI, a second antibody (anti-SBDP150; rabbit polyclonal) that recognizes only the calpain-cleaved N-terminal region (GMMPR) of the 150 kDa αII-spectrin breakdown product (SBDP) was also used (Saido *et al.* 1993; Nath *et al.* 1996b). Some immunoblots were immunolabeled with an antibody that recognizes erythroid αI-spectrin (Cat.# BYA10881; Accurate Chemical & Scientific Corp, Westbury, NY, USA). Following an overnight incubation at 4°C with the primary antibodies (FG 6090 Ab, 1 : 4000 for brain tissue and 1: 2000 for CSF; SBDP150 Ab, 1 : 1000; BYA10881, 1 : 400), blots were incubated for 1 h at ambient temperature in 3% non-fat milk that contained a horseradish peroxidase-conjugated goat anti-mouse IgG (1 : 10 000 dilution) or goat-anti-rabbit IgG (1 : 3000). Enhanced chemiluminescence (ECL; Amersham) reagents were used to visualize immunolabeling on Kodak Biomax ML chemiluminescent film.

Statisitical analyses

Semi-quantitative evaluation of protein levels detected by immunblotting was performed by computer-assisted densitometric scanning (AlphaImager 2000; Digital Imaging System, San Leandro, CA, USA). Data were acquired as integrated densitometric values and transformed to percentages of the densitometric levels obtained on scans from sham-injured animals visualized on the same blot. Data was evaluated by least squares linear regression followed by ANOVA. All values are given as mean ± SEM. Differences were considered significant if $p < 0.05$.

Results

Proteolysis of αII-spectrin in the cortex by calpain, but not caspase-3 after TBI

In the ipsilateral cortex, TBI resulted in decreased protein levels of αII-spectrin (280 kDa) that were associated with concomitant accumulation of calpain-generated 150 and 145 kDa αII-SBDPs (Fig. 1). However, there was little to no detectable increase in the caspase-3-genearated 120 kDa αII-SBDP. These results replicate our previous investigation that reported calpain but not caspase-3 processing of αII-spectrin following a moderate level of lateral controlled cortical impact TBI (Pike *et al.* 1998a). Decreased αII-spectrin (280 kDa) protein levels were 65%, 48% and 39% of sham-injured protein levels at 24 h, 48 h, and 72 h after TBI, respectively (Fig. 2). Increased 150 kDa αII-SBDP levels were 189%, 157%, and 153% of sham-injured levels at 24 h, 48 h and 72 h after TBI, respectively, while increased 145 kDa αII-SBDP levels were 237%, 203% and 198% of sham-injured levels at 24 h, 48 h and 72 h after TBI, respectively (Fig. 2).

In the contralateral cortex, traumatic brain injury resulted in no apparent alteration in protein levels of αII-spectrin (280 kDa) or in any apparent accumulation of calpain-generated 150 or 145 kDa αII-SBDPs, or in caspase-3 generated 120 kDa αII-SBDP as compared to sham-injured control animals (Fig. 1). These results are also in accord with our previous report that calpain-mediated processing of αII-spectrin is predominately confined to ipsilateral brain regions after moderate lateral controlled cortical impact TBI (Newcomb *et al.* 1997; Pike *et al.* 1998a).

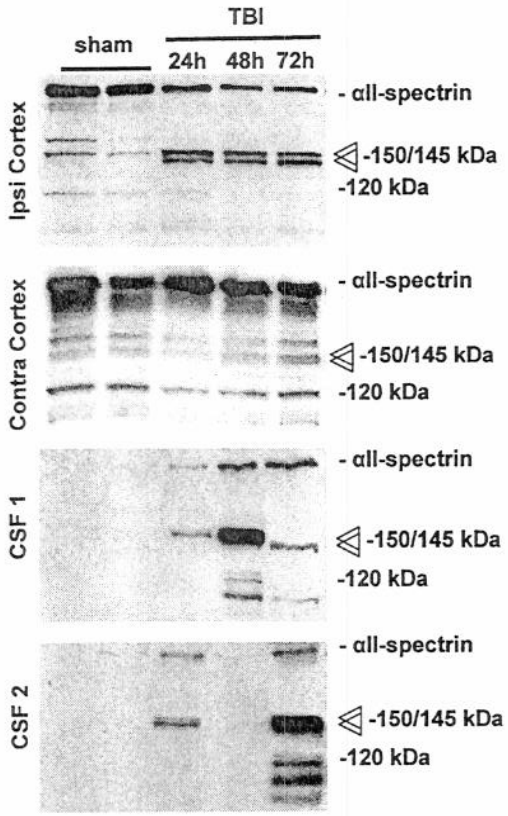

Fig. 1 Traumatic brain injury (TBI) results in prominent accumulation of αII-spectrin (280 kDa) and calpain-cleaved 150 kDa and 145 kDa αII-SBDPs in CSF (FG 6090 Ab). The caspase-3 generated 120 kDa fragment was also apparent in CSF of some animals. TBI caused proteolysis of constitutively expressed brain αII-spectrin (280 kDa) in ipsilateral but not contralateral cortex. Increases in the caspase-3-mediated 120 kDa αII-SBDP were not as apparent in ipsilateral or contralateral cortex after TBI. Immunolabeling of additional unknown bands at ~110 kDa and 95 kDa were also detected in CSF at 48 h and 72 h after injury. Both CSF1 and CSF2 are from two separate series of animals shown to illustrate that there was more variability in CSF levels of SBDPs than in brain levels, which may reflect individual differences in injury severity.

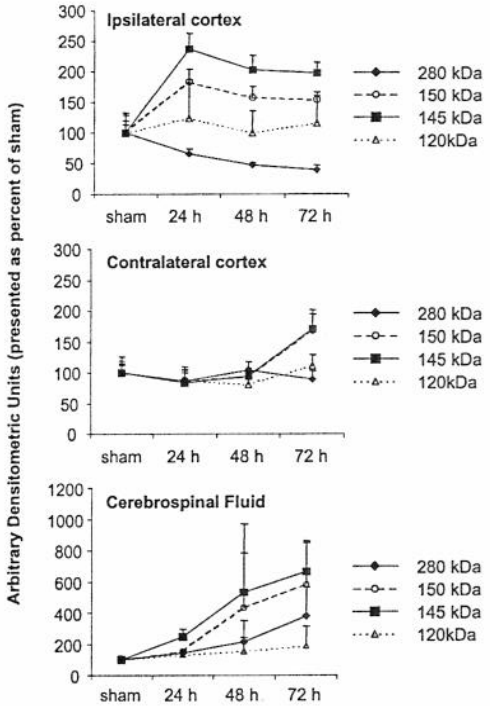

Fig. 2 Mean arbitrary densitometric units obtained from 280 kDa αII-spectrin and the 150 kDa and 145 kDa αII-SBDPs were converted to percent of sham-injured values. Decreases in 280 kDa αII-spectrin and increases in 150 kDa and 145 kDa αII-SBDPs (ipsilateral cortex) were associated with concomitant increases of these proteins in the CSF. Mean accumulation of the caspase-3 generated 120 kDa fragment in these tissues was relatively flat.

Delete 'both'

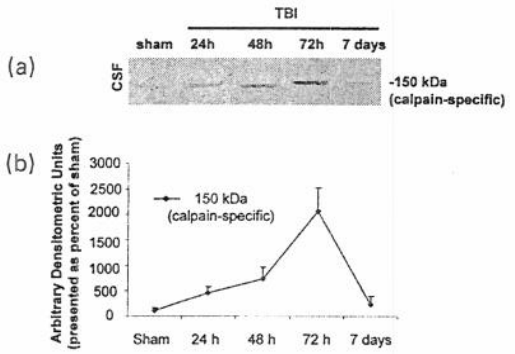

Fig. 3 N-terminal fragment-specific detection of calpain-generated SBDP150 in CSF after traumatic brain injury (SBDP150 Ab). (a) As with the FG 6090 Ab, the SBDP150 Ab detected a progressive increase in the calpain-cleaved 150 kDaA SBDP from 24 h to 72 h after TBI. Levels of 150 kDa SBDP had resolved to sham-injured control levels by seven days after TBI. (b) Mean arbitrary densitometric units of SBDP150 levels detected with anti-SBDP150 Ab.

Accumulation of calpain-mediated αII-SBDPs in CSF after TBI

Immunoblot analyses of CSF levels of non-erythroid αII-spectrin and αII-SBDPs (FG 6090 Ab) showed no detectable levels of these proteins in CSF of sham-injured control animals (Fig. 1). However, after TBI, accumulation of αII-spectrin (280 kDa) and calpain-generated 150 and 145 kDa SBDPs were markedly increased at 24 h, 48 h and 72 h, after injury (Fig. 1). In addition, there was an increase in the caspase-3-generated 120 kDa fragment in one animal at 48 h after TBI, and in another animal at 72 h after TBI (Fig. 1). Accumulation of αII-spectrin (280 kDa) protein levels was 143%, 212%, and 379% of sham-injured animals at 24 h, 48 h, and 72 h after TBI, respectively (Fig. 2). Similarly, accumulation of 150 kDa αII-SBDP after TBI was 155%, 434%, and 583% of sham-injured levels at 24 h, 48 h, and 72 h, respectively, while accumulation of 145 kDa αII-SBDP after TBI was 244%, 530%, and 665% of sham-injured levels at 24 h, 48 h and 72 h, respectively (Fig. 2). In contrast, although accumulation of the caspase-3 cleaved 120 kDa fragment was detected in two animals, the average response was relatively flat. In addition, several lower molecular weight species of αII-spectrin were detected. The protease(s) responsible for these lower molecular weight fragments are currently unknown. However, future identification of these bands may provide important new information regarding other neurochemical events in the brain after TBI.

To provide further confirmation of calpain-generated αII-SBDP accumulation in CSF after TBI, an additional group of animals ($n = 5$ per time-point) was injured as described above and immunoblots of CSF samples were probed with anti-SBDP150 Ab. In this experiment, an additional time-point (7 days post-TBI) was also examined. The SBDP150 Ab specifically recognizes only the calpain-cleaved 150 kDa αII-spectrin fragment and does not recognize the intact 280 kDa protein or other proteolytic fragments (Saido *et al.* 1993; Nath *et al.* 1996a). Results with the SBDP150 Ab were nearly identical to those obtained with the FG-6090 Ab (Fig. 3). The calpain-cleaved 150 kDa SBDP was nearly undetectable in CSF of sham-injured animals, and a progressive increase in immunoreactivity was observed from 24 h to 72 h after TBI. Importantly, this experiment also demonstrated that levels of calpain-cleaved 150 kDa SBDP were decreased back to sham-injured control levels by seven days after TBI (Fig. 3).

Linear regression analyses of Cortical versus CSF levels of αII-spectrin and αII-SBDPs

Least squares linear regression was calculated to determine the relationship between brain and CSF levels of αII-spectrin and αII-SBDPs over days post-injury. The slope of the regression lines for αII-spectrin and αII-SBDPs in brain and CSF were analyzed by ANOVA.

For cortical levels of 280 kDa αII-spectrin protein, the slope of the regression line was relatively steep and negative indicating large decreases over days in cortical levels of native αII-spectrin protein (Fig. 4). In contrast, the slope of the regression line for CSF levels of 280 kDa αII-spectrin was relatively steep and positive indicating large increases over days in CSF levels of αII-spectrin protein after TBI. In addition, ANOVA indicated that there was a significant difference ($F = 19.95$, $p < 0.001$) between cortical and CSF slopes for 280 kDa αII-spectrin protein level. This significance indicates that as brain levels of αII-spectrin decrease over days, CSF levels of αII-spectrin increase over days.

For cortical and CSF levels of 150 kDa αII-SBDP, both slopes of the regressions lines were positive indicating large increases in the calpain-cleaved 150 kDa αII-SBDP in brain and CSF over days (Fig. 4). ANOVA indicated no significant difference ($F = 1.86$, $p = 0.1873$) between slopes indicating that the relative accumulation of 150 kDa αII-SBDP in cortex and CSF were similar. However, the slope for CSF 150 kDa αII-SBDP was relatively steeper than the slope for cortical 150 kDa αII-SBDP. This result reflects the densitometric data (Fig. 2) indicating that, in the cortex, peak levels of the 150 kDa αII-SBDP accumulated rapidly (24 h) and were maintained at 48 h and 72 h post-injury. This result also reflects densitometric data (Fig. 2) indicating that CSF levels of the 150 kDa αII-SBDP accumulated more slowly early after injury (24 h) with a greater rate of further accumulation at 48 h and 72 h post-injury. Observed statistical differences in accumulation rates can be appreciated visually in the immunoblot data (Fig. 1). The stability of αII-spectrin and αII-SBDPs in CSF may be increased due to lack of endogenous proteases. For example,

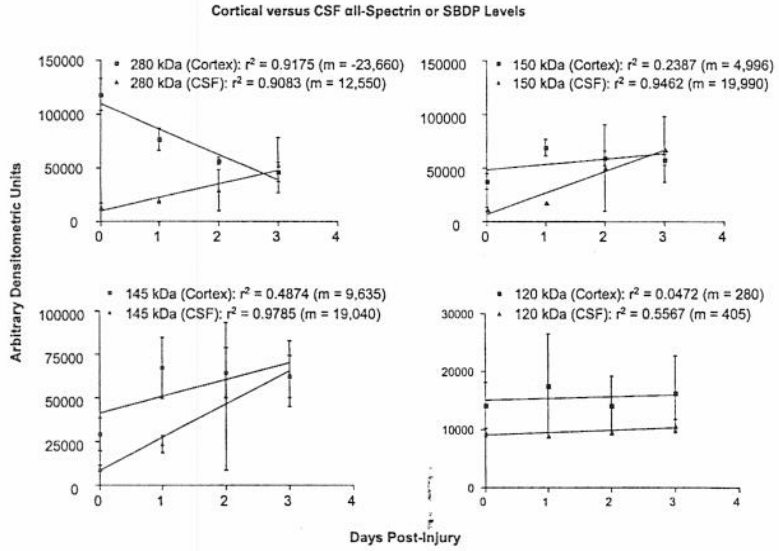

Fig. 4 Cortical versus CSF levels of αII-spectrin (280 kDa) and αII-SBDPs (150, 145, and 120 kDa) over days post-injury. Least squares regression lines of brain and CSF spectrin and SBDP levels were plotted on the same graph. Pearson correlation coefficients for each regression line are indicated. Results indicate that parenchymal decreases in levels of native αII-spectrin (280 kDa) are associated with increases in CSF accumulation while increased parenchymal levels of calpain-mediated αII-SBDPs (150 and 145 kDa) are associated with increased CSF accumulation. On average, there were no changes in parenchymal or CSF levels of the caspase-3-mediated 120 kDa αII-SBDP, although individual rats at different time points showed some increase in CSF levels of the 120 kDa product.

when CSF from TBI animals was stored in individual aliquots at either −85°C or at ambient laboratory temperature (~26°C) without protease inhibitors for 48 h, αII-SBDP levels from ambient temperature aliquots were only decreased by 28% compared to aliquots stored at −85°C (Fig. 5). Importantly, the relative stability of αII-SBDP protein in CSF at ambient temperature further indicates this protein as a useful biomarker after TBI.

For cortical and CSF levels of calpain-cleaved 145 kDa αII-SBDP, both slopes of the regression lines were steep and positive indicating large increases in the 145 kDa αII-SBDP in brain and CSF over days (Fig. 4). ANOVA indicated no significant difference ($F = 0.69$, $p = 0.4153$) between slopes indicating that the relative accumulation of 145 kDa αII-SBDP in cortex and CSF were similar as compared to the respective controls. Comparison of slopes for 150 kDa and 145 kDa αII-SBDPs in the brain revealed that the slope of the brain 145 kDa αII-SBDP over days was considerably steeper than the slope of the brain 150 kDa αII-SBDP. This result indicates that brain 145 kDa αII-SBDP protein levels accumulate at a greater rate over days than brain 150 kDa αII-SBDP protein levels. This observation is most likely the result of lower basal levels of brain 145 kDa αII-SBDP than brain 150 kDa αII-SBDP in sham-injured animals and of continued calpain digestion of the larger 150 kDa αII-SBDP to the smaller 145 kDa αII-SBDP over time.

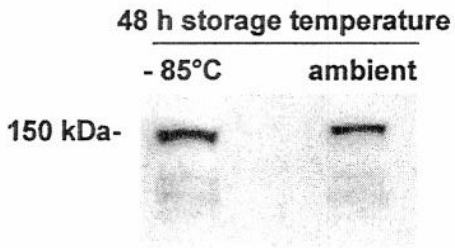

Fig. 5 Stability of αII-SBDP in CSF after prolonged storage in the absence of protease inhibitors at ambient laboratory temperature. The αII-SBDP protein levels only decreased by 28% when stored at ambient temperature (~26°C) for 48 h compared to identical samples stored at −85°C for 48 h. These results indicate that αII-SBDPs in CSF are relatively stable at room temperature. This is an important practical consideration for clinical utility.

For cortical and CSF levels of caspase-3-cleaved 120 kDa αII-SBDP, both slopes were nearly horizontal, indicating no increased accumulation of caspase-3-generated 120 kDa αII-SBDP over days after TBI (Fig. 4). In addition, ANOVA indicated no significant difference between slopes ($F = 0.002$, $p = 0.9621$).

Erythroid αI-spectrin versus non-erythroid αII-spectrin

After head injury, the most likely source of CSF contamination will be from blood. Both neurons and blood

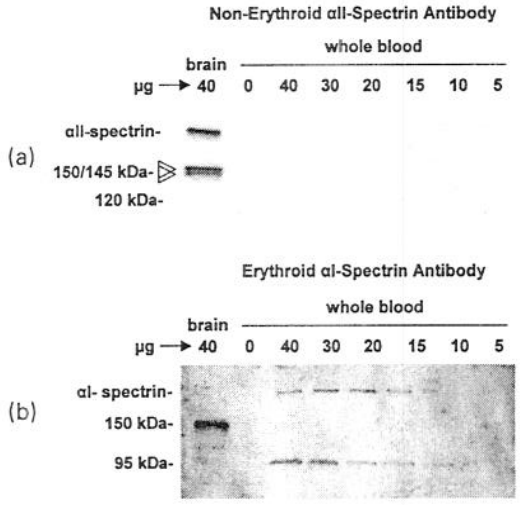

Fig. 6 (a) Non-erythroid αII-spectrin protein is not detected in whole blood. After TBI, the most probable source of non-CNS accumulation of proteins in the CSF is from blood. This immunoblot demonstrates that non-erythroid αII-spectrin is detectable in brain protein homogenates but not in blood protein homogenates. (b) In contrast, use of an erythroid αI-spectrin antibody on the same blot that has been stripped and re-probed reveals immunoreactivity for both blood and brain spectrin. These results demonstrate that potential blood contamination of CSF samples does not affect detection of brain-derived αII-spectrin.

contain the erythroid form αI-spectrin protein. However, erythrocytes do not contain non-erythroid αII-spectrin protein. To demonstrate that the source of αII-spectrin immunoreactivity in the CSF is not blood borne, we probed immunoblots containing various concentrations of whole blood proteins and brain protein with either an erythroid anti-αI-spectrin antibody or with an anti-αII-spectrin antibody (Fig. 6a,b). As predicted, no immunoreactivity was observed at any concentration of whole blood protein (0–40 μg) while brain spectrin was highly reactive to the non-erythroid anti-αII-spectrin antibody. In contrast, both the brain and blood protein samples were immunoreactive to the erythroid anti-αI-spectrin antibody. This result clearly indicates that use of the non-erythroid, but not the erythroid, anti-spectrin antibody can be used to discriminate non-blood borne spectrin protein in CSF samples.

Discussion

This paper provides the first evidence for accumulation of non-erythroid αII-spectrin protein and calpain-mediated αII-SBDPs in CSF after TBI. Detection of calpain-specific proteolytic fragments to αII-spectrin were confirmed with two antibodies, one that recognizes both intact αII-spectrin and calpain-specific SBDPs (FG 6090 Ab), and one that recognizes only the N-terminal region of calpain-cleaved 150 kDa SBDP (SBDP150 Ab). Results of this investigation indicate that CSF detection of αII-spectrin and αII-SBDPs can provide both a sensitive surrogate biochemical measure of TBI pathology and provide important information about specific neurochemical events that have occurred in the brain after TBI. To our knowledge, this is the first investigation of any CNS pathology to indicate that identification of accumulated CSF proteins or protein metabolic products can be used to infer specific neurochemical events (i.e. calpain activation) in the brain. Thus, use of αII-SBDPs as surrogate biochemical markers of TBI has important clinical ramifications for assessment of outcome after injury and for determination of specific pathological proteolytic cascades known to occur after TBI. Although other CNS proteins have been detected in CSF after brain injury (e.g. S-100B) and have been correlated with outcome, these proteins offer no insight into pathological mechanisms that have occurred in the brain after TBI. Obviously, identification of metabolic products with known neurochemical etiology will be beneficial for appropriate application of targeted therapeutics (such as calpain inhibitors) after TBI.

Calpain and caspase-3 cysteine proteases are important mediators of cell death and dysfunction in numerous CNS diseases and injuries including TBI. The calpains have historically been associated with necrotic (oncotic) cell death although recent evidence indicates a role in apoptotic cell death as well (Linnik *et al.* 1996; Nath *et al.* 1996a; Newcomb *et al.* 1998; Pike *et al.* 1998b). Numerous investigations have reported calpain activation after TBI (Saatman *et al.* 1996a, 2000; Kampfl *et al.* 1997; Newcomb *et al.* 1997; Posmantur *et al.* 1997; Pike *et al.* 1998a) and inhibitors of calpains have been shown to confer neuroprotection after TBI (Posmantur *et al.* 1997; Saatman *et al.* 1996b, 2000). Caspase-3 is a critical executioner of apoptosis and caspase-3 activation has been reported in *in vitro* (Shah *et al.* 1997; Allen *et al.* 1999; Pike *et al.* 2000b) and *in vivo* (Beer *et al.* 2000; Yakovlev *et al.* 1997; Pike *et al.* 1998a; Clark *et al.* 2000a) models of TBI. However, it should be noted that at least in our hands, the magnitude of calpain activation after TBI is much greater than that of caspase-3, and that at the moderate level of brain injury employed in the current study, caspase-3 is only transiently elevated in deep, non-cortical brain regions (Pike *et al.* 1998a). This result most likely accounts for the detection of relatively minimal amounts of the 120 kDa caspase-3-mediated αII-SBDP in CSF after TBI. In contrast to our injury model, Beer *et al.* (2000) have observed prominent levels of caspase-3 activation in the cortex after cortical impact TBI. However, while our cortical impact model is typically characterized by prominent tissue necrosis and progressive cortical cavitation to the gray–white interface (Kampfl *et al.* 1996; Newcomb *et al.* 1997;

Q5 change to 'a, b'

Q6 change to '2000b'

Dixon *et al.* 1998; Newcomb *et al.* 1999; Pike *et al.* 2000a), the model employed by Beer *et al.* (2000) was not. Thus, differences in injury magnitude may be important factors affecting calpain and/or caspase-3 activation after TBI, and this hypothesis warrants further investigation. However, it should be pointed out that although caspase-3 activation has not been a prominent feature in our model of cortical impact TBI, we have detected substantial levels of apoptotic cell death in the cortex after TBI (Newcomb *et al.* 1999). This apparent discrepancy between apoptotic cell death and caspase-3 activation raises the intriguing possibility that apoptosis may occur via a caspase-3-independent pathway after TBI. This observation also warrant further examination.

That different injury magnitudes may result in differential activation of calpain or caspase-3 proteases has important implications for targeted therapeutic intervention after TBI, and importantly, further validates the utility of using surrogate markers of TBI that have known neurochemical etiologies. For example, the current investigation detected CSF accumulation of the calpain-mediated αII-SBDP and not the caspase-3-mediated αII-SBDP. Based on this evidence, administration of calpain but not caspase-3 inhibitors would be predicted to have the most beneficial effect on outcome. However, other injury magnitudes may result in more caspase-3 activation indicating use of caspase-3 inhibitors or a combination of calpain/caspase-3 protease inhibitors. Thus, surrogate measures of TBI will result in selective pharmaceutical therapies based on clinical assessment of neuropathology, and this approach is a superior strategy to promiscuous prophylactic administration of unnecessary and potentially harmful compounds.

The most probable source of peripheral contamination of the CSF after TBI will be blood born. Indeed, we did detect visible red blood cell contamination of CSF after experimental TBI (which was removed by centrifugation). However, our control experiments with brain and whole blood immnuoblots (Fig. 6a,b) clearly demonstrated that the non-erythroid anti-αII-spectrin antibody did not detect any αII-spectrin protein in whole blood samples. Conversly, the erythroid αI-spectrin antibody labeled both brain and blood samples. These results indicate that the major source of potential peripheral CSF contamination after TBI, blood, is not detected by the non-erythroid anti-αII-spectrin antibody. This finding supports the utility of αII-spectrin and αII-SBDPs as surrogate biomarkers of injury after TBI, and importantly, as biomarkers of calpain and/or caspase-3 activation after TBI.

One caveat to the current investigation is the finding that there was more variability in levels of CSF SBDPs than there were in brain levels of SBDPs. This variability is indicated by the larger error bars in Fig. 2 and 4 and can be observed in individual animals in Fig. 1. The reason for the larger variability in CSF protein accumulation is unknown, but may reflect differences in individual animal's CSF circulation after TBI. For example, differences in increased intracranial pressure after TBI may restrict passage of CSF through various foramina that may preclude detection of secreted proteins into the cisterna magna (source of CSF in the present study). Additional studies should examine differences in intraventricular versus intracisternal levels of accumulated SBDPs.

Nonetheless, future studies focused on development of neuron-specific antibodies targeted against calpain-specific and caspase-3-specific αII-SBDPs (such as the SBDP150 Ab) will further strengthen the utility and specificity of αII-SBDPs as surrogate markers of brain injury. In addition, development of enzyme-linked immunosorbent assays (ELISA) will allow greater quantification of calpain and caspase-3 SBDPs and provide a more rapid and practical approach to CSF detection of these proteins.

Acknowledgements

This work was supported by National Institute of Health (NIH) R01 NS39091, NIH R01 NS40182, US Army DAMD17-99-1-9565 to RLH and by NIH award F32-NS10857 and the State of Florida Brain and Spinal Cord Rehabilitation Trust Fund (BSCIRTF) to BRP.

References

Allen J. W., Knoblach S. M. and Faden A. I. (1999) Combined mechanical trauma and metabolic impairment in vitro induces NMDA receptor-dependent neuronal cell death and caspase-3-dependent apoptosis. *FASEB J.* **13**, 1875–1882.

Beer R., Franz G., Srinivasan A., Hayes R. L., Pike B. R., Newcomb J. K., Zhao X., Schmutzhard E., Poewe W. and Kampfl A. (2000) Temporal profile and cell subtype distribution of activated caspase-3 following experimental traumatic brain injury. *J. Neurochem.* **75**, 1264–1273.

Buki A., Okonkwo D. O., Wang K. K. and Povlishock J. T. (2000) Cytochrome C release and caspase activation in traumatic axonal injury. *J. Neurosci.* **20**, 2825–2834.

Clark R. S., Kochanek P. M., Chen M., Watkins S. C., Marion D. W., Chen J., Hamilton R. L., Loeffert J. E. and Graham S. H. (1999) Increases in Bcl-2 and cleavage of caspase-1 and caspase-3 in human brain after head injury. *FASEB J.* **13**, 813–821.

Clark R. S., Kochanek P. M., Adelson P. D., Bell M. J., Carcillo J. A., Chen M., Wisniewski S. R., Janesko K., Whalen M. J. and Graham S. H. (2000a) Increases in Bcl-2 protein in cerebrospinal fluid and evidence for programmed cell death in infants and children after severe traumatic brain injury. *J. Pediatr.* **137**, 197–204.

Clark R. S., Kochanek P. M., Watkins S. C., Chen M., Dixon C. E., Seidberg N. A., Melick J., Loeffert J. E., Nathaniel P. D., Jin K. L. and Graham S. H. (2000b) Caspase-3 mediated neuronal death after traumatic brain injury in rats. *J. Neurochem.* **74**, 740–753.

Dixon C. E., Clifton G. L., Lighthall J. W., Yaghmai A. A. and Hayes R. L. (1991) A controlled cortical impact model of traumatic brain injury in the rat. *J. Neurosci. Meth.* **39**, 253–262.

Dixon C. E., Markgraf C. G., Angileri F., Pike B. R., Wolfson B., Newcomb J. K., Bismar M. M., Blanco A. J., Clifton G. L. and

Hayes R. L. (1998) Protective effects of moderate hypothermia on behavioral deficits but not necrotic cavitation following cortical impact injury in the rat. *J. Neurotrauma* **15**, 95–103.

Gennarelli T. A. (1994) Animate models of human head injury. *J. Neurotrauma* **11**, 357–368.

Goldstein M. (1990) Traumatic brain injury: a silent epidemic. *Ann. Neurol.* **27**, 327.

Goodman S. R., Zimmer W. E., Clark M. B., Zagon I. S., Barker J. E. and Bloom M. L. (1995) Brain spectrin: of mice and men. *Brain Res. Bull.* **36**, 593–606.

Goodman J. C. and Simpson R. K. Jr (1996) Biochemical monitoring in head injury. In: R. K. Narayan, J. E. Wilberger and J. T. Povlishock, eds. *Neurotrauma*, pp. 577–591. McGraw-Hill, New York.

Haber B. and Grossman R. G. (1980) Acetylcholine metabolism in intracranial and lumbar spinal cerebrospinal fluid and in blood. In: J. H. Wood, ed. *Neurobiology and Cerebrospinal Fluid*, pp. 345–350. Plenum, New York.

Harris A. S., Croall D. E. and Morrow J. S. (1988) The calmodulin-binding site in alpha-fodrin is near the calcium-dependent protease-I cleavage site. *J. Biol. Chem.* **263**, 15754–15761.

Inao S., Marmarou A., Clarke G. D., Anderson B. J., Fatouros P. P. and Young H. F. (1988) Production and clearance of lactate from brain tissue, cerebrospinal fluid, and serum following experimental brain injury. *J. Neurosurg.* **69**, 736–744.

Kampfl A., Posmantur R., Nixon R., Grynspan F., Zhao X., Liu S. J., Newcomb J. K., Clifton G. L. and Hayes R. L. (1996) Mu-calpain activation and calpain-mediated cytoskeletal proteolysis following traumatic brain injury. *J. Neurochem.* **67**, 1575–1583.

Kampfl A., Posmantur R. M., Zhao X., Schmutzhard E., Clifton G. L. and Hayes R. L. (1997) Mechanisms of calpain proteolysis following traumatic brain injury: implications for pathology and therapy: implications for pathology and therapy: a review and update. *J. Neurotrauma.* **14**, 121–134.

LaPlaca M. C., Raghupathi R., Verma A., Pieper A. A., Saatman K. E., Snyder S. H. and McIntosh T. K. (1999) Temporal patterns of poly (ADP-ribose) polymerase activation in the cortex following experimental brain injury in the rat. *J. Neurochem.* **73**, 205–213.

Linnik M. D., Markgraf C. G., Mason P. J., Velayo N. and Racke M. M. (1996) Calpain inhibition attenuates apoptosis in vitro and decreases infarct size in vivo. In: *Pharmacology of Cerebral Ischemia.* J. Krieglstein, ed. CRC Press, Boca Raton:pp. 33.–40.

Lyeth B. G., Jiang J. Y., Robinson S. E., Guo H. and Jenkins L. W. (1993) Hypothermia blunts acetylcholine increase in CSF of traumatically brain injured rats. *Mol. Chem. Neuropath.* **18**, 247–256.

Marion D. W. (1996) Outcome from severe head injury. In: R. K. Narayan, J. E. Wilberger and J. T. Povlishock, eds. *Neurotrauma*, pp. 767–777. McGraw-Hill, New York.

Meaney D. F., Ross D. T., Winkelstein B. A., Brasko J., Goldstein D., Bilston L. B., Thibault L. E. and Gennarelli T. A. (1994) Modification of the cortical impact model to produce axonal injury in the rat cerebral cortex. *J. Neurotrauma* **11**, 599–612.

Nath R., McGinnis K. J., Nadimpalli R., Stafford D. and Wang K. K. W. (1996a) Effects of ICE-like proteases and calpain inhibitors on neuronal apoptosis. *Neuroreport* **8**, 249–255.

Nath R., Raser K. J., Stafford D., Hajimohammadreza I., Posner A., Allen H., Talanian R. V., Yuen P., Gilbertson R. B. and Wang K. K. (1996b) Non-erythroid α-spectrin breakdown by calpain andinterleukin 1β-converting-enzyme-like protease (s) in apoptotic cells: contributory roles of both protease families in neuronal apoptosis. *Biochem. J.* **319**, 683–690.

Nath R., Probert A., McGinnis K. M. and Wang K. K. W. (1998) Evidence for activation of caspase-3-like protease in excitotoxin- and hypoxia/hypoglycemia-injured neurons. *J. Neurochem.* **71**, 186–195.

Nath R., Scott M., Nadimpalli R., Gupta R. and Wang K. K. (2000) Activation of apoptosis-linked caspase(s) in NMDA-injured brains in neonatal rats. *Neurochem. Int.* **36**, 119–126.

Newcomb J. K., Kampfl A., Posmantur R. M., Zhao X., Pike B. R., Liu S. J., Clifton G. L. and Hayes R. L. (1997) Immunohistochemical study of calpain-mediated breakdown products to alpha-spectrin following controlled cortical impact injury in the rat. *J. Neurotrauma.* **14**, 369–383.

Newcomb J. K., Zhao X., Pike B. R., Wang K. K. W. and Hayes R. L. (1998) Proteolytic mechanisms of cell injury following glucose-oxygen deprivation in primary septo-hippocampal cell cultures. *J. Neurotrauma.* **15**, 887.

Newcomb J. K., Zhao X., Pike B. R. and Hayes R. L. (1999) Temporal profile of apoptotic-like changes in neurons and astrocytes following controlled cortical impact injury in the rat. *Exp. Neurol.* **158**, 76–88.

Okonkwo D. O., Buki A., Siman R. and Povlishock J. T. (1999) Cyclosporin A limits calcium-induced axonal damage following traumatic brain injury. *Neuroreport.* **10**, 353–358.

Pike B. R., Zhao X., Newcomb J. K., Posmantur R. M., Wang K. K. W. and Hayes R. L. (1998a) Regional calpain and caspase-3 proteolysis of α-spectrin after traumatic brain injury. *Neuroreport.* **9**, 2437–2442.

Pike B. R., Zhao X., Newcomb J. K., Wang K. K. W., Posmantur R. M. and Hayes R. L. (1998b) Temporal relationships between de novo protein synthesis, calpain and caspase 3-like protease activation, and DNA fragmentation during apoptosis in septo-hippocampal cultures. *J. Neurosci. Res.* **52**, 505–520.

Pike B. R., Johnson E., Flint J., Glenn C. C. and Hayes R. L. (2000a) Prolonged calpain activation in regions of tissue atrophy after traumatic brain injury. *Restor. Neurol. Neurosci.* **16** (3, 4), 166.[abstract].

Pike B. R., Zhao X., Newcomb J. K., Glenn C. C., Anderson D. K. and Hayes R. L. (2000b) Stretch injury causes calpain and caspase-3 activation and necrotic and apoptotic cell death in septo-hippocampal cell cultures. *J. Neurotrauma.* **17**, 283–298.

Posmantur R., Kampfl A., Siman R., Liu J., Zhao X., Clifton G. L. and Hayes R. L. (1997) A calpain inhibitor attenuates cortical cytoskeletal protein loss after experimental traumatic brain injury in the rat. *Neuroscience.* **77**, 875–888.

Raabe A., Grolms C., Sorge O., Zimmermann M. and Seifert V. (1999) Serum S-100B protein in severe head injury. *Neurosurgery.* **45**, 477–483.

Raabe A. and Seifert V. (1999) Fatal secondary increase in serum S-100B protein after severe head injury. *J. Neurosurgery.* **91**, 875–877.

Riederer B. M., Zagon I. S. and Goodman S. R. (1986) Brain spectrin (240/235) and brain spectrin (240/235E): two distinct spectrin subtypes with different locations within mammalian neural cells. *J. Cell Biol.* **102**, 2088–2097.

Roberts-Lewis J. M., Savage M. J., Marcy V. R., Pinsker L. R. and Siman R. (1994) Immunolocalization of μ-calpain mediated spectrin degradation to vulnerable neurons in ischemic gerbil brain. *J. Neurosci.* **14**, 3934–3944.

Robinson S. E., Martin R. M., Davis T. R., Gyenes C. A., Ryland J. E. and Enters E. K. (1990) The effect of acetylcholine depletion on behavior following traumatic brain injury. *Brain Res.* **509**, 41–46.

Saatman K. E., Bozyczko-Coyne D., Marcy V., Siman R. and McIntosh T. K. (1996a) Prolonged calpain-mediated spectrin breakdown occurs regionally following experimental brain injury in the rat. *J. Neuropathol. Exp. Neurol.* **55**, 850–860.

Saatman K. E., Murai H., Bartus R. T., Smith D. H., Hayward N. J.,

Perri B. R. and McIntosh T. K. (1996b) Calpain inhibitor AK295 attenuates motor and cognitive deficits following experimental brain injury in the rat. *Proc. Natl Acad. Sci. USA* **93**, 3428–3433.

Saatman K. E., Zhang C., Bartus R. T. and McIntosh T. K. (2000) Behavioral efficacy of posttraumatic calpain inhibition is not accompanied by reduced spectrin proteolysis, cortical lesion, or apoptosis. *J. Cereb. Blood Flow Metab.* **20**, 66–73.

Saido T. C., Yokota M., Nagao S., Yamaura I., Tani E., Tsuchiya T., Suzuki K. and Kawashima S. (1993) Spatial resolution of fodrin proteolysis in postischemic brain. *J. Biol. Chem.* **268**, 25239–25243.

Shah P. T., Yoon K. W., Xu X. M. and Broder L. D. (1997) Apoptosis mediates cell death following traumatic injury in rat hippocampal neurons. *Neuroscience.* **79**, 999–1004.

Tapiola T., Pirttila T., Mikkonen M., Mehta P. D., Alafuzoff I., Koivisto K. and Soininen H. (2000) Three-year follow-up of cerebrospinal fluid tau, β-amyloid 42 and 40 concentrations in Alzheimer's disease. *Neurosci. Lett.* **280**, 119–122.

Wang K. K. W., Posmantur R. M., Nath R., McGinnis K. M., Whitton M., Talanian R. V., Glantz S. B. and Morrow J. S. (1998) Simultaneous degredation of αII and βII spectrin by caspase-3 (CPP32) in apoptotic cells. *J. Biol. Chem.* **273**, 22490–22497.

Yakovlev A. G., Knoblach S. M., Fan L., Fox G. B., Goodnight R. and Faden A. I. (1997) Activation of CPP32-like caspases contributes to neuronal apoptosis and neurological dysfunction after traumatic brain injury. *J. Neurosci.* **17**, 7415–7424.

Zemlan F. P., Rosenberg W. S., Luebbe P. A., Cambell T. A., Dean G. E., Weiner N. E., Cohen J. A., Rudick R. A. and Woo D. (1999) Quantification of axonal damage in traumatic brain injury: affinity purification and characterization of cerebrospinal fluid tau proteins. *J. Neurochem.* **72**, 741–750.

Zhang C., Raghupathi R., Saatman K. E., LaPlaca M. C. and McIntosh T. K. (1999) Regional and temporal alterations in DNA fragmentation factor (DFF)-like proteins following experimental brain trauma in the rat. *J. Neurochem.* **73**, 1650–1659.

Zhao X., Pike B. R., Newcomb J. K., Wang K. K., Posmantur R. M. and Hayes R. L. (1999) Maitotoxin induces calpain but not caspase-3 activation and necrotic cell death in primary septo-hippocampal cultures. *Neurochem. Res.* **24**, 371–382.

Zhao X., Newcomb J. K., Pike B. R., Wang K. K., d'Avella D. and Hayes R. L. (2000) Novel characteristics of glutamate-induced cell death in primary septohippocampal cultures: relationship to calpain and caspase-3 protease activation. *J. Cereb. Blood Flow Metab.* **20**, 550–562.

Journal of Cerebral Blood Flow and Metabolism
21:1281–1294 © 2001 The International Society for Cerebral Blood Flow and Metabolism
Published by Lippincott Williams & Wilkins, Inc., Philadelphia

Concurrent Assessment of Calpain and Caspase-3 Activation After Oxygen–Glucose Deprivation in Primary Septo-Hippocampal Cultures

Jennifer K. Newcomb-Fernandez, Xiurong Zhao, *Brian R. Pike, †Kevin K. W. Wang, ‡Andreas Kampfl, ‡Ronald Beer, *S. Michelle DeFord, and *Ronald L. Hayes

*University of Texas Health Science Center-Houston, Department of Neurosurgery, The Vivian L. Smith Center for Neurologic Research, Houston, Texas, *Evelyn F. and William L. McKnight Brain Institute of the University of Florida, Department of Neuroscience, Gainesville, Florida, and †Park-Davis Pharmaceutical Research, Warner-Lambert Company, Ann Arbor, Michigan, U.S.A.; and ‡University Hospital Innsbruck, Department of Neurology, Innsbruck, Austria*

Summary: The contributions of calpain and caspase-3 to apoptosis and necrosis after central nervous system (CNS) trauma are relatively unexplored. No study has examined concurrent activation of calpain and caspase-3 in necrotic or apoptotic cell death after any CNS insult. Experiments used a model of oxygen–glucose deprivation (OGD) in primary septo-hippocampal cultures and assessed cell viability, occurrence of apoptotic and necrotic cell death phenotypes, and protease activation. Immunoblots using an antibody detecting calpain and caspase-3 proteolysis of α-spectrin showed greater accumulation of calpain-mediated breakdown products (BDPs) compared with caspase-3–mediated BDPs. Administration of calpain and caspase-3 inhibitors confirmed that activation of these proteases contributed to cell death, as inferred by lactate dehydrogenase release. Oxygen–glucose deprivation resulted in expression of apoptotic and necrotic cell death phenotypes, especially in neurons. Immunocytochemical studies of calpain and caspase-3 activation in apoptotic cells indicated that these proteases are almost always concurrently activated during apoptosis. These data demonstrate that calpain and caspase-3 activation is associated with expression of apoptotic cell death phenotypes after OGD, and that calpain activation, in combination with caspase-3 activation, could contribute to the expression of apoptotic cell death by assisting in the degradation of important cellular proteins. **Key Words:** Apoptosis—Calpain—Caspases—Necrosis—Stroke—TBI.

Increased activation of calpain and caspase-3 occurs in many central nervous system (CNS) injuries and diseases. Caspase-3 is considered a key executioner in the apoptotic cell death cascade and shares numerous substrates with the Ca^{2+}-dependent protease calpain, including the cytoskeletal protein α-spectrin (Wang, 2000). Studies examining animal models of ischemia have reported increased calpain (Bartus et al., 1995; Roberts-Lewis et al., 1994; Yokota et al., 1995; Rami et al., 2000) or caspase-3 (Chen et al., 1998; Namura et al., 1998) activation after injury. Furthermore, inhibition of calpain (Hong et al., 1994; Markgraf et al., 1998) or caspase-3 (Fink et al., 1998; Himi et al., 1998) reduced infarct volume, substrate proteolysis, DNA fragmentation, and hippocampal cell death after focal and global ischemia. Activation of these proteases also has been observed in animal models of traumatic brain injury (TBI) (Newcomb et al., 1997; Pike et al., 1998*a*; Saatman et al., 1996; Yakovlev et al., 1997; Clark et al., 2000; Beer et al., 2000; Buki et al., 2000). Inhibition of calpain (Postmantur et al., 1997) or caspase-3 (Yakovlev et al., 1997) is protective in these models, although conflicting data has been reported (Clark et al., 2000; Saatman et al., 2000). However, few investigations have examined concurrent activation of calpain and caspase-3 after CNS injury or disease (Buki et al., 2000; Nath et al., 1998; Pike et al., 1998*a*).

Received February 6, 2001; final revision received July 23, 2001; accepted July 25, 2001.

Supported by NIH grants RO1 NS39091 and RO1 NS40182, US Army DAMD 17–99–1-9565, an endowment from the Vivian L. Smith Center for Neurologic Research, and the Austrian Science Fund P12287 MED.

Address correspondence and reprint requests to Ronald L. Hayes, PhD, Director, Center for Traumatic Brain Injury Studies, Professor of Neuroscience, Neurosurgery and Clinical and Health Psychology, Evelyn F. and William L. McKnight Brain Institute of the University of Florida, Department of Neuroscience, 100 Newell Dr., Box 100244, Gainesville, FL 32610, U.S.A.

Although apoptosis and necrosis occur after ischemia (Linnik et al., 1993) and TBI (Colicos and Dash, 1996; Newcomb et al., 1999; Rink et al., 1995), the relation between protease activation and the expression of apoptotic and necrotic cell death phenotypes is relatively unexplored. Traditionally, calpain activation has been associated with necrosis, and caspase-3 activation with apoptosis. Although caspase-3 activation has not been detected in models of necrosis (Wang et al., 1996; Zhao et al., 1999), calpain activation has been implicated in various models of apoptosis (Nath et al., 1996; Pike et al., 1998*b*; Squier et al., 1994; Vanags et al., 1996). However, inconsistencies in criteria associated with cell death phenotypes have complicated data interpretation (Charriaut-Marlangue and Ben-Ari, 1995).

Oxygen–glucose deprivation (OGD) is a widely used *in vitro* model of ischemia, which produces apoptotic (Kalda et al., 1998) and necrotic (Gwag et al., 1995; Goldberg and Choi, 1993) cell death phenotypes and increased calpain and caspase-3 activity (Nath et al., 1998). Currently, no study has investigated the concurrent activation of calpain and caspase-3 in archetypal necrotic and apoptotic cell death phenotypes after any CNS insult. The current study sought to determine the contributions of these proteases to apoptotic and necrotic cell death after OGD. The current findings demonstrate that coactivation of calpain and caspase-3 is usually associated with the expression of apoptotic cell death phenotypes after OGD.

MATERIALS AND METHODS

Primary septo-hippocampal cultures

Septi and hippocampi were dissected from 18-day-old rat fetuses, dissociated by trituration, and the dissociated cells were plated on poly-L-lysine coated 24-well culture plates, 6-well culture plates or 12-mm German Glass (Erie Scientific, Portsmouth, NH, U.S.A.) at a density of 4.36×10^5 cells/mL. Cultures were maintained in Delbecco's modified Eagle's medium (DMEM) with 10% fetal bovine serum in a humidified incubator in an atmosphere of 5% CO_2 at 37°C. After 5 days in culture, the media was changed to DMEM with 5% horse serum. Subsequent media changes were performed three times a week. Experiments were performed on days 10 to 11 *in vitro* when astroglia had formed a confluent monolayer beneath morphologically mature neurons. All animal studies conformed to the guidelines outlined in *Guide for the Care and Use of Laboratory Animals* from the National Institutes of Health and were approved by the University of Florida and the University of Texas-Houston Health Science Center Animal Welfare Committee.

Oxygen–glucose deprivation

To achieve oxygen–glucose deprivation (OGD), a technique similar to that described by Copin et al. (1998) was used. Normal media was replaced with low glucose media (Hank's balanced salt solution containing 1.8 mmol/L Ca^{2+}, 0.8 mmol/L Mg^{2+}, and 0.2 g/L d-glucose) and culture plates were placed in an airtight chamber (Billups-Rothenberg, Del Mar, CA, U.S.A.). The chamber was flushed with 95% N_2/5% CO_2 for 3 minutes, sealed, and placed in a 37°C incubator for the appropriate duration. Initial experiments that manipulated the amount of time (1 to 10 minutes) the chamber was flushed with 95% N_2/5% CO_2 confirmed that 3 minutes of flushing combined with the low glucose media produced an environment severe enough to result in a consistent model of cell injury. After the insult, low glucose media was replaced with DMEM (serum-free) and cultures were returned to a normoxic environment. Initial experiments deprived cells of oxygen and glucose for various durations (1 to 12 hours) and samples were collected 24 hours after the cultures had returned to a normal environment. These data suggested that 10 hours of OGD resulted in substantial cell death and protease activation. To examine the effects of altering the length of reperfusion (that is, duration of normoxia after OGD) samples were collected at various times (immediately through 48 hours) after 10 hours of OGD. Subsequent experiments focused on 10 hours of OGD combined with 24 hours of reperfusion, unless stated otherwise.

Chemical inducers of apoptotic or necrotic cell death phenotypes

To provide comparisons of OGD with classic apoptotic and necrotic profiles, cultures were treated with staurosporine, a general protein kinase inhibitor, or maitotoxin, a potent marine toxin that activates both voltage-sensitive and receptor-operated calcium channels (Wang et al., 1996). Cultures were challenged with 0.5 μmol/L staurosporine for 24 hours, a dose and duration that produces apoptotic but not necrotic neuronal cell death in this *in vitro* system (Pike et al., 1998*b*). Separate cultures were treated with maitotoxin (0.1 nmol/L) for 1 hour, a dose and duration that produces an exclusively necrotic cell death profile in neurons and glia and is associated with calpain, but not caspase-3 activation (Zhao et al., 1999).

Pharmacologic inhibition of calpain and caspase activation

Cultures were pretreated 1 hour before and were cotreated during OGD, with various doses of calpain inhibitor-3 (CI-3, [MDL28170], 1 to 300 μmol/L; CalBiochem, San Diego, CA, U.S.A.), the pan-caspase inhibitor (Z-D-DCB, 50 to 200 μmol/L; Bachem, Philadelphia, PA, U.S.A.) or the specific caspase-3 inhibitor (z-DEVD-fmk, 50 to 200 μmol/L; CalBiochem). Stock solutions (50 mmol/L) of CI-3 (in dimethyl sulfoxide), Z-D-DCB (in EtOH), and z-DEVD-fmk (in dimethyl sulfoxide) were added directly to the low glucose media for the 1-hour pretreatment, and then cells were deprived of oxygen. Initial experiments confirmed that incubating cells with low glucose media for 1 hour had no effect on control cells or injury magnitude in cells later exposed to OGD (data not shown). After OGD, low glucose media was replaced with DMEM (serum-free) containing fresh inhibitor. Samples were collected 12 or 24 hours after OGD for lactate dehydrogenase (LDH) release and immunoblot analyses. Western blot analyses confirmed whether the drugs and doses used inhibited activation of calpain and caspase-3–like proteases inferred by α-spectrin proteolysis.

Determination of lactate dehydrogenase activity

Lactate dehydrogenase activity assessed cell viability (Koh and Choi, 1987) in experiments examining the effects of OGD and protease inhibition. Lactate dehydrogenase released from damaged cells was measured by standard kinetic assay for pyruvate (Hoffmann-LaRoche Ltd., Basel, Switzerland). Briefly, culture medium was removed from each well and centrifuged at 5,000 *g* for 5 minutes. One hundred microliters of supernatant was transferred to each well of 96-well flat bottom plate and 100 μL of detection reagent was added. After incubation, the

absorbance of samples was measured at 490 nm using Bio-Rad model 450 microplate reader (Hercules, CA, U.S.A.).

Annexin V and propidium iodide staining

Control cells and cells exposed to OGD, staurosporine, or maitotoxin were simultaneously stained with Annexin V and propidium iodide (PI) to differentiate apoptotic and necrotic cell death phenotypes. Cells were rinsed with phosphate-buffered saline (PBS) and incubated in staining solution consisting of HEPES buffer, Annexin V fluorescein labeling reagent (Molecular Probes; Eugene, OR, U.S.A.), and PI (Molecular Probes) for 15 minutes in the dark. Stained cells were examined with a Zeiss Axiovert 135 fluorescence microscope (Oberkochen, Germany) fitted with a filter combination that allowed green and red fluorescing cells to be seen simultaneously. The number of apoptotic and necrotic cells was calculated (10 sequential 320× fields were counted and averaged per well) for n = 3 wells per condition.

DNA gel electrophoresis

DNA gel electrophoresis was performed as previously described (Zhao et al., 2000; Gong et al., 1994). At the appropriate time after injury, cells were collected by centrifugation, fixed in 70% cold ethanol, and stored in fixative at −20°C for 24 to 72 hours. After subsequent centrifugation and removal of ethanol, cell pellets were resuspended in phosphate-citrate buffer at room temperature for 1 hour, centrifuged, and the supernatant was concentrated by vacuum in a SpeedVac concentrator (ThermoSavant, Holbrook, NY, U.S.A.). The pellet was incubated in Nonidet NP-40 and DNase-free RNase followed by proteinase K. After the incubation, 6× loading buffer was added and the contents of the tube were transferred to a 1.5% agarose gel. Electrophoresis was performed in 1× 0.1 mol/L Tris, 0.09 mol/L boric acid, 1 mmol/L EDTA, pH 8.4 at 40 V for 2 hours. DNA was visualized and photographed under UV light after staining with 5 μg/mL ethidium bromide.

DNA fragmentation ELISA

Apoptotic cell death also was examined with an assay that allowed specific determination of mono- and oligonucleosomes in the cytoplasmic fraction of cell lysates (Cell Death Detection ELISA Plus; Hoffman-LaRoche Ltd., Basel, Switzerland). At the appropriate time after injury, cells were collected by centrifugation and 2 mL lysis buffer was mixed with the pellet. The solution was incubated for 30 minutes at room temperature and stored at −20°C for 24 to 72 hours. After thawing, diluted samples (5 μL sample + 15 μL lysis buffer) were added to each well of a streptavidin-coated, 96-well microtiter plate (separate studies confirmed that this dilution resulted in a suitable cell concentration, data not shown). Eighty microliters of reagent solution containing incubation buffer, anti–histone-biotin, and anti–DNA-POD was added to each well and incubated with the sample on a shaker for 2 hours. The solution was removed and wells were rinsed with incubation buffer to remove unbound antibody. The amount of POD retained in the immunocomplex—and thus the amount of DNA fragments—was determined colorimetrically with the substrate ABTS using a microplate reader (Bio-Rad Model 450) at 405 nm with a reference filter of 490 nm. Absorbance values were calculated and reported as percent of control.

Assessment of caspase-3 and calpain activity

The cytoskeletal protein α-spectrin contains sequence motifs preferred by calpain and caspase-3 proteases; thus, activation of these proteases can be assessed concurrently by immunoblot identification of calpain and/or caspase-3 signature cleavage products. Although calpains and caspases produce initial fragments of nearly identical size (150 kDa), calpains further process α-spectrin into a distinctive breakdown product (BDP) of 145 kDa (Harris et al., 1988; Nath et al., 1996), whereas caspase-3 produces a unique 120-kDa BDP (Wang et al., 1998*b*). Notably, the initial 150-kDa fragment produced by calpain differs from that produced by the caspases. Immunocytochemistry using antibodies specific for this calpain-mediated fragment (SBDP 150) or the 120-kDa fragment produced by caspase-3 (SBDP 120) allows detection of calpain- and/or caspase-3–mediated proteolysis of α-spectrin in individual cells. Caspase-3 activation also can be inferred by the appearance of BDPs to the proenzyme, because activation occurs when caspase-3 is proteolyzed into smaller subunits.

Sodium dodecyl sulfate-polyacrylamide gel electrophoresis and immunoblotting. Gel electrophoresis and immunoblotting were performed as described previously (Pike et al., 2000). At the appropriate time after injury, media was removed and cells were collected from each well with lysis buffer and sheared with a 25-gauge needle. Protein content was assayed by the Micro BCA method (Pierce, Rockford, IL, U.S.A.). For protein electrophoresis, equal amounts of total protein (25 μg) were prepared in 4× loading buffer and heated at 95°C for 10 minutes. For analysis of α-spectrin proteolysis, samples were resolved in a vertical electrophoresis chamber using a 4% stacking gel over a 6.5% acrylamide resolving gel. Separated proteins were laterally transferred to a nitrocellulose membrane (0.45 μm). For analysis of caspase-3 proteolysis, samples were resolved using a 4% to 20% gradient acrylamide gel or a Tris-Tricine gel (16.5% + 4% stacking). Separated proteins were laterally transferred to a nitrocellulose membrane (0.2 μm). Nitrocellulose membranes were stained with Panceau red (Sigma, St. Louis, MO, U.S.A.) to ensure even transfer of all samples to the membranes and to confirm that equal amounts of protein were loaded in each lane. Blots were blocked overnight in 5% nonfat milk in 20 mmol/L Tris, 0.15 mol/L NaCl, and 0.005% Tween-20 at 4°C.

Immunoblots were probed with an anti–α-spectrin monoclonal antibody (Affiniti Research Products, U.K.) that detects intact α-spectrin (MW_r = 240 kDa) and 150-, 145-, and 120-kDa BDP, as described previously (Pike et al., 2000). Separate blots were probed with a caspase-3 polyclonal antibody (1:500; Santa Cruz Biotechnology, Santa Cruz, CA, U.S.A.) that detects the caspase-3 proenzyme (32 kDa) and proteolytic fragments. After incubation in primary antibody for 2 hours at room temperature, blots were incubated in peroxidase-conjugated goat anti-rabbit IgG (1:3000) for 1 hour. Enhanced chemiluminescence reagents (ECL; Amersham, Buckinghamshire, U.K.) were used to visualize immunolabeling on Hyperfilm (Hyperfilm ECL; Amersham).

Semiquantitative evaluation of protein levels detected by immunoblotting was performed through computer-assisted, one-dimensional densitometric scanning (AlphaImager 2000 Digital Imaging System; San Leandro, CA, U.S.A.). Data were acquired as integrated densitometric values and transformed to percentages of the densitometric values obtained from control samples. Data from multiple Western blots (n = 4) were combined and analyzed statistically.

Calpain- and caspase-3–mediated α-spectrin BDPs in individual cells. Cells were cultured on German Glass for immunocytochemistry protocols. Control cultures or cells exposed to OGD, staurosporine, or maitotoxin were fixed in 4% paraformaldehyde for 5 minutes and rinsed in PBS. Cells were blocked in 10% normal goat serum in PBS for 30 minutes at 37°C and incubated simultaneously in primary antibodies specific for SBDP 150 (1:100, polyclonal, made in rabbit; gift

from T.C. Saido, Japan, (Saido et al., 1993)) and SBDP 120 (1:100, polyclonal, made in chicken; gift from Kevin Wang, Parke-Davis, Ann Arbor, MI (Buki et al., 2000)) for 30 minutes at 37°C. After rinsing in PBS/0.05% Tween 20, cells were incubated in secondary antibodies linked to Alexa Fluor 488 (1:50, goat α-chicken; Molecular Probes, Eugene, OR, U.S.A.) or Alexa Fluor 568 (1:50, goat α-rabbit; Molecular Probes) for 30 minutes at 37°C. To assess nuclear morphology (that is, characteristics of necrotic or apoptotic alterations) cells were counterstained with the DNA dye, 4′ 6-diamidino-2-phenylindole, dihydrochloride (DAPI, 1:500; Molecular Probes). German Glass were mounted onto glass slides with Fluoromount-G (Southern Biotechnology Associates; Birmingham, AL, U.S.A.).

Cells were examined under oil immersion at 1000× magnification with a Zeiss Axiovert 135 fluorescence microscope equipped as described above. DAPI staining was viewed with a UV2A filter (Zeiss). Nuclear morphology was assessed in cells immunoreactive for SBDP 150, or SBDP 120, or both, and cells were categorized (blind to treatment condition) as healthy, apoptotic, or necrotic. Nuclei of healthy cells can be identified by a homogenous and diffuse fluorescent chromatin, whereas cells classified as apoptotic fluoresce intensely and are characterized by highly condensed chromatin, visibly shrunken and often irregular shaped nuclei, margination of chromatin along the periphery of the nuclear envelope, or by the separation of the nucleus into discrete nuclear fragments (apoptotic bodies). In contrast, necrotic cells fluoresce brightly with pyknotic chromatin where nuclei have maintained their basic morphology or have become rounded or swollen in appearance. These cells also fail to exhibit apoptotic morphology (Schmechel, 1999; Purnanam and Boustany, 1999). Using these criteria, the number of healthy, apoptotic, and necrotic SBDP 150 and SBDP 120 immunoreactive cells were quantified in control and OGD cultures.

Analysis of cell types

Control cells or cells exposed to OGD were prepared for immunocytochemistry as described above. Cells were labeled with both neuronal nuclear marker (NeuN) and microtubule-associated protein (MAP)2 or GFAP (glial fibrillary acidic protein) to evaluate neuronal and astroglial morphology, respectively. Using both NeuN and MAP2 allowed clear visualization of the neuronal cell body and processes. All cells were blocked in 10% normal goat serum in PBS and were incubated in primary antibodies specific for NeuN (1:1000, monoclonal; Chemicon, Temecula, CA, U.S.A.) and MAP2 (1:1000, monoclonal; Sternberger Monoclonals, Lutherville, MD, U.S.A.) or GFAP (1:1000, monoclonal; Sigma). After rinsing in PBS/0.05% Tween 20, cells were incubated in secondary antibody linked to Alexa Fluor 488 (1:50, goat α-mouse; Molecular Probes). Cells were counterstained with DAPI and mounted onto glass slides with Fluoromount-G.

Samples immunolabeled with NeuN and MAP2 were examined under low magnification to assess neuronal loss after OGD (10 sequential 320× fields were counted and added per sample, n = 6). Samples immunolabeled with GFAP also were examined under low magnification, however quantitative data on loss of GFAP-positive cells could not be obtained because of the high density of these cells and the inability to differentiate individual glia. Under high magnification (1000×), DAPI staining was examined in NeuN- and/or MAP2-positive cells and GFAP-positive cells (50 random immunoreactive cells per sample) to assess the nuclear morphology of neurons and astroglia, respectively. Values for healthy, apoptotic, and necrotic neurons and astroglia were calculated for control and OGD cells using the criteria described above.

Statistical analysis

Data were evaluated by one-way analysis of variance and *post hoc* least significant difference *t* test. Values are given as mean ± SD. Differences were considered significant at $P \leq 0.05$.

RESULTS

Effects of oxygen–glucose deprivation on primary mixed septo-hippocampal cultures

Effects of oxygen–glucose deprivation duration and reperfusion. An initial set of experiments (data not shown) was conducted to evaluate duration of OGD on cell viability. Primary mixed septo-hippocampal cultures were deprived of oxygen and glucose for 1, 6, 8, 10, or 12 hours and media was collected 24 hours after cultures were returned to normal conditions for analysis of LDH release. Reported as percent of control, significant increases in LDH release ($P < 0.01$) occurred after 6 (204% ± 18.1%), 8 (233% ± 30.1%), 10 (895% ± 43.1%), and 12 (725% ± 70.5%) hours of OGD. Subsequent experiments (data not shown) investigated the effect of reperfusion length on cell viability. Samples were subjected to OGD for 10 hours and media were collected immediately or after 3, 12, 24, or 48 hours of reperfusion for analysis of LDH release. Significant increases in LDH release were evident immediately after injury (172% ± 15.2%, $P < 0.05$) compared with control cultures. Moreover, increasing the length of reperfusion resulted in a time-dependent and significant increase in LDH release ($P < 0.001$) at all later times tested—3 (367% ± 51.7%), 12 (561% ± 5.6%), 24 (674% ± 14.7%), and 48 (784% ± 5.6%) hours after injury, compared with control samples.

Characterization of cell death phenotypes after oxygen-glucose deprivation. To distinguish apoptotic and necrotic cell death, control cells and cells subjected to OGD (10 hours + 24 hours of reperfusion) were stained with Annexin V and PI (data not shown). Staurosporine- (0.5 mmol/L for 24 hours) and maitotoxin- (0.1 nmol/L for 1 hour) treated cells were used as positive controls of apoptosis and necrosis, respectively. Values are reported as total apoptotic or necrotic cells per well (10, 320× fields). Uninjured control cultures contained few apoptotic (78.0 ± 40.0) or necrotic (8.3 ± 2.1) cells. Cultures subjected to OGD contained significantly ($P < 0.001$) more apoptotic (356.3 ± 32.0) and necrotic (180.7 ± 37.4) cells compared with control cultures. In comparison, staurosporine treatment produced a significant increase ($P < 0.001$) in apoptotic cells (389.3 ± 37.5) with fewer necrotic cells (38.3 ± 14.4), whereas maitotoxin treatment resulted in a significant increase ($P < 0.001$) in necrotic cells (597.0 ± 73.4) with fewer apoptotic cells (13.7 ± 3.8) compared with control cultures.

Examination of DAPI staining (10, 1000× fields) revealed morphologic changes in chromatin staining that

were clearly distinguishable from the classic necrotic phenotype (Fig. 1A and 1B). These nonnecrotic changes showed different evolutionary stages of chromatin margination, condensation, and formation of apoptotic bodies. Thus, these nuclear profiles were termed apoptoticlike. Most stained nuclei in control cultures were healthy; however, some apoptoticlike nuclei were observed and were probably because of spontaneous apoptosis (Fig. 1A). Compared with control cultures, OGD cultures contained significantly less healthy nuclei ($P < 0.001$) and significantly more apoptoticlike nuclei ($P < 0.001$). Necrotic nuclei were rarely observed in either control or OGD cultures. Figure 1B shows a representation of the typical distribution of cell death phenotypes after OGD in this culture system. Nuclei exhibiting apoptoticlike morphology were frequently detected after OGD, as well as cells with healthy nuclei. Surprisingly, examination of DAPI staining in OGD cultures failed to reveal a substantial number of necrotic cells, in contrast with data collected with Annexin V and PI staining. This reduction in necrotic cells may be caused by the frequent rinses and incubations performed during the immunocytochemistry and DAPI staining protocol that may have caused many necrotic cells to detach and go undetected by DAPI in the culture system. However, quite similar data were obtained using these separate techniques to calculate the number of apoptoticlike cells per sample. If values are adjusted to reflect the different field magnifications (320× for Annexin and 1000× for DAPI), the average number of apoptoticlike cells per sample is similar for Annexin (356.3 cells per sample) and DAPI (332.8 cells per sample, data not shown). These data stress the reliability of the authors' assessments of the contribution of apoptosis to cell death in the culture system.

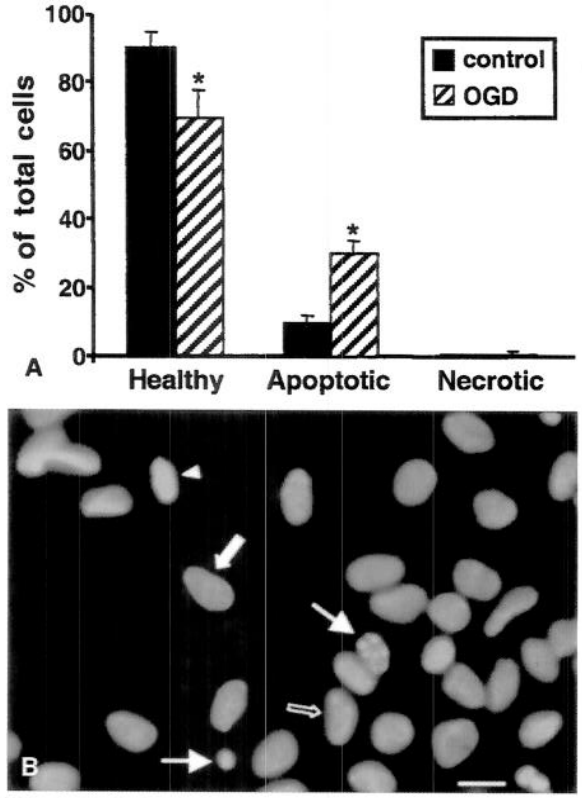

FIG. 1. Analysis of nuclear morphology after oxygen–glucose deprivation (OGD). **(A)** Control cultures and cultures deprived of oxygen and glucose (10 hours + 24 hours of reperfusion) were stained with DAPI, and cells were characterized as healthy, apoptoticlike, or necrotic based on nuclear morphology. Control cultures contained mostly healthy nuclei (90.1% ± 6.1%), although apoptoticlike nuclei (9.6% ± 2.9%) were detected. Compared with control cultures, OGD contained significantly fewer healthy nuclei (69.3% ± 10.5%) and significantly more apoptoticlike nuclei (30.0% ± 5.4%). No significant differences were observed in the percentage of necrotic cells between control (0.3% ± 0.2%) and OGD (0.7% ± 1.0%) cultures. *$P < 0.001$. **(B)** DAPI staining of septo-hippocampal cultures after OGD. Representative image illustrating the typical distribution of cell death phenotypes after OGD (10 hours + 24 hours of reperfusion). Nuclei exhibiting apoptoticlike morphology such as chromatin condensation (arrowhead), irregular-shaped nuclei (open arrow), and the formation of apoptotic bodies (thin arrows) were frequently detected after OGD. Healthy nuclei (wide arrow) also were observed after injury. Scale bar = 1 μm.

As an additional indicator of internucleosomal fragmentation, the amount of mono- and oligonucleosomes in the cytoplasmic fraction of cell lysates was quantitatively assessed (Fig. 2B). Control cultures showed little DNA fragmentation, whereas cells deprived of oxygen and glucose for 10 hours contained significantly more mono- and oligonucleosomes after 24 ($P < 0.001$) and 48 ($P < 0.001$) hours of reperfusion, but not after 3 or 12 hours of reperfusion. In comparison, staurosporine treatment resulted in a significant increase ($P < 0.001$) in mono- and oligonucleosomes, whereas samples exposed to maitotoxin were not statistically different from control samples.

Induction of cell death by oxygen–glucose deprivation in neurons and glia. To identify the type of cell (that is, neuron vs. astroglia) affected by OGD, primary mixed septo-hippocampal cultures were stained with NeuN and MAP2 (for neurons) or GFAP (for astroglial)

Condensation and aggregation of chromatin, as shown with DAPI staining (Fig. 1B), may occur independently of endonuclease activation (Oberhammer et al., 1993). Therefore, two separate techniques were used to qualitatively (Fig. 2A) and quantitatively (Fig. 2B) assess internucleosomal DNA fragmentation, and thus endonuclease activation, after OGD. DNA electrophoresis (Fig. 2A) revealed a robust ladder pattern, characteristic of internucleosomal DNA fragmentation, after 10 hours of OGD with 12, 24, and 48 hours of reperfusion. Faint bands also were detected after 3 hours of reperfusion. Staurosporine treatment produced a characteristic DNA ladder pattern, whereas control samples and cells subjected to maitotoxin failed to show any internucleosomal fragments.

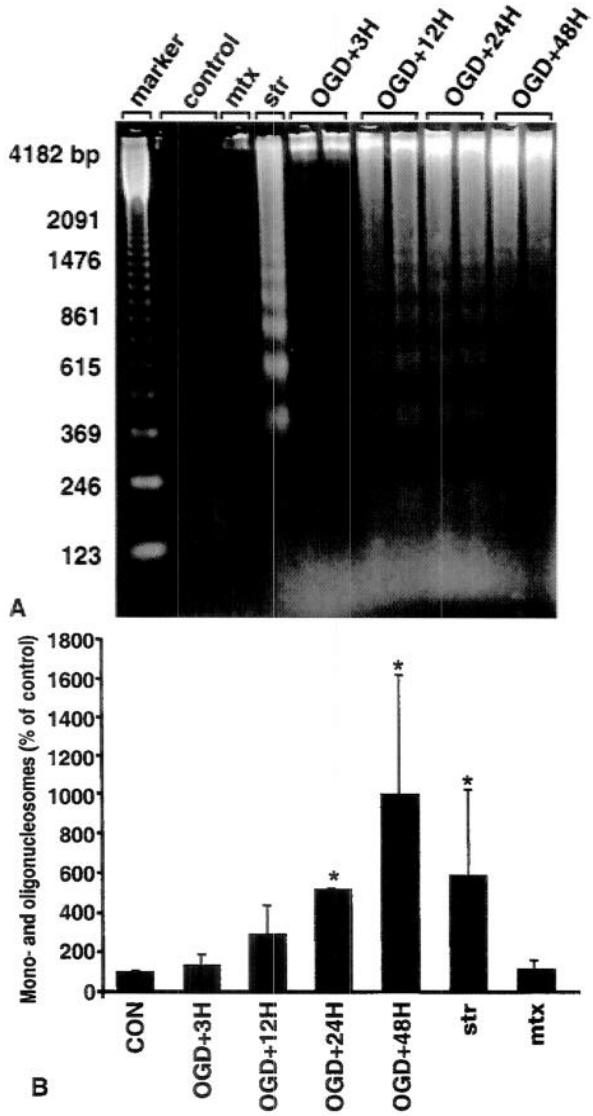

FIG. 2. Assessment of internucleosomal DNA fragmentation after oxygen–glucose deprivation (OGD). **(A)** DNA electrophoresis. Samples collected from control and maitotoxin (mtx)-treated cultures showed no internucleosomal DNA fragmentation, whereas staurosporine (str) treatment produced a characteristic DNA ladder pattern. Cultures subjected to OGD for 10 hours and collected 3 hours after injury exhibited a faint ladder. Prominent DNA laddering was observed 12, 24, and 48 hours after injury. **(B)** DNA fragmentation assay. DNA fragmentation was quantitatively assessed by detection of mono- and oligonucleosomes in the cytoplasmic fraction of cell lysates. Analysis of control cultures demonstrated little DNA fragmentation, similar to cells deprived of oxygen and glucose for 10 hours after 3 (129% ± 46.8%) or 12 (287% ± 163.0%) hours of reperfusion. However, a significant increase in mono- and oligonucleosomes was detected in cells deprived of oxygen and glucose for 10 hours after 24 (513% ± 5.6%) and 48 (998% ± 606.9%) hours of reperfusion. Staurosporine (str) treatment resulted in a significant increase (582% ± 441.7%) in mono- and oligonucleosomes, whereas samples exposed to maitotoxin (mtx) were not statistically different from control samples (111% ± 58.1%). $^*P < 0.001$.

and counterstained with DAPI (Fig. 3). Low magnification examination of NeuN and MAP2 staining in OGD cultures revealed a significant loss (68% ± 9.3% of control values, $P < 0.001$) of immunoreactive (IR) neurons (data not shown). Examination of GFAP staining in cells subjected to OGD showed that OGD had a modest effect on astroglia that was not readily apparent under low magnification.

High magnification (1000×) examination of NeuN, or MAP2 IR cells, or both (Fig. 3), showed that the majority of positive cells in control cultures possessed large cell bodies and several intact processes that were intensely labeled for both neuronal markers (Fig. 3A). These cells contained healthy, oval-shaped nuclei with diffuse chromatin distribution (Fig. 3B). In contrast, NeuN and MAP2 staining of OGD cultures showed a substantial number of neurons with shrunken cell bodies and fragmented processes (Fig. 3C). Nuclei of these neurons were shrunken, irregularly shaped, and possessed highly condensed chromatin (Fig. 3D). Apoptoticlike nuclei that were not IR for NeuN or MAP2 also were observed (Fig. 3D). These cells may have been apoptotic astroglia, or more likely, neurons in an advanced stage of apoptosis in which the phenotype is most apparent and degeneration of cellular proteins may compromise the retention of epitopes necessary for cell type identification. Quantitative analysis of DAPI staining in NeuN, or MAP2 IR cells, or both (50 random IR cells per sample), demonstrated that the majority of positive cells in control cultures exhibited healthy nuclear morphology (83.3% ± 4.4%). Although cells with apoptoticlike nuclei (16.7% ± 1.8%) were occasionally observed, neurons with necrotic nuclei were not detected in this set of control cultures. Analysis of DAPI staining in OGD cultures revealed a significantly lower percentage of healthy nuclei (57.3% ± 9.3%, $P < 0.001$) and significantly higher percentage of apoptoticlike nuclei (40.3% ± 8.6%, $P < 0.001$), compared with control cultures. Although OGD cultures also contained more necrotic nuclei (2.3% ± 1.5%) than control cultures, necrotic cells were rarely observed.

Examination of GFAP staining in control and OGD cultures showed that most GFAP-positive cells were healthy astroglia with large cell bodies, extensive processes, and diffuse and even immunoreactivity (Fig. 3E and 3G, respectively). Astroglial nuclei were large and oval-shaped with even chromatin distribution (Fig. 3F and 3H). Although most IR cells in OGD cultures appeared healthy, cells with shrunken cell bodies, broken processes, and aggregated GFAP immunoreactivity also were observed (Fig. 3G).

These cells possessed shrunken nuclei with highly condensed chromatin and apoptotic bodies (Fig. 3H). Quantitative assessment of DAPI staining in GFAP IR cells (50 random IR cells per sample) showed that most GFAP-positive cells in control (98.3% ± 12.7%) and

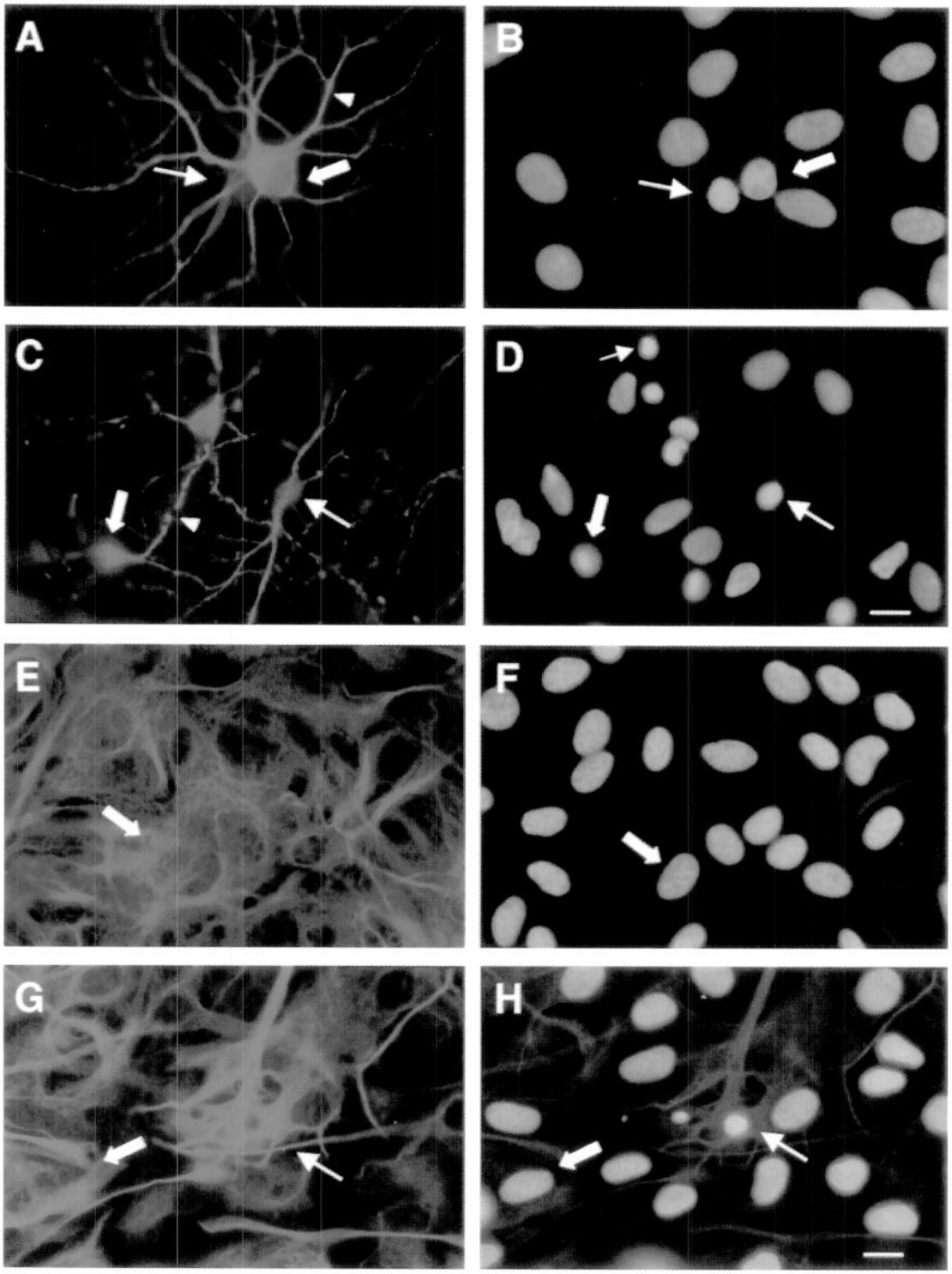

FIG. 3. Neuronal and glial morphology after oxygen–glucose deprivation (OGD). Cultures were immunolabeled with NeuN and MAP2 or GFAP (glial fibrillary acidic protein) and were counterstained with DAPI to assess morphologic and nuclear changes after OGD (10 hours + 24 hours of reperfusion). Cells were examined under high magnification (1000×). **(A)** NeuN/MAP2 immunoreactive (IR) cells in control cultures possessed large cell bodies (thin arrow, wide arrow) and several intact processes (arrowhead) that were intensely labeled for both neuronal markers. **(B)** These cells contained healthy, oval-shaped nuclei with diffuse chromatin distribution (thin arrow, wide arrow). **(C)** Cultures deprived of oxygen and glucose showed a substantial number of neurons with shrunken cell bodies (thin arrow, wide arrow) and fragmented processes (arrowhead). **(D)** Neuronal nuclei were shrunken, irregularly shaped and possessed highly condensed chromatin (thin arrow, wide arrow). Apoptotic nuclei not IR for NeuN or MAP2 also were observed (small arrow). **(E)** Control cultures contained healthy astroglia with large cell bodies, extensive processes, and diffuse and even immunoreactivity (arrow). **(F)** Nuclei were large and oval-shaped with even chromatin distribution (arrow). **(G)** OGD cultures contained a majority of healthy GFAP-positive cells (wide arrow), but cells with shrunken cell bodies, broken processes, and aggregated GFAP immunoreactivity also were observed (thin arrow) and characterized as apoptoticlike. **(H)** Nuclei in healthy astroglia resembled those detected in control cultures (wide arrow). Apoptotic astroglia contained shrunken nuclei with highly condensed chromatin and apoptotic bodies (thin arrow). Scale bars = 1 μm.

OGD (91.4% ± 27.2%) cultures possessed healthy nuclei. DAPI staining revealed some effects of OGD, including a decreased percentage of healthy nuclei and an increased percentage of apoptoticlike nuclei (8.4% ± 2.0%), compared with control cells (1.6% ± 1.5%), but these differences were not statistically significant. Necrotic nuclei were rarely observed in either control (0.2% ± 0.5%) or OGD (0.2% ± 0.5%) cultures.

Calpain and caspase-3 proteolysis of α-spectrin after oxygen–glucose deprivation

Western blots. Activation of calpain and caspase-3 after OGD was assessed with Western blots examining proteolysis of α-spectrin (Fig. 4A and 4B). After 10 hours of OGD, samples were collected immediately (0 hour), 3, 12, 24, or 48 hours after cultures were returned to a normal environment. Control samples and samples deprived of oxygen and glucose for 10 hours and collected immediately after injury showed no evidence of calpain-mediated proteolysis of α-spectrin. However, 3 hours after reperfusion, proteolysis of α-spectrin into 150-kDa and calpain-mediated 145-kDa BDPs was significantly increased over control values ($P < 0.001$). Degradation of α-spectrin continued and proteolysis into the 145-kDa BDP also was increased after 12, 24, and 48 hours of reperfusion ($P < 0.001$). Modest degradation of native α-spectrin was observed after 48 hours of reperfusion ($P < 0.01$). Slight increases in caspase-3–mediated proteolysis were detected after injury, but formation of the 120-kDa BDP was variable and did not differ significantly from control. However, immunoblots detected proteolysis of the caspase-3 proenzyme to the activated isoform (Fig. 4C), suggesting that analyses of autolytic

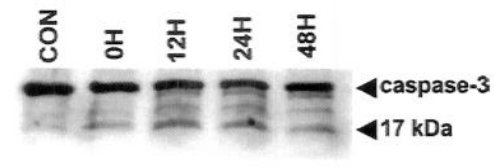

C

B Arbitrary densitometric units

Arbitrary densitometric units

FIG. 4. Calpain- and caspase-3–mediated proteolysis of α-spectrin after oxygen–glucose deprivation (OGD). **(A)** Representative Western blot showing calpain- and caspase-3–mediated proteolysis of α-spectrin after OGD. Control samples and samples collected immediately (0 hour) after injury showed no evidence of calpain-mediated proteolysis of α-spectrin. Accumulation of the 150- and 145-kDa BDPs was detected 3, 12, 24, and 48 hours after OGD. Moderate increases in the caspase-3–mediated BDP were detected after injury, but formation of the 120-kDa BDP was variable. **(B)** Calpain- and caspase-3–mediated proteolysis of α-spectrin semiquantitative analysis. Data from multiple Western blots analyzing α-spectrin proteolysis were acquired as integrated densitometric values and transformed to percentages of the densitometric values obtained from control samples. Formation of the 150- and 145-kDa BDPs was increased after OGD with 3, 12, 24, and 48 hours of reperfusion, whereas modest degradation of native α-spectrin (240 kDa) was detected after 48 hours of reperfusion. Accumulation of the caspase-3–mediated 120-kDa BDP was variable. *$P < 0.01$. †$P < 0.001$. **(C)** Activation of caspase-3 after OGD. Proteolysis of caspase-3 (32 kDa) to the activated isoform (17 kDa) was examined after 10 hours of OGD and 0, 12, 24, or 48 hours of reperfusion. Degradation of the proenzyme (32 kDa) was evident 12, 24, and 48 hours after injury. Proteolysis of caspase-3 into the 17-kDa subunit was detected with all lengths of reperfusion examined.

activation of the caspase-3 proenzyme may be more sensitive than analyses of processing of cytoskeletal protein substrates.

Immunocytochemistry. Primary mixed septo-hippocampal cultures were double-labeled with antibodies specific for calpain (SBDP 150) and caspase-3 (SBDP 120) mediated α-spectrin proteolytic fragments and were counterstained with DAPI (Fig. 5). Across all treatment conditions, cells with evidence of nuclear damage exhibited strong immunoreactivity, whereas most healthy cells showed faint or no immunoreactivity. Cultures deprived of oxygen and glucose had significantly increased cellular colocalization of SBDP 150 and SBDP 120 (93.5 ± 16.7 cells per sample, $P < 0.001$), compared with control cultures (23 ± 8.6 cells per sample). Although OGD cultures contained substantially more IR cells than control cultures, examination of immunocytochemistry showed a similar distribution of protease activation, regardless of treatment condition (Fig. 5A and 5C). Virtually all IR cells in control and OGD cultures showed concurrent calpain and caspase-3 proteolysis in varying magnitudes (Fig. 5A and 5C). Immunolabeling in control (Fig. 5A) and OGD (Fig. 5C) cultures resulted in subcellular localization of BDPs unique from staurosporine (Fig. 5E) or maitotoxin cultures (Fig. 5G). In control and OGD cells, SBDP 150 was localized exclusively within the cell body, that is, near the nuclear membrane. Conversely, SBDP 120 immunoreactivity was detected throughout the entire cell body, specifically along the outer boundary of the cell membrane, and in the proximal processes (Fig. 5A and 5C). The nuclei of IR cells were shrunken, irregularly shaped, possessed condensed chromatin, and were considered apoptoticlike (Fig. 5B and 5D). Staurosporine injured cells were immunoreactive for both SBDP 120 and SBDP 150 in cells exhibiting apoptoticlike nuclear morphology (Fig. 5E and 5F). Notably, different relative magnitudes of caspase-3 and calpain activation were evident in individual cells, but distinct localization of BDPs was not as apparent as the immunoreactivity in control and OGD cells. Maitotoxin-injured cells showed predominantly calpain-mediated BDPs in cells exhibiting the classic necrotic nuclear morphology of rounded, brightly fluoresced nuclei with pyknotic chromatin (Fig. 5G and 5H).

Quantitative analysis of DAPI staining in cells immunoreactive for SBDP 150 or SBDP 120 (data not shown) revealed that the majority of IR cells possessed apoptoticlike nuclei in control (95.7% ± 38.7%) and OGD (97.9% ± 17.2%) cultures. Few IR cells exhibiting a necrotic cell death phenotype were observed in control (1.4% ± 3.7%) or OGD (1.4% ± 1.5%) cultures. Occasionally, IR cells with healthy nuclei were present in control (2.9% ± 3.2%) and OGD (0.7% ± 1.0%) cultures. However, these cells may have been in the initial stages of cell death in which nuclear changes were not yet apparent.

Effects of calpain and caspase inhibitors

Preliminary experiments using protease inhibitors in cultures subjected to 10 hours of OGD and 24 hours of reperfusion data failed to show protection against cell death when LDH release was assayed (data not shown). These data suggested that 24 hours of reperfusion was too long a period to allow the inhibitors to be effective, or that the inhibitors became toxic after such long periods. Moreover, the current data demonstrated robust cell death, DNA fragmentation (Fig. 2), and protease activation (Fig. 4) with 10 hours of OGD and 12 hours of reperfusion. In an attempt to show protection and therefore involvement of calpain and caspase-3, cells were subjected to 10 hours of OGD with 12 hours of reperfusion in the presence of protease inhibitors. Lactate dehydrogenase analysis (Fig. 6A) showed significant decreases in release with CI-3 (100 μmol/L; $P < 0.001$) compared with vehicle-treated cultures. The specific caspase-3 inhibitor, DEVD-fmk (100 μmol/L, $P < 0.05$), also inhibited LDH release; however, decreases were not statistically significant compared with vehicle-treated cultures. The pan-caspase inhibitor, Z-D-DCB (100 μmol/L), had no effect on LDH release. Dimethyl sulfoxide also decreased LDH release, but this effect was not significantly different from the OGD and media cultures.

Consistent with the LDH data, Western blot analyses of these samples (Fig. 6B) showed that CI-3 decreased proteolysis of native 240 kDa α-spectrin and almost completely blocked the formation of the 150/145 kDa doublet. Z-D-DCB also inhibited formation of the 145 kDa BDP to a small extent, but had only a minor effect on the caspase-3–mediated BDP (120 kDa). Surprisingly, DEVD-fmk dramatically reduced the calpain-mediated BDP, but only had a modest effect on the 120 kDa band. Subsequent experiments investigating combined inhibition using CI-3 and DEVD-fmk failed to show a synergistic mechanism. Future experiments should examine more extensive dosing protocols.

DISCUSSION

Although numerous studies have investigated calpain and caspase-3 activation after acute CNS trauma, no study has examined the relation between protease activation and expression of cell death phenotypes. In the current study, the authors detected prominent expression of apoptoticlike cell death phenotypes following a model of OGD, especially in neurons. Moreover, coactivation of calpain and caspase-3 was almost always detected in cells exhibiting apoptoticlike cell death phenotypes.

Oxygen–glucose deprivation resulted in both apoptosis and necrosis in this culture system. Although apop-

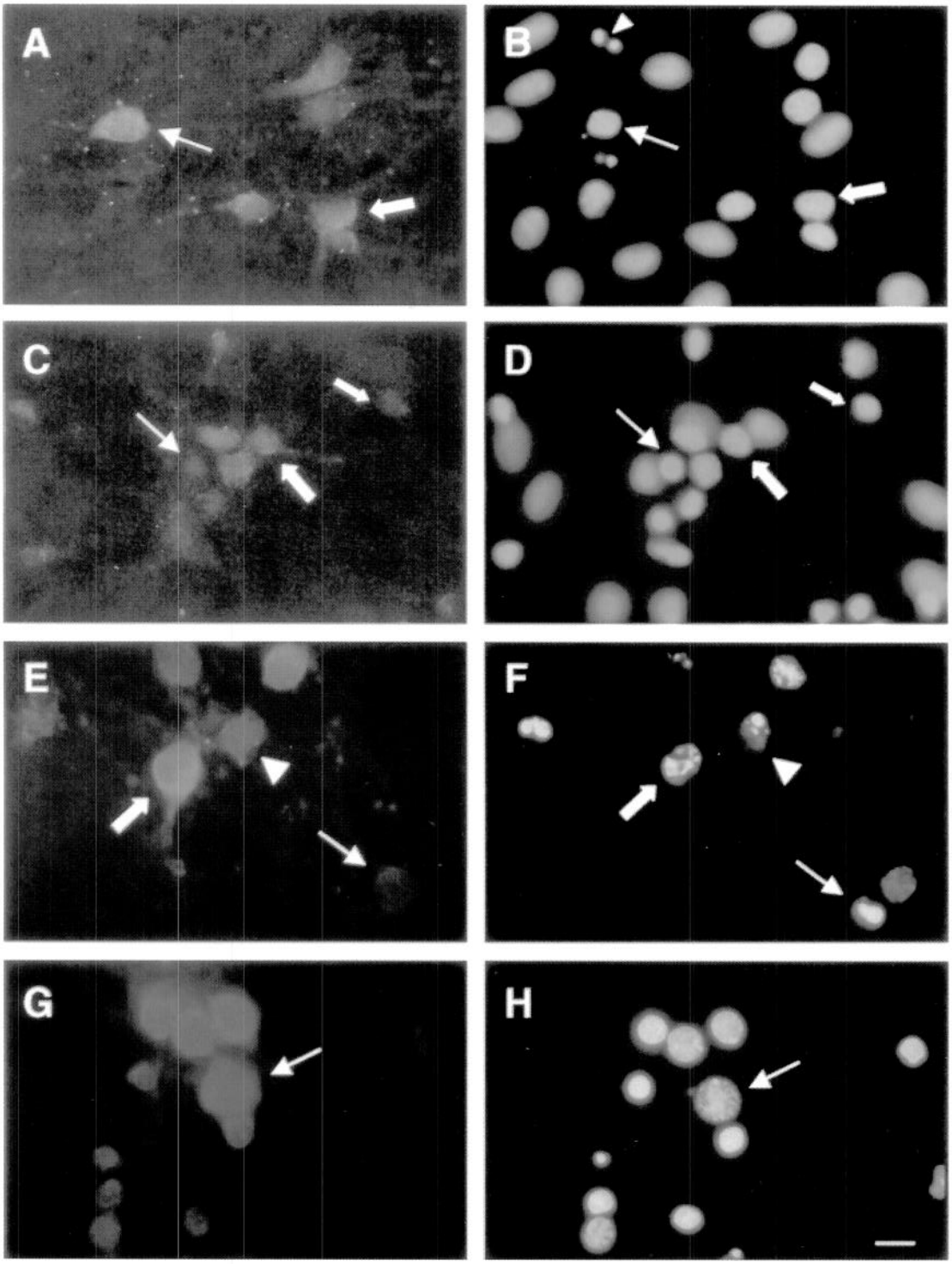

FIG. 5. Calpain and caspase-3 proteolysis of α-spectrin in individual cells following oxygen–glucose deprivation (OGD). Primary mixed septo-hippocampal cultures were immunolabeled with antibodies specific for calpain- (SBDP 150, red fluorescence) and caspase-3 (SBDP 120, green fluorescence)–mediated α-spectrin fragments, and counterstained with DAPI. **(A)** The majority of cells in control cultures were not immunoreactive (IR) for α-spectrin BDPs; however, cells that were IR exhibited both calpain- and caspase-3–mediated BDPs (thin arrow, wide arrow). **(B)** Nuclei of IR cells were shrunken and exhibited chromatin condensation (thin arrow, wide arrow) and apoptotic bodies were also evident (arrowhead). **(C)** OGD cultures also showed concurrent calpain and caspase-3 proteolysis (thin arrow, wide arrows). In addition, IR cells from control (A) and OGD (C) cultures showed subcellular localization of BDPs; SBDP 150 was detected exclusively within the cell body, while SBDP 120 was observed throughout the entire cell body and the proximal processes (A, C, all arrows). **(D)** Nuclei of IR cells in OGD cultures were shrunken, irregularly shaped, and possessed highly condensed chromatin (wide arrows). Nuclei with chromatin margination along the periphery of the nuclear membrane were also detected (thin arrow). **(E)** Staurosporine-injured cells were IR for SBDP 120 and SBDP 150 and different relative magnitudes of protease activation were evident in individual cells (thin arrow, wide arrow, arrowhead). **(F)** IR cells exhibited nuclear morphology consistent with apoptosis (thin arrow, wide arrow, arrowhead). **(G)** Maitotoxin-injured cells exhibited calpain-mediated BDPs (arrow). **(H)** Nuclei of IR cells were rounded, brightly fluoresced, exhibited pyknotic chromatin, and were considered necrotic (arrow). Scale bar = 1 μm.

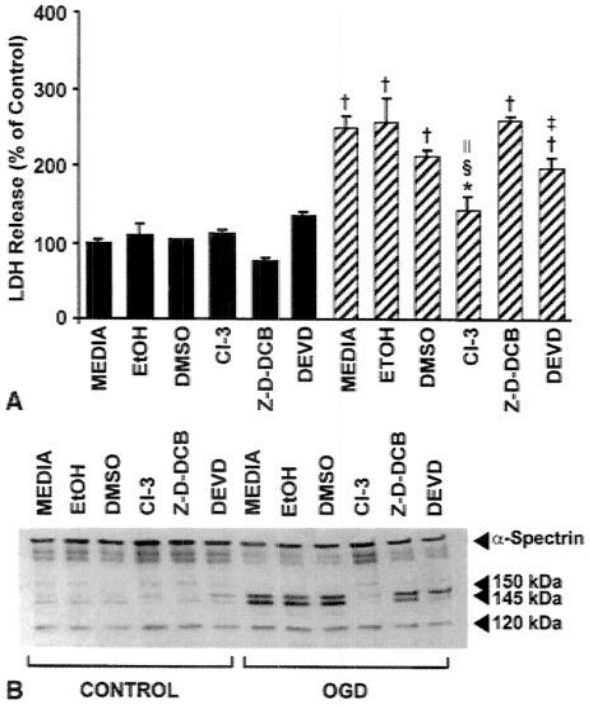

FIG. 6. (A) Effect of protease inhibition on lactate dehydrogenase (LDH) release following oxygen–glucose deprivation (OGD). Cultures were subjected to OGD (10 hours + 12 hours of reperfusion) alone, or combined with varying doses of protease inhibitors. Cell viability was assessed by measuring LDH release and expressed as percent of control. Significant decreases in LDH release were detected with administration of CI-3 (100 μmol/L) compared to vehicle-treated cultures. DEVD-fmk (100 μmol/L) also inhibited LDH release; however, decreases were not statistically significant compared to vehicle-treated cultures. Z-D-DCB (100 μmol/L) had no effect on cell viability. DMSO (2 μL/mL) also decreased LDH release, but its effect was not significantly different from the OGD/media cultures. $^{*}P < 0.05$ and $\dagger P < 0.001$ compared to control; $\ddagger P < 0.05$ and $\S P < 0.001$ compared to OGD/media; $^{\|}P < 0.01$ compared to vehicle-treated OGD. **(B)** Effect of protease inhibition on α-spectrin proteolysis. Western blot analyses of α-spectrin proteolysis assessed inhibition of appropriate proteases. CI-3 (100 μmol/L) decreased proteolysis of native 240 kDa α-spectrin and the formation of the 150/145 kDa doublet. Z-D-DCB (100 μmol/L) had a small effect on the accumulation of the 145 kDa and 120 kDa BDPs. DEVD-fmk (100 μmol/L) substantially reduced the formation of the 145 kDa BDP, but had only a modest effect on the formation of the 120 kDa BDP.

totic and necrotic cell death have been observed in some models of *in vitro* ischemia (Kalda et al., 1998), other models do not observe apoptosis unless glutamate receptor antagonists are used (Gottron et al., 1997; Gwag et al., 1995; Lobner and Choi, 1996). Variations in cell culture methodology, including culture age at time of injury and glial density, may be responsible for these discrepancies. Consistent with the prominent role of apoptosis in development, younger cultures, such as those used in this study, are more susceptible to apoptosis after cyclosporine or staurosporine treatment (McDonald et al., 1997), whereas older neurons are more vulnerable to *N*-methyl-d-aspartate toxicity (McDonald et al., 1997) and hypoxia (Di Loreto and Balestrino, 1997). In contrast to this article, studies that detected only necrosis after OGD used neuronally enhanced cell cultures (Goldberg and Choi, 1993; Gottron et al., 1997; Lobner and Choi, 1996). Increased sensitivity to glutamate toxicity and OGD has been observed in neuronally enhanced cultures (Zhao et al., 2000; Dugan et al., 1995), suggesting that the absence of glia may intensify a neuron's response to injury. It is conceivable that higher glial concentrations in the current model of OGD blunted the effects of deprivation and resulted in a slower and milder injury. Notably, *in vitro* studies have shown that the same insult can produce apoptosis or necrosis depending on its severity (Bonfoco et al., 1995).

Cell death after OGD was associated with concurrent activation of calpain and caspase-3. Although immunocytochemical experiments revealed robust caspase-3–mediated proteolysis of α-spectrin (120 kDa), Western blots failed to detect consistent increases in this proteolytic fragment. Use of different primary antibodies (monoclonal versus polyclonal) and methods of detection (enhanced chemiluminescence reagents versus fluorescence) may be responsible for these inconsistencies. Western blots using an antibody to the activated caspase-3 17-kDa subunit did provide evidence of caspase-3 activation, confirming immunohistochemical observations of caspase-3 activation and suggesting that Western blot assessments of proenzyme processing may be more sensitive than measures of substrate degradation in some model systems.

Cells phenotypically showing apoptoticlike nuclear profiles exhibited prominent expression of calpain and caspase-3, suggesting that there may be as yet undefined interactions between these two proteases in the expression of the apoptotic phenotype. Calpain and caspase-3 share a variety of substrates that are proteolyzed during apoptosis (Wang, 2000). In addition, these proteases cleave proteins important to each other's regulation—that is, caspase-3–mediated proteolysis of calpastatin, calpain-mediated proteolysis of pro-caspase-3 and pro-caspase-9 (Wang et al., 1998*a*; McGinnis et al., 1999; Wolf et al., 1999). Furthermore, calpains, but not caspases, promote apoptoticlike events during platelet activation (Wolf et al., 1999). Additional evidence for calpain's involvement in apoptotic cell death in CNS injury is provided by recent studies examining *in vivo* TBI and ischemia. Calpain-mediated breakdown products have been detected in the injured cortex after TBI (Beer et al., 2000; Pike et al., 1998*a*), a site associated with prominent apoptotic cell death (Beer et al., 2000; Newcomb et al., 1999), although evidence of caspase-3 activation in this region has yielded conflicting data

(Beer et al., 2000; Pike et al., 1998*a*). These discrepancies may be attributable to differences in injury magnitude, animal age, or species; these issues currently are being addressed in both laboratories. After *in vivo* ischemia, approximately 50% of TUNEL-positive cells failed to show caspase-3 activation (Namura et al., 1998), suggesting that other proteases, such as calpain, are involved in the apoptotic changes observed after injury.

Inhibition of calpain substantially decreased LDH release after OGD with 12 hours of reperfusion, suggesting that calpain activation contributes to cell death in this model. Inhibition of caspase-3 with DEVD-fmk also reduced LDH release, although this drug also showed marked inhibition against calpain activation. Thus, the current study did not allow for comparisons of the relative contribution of these two proteases to cell death in this model. It is unclear why DEVD-fmk showed substantial calpain inhibition and only modest caspase-3 inhibition, but these data suggest that this agent is not a specific inhibitor of caspase-3 activation, at least in this model system. Although not directly addressed in this study, future experiments must more rigorously investigate the relative contribution of calpain and caspase-3 to the expression of apoptotic cell death phenotypes.

Although the current study relied in part on morphologic characteristics of cell death phenotypes, a number of observations suggest that biochemical markers ultimately may be more useful indicators of cell death, especially in acute neurologic insults characterized by heterogeneous or ambiguous cell death phenotypes. In this study, appearance of necrotic cell death depended on method of detection. Using chromatin dyes to distinguish necrotic and apoptotic nuclear morphology is problematic because nuclei may exhibit characteristics either of both types (Colicos and Dash, 1996) or neither type (Zhao et al., 2000) of cell death. In fact, most techniques used to differentiate apoptosis also have been reported to label necrosis, perhaps because late events are similar in both types of cell death (Choi, 1996). Some investigators have argued that necrosis and apoptosis may not be phenotypically distinct events, but rather represent a morphologic continuum (Bonfoco et al., 1995; Portera-Cailliau et al., 1997). This issue is further complicated by evidence showing that the same insult can cause apoptosis and necrosis in different cell populations (Sloviter et al., 1996) or can result in an acute necrotic death with a delayed apoptotic death (Ankarcrona et al., 1995; Pang and Geddes, 1997).

In summary, the current data demonstrate that coactivation of calpain and caspase-3 is a reliable characteristic of apoptotic cell death in the current model system. These observations strongly suggest that calpain activation, in combination with caspase-3 activation, could contribute to the expression of apoptotic cell death by assisting in the proteolytic degradation of important cellular proteins (Wang, 2000). Finally, interactions between these two cysteine proteases could be important determinants of cell death.

REFERENCES

Ankarcrona M, Dypbukt JM, Bonfoco E, Zhivotovsky B, Orrenius S, Lipton SA, Nicotera P (1995) Glutamate-induced neuronal death: a succession of necrosis or apoptosis depending on mitochondrial function. *Neuron* 15:961–973

Bartus RT, Dean RL, Cavanaugh K, Eveleth D, Carriero DL, Lynch G (1995) Time-related neuronal changes following middle cerebral artery occlusion: implications for therapeutic intervention and the role of calapin. *J Cereb Blood Flow Metab* 15:969–979

Beer R, Franz G, Srinivasan A, Hayes RL, Pike BR, Newcomb JK, Zhao X, Schmutzhard E, Poewe W, Kampfl A (2000) Temporal profile and cell subtype distribution of activated caspase-3 following experimental traumatic brain injury. *J Neurochem* 75:1264–1273

Bonfoco E, Krainc D, Ankarcrona M, Nicotera P, Lipton S (1995) Apoptosis and necrosis: two distinct events induced, respectively, by mild and intense insults with N-methyl-D-aspartate or nitric oxide/superoxide in cortical cell cultures. *Proc Natl Acad Sci U S A* 92:7162–7166

Buki A, Okonkwo DO, Wang KKW, Povlishock JT (2000) Cytochrome c release and caspase activation in traumatic axonal injury. *J Neurosci* 20:2825–2834

Charriaut-Marlangue C, Ben-Ari Y (1995) A cautionary note on the use of TUNEL stain to determine apoptosis. *Neuroreport* 7:61–64

Chen J, Nagayama T, Jin K, Stetler A, Zhu RL, Graham SH, Simon RP (1998) Induction of caspase-3 like protease may mediate delayed neuronal death in the hippocampus after transient cerebral ischemia. *J Neurosci* 18:4914–4928

Choi DW (1996) Ischemia-induced neuronal apoptosis. *Curr Opin Neurobiol* 6:667

Clark RSB, Kochanek PM, Watkins SC, Chen M, Dixon CE, Seidberg NA, Melick J, Loeffert JE, Nathaniel PD, Jin KL, Graham SH (2000) Caspase-3 mediated neuronal death after traumatic brain injury in rats. *J Neurochem* 74:740–753

Colicos MA, Dash PK (1996) Apoptotic morphology of dentate gyrus granule cells following experimental cortical impact injury in rats: possible role in spatial memory deficits. *Brain Res* 739:120–131

Copin JC, Li Y, Reola LF, Chan PH (1998) Trolox and 6, 7-dinitroquinoxaline-2–3dione prevent necrosis but not apoptosis in cultured neurons subjected to oxygen deprivation. *Brain Res* 784:25–36

Di Loreto S, Balestrino M (1997) Development of vulnerability to hypoxic damage in *in vitro* hippocampal neurons. *Int J Dev Neurosci* 15:225–230

Dugan LL, Bruno VMG, Amagasu SM, Giffard RG (1995) Glia modulate the response of murine cortical neurons to excitotoxicity: glia exacerbate AMPA toxicity. *J Neurosci* 15:4545–4555

Fink K, Namura S, Shimizu-Sasamata M, Endres M, Ma J, Dalkara T, Yuan J, Moskowitz MA (1998) Prolonged therapeutic window for ischemic brain damage caused by delayed caspase activation. *J Cereb Blood Flow Metab* 18:1071–1076

Goldberg MP, Choi DW (1993) Combined oxygen and glucose deprivation in cortical cell culture: calcium-dependent and calcium-independent mechanisms of neuronal injury. *J Neurosci* 13:3510–3524

Gong J, Traganos F, Darzynkiewicz Z (1994) A selective procedure for DNA extraction from apoptotic cells applicable for gel electrophoresis and flow cytometry. *Anal Biochem* 218:314–319

Gottron FJ, Ying HS, Choi DW (1997) Caspase inhibition selectively reduces the apoptotic component of oxygen-glucose deprivation-induced cortical neuronal death. *Mol Cell Neurosci* 9:159–169

Gwag BJ, Lobner D, Koh JY, Wie MB, Choi DW (1995) Blockade of glutamate receptors unmasks neuronal apoptosis after oxygen-glucose deprivation *in vitro*. *Neuroscience* 68:615–619

Harris AS, Croall DE, Morrow JS (1988) The calmodulin-binding site in alpha-fodrin is near the calcium-dependent protease-1 cleavage site. *J Biol Chem* 263:15754–15761

Himi T, Ishizaki Y, Murota S (1998) A caspase inhibitor blocks ischemia-induced delayed neuronal death in the gerbil. *Eur J Neurosci* 10:777–781

Hong SC, Goto Y, Lanzino G, Soleau S, Kassell NF, Lee KS (1994) Neuroprotection with a calpain inhibitor in a model of focal cerebral ischemia. *Stroke* 25:663–669

Kalda A, Eriste E, Vassiljev V, Zharkovsky A (1998) Medium transitory oxygen-glucose deprivation induced both apoptosis and necrosis in cerebellar granule cells. *Neurosci Lett* 240:21–24

Koh JY, Choi DW (1987) Quantitative determination of glutamate mediated cortical neuronal injury in cell culture by lactate dehydronase efflux assay. *J Neurosci Meth* 20:83–90

Linnik MD, Zobrist RH, Hatfield MD (1993) Evidence supporting a role for programmed cell death in focal cerebral ischemia in rats. *Stroke* 24:2002–2009

Lobner D, Choi DW (1996) Preincubation with protein synthesis inhibitors protects cortical neurons against oxygen-glucose deprivation-induced death. *Neuroscience* 72:335–341

Markgraf CG, Velayo NL, Johnson MP, McCarty DR, Medhi S, Koehl JR, Chmielewski PA, Linnik MD (1998) Six-hour window of opportunity for calpain inhibition in focal cerebral ischemia in rats. *Stroke* 29:152–158

McDonald JW, Behrens MI, Chung C, Bhattacharyya T, Choi DW (1997) Susceptibility to apoptosis is enhanced in immature cortical neurons. *Brain Res* 759:228–232

McGinnis KM, Gnegy ME, Park YH, Mukerjee N, Wang KKW (1999) Procaspase-3 and poly(ADP)ribose polymerase (PARP) are calpain substrates. *Biochem Biophys Res Comm* 263:94–99

Namura S, Zhu J, Fink K, Endres M, Srinivasan A, Tomaselli KJ, Yuan J, Moskowitz MA (1998) Activation and cleavage of caspase-3 in apoptosis induced by experimental cerebral ischemia. *J Neurosci* 18:3659–3668

Nath R, Raser KJ, Stafford D, Hajimohammadreza I, Posner A, Allen H, Talanian RV, Yuen P, Gilbertsen RB, Wang KKW (1996) Non-erythroid alpha-spectrin breakdown by calpain and interleukin 1 beta-converting-enzyme-like protease(s) in apoptotic cells: contributory roles of both protease families in neuronal apoptosis. *Biochem J* 319:683–690

Nath R, Probert A, McGinnis KM, Wang KKW (1998) Evidence for activation of caspase-3-like protease in excitotoxin- and hypoxia/hypoglycemia-injured neurons. *J Neurochem* 71:186–195

Newcomb JK, Kampfl A, Posmantur RM, Zhao X, Pike BR, Liu SJ, Clifton GL, Hayes RL (1997) Immunohistochemical study of calpain-mediated breakdown products to α-spectrin following controlled cortical impact injury in the rat. *J Neurotrauma* 14:369–383

Newcomb JK, Zhao X, Pike BR, Hayes RL (1999) Temporal profile of apoptotic-like changes in neurons and astrocytes following controlled cortical impact injury in the rat. *Exp Neurol* 158:76–88

Oberhammer F, Fritsch G, Schmied M, Pavelka M, Printz D, Purchio R, Lassman H, Schulte-Hermann R (1993) Condensation of chromatin at the membrane of an apoptotic nuclease is not associated with activation of an endonuclease. *J Cell Sci* 104:317–326

Pang Z, Geddes JW (1997) Mechanisms of cell death induced by the mitochondrial toxin 3-nitropropionic acid: acute excitotoxic necrosis and delayed apoptosis. *J Neurosci* 17:3064–3073

Pike BR, Zhao X, Newcomb JK, Posmantur RM, Wang KKW, Hayes RL (1998*a*) Regional calpain and caspase-3 proteolysis of α-spectrin after traumatic brain injury. *Neuroreport* 9:2437–2442

Pike BR, Zhao X, Newcomb JK, Wang KKW, Posmantur RM, Hayes RL (1998*b*) Temporal relationship between *de novo* protein synthesis, calpain and caspase-3 like protease activation, and DNA fragmentation during apoptosis in septo-hippocampal cultures. *J Neurosci Res* 52:505–520

Pike BR, Zhao X, Newcomb JK, Glenn CC, Anderson DK, Hayes RL (2000) Stretch injury causes calpain and caspase-3 activation and necrotic and apoptotic cell death in septo-hippocampal cell cultures. *J Neurotrauma* 17:283–298

Portera-Cailliau C, Price DL, Martin LJ (1997) Excitotoxic neuronal death in the immature brain is an apoptosis-necrosis morphological continuum. *J Comp Neurol* 378:70–87

Posmantur RM, Kampfl A, Simon R, Liu SJ, Zhao X, Clifton GL, Hayes RL (1997) A calpain inhibitor attenuates cortical cytoskeletal protein loss after experimental brain injury in the rat. *Neuroscience* 77:875–888

Purnanam KL, Boustany R-M (1999) Assessment of cell viability and histochemical methods in apoptosis. In: *Apoptosis in neurobiology* (Hannun YA, Boustany R-M, eds), Boca Raton, FL: CRC Press, pp 129–152

Rami A, Agarwal R, Botez G, Winckler J (2000) α-Calpain activation, DNA fragmentation, and synergistic effects of caspase and calpain inhibitors in protecting hippocampal neurons from ischemic damage. *Brain Res* 866:299–312

Rink A, Fung KM, Trojanowski JQ, Lee VMY, Neugebauer E, McIntosh TK (1995) Evidence of apoptotic cell death after experimental traumatic brain injury in the rat. *Am J Path* 147:1575–1583

Roberts-Lewis JM, Savage MJ, Marcy V, Pinsker LR, Simon R (1994) Immunolocalization of μ-calpain mediated spectrin degradation to vulnerable neurons in ischemic gerbil brain. *J Neurosci* 14:3934–3944

Saatman KE, Bozyczko-Coyne D, Marcy V, Simon R, McIntosh TK (1996) Prolonged calpain-mediated spectrin breakdown occurs regionally following experimental brain injury in the rat. *J Neuropathol Exp Neurol* 55:850–860

Saatman KE, Zhang C, Bartus RT, McIntosh TK (2000) Behavioral efficacy of posttraumatic calpain inhibition is not accompanied by reduced spectrin proteolysis, cortical lesion, or apoptosis. *J Cereb Blood Flow Metab* 20:66–73

Saido TC, Yokota M, Nagao S, Yamaura I, Tani E, Tsuchiya T, Suzuki K, Kawashima S (1993) Spatial resolution of fodrin proteolysis in postischemic brain. *J Biol Chem* 268:25239–25243

Schmechel DE (1999) Assessment of ultrastructural changes associated with apoptosis. In: *Apoptosis in neurobiology* (Hannun YA, Boustany R-M, eds), Boca Raton, FL: CRC Press, pp 153–181

Sloviter RS, Dean E, Sollas AL, Goodman JH (1996) Apoptosis and necrosis induced in different hippocampal neuron populations by repetitive perforant path stimulation in the rat. *J Comp Neurol* 366:516–533

Squier MK, Miller AC, Malkinson AM, Cohen JJ (1994) Calpain activation in apoptosis. *J Cell Physiol* 159:229–237

Vanags DM, Porn-Ares MI, Coppola S, Burgess DH, Orrenius S (1996) Protease involvement in fodrin cleavage and phosphatidylserine exposure in apoptosis. *J Biol Chem* 271:31075–31081

Wang KKW, Nath R, Raser KJ, Hajimohammadreza I (1996) Maitotoxin induces calpain activation in SH-SY5Y neuroblastoma cells and cerebrocortical cultures. *Arch Biochem Biophys* 331:208–214

Wang KKW, Posmantur RM, Nadimpalli R, Nath R, Nixon R, Talanian RV, Allen H (1998*a*) Caspase-mediated fragmentation of calpain inhibitor protein calpastatin during apoptosis. *Arch Biochem Biophys* 356:187–196

Wang KKW, Posmantur RM, Nath R, McGinnis KM, Whitton M, Talanian RV, Glartz SB, Morrow JS (1998*b*) Simultaneous degradation of αII- and βII-spectrin by caspase 3 (CPP32) apoptotic cells. *J Biol Chem* 273:22490–22497

Wang KKW (2000) Calpain and caspase: can you tell the difference? *Trends Neurosci* 23:20–26

Wolf BB, Goldstein JC, Stennicke HR, Beere H, Amarante-Mendes GP, Salvesen GS, Green DR (1999) Calpain functions in a caspase-independent manner to promote apoptotic-like events during platelet activation. *Blood* 94:1683–1692

Yakovlev AG, Knoblach SM, Fan L, Fox GB, Goodnight R, Faden AI (1997) Activation of CPP32-like caspases contributes to neuronal apoptosis and neurological dysfunction after traumatic brain injury. *J Neurosci* 17:7415–7424

Yokota M, Saido TC, Tani E, Kawashima S, Suzuki K (1995) Three distinct phases of fodrin proteolysis induced in postischemic hippocampus. Involvement of calpain and unidentified protease. *Stroke* 26:1901–1907

Zhao X, Pike BR, Newcomb JK, Wang KKW, Postmantur RM, Hayes RL (1999) Maitotoxin induces calpain but not caspase-3 activation

and necrotic cell death in primary septo-hippocampal cultures. *Neurochem Res* 24:371–382

Zhao X, Newcomb JK, Pike BR, Posmantur RM, Wang KKW, Hayes RL (2000) Novel characteristics of glutamate-induced cell death in primary septo-hippocampal cultures: relationship to calpain and caspase-3 protease activation. *J Cereb Blood Flow Metab* 20:550–562

JOURNAL OF NEUROTRAUMA
Volume 21, Number 9, 2004

Pp. 1183–1195

Cell-Specific Upregulation of Survivin after Experimental Traumatic Brain Injury in Rats

ERIK A. JOHNSON,[1,2] STANISLAV I. SVETLOV,[1,2] BRIAN R. PIKE,[1,2] PAUL J. TOLENTINO,[1,4] GERALD SHAW,[1,2,5] KEVIN K.W. WANG,[1,2,6] RONALD L. HAYES,[1,2,4,6] and JOSE A. PINEDA[1,3]

ABSTRACT

In this study, we examined the expression and cellular localization of survivin and proliferating cell nuclear antigen (PCNA) after controlled cortical impact traumatic brain injury (TBI) in rats. There was a remarkable and sustained induction of survivin mRNA and protein in the ipsilateral cortex and hippocampus of rats after TBI, peaking at five days post injury. In contrast, both survivin mRNA and protein were virtually undetectable in craniotomy control animals. Concomitantly, expression of PCNA was also significantly enhanced in the ipsilateral cortex and hippocampus of these rats with similar temporal and spatial patterns. Immunohistochemistry revealed that survivin and PCNA were co-expressed in the same cells and had a focal distribution within the injured brain. Further analysis revealed a frequent co-localization of survivin and GFAP, an astrocytic marker, in both the ipsilateral cortex and hippocampus, while a much smaller subset of cells showed co-localization of survivin and NeuN, a mature neuronal marker. Neuronal localization of survivin was observed predominantly in the ipsilateral cortex and contralateral hippocampus after TBI. PCNA protein expression was detected in both astrocytes and neurons of the ipsilateral cortex and hippocampus after TBI. Collectively these data demonstrate that the anti-apoptotic protein survivin, previously characterized in cancer cells, is abundantly expressed in brain tissues of adult rats subjected to TBI. We found survivin expression in both astrocytes and a sub-set of neurons. In addition, the expression of survivin was co-incident with PCNA, a cell cycle protein. This suggests that survivin may be involved in regulation of neural cell proliferative responses after traumatic brain injury.

Key words: astrocyte; neuron; PCNA; survivin; traumatic brain injury

INTRODUCTION

TRAUMATIC BRAIN INJURY (TBI) is a major health care issue that can lead to permanent motor, cognitive and behavioral deficits. These deficits are the result of neural tissue injury and cell death, most of which occurs within the first days after injury (Raghupathi et al., 2000). The ability of this tissue to resist injury and recover depends

[1]Center for Traumatic Brain Injury Studies, E.F and W.L. McKnight Brain Institute of the University of Florida, Gainesville, Florida.

Departments of [2]Neuroscience, [3]Pediatrics, [4]Neurosurgery, [5]Anatomy and Cell Biology, and [6]Psychiatry, University of Florida, Gainesville, Florida.

188

largely on two factors, the survival potential of the cells and the proliferative ability of the cells in the affected area. Therefore, proliferation of cells in response to injury is important in the compensatory/reparative process. Astrocytes multiply possibly to support surviving neurons and prevent further tissue damage through formation of the glial scar (Ridet et al., 1997; Bush et al., 1999; Smith et al., 2001). Microglia increase to remove cellular debris and promote recovery (Giulian, 1991). Neurons may be replenished by neural stem cells in the dentate gyrus and subventricular zones (Doetsch et al., 1999; Cameron and McKay, 2001; Kernie et al., 2001; Yagita et al., 2001; Peterson, 2002). Consistent with these findings, cell cycle protein expression has been shown after TBI (Kaya et al., 1999a). However, studies have not investigated the role of survivin, a pro-mitotic and anti-apoptotic protein, in the adult brain after TBI.

Survivin is a novel member of the inhibitor of apoptosis protein (IAP) family that can inhibit activated caspases (Ambrosini et al., 1997; LaCasse et al., 1998; Takahashi et al., 1998; Tamm et al., 1998; Deveraux and Reed, 1999; Li and Altieri, 1999; Muchmore et al., 2000; Jiang et al., 2001). Survivin is also an evolutionarily conserved chromosomal passenger protein that is required for proper completion of mitosis. Survivin is present during normal tissue development (Adida et al., 1998; Kobayashi et al., 1999) but is absent in most adult tissues including the brain (Ambrosini et al., 1997; Kobayashi et al., 1999). Many cancer cell lines and cancer tumors, such as neural derived neuroblastoma and glioblastoma, which proliferate at high rates, exhibit survivin over-expression (Altieri et al., 1999; Sasaki et al., 2002). In addition, blocking survivin expression with anti-sense oligonucleotides in these cell lines leads to cell death (Shankar et al., 2001).

In this paper, we demonstrate the induction of survivin expression at the levels of mRNA and protein in the cortex and hippocampus of rats after traumatic brain injury. Survivin protein was primarily localized to astrocytes and in a small subset of neurons as indicated by its co-localization with GFAP and NeuN. In addition, a remarkable induction of proliferating cell nuclear antigen (PCNA) was observed after TBI and also localized to astrocytes and neurons. Finally, survivin and PCNA were co-expressed in single cells suggesting a possible role for survivin in regulation of cellular proliferative responses following TBI.

MATERIALS AND METHODS

Induction of Controlled Cortical Impact Brain Injury

The surgical and cortical impact injury procedures were conducted as previously described (Dixon et al., 1991; Pike et al., 1998). Briefly, adult male Sprague-Dawley rats (250–300 g) were anesthetized with 4% isoflurane (Halocarbon Laboratories; River Edge, NJ) in 1:1 O_2/N_2O for 4 min and maintained during surgery with 2.5% isoflurane. Core body temperature was continuously monitored using a rectal thermistor probe and maintained at 36.5–37.5°C using an adjustable heating pad. A unilateral craniotomy (ipsilateral to injury) was performed over the right cortex between the sagittal suture, bregma, and lambda while leaving the dura intact. Traumatic insult was generated by impacting the exposed cortex with a 5-mm-diameter aluminum tip at a velocity of 4 m/sec, a 150-msec dwell time, and a 1.6-mm compression. Craniotomy control animals received the cra-niotomy but not the impact injury. All procedures were performed according to guidelines established by the University of Florida Institutional Animal Care and Use Committee (IACUC) and the National Institutes of Health (NIH).

Quantitative Real-Time Polymerase Chain Reaction (Q-PCR)

Survivin primers were generated using GeneBank locus AF 276775: forward primer 5′ TAAGC CACTT GTCCC AGCTT 3′, and reverse primer 5′ AGGAT GGTAC CCCAT TACCT 3′. GAPDH: forward primer 5′ GGCTG CCTTC TCTTG TGAC 3′ and the reverse primer 5′ CACCA CTTCG TCCGC CGG 3′. Cortical and hippocampal tissues from the ipsilateral and contralateral hemispheres were rapidly excised at either 1, 2, 3, 5, 7, or 14 days and "snap-frozen" with liquid nitro-

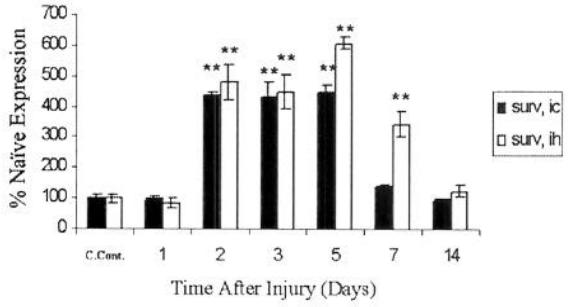

FIG. 1. Survivin mRNA induction in rat brain after traumatic brain injury. Rats were subjected to craniotomy followed by controlled cortical impact brain injury. Total RNA was isolated from injured (ipsilateral) cortex (ic) and hippocampus (ih) at indicated post-injury times. cDNA was synthesized, and quantitative PCR using survivin primers was performed. Data are given as percent of survivin expression over craniotomy controls (C. Cont.); each time point represents mean ± SEM of four independent measurements in craniotomy control or TBI group. $^{**}p < 0.01$ versus craniotomy control (one-way ANOVA test with *post hoc* Bonferroni analysis).

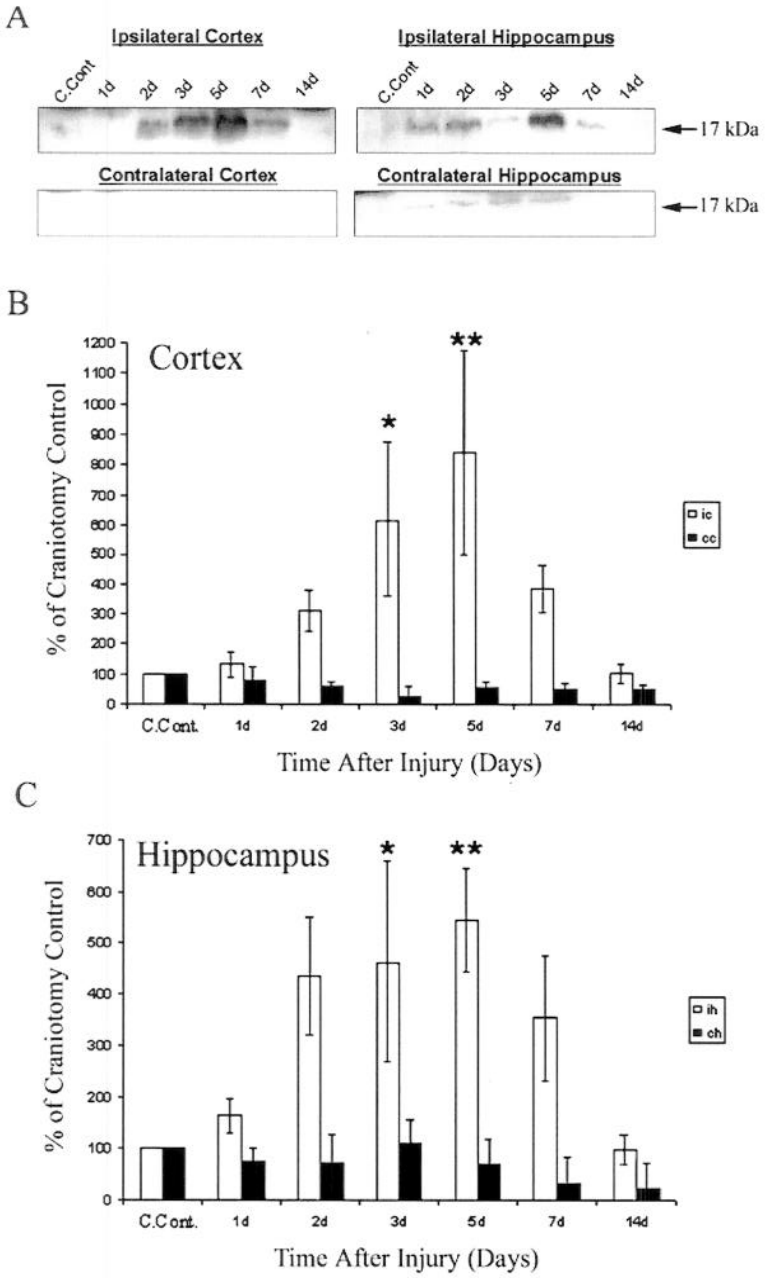

FIG. 2. Expression of survivin protein after TBI in rats. Brain tissue homogenate proteins (40 μg) were separated using SDS-PAGE, immunoblotted with survivin antibody, and visualized. **(A)** Representative Western blot of survivin (17-kDa protein) in ipsilateral cortex (ic) and hippocampus (ih), contralateral cortex (cc) and hippocampus (ch) obtained from injured rats, and from craniotomy control rats without cortical impact (C. Cont.). Densitometry analysis representation of survivin-positive bands in ipsilateral (ic) and contralateral (cc) cortex **(B)** and ipsilateral (ih) and contralateral (ch) hippocampus **(C)** after TBI is shown as percent of craniotomy control values. Each data point represents the mean ± SEM of four to six independent experiments. $*p < 0.05$, $**p < 0.001$ versus craniotomy control (one-way ANOVA test with *post hoc* Bonferroni analysis).

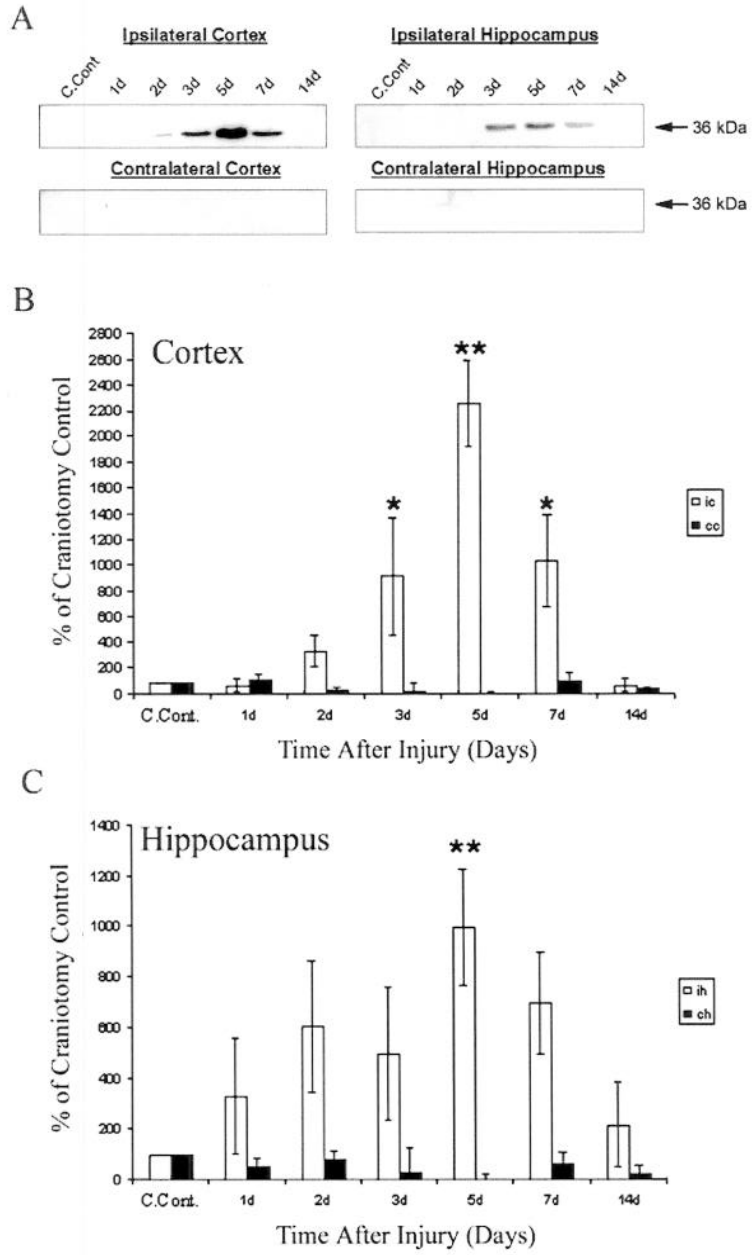

FIG. 3. Expression of PCNA after TBI in rats. PVDF membranes visualized for survivin were stripped and re-probed with PCNA antibody. Representative western blots showing PCNA (36 kDa) **(A)** and densitometry analysis of PCNA-positive bands **(B,C)** are presented. Experimental conditions, sample size and abbreviations are identical to those in Figure 2. $*p < 0.05$, $**p < 0.01$ versus craniotomy control (one-way ANOVA test with *post hoc* Bonferroni analysis).

gen. Total RNA was isolated from the samples using TRIzol reagent (Invitrogen, Carlsbad, CA) according to the manufacturer's instructions. cDNA synthesis was performed using 1 μg of total RNA with the SuperScript™ First-Strand Synthesis System for RT-PCR kit (Invitrogen/Life Technologies, Carlsbad, CA) according to the manufacturer's instructions. Q-PCR was performed as previously described (Tolentino et al., 2002) using the LightCycler-FastStart DNA Master SYBR Green I reaction mix (Roche Diagnostics, Indianapolis, IN) in combination with 0.5 μM primers, 2.5 mM $MgCl_2$ in the Light Cycler rapid thermal cycler system (Roche Diag-

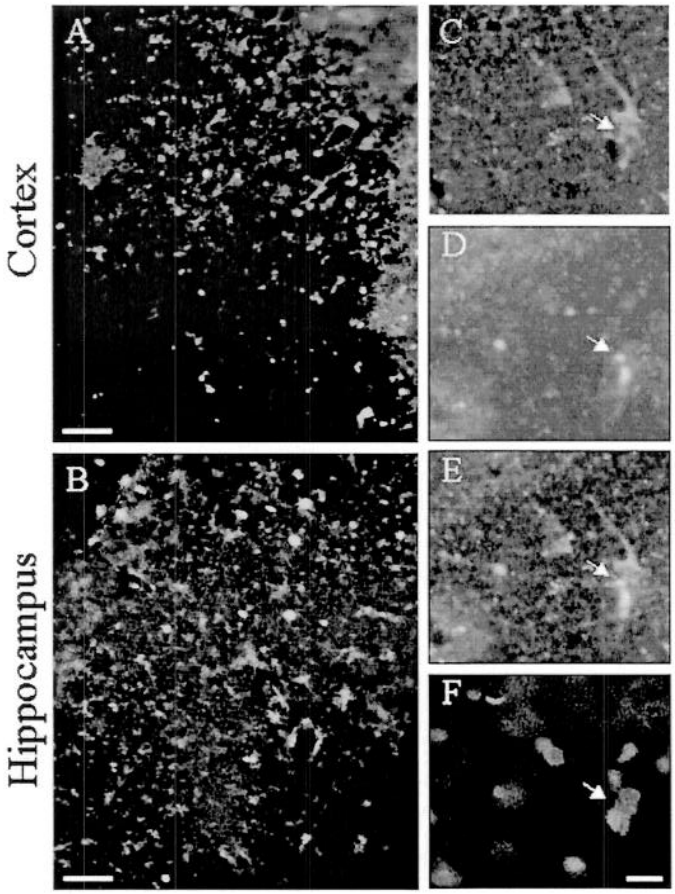

FIG. 4. Immunohistochemistry of survivin and PCNA. Double fluorescent immunostaining for survivin (red) and PCNA (green) was performed in the ipsilateral cortex **(A)** and hippocampus **(B)** at 5 day post-injury. Survivin is expressed in the cytoplasm **(C,** red), while PCNA is expressed in the nucleus **(D,** green). The white arrow indicates the typical focal co-expression of survivin and PCNA as shown in merged survivin and PCNA images **(E)**. PCNA expression was co-incident with DAPI staining **(F,** blue, white arrow). Original magnification, ×200; bar = 50 μm (A,B); original magnification ×400, bar = 20 μm (C–F).

nostics, Indianapolis, IN). Briefly, the primers were amplified then quantified by online monitoring and identification of the crossing point value (CPV) which is the exact time point at which the logarithmic linear phase could be distinguished from the background. The survivin primer sets were subjected to serial dilution and linear regression analysis of the logarithm of the dilution factor versus the CPV generated a standard curve for each transcript-speci-fic template. Results are presented as percentage of cranio-tomy control. Data were analyzed by ANOVA with a post-hoc Bonferroni-test and are given as mean ± SEM. Differences were considered significant at the level of $p \leq 0.05$.

Western Blot Analyses

Brain tissue was removed as described above, rinsed with cold PBS, snap frozen in liquid nitrogen and homogenized in ice-cold triple detergent lysis buffer containing a Complete™ protease inhibitor cocktail (Roche Biochemicals, Indianapolis, IN). Protein concentration was determined by bicinchoninic acid (BCA) micro protein assays (Pierce, Inc., Rockford, IL). Forty micrograms of protein per well was loaded and separated by SDS-PAGE, transferred to PVDF membranes and probed with goat-anti-rabbit survivin antibody (Novus Biologicals; Littleton, CO; 1:1000). After incubation with goat anti-rabbit HRP-labeled secondary antibody (Biorad, Hercules, CA), the membranes were developed using Enhanced Chemiluminescence Plus reagents (ECL Plus; Amersham, Arlington Heights, IL). For further PCNA analysis, developed PVDF membranes were incubated in stripping buffer, rinsed twice in TBST and incubated with PCNA antibody (Santa Cruz Biotech; Santa Cruz, CA;

1:1000) as described above. Semi-quantitative, densitometric analysis was performed using the AlphaImager™ 2000 Digital Imaging System (San Leandro, CA). Transformed data (experimental densitometry value/ craniotomy control densitometry value × 100) was evaluated by ANOVA and a post-hoc Bonferroni-test. Values are expressed as percentage of craniotomy controls and are given as mean ± SEM. Differences were considered significant at the level of $p \leq 0.05$.

Characterization of Survivin Antibody (R51)

First, we compared the specificity of the survivin antibody developed within our group (R51; Dr. G. Shaw) and a commercially available survivin antibody (Chemicon; Temecula, CA). Our antibody showed characteristic staining of the cleavage furrow between dividing HeLa cells consistent with other reports (Li et al., 1998, 1999; Uren et al., 2000). In addition, double labeling with both survivin antibodies showed co-localization at the cleavage furrow. The peptides used to develop our survivin antibody are specific to survivin and do not recognize other IAP family proteins according to SDSC Biology Workbench BLASTP (2.2.2) (Altschul et al., 1997) and CLUSTAL W (1.81) analysis (Higgins et al., 1992; Thompson et al., 1994), resulting in the survivin antibody's specificity.

Immunohistochemistry (IHC)

Animals were transcardially perfused with 2% Heparin (Elkins-Sinn, Inc.; Cherry Hill, NJ) in 0.9% saline solution (pH 7.4) followed by 4% paraformaldehyde in 0.1 M phosphate buffer (pH 7.4). The brains were post-fixed in 4% paraformaldehyde and stored in 0.1M PBS or cryobuffer. Forty micron sections were fluorescent immunolabeled with two primary antibodies in the following experiments: survivin (1:500)/GFAP for astrocytes (Sternberger; Lutherville, MD; 1:1000), survivin/NeuN for mature neurons (Chemicon; Temecula, CA; 1:1000), survivin/PCNA (Santa Cruz Biotech; Santa Cruz, CA; 1:200), PCNA/GFAP and PCNA/NeuN. The nuclear dye DAPI (in Vectashield; H-1200; Vector Laboratories; Burlingame, CA) was used to label the nuclei. The first primary antibody was incubated at 4°C for 24–48 h in a 2% goat serum/2% horse serum/0.2% Triton-X 100 in 0.1 M PBS (block) solution followed by the second primary antibody at 4°C for 1 h in block solution. Fluorescent-tagged secondary antibody (Molecular Probes; Eugene, OR) was used for visualization. For double-labeling using same species antibodies, we used the tyramide signal amplification (TSA) kit (PerkinElmer Life Sciences, Boston, MA) according to the manufacturer's instructions and as previously described (Stone et al., 2002). The sections were viewed and digitally captured with a Zeiss Axioplan 2 microscope (Zeiss, Thornwood, NY) AU1 equipped with a SPOT Real Time Slider high-resolution color CCD digital camera (Diagnostic Instruments, Inc., Sterling Heights, MI). The number of animals used for dual-labeling IHC is as follows: survivin × PCNA = 4, survivin × GFAP = 6, survivin × NeuN = 4, PCNA × GFAP = 4, and PCNA × NeuN = 4. Cell counts were obtained by comparing the number of double-labeled cells to total single-labeled cells in the following groups: survivin/NeuN positive cells to total NeuN positive cells, survivin/PCNA positive cells to total PCNA positive cells, PCNA/NeuN positive cells to total NeuN positive cells, and survivin/GFAP positive cells to total GFAP positive cells. Percentages were calculated by dividing the number of double-labeled cells with the total number of single-labeled cells. For each group, representative photomicrographs were selected and counted. Cells were counted in a total area of at least 188,000 μm^2 for each group, with no distinction made between cortical and hippocampal regions.

RESULTS

Induction of Survivin Expression after TBI

Q-PCR analysis revealed an initial increase in survivin mRNA at 2 days post injury in the ipsilateral cortex and hippocampus. These transcripts remained elevated in both regions, reached maximum levels at day 5 post-injury and declined at 7 days in the cortex and at 14 days in the hippocampus. All experimental animals remained alive and exhibited slightly impaired motor and cognitive impairments (data not shown). Cortical mRNA levels reached a maximum of 448 ± 10.0%, whereas hippocampal mRNAs attained 606 ± 10.0% compared to craniotomy control values (Fig. 1). To determine if the F1 induction of survivin mRNA resulted in corresponding increases in survivin protein, western blot analysis was performed. Survivin (17-kDa protein) was readily detectable in the ipsilateral cortex and hippocampus of TBI rats, while it was negligible in contralateral cortex and hippocampus (Fig. 2A). Survivin was expressed in a F2 time-dependent manner with a maximum increase at 5 days after injury followed by a gradual decline by 14 days. Specifically, the levels of survivin in cortical tissue were 616 ± 257% at 3 days and 839 ± 339% at 5 days compared to craniotomy controls (Fig. 2B). Similar increases of survivin protein in the ipsilateral hippocampus were detected at 3 d and 5 days post injury: 464 ± 196% and 545 ± 102% compared to craniotomy control, respectively (Fig. 2C).

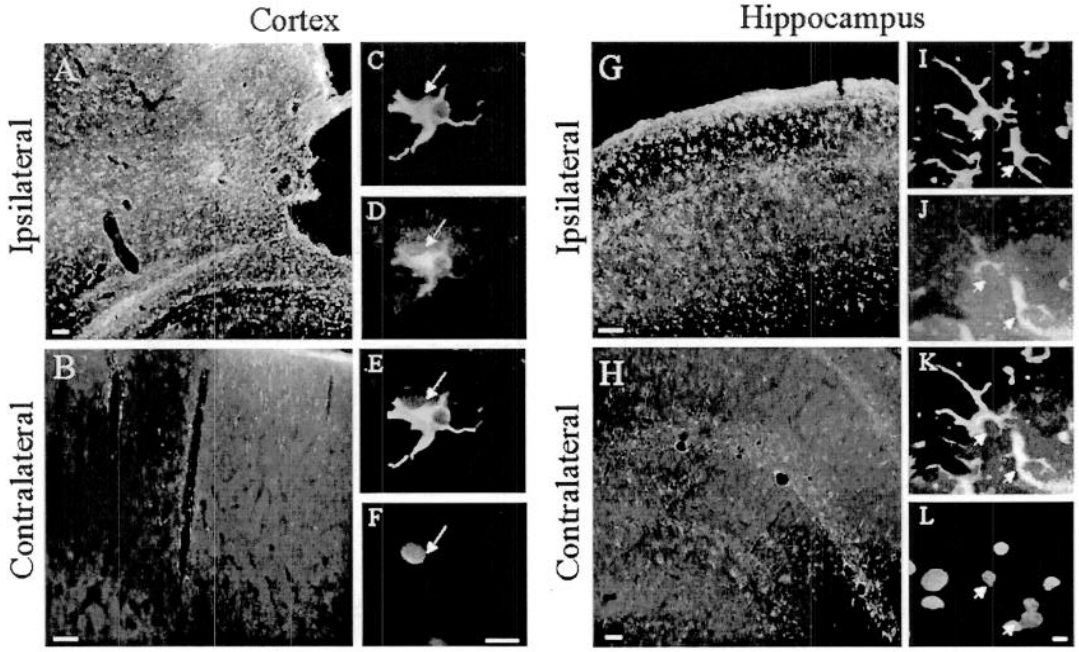

FIG. 5. Co-localization of survivin and GFAP in brain tissue after TBI. Fluorescent immunohistochemistry for survivin (green) and GFAP (red) was performed in the ipsilateral and contralateral cortex **(A,B)** and in the CA1 and dentate gyrus regions of the hippocampus **(G,H)** at 5 day post-injury. The injury has completely destroyed the cortex in G leaving only the hippocampus in this picture. Survivin was expressed in the cytoplasm **(D,J,** green) of GFAP-positive astrocytes **(C,I,** red) of the ipsilateral cortex and hippocampus and was found to co-localize to these cells as shown in merged C/D and I/J images **(E,K,** respectively, yellow). White arrows indicate typical survivin-positive astrocytes. Nuclei are shown using DAPI **(F,L,** blue). Original magnification, ×100, bar = 50 μm (A,B,G,H); ×400, bar = 20 μm (C–F and I–L).

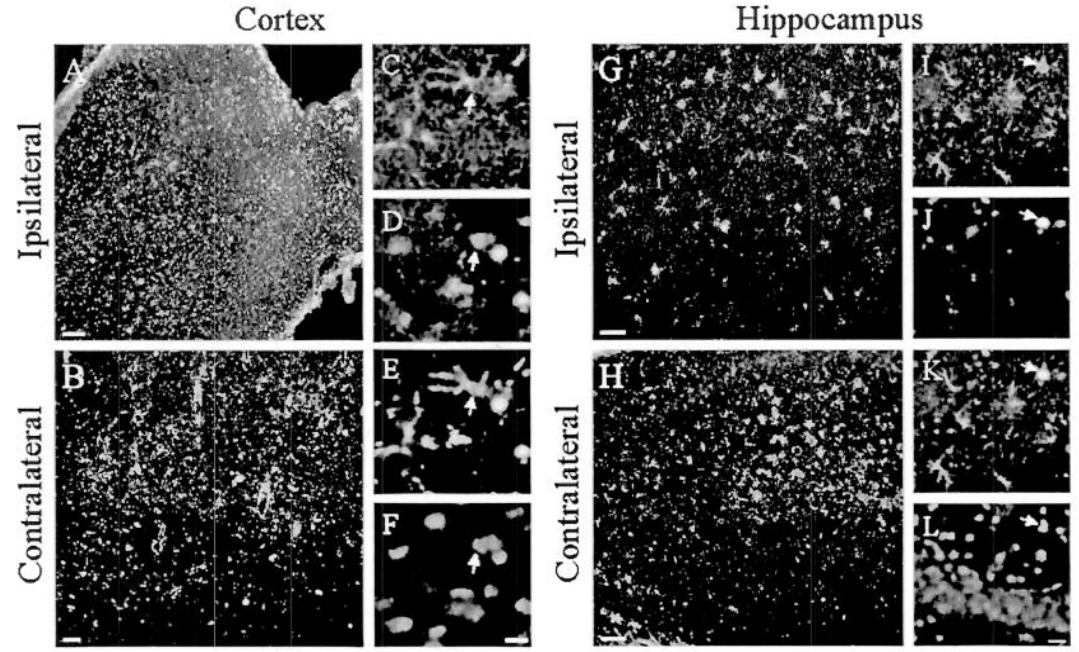

FIG. 6. Co-localization of PCNA and GFAP in brain tissue after TBI. Double immunostaining for PCNA (green) and GFAP (red) was performed in the ipsilateral and contralateral cortex **(A,B)** and the CA1 and dentate gyrus regions of the hippocampus **(G,H)** at 5 day post-injury. PCNA is present in GFAP-positive cells of ipsilateral cortex **(C,D)** and, to a lesser extent hippocampus **(I,J)**. **(E,K)** Merged C/D and I/J, respectively. White arrows indicate typical PCNA-positive astrocytes. PCNA expression was co-incident with DAPI staining **(F,L,** blue). Original magnification, ×100; bar = 50 μm (A,B,G,H); ×400, bar = 20 μm (C–F, and I–L).

PCNA Expression after TBI

For detection of proliferating cell nuclear antigen (PCNA), PVDF membranes immunostained for survivin were stripped and re-probed using a PCNA-specific antibody. PCNA (36-kDa protein) was significantly detectable in the ipsilateral cortex and hippocampus of TBI rats, but only negligible amounts were observed in the contralateral cortex and hippocampus (Fig. 3A). The temporal patterns exhibited by PCNA protein were similar to that of survivin protein. Namely, PCNA expressed in a time-dependant fashion with a maximum increase at 5 days after injury followed by a gradual decline by 14 days. The levels of PCNA in ipsilateral cortical tissue were raised over craniotomy control by 919 ± 459% at 3 days, 2263 ± 333% at 5 days, and 1035 ± 356% at 7 days post injury (Fig. 3B). Similar increases of PCNA protein in ipsilateral hippocampus were detected at 5 days post injury with a maximum of 1006 ± 229% compared to craniotomy controls (Fig. 3C). No significant increase was found in the contralateral regions when compared to craniotomy controls (Fig. 3A).

F3

Co-Expression of Survivin and PCNA following TBI

To examine spatial co-localization of survivin and PCNA, double-label immunohistochemistry of brain tissue sections was performed on day 5 post injury, when peak expression of these proteins was observed.

At this time point, a remarkable survivin and PCNA immunoreactivity was found in the ipsilateral cortex (Fig. 4A) and ipsilateral hippocampus (Fig. 4B) consistent with data obtained using Western blot analyses. Within both regions, focal co-expression patterns of survivin and PCNA in single cells were detected, which was demonstrated by both separate fluorescent visualization of individual proteins and by merging the images of double-stained slides (Fig. 4C–E). However, the dual expression of survivin and PCNA occurred infrequently as survivin and PCNA immunoreactivity could readily be found separately (Fig. 4C–E). Approximately 12% of the total number of PCNA-positive cells also labeled with survivin. The nuclear morphology of dual survivin and PCNA-positive cells was ambiguous as indicated by DAPI staining (Fig. 4F). Therefore, DAPI staining was simply used for cell identification in all subsequent experiments.

F4

Survivin and PCNA Are Expressed in Astrocytes after TBI

To determine the cell types expressing survivin and PCNA, double-label immunohistochemistry for these proteins and GFAP, a marker of astrocytes, was performed on day 5 post injury.

In accordance with Western blot data, remarkable survivin-positive immunoreactivity was observed in the ipsilateral cortex and hippocampus proximal to the injury cavity (Fig. 5A,G, green) but not in the contralateral areas (Fig. 5B,H). Survivin was co-localized with GFAP in the cells of injured cortex and hippocampus, which strongly suggested primary accumulation of survivin in cells of astrocytic lineage (Fig. 5C–E,I–L). Survivin was uniformly distributed in the cytoplasm and processes of astrocytes in both cortex and hippocampus (Fig. 5D,J). DAPI staining is shown in Figure 5F,L3. Approximately 88% of the total number of GFAP-positive cells also labeled with survivin.

F5

PCNA-positive immunoreactivity staining was observed in the ipsilateral cortex (Fig. 6A, green) and hippocampus (Fig. 6G, green) of injured brain, while contralateral cortex and hippocampus exhibited negligible PCNA immunoreactivity (Fig. 6B,H). PCNA (Fig. 6C,I) was partially co-localized with GFAP (Fig. 6D,J, red) in both regions, and was characteristically distributed in the nucleus of the cells in both cortex and hippocampus (Fig. 6E,K). DAPI staining is shown in Figure 6F,L.

F6

Taken together, double-label immunohistochemistry data provides evidence that both survivin and PCNA can be detected in GFAP-positive astrocytes following traumatic insult. Since survivin and PCNA immunoreactivity was not exclusively localized in GFAP-positive cells, we next addressed a question what other cell type might express survivin after TBI. We suggested that a certain population of mature neurons might express survivin in response to injury.

Survivin and PCNA Are Expressed in a Sub-Set of Neurons after TBI

As can be seen in Figure 7, survivin and PCNA were each co-expressed with NeuN, a marker of mature neurons. NeuN-positive cells were found to express survivin in the ipsilateral cortex distal to the injury cavity (Fig. 7A–D) and in the contralateral hippocampus (Fig. 7E–H). It should be noted, however, that NeuN-positive cells that also expressed survivin occurred infrequently. For example, we estimated the number of dual survivin/NeuN positive cells as 0.1–1.5% of the total number of NeuN-positive cells in these regions. Survivin immunoreactivity was negligible in either hemisphere of craniotomy control brains (Fig. 7Q,R). No co-localization of survivin and NeuN was observed in ipsilateral hippocampus (data not shown). As can be seen in Figure 7B,F, survivin was predominantly localized to the cytoplasm and axons of NeuN-positive neurons. DAPI staining is shown in Figure 7D,H.

F7

PCNA-positive neurons were found in the ipsilateral cortex (Fig. 7I–L) and hippocampus after TBI (Fig.

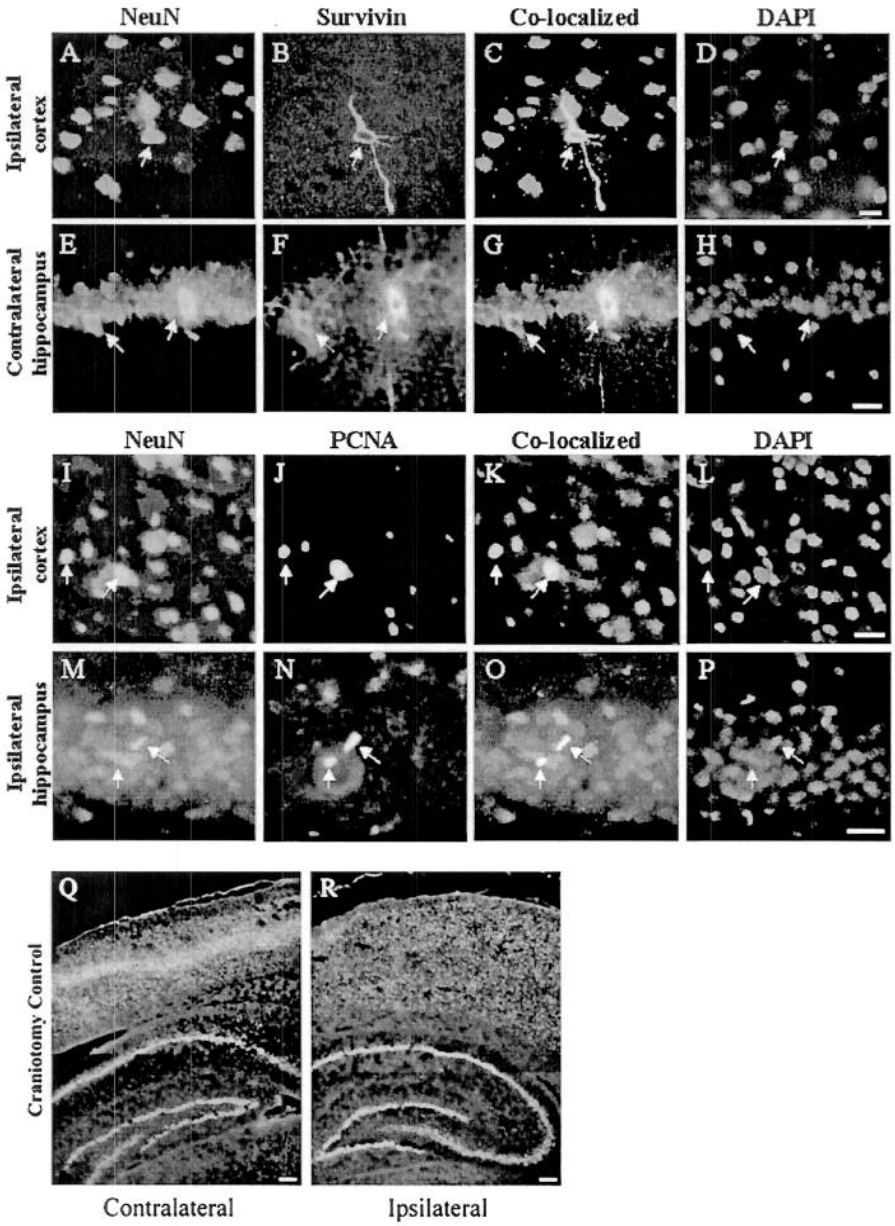

FIG. 7. A sub-set of NeuN-positive neurons express survivin and PCNA after TBI. Double fluorescent immunohistochemistry for survivin (green) and NeuN (red) in the ipsilateral cortex **(A,B)** and the CA1 pyramidal layer of the contralateral hippocampus **(E,F)** was performed. Survivin is expressed in the cytoplasm and, to a limited extent, in the processes of NeuN-positive neurons (merged images **C/G**). Dual staining for PCNA (green) and NeuN (red) is shown in the ipsilateral cortex **(I,J)** and the CA1 pyramidal layer of the ipsilateral hippocampus **(M,N)**. The nuclei are shown using DAPI staining (**D,H,** blue). PCNA is expressed in the nucleus of NeuN-positive neurons (merged images **K/O**). PCNA expression was co-incident with DAPI staining in these examples (**L,P,** blue). White arrows indicate focal co-localization of survivin/NeuN and PCNA/NeuN. Survivin/NeuN co-localization of survivin (green) and NeuN (red) was seen only in TBI rats as opposed to either hemisphere of craniotomy control **(Q,R)**. Original magnification, ×400, bar = 20 μm (A–P); original magnification, ×50, bar = 100,000 μm (Q,R).

7M–P), whereas craniotomy control tissue exhibited only trace amounts of PCNA (data not shown). Similar to the survivin/NeuN co-localization data, dual PCNA/NeuN immunostaining was a rare event accounting for approximately 4% of the total number of NeuN positive cells. PCNA was distributed in the nuclei of these neurons (Fig. 7K,O) although the nuclear morphology of these cells was not clearly resolved by DAPI staining (Fig. 7L,P).

DISCUSSION

Traumatic brain injury (TBI) sets into motion various biochemical cascades that induce neural tissue injury and cell death. Conversely, several proteins expressed in neural cells after TBI are directed to resist cell death and promote recovery in the injured CNS (Ridet et al., 1997; Chen and Swanson, 2003). Survivin is a multi-functional protein that inhibits apoptosis and is also required for the proper completion of mitosis. Anti-apoptotic and pro-mitogenic roles for survivin have been documented in proliferating cells of neural origin *in vitro*, such as in neuroblastoma and glioma cells (LaCasse et al., 1998; Tamm et al., 1998; Deveraux and Reed, 1999; Conway et al., 2000; Shin et al., 2001; Sasaki et al., 2002). However, no studies have investigated the potential role of survivin in the adult brain after TBI, when a sub-population of CNS cells may initiate a cell cycle-related process in response to injury.

In the present paper, we demonstrate the induction of survivin expression in rat brain subjected to TBI. The expression of survivin was time-dependent and cell-specific, and was present in astrocytes and, to a much lesser extent, in neurons in brain cortex and hippocampus. Induction of survivin in these cells was accompanied by occasional expression of PCNA, a cell cycle protein involved in mitotic G1/S progression. Our present data are the first to show that survivin mRNA and protein are significantly up-regulated after traumatic brain injury in rats. PCNA expression after TBI has been described previously (Miyake et al., 1992; Chen et al., 2003), suggesting its role in mechanisms of brain recovery after injury. The concurrent up-regulation of survivin with a similar temporal profile as PCNA shown herein further suggests that survivin may play a role in cellular proliferation after TBI.

Brain injury evoked the expression of survivin and PCNA in a time-dependent manner (Figs. 2 and 3). Western blot analysis revealed maximal co-expression of both survivin and PCNA at five days post injury. Immunohistochemistry at this time point, demonstrated co-localization of these proteins (Fig. 4), although most cells were labeled separately with PCNA and survivin. In fact, only 12% of the total number of PCNA-positive cells were also survivin positive. It has been reported that PCNA is expressed predominantly in G1/S (Bravo et al., 1987), while survivin is found at the G2/M phase of the cell cycle (Bravo et al., 1987; Otaki et al., 2000). Hence, a lack of strict co-localization of survivin and PCNA in our study may be explained by their expression at different points in the cell cycle.

In our experimental model, we observed survivin- as well as PCNA-positive astrocytes in the proximal area of the injury and in the ipsilateral hippocampus. Proliferation of astrocytes is well documented after TBI as shown by cell labeling with BrdU as well as expression of PCNA (Latov et al., 1979; Dunn-Meynell and Levin, 1997; Carbonell and Grady, 1999; Norton, 1999; Csuka et al., 2000; Kernie et al., 2001; Chen et al., 2003). Because survivin and PCNA were expressed in astrocytes following TBI (Figs. 5 and 6), it is possible that survivin plays an important role linking astrocyte survival and proliferation after traumatic insult. Astrocyte proliferation has been implicated in the formation of the glial scar observed after injury (Latov et al., 1979) and creates a non-permissive environment for repair (Sykova et al., 1999). However, glial proliferation may also enhance neuronal survival (Smith et al., 2001; Wei et al., 2001).

Of particular interest is a sub-set of NeuN-positive neurons found to express survivin only after TBI (Fig. 7). These cells were much less abundant than survivin-positive astrocytes, and their functional significance is currently unknown. However, both neurons and astrocytes have been documented previously to express cell cycle proteins after various insults such as exposure to β-amyloid–activated microglia (Wu et al., 2000), TBI (Kaya et al., 1999a,b), chlorine toxicity (Magavi et al., 2000), or as a consequence of Alzheimer's disease (Yang et al., 2001). These papers underscore the significant controversy that exists regarding the function of cell cycle proteins such as PCNA in neurons after different types of injury. We are currently conducting further studies which will elucidate the roles for PCNA and survivin in neurons after TBI.

It should be noted that dual staining of survivin and PCNA could not be directly attributed to a specific cell type due to the technical difficulties of triple labeling antibody-based IHC. Therefore, we cannot rule out the possibility that other cell types, such as endothelial (Conway et al., 2003) or inflammatory cells (Hill-Felberg et al., 1999), may also contribute to survivin and PCNA expression after TBI. The appearance of survivin and PCNA separately in neurons (NeuN-positive) and astrocytes (GFAP-positive) along with co-localization of survivin with PCNA in the same cells provide correlative data to suggest an activation of cell cycle-like program in astrocytes and possibly in a small subtype of neurons after

TBI. In our experiments, survivin co-localization with PCNA does suggest that survivin may be associated with a pro-mitotic process. In an attempt to clarify these protein's roles after TBI, we analyzed the nuclear morphology of survivin-positive cells to define the apoptotic or mitotic architecture of nuclei. DAPI staining proved too ambiguous in identifying apoptotic versus mitotic phenotypes likely due to the thickness of the brain sections (40 μm). Further studies using direct markers of mitosis such as BrdU incorporation as well as simultaneous labeling with cell death related proteins is required to delineate anti-apoptotic and pro-mitotic activities of survivin and PCNA in these cells.

In conclusion, our data demonstrate the induction of survivin in the rat brain following TBI. Expression of survivin occurred predominantly in astrocytes as compared to neurons in a time-dependant fashion and was accompanied by expression of PCNA. Taken together, these results suggest that survivin plays a role in neural cell responses following traumatic brain injury in rats. Future studies will investigate the implications of these findings to the pathophysiology of TBI.

ACKNOWLEDGMENTS

We thank Barbara O'Steen and Tao Fan, M.D., for technical assistance. This work was funded by grants NIH RO1 NS39091, NIH RO1 NS40182, DAMD 17-99-1-9565, and DAMD 17-01-1-0765.

REFERENCES

ADIDA, C., CROTTY, P.L., McGRATH, J., BERREBI, D., DIEBOLD, J., and ALTIERI, D.C. (1998). Developmentally regulated expression of the novel cancer anti-apoptosis gene survivin in human and mouse differentiation. Am. J. Pathol. **152,** 43–49.

ALTIERI, D.C., MARCHISIO, P.C., and MARCHISIO, C. (1999). Survivin apoptosis: an interloper between cell death and cell proliferation in cancer. Lab. Invest. **79,** 1327–1333.

ALTSCHUL, S.F., MADDEN, T.L., SCHAFFER, A.A., et al. (1997). Gapped BLAST and PSI-BLAST: a new generation of protein database search programs. Nucleic Acids Res. **25,** 3389–3402.

AMBROSINI, G., ADIDA, C., and ALTIERI, D.C. (1997). A novel anti-apoptosis gene, survivin, expressed in cancer and lymphoma. Nat. Med. **3,** 917–921.

BRAVO, R., FRANK, R., BLUNDELL, P.A., and MACDONALD-BRAVO, H. (1987). Cyclin/PCNA is the auxiliary protein of DNA polymerase-delta. Nature **326,** 515–517.

BUSH, T.G., PUVANACHANDRA, N., HORNER, C.H., et al. (1999). Leukocyte infiltration, neuronal degeneration, and neurite outgrowth after ablation of scar-forming, reactive astrocytes in adult transgenic mice. Neuron **23,** 297–308.

CAMERON, H.A., and McKAY, R.D. (2001). Adult neurogenesis produces a large pool of new granule cells in the dentate gyrus. J. Comp. Neurol. **435,** 406–417.

CARBONELL, W.S., and GRADY, M.S. (1999). Regional and temporal characterization of neuronal, glial, and axonal response after traumatic brain injury in the mouse. Acta Neuropathol. (Berl.) **98,** 396–406.

CHEN, X.H., IWATA, A., NONAKA, M., BROWNE, K.D., and SMITH, D.H. (2003). Neurogenesis and glial proliferation persist for at least one year in the subventricular zone following brain trauma in rats. J. Neurotrauma **20,** 623–631.

CHEN, Y., and SWANSON, R.A. (2003). Astrocytes and brain injury. J. Cereb. Blood Flow Metab. **23,** 137–149.

CONWAY, E.M., POLLEFEYT, S., CORNELISSEN, J., et al. (2000). Three differentially expressed survivin cDNA variants encode proteins with distinct antiapoptotic functions. Blood **95,** 1435–1442.

CSUKA, E., HANS, V.H., AMMANN, E., TRENTZ, O., KOSSMANN, T., and MORGANTI-KOSSMANN, M.C. (2000). Cell activation and inflammatory response following traumatic axonal injury in the rat. Neuroreport **11,** 2587–2590.

DEVERAUX, Q.L., and REED, J.C. (1999). IAP family proteins—suppressors of apoptosis. Genes Dev. **13,** 239–252.

DIXON, C.E., CLIFTON, G.L., LIGHTHALL, J.W., YAGHMAI, A.A., and HAYES, R.L. (1991). A controlled cortical impact model of traumatic brain injury in the rat. J. Neurosci. Methods **39,** 253–262.

DOETSCH, F., CAILLE, I., LIM, D.A., GARCIA-VERDUGO, J.M., and ALVAREZ-BUYLLA, A. (1999). Subventricular zone astrocytes are neural stem cells in the adult mammalian brain. Cell **97,** 703–716.

DUNN-MEYNELL, A.A., and LEVIN, B.E. (1997). Histological markers of neuronal, axonal and astrocytic changes after lateral rigid impact traumatic brain injury. Brain Res. **761,** 25–41.

GIULIAN, D. (1991). Microglia—neuron interactions after injury to the central nervous system, in: *Peripheral Signaling of the Brain: Role in Neural-Immune Interactions, Learning and Memory.* R. Frederickson, J. McGaugh, and D. Felton (eds.) Lewiston, NY: Hogrefe and Huber, pps. 73–82.

HIGGINS, D.G., BLEASBY, A.J., and FUCHS, R. (1992). CLUSTAL V: improved software for multiple sequence alignment. Comput. Appl. Biosci. **8,** 189–191.

HILL-FELBERG, S.J., McINTOSH, T.K., OLIVER, D.L., RAGHUPATHI, R., and BARBARESE, E. (1999). Concurrent loss and proliferation of astrocytes following lateral fluid percussion brain injury in the adult rat. J. Neurosci. Res. **57,** 271–279.

JIANG, X., WILFORD, C., DUENSING, S., MUNGER, K,, JONES, G., and JONES, D. (2001). Participation of Survivin in mitotic and apoptotic activities of normal and tumor-derived cells. J. Cell. Biochem. **83,** 342–354.

KAYA, S.S., MAHMOOD, A., LI, Y., YAVUZ, E., and CHOPP, M. (1999a). Expression of cell cycle proteins (cyclin D1 and cdk4) after controlled cortical impact in rat brain. J. Neurotrauma **16,** 1187–1196.

KAYA, S.S., MAHMOOD, A., LI, Y., YAVUZ, E., GOKSEL, M., and CHOPP, M. (1999b). Apoptosis and expression of p53 response proteins and cyclin D1 after cortical impact in rat brain. Brain Res. **818,** 23–33.

KERNIE, S.G., ERWIN, T.M., and PARADA, L.F. (2001). Brain remodeling due to neuronal and astrocytic proliferation after controlled cortical injury in mice. J. Neurosci. Res. **66,** 317–326.

KOBAYASHI, K., HATANO, M., OTAKI, M., OGASAWARA, T., and TOKUHISA, T. (1999). Expression of a murine homologue of the inhibitor of apoptosis protein is related to cell proliferation. Proc. Natl. Acad. Sci. USA **96,** 1457–1462.

LACASSE, E.C., BAIRD, S., KORNELUK, R.G., and MACKENZIE, A.E. (1998). The inhibitors of apoptosis (IAPs) and their emerging role in cancer. Oncogene **17,** 3247–3259.

LATOV, N., NILAVER, G., ZIMMERMAN, E.A., et al. (1979). Fibrillary astrocytes proliferate in response to brain injury: a study combining immunoperoxidase technique for glial fibrillary acidic protein and radioautography of tritiated thymidine. Dev. Biol. **72,** 381–384.

LI, F., and ALTIERI, D.C. (1999). The cancer antiapoptosis mouse survivin gene: characterization of locus and transcriptional requirements of basal and cell cycle-dependent expression. Cancer Res. **59,** 3143–3151.

LI, F., AMBROSINI, G., CHU, E.Y., et al. (1998). Control of apoptosis and mitotic spindle checkpoint by survivin. Nature **396,** 580–584.

LI, F., ACKERMANN, E.J., BENNETT, C.F., et al. (1999). Pleiotropic cell-division defects and apoptosis induced by interference with survivin function. Nat. Cell. Biol. **1,** 461–466.

MAGAVI, S.S., LEAVITT, B.R., and MACKLIS, J.D. (2000). Induction of neurogenesis in the neocortex of adult mice. Nature **405,** 951–955.

MIYAKE, T., OKADA, M., and KITAMURA, T. (1992). Reactive proliferation of astrocytes studied by immunohistochemistry for proliferating cell nuclear antigen. Brain Res. **590,** 300–302.

MUCHMORE, S.W., CHEN, J., JAKOB, C., et al. (2000). Crystal structure and mutagenic analysis of the inhibitor-of-apoptosis protein survivin. Mol. Cell. **6,** 173–182.

NORTON, W.T. (1999). Cell reactions following acute brain injury: a review. Neurochem. Res. **24,** 213–218.

OTAKI, M., HATANO, M., KOBAYASHI, K., et al. (2000). Cell cycle–dependent regulation of TIAP/m-survivin expression. Biochim. Biophys. Acta **1493,** 188–194.

PETERSON, D.A. (2002). Stem cells in brain plasticity and repair. Curr. Opin. Pharmacol. **2,** 34–42.

PIKE, B.R., ZHAO, X., NEWCOMB, J.K., POSMANTUR, R.M., WANG, K.K., and Hayes, R.L. (1998). Regional calpain and caspase-3 proteolysis of alpha-spectrin after traumatic brain injury. Neuroreport **9,** 2437–2442.

RAGHUPATHI, R., GRAHAM, D.I., MCINTOSH, T.K. (2000). Apoptosis after traumatic brain injury. J. Neurotrauma **17,** 927–938.

RIDET, J.L., MALHOTRA, S.K., PRIVAT, A., and GAGE, F.H. (1997). Reactive astrocytes: cellular and molecular cues to biological function. Trends Neurosci. **20,** 570–577.

SASAKI, T., LOPES, M.B., HANKINS, G.R., and HELM, G.A. (2002). Expression of survivin, an inhibitor of apoptosis protein, in tumors of the nervous system. Acta Neuropathol. (Berl.) **104,** 105–109.

SHANKAR, S.L., MANI, S., O'GUIN, K.N., KANDIMALLA, E.R., AGRAWAL, S., and SHAFIT-ZAGARDO, B. (2001). Survivin inhibition induces human neural tumor cell death through caspase-independent and -dependent pathways. J. Neurochem. **79,** 426–436.

SHIN, S., SUNG, B.J., CHO, Y.S., et al. (2001). An anti-apoptotic protein human survivin is a direct inhibitor of caspase-3 and -7. Biochemistry **40,** 1117–1123.

SMITH, C., BERRY, M., CLARKE, W.E., and LOGAN, A. (2001). Differential expression of fibroblast growth factor–2 and fibroblast growth factor receptor 1 in a scarring and non-scarring model of CNS injury in the rat. Eur. J. Neurosci. **13,** 443–456.

STONE, J.R., OKONKWO, D.O., SINGLETON R.H., MUTLU, L.K., HELM, G.A., and POVLISHOCK, J.T. (2002). Caspase-3–mediated cleavage of amyloid precursor protein and formation of amyloid Beta peptide in traumatic axonal injury. J. Neurotrauma **19,** 601–614.

SYKOVA, E., VARGOVA, L., PROKOPOVA, S., and SIMONOVA, Z. (1999). Glial swelling and astrogliosis produce diffusion barriers in the rat spinal cord. Glia **25,** 56–70.

TAKAHASHI R., DEVERAUX, Q., TAMM, I., et al. (1998). A single BIR domain of XIAP sufficient for inhibiting caspases. J. Biol. Chem. **273,** 7787–7790.

TAMM, I., WANG, Y., SAUSVILLE, E., et al. (1998). IAP-family protein survivin inhibits caspase activity and apoptosis induced by Fas (CD95), Bax, caspases, and anticancer drugs. Cancer Res. **58,** 5315–5320.

THOMPSON, J.D., HIGGINS, D.G., and GIBSON, T.J. (1994). CLUSTAL W: improving the sensitivity of progressive multiple sequence alignment through sequence weighting, position-specific gap penalties and weight matrix choice. Nucleic Acids Res. **22,** 4673–4680.

TOLENTINO, P.J., DEFORD, S.M., NOTTERPEK, L., et al. (2002). Up-regulation of tissue-type transglutaminase after traumatic brain injury. J. Neurochem. **80,** 579–588.

UREN, A.G., WONG, L., PAKUSCH, M., et al. (2000). Survivin and the inner centromere protein INCENP show similar cell-cycle localization and gene knockout phenotype. Curr. Biol. **10,** 1319–1328.

WEI, L.H., HUANG, C.Y., CHENG, S.P., CHEN, C.A., and HSIEH, C.Y. (2001). Carcinosarcoma of ovary associated with previous radiotherapy. Int. J. Gynecol. Cancer **11,** 81–84.

WU, Q., COMBS, C., CANNADY, S.B., GELDMACHER, D.S., and HERRUP, K. (2000). Beta-amyloid activated microglia induce cell cycling and cell death in cultured cortical neurons. Neurobiol. Aging **21,** 797–806.

YAGITA, Y., KITAGAWA, K., OHTSUKI, T., et al. (2001). Neurogenesis by progenitor cells in the ischemic adult rat hippocampus. Stroke **32,** 1890–1896.

YANG, Y., GELDMACHER, D.S., and HERRUP, K. (2001). DNA replication precedes neuronal cell death in Alzheimer's disease. J. Neurosci. **21,** 2661–2668.

Address reprint requests to:
Jose A. Pineda, Ph.D.
E.F and W.L. McKnight Brain Institute
University of Florida
100 S Newell Dr., Bldg. 59
L1-118 Dept. of Pediatrics
Gainesville, FL 32610

E-mail: pinedja@peds.ufl.edu

Exp Brain Res (2005) 167: 17–26
DOI 10.1007/s00221-005-2362-2

RESEARCH ARTICLE

Erik A. Johnson · Stanislav I. Svetlov
Kevin K. W. Wang · Ronald L. Hayes · Jose A. Pineda

Cell-specific DNA fragmentation may be attenuated by a survivin-dependent mechanism after traumatic brain injury in rats

Received: 3 December 2004 / Accepted: 23 March 2005 / Published online: 29 September 2005

Abstract Survivin attenuates apoptosis by inhibiting cleavage of some cell proteins by activated caspase-3. We recently discovered strong up-regulation of survivin, primarily in astrocytes and a sub-set of neurons, after traumatic brain injury (TBI) in rats. In this study we characterized co-expression of survivin with activated caspase-3 and downstream DNA fragmentation (TUNEL) in astrocytes and neurons after TBI. Western blot analysis revealed significant time-dependent increases in active caspase-3 between 5 and 14 days post-injury. No difference was observed between the proportion of survivin-positive and survivin-negative cells labeled with active caspase-3 at 5 or 7 days post-injury, as indicated by dual fluorescent immunostaining. Labeling of survivin-negative cells with TUNEL was, however, significantly greater than for survivin-positive cells, suggesting that expression of survivin may attenuate DNA cleavage and progression of apoptosis. A higher proportion of astrocytes than neurons accumulated active caspase-3. In contrast, co-localization with TUNEL was significantly higher for neurons than for astrocytes. These data suggest that survivin expression may attenuate DNA cleavage and cell death, and that this mechanism operates in a cell type-specific manner after TBI.

Keywords Astrocyte · Neuron · Caspase-3 · Survivin · Traumatic brain injury · Inhibitor of apoptosis protein

Abbreviations IAP: Inhibitor of apoptosis protein · IHC: Immunohistochemistry · TBI: Traumatic brain injury

E. A. Johnson · S. I. Svetlov · K. K. W. Wang
R. L. Hayes · J. A. Pineda
Center for Traumatic Brain Injury Studies (CTBIS),
E.F and W.L. McKnight Brain Institute of the University of Florida, Gainesville, FL 32610, USA
E-mail: erikj@ufbi.ufl.edu
E-mail: svetlov@mbi.ufl.edu
E-mail: kwang@psychiatry.ufl.edu
E-mail: hayes@ufbi.ufl.edu

E. A. Johnson · S. I. Svetlov
K. K. W. Wang · R. L. Hayes
Department of Neuroscience, E.F and W.L. McKnight Brain Institute of the University of Florida, 100 S Newell Dr. Bldg. 59, L1 100, Gainesville, FL 32610, USA

J. A. Pineda (✉)
Department of Pediatrics, E.F and W.L. McKnight Brain Institute of the University of Florida, 100 S Newell Dr. Bldg. 59, L1-118, Gainesville, FL 32610, USA
E-mail: pineda_J@kids.wustl.edu
Tel.: +1-314-4542545
Fax: +1-314-3610733

J. A. Pineda
Department of Pediatrics, Washington University School of Medicine, Campus Box 8116, St. Louis, MO 63110, USA

R. L. Hayes
Department of Anatomy and Cell Biology, E.F and W.L. McKnight Brain Institute of the University of Florida, Gainesville, FL 32610, USA

K. K. W. Wang · R. L. Hayes
Department of Psychiatry, E.F and W.L. McKnight Brain Institute of the University of Florida, c100 S Newell Dr. Bldg. 59, L4-100, Gainesville, FL 32610, USA

Introduction

Traumatic insult to the brain results in neural tissue injury through cell-death processes, including apoptosis. Apoptosis in damaged neural tissues is executed mainly by caspase-3 (Juan et al. 1997), activation of which results in the proteolytic cleavage of many intracellular substrates, such as alpha-II-spectrin, DFF45, PARP and Bcl-2 (Eldadah and Faden 2000). Most importantly, cleavage of deoxyribonuclease inhibitors promotes DNA fragmentation (Enari et al. 1998; Liu et al. 1998). In contrast, cleavage of vital cellular proteins by activated caspases and the progression of apoptosis is attenuated by IAPs (Deveraux et al. 1997; Roy et al. 1997; Takahashi et al. 1998; Maier et al. 2002) including

survivin (Ambrosini et al. 1998; Tamm et al. 1998; Shankar et al. 2001; Shin et al. 2001).

Although survivin does not prevent the activation of caspases from their inactive proforms, evidence shows that survivin can bind and inhibit the activity of caspase-3, caspase-7, and caspase-9 (Tamm et al. 1998; Kobayashi et al. 1999; O'Connor et al. 2000; Shin et al. 2001). Previous work in our laboratory has revealed significant up-regulation of survivin mRNA and protein primarily in astrocytes and a sub-set of neurons after TBI (Johnson et al. 2004). Relationships between survivin, apoptosis—specifically the accumulation of active caspase-3—and downstream DNA fragmentation (TUNEL) after TBI have not been investigated, however.

In this work we have demonstrated that activation of caspase-3 in injured rat brain occurs in a similar time-dependent fashion to survivin expression. Although no difference was observed in active caspase-3 expression in survivin-positive cells compared with survivin-negative cells, significantly lower TUNEL labeling was found in cells that expressed survivin. The proportion of astrocytes labeled with TUNEL was, moreover, significantly lower compared with neurons. These data, with our previous findings, suggest that survivin expression may attenuate DNA cleavage, in a cell-specific manner, after TBI.

Materials and methods

Induction of controlled cortical impact brain injury

Surgical and cortical impact injury procedures were conducted as previously described (Dixon et al. 1991; Pike et al. 1998). Briefly, adult male Sprague–Dawley rats (250–300 g) were anesthetized with 4% isoflurane (Halocarbon Laboratories; River Edge, NJ, USA) in 1:1 O_2/N_2O for 4 min and maintained during surgery with 2.5% isoflurane. Core body temperature was continuously monitored, by use of a rectal thermistor probe, and maintained at 36.5–37.5°C using an adjustable heating pad. A unilateral craniotomy (ipsilateral to injury) was performed over the right cortex between the sagittal suture, bregma and lambda, leaving the dura intact. Traumatic insult was generated by impacting the exposed cortex with a 5 mm diameter aluminium tip at a velocity of 4 m s^{-1}, a 150 ms dwell time and 1.6 mm compression. Craniotomy control animals received the craniotomy but not the impact injury. All procedures were performed according to guidelines established by the University of Florida Institutional Animal Care and Use Committee (IACUC) and the National Institutes of Health (NIH).

Western blot analyses

Ipsilateral and contralateral neocortex (−500 mm^2 centered on the craniotomy and excised to the corpus callosum) and the hippocampus were removed, rinsed with cold PBS, snap frozen in liquid nitrogen, and homogenized in ice-cold triple detergent lysis buffer containing a Complete protease inhibitor cocktail (Roche Biochemicals; Indianapolis, IN, USA). Protein concentration was determined by bicinchoninic acid (BCA) micro protein assays (Pierce Inc., Rockford, IL, USA). Forty micrograms of protein per well was loaded and separated by SDS–PAGE, transferred to PVDF membranes and probed with a goat-anti-rabbit antibody that recognized only active caspase-3 (Cell Signaling Technology; Beverly, MA, USA; 9661L; 1:1000). After incubation with goat anti-rabbit HRP-labeled secondary antibody (Biorad; Hercules, CA, USA), the membranes were developed using Enhanced Chemiluminescence Plus reagents (ECL Plus, Amersham; Arlington Heights, IL, USA). Semi-quantitative, densitometric analysis was performed using the AlphaImager 2000 Digital Imaging System (San Leandro, CA, USA). For both craniotomy controls and experimental groups $n=6$. Transformed data (experimental densitometry value/craniotomy control densitometry value×100) were evaluated by ANOVA and a post-hoc Dunnet test. Craniotomy control tissues from the ipsilateral hemisphere were used for statistical comparison, because of the small but detectable proteolytic activity present in the contralateral hemisphere after TBI. Values are expressed as percentage of craniotomy controls and are given as mean ± SEM. Differences were considered significant at the level of $P \leq 0.05$.

Immunohistochemistry (IHC)

Animals were sacrificed 5 or 7 days post-injury after being anesthetized with 4% isoflurane (Halocarbon Laboratories; River Edge, NJ, USA) in 1:1 O_2/N_2O for 4 min. The brains were blocked in OCT (Ted Pella; Redding, CA, USA), snap frozen in liquid nitrogen, and cut on a Leica CM3050 cryostat. Five-micron sections were attached to Fropen (Ted Pella)-treated coverslips, fixed in cold methanol for 20 min at –20°C, and fluorescent immunolabeled with two primary antibodies in subsequent experiments—active caspase-3 (1:100)/GFAP for astrocytes (Sternberger; Lutherville, MD, USA; 1:1000), active caspase-3/NeuN for mature neurons (Chemicon; Temecula, CA, USA; 1:1000) and active caspase-3/survivin (G. Shaw; 1:250). The survivin antibody created in-house has previously been characterized (Johnson et al. 2004). Sections were also labeled with the Apoptag Cell Death Labeling kit (terminal deoxynucleotidyl transferase-mediated biotinylated dUTP nick-end labeling or TUNEL), in accordance with the manufacturer's instructions, to mark double-stranded DNA breaks. This kit was used in conjunction with the antibodies TUNEL/GFAP, TUNEL/NeuN, and TUNEL/survivin. Fluorescent IHC labeling was conducted as described elsewhere (Johnson et al. 2004). Briefly, the first primary antibody was incubated at 4°C

for 24–48 h in 10% goat serum/0.2% Triton-X 100 in 0.1 mol L^{-1} PBS (block) solution, followed by the second primary antibody at 4°C for 1 h in block solution. Fluorescent-tagged secondary antibody (Molecular Probes; Eugene, OR, USA) was used for visualization. For double-labeling IHC using same-species antibodies we used a biotin/streptavidin antibody procedure that relied on steric hindrance to block same-species binding sites. Control sections showed the secondary/tertiary complex was sufficient for steric blockage (data not shown). After an endogenous biotin blocking step (Vector Laboratories; Burlingame, CA, USA), the first primary antibody was incubated as described above, followed sequentially by a biotin-conjugated secondary antibody and fluorescent-labeled streptavidin (Molecular Probes), both steps at room temperature for 1 h in block solution. The second antigen was then labeled as described above. Sections were viewed and digitally captured with a Zeiss Axioplan Two microscope equipped with a SPOT Real Time Slider high-resolution color CCD digital camera (Diagnostic Instruments; Sterling Heights, MI, USA). A Bio-Rad 1024 ES confocal microscope was used to confirm single-cell localization of the label pairings. The settings for these images were: power = 100% for the red field: iris = 2.7–5.2, gain = 1400, Blev = −3; for the green field: iris = 3.0–5.7, gain = 1400, Blev = −3. The number of animals used for each label pairing for dual-labeling IHC was four ($n = 4$).

IHC quantification

Cell quantification was performed by comparing the number of double-labeled cells with the total number of single-labeled cells in six groups: active caspase-3/NeuN-positive cells to total NeuN-positive cells, active caspase-3/survivin-positive cells to total survivin-positive cells, active caspase-3/GFAP-positive cells to total GFAP-positive cells, TUNEL/NeuN-positive cells to total NeuN-positive cells, TUNEL/survivin-positive cells to total survivin-positive cells, and TUNEL/GFAP-positive cells to total GFAP-positive cells. Percentages were calculated by dividing the number of double-labeled cells by the total number of single-labeled cells. For each label pairing, representative photomicrographs were selected and counted. Cells were counted in a total area of 188,000 μm^2 for each label pairing in both cortical and hippocampal regions. These numbers were then transformed into percentages of either total cells or total cell type. Individual comparisons between groups were made using an unpaired Student t-test. Results were

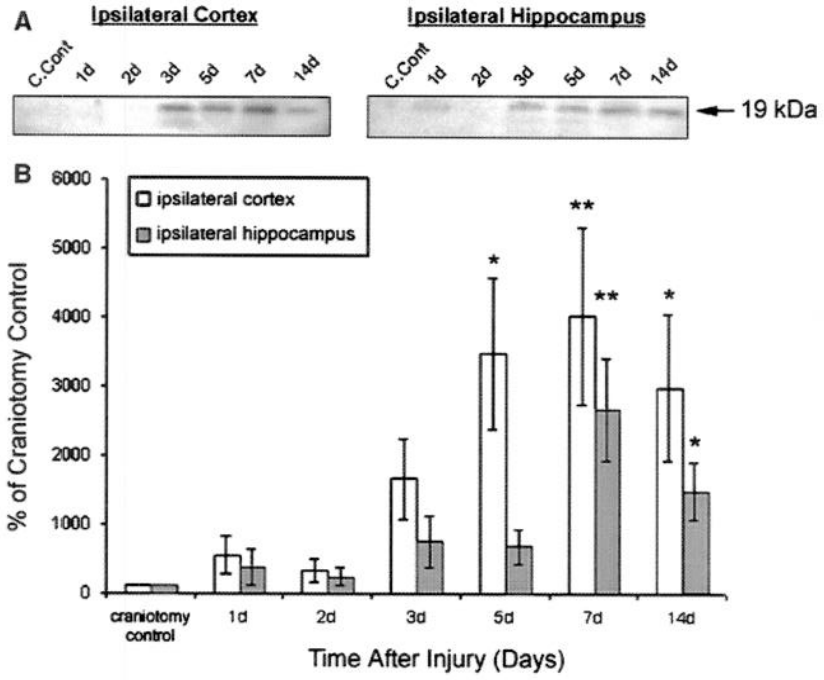

Fig. 1 Caspase-3 activation in rat brain after TBI. Rats were subjected to craniotomy then controlled cortical impact brain injury. Brain tissue homogenate proteins (40 μg) were separated using SDS–PAGE, immunoblotted with an antibody specific for active caspase-3, and visualized as described in detail under "Materials and methods". Representative western blots of active caspase-3 (19 kDa) in ipsilateral cortex and hippocampus obtained from injured rats and from craniotomy control rats without cortical impact (*craniotomy control*) revealed accumulation of active caspase-3 after *TBI* (**A**). Densitometric analysis of the active caspase-3 bands in ipsilateral cortex and hippocampus after *TBI* shows significant increases in a time-dependent manner (**B**). Data are given as percentage of the active fragment of caspase-3 relative to craniotomy controls; each craniotomy control and *TBI* time point represents data from an $n = 6$ individual animals and is reported as mean ± SEM. $^*P < 0.05$; $^{**}P < 0.01$ versus craniotomy control (one-way ANOVA test with post hoc Dunnet analysis)

considered significant at $P < 0.05$. Two additional blinded observers were used to count representative samples. Inter-rater reliability was calculated using Ebel's (1951) inter-rater reliability formula. The intra-class correlation (ICC) value achieved was 0.97, indicating little variation between raters.

Results

Caspase-3 is activated in the same brain regions as survivin after TBI

To determine the temporal and regional profile of caspase-3 activation, Western blot analysis was performed on cortical and hippocampal TBI samples. Active caspase-3 (19 kDa protein) was readily detectable in the ipsilateral cortex and hippocampus of rats subjected to TBI (Fig. 1A). Caspase-3 activation occurred in a time-dependant manner in the ipsilateral cortex and hippocampus with prominent activation occurring between 5 and 14 days post-injury, with peak accumulation occurring at 7 days post-injury. In the ipsilateral cortex, significant increases in active caspase-3 levels reached $3468 \pm 1088\%$ at 5 days, $4019 \pm 1291\%$ at 7 days and $2984 \pm 1058\%$ at 14 days post-injury, compared with craniotomy controls. Similar increases in caspase-3 activation were detected in the ipsilateral hippocampus with increases of $671 \pm 257\%$ at 5 days, $2662 \pm 738\%$ at 7 days and

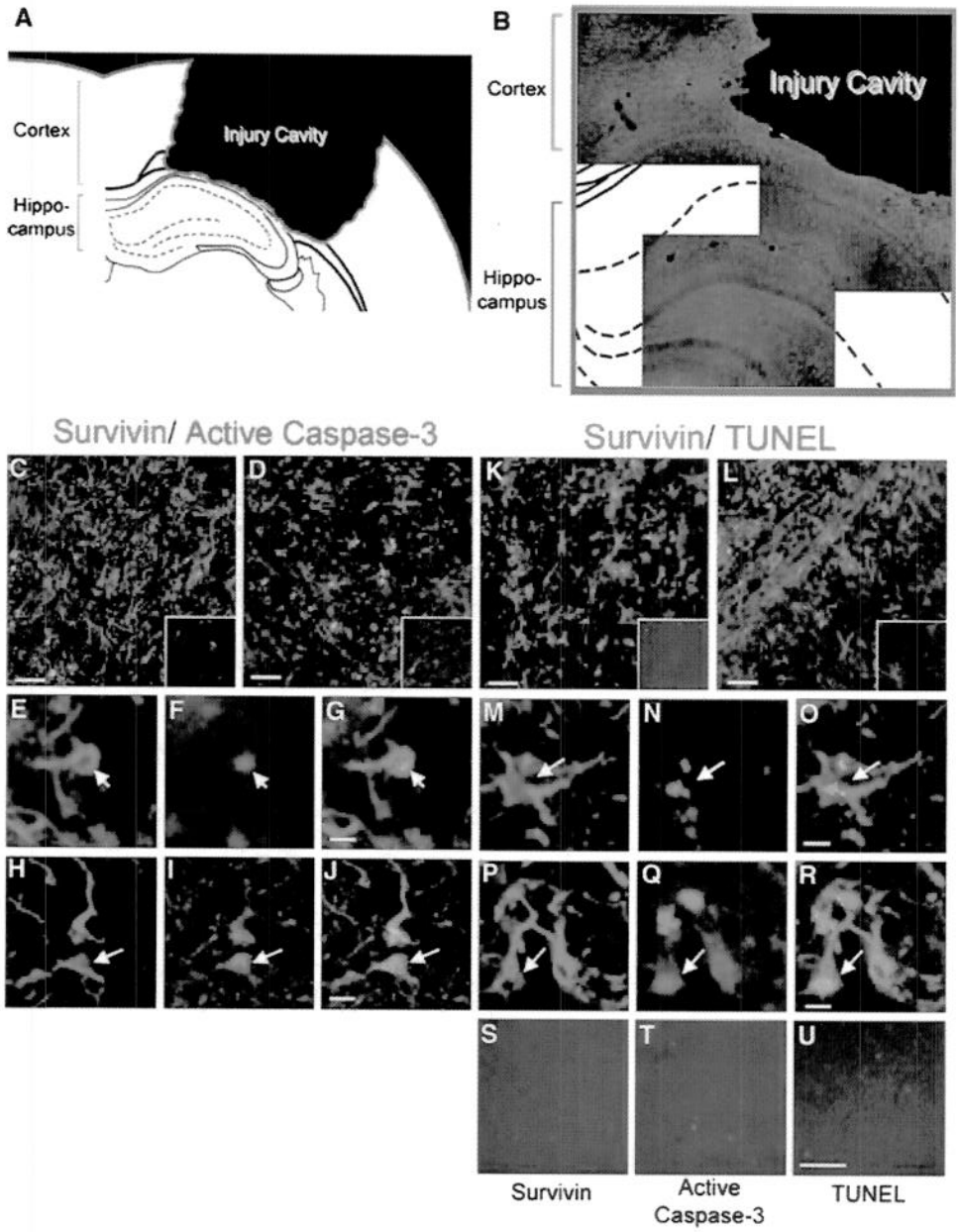

Fig. 2 Co-expression of survivin and apoptosis markers in rat brain after TBI. Substantial cavitation is produced 5 days post-TBI with this model (**A**). Extensive damage occurs in both cortical and hippocampal areas as indicated by increased GFAP-positive astrocytosis (*red*, **B**). Double-fluorescent immunostaining for survivin (*red*) and active caspase-3 (*green*, **C–J**) or TUNEL (*green*, **K–R**) was performed in the ipsilateral cortex (**C**, **K**) and hippocampus (**D**, **L**) at 5 days post-injury as described in detail under "Materials and methods". *Insets* in C, D, K and L show reduced labeling of survivin, active caspase-3, and TUNEL in craniotomy control tissue. Survivin is expressed in both the cytoplasm and in the nucleus (*red*, **E**, **H**, **M**, and **P**), whereas active caspase-3 (*green*, **F**, **I**) and TUNEL (*green*, **N**, **Q**) labeling is found predominantly in the nucleus. The *white arrow* indicates the typical focal co-localization of survivin and active caspase-3 (**G**, **J**) and survivin and TUNEL (**O**, **R**), as shown in the merged images. Immunostaining of naïve tissue (*negative control*) did not reveal strong immunoreactivity for survivin (**S**), active caspase-3 (**T**) or TUNEL (**U**). Photomicrographs in **B–G**, **K–O** and **S–U** were acquired using conventional fluorescent microscopy whereas photomicrographs in **H–J** and **P–R** were acquired using confocal microscopy. Magnification: 200 times, scale bar 50 μm (**C**, **D**, **K**, **L**, and **S–U**); 200 times, scale bar 10 μm (**E–J**, **M–R**)

1487 ± 405% at 14 days post-injury, compared with craniotomy controls (Fig. 1B).

Survivin expression correlates with decreased TUNEL labeling but not active caspase-3 expression

The IHC was performed on brain sections five days post-injury to investigate the expression of active caspase-3 and TUNEL labeling at peak survivin expression (Johnson et al. 2004). A large cavity, involving the cortex and encroaching on the hippocampus, develops 5 days post-injury (Fig. 2A). Strong GFAP-immunoreactivity (red), indicative of astrocytosis, is seen around the leading edge of the cavity and projecting into deeper cortical and hippocampal structures (Fig. 2B). The IHC revealed moderate co-localization of survivin with active caspase-3 and TUNEL in the ipsilateral cortex (Figs. 2C and 2K) and ipsilateral hippocampus (Figs. 2D and 2L) of injured animals. These data are summarized in Table 1. Survivin was found primarily in the cytoplasm, and to a lesser extent in the nucleus of the ipsilateral cortex (Figs. 2E and 2M). A similar pattern was seen in the ipsilateral hippocampus (data not shown). Active caspase-3 (Fig. 2F) and TUNEL (Fig. 2N) labeling were both found in the nucleus in both regions. Survivin co-localization with active caspase-3 and TUNEL is shown at high magnification in Figs. 2G and 2O, respectively. Confocal microscopy was used to ensure single-cell co-localization of survivin, active caspase-3, and TUNEL (Figa. 2H–2J and 2P–2R). These labeling patterns were specific to the injury condition and were not observed in naïve (negative control) tissues (Fig. 2S–2U).

Quantitative analysis revealed no significant difference between accumulation of active caspase-3 by survivin-positive cells and survivin-negative cells at 5 days post-injury in either the cortex or hippocampus (Fig. 3). A significantly higher proportion of TUNEL labeling was, however, observed in survivin-negative cells compared with survivin-positive cells in both regions ($P < 0.01$) (Fig. 3, Table 1a). At 7 days post-injury, there was no significant difference between accumulation of active caspase-3 and TUNEL labeling by survivin-positive and survivin-negative cells in either the cortex or hippocampus (Table 1b).

To verify that caspase-3 activation does not necessarily result in irreversible cell death, probably because of survivin inhibition, quantification data were gathered for cells that accumulate active caspase-3 and are TUNEL label-positive and compared with data for active caspase-3-positive cells that were not labeled with TUNEL. Indeed, we found that the number of dual-labeled active caspase-3 and TUNEL cells was not statistically different from the number of those cells labeled with active caspase-3 only (Fig. 3). This finding further supports the notion that several counteractive factors, including survivin, may inhibit active caspase-3 and reduce cell death after TBI.

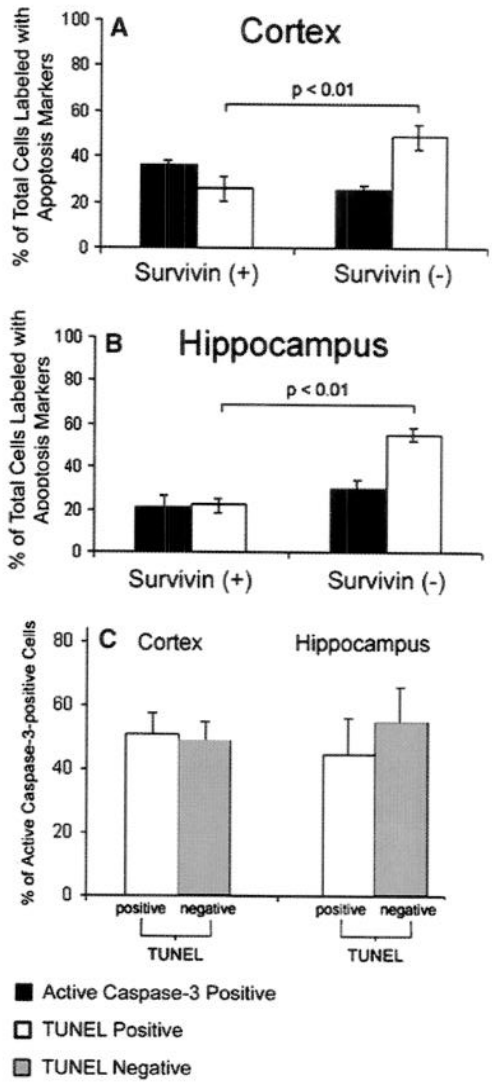

Fig. 3 Survivin expression decreases the accumulation of TUNEL but not active caspase-3. Cells were quantified and visualized as described in detail under "Materials and methods". The proportion of cells expressing active caspase-3 and labeling with TUNEL was compared in two cell populations, survivin-positive and survivin-negative, in the ipsilateral cortex (**A**) and hippocampus (**B**). No differences were found between the proportions of survivin-positive and survivin-negative cells expressing active caspase-3 in either the cortex (**A**, *black bars*) or hippocampus (**B**, *black bars*). Significantly more survivin-negative than survivin-positive cells were TUNEL-positive in both the cortex ($P < 0.01$, **A**, *white bars*) and hippocampus ($P < 0.001$, **B**, *white bars*). No differences were found between the proportions of TUNEL-positive (**C**, *white bars*) and TUNEL-negative cells (**C**, *gray bars*) that also labeled with active caspase-3. Each bar represents data from an $n = 4$ (**A**, *cortex*) or 3 (**B**, *hippocampus*) individual animals, analyzed using an unpaired Student *t*-test and reported as mean ± SEM

Astrocytes and neurons demonstrate cell specific differences in active caspase-3 and TUNEL labeling

To determine the cell types that express active caspase-3 or positive TUNEL labeling after TBI, dual IHC was

Table 1 Cell Quantification Data for Immunohistochemistry Labeling Pairs. This table summarizes the results from all cell count experiments investigating survivin IHC, active caspase-3 IHC, cell type, and DNA fragmentation marker (TUNEL). The numbers given are percentages calculated as described in the Materials and methods. Each percentage represents data from an $n=4$ (cortex) or $n=3$ (hippocampus) individual animals, analyzed using an unpaired Student t test and reported as mean + SEM at either five days post-injury (A) or seven days post-injury (B)

		Survivin(+)	Survivin(−)	GFAP(+)	NeuN(+)	TUNEL(+)	TUNEL(−)
A							
Active Caspase-3(+)	Cortex	37 ± 2	26 ± 6	$50\pm7^{\#\#\#}$	7 ± 1	51 ± 6	49 ± 6
	Hippocampus	21 ± 5	22 ± 3	29 ± 4	15 ± 2	45 ± 11	55 ± 11
TUNEL(+)	Cortex	$25\pm2^{**}$	49 ± 5	$11\pm2^{\#\#\#}$	46 ± 2		
	Hippocampus	$30\pm4^{**}$	55 ± 3	$19\pm0.2^{\#\#\#}$	60 ± 3		
B							
Active Caspase-3(+)	Cortex	36 ± 2	39 ± 11	$36\pm3^{\#\#\#}$	11 ± 1	48 ± 4	52 ± 4
	Hippocampus	37 ± 2	22 ± 6	$31\pm3^{\#\#}$	15 ± 3	$62\pm5^{\$\$}$	38 ± 5
TUNEL(+)	Cortex	20 ± 5	25 ± 10	$19\pm1^{\#\#\#}$	74 ± 5		
	Hippocampus	20 ± 3	31 ± 10	$28\pm7^{\#\#\#}$	80 ± 2		

** $p<0.01$ versus survivin-negative cells
$p<0.01$ versus NeuN-positive cells
$p<0.001$ versus NeuN-positive cells
$$ $p<0.01$ versus TUNEL-negative cells (unpaired Student t test)

performed with GFAP, a marker of astrocytes, and NeuN, a marker of mature neurons.

Co-localization of GFAP was observed with both active caspase-3 and TUNEL labeling in the ipsilateral cortex (Figs. 4A and 4I, respectively) and ipsilateral hippocampus (Figs. 4B and 4J, respectively). The GFAP is expressed in the cytoplasm (Figs. 4C and 4K) whereas active caspase-3 (Fig. 4D) and TUNEL (Fig. 4L) are expressed in the nucleus. Higher magnification photomicrographs of the ipsilateral cortex show a typical astrocyte expressing active caspase-3 (Figs. 4C–4E) or labeling with TUNEL (Figs. 4K–4M). Co-localization of these antibodies was confirmed by confocal microscopy on similar astrocytes (Fig. 4F–4H and 4N–4P).

Modest accumulation of active caspase-3 and substantial labeling with TUNEL were observed for NeuN-

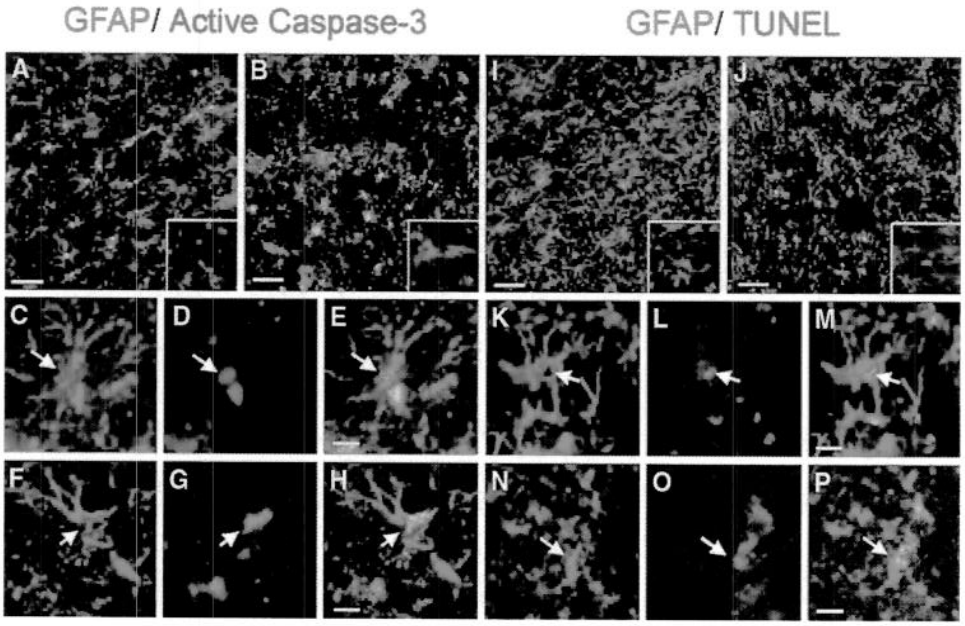

Fig. 4 Astrocytes express active caspase-3 and label with TUNEL after TBI in rats. Double-fluorescent immunostaining for GFAP (*red*) and active caspase-3 (*green*, **A**–**H**) or TUNEL (*green*, **I**–**P**) was performed in the ipsilateral cortex (**A**, **I**) and hippocampus (**B**, **J**) at 5 days post-injury as described in detail under "Materials and methods". The *insets* in **A**, **B**, **I** and **J** show reduced labeling of active caspase-3 and TUNEL in craniotomy control tissue. GFAP is expressed in the cytoplasm (**C**, **F**, **K**, and **N**, *red*) whereas active caspase-3 (**D**, **G**, *green*) and TUNEL (**L**, **O**, *green*) are expressed in the nucleus. The *white arrow* indicates the typical focal co-expression of GFAP and active caspase-3 (**E**, **H**) and TUNEL (**M**, **P**) as shown in the merged images. Photomicrographs in **A**–**E** and **I**–**M** were acquired using conventional fluorescent microscopy whereas photomicrographs in **F**–**H** and **N**–**P** were acquired using confocal microscopy. Magnification: 200 times, scale bar 50 μm (**A**, **B**, **I**, and **J**); 200 times, scale bar 10 μm (**C**–**H**,and **K**–**P**)

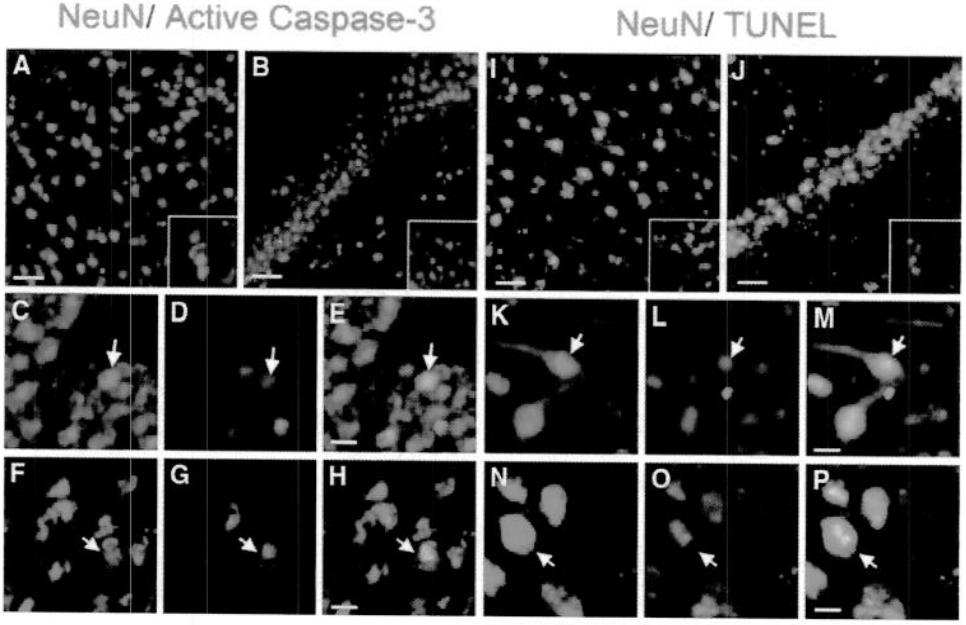

Fig. 5 Neurons express active caspase-3 and label with TUNEL after TBI in rats. Dual-fluorescent immunostaining for NeuN (*red*) and active caspase-3 (*green*, **A**–**H**) or TUNEL (*green*, **I**–**P**) was performed in the ipsilateral cortex (**A**, **I**) and hippocampus (**B**, **J**) at 5 days post-injury as described in detail under "Materials and methods". The *insets* in **A**, **B**, **I** and **J** show reduced labeling of active caspase-3 and TUNEL in craniotomy control tissue. The NeuN is expressed primarily in the nucleus but also in the cytoplasm (**C**, **F**, **K**, and **N**, *red*), whereas active caspase-3 (**D**, **G**, *green*) and TUNEL (**L**, **O**, *green*) are found in the nucleus. The *white arrow* indicates the typical focal co-localization of NeuN and active caspase-3 (**E**, **H**) and NeuN and TUNEL (**M**, **P**), as shown in the merged images. Photomicrographs in **A**–**E** and **I**–**M** were acquired using conventional fluorescent microscopy whereas photomicrographs in **F**–**H** and **N**–**P** were acquired using confocal microscopy. Magnification: 200 times, scale bar 50 μm (**A**, **B**, **I**, and **J**); 200 times, scale bar 10 μm (**C**–**H**,and **K**–**P**)

positive cells in the ipsilateral cortex (Figs. 5A and 5I, respectively) and ipsilateral hippocampus (Figs. 5B and 5J). Specifically, both active caspase-3 (Fig. 5D) and TUNEL (Fig. 5L) were present in neuronal nuclei (Fig. 5C and 5K), which was indicated by co-localization with NeuN in the ipsilateral cortex (Figs. 5E and 5M). Confocal microscopy was used to ensure single cell co-localization of NeuN with active caspase-3 and TUNEL (Figs. 5F–5H and 5N–5P).

Quantitative analysis revealed a substantially different expression profile of active caspase-3 and TUNEL in neurons and astrocytes. A significantly higher number of astrocytes accumulated active caspase-3, compared with neurons in the cortex ($P < 0.001$), but this difference was not statistically significant in the hippocampus (Table 1a). Conversely, a significantly greater number of neurons were labeled with TUNEL compared with astrocytes in both the cortex and hippocampus ($P < 0.001$) (Fig. 6, Table 1a). A similar expression profile of active caspase-3 and TUNEL was observed in astrocytes and neurons 7 days post-injury (Table 1b).

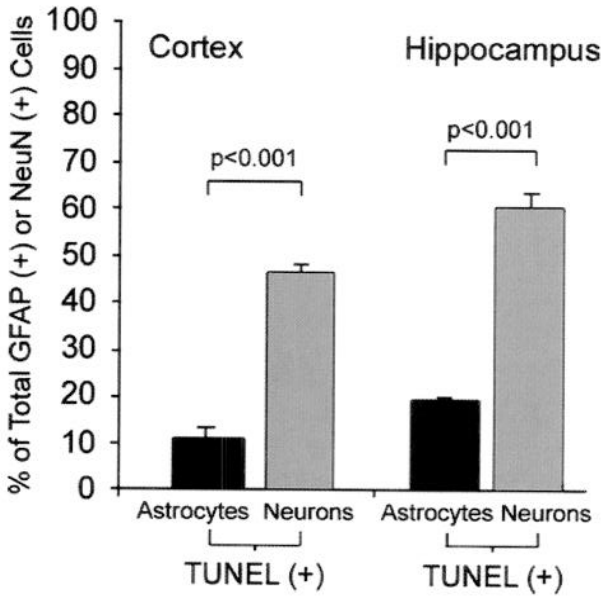

Fig. 6 TUNEL labeling is cell-specific after TBI in rats. Cells were quantified and visualized as described in detail under "Materials and methods". The proportion of NeuN-positive (neurons) and GFAP-positive (astrocytes) with TUNEL-positive labeling was compared in the ipsilateral cortex and hippocampus. Significantly more TUNEL labeling was seen in neurons (*gray bars*) than in astrocytes (*black bars*) in both the cortex ($P < 0.001$) and hippocampus ($P < 0.001$). Each bar represents an $n = 4$ (*cortex*) or 3 (*hippocampus*) individual animals reported as mean ± SEM and analyzed using an unpaired Student *t*-test

Discussion

Caspase-3 activation is a prominent feature of apoptosis and its role in DNA fragmentation after TBI has been well documented (Nicholson et al. 1995; Tewari et al.

1995; Pike et al. 1998; Tang and Kidd 1998; Wolf et al. 1999; Beer et al. 2000; Buki et al. 2000; Clark et al. 2000). Survivin is an inhibitor of apoptosis protein (IAP), which can inhibit active caspase-3 and thereby modulate cell death in a variety of tissues, including the CNS (Shankar et al. 2001; Sasaki et al. 2002; Van Haren et al. 2004). No studies have investigated the potential anti-apoptotic role of survivin in the adult brain after TBI, however.

In this paper we characterize the relationship between survivin expression and two apoptosis events—accumulation of active caspase-3 and downstream DNA fragmentation (as shown by TUNEL labeling) in rat brain subjected to TBI. Although use of TUNEL labeling alone cannot definitively confirm apoptosis, TUNEL in conjunction with active caspase-3 is regarded a reliable tool to assess apoptosis progression (Lei et al. 2004; Marciano et al. 2004; Nakase et al. 2004). The appearance of active caspase-3 was time-dependent and region-specific after injury (Fig. 1); the pattern was similar to that of survivin expression after TBI. These findings suggest that survivin may interact with active caspase-3 after TBI and possibly reduce the deleterious consequences of caspase-3-mediated cell death (Tamm et al. 1998; Kobayashi et al. 1999; O'Connor et al. 2000; Shin et al. 2001). Other IAPs, for example XIAP and NAIP, are up-regulated in concert with caspase activation after brain injury (Keane et al. 2001). In addition, survivin expression is up-regulated by the pro-survival PI3-kinase/Akt pathway, which is activated after TBI (Kitagawa et al. 1999; Xia et al. 2002; Kim et al. 2004).

Survivin-positive cells expressed active caspase-3 and were labeled with TUNEL (Fig. 2), although there was no significant difference between accumulation of active caspase-3 in survivin-positive and survivin-negative cells (Fig. 3). These data are in accordance with the ability of survivin (Tamm et al. 1998) and other IAPs (Shankar et al. 2001; Maier et al. 2002) to inhibit the activity, but not the activation, of caspase-3. In contrast, fewer survivin-positive cells than survivin-negative cells exhibited DNA fragmentation (TUNEL labeling) 5 days post-injury (Fig. 3). These data suggest that survivin expression may attenuate the apoptotic cascade by inhibiting cleavage of caspase-3-specific substrates that result in DNA fragmentation. Furthermore, the finding that active caspase-3 accumulation led to positive TUNEL labeling in 51% of all active caspase-3-positive cells (Fig. 3) is consistent with the observation that endogenous factors, including survivin, may inhibit active caspase-3 and attenuate DNA fragmentation after TBI. In cancer cells, for example, survivin and other endogenous factors play important roles in tumor survival (Lu et al. 1998; Altieri et al. 1999; Grossman et al. 1999; Jiang et al. 2001; Chiou et al. 2003). In addition, survivin antisense treatment increases DNA fragmentation in neuroblastoma and oligodendroglioma (Shankar et al. 2001).

We next investigated the labeling patterns of active caspase-3 and TUNEL in astrocytes and neurons. Recent data show that a large majority of astrocytes, but few neurons, express survivin after TBI (Johnson et al. 2004). In this work both astrocytes and neurons expressed active caspase-3 and TUNEL-positive labeling post-injury, but the prevalence of this labeling was dramatically different (Figs. 4 and 5). A higher proportion of astrocytes accumulated active caspase-3, but fewer astrocytes than neurons were labeled with TUNEL (Fig. 6). It is presently unclear why so few neurons were labeled with active caspase-3 in these experiments (Table 1). One possibility could be caspase-3-mediated loss of NeuN antigenicity (Unal-Cevik et al. 2004), although other groups have detected prominent caspase-3 activation in apoptotic neurons after TBI (Beer et al. 2000). Caspase-independent necrosis may also be a major contributor to neuronal cell death after TBI (Newcomb et al. 1999; Wennersten et al. 2003). Taken together, these findings suggest an intriguing correlation between accumulation of survivin and low levels of DNA fragmentation. These phenomena seemed, moreover, to be cell-specific—astrocytes frequently expressed survivin and there was less evidence of DNA fragmentation whereas for neurons there was more evidence of DNA fragmentation and survivin was expressed less frequently.

These studies also revealed that active caspase-3 immunoreactivity is found primarily, though not exclusively, in the nucleus of both neurons and astrocytes 5 days post-injury. Although the cytoplasmic (Namura et al. 1998; Beer et al. 2000; Clark et al. 2000) and nuclear (Velier et al. 1999; Kamada et al. 2005; Noyan-Ashraf et al. 2005) distribution of active caspase-3 have both been characterized, the ramifications of active caspase-3 nuclear translocation and its role in apoptosis after TBI are unknown. Studies are in progress to determine the relationship between the nuclear translocation of active caspase-3 and another pro-apoptotic event, nuclear translocation of caspase-3 cleaved DFF40.

Cell-specific survivin expression may explain the lower incidence of TUNEL labeling in astrocytes than in neurons (Fig. 6). Cell type-specific expression of IAPs after TBI has been reported. For example, XIAP is expressed primarily by neurons (Lotocki et al. 2003) and a subset of oligodendrocytes (Keane et al. 2001) after brain injury. The NAIP is expressed in neurons after ischemia (Xu et al. 1997) and TBI (Hutchison et al. 2001). Last, RIAP-2 is abundantly expressed in neurons, as opposed to astrocytes, after kainic acid treatment (Belluardo et al. 2002). Figure 7 shows a putative mechanism for apoptosis inhibition by survivin. After upstream caspase activation and cleavage of procaspase-3 to active caspase-3, survivin acts to attenuate the apoptotic cascade and consequent DNA cleavage by inhibiting caspase-3 activity.

In conclusion, our data are consistent with other TBI findings showing activation of apoptotic cascades, including accumulation of active caspase-3, in both neurons and astrocytes, with concurrent loss of cortical and hippocampal tissues (Smith et al. 1997; Conti et al.

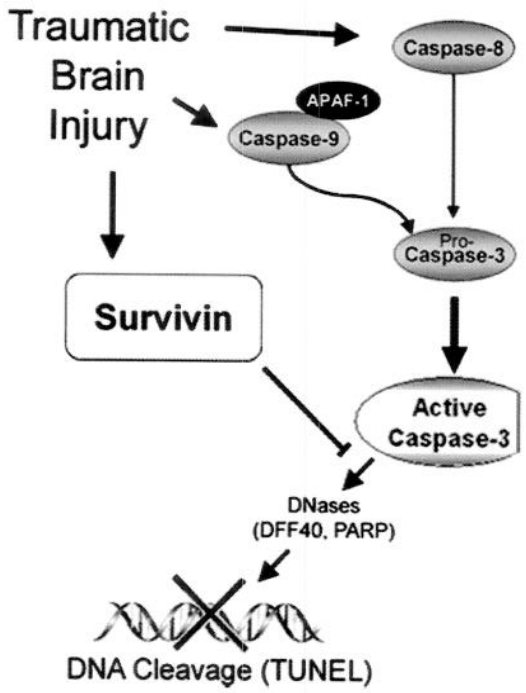

Fig. 7 Putative mechanism of apoptosis inhibition by survivin after TBI. The TBI induces activation of upstream caspases-8 and caspases-9 that can process pro-caspase-3 to its active form. Once activated, caspase-3 can cleave several intracellular substrates and activate restrictases that may lead to DNA fragmentation. Concomitant survivin expression is up-regulated in response to the same TBI signals. Survivin inhibits the activity of active caspase-3, which results in the attenuation of DNA fragmentation

1998; Newcomb et al. 1999; Raghupathi et al. 2000; Larner et al. 2004). Our data also demonstrate for the first time that accumulation of active caspase-3 in the rat brain after TBI follows a similar timeframe, region, and cell type expression pattern as survivin. These data suggest that DNA cleavage may be attenuated by expression of survivin protein, in a cell-specific fashion, after TBI. Namely, astrocytes have significantly lower TUNEL and more frequent survivin labeling than neurons, suggesting a more robust anti-apoptotic role for survivin in astrocytes. Taken together, these results suggest that survivin may be a part of the counteracting mechanisms reducing DNA fragmentation and cell death after TBI in rats.

Acknowledgments We thank Barbara O'Steen and Jeremy Flint for technical assistance. We also thank Edward Lin and Karie Johnson, MESS ATC for assistance with cell quantification. This work was funded by grants NIH RO1 NS39091, NIH RO1 NS40182, DAMD 17-99-1-9565, DAMD 17-01-1-0765, and DAMD 17-03-1-0066.

References

Altieri DC, Marchisio PC, Marchisio C (1999) Survivin apoptosis: an interloper between cell death and cell proliferation in cancer. Lab Invest 79:1327–1333

Ambrosini G, Adida C, Sirugo G, Altieri DC (1998) Induction of apoptosis and inhibition of cell proliferation by survivin gene targeting. J Biol Chem 273:11177–11182

Beer R, Franz G, Srinivasan A, Hayes RL, Pike BR, Newcomb JK, Zhao X, Schmutzhard E, Poewe W, Kampfl A (2000) Temporal profile and cell subtype distribution of activated caspase-3 following experimental traumatic brain injury. J Neurochem 75:1264–1273

Belluardo N, Korhonen L, Mudo G, Lindholm D (2002) Neuronal expression and regulation of rat inhibitor of apoptosis protein-2 by kainic acid in the rat brain. Eur J Neurosci 15:87–100

Buki A, Okonkwo DO, Wang KK, Povlishock JT (2000) Cytochrome c release and caspase activation in traumatic axonal injury. J Neurosci 20:2825–2834

Chiou SK, Jones MK, Tarnawski AS (2003) Survivin—an anti-apoptosis protein: its biological roles and implications for cancer and beyond. Med Sci Monit 9:PI25–PI29

Clark RS, Kochanek PM, Watkins SC, Chen M, Dixon CE, Seidberg NA, Melick J, Loeffert JE, Nathaniel PD, Jin KL, Graham SH (2000) Caspase-3 mediated neuronal death after traumatic brain injury in rats. J Neurochem 74:740–753

Conti AC, Raghupathi R, Trojanowski JQ, McIntosh TK (1998) Experimental brain injury induces regionally distinct apoptosis during the acute and delayed post-traumatic period. J Neurosci 18:5663–5672

Deveraux QL, Takahashi R, Salvesen GS, Reed JC (1997) X-linked IAP is a direct inhibitor of cell-death proteases. Nature 388:300–304

Dixon CE, Clifton GL, Lighthall JW, Yaghmai AA, Hayes RL (1991) A controlled cortical impact model of traumatic brain injury in the rat. J Neurosci Methods 39:253–262

Ebel RL (1951) Estimation of the reliability of ratings. Psycometrika 16:407–424

Eldadah BA, Faden AI (2000) Caspase pathways, neuronal apoptosis, and CNS injury. J Neurotrauma 17:811–829

Enari M, Sakahira H, Yokoyama H, Okawa K, Iwamatsu A, Nagata S (1998) A caspase-activated DNase that degrades DNA during apoptosis, and its inhibitor ICAD. Nature 391:43–50

Grossman D, McNiff JM, Li F, Altieri DC (1999) Expression and targeting of the apoptosis inhibitor, survivin, in human melanoma. J Invest Dermatol 113:1076–1081

Hutchison JS, Derrane RE, Johnston DL, Gendron N, Barnes D, Fliss H, King WJ, Rasquinha I, MacManus J, Robertson GS, MacKenzie AE (2001) Neuronal apoptosis inhibitory protein expression after traumatic brain injury in the mouse. J Neurotrauma 18:1333–1347

Jiang X, Wilford C, Duensing S, Munger K, Jones G, Jones D (2001) Participation of Survivin in mitotic and apoptotic activities of normal and tumor-derived cells. J Cell Biochem 83:342–354

Johnson EA, Svetlov SI, Pike BR, Tolentino PJ, Shaw G, Wang KKW, Hayes RL, Pineda JA (2004) Cell-specific Upregulation of Survivin After Experimental Traumatic Brain Injury in Rats. J Neurotrauma 21:1183–1195

Juan TS, McNiece IK, Argento JM, Jenkins NA, Gilbert DJ, Copeland NG, Fletcher FA (1997) Identification and mapping of Casp7, a cysteine protease resembling CPP32 beta, interleukin-1 beta converting enzyme, and CED-3. Genomics 40:86–93

Kamada S, Kikkawa U, Tsujimoto Y, Hunter T (2005) Nuclear translocation of caspase-3 is dependent on its proteolytic activation and recognition of a substrate-like protein(s). J Biol Chem 280:857–860

Keane RW, Kraydieh S, Lotocki G, Alonso OF, Aldana P, Dietrich WD (2001) Apoptotic and antiapoptotic mechanisms after traumatic brain injury. J Cereb Blood Flow Metab 21:1189–1198

Kim S, Kang J, Qiao J, Thomas RP, Evers BM, Chung DH (2004) Phosphatidylinositol 3-kinase inhibition down-regulates survivin and facilitates TRAIL-mediated apoptosis in neuroblastomas. J Pediatr Surg 39:516–521

Kitagawa H, Warita H, Sasaki C, Zhang WR, Sakai K, Shiro Y, Mitsumoto Y, Mori T, Abe K (1999) Immunoreactive Akt, PI3-K and ERK protein kinase expression in ischemic rat brain. Neurosci Lett 274:45–48

Kobayashi K, Hatano M, Otaki M, Ogasawara T, Tokuhisa T (1999) Expression of a murine homologue of the inhibitor of apoptosis protein is related to cell proliferation. Proc Natl Acad Sci USA 96:1457–1462

Larner SF, Hayes RL, McKinsey DM, Pike BR, Wang KK (2004) Increased expression and processing of caspase-12 after traumatic brain injury in rats. J Neurochem 88:78–90

Lei B, Popp S, Capuano-Waters C, Cottrell JE, Kass IS (2004) Lidocaine attenuates apoptosis in the ischemic penumbra and reduces infarct size after transient focal cerebral ischemia in rats. Neuroscience 125:691–701

Liu X, Li P, Widlak P, Zou H, Luo X, Garrard WT, Wang X (1998) The 40-kDa subunit of DNA fragmentation factor induces DNA fragmentation and chromatin condensation during apoptosis. Proc Natl Acad Sci USA 95:8461–8466

Lotocki G, Alonso OF, Frydel B, Dietrich WD, Keane RW (2003) Monoubiquitination and cellular distribution of XIAP in neurons after traumatic brain injury. J Cereb Blood Flow Metab 23:1129–1136

Lu CD, Altieri DC, Tanigawa N (1998) Expression of a novel antiapoptosis gene, survivin, correlated with tumor cell apoptosis and p53 accumulation in gastric carcinomas. Cancer Res 58:1808–1812

Maier JK, Lahoua Z, Gendron NH, Fetni R, Johnston A, Davoodi J, Rasper D, Roy S, Slack RS, Nicholson DW, MacKenzie AE (2002) The neuronal apoptosis inhibitory protein is a direct inhibitor of caspases 3 and 7. J Neurosci 22:2035–2043

Marciano PG, Brettschneider J, Manduchi E, Davis JE, Eastman S, Raghupathi R, Saatman KE, Speed TP, Stoeckert CJ, Jr, Eberwine JH, McIntosh TK (2004) Neuron-specific mRNA complexity responses during hippocampal apoptosis after traumatic brain injury. J Neurosci 24:2866–2876

Nakase T, Sohl G, Theis M, Willecke K, Naus CC (2004) Increased apoptosis and inflammation after focal brain ischemia in mice lacking connexin43 in astrocytes. Am J Pathol 164:2067–2075

Namura S, Zhu J, Fink K, Endres M, Srinivasan A, Tomaselli KJ, Yuan J, Moskowitz MA (1998) Activation and cleavage of caspase-3 in apoptosis induced by experimental cerebral ischemia. J Neurosci 18:3659–3668

Newcomb JK, Zhao X, Pike BR, Hayes RL (1999) Temporal profile of apoptotic-like changes in neurons and astrocytes following controlled cortical impact injury in the rat. Exp Neurol 158:76–88

Nicholson DW, Ali A, Thornberry NA, Vaillancourt JP, Ding CK, Gallant M, Gareau Y, Griffin PR, Labelle M, Lazebnik YA, et al. (1995) Identification and inhibition of the ICE/CED-3 protease necessary for mammalian apoptosis. Nature 376:37–43

Noyan-Ashraf MH, Brandizzi F, Juurlink BH (2005) Constitutive nuclear localization of activated caspase 3 in subpopulations of the astroglial family of cells. Glia 49:588–593

O'Connor DS, Schechner JS, Adida C, Mesri M, Rothermel AL, Li F, Nath AK, Pober JS, Altieri DC (2000) Control of apoptosis during angiogenesis by survivin expression in endothelial cells. Am J Pathol 156:393–398

Pike BR, Zhao X, Newcomb JK, Posmantur RM, Wang KK, Hayes RL (1998) Regional calpain and caspase-3 proteolysis of alpha-spectrin after traumatic brain injury. Neuroreport 9:2437–2442

Raghupathi R, Graham DI, McIntosh TK (2000) Apoptosis after traumatic brain injury. J Neurotrauma 17:927–938

Roy N, Deveraux QL, Takahashi R, Salvesen GS, Reed JC (1997) The c-IAP-1 and c-IAP-2 proteins are direct inhibitors of specific caspases. EMBO J 16:6914–6925

Sasaki T, Lopes MB, Hankins GR, Helm GA (2002) Expression of survivin, an inhibitor of apoptosis protein, in tumors of the nervous system. Acta Neuropathol (Berl) 104:105–109

Shankar SL, Mani S, O'Guin KN, Kandimalla ER, Agrawal S, Shafit-Zagardo B (2001) Survivin inhibition induces human neural tumor cell death through caspase-independent and -dependent pathways. J Neurochem 79:426–436

Shin S, Sung BJ, Cho YS, Kim HJ, Ha NC, Hwang JI, Chung CW, Jung YK, Oh BH (2001) An anti-apoptotic protein human survivin is a direct inhibitor of caspase-3 and −7. Biochemistry 40:1117–1123

Smith DH, Chen XH, Pierce JE, Wolf JA, Trojanowski JQ, Graham DI, McIntosh TK (1997) Progressive atrophy and neuron death for one year following brain trauma in the rat. J Neurotrauma 14:715–727

Takahashi R, Deveraux Q, Tamm I, Welsh K, Assa-Munt N, Salvesen GS, Reed JC (1998) A single BIR domain of XIAP sufficient for inhibiting caspases. J Biol Chem 273:7787–7790

Tamm I, Wang Y, Sausville E, Scudiero DA, Vigna N, Oltersdorf T, Reed JC (1998) IAP-family protein survivin inhibits caspase activity and apoptosis induced by Fas (CD95), Bax, caspases, and anticancer drugs. Cancer Res 58:5315–5320

Tang D, Kidd VJ (1998) Cleavage of DFF-45/ICAD by multiple caspases is essential for its function during apoptosis. J Biol Chem 273:28549–28552

Tewari M, Quan LT, O'Rourke K, Desnoyers S, Zeng Z, Beidler DR, Poirier GG, Salvesen GS, Dixit VM (1995) Yama/CPP32 beta, a mammalian homolog of CED-3, is a CrmA-inhibitable protease that cleaves the death substrate poly(ADP-ribose) polymerase. Cell 81:801–809

Unal-Cevik I, Kilinc M, Gursoy-Ozdemir Y, Gurer G, Dalkara T (2004) Loss of NeuN immunoreactivity after cerebral ischemia does not indicate neuronal cell loss: a cautionary note. Brain Res 1015:169–174

Van Haren K, van der Voorn JP, Peterson DR, van der Knaap MS, Powers JM (2004) The life and death of oligodendrocytes in vanishing white matter disease. J Neuropathol Exp Neurol 63:618–630

Velier JJ, Ellison JA, Kikly KK, Spera PA, Barone FC, Feuerstein GZ (1999) Caspase-8 and caspase-3 are expressed by different populations of cortical neurons undergoing delayed cell death after focal stroke in the rat. J Neurosci 19:5932–5941

Wennersten A, Holmin S, Mathiesen T (2003) Characterization of Bax and Bcl-2 in apoptosis after experimental traumatic brain injury in the rat. Acta Neuropathol (Berl) 105:281–288

Wolf BB, Schuler M, Echeverri F, Green DR (1999) Caspase-3 is the primary activator of apoptotic DNA fragmentation via DNA fragmentation factor-45/inhibitor of caspase-activated DNase inactivation. J Biol Chem 274:30651–30656

Xia XG, Hofmann HD, Deller T, Kirsch M (2002) Induction of STAT3 signaling in activated astrocytes and sprouting septal neurons following entorhinal cortex lesion in adult rats. Mol Cell Neurosci 21:379–392

Xu DG, Crocker SJ, Doucet JP, St-Jean M, Tamai K, Hakim AM, Ikeda JE, Liston P, Thompson CS, Korneluk RG, MacKenzie A, Robertson GS (1997) Elevation of neuronal expression of NAIP reduces ischemic damage in the rat hippocampus. Nat Med 3:997–1004

JOURNAL OF NEUROTRAUMA
Volume 22, Number 6, 2005

Pp. 629–644

Rapid Discovery of Putative Protein Biomarkers of Traumatic Brain Injury by SDS–PAGE–Capillary Liquid Chromatography–Tandem Mass Spectrometry

WILLIAM E. HASKINS,[1,2,4] FIRAS H. KOBEISSY,[1,2,3] REGINA A. WOLPER,[1,2,4] ANDREW K. OTTENS,[1,2,4] JASON W. KITLEN,[2,4] SCOTT H. McCLUNG,[5] BARBARA E. O'STEEN,[2,4] MARJORIE M. CHOW,[5] JOSE A. PINEDA,[2] NANCY D. DENSLOW,[1,5] RONALD L. HAYES,[2,3,4] and KEVIN K.W. WANG[1,2,3,4]

ABSTRACT

We report the rapid discovery of putative protein biomarkers of traumatic brain injury (TBI) by SDS–PAGE–capillary liquid chromatography–tandem mass spectrometry (SDS–PAGE–Capillary LC–MS^2). Ipsilateral hippocampus (IH) samples were collected from naive rats and rats subjected to controlled cortical impact (a rodent model of TBI). Protein database searching with 15,558 uninterpreted MS^2 spectra, collected in 3 days via data-dependent capillary LC-MS^2 of pooled cyanine dye-labeled samples separated by SDS-PAGE, identified more than 306 unique proteins. Differential proteomic analysis revealed differences in protein sequence coverage for 170 mammalian proteins (57 in naive only, 74 in injured only, and 39 of 64 in both), suggesting these are putative biomarkers of TBI. Confidence in our results was obtained by the presence of several known biomarkers of TBI (including αII-spectrin, brain creatine kinase, and neuron-specific enolase) in our data set. These results show that SDS-PAGE prior to *in vitro* proteolysis and capillary LC-MS^2 is a promising strategy for the rapid discovery of putative protein biomarkers associated with a specific physiological state (i.e., TBI) without *a priori* knowledge of the molecules involved.

Key words: controlled cortical impact (CCI); differential in-gel electrophoresis (DIGE); sodium dodecyl sulfate–polyacrylamide gel electrophoresis (SDS-PAGE); tandem mass spectometry (MS^2); traumatic brain injury (TBI)

INTRODUCTION

TRAUMATIC BRAIN INJURY (TBI), defined as brain damage due to mechanical force applied to the head, has an incidence of approximately 2 million persons annually in the United States with an annual economic cost of $25 billion. Thus, accurate diagnosis following TBI is crucial for appropriate clinical management of TBI patients and for reducing costs. Current assessment tools of TBI include computed tomography and magnetic resonance imaging. Despite the accuracy of these techniques, TBI survivors suffer long-term impairment due to late di-

[1]Center of Neuroproteomics and Biomarkers Research, [2]Center for Traumatic Brain Injury Studies, Departments of [3]Psychiatry and [4]Neuroscience, and [5]Interdisciplinary Center of Biotechnology Research University of Florida, Gainesville, Florida.

agnosis and unguided clinical management. Therefore, increased interest in the discovery of biomarkers that are indicative of injury severity and anatomical localization has been realized in recent years.

Several laboratories have examined a number of biological molecules in cerebral spinal fluid (CSF) and blood from TBI patients in an effort to discover TBI-specific molecules (Pike et al., 2002; Varma et al., 2003; Zemlan et al., 2002; Berger et al., 2002; Raabe et al., 2003). For example, our laboratory reported the discovery of nonerythroid αII-spectrin and its protease-specific degradation products as biomarkers of TBI (Pike et al., 2002). However, a major limitation of currently described biomarkers is a lack of TBI specificity and a poor understanding of the biochemical mechanisms of brain trauma. Thus, the discovery of novel protein biomarkers of TBI that serve as reliable indicators of injury severity would be highly beneficial for predicting outcome and managing patients (Denslow et al., 2003). Moreover, novel biomarkers of TBI, particularly neurodegenerative and neuroprotective proteins, provide insights on pathophysiology and may serve as therapeutic targets for various neurological diseases.

Rapid discovery of protein biomarkers in complex samples by state-of-the-art mass spectrometry methods, capable of identifying thousands of proteins in a single sample by protease-specific peptide sequences, is precluded by several limitations. "Shotgun" capillary liquid chromatography (LC)–tandem mass spectrometry (MS^2) methods (McDonald and Yates, 2002) require extended analysis times for each sample (days) and information about post-translational modifications (PTMs), particularly protein degradation, is often lost during *in vitro* proteolysis (e.g., trypsination). Liquid-phase protein separation (e.g., 2D gels and LC-LC) prior to *in vitro* proteolysis and capillary LC-MS^2, preserves more information about PTMs, but can require 10–100-fold more sample and even greater analysis times for complete characterization (weeks). Reproducible replicate analysis, required for preliminary biomarker validation, and limited resources (e.g., mass spectrometer time) further compound these problems.

Recently, the large dynamic range and high quantum yield of cyanine dye-labeled proteins were combined with 2D gels in order to improve gel-to-gel reproducibility and reduce analysis time via sample multiplexing (Gharbi et al., 2002; Leimgruber et al., 2002; Macdonald et al., 2001, Tonge et al., 2001). This technique, differential in-gel electrophoresis (DIGE), provides quantitative information complementary to isotope coded affinity tag (ICAT)–capillary LC–MS^2 approaches (Gygi et al., 1999), while preserving more information about PTMs. DIGE also provides a reduction in analysis time because only gel spots with a significant difference in the ratio of their fluorescence signals need to be targeted for protein identification by mass spectrometry (Gharbi et al., 2002; Kernec et al., 2001; Shaw et al., 2003; Tonge et al., 2001; Yan et al., 2002). However, poorly resolved proteins elude identification, while well-resolved, multiply labeled, proteins produce redundant identifications. Given our emphasis on rapid analysis, rather than more comprehensive characterization, we selected the limited resolving power of SDS-PAGE as an effective means to reduce redundant identifications and accelerate the discovery of putative protein biomarkers.

In this report, we describe the application of a novel differential analysis strategy, SDS-PAGE–capillary liquid chromatography–tandem mass spectrometry (SDS-PAGE–Capillary LC–MS^2), to the discovery of putative protein biomarkers of TBI in hippocampus tissue. Herein, protein database searching of uninterpreted MS^2 spectra, collected via data-dependent capillary LC–MS^2 of pooled cyanine dye-labeled samples separated by SDS-PAGE, was combined with differential proteomic analysis. We hypothesized that a subset of putative protein biomarkers of TBI, including some with PTMs, would be rapidly revealed by comparing the protein sequence coverage of naive and injured samples.

MATERIALS AND METHODS

Chemicals and Reagents

The chemicals and reagents used are described elsewhere (Haskins et al., 2001). Tryptic digests were purchased from Michrom Bioresources (Auburn, CA) for use as quality control standards. Cyanine dye labeling reagents were purchased from Amersham Biosciences (Piscataway, NJ).

Controlled Cortical Impact

The controlled cortical impact (CCI) device used to model TBI in male Sprague-Dawley rats was described in detail elsewhere (Pike et al., 2002). The magnitude of injury used in these studies produces significant cortical contusions and less overt injury that often extends into the region of the hippocampus (Posmantur et al., 1997; Dixon et al., 1991). Although overt hippocampal damage is not usually associated with this model, there is evidence of increased pathological calpain-mediated proteolysis in the hippocampus following cortical impact injury (Newcomb et al., 1997). Cortical impact injury is usually associated with intraparenchymal hemorrhage and dural disruption, but extensive subdural hemorrhage is not a primary feature of this model. The

adult rats were anesthetized with 4% isoflurane in a carrier gas of 1:1 O_2/N_2O (4 min) followed by maintenance anesthesia of 2.5% isoflurane in the same carrier gas. Core body temperature was monitored continuously by a rectal thermistor probe and maintained at 37 ± 1°C by placing an adjustable temperature controlled heating pad beneath the rats. Animals were mounted in a stereotactic frame in a prone position and secured by ear and incisor bars. A midline cranial incision was made, the soft tissues were reflected, and a unilateral (ipsilateral to site of impact) craniotomy (7 mm diameter) was performed adjacent to the central suture, midway between bregma and lambda. The dura mater was kept intact over the cortex. Brain trauma was produced by impacting the right cortex (ipsilateral cortex) with a 5-mm-diameter aluminum impactor tip (housed in a pneumatic cylinder) at a velocity of 3.5 m/sec with a 1.6-mm compression and 150-msec dwell time (compression duration). Velocity was controlled by adjusting the pressure (compressed N_2) supplied to the pneumatic cylinder. Velocity and dwell time were measured by a linear velocity displacement transducer (Lucas Shaevitz™ model 500 HR, Detroit, MI) that produced an analog signal that was recorded by a storage-trace oscilloscope (BK Precision, model 2522B, Placentia, CA). At 48 h post-injury, the animals were anesthetized with 4% isoflurane in a carrier gas of 1:1 O_2/N_2O (4 min) and subsequently sacrificed by decapitation. Hippocampus samples were rapidly dissected, washed with saline solution, snap-frozen in liquid nitrogen, and stored at −80°C until further processing. Naive animals underwent identical surgical procedures but did not receive an impact injury. Appropriate pre- and post-injury management was maintained to insure compliance with guidelines set forth by the University of Florida Institutional Animal Care and Use Committee and the National Institutes of Health guidelines detailed in the *Guide for the Care and Use of Laboratory Animals*.

Sample preparation. Hippocampus samples were homogenized in a glass tube with a Teflon dounce pestle in 15 volumes of ice-cold detergent-free buffer (50 mM Tris-HCl, pH 7.4, 1 mM EDTA, 2 mM EGTA, 0.33 M sucrose, 1 mM DTT) containing a broad-range protease inhibitor cocktail (Roche Molecular Biochemicals, no. 1-836-145) and sonicated. Samples were then centrifuged at 9000*g* for 5 min at 4°C. The supernatant was stored at −80°C. The protein concentration of each sample was determined by DC protein assay (Biorad, Hercules, CA) with albumin standards. Proteins were diluted to 5 μg/μL in DIGE lysis buffer containing a 1% protease inhibitor cocktail (P8340, Sigma, St. Louis, MO) to prevent proteolysis during labeling.

SDS-PAGE. The Cyanine dye labeling reaction was performed with minimal labeling conditions (50 μg of protein at 5 μg/μL) per the manufacturer's instructions unless stated otherwise (Amersham, Piscataway, NJ). Labeled proteins from pooled and individual (naive or injured) samples were reduced with 5 mM DTT, alkylated with 55 mM iodoacetamide, and heated to 95°C for 2 min prior to separation with Tris-tricine SDS-PAGE gels (10–20% polyacrylamide, Invitrogen, Carlsbad, CA) at 4°C. Fluorescence imaging was performed with 1-sec exposure times (ProExpress, PerkinElmer, Boston, MA). Alternatively, unlabeled proteins were separated with the same gel system and stained with Coomassie blue. In both cases, image analysis (ImageJ, NIH) was performed to target specific regions of the gel; however, 1.5 mm × 4 mm gel slices spanning the entire gel lane were excised and stored at −80°C for trypsinization.

In vitro *proteolysis*. Excised gel bands were destained, reduced with 5 mM DTT, and alkylated with 55 mM iodoacetamide prior to overnight digestion with 400 ng of trypsin (Trypsin gold, Promega, Madison, WI) in 100 mM NH_4HCO_3.

Preparation of capillary LC columns with integrated electrospray emitters. The preparation of capillary LC columns with integrated electrospray emitters is described elsewhere (Haskins et al., 2001); however, 5 cm of 3-μm C18 particles (Alltima C18, Alltech, Deerfield, IL) and 50-μm-i.d. capillary LC columns were used in this work.

Automated two-pressure capillary LC-MS^2 system. The capillary LC-MS^2 system is described elsewhere (Haskins et al., 2001). The system utilizes 2 six-port valves to select the pump and flow path for preconcentration, desalting, and separation/electrospray steps. During the preconcentration and desalting steps the high-flow-rate pump was selected without splitting of the sample in order to minimize the sample loading time. During the separation/electrospray step, the low-flow-rate pump was selected with splitting of the gradient in order to maximize the separation and electrospray efficiency and to minimize the delay time of the gradient, respectively.

In this work, 4.5 μL from a 12-μL sample of tryptic peptides was transferred into a 2-μL sample loop with an autosampler and analyzed every 38 min by preconcentrating/desalting at 600 nL/min and separating/electrospraying at 60 nL/min. All measurements were made with the following capillary LC-MS^2 parameters, unless specified otherwise: preconcentration time = 3.3 min (2.0 μL), desalting time = 3.3 min (2.0 (L), separa-

tion/electrospray time = 30 min (10 min pump gradient from 5% to 45% mobile phase B; mobile phase A = 2% acetonitrile: 1% acetic acid; mobile phase B = 98% acetonitrile: 1% acetic acid), re-equilibration time = 1.4 min. The mass spectrometer was a QIT (LCQ-Deca XP+, ThermoFinnigan, San Jose, CA) with the following parameters, unless specified otherwise: automatic gain control (AGC) on, max AGC time = 300 msec, q = 0.25, isolation width = 3 *m/z*, normalized collision energy = 35%, activation time = 0.25 msec and the default number of microscans and target count values. Data-dependent MS/MS spectra (MS, 4 × MS/MS) were collected using a precursor ion window of *m/z* 400–1800 and a product ion window calculated for z = +2.

Differential proteomic analysis. Protein database searching (RefSeq 785,143 sequences (Pruitt and Maglott, 2001) with uninterpreted MS^2 spectra and differential proteomic analysis of unmodified proteins were performed with Sequest (Yates et al., 1998) and DTASelect (Tabb et al., 2002), respectively. The default precursor and product ion tolerances of 1.5 and 0.0 were selected for Sequest, while only singly, doubly, and triply charged tryptic peptide sequences with Xcorr > 1.8, 2.5, and 3.5 were considered significant for DTASelect. No molecular mass constraints were placed on protein identification by protein database searching. A TBI database containing unmodified peptide and protein sequences that were observed in naive only, injured only, or both conditions was constructed in-house (from the DTASelect files via Microsoft Access 2002) as a function of the 1D-DIGE gel position (gel slices were numbered 1–50 from high to low molecular mass). PTMs were investigated with Mascot (Perkins et al., 1999) using the same protein database as Sequest but with the recommended precursor and product ion tolerances of 2.0 and 0.8, respectively. PTMs were considered significant if the Mascot score indicated homology with greater than 95% probability.

RESULTS

SDS-PAGE-Capillary LC-MS²

Naive and injured hippocampal protein samples were processed and labeled with Cy-3 and Cy-5 dye separately. Labeled proteins from pooled and individual samples were separated side-by-side, and naive and injured samples were run on separate lanes (Fig. 1). Our results show the consistency in protein loading, cyanine dye labeling, and separation efficiency. Alternatively, unlabeled proteins were separated with the same gel system and stained with Coomassie blue (data not shown). In general, we did not find a significant advantage of cyanine-dye labeling for our purposes. Fifty 1.5 mm × 4 mm gel slices spanning each (naive or injured) gel lane were excised, trypsinized and subjected to automated capillary LC-MS^2. We collected 15,558 uninterpreted MS^2 spectra in 3 days for pooled cyanine dye-labeled samples separated by SDS-PAGE. Protein database searching identified more than 306 unique proteins. Overall, we obtained 156 ± 60 MS^2 spectra per gel slice and 1–3 tryptic peptide sequences per protein. Figure 2 shows the correlation between the database-derived molecular mass ($M_r$calc), and SDS-PAGE–predicted molecular mass ($M_r$obs). The migration of proteins in the SDS-PAGE gel inversely correlates with $M_r$calc for unmodified proteins identified by capillary LC-MS^2 and database searching (solid line), as expected. Accordingly, $M_r$obs directly correlates with $M_r$calc. In addition, protein sequence coverage shows an inverse correlation with $M_r$calc (dashed line). That is, the higher the molecular mass of the protein, the less sequence coverage is obtained. However, it is important to note that we have successfully identified (by peptide sequences rather than by peptide masses) more than 20 proteins of high molecular mass (150–300 kDa). In contrast, proteins in this molecular mass range are almost impossible to visualize and identify by 2D gels (Fountoulakis et al., 1999b).

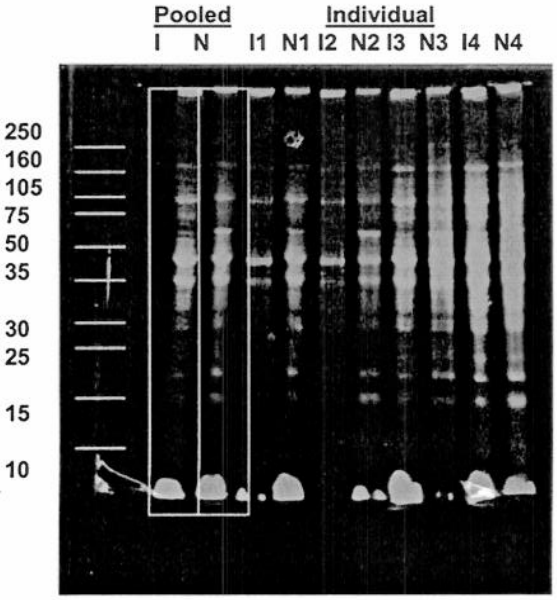

FIG. 1. Cyanine-dye labeled proteins separated by SDS-PAGE. Fluorescence image of 25 μg of Cy3– and Cy5–labeled proteins from naive (N) and injured (I) ipsilateral hippocampus (IH) samples separated on a Tris-tricine SDS-PAGE gel (10–20% polyacrylamide).

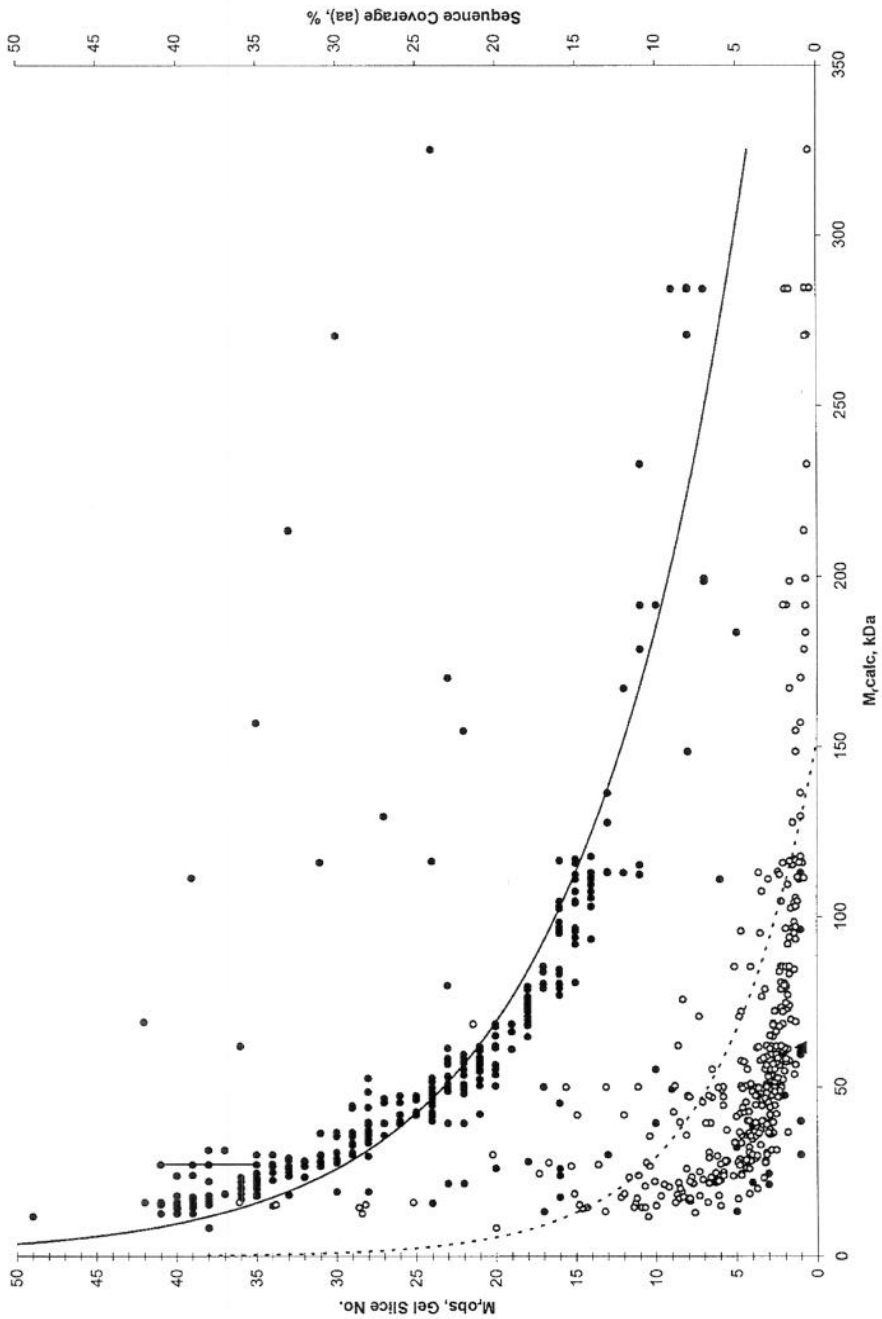

FIG. 2. Correlation between the database-derived molecular mass ($M_r$calc), and SDS-PAGE-predicted molecular mass ($M_r$obs). The migration of proteins in the SDS-PAGE gel inversely correlates with $M_r$calc for unmodified proteins identified by capillary LC-MS^2 and database searching (solid line), as expected. Accordingly, $M_r$obs directly correlates with $M_r$calc. In addition, protein sequence coverage shows an inverse correlation with $M_r$calc (dashed line).

TABLE 1. DIFFERENTIAL PROTEOMIC ANALYSIS OF MAMMALIAN PROTEIN

RefSeq accession number	*Protein description*	*$M_r$calc (kDa)*	*$M_r$obs (kDa)*
Protein appears in naïve animals only			
NM_022007	FXYD domain-containing ion transport regulator 7 [*Mus musculus*]	8	13–17
NM_181029	casein alpha-S1 [*Bos taurus*]	25	>250
NM_012966	heat shock 10 kDa protein 1 (chaperonin 10) [*Rattus norvegicus*]	11	10–13
NM_017236	phosphatidylethanolamine binding protein [*Rattus norvegicus*]	21	15–25
NM_018947	cytochrome c [*Homo sapiens*]	12	<10
NM_057114	peroxiredoxin 1 [*Rattus norvegicus*]	22	15–25
NM_022511	profilin [*Rattus norvegicus*]	15	10–15
NM_174294	casein kappa [*Bos taurus*]	21	>250
NM_028207	dual specificity phosphatase 3 [*Mus musculus*]	20	15–25
NM_016956	hemoglobin, beta adult minor chain; beta min; beta minor globin [*Mus musculus*]	16	10–15
NM_017169	thioredoxin peroxidase 1 [*Rattus norvegicus*]	22	15–25
NM_017055	transferrin [*Rattus norvegicus*]	76	50–75
NM_182839	RIKEN cDNA 2900041A09 [*Mus musculus*]	23	17–27
NM_010471	hippocalcin [*Mus musculus*]	22	15–25
NM_023716	tubulin, beta [*Mus musculus*]	50	35–50
NM_021316	BM88 antigen [*Mus musculus*]	15	15–25
NM_053511	neural F box protein NFB42 [*Rattus norvegicus*]	34	30–35
NM_009610	Actin, gamma 2 (smooth muscle) [*Mus musculus*]	42	40–60
NM_022922	triosephosphate isomerase 1 [*Rattus norvegicus*]	27	17–27
NM_019131	tropomyosin 1, alpha [*Rattus norvegicus*]	29	27–33
NM_012498	aldehyde reductase 1 [*Rattus norvegicus*]	36	13–17
NM_000410	hemochromatosis protein 1 [*Homo sapiens*]	10	35–50
NM_017025	lactate dehydrogenase A [*Rattus norvegicus*]	36	27–33
NM_008617	malate dehydrogenase, mitochondrial [*Mus musculus*]	35	27–33
NM_023716	RIKEN cDNA 2410129E14 gene [*Mus musculus*]	50	35–50
NM_002634	prohibitin [*Homo sapiens*]	30	17–27
NM_011553	t-complex protein 10b [*Mus musculus*]	49	>250
NM_001069	tubulin, beta polypeptide [*Homo sapiens*]	50	35–50
NM_002301	lactate dehydrogenase C [*Homo sapiens*]	36	27–33
NM_012949	enolase 3, beta; [*Rattus norvegicus*]	47	35–50
NM_014364	glyceraldehyde-3-phosphate dehydrogenase, testis-specific [*Homo sapiens*]	44	27–33
NM_013506	eukaryotic translation initiation factor 4A2 [*Mus musculus*]	46	35–50
NM_133977	transferrin; hypotransferrinemia with hemochromatosis [*Mus musculus*]	77	50–75
NM_003026	SH3-domain GRB2-like 2 [*Homo sapiens*]	40	33–40
NM_139254	tubulin, beta 3 [*Rattus norvegicus*]	50	35–50
NM_022399	calreticulin [*Rattus norvegicus*]	48	35–50
NM_031140	vimentin [*Rattus norvegicus*]	54	35–50
NM_012497	aldolase C, fructose-biphosphate [*Rattus norvegicus*]	39	33–40
NM_031034	guanine nucleotide binding protein (G protein) alpha 12 [*Rattus norvegicus*]	44	30–35
XM_236277	protein phosphatase PP2A [*Rattus norvegicus*]	65	50–75
NM_019225	solute carrier family 1, member 3 [*Rattus norvegicus*]	60	>250
NM_017009	glial fibrillary acidic protein [*Rattus norvegicus*]	50	35–50
NM_025407	ubiquinol-cytochrome c reductase core protein 1 [*Mus musculus*]	53	35–50
NM_145614	dihydrolipoamide S-acetyltransferase [*Mus musculus*]	68	50–75

TABLE 1. DIFFERENTIAL PROTEOMIC ANALYSIS OF MAMMALIAN PROTEIN (*CONTINUED*)

RefSeq accession number	*Protein description*	*$M_r$calc (kDa)*	*$M_r$obs (kDa)*
NM_022229	heat shock protein 60 (chaperonin) [*Rattus norvegicus*]	61	40–60
NM_145518	NADH dehydrogenase (ubiquinone) Fe-S protein 1 [*Mus musculus*]	80	50–75
NM_175199	heat shock protein 12A [*Mus musculus*]	75	50–75
NM_008449	kinesin heavy chain 5C, neuron-specific [*Mus musculus*]	109	80–130
NM_031715	phosphofructokinase, muscle [*Rattus norvegicus*]	86	60–90
NM_145779	pregnancy-zone protein [*Rattus norvegicus*]	167	115–205
NM_013559	HSP105 [*Mus musculus*]	97	80–130
NM_031604	H^+ transporting ATPase, lysosomal (vacuolar proton pump) [*Rattus norvegicus*]	96	>250
NM_021343	spermatogenesis associated factor [*Mus musculus*]	97	75–105
NM_007804	cut-like 2 [*Mus musculus*]	155	35–50
NM_152296	ATPase, Na^+/K^+ transporting, alpha 3 polypeptide [*Homo sapiens*]	112	80–130
NM_054004	TBP-interacting protein 120A [*Rattus norvegicus*]	136	105–160
NM_019167	beta-spectrin 3 [*Rattus norvegicus*]	271	>250
Protein appears in injured animals only			
NM_003509	H2A histone family, member C [*Homo sapiens*]	14	10–15
NM_080777	synuclein, beta [*Rattus norvegicus*]	15	10–15
NM_000976	ribosomal protein L12 [*Homo sapiens*]	18	15–25
NM_025562	RIKEN cDNA 2010003O14 [*Mus musculus*]	17	13–17
NM_016068	CGI-135 protein [*Homo sapiens*]	17	13–17
NM_025313	RIKEN cDNA 0610008F14 [*Mus musculus*]	18	10–15
NM_026369	actin-related protein 2/3 complex, subunit 5 [*Mus musculus*]	16	13–17
NM_012038	visinin-like 1 [*Mus musculus*]	22	15–25
NM_009923	cyclic nucleotide phosphodiesterase 1 [*Mus musculus*]	47	35–50
NM_133796	Rho GDP dissociation inhibitor (GDI) alpha [*Mus musculus*]	23	17–27
NM_014231	VAMP-1A; synaptobrevin [*Homo sapiens*]	13	10–15
NM_017101	peptidylprolyl isomease A (cyclophilin A) [*Rattus norvegicus*]	18	10–15
NM_009001	RAB3A, member RAS oncogene family [*Mus musculus*]	25	15–25
NM_000518	beta globin [*Homo sapiens*]	16	10–15
NM_024349	adenylate kinase [*Rattus norvegicus*]	21	15–25
NM_031603	14-3-3 epsilon [*Rattus norvegicus*]	29	15–25
NM_017051	superoxide dismutase 2, mitochondrial [*Rattus norvegicus*]	25	15–25
NM_026267	RIKEN cDNA 1200016B17 [*Mus musculus*]	30	30–35
NM_008907	peptidylprolyl isomerase A; cyclophilin A [*Mus musculus*]	18	13–17
NM_053610	peroxiredoxin 5 precursor [*Rattus norvegicus*]	22	13–17
NM_016131	ras-related GTP-binding protein RAB10 [*Homo sapiens*]	23	15–25
NM_011670	ubiquitin carboxy-terminal hydrolase L1; gracile axonal dystrophy; protein gene product 9.5 [*Mus musculus*]	25	15–25
NM_019376	14-3-3 protein gamma [*Rattus norvegicus*]	28	17–27
NM_011739	14-3-3 theta [*Mus musculus*]	28	17–27
NM_010312	guanine nucleotide-binding protein, beta-2 subunit [*Mus musculus*]	37	30–35
NM_023200	protein phosphatase-1 regulatory subunit 7 [*Mus musculus*]	41	35–50
NM_019632	N-ethylmaleimide sensitive fusion protein attachment protein beta; brain protein I47 [*Mus musculus*]	34	27–33
NM_017327	GTP-binding protein alpha o; RATBPGTPC [*Rattus norvegicus*]	40	30–35
NM_026646	RIKEN cDNA 1300006L01 [*Mus musculus*]	35	30–35
NM_005165	aldolase C, fructose-bisphosphate; Aldolase C, fructose-bisphosphatase [*Homo sapiens*]	39	33–40

(*continued*)

TABLE 1. DIFFERENTIAL PROTEOMIC ANALYSIS OF MAMMALIAN PROTEIN (*CONTINUED*)

RefSeq accession number	*Protein description*	*$M_r$calc (kDa)*	*$M_r$obs (kDa)*
NM_025942	RIKEN cDNA 2810409H07 [*Mus musculus*]	45	35–50
NM_019291	carbonic anhydrase 2 [*Rattus norvegicus*]	37	27–33
NM_017215	solute carrier family 1, member 2 [*Rattus norvegicus*]	62	>250
NM_005917	cytosolic malate dehydrogenase [*Homo sapiens*]	36	17–27
NM_006032	copine 6; neuronal copine; N-copine [*Homo sapiens*]	62	50–75
NM_006136	F-actin capping protein alpha-2 [*Homo sapiens*]	33	27–33
NM_002074	G protein, beta-1 subunit; transducin beta chain 1I [*Homo sapiens*]	37	30–35
NM_014203	adaptin, alpha A; [*Homo sapiens*]	108	80–130
NM_002635	phosphate carrier precursor isoform 1b; mitochondrial [*Homo sapiens*]	40	>250
NM_018754	stratifin; 14-3-3 sigm [*Mus musculus*]	28	17–27
NM_024221	pyruvate dehydrogenase (lipoamide) beta [*Mus musculus*]	39	30–35
NM_025899	ubiquinol cytochrome c reductase core protein 2 [*Mus musculus*]	48	35–50
NM_002300	lactate dehydrogenase B [*Homo sapiens*]	37	27–33
NM_012570	glutamate dehydrogenase 1; memory related gene 2 [*Rattus norvegicus*]	61	40–60
NM_138828	apolipoprotein E [*Rattus norvegicus*]	36	27–33
NM_013681	synapsin II [*Mus musculus*]	52	40–60
NM_033235	malate dehydrogenase 1[*Rattus norvegicus*]	36	27–33
NM_011861	protein kinase C and casein kinase substrate in neurons 1 [*Mus musculus*]	51	40–60
NM_004077	citrate synthase precursor; citrate synthase, mitochondrial [*Homo sapiens*]	52	35–50
NM_007505	ATP synthase, H^+ transporting, mitochondrial F1 complex, alpha subunit, isoform 1 [*Mus musculus*]	60	35–50
NM_057118	contactin 1 [*Rattus norvegicus*]	113	105–160
NM_010481	heat shock protein, A [*Mus musculus*]	74	50–75
NM_019703	phosphofructokinase [*Mus musculus*]	86	60–90
NM_012491	adducin 2, beta [*Rattus norvegicus*]	81	80–130
NM_003178	synapsin IIb [*Homo sapiens*]	52	40–60
NM_009947	copine VI; copine 6; neuronal copine [*Mus musculus*]	62	50–75
NM_011393	solute carrier family 1, member 2; glial high affinity glutamate transporter [*Mus musculus*]	61	>250
NM_153781	brain glycogen phosphorylase [*Mus musculus*]	97	75–105
NM_006644	heat shock 105 kD [*Homo sapiens*]	92	80–130
NM_031783	neurofilament, light polypeptide [*Rattus norvegicus*]	61	50–75
NM_006950	synapsin Ia [*Homo sapiens*]	74	50–75
NM_013066	microtubule-associated protein 2 [*Rattus norvegicus*]	199	>250
NM_021979	heat shock 70 kDa protein 2 [*Homo sapiens*]	70	50–75
NM_012607	neurofilament, heavy polypeptide [*Rattus norvegicus*]	115	115–205
NM_181092	synaptic Ras GTPase activating protein 1 [*Rattus norvegicus*]	128	105–160
NM_005348	heat shock 90 kDa protein 1, alpha [*Homo sapiens*]	85	75–105
NM_010438	hexokinase 1; downeast anemia [*Mus musculus*]	106	80–130
NM_000477	albumin precursor [*Homo sapiens*]	69	10–15
NM_001385	dihydropyrimidinase [*Homo sapiens*]	57	50–75
NM_001127	Seta-adaptin [*Homo sapiens*]	105	80–130
NM_003334	ubiquitin-activating enzyme E1 [*Homo sapiens*]	118	80–130
NM_001835	Clathrin, heavy chain [*Homo sapiens*]	179	115–205
NM_005657	tumor protein p53 binding protein, 1 [*Homo sapiens*]	214	15–25
NM_002374	microtubule-associated protein 2a [*Homo sapiens*]	199	>250

TABLE 1. DIFFERENTIAL PROTEOMIC ANALYSIS OF MAMMALIAN PROTEIN (*CONTINUED*)

RefSeq accession number	*Protein description*	*$M_r$calc (kDa)*	*$M_r$obs (kDa)*
Higher sequence coverage in injured than naïve (protein appears in both)			
NM_005530	mitochondrial; isocitrate dehydrogenase (NAD^+) alpha [*Homo sapiens*]	40	30–35
NM_024398	mitochondrial aconitase [*Rattus norvegicus*]	85	60–90
NM_005566	lactate dehydrogenase A [*Homo sapiens*]	37	27–33
NM_057143	fertility protein SP22 [*Rattus norvegicus*]	200	15–25
NM_013083	heat shock 70 kD protein 5 [*Rattus norvegicus*]	72	50–75
NM_019169	synuclein, alpha [*Rattus norvegicus*]	15	10–15
NM_024398	mitochondrial aconitase [*Rattus norvegicus*]	85	60–90
XM_237718	tubulin alpha 6 [*Rattus norvegicus*]	50	35–50
NM_171983	alpha-spectrin 2 [*Rattus norvegicus*]	285	>250
NM_139325	enolase 2, gamma; neuronal [*Rattus norvegicus*]	50	35–50
NM_006597	heat shock 70 kDa protein 8 isoform 1 [*Homo sapiens*]	71	50–75
NM_015981	CaM kinase II alpha subunit; isoform 1 [*Homo sapiens*]	55	40–60
NM_011738	14-3-3 eta [*Mus musculus*]	28	17–27
NM_017042	protein phosphatase 3 (calcineurin) subunit A beta [*Rattus norvegicus*]	59	40–60
NM_005507	cofilin 1 (non-muscle) [*Homo sapiens*]	19	15–25
NM_146100	hypothetical protein MGC25352 [*Mus musculus*]	55	50–75
XM_217040	tubulin alpha-1 [*Rattus norvegicus*]	50	35–50
Same sequence coverage in naïve and injured			
NM_006870	destrin [*Homo sapiens*]	19	15–25
NM_173102	tubulin, beta 5 [*Rattus norvegicus*]	50	35–50
NM_006000	tubulin, alpha 1; testis-specific [*Homo sapiens*]	50	35–50
NM_001102	actinin, alpha 1 [*Homo sapiens*]	103	80–130
NM_008634	microtubule-associated protein 1b [*Mus musculus*]	270	27–33
NM_008084	glyceraldehyde-3-phosphae dehydrogenase [*Mus musculus*]	36	30–35
NM_023964	glyceraldehyde-3-phosphate dehydrogenase type 2 [*Rattus norvegicus*]	47	30–35
NM_153629	(NM_153629) heat shock 70 kDa protein 4 [*Rattus norvegicus*]	94	80–130
NM_012529	(NM_012529) creatine kinase, brain [*Rattus norvegicus*]	43	33–40
NM_012734	hexokinase 1 [*Rattus norvegicus*]	103	75–105
NM_009497	vesicle-associated membrane protein 2; synaptobrevin II [*Mus musculus*]	13	10–15
NM_016774	ATP synthase, H^+ transporting mitochondrial F1 complex, beta subunit [*Mus musculus*]	58	35–50
NM_010777	(NM_010777) myelin basic protein; myelin deficient [*Mus musculus*]	27	10–27
NM_031728	synaptosomal-associated protein (AP180) [*Rattus norvegicus*]	94	80–130
NM_000517	alpha 2 globin [*Homo sapiens*]	15	10–15
NM_002965	S100 A9; calgranulin B [*Homo sapiens*]	13	I: >250, N: 60–90
NM_030873	profilin II [*Rattus norvegicus*]	15	10–15
NM_012673	thymus cell surface antigen [*Rattus norvegicus*]	18	15–25
NM_012635	(NM_012635) pancreatic trypsin 1 [*Rattus norvegicus*]	26	75–105
NM_013177	Glutamate oxaloacetate transaminase 2 mitochondrial [*Rattus norvegicus*]	27	33–40
NM_012504	ATPase, Na^+K^+ transporting, alpha 1 [*Rattus norvegicus*]	113	105–160
NM_010324	glutamate oxaloacetate transaminase 1, cytosolic [*Mus musculus*]	26	33–40
NM_080583	adaptor-related protein complex 2, beta 1 subunit; beta adaptin [*Rattus norvegicus*]	105	75–105

(*continued*)

TABLE 1. DIFFERENTIAL PROTEOMIC ANALYSIS OF MAMMALIAN PROTEIN (*CONTINUED*)

RefSeq accession number	*Protein description*	*$M_r$calc (kDa)*	*$M_r$obs (kDa)*
NM_026508	(NM_026508) RIKEN cDNA 2410002K23 [*Mus musculus*]	80	75–105
NM_006310	puromycin-sensitive aminopeptidase; metalloproteinase MP100 [*Homo sapiens*]	99	75–105
Higher sequence coverage in naïve than injured (protein appears in both)			
NM_030773	beta tubulin 1, class VI [*Homo sapiens*]	50	35–50
NM_019299	clathrin, heavy polypeptide (Hc) [*Rattus norvegicus*]	192	160–250
NM_003127	alpha-spectrin 2 (alpha-fodrin) [*Homo sapiens*]	284	>250
NM_013096	hemoglobin, alpha 1 [*Rattus norvegicus*]	15	10–15
NM_018753	14-3-3 protein beta [*Mus musculus*]	28	17–27
NM_000944	protein phosphatase 3 (calcineurin A alpha) [*Homo sapiens*]	59	40–60
NM_057213	ATPase, H^+ transporting, lysosomal beta 2 [*Rattus norvegicus*]	57	40–60
NM_138548	nucleoside diphosphate kinase (NM23A) [*Rattus norvegicus*]	17	10–15
NM_033234	Hemoglobin, beta [*Rattus norvegicus*]	16	10–15
NM_053543	neurochondrin [*Rattus norvegicus*]	79	50–75
NM_003406	14-3-3 zeta [*Homo sapiens*]	28	17–27
NM_031353	voltage-dependent anion channel 1 [*Rattus norvegicus*]	31	27–33
NM_138597	ATP synthase, H^+ transporting, mitochondrial F1 complex, O subunit [*Mus musculus*]	23	15–25
NM_053291	phosphoglycerate kinase 1 [*Rattus norvegicus*]	45	35–50
NM_000034	aldolase A; fructose-biphosphate aldolase [*Homo sapiens*]	39	33–40
NM_017245	translation elongation factor 2 [*Rattus norvegicus*]	95	75–105
NM_023119	enolase 1, alpha non-neuron [*Mus musculus*]	47	35–50
NM_005918	mitochondrial malate dehydrogenase [*Homo sapiens*]	36	27–33
NM_053297	/pyruvate kinase, muscle [*Rattus norvegicus*]	58	40–60
NM_080689	dynamin 1 [*Rattus norvegicus*]	96	75–105
NM_011123	myelin proteolipid protein [*Mus musculus*]	30	I, N: 15–30, N: 105–160
NM_134326	albumin [*Rattus norvegicus*]	69	50–75

The RefSeq (Pruitt and Maglott, 2001) accession number, protein description, database-derived molecular mass ($M_r$calc), and SDS-PAGE-predicted molecular mass ($M_r$obs) are shown for putative protein biomarkers of TBI.

Differential proteomic analysis of the gel slices (high to low $M_r$obs) revealed differences in protein sequence coverage for 170 mammalian proteins (57 in naive only, 74 in injured only, and 39 of 64 in both) as listed in Table 1. Inspection of the proteins falling into each of the three categories of protein markers shows that several well-studied proteins involved in TBI were observed in both naive and injured samples, including brain creatine kinase (CKB), αII-spectrin, neuron-specific enolase (NSE), α-synuclein (α-Syn), microtubule associated protein 2a and 2b (MAP2), neurofilament (NF), proteolipid protein (PLP), and myelin basic protein (MBP). The injured-to-naive ratio of protein sequence coverage suggests putative biomarkers that may exhibit significant differences in protein concentration between naive and injured samples. However, protein sequence coverage is only a semi-quantitative measure of protein concentration. This is particularly true for protein identifications based on single tryptic peptide sequences, and it is even more pronounced for degraded proteins. However, proteins observed only in naive samples, or proteins observed with greater sequence coverage in naive samples than in injured samples, suggest a subset of putative biomarkers that are down-regulated, released, or degraded during TBI, for example, (αII-spectrin (Pike et al., 2002), MAP2 (Huh et al., 2003), NF (Posmantur et al., 1996, 1998) and PLP (Banik et al., 1985; Domanska-Janik et al., 1992). Likewise, proteins observed only in injured samples, or proteins observed with greater sequence coverage in injured samples than in naive samples, suggest a subset of putative biomarkers that are up-regulated, accumulated, or aggregated during TBI, for example, NSE (Varma et al., 2003), amyloid precursor protein, amyloid β 1-42, tau (Franz et al., 2003), and α-Syn (Uryu et al., 2003; Bramlett and Dietrich 2003; Newell et al., 1999; Smith et al., 2003). Since the fragments of degraded proteins, for ex-

ample, breakdown products of αII-spectrin (Pike et al., 2002) may also be observed, it is important to relate $M_r$calc to $M_r$obs for putative protein biomarkers of TBI.

In order to evaluate whether any of our biomarkers were fragments of degraded proteins rather than intact proteins, we performed differential proteomic analysis as a function of $M_r$obs. Degraded protein biomarkers may not be revealed by differences in protein sequence coverage using current differential proteomic analysis tools, even when proteins are separated prior to *in vitro* proteolysis and capillary LC-MS^2, because $M_r$obs, which is encoded in SDS-PAGE–Capillary LC–MS^2 data, may not be preserved during data reduction. For example, MBP was identified by database searching ($M_r$calc = 27 kDa) in both naive and injured samples with a sequence coverage of 13.6%, incorrectly suggesting that it is not a putative biomarker of TBI. However, the vertical line in Figure 2 illustrates that MBP was observed in gel slices 35–41 ($M_r$obs ~ 27 kDa to 10 kDa, respectively) in injured (and not naive) samples, suggesting possible degradation, as confirmed by Western blot (Liu et al., unpublished observations).

Classification of Putative Protein Biomarkers of TBI

Stratification of the putative protein biomarkers discovered in this work, based on function and distribution, suggests several classes of proteins are of interest (Figs. 3 and 4). Careful examination of the fraction of proteins from each class that were observed in naive only, injured only, and both naive and injured samples highlights the most promising classes for biomarkers of TBI. For example, Figure 3 shows that 10% of the putative biomarkers observed only in injured samples were neuronal proteins including: PLP, Syn (α and β), NSE, NF (light and heavy), synapsin (I and II), vesicle associated membrane protein 1, and apolipoprotein E. Other promising classes of biomarkers observed only in injured samples include heat shock proteins (e.g., chaperonin 10) and kinases (e.g., calcium/calmodulin protein kinase II). These observations are reflected by peaks in the line plot shown in Figure 4. Thus, neuronal proteins, heat shock proteins, and kinases are a promising class of biomarkers that are up-regulated, accumulated, or aggregated during TBI. In contrast, the valley for dehydrogenases (e.g., lactate dehydrogenase) only in naive samples indicates a promising class of biomarkers that are down-regulated, released, or degraded. A complete discussion of the putative protein biomarkers discovered in this work is beyond the scope of this paper. While some ambiguity is expected, for example, glutamate dehydrogenase was observed only in injured samples while the neuronal protein glial fibrillary acidic protein (GFAP) was observed only in naive samples, the classification of putative protein biomarkers of TBI, combined with differential analysis methods such as this one, provides direction for biomarker research.

Preliminary Validation

The relative concentration of several putative protein biomarkers of TBI was investigated by targeted capillary LC-MS^2 (Haskins et al., 2001) of selected tryptic peptides (Fig. 4). Two- to ten-fold changes in tryptic peptide concentration for injured versus naive samples reflect the semi-quantitative differences in protein sequence coverage observed. For example, glutamate dehydrogenase (memory related gene 2), shown in Figure 5C, was ~10-fold higher in injured samples than in naive samples: corresponding to 2.9% protein sequence coverage in injured samples and 0.0% protein sequence coverage in naive samples (i.e., no tryptic peptides were observed in naive samples). A high yield of sequence-specific b- and y-type product ions was observed following isolation and fragmentation of selected tryptic precursor ions by collision-induced dissociation. Absolute quantification (AQUA) (Gerber et al., 2003) of these proteins can be readily achieved by incorporating an isotopically labeled tryptic peptide as an internal standard during trypsin digestion (publication in preparation). Assuming that the analytical variability exceeds the biological variability in pooled samples such as these, a false-positive rate as high as 30% is expected for data-dependent capillary LC-MS^2 of complex mixtures (unpublished work). While only a 29% overlap of proteins conserved between naive and injured samples underscores the need for higher-resolution protein separation methods, this must be balanced with the need for faster results. Indeed, preliminary validation of biomarkers is a significant bottleneck for proteomics as the speed of discovery continues to outpace the speed of validation (Bodovitz and Joos, 2004).

Comparison with Previous Work

This is the first report of SDS-PAGE–Capillary LC–MS^2 for biomarker discovery. Several of the putative protein biomarkers described herein at 48 h post-injury were suggested previously by a microarray- and RNA-based gene expression experiment (Matzilevich et al., 2002) In 10 oligonucleotide array pairs, 261 of 8800 genes were significantly affected at 24 h post-injury, including NF (light), MAP2, GFAP, and beta-tubulin.

More recently, a proteomics approach using 2D gels and database searching of 2D gel images (Fountoulakis et al., 1999a) at 24 h post-injury was presented (Jenkins et al., 2002). In that work, 50 (<95 kDa proteins) of

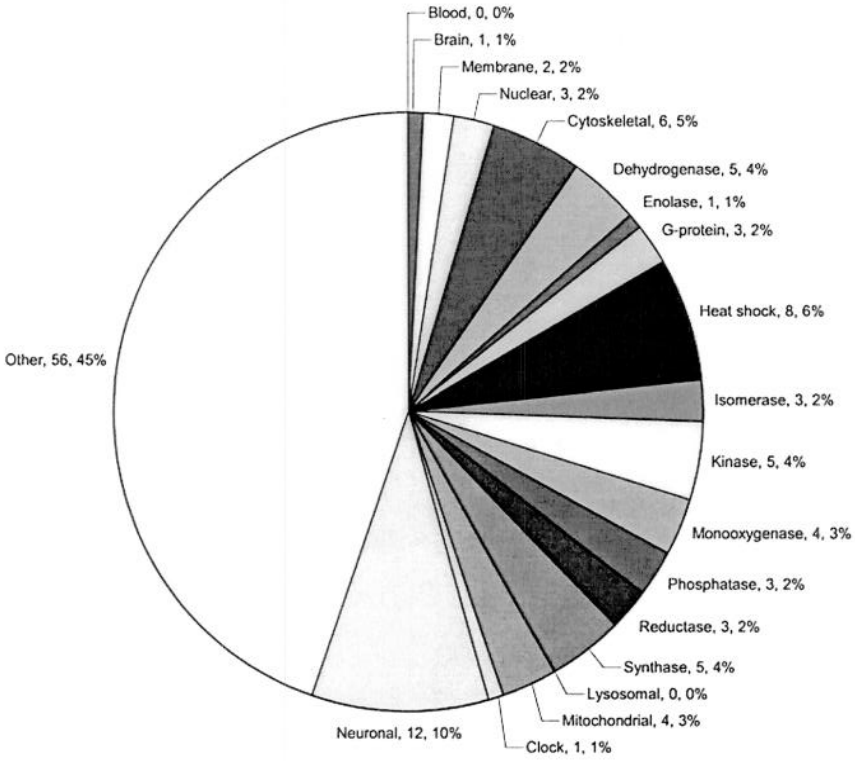

FIG. 3. Stratification of the putative protein biomarkers discovered in injured hippocampus only. Protein class, number of proteins, fraction of protein biomarkers. Proteins were sorted into classes based on function and localization with increasingly stringent specificity: blood, brain < membrane < nuclear < cytoskeletal < dehydrogenase, enolase, clock, G-protein, heat shock, isomerase, kinase, monooxygenase, phosphatase, reductase < synthase < lysosomal, mitochondrial < neuronal.

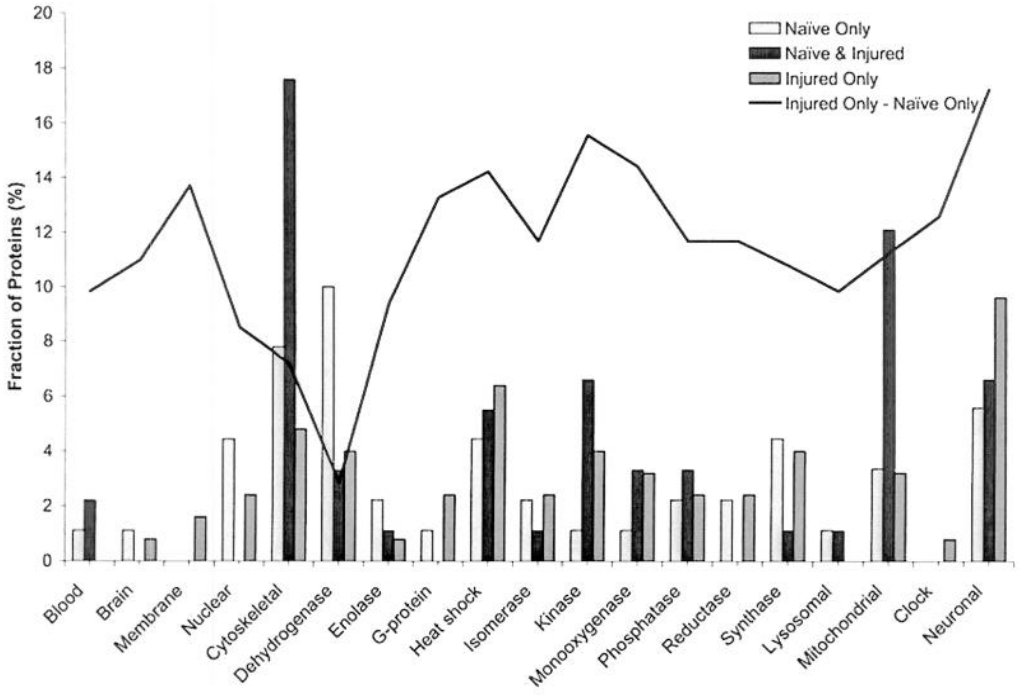

FIG. 4. Stratification of putative protein biomarkers discovered in naive only, injured only, and both naive and injured hippocampal samples. The fractions of biomarkers in "Naive Only" (light grey columns), "Injured Only" (dark grey), and both "Naive and Injured" samples (black). were plotted against each function and localization class. In addition, the difference in the fraction between the "Injured Only" group and the "Naive Only" group was plotted as a line graph on the same scale. Peaks in the line plot suggest classes of proteins that are elevated, upregulated, or aggregated (e.g., neuronal, kinase) in injured hippocampus, while valleys in the line plot are those that are down-regulated, released, or degraded (e.g., dehydrogenase) in injured hippocampus.

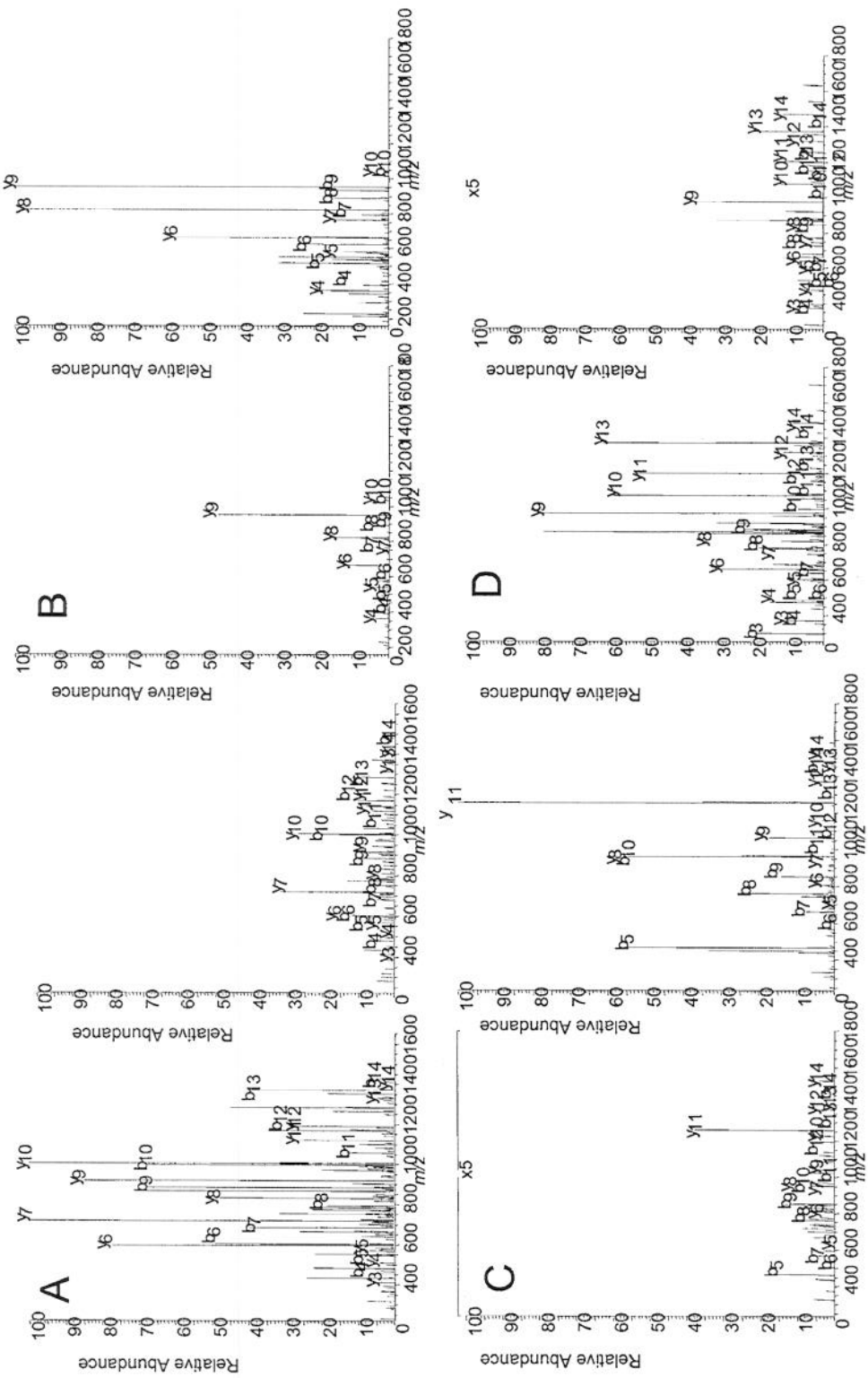

FIG. 5. Representative targeted MS^2 spectra collected in naive (left) and injured (right) hippocampus samples. (**A**) CKB-rat, (**B**) α-Syn, (**C**) Memory-related gene 2, (**D**) αII-Spectrin. The tryptic peptide sequences corresponding to these spectra are LAVEALSSLDGDLSGR (A), KEGVLYVGSK (B), HGGTIPVVPTAEFQDR (C), and DLAALGDKVNSLGETAQR (D), respectively.

~1500 protein spots were tentatively identified by matching the 2D gel-derived molecular masses and isoelectric points of the protein spots with a rat brain database of 210 proteins. However, only six putative protein biomarkers were revealed by significant changes across six of six gel pairs (individual rather than pooled samples). Interestingly, an increase in the mitochondrial protein Cu/Zn superoxide dismutase, and a decrease in the cytoskeletal proteins α- and β-tubulin, were also observed in this work.

Confidence in previously reported putative biomarkers is significantly strengthened by sequence-specific discovery of these proteins by SDS-PAGE–Capillary LC–MS^2. Protease-specific peptide sequences provide a means to unambiguously identify putative protein biomarkers and various PTMs (e.g., degradation) from large protein databases (e.g., RefSeq 785,143 sequences) (Pruitt and Maglott, 2001). In contrast, microarray experiments suffer from our incomplete understanding of the interaction between transcription and translation; that is, RNA levels do not accurately reflect protein levels, and database searching of 2D gel images suffers from a low success rate for protein identification. Despite the limitations of these techniques, the unambiguous identification of several previously reported putative biomarkers by SDS-PAGE–Capillary LC–MS^2 provides evidence for the validity of this approach to biomarker discovery.

DISCUSSION

Using differential proteomic analysis, we revealed differences in protein sequence coverage for 170 mammalian proteins (57 in naive only, 74 in injured only, and 39 of 64 in both). Our data suggest that these are putative biomarkers of TBI in hippocampus tissue, as these are expected to either accumulate in the CSF and blood, or form aggregate in the extracellular compartment of the brain. However, we must further establish if these markers can distinguish TBI from various other brain diseases, and the kinetics for their degradation and clearance from tissue to CSF and blood must be favorable in order to obtain reliable indicators of injury severity. A subset of the putative protein biomarkers of TBI described herein, particularly the neuronal proteins, are expected to meet these criteria for biomarker validation. In the meantime, these biomarkers may also find use in the laboratory setting. For example, β3-tubulin and GFAP are used to distinguish neuronal differentiation in stem cell research (Kornblum and Geschwind, 2001). Lastly, this work provides proof-of-principle for more rapid and comprehensive sequence-specific biomarker discovery strategies incorporating protein separation prior to capillary LC-MS^2.

ACKNOWLEDGMENTS

We thank Professor Steven Gygi (Harvard Medical), Dr. David Tabb (Oak Ridge National Laboratory), and Drs. Anu Waghray and Clair Ringger (University of Florida) for insightful discussion. This work was supported by DoD grants DAMD17-03-1-0066, DAMD17-01-1-0765, and DAMD17-99-1-9565; NIH grants R01 NS39091 and R01 NS40182.

REFERENCES

BANIK, N.L., McALHANEY, W.W., and HOGAN, E.L. (1985). Calcium-stimulated proteolysis in myelin: evidence for a Ca^{2+}-activated neutral proteinase associated with purified myelin of rat CNS. J Neurochem. **45,** 581–588.

BERGER, R.P., PIERCE, M.C., WISNIEWSKI, S.R., et al. (2002). Neuron-specific enolase and S100B in cerebrospinal fluid after severe traumatic brain injury in infants and children. Pediatrics **109,** E31.

BODOVITZ, S., and JOOS, T. (2004). The proteomics bottleneck: strategies for preliminary validation of potential biomarkers and drug targets. Trends Biotechnol. **22,** 4–7.

BRAMLETT, H.M. and DIETRICH, W.D. (2003). Synuclein aggregation: possible role in traumatic brain injury. Exp. Neurol. **184,** 27–30.

BUKI, A., OKONKWO, D.O., WANG, K.K.W., and POVLISHOCK, J.T. (2000). Cytochrome c release and caspase activation in traumatic axonal injury. J. Neurosci. **20,** 2825–2834.

DENSLOW, N., MICHEL, M.E., TEMPLE, M.D., HSU, C.Y., SAATMAN, K., and HAYES, R.L. (2003). Application of proteomics technology to the field of neurotrauma. J. Neurotrauma **20,** 401–407.

DIXON, C.E., CLIFTON, G.L., LIGHTHALL, J.W., YAGHAMAI, A.A., and HAYES, R.L. (1991). A controlled cortical impact model of traumatic brain injury in the rat. J. Neurosci. Methods **39,** 253–262.

DOMANSKA-JANIK, K., DE NECHAUD, B., INOMATA, M., KAWASHIMA, S., and ZALEWSKA, T. (1992). Calcium-activated neutral protease (CANP). in normal and dysmyelinating mutant paralytic tremor rabbit myelin. Mol. Chem. Neuropathol. **16,** 273–288.

FOUNTOULAKIS, M., SCHULLER, E., HARDMEIER, R., BERNDT, P., and LUBEC, G. (1999a). Rat brain proteins: two-dimensional protein database and variations in the expression level. Electrophoresis **20,** 3572–3579.

FOUNTOULAKIS, M., SCHULLER, E., HARDMEIER, R., BERNDT, P. and, LUBEC, G. (1999b). Rat brain proteins: two-dimensional protein database and variations in the expression level. Electrophoresis **20,** 3572–3579.

FRANZ, G., BEER, R., KAMPFL, A., et al. (2003). Amyloid beta 1–42, and tau in cerebrospinal fluid after severe traumatic brain injury. Neurology **60,** 1457–1461.

GERBER, S.A., RUSH, J., STEMMAN, O., KIRSCHNER, M.W., and GYGI, S.P. (2003). Absolute quantification of proteins and phosphoproteins from cell lysates by tandem MS. Proc. Natl. Acad. Sc.i USA **100,** 6940–6945.

GHARBI, S., GAFFNEY, P., YANG, A., et al. (2002). Evaluation of two-dimensional differential gel electrophoresis for proteomic expression analysis of a model breast cancer cell system. Mol. Cell. Proteomics **1,** 91–98.

GYGI, S.P., RIST, B., GERBER, S.A., TURECEK, F., GELB, M.H., and AEBERSOLD, R. (1999). Quantitative analysis of complex protein mixtures using isotope-coded affinity tags. Nat. Biotechnol. **17,** 994–999.

HASKINS, W.E., WANG, Z.Q., WATSON, C.J., et al. (2001). Capillary LC-MS^2 at the attomole level for monitoring and discovering endogenous peptides in microdialysis samples collected *in vivo*. Anal. Chem. **73,** 5005–5014.

HUH, J.W., RAGHUPATHI, R., LAURER, H.L., HELFAER, M.A., and SAATMAN, K.E. (2003). Transient loss of microtubule-associated protein 2 immunoreactivity after moderate brain injury in mice. J. Neurotrauma **20,** 975–984.

JENKINS, L.W., PETERS, G.W., DIXON, C.E., et al. (2002). Conventional and functional proteomics using large format two-dimensional gel electrophoresis 24 hours after controlled cortical impact in postnatal day 17 rats. J. Neurotrauma **19,** 715–740.

KERNEC, F., UNLU, M., LABEIKOVSKY, W., MINDEN, J.S., and KORETSKY, A.P. (2001). Changes in the mitochondrial proteome from mouse hearts deficient in creatine kinase. Physiol. Genomics **6,** 117–128.

KORNBLUM, H.I., and GESCHWIND, D.H. (2001). Molecular markers in CNS stem cell research: hitting a moving target. Nat. Rev. Neurosci. **2,** 843–846.

LEIMGRUBER, R.M., MALONE, J.P., RADABAUGH, M.R., LAPORTE, M.L., VIOLAND, B.N., and MONAHAN, J.B. (2002). Development of improved cell lysis, solubilization and imaging approaches for proteomic analyses. Proteomics **2,** 135–144.

MACDONALD, N., CHEVALIER, S., TONGE, R., et al. (2001). Quantitative proteomic analysis of mouse liver response to the peroxisome proliferator diethylhexylphthalate (DEHP). Arch. Toxicol. **75,** 415–424.

MATZILEVICH, D.A., RALL, J.M., MOORE, A.N., GRILL, R.J., and DASH, P.K. (2002). High-density microarray analysis of hippocampal gene expression following experimental brain injury. J. Neurosci. Res. **67,** 646–663.

McDONALD, W.H., and YATES, J.R. (2002). Shotgun proteomics and biomarker discovery. Dis. Markers **18,** 99–105.

NEWCOMB, J.K., KAMPFL, A., POSMANTUR, R.M., et al. (1997). Immunohistochemical study of calpain-mediated breakdown products to a-spectrin following controlled cortical impact injury in the rat. J. Neurotrauma **14,** 369–383.

NEWELL, K.L., BOYER, P., GOMEZ-TORTOSA, E., et al. (1999). Alpha-synuclein immunoreactivity is present in axonal swellings in neuroaxonal dystrophy and acute traumatic brain injury. J. Neuropathol. Exp. Neurol. **58,** 1263–1268.

PERKINS, D.N., PAPPIN, D.J., CREASY, D.M., and COTTRELL, J.S. (1999). Probability-based protein identification by searching sequence databases using mass spectrometry data. Electrophoresis **20,** 3551–3567.

PIKE, B.R., FLINT, J., DUTTA, S., WANG, D.S., WANG, K.K.W., and HAYES, R.L. (2002). Accumulation of spectrin and calpain-cleaved spectrin breakdown products in CSF after traumatic brain injury. J. Neurochem. **81,** 73.

POSMANTUR, R.M., KAMPFL, A., LIU, S.J., et al. (1996). Cytoskeletal derangements of cortical neuronal processes three hours after traumatic brain injury in rats: an immunofluorescence study. J. Neuropathol. Exp. Neurol. **55,** 68–80.

POSMANTUR, R., KAMPFL, A., SIMAN, R., et al. (1997). A calpain inhibitor attenuates cortical cytoskeletal protein loss after experimental traumatic brain injury in the rat. Neuroscience **77,** 875–888.

POSMANTUR, R.M., ZHAO, X., KAMPFL, A., CLIFTON, G.L., and HAYES, R.L. (1998). Immunoblot analyses of the relative contributions of cysteine and aspartic proteases to neurofilament breakdown products following experimental brain injury in rats. Neurochem. Res. **10,** 1265–1276.

PRUITT, K.D., and MAGLOTT, D.R. (2001). RefSeq and LocusLink: NCBI gene-centered resources. Nucleic Acids Res. **29,** 137–140.

RAABE, A., KOPETSCH, O., WOSZCZYK, A., et al. (2003). Serum S-100B protein as a molecular marker in severe traumatic brain injury. Restor. Neurol. Neurosci. **21,** 159–169.

SHAW, J., ROWLINSON, R., NICKSON, J., et al. (2003). Evaluation of saturation labeling two-dimensional difference gel electrophoresis fluorescent dyes. Proteomics **3,** 1181–1195.

SMITH, D.H., URYU, K., SAATMAN, K.E., TROJANOWSKI, J.Q., and McINTOSH, T.K. (2003). Protein accumulation in traumatic brain injury. Neuromol. Med. **4,** 59–72.

TABB, D.L., McDONALD, W.H., and YATES, J.R. (2002). DTASelect and contrast: tools for assembling and comparing protein identifications from shotgun proteomics. J. Proteome Res. **1,** 21–26.

TONGE, R., SHAW, J., MIDDLETON, B., et al. (2001). Validation and development of fluorescence two-dimensional differential gel electrophoresis proteomics technology. Proteomics **1,** 377–396.

URYU, K., GIASSON, B.I., LONGHI, L., et al. (2003). Age-dependent synuclein pathology following traumatic brain injury in mice. Exp. Neurol. **184,** 214–224.

VARMA, S., JANESKO, K.L., WISNIEWSKI, S.R., et al. (2003). F-2–isoprostane and neuron-specific enolase in cerebrospinal fluid after severe traumatic brain injury in infants and children. J. Neurotrauma **20,** 781–786.

YAN, J.X., DEVENISH, A.T., WAIT, R., STONE, T., LEWIS, S., and FOWLER, S. (2002). Fluorescence two-dimensional difference gel electrophoresis and mass spectrometry based proteomic analysis of *Escherichia coli*. Proteomics **2,** 1682–1698.

YATES, J.R., MORGAN, S.F., GATLIN, C.L., GRIFFIN, P.R., and ENG, J.K. (1998). Method to compare collision-induced dissociation spectra of peptides: potential for library searching and subtractive analysis. Anal. Chem. **70,** 3557–3565.

ZELMAN, F.P., JAUCH, E.C., MULCHAHEY, J.J., et al. (2002). C-tau biomarker of neuronal damage in severe brain-injured patients: association with elevated intracranial pressure and clinical outcome. Brain Res. **947,** 131–139.

Address reprint requests to:
Kevin K.W. Wang, Ph.D.
McKnight Brain Institute, L4-100F
University of Florida (P.O. Box 100256)
100 S. Newell Dr.
Gainesville, FL 32610

E-mail: kwang@psychiatry.ufl.edu

Journal of Neurochemistry, 2001, **78**, 862–873

Temporal and spatial profile of caspase 8 expression and proteolysis after experimental traumatic brain injury

Ronny Beer,* Gerhard Franz,* Stanislaw Krajewski,† Brian R. Pike,‡ Ronald L. Hayes,‡ John C. Reed,† Kevin K. Wang,§ Christian Klimmer,* Erich Schmutzhard,* Werner Poewe* and Andreas Kampfl*

**Department of Neurology, University Hospital Innsbruck, Austria*

†The Burnham Institute, La Jolla, California, USA

‡Center for Traumatic Brain Injury Studies, Department of Neuroscience, Evelyn F. and William L. McKnight Brain Institute of the University of Florida, Gainesville, Florida, USA

§Department of Neuroscience Therapeutics, Pfizer Inc., Ann Arbor, Michigan, USA

Abstract

Recent studies have demonstrated that the downstream caspases, such as caspase 3, act as executors of the apoptotic cascade after traumatic brain injury (TBI) *in vivo*. However, little is known about the involvement of caspases in the initiation phase of apoptosis, and the interaction between these initiator caspases (e.g. caspase 8) and executor caspases after experimental brain injuries *in vitro* and *in vivo*. This study investigated the temporal expression and cell subtype distribution of procaspase 8 and cleaved caspase 8 p20 from 1 h to 14 days after cortical impact-induced TBI in rats. Caspase 8 messenger RNA levels, estimated by semi-quantitaive RT-PCR, were elevated from 1 h to 72 h in the traumatized cortex. Western blotting revealed increased immunoreactivity for procaspase 8 and the proteolytically active subunit of caspase 8, p20, in the ipsilateral cortex from 6 to 72 h after injury, with a peak at 24 h after TBI. Similar to our previous studies, immunoreactivity for the p18 fragment of activated caspase 3 also increased in the current study from 6 to 72 h after TBI, but peaked at a later timepoint (48 h) as compared with proteolyzed caspase 8 p20. Immunohistologic examinations revealed increased expression of caspase 8 in neurons, astrocytes and oligodendrocytes. Assessment of DNA damage using TUNEL identified caspase 8- and caspase 3-immunopositive cells with apoptotic-like morphology in the cortex ipsilateral to the injury site, and immunohistochemical investigations of caspase 8 and activated caspase 3 revealed expression of both proteases in cortical layers 2–5 after TBI. Quantitative analysis revealed that the number of caspase 8 positive cells exceeds the number of caspase 3 expressing cells up to 24 h after impact injury. In contrast, no evidence of caspase 8 and caspase 3 activation was seen in the ipsilateral hippocampus, contralateral cortex and hippocampus up to 14 days after the impact. Our results provide the first evidence of caspase 8 activation after experimental TBI and suggest that this may occur in neurons, astrocytes and oligodendrocytes. Our findings also suggest a contributory role of caspase 8 activation to caspase 3 mediated apoptotic cell death after experimental TBI *in vivo*.

Keywords: apoptosis, astrocyte, caspase 8, neuron, oligodendrocyte, traumatic brain injury.

J. Neurochem. (2001) **78**, 862–873.

Traumatically evoked brain injury is a major cause of morbidity and mortality (Thurman *et al.* 1999). Studies over the last two decades have demonstrated that a significant amount of CNS damage after traumatic brain injury (TBI) occurs as a result of secondary autodestructive insults (Hayes *et al.* 1992; Faden 1996; McIntosh *et al.* 1998). Secondary injury involves a complex cascade of biochemical events that contributes to delayed tissue damage and cell death (Kermer *et al.* 1999; Graham *et al.* 2000). Importantly, recent research reported on a potential role for apoptosis in

Received April 25, 2001; revised manuscript received May 25, 2001; accepted May 28, 2001.

Address correspondence and reprint requests to Andreas Kampfl MD, Department of Neurology, University Hospital Innsbruck, Anichstrasse 35, A-6020 Innsbruck, Austria. E-mail: andreas.kampfl@uibk.ac.at

Abbreviations used: CNPase, 2′,3′-cyclic-nucleotide-3′-phosphodiesterase; FCS, fetal calf serum; GFAP, glial fibrillary acidic protein; NeuN, neuron specific nuclear protein (neuronal nuclei); PBS, phosphate buffered saline; TBI, traumatic brain injury; TBS, Tris-buffered saline; TUNEL, terminal deoxynucleotidyl transferase (TdT)-mediated deoxyuridine-biotin nick-end labeling.

cell degeneration after cerebral and spinal cord ischemia (Nitatori *et al.* 1995; Kato *et al.* 1997; Charriaut-Marlangue *et al.* 1998), traumatic spinal cord injury (Crowe *et al.* 1997; Liu *et al.* 1997), and TBI *in vitro* (Shah *et al.* 1997; Pike *et al.* 2000) and *in vivo* (Rink *et al.* 1995; Conti *et al.* 1998; Newcomb *et al.* 1999; Beer *et al.* 2000b).

Although a potential role for apoptosis in neuronal and glial cell damage after TBI has been suggested, little is known about the molecular mechanisms involved. However, recent evidence implicates a distinct class of proteases, referred to as caspases. So far, 14 mammalian caspases have been described (Nicholson 1999). Based on their proteolytic specifities, caspases further divide into three groups: the inflammatory caspases (e.g. caspase 1), which mediate cytokine maturation (Cerretti *et al.* 1992); the caspases involved in apoptotic cell death, which segregate into initiator enzymes, such as caspase 8 and caspase 9; executioner caspases, such as caspase 3 (Cohen 1997; Cryns and Yuan 1998). Caspases are synthesized as inactive pro-enzymes that contain three domains (Nicholson 1999), an N-terminal prodomain (approximately 3–24 kDa), a large subunit (approximately 17–21 kDa) and a small subunit (approximately 10–13 kDa). Depending on the cell type, procaspases have been shown to reside in various subcellular localizations (Qin *et al.* 2001; Shikama 2001) and are activated through proteolytic processing and association of the large and small subunits to form a catalytic heterotetramer (Walker *et al.* 1994).

Activation of the executioner caspase 3 has been shown in numerous chronic and acute disorders of the nervous system. For example, caspase 3 processing has been demonstrated in Alzheimer's (Stadelmann *et al.* 1999; Khan *et al.* 2000) and Parkinson's disease (Mogi *et al.* 2000). Further, caspase 3 mediated neuronal and glial cell degeneration has been found in experimental models of cerebral and spinal cord ischemia (Hayashi *et al.* 1998; Namura *et al.* 1998) and spinal cord injury (Springer *et al.* 1999). Importantly, recent data have also suggested a contributory role for activated caspase 3 in apoptotic degeneration of neurons, astrocytes and oligodendrocytes after TBI *in vivo* (Yakovlev *et al.* 1997; Beer *et al.* 2000b; Clark *et al.* 2000).

Current evidence also indicates that in receptor-triggered apoptosis the main pathway for caspase 3 activation is direct activation by caspase 8 (Scaffidi *et al.* 1998; Stennicke *et al.* 1998). Importantly, recent data suggest that receptor-mediated apoptosis indeed occurs in acute CNS injuries (Ertel *et al.* 1997; Felderhoff-Mueser *et al.* 2000). For example, increased expression of Fas and caspase 8 has been shown after experimental spinal cord ischemia (Matsushita *et al.* 2000). In addition, increased Fas and Fas ligand immunoreactivity (Beer *et al.* 2000a) and caspase 3 activation have been reported following TBI in the rat (Beer *et al.* 2000b; Clark *et al.* 2000), suggesting a putative link between the activation of caspase 8 and caspase 3 after TBI *in vivo*. However, to our knowledge no study to date has concurrently investigated changes in the expression and activity of both caspase 8 and caspase 3 in trauma-induced CNS degeneration.

To further investigate potential changes of caspase 8 and caspase 3 expression after experimental TBI, rodents were subjected to a widely used model of experimental brain injury: lateral cortical impact injury (Dixon *et al.* 1991; Franz *et al.* 1999; Beer *et al.* 2000a,b). The present study employed semiquantitative RT-PCR and western blot analyses of procaspase 8, cleaved caspase 8 p20, and processed caspase 3 to determine the relative temporal profile of caspase 8 to caspase 3 expression and activation from 1 h to 14 days after experimental TBI. Immunohistochemical examinations were performed to investigate the cell subtype distribution of caspase 8 after impact injury *in vivo*. Further, TUNEL was used to assess whether caspase 8 and caspase 3 immunopositive cells exhibit morphological features of DNA damage consistent with apoptotic phenotype after TBI in the rat.

Materials and methods

Rat model of traumatic brain injury

A controlled cortical impact device was used to induce a moderate level of TBI, as previously described (Dixon *et al.* 1991; Franz *et al.* 1999). In brief, adult male Sprague–Dawley rats (250–350 g) were intubated and anesthesized with 2% halothane in a 2 : 1 mixture of N_2O/O_2. Core body temperature was monitored continuously using a rectal thermistor probe and maintained at 36.5–37.5°C by a heating pad. Animals were mounted in a stereotaxic frame on the injury device in a prone position secured by ear and incisor bars. A midline incision was made, the soft tissues were reflected, and two 7-mm craniotomies were made adjacent to the central suture, midway between lambda and bregma. The dura was kept intact over the cortex. Injury was induced by impacting the right (ipsilateral) cortex with a 6-mm diameter aluminum tip at a rate of 4 m/s. The injury device was set to produce a tissue deformation of 2 mm. Impact velocity was measured directly by a linear variable differential transformer (Shaevitz Model 500 HR; Shaevitz, Detroit, MI, USA), which produces an analog signal that was recorded by a PC-based data acquisition system for analysis of time/displacement parameters of the impactor. This magnitude of injury has previously been associated with significant cell degeneration restricted to the contusion site (Franz *et al.* 1999; Beer *et al.* 2000a,b). After trauma, animals were extubated and immediately assessed for recovery of reflexes (Dixon *et al.* 1991). Sham-injured animals underwent identical surgical procedures but did not receive impact injury. Naive animals were not exposed to any injury-related surgical procedures. Ninety animals were used in this study (naive rats, $n = 10$; sham-injured rats, $n = 12$; injured rats, $n = 68$). Animal care and experimental protocols complied with the guidelines outlined in the *Guide for the Care and Use of Laboratory Animals*, Austrian Department of Health and Science, and were approved by the University of Innsbruck Medical School Animal

Table 1 Systemic parameters

	Prior to craniotomy ($n = 20$)	Post surgery	
		sham ($n = 4$)	injured ($n = 16$)
MABP (mmHg)	101 ± 5	97 ± 8	103 ± 6
pH	7.46 ± 0.01	7.43 ± 0.02	7.44 ± 0.02
PaO_2 (mmHg)	142 ± 4	79 ± 12	85 ± 9
$PaCO_2$ (mmHg)	43 ± 6	41 ± 3	42 ± 5
Rectal temperature (°C)	37.1 ± 0.2	37.3 ± 0.2	36.9 ± 0.1

Values are mean ± SD; MABP, mean arterial blood pressure.

Welfare Committee. Importantly, all efforts were made to minimize animal suffering and to reduce the number of animals used.

Assessment of physiologic parameters

In a subgroup of animals (sham-injured rats, $n = 4$; injured rats, $n = 16$) systemic parameters were monitored as described by Dixon *et al.* (1991). Briefly, a 22-gauge Teflon catheter was advanced into the abdominal aorta through a left femoral arteriotomy for arterial blood pressure measurement and arterial blood sampling. Blood samples (100 μL) were analyzed for pH, arterial oxygen pressure (PaO_2), and arterial pressure of carbon dioxide ($PaCO_2$), (Table 1) using an AVL Omni 4 (Diamond Diagnostics, Holliston, MA, USA) blood gas analyzer before craniotomy and 5 min after surgery. All parameters were within the normal physiological range (Table 1) (Krinke 2000).

Sample preparation

All animals were given a lethal dose of phenobarbital intraperitoneally (20 mg/kg; Tyrol Pharma, Kundl, Austria) and subsequently killed by decapitation 6 h, 24 h, 48 h, 72 h, 7 days and 14 days after TBI ($n = 4$ for each time after injury, $n = 4$ for naive and sham-injured animals). Both cortices and hippocampi (ipsilateral and contralateral to the injury site) were removed. Excision of both cortices beneath the craniotomies extended ~4-mm laterally, ~7-mm rostrocaudally, and to a depth extending to the white matter. All samples were immediately frozen in liquid nitrogen. The microdissected tissue was homogenized at 4°C in ice-cold homogenization buffer containing 20 mM piperazine-*N*,*N*′-bis(2-ethanesulfonic acid) (pH 7.1), 2 mM EGTA, 1 mM EDTA, 1 mM dithiothreitol, 0.3 mM phenylmethylsulfonylfluoride (PMSF), and 0.1 mM leupeptin. Chelators and protease inhibitors (Sigma, St Louis, MO, USA) were added to prevent endogenous *in vitro* activation of proteases and subsequent artifactual degradation of caspase 8 and caspase 3 during tissue processing.

Sodium dodecyl sulfate–polyacrylamide gel electrophoresis, immunoblotting and quantification

Protein concentrations were determined by bicinchoninic acid microprotein assay (Sigma) with albumin standards. Protein-balanced samples were prepared for polyacrylamide gel electrophoresis in two-fold loading buffer containing 0.25 M Tris (pH 6.8), 0.2 M dithiothreitol, 2% sodium dodecyl sulfate, 0.005% bromophenol blue and 5% glycerol in distilled water. Samples were heated for 5 min at 95°C. Sixty micrograms of protein per lane was routinely resolved on 16% Tris/glycine gels (Invitrogen, Groningen, the Netherlands). After separation, proteins were transferred to nitrocellulose membranes using western blotting with transfer buffer made up of 0.192 M glycine and 0.025 M Tris (pH 8.3). Coomassie blue (Bio-Rad, Hercules, CA, USA) and Ponceau red (Sigma) stainings were performed to confirm that equal amounts of protein were loaded in each lane. Five percent non-fat milk in phosphate buffered saline (PBS) with 0.05% Tween 20 was used to reduce non-specific binding. Immunoblots were probed with either a mouse monoclonal antibody (Santa Cruz Biotechnology, Santa Cruz, CA, USA), reacting with the p20 subunit and precursor of caspase 8, diluted 1 : 1000, or a rabbit polyclonal antiserum (CM1; IDUN Pharmaceuticals, La Jolla, CA, USA; dilution 1 : 5000), directed against the p18 subunit of activated caspase 3. Specifity and sensitivity of CM1 has been described in detail in previous investigations (Namura *et al.* 1998; Srinivasan *et al.* 1998; Beer *et al.* 2000b). After incubation with primary antibodies overnight at 4°C, nitrocellulose membranes (Amersham Pharmacia Biotech, Uppsala, Sweden) were incubated with secondary antibodies linked to horseradish peroxidase (Amersham Pharmacia Biotech) for 1 h at 20°C (automated climate control). Enhanced chemiluminescence reagents (Amersham Pharmacia Biotech) were used to visualize the immunolabeling on X-ray film. In each blot, the constitutively expressed protein α-tubulin (Sigma) was used as an internal standard to further indicate that sample processing was carried out correctly.

Semiquantitative RT-PCR

Total RNA was isolated from frozen ipsilateral and contralateral cortex and hippocampus of naive ($n = 2$), sham-injured ($n = 4$), and injured animals (1 h, 6 h, 24 h, 48 h and 72 h; $n = 4$ for each time point after injury) with Trizol reagent (Life Technologies, Rockville, MD, USA). Ten micrograms of total RNA was treated with 1 U of amplification grade DNase I (Life Technologies) to eliminate residual genomic DNA and was reverse transcribed into first-strand cDNA using Superscript II reverse transcriptase (Life Technologies) with oligo(dT) as primer. The resulting cDNAs were diluted to 100 μL and subjected to PCR analysis. Each PCR mixture contained equal amounts of diluted cDNA corresponding to 200 ng of total RNA, 100 pM of each primer, 10 pM dNTPs, onefold Ampli-Taq reaction buffer and 2.5 U Ampli-Taq-Gold DNA polymerase (PE Biosystems, Foster City, CA, USA). All cDNAs were amplified with primers specific for the housekeeping

gene glyceraldehyde-3-phosphate dehydrogenase (GAPDH; GenBank Acc. No. X02231; 5′-CCCACGGCAAGTTCAACGG-3′ and 5′-CTTTCCAGAGGGGCCATCCA), and caspase 8 (GenBank Acc. No. AF279308; 5′-ACTGGCTGCCCTCAAGTTCCTGTGC-3′ and 5′-TCCCTCACCATTTCCTCTGGGCTGC-3′). PCR amplification was carried out for 34 cycles of 45 s at 94°C, 45 s at 60°C, and 45 s at 72°C, followed by a final step of 10 min at 72°C in the UNO II Thermocycler (Biometra, Göttingen, Germany). The number of cycles and reaction temperature conditions were optimized to provide a linear relationship between the quantity of input template and the quantity of PCR product. PCR products were analyzed by agarose gel electrophoresis in 2% NuSieve agarose gels (FMC BioProducts, Rockland, ME, USA) and visualized by ethidium-bromide staining. The identity of the PCR products obtained was confirmed by Southern blot analysis using an internal oligonucleotide as hybridization probe.

Immunohistochemistry

Prior to perfusion, animals from all treatment groups were given a lethal injection of phenobarbital (20 mg/kg intraperitoneally). Rats were transcardially perfused through the left ventricle (120 mL of 0.9% saline and 200 mL of 4% paraformaldehyde) at 6 h, 24 h, 48 h, 72 h, 7 days and 14 days after TBI ($n = 4$ for each time point after injury; $n = 4$ for sham-injured and naive animals). The brains were removed, grossly sectioned coronally at 2-mm intervals, processed through graded alcohols and xylene substitute (Histoclear; National Diagnostics, Atlanta, GA, USA), and routinely embedded in paraffin. Sections were cut at 3–4 μm on a rotary microtome, mounted on aminoalkylsilated glass slides, and processed for immunohistochemistry as follows: deparaffinized and rehydrated sections were microwaved in 10 mM sodium citrate buffer, pH 6.0, and allowed to cool to room temperature. Endogenous peroxidase was blocked by treatment with 0.3% H_2O_2 in methanol followed by incubation with 10% fetal calf serum (FCS) in Tris-buffered saline (TBS) for 60 min. Rabbit polyclonal antibodies against caspase 8 (The Burnham Institute, La Jolla, CA, USA) and caspase 3 p18 (IDUN Pharmaceuticals) were diluted 1 : 5000 in 10% FCS and permitted to bind overnight at 4°C.

Rabbit antiserum against caspase 8 was generated as previously described (Krajewska *et al.* 1997) using recombinant catalytic C-terminal fragment of human caspase 8 protein using construct pET15b MGS H_6-Ser216-TAA. This protein was expressed in BL 21 (DE3) cells by induction with 1 mM IPTG. After cell growth and lysis, the clarified cell lysate was applied to an Ni-NTA column and eluted with an imidazole gradient. The pooled caspase 8 fractions were dialyzed against 50 mM Tris at pH 8.8 and applied to a FPLC Mono Q HR 10/10 column (Amersham Pharmacia Biotech) and eluted with an NaCl gradient. New Zealand white female rabbits were injected subcutaneously with a mixture of recombinant protein (0.1–0.15 mg protein per immunization) and 0.5 mL Freund's complete adjuvant with the dose divided over 10 injection sites, and then boosted three times at weekly intervals followed by another 3–20 boostings at monthly intervals with 0.15 mg each of recombinant protein immunogen in Freund's incomplete adjuvant. Antiserum specificity was confirmed by pre-absorption with full-length or fully cleaved caspase 8 protein, respectively. This polyclonal antibody reacts with the unprocessed zymogen form of caspase 8 and detects the processed large subunit (p20) of active caspase 8. In addition, specificity of the caspase 8 antiserum has been described recently (Stoka *et al.* 2001).

Biotinylated goat anti-rabbit (Vector Laboratories, Burlingame, CA, USA) was then applied at a dilution of 1 : 200 in 3% rat serum in TBS for 1 h at room temperature followed by avidin-peroxidase (Sigma), diluted 1 : 100 in TBS, also for 1 h at room temperature. The reaction was visualized by treatment with 0.05% 3,3′-diaminobenzidine tetrahydrochloride solution in TBS containing 0.05% H_2O_2. The color reaction was stopped with several washes of TBS. Immunostaining results were confirmed by the use of pre-immune serum from the same animals and by pre-absorption of the polyclonal antibodies with the relevant protein.

For double immunostaining using brightfield chromagens, sections were pretreated with the rabbit polyclonal antiserum against caspase 8 as described above. Sections were then incubated with a mouse anti-neuron-specific nuclear protein (NeuN) antibody (Wolf *et al.* 1996) (Chemicon, Temecula, CA, USA) for neuronal staining. For staining of astrocytes, oligodendrocytes and microglia, a mouse anti-GFAP (Debus *et al.* 1983) (Roche Molecular Biochemicals, Mannheim, Germany), a mouse anti-CNPase (Sprinkle 1989) (Sternberger Monoclonals Inc., Lutherville, MD, USA) and an anti-ED1 monoclonal antibody (Graeber *et al.* 1990) (Serotec, Kidlington, Oxford, UK) were used. All antibodies were diluted 1 : 500 in 10% FCS in TBS and allowed to bind overnight at 4°C. After being rinsed, sections were incubated with a biotinylated horse anti-mouse antibody (Vector Laboratories) at a dilution of 1 : 200 for 1 h at room temperature followed by incubation with an alkaline phosphatase avidin-biotin substrate and then reaction with blue chromagen (Vector Blue; Vector Laboratories). Sections were dehydrated through graded ethanol, cleared in a xylene substitute (Histoclear; National Diagnostics, Atlanta, GA, USA), mounted in Permount (Fisher Scientific, Nepean, Ontario, Canada) and coverslipped. Sections without primary antibodies were similarly processed to control for binding of the secondary antibodies. On control sections no specific immunoreactivity was detected.

Histochemical detection of DNA fragmentation (terminal deoxynucleotidyl transferase-mediated deoxyuridine-biotin nick end labeling)

To confirm the presence of cell degeneration by an apoptotic mechanism, terminal deoxynucleotidyl transferase-mediated deoxyuridine-biotin nick end labeling (TUNEL) was performed as described by Gavrieli *et al.* (1992) with minor modifications. Briefly, for double-label experiments, dewaxed and rehydrated sections of all animal groups from regions between −1.5 and −3.4 mm bregma were stained with primary and secondary antisera as described earlier. Immunohistochemical staining was visualized by exposure to 3-amino-9-ethylcarbazole in *N,N′*-dimethylformamide (Sigma). Sections were then rinsed thoroughly and incubated with labeling mix (TdT buffer containing 100 U/mL TdT and 20 nM/mL biotin-conjugated 16 deoxyuridine) in a humidified chamber for 60 min at 37°C. After three washes in TBS, slides were incubated in Converter alkaline phosphatase for 15 min in a humidified chamber at 37°C. All reagents were purchased from Roche Molecular Biochemicals. The reaction was visualized by treatment for 3 min with 5-bromo-4-chloro-3-indolyl phosphate/nitro blue tetrazolium substrate system (Dako Corporation, Carpinteria, CA, USA). Primary antibody, labeling mix or

secondary antibody were omitted in control sections. Sections were mounted using an aqueous mounting fluid (Dako Corporation) and examined under the light microscope.

Statistical analysis

Semiquantitative evaluation of RT-PCR band density and of immunoreactivity detected by western blotting was performed using computer-assisted two-dimensional densitometric scanning with a MacIntosh computer using the public domain NIH IMAGE program (developed at the US National Institutes of Health and available on the internet at http://rsb.info.nih.gov/nih-image/). Relative band densities on RT-PCR and western blots ($n = 1$/blot) were expressed as arbitrary densitometric units for each time point. This procedure was performed for the data of four independent experiments for a total of four different animals per time point. Data acquired in arbitrary densitometric units were transformed to percentages of the densitometric levels observed for scans from sham animals on the same agarose gel (for RT-PCR analysis) and same blot. Group differences were determined by ANOVA and Tukey's *post hoc* honestly significant difference (HSD) test. Values given are means ± SD of four independent experiments. Differences were considered significant when $p \leq 0.05$. For quantitative analysis of immunohistochemistry, the numbers of caspase 8 and caspase 3 positive cells of three non-consecutive sections (each separated by at least 50 μm) of four different animals for each time point were counted by an independent observer in the entire anatomic regions of the cortex from the primary injury zone at bregma − 3.4 mm ± 0.2 mm (Paxinos and Watson 1997) using light microscopy at a magnification of 100×. The total number of caspase 8- and caspase 3-immunopositive cells was obtained for each section. Further, the numbers of cells labeled with anti-caspase 8 antibody and NeuN, GFAP and CNPase were counted on sections (three sections per animal) processed for double-label immunohistochemistry. Values for each animal (four animals per time point) were averaged to calculate the mean number of immunopositive cells per time point (6–72 h after TBI). Cell counts (caspase 8 vs. caspase 3 and double-labeled neurons vs. double-labeled glia) were analyzed with ANOVA and Bonferroni's *post hoc* analysis for selected pairs of columns. Values given are means ± SD of four different animals. Differences were considered significant when $p \leq 0.05$.

Results

Caspase 8 messenger RNA levels increase after TBI

Caspase 8 messenger RNA was detected by semiquantitative RT-PCR analysis in cortical and hippocampal samples (not shown) of sham and injured animals, respectively (Fig. 1). Cortical impact injury resulted in an increase of caspase 8 messenger RNA levels in the ipsilateral cortex (Fig. 1). Starting at 1 h after injury, a significant increase in caspase 8 messenger RNA levels was observed. Rising rapidly, band intensity reached a maximum level by 6 h after the trauma (386% increase relative to sham animals) and remained thereafter at a steady-state level (332% increase relative to sham animals) at 24 h after TBI. Caspase 8 messenger RNA levels then declined thereafter to a level of approximately

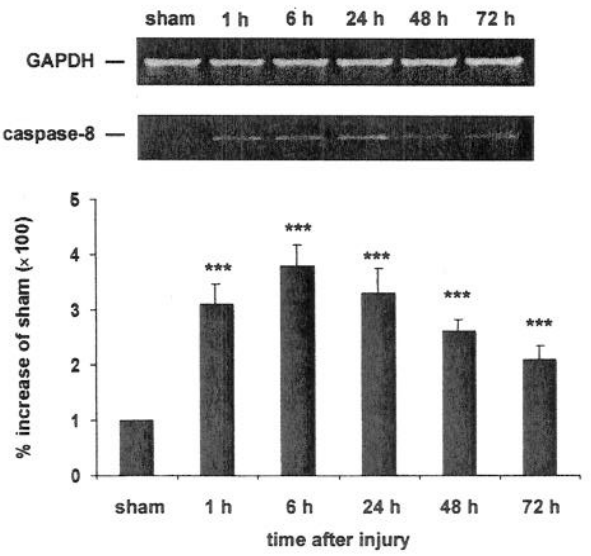

Fig. 1 RT-PCR analysis of caspase 8 mRNA in the ipsilateral cortex following TBI. Cortical samples of single control animals (sham) and single injured animals were prepared for RT-PCR at the indicated times after TBI *in vivo*. Values are presented as percentages of the densitometric levels observed on scans from sham animals visualized on the same agarose gel. Data are mean ± SD values of four independent experiments. Levels of caspase 8 mRNA increased within 1 h after TBI as compared with controls. Levels of caspase 8 mRNA peaked at 6 h after TBI and remained elevated as late as 72 h after the injury. ***$p < 0.001$.

two-fold (220% increase relative to sham animals) above controls at 72 h after the impact. No statistically significant increases in caspase 8 messenger RNA levels were observed in cortical samples contralateral to the injury site and hippocampal samples ipsi- and contralateral to the injury site from 1 h to 72 h after the impact (data not shown).

Proteolytic processing of caspase 8 and caspase 3 occurs after TBI

To determine whether caspase 8 and caspase 3 are activated after TBI, brain extracts from cortex and hippocampus ipsi- and contralateral to the injury site were examined for the expression of the p55 subunit (procaspase 8), the p20 subunit (processed caspase 8) and of the p18 subunit (cleaved caspase 3) by western blotting. Cortical impact injury resulted in an increase of p55 and p20 caspase 8 immunoreactivity in the ipsilateral cortex (Fig. 2a). The p55 and p20 caspase 8 immunoreactivity increased within 6 h after TBI and peaked at 24 h after the impact (376% increase relative to sham animals for p55, and 653% increase as compared with sham animals for p20, respectively), declining thereafter. After 7 and 14 days, no significant increases were evident in the p55 and p20 fragments when compared with levels in sham-injured control animals. Similar to a previous study (Beer *et al.*

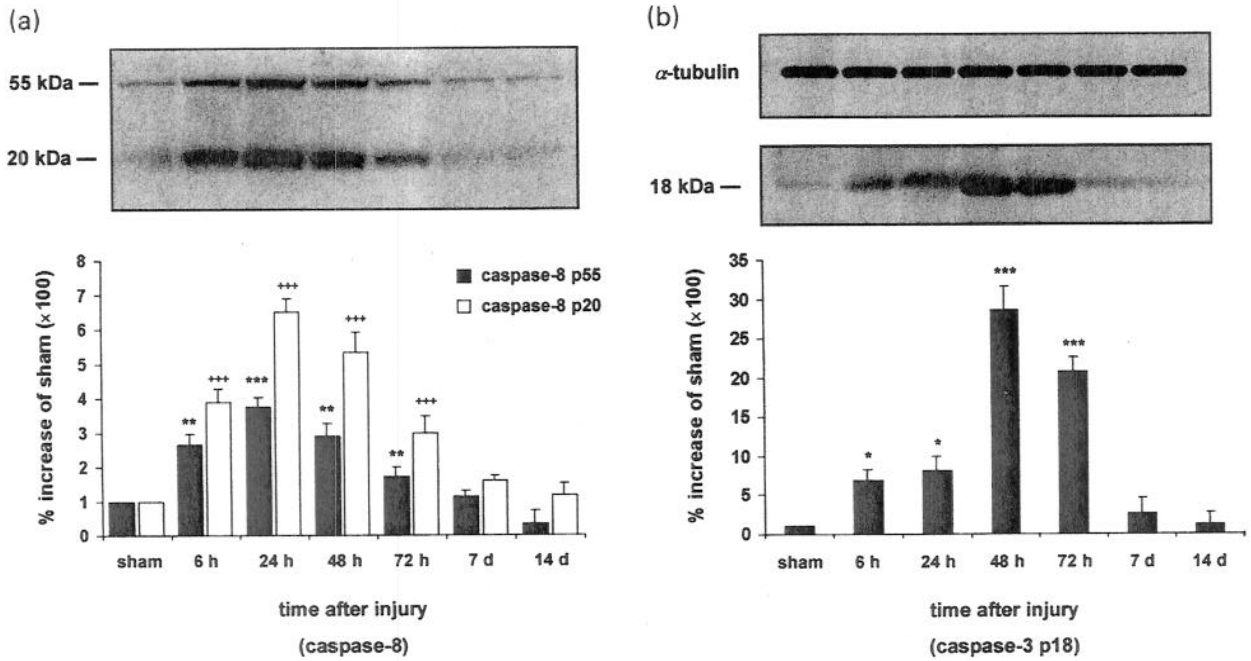

Fig. 2 Time-course of caspase 8 (a) and caspase 3 p18 (b) protein expression after TBI. Samples from single control (sham) and single injured animals were prepared for western blotting between 6 h and 14 days after TBI. Levels of protein are expressed as arbitrary densitometric units. Data were transformed to percentages of the densitometric levels observed on scans from sham animals visualized on the same blot. Values given are mean ± SD of four independent experiments. (a) Ipsilateral cortex: immunoblots demonstrated that procaspase 8 (p55) is constitutively expressed in sham-injured brains. Following TBI, immunoreactivity of p55 (filled bars) (**$p < 0.01$) and p20 (processed caspase 8; open bars) ($^{+++}p < 0.001$) increased significantly at 6 h after TBI and peaked at 24 h post injury. Immunoreactivity of p55 (*$p < 0.05$) and p20 ($^{+++}p < 0.001$) was still significantly increased up to 72 h post trauma. (b) Ipsilateral cortex: the proteolytically active p18 fragment of caspase 3 increased significantly within 6 h after TBI (*$p < 0.05$). p18 immunoreactivity peaked at 48 h after TBI (***$p < 0.001$) and was still significantly elevated at 72 h after impact injury (***$p < 0.001$). α-tubulin was used as an internal standard.

2000b), immunoreactivity for activated caspase 3 (p18) increased within 6 h after TBI in the traumatized cortex (Fig. 2b). However, the maximal increase of p18 immunoreactivity was seen at later times (48 h after TBI; 2850% increase relative to sham animals), when compared with caspase 8 p20. Caspase 3 p18 immunoreactivity then declined to a 2060% increase relative to sham at 72 h after TBI. Similar to proteolyzed caspase 8, no statistically significant differences in caspase 3 p18 immunoreactivity were observed between cortical samples ipsilateral to the injury site at 7 and 14 days after TBI and in cortical samples from sham-injured animals. In addition, no significant increases in p55, p20 and p18 immunoreactivity were seen between sham and injured animals in cortical samples contralateral to the injury site and hippocampal samples ipsi- and contralateral to the injury site between 6 h and 14 days after TBI (data not shown).

Caspase 8 is expressed in traumatized cortical neurons, astrocytes and oligodendrocytes

Ipsilateral and contralateral cortical and hippocampal tissues were examined rostrocaudally from + 0.2 to − 3.8 mm bregma. No caspase 8 immunoreactivity was present in the tissue from sham-injured (Fig. 3a) or naive (data not shown) control rats. Positive immunoreactivity for caspase 8 was found throughout the ipsilateral cortex at the primary injury zone (from − 1.5 to − 3.4 mm bregma) from 6 h to 72 h after the trauma (Figs 3b and c; time point = 24 h after TBI; − 3.4 mm bregma). To further investigate if caspase 8 is expressed in glial and/or neuronal cells, we performed double-labeling experiments for caspase 8 using the neuronal cell specific marker NeuN, the astrocytic marker GFAP, the microglial marker ED-1, and the oligodendroglial marker CNPase. These immunohistochemical analyses of caspase 8-positive cells from 6 to 72 h after TBI (Figs 3i–k; time point = 24 h after trauma; − 3.4 mm bregma) identified labeling with NeuN, GFAP and CNPase, and demonstrated the expression of caspase 8 in cortical neurons (Fig. 3i), astrocytes (Fig. 3j) and oligodendrocytes (Fig. 3k), respectively. Interestingly, immunoreactivity for caspase 8 was observed to be mainly cytosolic in neurons (Figs 3g and i), but appeared rather nuclear in astrocytes (Fig. 3j) and oligodendrocytes (Fig. 3k). No caspase 8 immunoreactivity was detected in microglial cells.

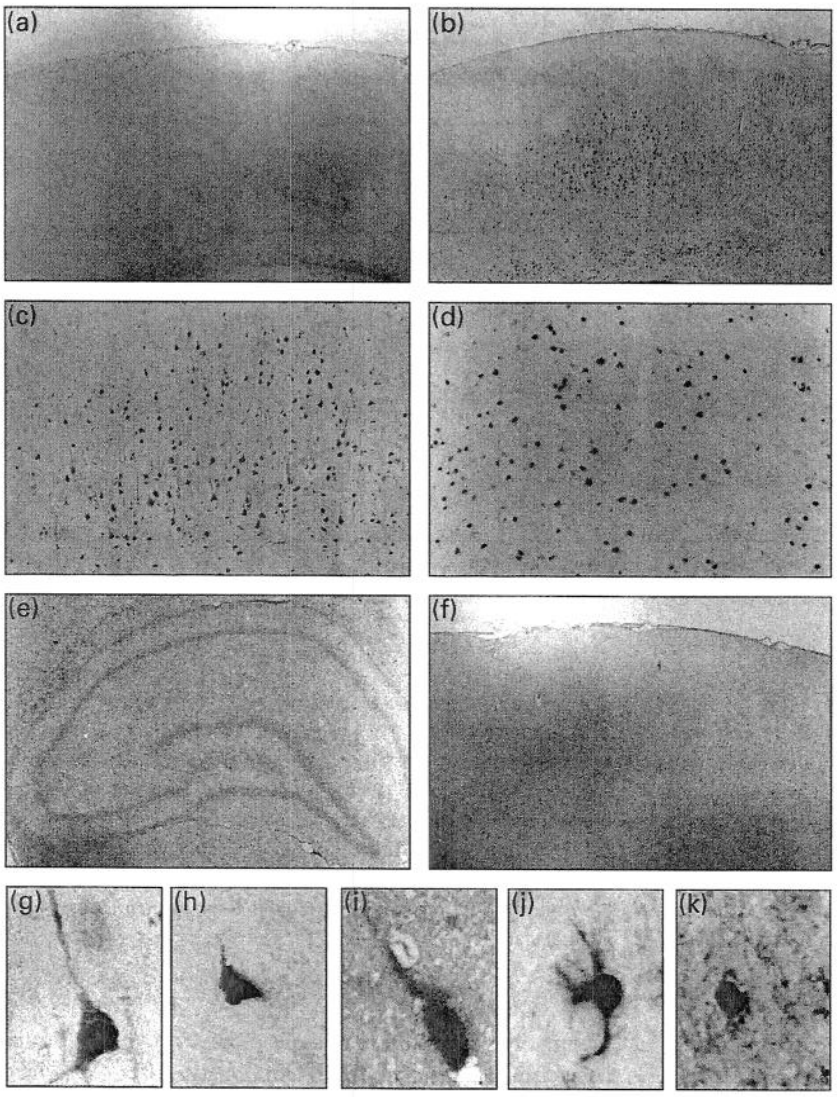

Fig. 3 Cell subtype distribution of caspase 8 in the traumatized cortex (− 3.4 mm bregma) at 24 h after TBI. Sham injured brains showed no specific caspase 8 immunolabeling (a). Low (b), intermediate (c) and high magnification (g) photomicrographs revealed specific caspase 8 expression in the ipsilateral cortex following cortical impact injury. Cells immunopositive for activated caspase 3 are found within similar brain regions (d and h). Double immunostaining experiments with caspase 8 (brown color; i, j and k) and NeuN (blue color; i), GFAP (blue color; j), and CNPase (blue color; k) provided evidence that caspase 8 is expressed in cortical neurons (i), astrocytes (j), and oligodendrocytes (k) after TBI. Magnifications: (a) and (b), 40×; (c) and (d), 100×; (e), 20×; (f), 40×; (g–k), 1000×.

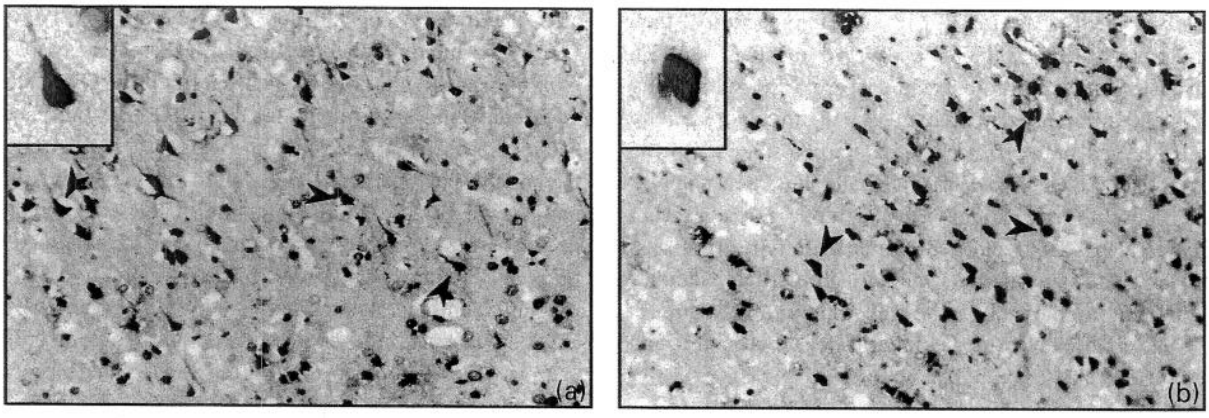

Fig. 4 Appearance of caspase 8 and processed caspase 3 p18 in TUNEL-positive cells. Combined immunohistochemistry for caspase 8 (red color; a) and TUNEL (dark blue color; a) (24 h after TBI) and caspase 3 p18 (red color; b) and TUNEL (dark blue; b) (48 h after TBI) demonstrated caspase 8 (a) and activated caspase 3 (b) in cells with gross nuclear apoptotic-like morphology. TUNEL-positive cells exhibited chromatin condensation and nuclear fragmentation (arrows). Magnifications: (a) and (b), 200×; inserts, 1000×.

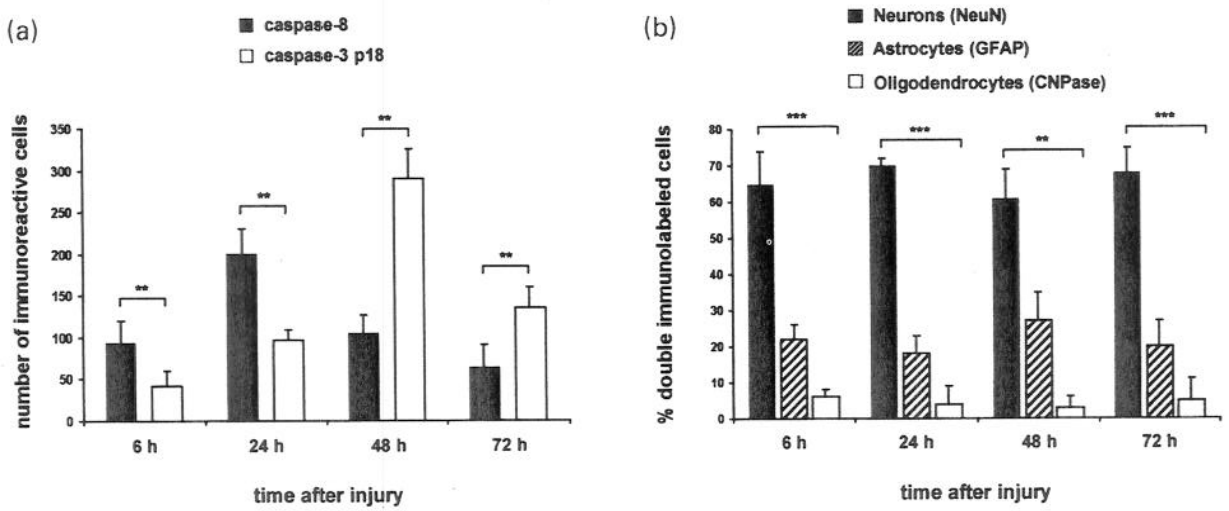

Fig. 5 Quantification of caspase 8 and caspase 3 p18 positive cells in the ipsilateral cortex after TBI (a) and quantification of caspase 8 cell subtype staining (b). Cells were counted in the entire anatomic regions of the cortex at the primary injury zone (bregma − 3.4 mm). (a) The number of caspase 8 positive cells (filled bars) was significantly greater than that of caspase 3 p18 positive cells (open bars) before 48 h after TBI. (b) Quantitative analysis was conducted of caspase 8 and NeuN (filled bars), caspase 8 and GFAP (hatched bars), and caspase 8 and CNPase (open bars) immunopositive cells. Columns indicate double-labeled neurons (filled bars), double-labeled astrocytes (hatched bars), and double-labeled oligodendrocytes (open bars) as percentages of caspase 8-positive cells from 6 to 72 h after TBI. Cell counts of caspase 8-positive neurons were significantly higher as compared with caspase 8-positive glia (i.e. astrocytes and oligodendrocytes at 6, 24, 48 and 72 h after TBI, respectively). Cell counts were evaluated by ANOVA with Bonferroni's *post hoc* analysis (**$p < 0.01$, ***$p < 0.001$). Values given are mean ± SD of four different animals per time point.

Caspase 8 immunoreactivity was absent in ipsilateral hippocampal samples (Fig. 3e) and contralateral samples of cortex (Fig. 3f) and hippocampus (data not shown) at all times investigated.

Caspase 8- and caspase 3-immunopositive cells exhibit nuclear apoptotic-like morphology

To verify further an apoptotic component of post-traumatic cell death and to support the possibility that caspase 8 and caspase 3 are associated with trauma-induced apoptosis, sections immunopositive for caspase 8 and caspase 3 p18 were stained with TUNEL to assess DNA damage. Double-labeling experiments demonstrated that a substantial proportion of TUNEL positive cells with shrunken morphology, condensed nuclei and chromatin margination also expressed caspase 8 (Fig. 4a) and activated caspase 3 (Fig. 4b) in layers 2–5 of the injured parietal cortex after TBI. However, cells with either caspase 8 or activated caspase 3 reactivity or gross apoptotic-like morphology alone were also detected.

Quantification of caspase 8- and caspase 3-positive cells and caspase 8 cell subtype staining after TBI

Activated caspase 3 was detected in the ipsilateral traumatized cortex from 6 to 72 h after impact injury. Similar to our findings for caspase 8, p18 positive cells were seen within cortical layers 2–5 at the primary impact zone (Fig. 3d) (Beer *et al.* 2000b). In contrast to caspase 8, the intracellular localization of activated caspase 3 was predominantly nuclear (Fig. 3h). Quantitative analysis of caspase 8- and p18-positive cells revealed that the number of caspase 8- and p18-labeled cells increased up to 24 and 48 h after trauma, respectively, with the number of caspase 8-positive cells being significantly higher until 24 h after TBI (Fig. 5a).

Quantification of caspase 8 and NeuN, GFAP and CNPase revealed that the number of caspase 8-positive neurons is significantly higher as compared with glia (i.e. astrocytes and mature oligodendrocytes) from 6 to 72 h after injury, respectively (Fig. 5b).

Discussion

Our results provide the first evidence for caspase 8 expression and processing after experimental TBI. Proteolyzed caspase 8 appeared in samples of the traumatized cortex from 6 to 72 h after impact injury. Furthermore, double labeling experiments revealed expression of caspase 8 in neurons, astrocytes and oligodendrocytes after experimental brain injury. Moreover, our data indicate that expression of caspase 8 and cleaved caspase 3 p18 is associated with apoptotic-like cell death phenotypes detected in TUNEL-positive cells. Finally, our results suggest that caspase 8 may at least in part contribute to caspase 3-mediated cell death after experimental TBI in the rat.

Reverse transcription PCR and western blotting data revealed increased expression of caspase 8 messenger RNA and increased immunoreactivity for procaspase 8 and caspase 8 p20 in the ipsilateral cortex from 1 h to 72 h after the impact. Similar to our results, current data also suggest that caspase 8 messenger RNA, procaspase 8 and activated caspase 8 are over-expressed at early time points after experimental spinal cord ischemia (Matsushita *et al.* 2000) and focal cerebral ischemia (Harrison *et al.* 2001) in the mouse. Moreover, increased expression of proteolyzed caspase 8 has also been described after experimental focal ischemia in the rat up to 48 h after the insult (Velier *et al.* 1999). In this regard, it is noteworthy that cortical impact injury may produce focal ischemia in the cortex ipsilateral to the injury site (Bryan *et al.* 1995). Thus, reduced cerebral blood flow may have also contributed to activation of caspase 8 in our experiments. Taken together, these data demonstrate that caspase 8 is up-regulated and activated as an early event after various acute CNS injuries *in vivo*.

Previous reports on the cell subtype distribution have found increased immunoreactivity for caspase 8 in neurons after focal ischemia in the rat (Velier *et al.* 1999). In addition, recent data provided evidence that caspase 8 is also over-expressed in neurons following experimental spinal cord ischemia in the mouse (Matsushita *et al.* 2000) and in oligodendrocytes undergoing staurosporine-induced apoptosis *in vitro* (Gu *et al.* 1999). These findings indicate that whereas caspase 8 has been reported only to be weakly expressed in normal brain parenchyma (Velier *et al.* 1999), the brain readily over-expresses caspase 8 after a variety of pathological stimuli. Our immunohistochemical results, however, are the first to show that caspase 8 is over-expressed in neurons, astrocytes and oligodendrocytes after experimental brain injury *in vivo*. Moreover, our findings suggest that caspase 8 expression is mainly cytosolic in neurons, but has a rather nuclear distribution in astrocytes and oligodendrocytes after TBI *in vivo*. In this regard it is noteworthy that caspase 8 can be expressed in both the nuclear and cytosolic compartment (Xerri *et al.* 2000). Therefore, future studies are needed to further investigate the significance of caspase 8 expression in different subcellular compartments of CNS cells after experimental brain injuries *in vivo*.

The exact mechanisms leading to the activation of caspase 8 after CNS injuries have yet not been determined. Recent data suggest that caspase 8 may be activated by receptor-mediated mechanisms including the tumor necrosis factor receptor type-1 (TNF-R1) (Schulze-Osthoff *et al.* 1998) and Fas signaling pathways (Muzio *et al.* 1996; Medema *et al.* 1997). For example, it has been reported that over-expression of α-TNF and Fas ligand may induce apoptosis after experimental cerebral ischemia and brain trauma *in vivo* (Kokaia *et al.* 1998; Shohami *et al.* 1996; Martin-Villalba *et al.* 1999). Moreover, increased Fas expression has been implicated in glutamate-induced apoptotic cell death of CNS neurons *in vitro* (Li *et al.* 1998). Importantly, excessive excitatory amino acid release with subsequent neurotoxicity also has been described after TBI *in vivo* (for review see Globus *et al.* 1995). Finally, recent data by Beer *et al.* (2000a) indicate that the Fas/Fas ligand system is also up-regulated in similar brain regions and at similar times after TBI as caspase 8 expression seen in our study (cortical layers 2–5, and 15 min to 72 h after impact injury, respectively). Taken together, these results suggest that excitatory amino acids and the Fas/Fas ligand system may indeed participate in activation of caspase 8 after TBI. In this regard, it is noteworthy that coexpression of Fas and caspase 8 has been observed in spinal cord neurons after experimental spinal cord ischemia *in vivo* (Matsushita *et al.* 2000).

Recent data suggest that cell loss induced by traumatic spinal cord injury and TBI may be attributed in part to apoptotic mechanisms (for a review see Beattie *et al.* 2000; Raghupathi *et al.* 2000). Moreover, several *in vivo* and *in vitro* studies have documented the significance of caspases in apoptotic cell degeneration following acute CNS injuries (for reviews see Eldadah and Faden 2000; Mattson *et al.* 2000). In addition, it has also been reported that caspase 3 is activated after experimental cerebral ischemia (Namura *et al.* 1998; Velier *et al.* 1999), fluid percussion (Yakovlev *et al.* 1997), and cortical impact models of TBI (Beer *et al.* 2000b; Clark *et al.* 2000). Our western blotting data also indicate that caspase 3 is activated after TBI, and our double-labeling immunohistochemical studies using TUNEL and p18 antiserum demonstrated caspase 3-positive cells with gross DNA damage in the traumatized cortex, suggesting a mechanistic link between caspase 3 activation and apoptosis.

Recent evidence from *in vitro* studies suggests that caspase 3 can be activated directly by caspase 8 (Stennicke *et al.* 1998). However, coexpression of caspase 8 and activated caspase 3 after various CNS injuries *in vivo* has not been studied extensively. One recent report indicated that caspase 8 and activated caspase 3 are coexpressed within CNS cells after experimental spinal cord ischemia up to 24 h after the insult (Matsushita *et al.* 2000). Our present findings provide further evidence of expression of both, caspase 8 and activated caspase 3 in multiple cortical CNS cell populations after TBI *in vivo*. Importantly, the expression of caspase 8 and activated caspase 3 in similar cortical brain regions suggests that caspase 8 may participate in caspase 3 activation in cortical CNS cells after TBI. Moreover, the greater number of caspase 8 positive cells (compared with caspase 3 immunoreactive cells) at early time points (6 and 24 h post trauma) followed by a greater number of caspase 3 positive cells (compared with caspase 8 positive cells) at later time points (48 h and 72 h post trauma) supports the hypothesis that caspase 8 may indeed be upstream of caspase 3. However, it was of interest that

caspase 8 immunoreactivity is found also in cells with evidence of DNA damage as indicated by TUNEL. In this regard it is noteworthy that caspase 8 may also function as an amplifying executioner caspase in drug-induced apoptosis *in vitro* (Engels *et al.* 2000). Therefore, future studies have to investigate the exact role of caspase 8 in the activation and/or execution phase of the apoptotic cascade after acute CNS injuries *in vivo*. This also implicates the need for further investigations on the significance of caspase 8 independent activation of caspase 3, including the mitochondrial pathway (Eldadah and Faden 2000).

Our study failed to detect increased expression of caspase 8, activated caspase 3 and apoptotic CNS morphology in the hippocampus ipsilateral to the injury site from 6 h to 14 days after the trauma. This is in contrast to previous reports, which clearly describe features of apoptotic neuronal degeneration in the hippocampus following fluid percussion injury (Yakovlev *et al.* 1997; Conti *et al.* 1998) and cortical impact injury (Clark *et al.* 2000; Colicos and Dash 1996). However, previous studies from our laboratory (Franz *et al.* 1999; Beer *et al.* 2000a,b) have shown that cortical impact injury may not necessarily be associated with hippocampal neuronal degeneration. Probable reasons for discrepancies in the appearance of hippocampal damage may be subtle methodological differences in animal models of TBI. For example, differences in angulation and velocity of the impact devices could account for the presence or absence of hippocampal cell degeneration.

In conclusion, our results provide evidence for induction of caspase 8 expression in cortical neurons and glial cells after TBI *in vivo*. Moreover, our data raise the possibility that caspase 8 may contribute to caspase 3 activation after impact injury in the rat. In addition to these *in vivo* findings, we also provided evidence that caspase 8 and activated caspase 3 may participate in mechanisms of apoptotic CNS cell degeneration in the traumatized cortex. However, future studies are needed to further elucidate the precise role of caspase 8 and activated caspase 3 for cellular CNS degeneration after TBI, including the significance of apoptotic cell death on functional outcome after acute brain injuries *in vivo*.

Acknowledgements

This study was supported by grants from the Austrian Science Fund (FWF; P12287-MED) to AK, the National Institutes of Health to SK (NS36821) and RLH (R01 NS40182; R01 NS39091), and the US Army (DAMD17-9-1-9565) to RLH.

The authors thank Dr Guy Salvesen (The Burnham Institute, La Jolla, CA, USA) for providing caspase 8 recombinant protein and are indebted to Helene Breitschopf, Marianne Leissner (Brain Research Institute, University of Vienna, Vienna, Austria), and Kathrin Schanda for expert technical assistance.

References

Beattie M. S., Farooqui A. A. and Bresnahan J. C. (2000) Review of current evidence for apoptosis after spinal cord injury. *J. Neurotrauma* **17**, 915–925.

Beer R., Franz G., Schöpf M., Reindl M., Zelger B., Schmutzhard E., Poewe W. and Kampfl A. (2000a) Expression of Fas and Fas ligand after experimental traumatic brain injury in the rat. *J. Cereb. Blood Flow Metab.* **20**, 669–677.

Beer R., Franz G., Srinivasan A., Hayes R. L., Pike B. R., Newcomb J. K., Zhao X., Schmutzhard E., Poewe W. and Kampfl A. (2000b) Temporal profile and cell subtype distribution of activated caspase-3 following experimental traumatic brain injury. *J. Neurochem.* **75**, 1264–1273.

Bryan R. M., Cherian L. and Robertson C. (1995) Regional cerebral blood flow after controlled cortical impact injury in rats. *Anesth. Analg.* **80**, 687–695.

Cerretti D. P., Kozlosky C. J., Mosley B., Nelson N., Van Ness K., Greenstreet T. A., March C. J., Kronheim S. R., Druck T. and Cannizzaro L. A. (1992) Molecular cloning of the interleukin-1 beta converting enzyme. *Science* **256**, 97–100.

Charriaut-Marlangue C., Remolleau S., Aggoun-Zouaoui D. and Ben-Ari Y. (1998) Apoptosis and programmed cell death: a role in cerebral ischemia. *Biomed. Pharmacother.* **52**, 264–269.

Clark R. S., Kochanek P. M., Watkins S. C., Chen M., Dixon C. E., Seidberg N. A., Melick J., Loeffert J. E., Nathaniel P. D., Jin K. L. and Graham S. H. (2000) Caspase-3 mediated neuronal death after traumatic brain injury in rats. *J. Neurochem.* **74**, 740–753.

Cohen G. M. (1997) Caspases: the executioners of apoptosis. *Biochem. J.* **326**, 1–16.

Colicos M. A. and Dash P. K. (1996) Apoptotic morphology of dentate gyrus granule cells following experimental cortical impact injury in rats: possible role in spatial memory deficits. *Brain Res.* **739**, 120–131.

Conti A. C., Raghupathi R., Trojanowski J. Q. and McIntosh T. K. (1998) Experimental brain injury induces regionally distinct apoptosis during the acute and delayed post-traumatic period. *J. Neurosci.* **18**, 5663–5672.

Crowe M. J., Bresnahan J. C., Shuman S. L., Masters J. N. and Beattie M. S. (1997) Apoptosis and delayed degeneration after spinal cord injury in rats and monkeys. *Nat. Med.* **3**, 73–76.

Cryns V. and Yuan J. (1998) Proteases to die for. *Genes Dev.* **12**, 1551–1570.

Debus E., Weber K. and Osborn M. (1983) Monoclonal antibodies specific for glial fibrillary acidic (GFA) protein and for each of the neurofilament triplet polypeptides. *Differentiation* **25**, 193–203.

Dixon C. E., Clifton G. L., Lighthall J. W., Yaghmai A. A. and Hayes R. L. (1991) A controlled cortical impact model of traumatic brain injury in the rat. *J. Neurosci. Meth.* **39**, 253–262.

Eldadah B. A. and Faden A. I. (2000) Caspase pathways, neuronal apoptosis, and CNS injury. *J. Neurotrauma* **17**, 811–829.

Engels I. H., Stepczynska A., Stroh C., Lauber K., Berg C., Schwenzer R., Wajant H., Jänicke R. U., Porter A. G., Belka C., Gregor M., Schulze-Osthoff K. and Wesselborg S. (2000) Caspase-8/FLICE functions as an executioner caspase in anticancer drug-induced apoptosis. *Oncogene* **19**, 4563–4573.

Ertel W., Keel M., Stocker R., Imhof H. G., Leist M., Steckholzer U., Tanaka M., Trentz O. and Nagata S. (1997) Detectable concentrations of Fas ligand in cerebrospinal fluid after severe head injury. *J. Neuroimmunol.* **80**, 93–96.

Faden A. I. (1996) Pharmacologic treatment of acute traumatic brain injury. *J. Am. Med. Assoc.* **276**, 569–570.

Felderhoff-Mueser U., Taylor D. L., Greenwood K., Kozma M., Stibenz D., Joashi U. C., Edwards A. D. and Mehmet H. (2000) Fas/CD95/APO-1 can function as a death receptor for neuronal cells in vitro

and in vivo and is upregulated following cerebral hypoxic-ischemic injury to the developing rat brain. *Brain Pathol.* **10**, 17–29.

Franz G., Reindl M., Patel S. C., Beer R., Unterrichter I., Berger T., Schmutzhard E., Poewe W. and Kampfl A. (1999) Increased expression of apolipoprotein D following experimental traumatic brain injury. *J. Neurochem.* **73**, 1615–1625.

Gavrieli Y., Sherman Y. and Ben-Sasson S. A. (1992) Identification of programmed cell death in situ via specific labeling of nuclear DNA fragmentation. *J. Cell Biol.* **119**, 493–501.

Globus M. Y., Alonso O., Dietrich W. D., Busto R. and Ginsberg M. D. (1995) Glutamate release and free radical production following brain injury: effects of posttraumatic hypothermia. *J. Neurochem.* **65**, 1704–1711.

Graeber M. B., Streit W. J., Kiefer R., Schoen S. W. and Kreutzberg G. W. (1990) New expression of myelomonocytic antigens by microglia and perivascular cells following lethal motor neuron injury. *J. Neuroimmunol.* **27**, 121–132.

Graham D. I., McIntosh T. K., Maxwell W. L. and Nicoll J. A. (2000) Recent advances in neurotrauma. *J. Neuropathol. Exp. Neurol.* **59**, 641–651.

Gu C., Casaccia-Bonnefil P., Srinivasan A. and Chao M. V. (1999) Oligodendrocyte apoptosis mediated by caspase activation. *J. Neurosci.* **19**, 3043–3049.

Harrison D. C., Davis R. P., Bond B. C., Campbell C. A., James M. F., Parsons A. A. and Philpott K. L. (2001) Caspase mRNA expression in a rat model of focal cerebral ischemia. *Brain Res. Mol. Brain Res.* **89**, 133–146.

Hayashi T., Sakurai M., Abe K., Sadahiro M., Tabayashi K. and Itoyama Y. (1998) Apoptosis of motor neurons with induction of caspases in the spinal cord after ischemia. *Stroke* **29**, 1007–1012.

Hayes R. L., Jenkins L. W. and Lyeth B. G. (1992) Neurotransmitter-mediated mechanisms of traumatic brain injury: acetylcholine and excitatory amino acids. *J. Neurotrauma* **9**, S173–S187.

Kato H., Kanellopoulos G. K., Matsuo S., Wu Y. J., Jacquin M. F., Hsu C. Y., Kouchoukos N. T. and Choi D. W. (1997) Neuronal apoptosis and necrosis following spinal cord ischemia in the rat. *Exp. Neurol.* **148**, 464–474.

Kermer P., Klocker N. and Bähr M. (1999) Neuronal death after brain injury. Models, mechanisms, and therapeutic strategies in vivo. *Cell Tissue Res.* **298**, 383–395.

Khan S. M., Cassarino D. S., Abramova N. N., Keeney P. M., Borland M. K., Trimmer P. A., Krebs C. T., Bennett J. C., Parks J. K., Swerdlow R. H., Parker W. D. and Bennett J. P. (2000) Alzheimer's disease cybrids replicate beta-amyloid abnormalities through cell death pathways. *Ann. Neurol.* **48**, 148–155.

Kokaia Z., Andsberg G., Martinez-Serrano A. and Lindvall O. (1998) Focal cerebral ischemia in rats induces expression of P75 neurotrophin receptor in resistant striatal cholinergic neurons. *Neuroscience* **84**, 1113–1125.

Krajewska M., Wang H. G., Krajewski S., Zapata J. M., Shabaik A., Gascoyne R. and Reed J. C. (1997) Immunohistochemical analysis of in vivo patterns of expression of CPP32 (Caspase-3), a cell death protease. *Cancer Res.* **57**, 1605–1613.

Krinke G. J. (2000) Part 6: Physiology in, *The Laboratory Rat* (Bullock, G., Bunton, T., eds). San Diego, Academic Press.

Li Y., Maher P. and Schubert D. (1998) Phosphatidylcholine-specific phospholipase C regulates glutamate-induced nerve cell death. *Proc. Natl Acad. Sci. USA* **95**, 7748–7753.

Liu X. Z., Xu X. M., Du Hu R. C., Zhang S. X., McDonald J. W., Dong H. X., Wu Y. J., Fan G. S., Jacquin M. F., Hsu C. Y. and Choi D. W. (1997) Neuronal and glial apoptosis after traumatic spinal cord injury. *J. Neurosci.* **17**, 5395–5406.

McIntosh T. K., Saatman K. E., Raghupathi R., Graham D. I., Smith D. H., Lee V. M. and Trojanowski J. Q. (1998) The Dorothy Russell Memorial Lecture. The molecular and cellular sequelae of experimental traumatic brain injury: pathogenetic mechanisms. *Neuropathol. Appl. Neurobiol.* **24**, 251–267.

Martin-Villalba A., Herr I., Jeremias I., Hahne M., Brandt R., Vogel J., Schenkel J., Herdegen T. and Debatin K. M. (1999) CD95 ligand (Fas-L/APO-1L) and tumor necrosis factor-related apoptosis-inducing ligand mediate ischemia-induced apoptosis in neurons. *J. Neurosci.* **19**, 3809–3817.

Matsushita K., Wu Y., Qiu J., Lang-Lazdunski L., Hirt L., Waeber C., Hyman B. T., Yuan J. and Moskowitz M. A. (2000) Fas receptor and neuronal cell death after spinal cord ischemia. *J. Neurosci.* **20**, 6879–6887.

Mattson M. P., Culmsee C. and Yu Z. F. (2000) Apoptotic and anti-apoptotic mechanisms in stroke. *Cell Tissue Res.* **301**, 173–187.

Medema J. P., Scaffidi C., Kischkel F. C., Shevchenko A., Mann M., Krammer P. H. and Peter M. E. (1997) FLICE is activated by association with the CD95 death-inducing signaling complex (DISC). *EMBO J.* **16**, 2794–2804.

Mogi M., Togari A., Kondo T., Mizuno Y., Komure O., Kuno S., Ichinose H. and Nagatsu T. (2000) Caspase activities and tumor necrosis factor receptor R1 (p55) level are elevated in the substantia nigra from parkinsonian brain. *J. Neural. Transm.* **107**, 335–341.

Muzio M., Chinnaiyan A. M., Kischkel F. C., O'Rourke K., Shevchenko A., Ni J., Scaffidi C., Bretz J. D., Zhang M., Gentz R., Mann M., Krammer P. H., Peter M. E. and Dixit V. M. (1996) FLICE, a novel FADD-homologous ICE/CED-3-like protease, is recruited to the CD95 (Fas/APO-1) death-inducing signaling complex. *Cell* **85**, 817–827.

Namura S., Zhu J., Fink K., Endres M., Srinivasan A., Tomaselli K. J., Yuan J. and Moskowitz M. A. (1998) Activation and cleavage of caspase-3 in apoptosis induced by experimental cerebral ischemia. *J. Neurosci.* **18**, 3659–3668.

Newcomb J. K., Zhao X., Pike B. R. and Hayes R. L. (1999) Temporal profile of apoptotic-like changes in neurons and astrocytes following controlled cortical impact injury in the rat. *Exp. Neurol.* **158**, 76–88.

Nicholson D. W. (1999) Caspase structure, proteolytic substrates, and function during apoptotic cell death. *Cell Death Differ.* **6**, 1028–1042.

Nitatori T., Sato N., Waguri S., Karasawa Y., Araki H., Shibanai K., Kominami E. and Uchiyama Y. (1995) Delayed neuronal death in the CA1 pyramidal cell layer of the gerbil hippocampus following transient ischemia is apoptosis. *J. Neurosci.* **15**, 1001–1011.

Paxinos G. and Watson C. (1997). *The Rat Brain in Stereotaxic Coordinates*, 4th edn. San Diego, CA: Academic Press.

Pike B. R., Zhao X., Newcomb J. K., Glenn C. C., Anderson D. K. and Hayes R. L. (2000) Stretch injury causes calpain and caspase-3 activation and necrotic and apoptotic cell death in septo-hippocampal cell cultures. *J. Neurotrauma* **17**, 283–298.

Qin Z. H., Wang Y., Kikly K. K., Sapp E., Kegel K. B., Aronin N. and DiFiglia M. (2001) Pro-caspase-8 is predominatly localized in mitochondria and released into cytoplasm upon apoptotic stimulation. *J. Biol. Chem.* **276**, 8079–8086.

Raghupathi R., Graham D. I. and McIntosh T. K. (2000) Apoptosis after traumatic brain injury. *J. Neurotrauma* **17**, 927–938.

Rink A., Fung K. M., Trojanowski J. Q., Lee V. M., Neugebauer E. and McIntosh T. K. (1995) Evidence of apoptotic cell death after experimental traumatic brain injury in the rat. *Am. J. Pathol.* **147**, 1575–1583.

Scaffidi C., Fulda S., Srinivasan A., Friesen C., Li F., Tomaselli K. J.,

Debatin K. M., Krammer P. H. and Peter M. E. (1998) Two CD95 (APO-1/Fas) signaling pathways. *EMBO J.* **17**, 1675–1687.

Schulze-Osthoff K., Ferrari D., Los M., Wesselborg S. and Peter M. E. (1998) Apoptosis signaling by death receptors. *Eur. J. Biochem.* **254**, 439–459.

Shah P. T., Yoon K. W., Xu X. M. and Broder L. D. (1997) Apoptosis mediates cell death following traumatic injury in rat hippocampal neurons. *Neuroscience* **79**, 999–1004.

Shikama Y. (2001) Comprehensive studies on subcellular localizations and cell death-inducing activities of eight gfp-tagged apoptosis-related caspases. *Exp. Cell Res.* **264**, 315–325.

Shohami E., Bass R., Wallach D., Yamin A. and Gallily R. (1996) Inhibition of tumor necrosis factor alpha (TNF alpha) activity in rat brain is associated with cerebroprotection after closed head injury. *J. Cereb. Blood Flow Metab.* **16**, 378–384.

Springer J. E., Azbill R. D. and Knapp P. E. (1999) Activation of the caspase-3 apoptotic cascade in traumatic spinal cord injury. *Nat. Med.* **8**, 943–946.

Sprinkle T. J. (1989) 2′,3′-cyclic nucleotide 3′-phosphodiesterase, an oligodendrocyte-Schwann cell and myelin-associated enzyme of the nervous system. *Crit. Rev. Neurobiol.* **4**, 235–301.

Srinivasan A., Roth K. A., Sayers R. O., Shindler K. S., Wong A. M., Fritz L. C. and Tomaselli K. J. (1998) In situ immunodetection of activated caspase-3 in apoptotic neurons in the developing nervous system. *Cell Death Differ.* **5**, 1004–1016.

Stadelmann C., Deckwerth T. L., Srinivasan A., Bancher C., Bruck W., Jellinger K. and Lassmann H. (1999) Activation of caspase-3 in single neurons and autophagic granules of granulovacuolar degeneration in Alzheimer's disease. Evidence for apoptotic cell death. *Am. J. Pathol.* **155**, 1459–1466.

Stennicke H. R., Jurgensmeier J. M., Shin H., Deveraux Q., Wolf B. B., Yang X., Zhou Q., Ellerby H. M., Ellerby L. M., Bredesen D., Green D. R., Reed J. C., Froelich C. J. and Salvesen G. S. (1998) Pro-caspase-3 is a major physiologic target of caspase-8. *J. Biol. Chem.* **273**, 27084–27090.

Stoka V. V., Turk B., Schendel S. L., Kim T. H., Cirman T., Snipas S. J., Ellerby L. M., Bredesen D., Freeze H., Abrahamson M., Bromme D., Krajewski S., Reed J. C., Yin X. M., Turk V. V. and Salvesen G. S. (2001) Lysosomal protease pathways to apoptosis: cleavage of bid, not pro-caspases, is the most likely route. *J. Biol. Chem.* **276**, 3149–3157.

Thurman D. J., Alverson C., Dunn K. A., Guerrero J. and Sniezek J. E. (1999) Traumatic brain injury in the United States: a public health perspective. *J. Head Trauma Rehabil.* **14**, 602–615.

Velier J. J., Ellison J. A., Kikly K. K., Spera P. A., Barone F. C. and Feuerstein G. Z. (1999) Caspase-8 and caspase-3 are expressed by different populations of cortical neurons undergoing delayed cell death after focal stroke in the rat. *J. Neurosci.* **19**, 5932–5941.

Walker N. P., Talanian R. V., Brady K. D., Dang L. C., Bump N. J., Ferenz C. R., Franklin S., Ghayur T., Hackett M. C. and Hammill L. D. (1994) Crystal structure of the cysteine protease interleukin-1 beta-converting enzyme: a (p20/p10), 2 homodimer. *Cell* **78**, 343–352.

Wolf H. K., Buslei R., Schmidt-Kastner R., Schmidt-Kastner P. K., Pietsch T., Wiestler O. D. and Bluhmke I. (1996) NeuN: a useful neuronal marker for diagnostic histopathology. *J. Histochem. Cytochem.* **44**, 1167–1171.

Xerri L., Palmerini F., Devilard E., Defrance T., Bouabdallah R., Hassoun J. and Birg F. (2000) Frequent nuclear localization of ICAD and cytoplasmic co-expression of caspase-8 and caspase-3 in human lymphomas. *J. Pathol.* **192**, 194–202.

Yakovlev A. G., Knoblach S. M., Fan L., Fox G. B., Goodnight R. and Faden A. I. (1997) Activation of CPP32-like caspases contributes to neuronal apoptosis and neurological dysfunction after traumatic brain injury. *J. Neurosci.* **17**, 7415–7424.

Biomarkers of Proteolytic Damage Following Traumatic Brain Injury

Jose A. Pineda[1,3]; Kevin K.W. Wang[1,2,4]; Ronald L. Hayes[1,2,4]

[1]Center for Traumatic Brain Injury Studies, Evelyn F. and William L. McKnight Brain Institute of The University of Florida, Gainesville.
Departments of [2]Neuroscience, [3]Pediatrics, and [4]Psychiatry, University of Florida, Gainesville.

Corresponding author:
Jose A. Pineda, MD, PICU, PO Box 100296, Gainesville, FL 32610-0296 (E-mail: pinedja@peds.ufl.edu)

The history of numerous failed clinical trials designed to identify therapeutic agents to assist in improving outcomes after traumatic brain injury points to the critical importance of understanding biochemical markers of injury. Such biomarkers should be readily accessible, provide information specific to the pathologic disruptions occurring in the central nervous system, and allow improved monitoring of the progression of secondary damage. Additionally, these biomarkers should may provide investigators a window on the individual patient's response to treatment, and should contribute to prediction of outcome. Most research on this topic to date has focused on neuron-specific enolase (NSE) and S-100 proteins but these have not proven to be satisfactory for a variety of reasons. A different approach is provided by the study of 2 important proteases, caspase-3 and calpain. This paper reports the current state of knowledge concerning caspase and calpain as specific markers of TBI, and discusses all-spectrin, a principal substrate for both caspase and calpain, as well as initial findings regarding neurofilament 68 protein (NF-68).

Brain Pathol 2004;14:202-209.

INTRODUCTION

Brain injury resulting from traumatic, ischemic and/or chemical etiology is a significant international health concern, representing a potentially catastrophic debilitating medical emergency with poor prognosis for long-term disability. It represents a major problem to military care, accounting for 25% of all combat casualties and is the leading cause of death (approaching 50% incidence) among wounded soldiers reaching Echelon I medical treatment (10). In civilian life, the incidence of brain injury and resultant long-term disabilities caused by traumatic insults (eg, automobile accidents, gunshots, sports) and ischemic events (eg, strokes, cerebral hemorrhage, cardiac arrest) are several orders of magnitude greater. There are more than 1 million traumatic brain injury (TBI) cases that are treated and released from an emergency department annually in the United States, resulting in more than 230 000 hospitalizations, 50 000 deaths and 80 000 disabilities. Among all age groups, the top 3 causes of TBI are motor vehicle accidents, falls and violence (1). Despite modern automobile design and injury prevention campaigns, important causes of TBI in children such as ejections from cars during traffic accidents, have increased in recent years (111). The current estimate is that 5.3 million Americans live with a TBI-related disability. TBI is the greatest cause of death and disability in young people less than 24-years-old (2).

With the exception of supportive measures, there are currently no approved drug treatments for TBI (76). There have been a large number of clinical trials studying potential therapies for traumatic brain injury (TBI) that have resulted in negative findings with a cost of over $200 million (17, 31). Many investigators have pointed out that the absence of biochemical markers of injury could have contributed to these failures (76, 104). Unlike other organ-based diseases where rapid diagnosis employing biomarkers (usually involving blood tests) prove invaluable to guide treatment of the disease, no such rapid, definitive diagnostic tests exist for TBI to provide physicians with quantifiable neurochemical markers to help determine the seriousness of the injury, the anatomical and cellular pathology of the injury, and to guide implementation of appropriate triage and medical management.

CRITERIA FOR BIOCHEMICAL/ SURROGATE MARKERS

In the course of research on biomarkers, our laboratories have developed criteria for biomarker development. Useful biomarkers should employ readily accessible biological material such as CSF or blood (CSF is routinely accessible in severely injured TBI patients), predict the magnitude of injury and resulting functional deficits and possess high sensitivity and specificity, have a rapid appearance in blood and be released in a time-locked sequence after injury. Ideally, biomarkers should employ biological substrates unique to the CNS and provide information on injury mechanisms, a criterion often used to distinguish biochemical markers from surrogate markers of injury, which usually do not provide information on injury mechanisms. Potential gender and age related differences on biomarker profiles are also important and should be taken into account when developing useful biochemical markers (43).

USES OF BIOMARKERS

Biomarkers would have important applications in diagnosis, prognosis and clinical research of brain injuries. Simple, rapid diagnostic tools will immensely facilitate allocation of the major medical resources required to treat TBI and other brain injuries. Accurate diagnosis in acute care environments can significantly enhance decisions about patient management including decisions whether to admit or discharge, or administer other time consuming and expensive tests including computer tomography (CT) and magnetic resonance imaging (MRI) scans. Biomarkers could have important prognostic functions especially in patients suffering mild TBI, which make up an estimated 80% of the 2.5 to 6.5 million individuals who suffer from lifelong impairment as a result of TBI (3, 82). Ac-

190

curate identification of these patients could facilitate development of guidelines for return to duty, work or sports activities and also provide opportunities for counseling of patients suffering from these deficits. Biomarkers could provide major opportunities for the conduct of clinical research including confirmation of injury mechanism(s) and drug target identification. The temporal profile of changes in biomarkers could guide timing of treatment and assist in monitoring the response to therapy and intervention. Finally, biomarkers could provide a clinical trial outcome measure obtainable much more cheaply and readily than conventional neurological assessments, thereby significantly reducing the risks and costs of human clinical trials. Relevant, easily available biomarkers are needed in order to maximize chances of success in developing long awaited effective drugs for TBI (76).

CURRENT STATUS OF RESEARCH ON MARKERS OF TRAUMATIC BRAIN INJURY

Analysis of specific biochemical markers has provided useful information on the mechanism and diagnosis of specific organ dysfunction in humans (112). However, although analysis of cerebrospinal fluid, cerebral microdialysis samples, and brain tissue specimens has provided insight into the mechanisms of brain injury (61, 63), there are no biomarkers of proven clinical utility for TBI.

TBI is difficult to assess and clinical examinations are of restricted value during the first hours and days after injury. Conventional diagnoses of TBI are based on neuroimaging techniques such as CT scanning, MRI and single-photon emission CT scanning (46, 58, 72). CT scanning has low sensitivity to detect diffuse brain damage, and the availability of MRI is limited (60, 64). Single-photon emission CT scanning detects regional blood-flow abnormalities not necessarily related to structural damage.

A recent review of biomarkers of TBI highlighted the need for biomarker development (43). The most studied potential biochemical markers for TBI include creatine kinase (CK), glial fibrillary acidic protein (GFAP), lactate dehydrogenase (LDH), myelin basic protein (MBP), neuron-specific enolase (NSE) and S-100 proteins. The bulk of research in TBI has focused on NSE and S-100β. The specificity of NSE for brain is high (49) , sex- and age-related variability is low (30, 51, 74, 85, 97, 120, 121, 134), and NSE is rapidly detectible in serum after TBI (129). However, studies relating NSE serum levels to admission GCS in patients with severe TBI show conflicting results. Similar data have been reported concerning relationships with CT scan findings, ICP and long-term outcomes. In mild TBI, NSE failed to separate patients from controls (12, 44, 108, 132). Thus, NSE is predominantly used as a marker for tumors (24). NSE is also released in the blood by hemolysis, which could be a major source of error (24).

The S-100 protein family now consists of 19 members, of which S-100β is the one viewed as a marker of brain damage (49, 65), although it is present in other tissues such as adipocytes and chondrocytes (40). Investigators have reported that S-100β serum levels correlate to GCS scores, neuroradiologic findings at admission and long-term outcomes (98, 99, 130). However, investigators have recently raised questions about the utility of S-100β reporting that high serum levels of S-100β are detectible in trauma patients not having head injuries, a factor not adequately controlled for in earlier studies (4). In addition, serum levels of S-100β following mild TBI do not show strong correlations with neuropsychological outcome (107). Research in this area continues and recent reports have indicated the potential utility of measures of blood GFAP (71), spinal fluid interleukin-6 (115) and cleaved tau protein in serum (45, 114) and spinal fluid (136) following brain injury.

Investigators have also generally recognized the need for more objective assessments of outcome following stroke, including biochemical markers (29, 68). The approval of tPA as a treatment for acute stroke has additionally highlighted the potential utility of biochemical markers. Use of tPA may be hindered by diagnostic concerns because neurological deficits accompanying stroke can mimic those seen during transient ischemic attacks, complex migraine, space-occupying lesions and post-ictal paralysis. A reliable biochemical marker might give assurance to physicians considering administering thrombolytic agents for acute stroke (41, 50).

Previously reported biomarkers of cerebral ischemia include NSE, brain specific creatine kinase enzyme (CPK-BB), S-100β and inflammatory cytokines such as IL-6 (88). NSE and S-100β have been the most studied. After cardiac arrest, NSE elevations in serum and CSF have been correlated with neurological recovery (28, 67, 106). Serum and CSF NSE values were reported to be elevated in rodent models of focal ischemia in proportion to the eventual infarct volume (26, 27, 42). In clinical trials, peak serum NSE values also predicted infarct volumes as shown by CT. Correlating serum NSE values with functional outcome was less successful (26, 27, 70), possibly because functional neurological deficit is influenced as much by location of brain injury as by infarct size (70). S-100β protein has been studied most extensively for characterization of ischemic injuries after cardiac surgery, and several reports have documented post-operative serum elevations (5, 113, 128). However, many of these reports do not include careful studies of neurological outcome, and several investigators have recently criticized the diagnostic utility of S-100β during cardiac surgery (4).

PROTEOLYTIC DAMAGE AND THE PATHOBIOLOGY OF TRAUMATIC BRAIN INJURY

After TBI, brain cells can deteriorate by more than one pathway, and many genes and proteins may be involved. Programmed cell death is an evolutionarily conserved form of cell suicide that occurs widely throughout development (15). This type of cell death often has the morphological appearance of apoptosis (119). Apoptosis occurs following TBI in animals (22, 59, 131) and humans (18, 19). Studies of apoptosis pose special challenges since there are multiple apoptotic pathways, and apoptosis is extremely sensitive to a number of variables including injury type and magnitude (13, 16, 100), cell type (38, 57) and stimulation/antagonism of specific receptors (16, 21, 25, 38, 39, 48).

The molecular events occurring after TBI are just beginning to be understood. Elevated neuronal calcium levels activate a number of calcium-dependent enzymes such as phospholipases (83), kinases (133), phosphatases (75), and proteases (7, 80), all of which can modulate post-TBI cytoskel-

etal protein loss. Caspase-3 is a member of the caspase family of cysteine proteases. Activated caspase-3 has many cellular targets that, when interrupted and/or activated, produce the morphologic features of apoptosis (20). Calpains are calcium-activated, neutral cysteine proteases with relative selectivity for proteolysis of a subset of cellular proteins. Calpain activation has been implicated in different models of apoptosis and in different cell types, including neurons (92). Understanding of the contributions of calpains and caspases to cell injury/death following TBI may have important diagnostic and therapeutic implications.

CONTRIBUTIONS OF CASPASE-3 AND CALPAIN TO CELL DEATH FOLLOWING TRAUMATIC BRAIN INJURY

Numerous studies from our own (8, 90, 92) and other laboratories (32, 36, 73) have provided evidence that the caspase family of cysteine proteases is an important intracellular effector of apoptosis in various cell lines and apoptotic models. Caspase-3-like proteases have been shown to cleave a variety of cytoplasmic, nuclear and cytoskeletal proteins during apoptosis, including αII-spectrin (69, 77, 78, 122), poly(ADP-ribose) polymerase (PARP: 51) and others (52-57). In vitro studies in our laboratories using a model of stretch injury have demonstrated caspase-3 processing of α-spectrin to the apoptotic-linked 120-kDa fragment 24 hours after moderate, but not mild or severe injury (8). In vivo studies have provided evidence of caspase-3 activation following TBI. First, Clark et al demonstrated cleavage of capsase-3 to its p18 and p12 subunits in humans (19). Yakovlev et al reported that TBI increased caspase-3, but not caspase-1 activity (131). Caspase-3 inhibition reduced DNA fragmentation and TUNEL staining and improved behavioral outcome. We have also concurrently examined caspase-3 and calpain activation after TBI. Distinct regional and temporal patterns of calpain/caspase-3 processing of αII-spectrin in brain regions ipsilateral to the site of injury after TBI have been observed. Caspase-3-mediated breakdown products (BDP's) to αII-spectrin were absent in the cortex but showed significant increases in hippocampus and striatum early after TBI (91). Immunohistochemical examinations revealed increased expression of the proteolitically active subunit of caspase-3, p18, in neurons, astrocytes, and oligodendrocytes from 6 to 72 hours following controlled cortical impact injury. Moreover, concurrent assessment of nuclear histopathology using hematoxylin identified p18-immunopositive cells exhibiting apoptotic-like morphological profiles in the cortex ipsilateral to the injury site (8).

Calpains are Ca^{2+} activated cysteine proteases that have been implicated in a variety of neuropathological conditions (55, 127). Intracellular substrates of activated calpain include cytoskeletal proteins, calmodulin-binding proteins, enzymes involved in signal transduction, membrane proteins and transcription factors (110, 118, 126). While calpain activation has historically been associated with necrotic cell death (81), calpain activation has also been implicated in different models of apoptosis and in different cell types, including neurons (9, 52, 77, 117, 123). Research in our own and other laboratories have documented calpain activation following TBI in vivo (55). TBI results in altered Ca^{2+} homeostasis (135) and activates several Ca^{2+}-dependent enzymes including the calpains. Overactivation of calpains occurs in many neurodegenerative diseases and injuries to the CNS (6, 55, 127). Increased calpain activity following TBI has been inferred by a variety of techniques (54, 80, 93, 96), including protection by calpain inhibitors (94, 109).

Pathological calpain activation is believed to occur when intracellular free calcium levels surpass a certain threshold. Importantly, increases in free calcium via voltage and receptor gated calcium channels have been reported in CNS trauma in vivo (21, 48, 56). Calpains are located throughout the neuron, in somatodendritic regions and in axons (57). Calpain may also be a constituent of myelin (116). Therefore, pathological calpain activity and subsequent substrate proteolysis can have profound effects on neuronal structure and function.

Cytoskeletal alterations after experimental brain injury have pointed to the likelihood of calpain mediated proteolysis. Preferred substrates for calpains include the cytoskeletal protein spectrin (47, 66), microtubule associated protein-2 (MAP-2)(34), and neurofilament proteins (22, 23, 84, 105). Increased degradation of MAP2 (33, 131), the neurofilament triplet proteins (53, 86) and spectrin (79) have been reported in cerebral ischemia. In addition, loss of MAP-2 (62), neurofilament 68 (NF 68) and neurofilament 200 (NF 200)(93-95) have been reported following TBI in vivo. Additional evidence that calpain is activated in neurons following experimental brain injury has been provided by the use of antibodies which bind specifically to calpain mediated BDP's of cytoskeletal proteins in models of TBI (80).

αII-SPECTRIN DEGRADATION-A PROTOTYPE BIOMARKER

Our research program to develop biomarkers for TBI has focused on α-spectrin degradation as a prototypical biochemical marker (35, 103). αII-spectrin (280 kDa) is the major structural component of the cortical membrane cytoskeleton and is particularly abundant in axons and presynaptic terminals (37, 102). Importantly, αII-spectrin is a major substrate for both calpain and caspase-3 cysteine proteases (125). Our laboratory has provided considerable evidence that αII-spectrin is processed by calpains and/or caspase-3 to signature cleavage products in vivo after TBI (8, 14, 80, 91) and also in vitro after mechanical stretch injury (90). Calpain produces 2 major αII-spectrin breakdown products of 150 kDa and 145 kDa (SBDP150 and SBDP145) in a sequential manner. On the other hand, caspase-3 initially produces a 150 kDa SBDP that is further cleaved into a 120 kDa fragment (SBDP120)(124). Immunoblots of αII-spectrin degradation thus provide concurrent information on the activation of calpain and caspase-3, potentially important regulators of cell death following TBI. The calcium sensitivity and low basal levels of calpain optimize its utility as a marker of cell injury. Although not found in erythrocytes and thus robust to confounding by blood contamination, αII-spectrin is not specific to the CNS (89). Following injury, native αII-spectrin protein was decreased in brain tissue and increased in CSF from 24 hours to 72 hours after injury. Calpain-specific breakdown products increased in both brain and CSF after injury. Caspase-3-specific breakdown products increased in some animals, but to a lesser degree (89).

Recent efforts in our laboratory have expanded our studies of the potential clinical utility of αII-spectrin degradation as a

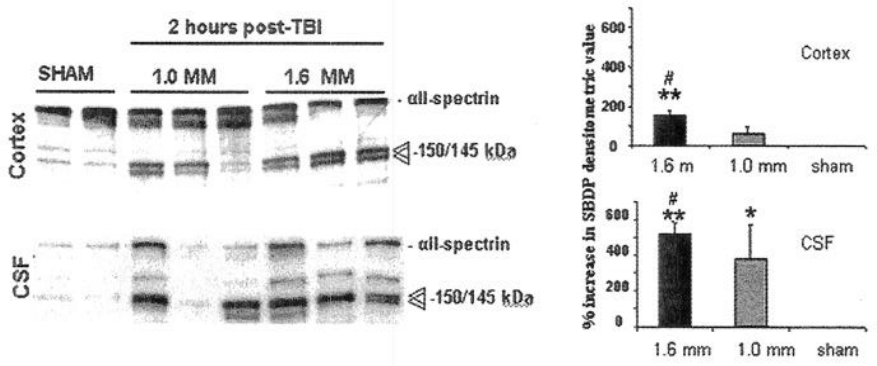

Figure 1. *Accumulation of calpain-specific SBDPs is sensitive to injury magnitude after controlled cortical impact.* Animals were injured using a model of controlled cortical impact at two magnitudes of injury. Accumulation of brain cortex and spinal fluid levels of αII-SBDP were measured by densitometric analysis at 2 hours post-injury. The 1.6 mm injury magnitude produced the highest levels of αII-SBDP accumulation in cortex and CSF compared to 1.0 mm injury and to sham-injured controls. However, statistical significance ($p<0.05$) between 1.6 mm and 1.0 mm injuries was only achieved at 2 hours but not at 6 or 24 hours post-injury (data not shown). This finding could indicate a critical window for discriminating injury magnitude using αII-SBDP as a biomarker. CSF levels of αII-SBDP were greater in CSF than in cortex, particularly for the 1.6 mm injury. This most likely reflects a greater ratio of SBDP to total protein in CSF relative to cortex and indicates that low abundance proteins may be more easily detected in CSF after brain injury (n = 6 per group).

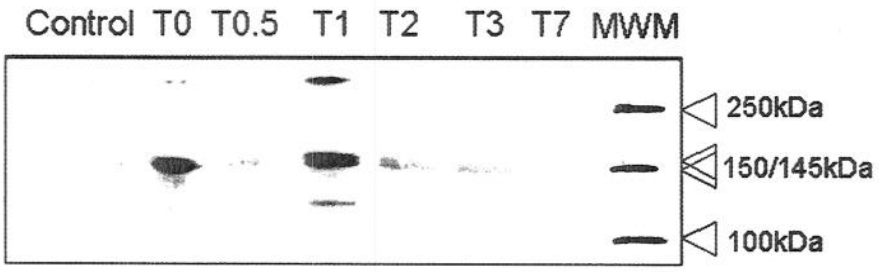

Figure 2. Western blot analysis of cerebrospinal fluid (CSF) samples from a 9-year-old patient diagnosed with severe head injury αII-spectrin breakdown products reflecting caspase-3 (150kDa and 120kDa bands) and calpain (150kDa and 145kDa bands) activity were identified as early as 12 hours after injury and persisted for at least 3 days after injury. Increased protein expression one day after injury may reflect clinical evidence of increased brain swelling and intracranial hypertension. CSF from a child with chronic hydrocephalus and no acute brain injury was used as control. T0 = admission to the intensive care unit; T0.5 = 12 hours after injury; T1 = 24 hours after injury; T2: 2 days after injury; T3: 3 days after injury; T7 = 7 days after injury; MWM = molecular weight marker.

biomarker for TBI (Figure 1). These studies focused on determining whether changes in αII-spectrin breakdown products in CSF could be useful indicators of the magnitude of brain injury. Our studies have provided the first evidence that protein degradation of a structural cytoskeletal protein can be a reliable marker of CNS injury. Equally important, our data suggests that there may be a critical period following injury during which these markers predict injury magnitude. Our laboratory has also provided the first human data on the potential utility of αII-spectrin as a biomarker (Figure 2). These preliminary studies indicate that αII-spectrin degradation is also detected in brain injury patients but not in chronic hydrocephalic controls. Equally important, our data suggests that secondary increases in levels of breakdown products in CSF may reflect secondary deterioration in the clinical status of the patient. Thus, biomarkers such as αII-spectrin degradation may provide useful information for management of head injury patients in critical care environments. However, it is not known whether BDP's and other biomarkers that discriminate magnitudes of injury at the biochemical level (ie, magnitude differences in CSF/serum levels of a biomarker) will be useful as predictors of clinically relevant measures of outcome. That is, 2 different injury magnitudes may produce significantly different biochemical responses in the brain that are discernable in CSF or serum, but these same injury magnitudes may not result in functionally different behavioral, pathological, or other

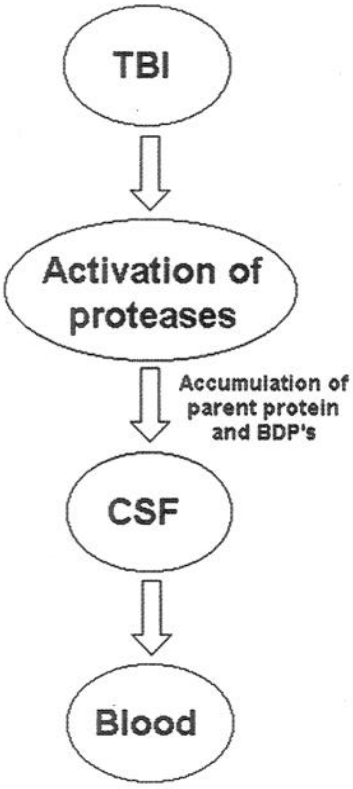

Figure 3. *Development of biomarkers of protease activity. Brain injury leads to activation of proteases after traumatic brain injury.* Proteolytic processing of cytoskeletal proteins (i.e. αII-spectrin) leads to accumulation of both the parent protein as well as signature breakdown products (BDP's). Initial characterization will most likely require analysis of cerebrospinal fluid (CSF). Antibodies will then be developed so that an easily accessible biomarker of protease activity is available for sampling from peripheral blood.

clinical outcome measures. Thus, biomarkers that do not correlate with clinically relevant outcome measures will not be useful for assessment of functional ability, functional recovery, or for gauging effects of therapy on outcome. In addition, preliminary results from our laboratories suggest that there is a spontaneous susceptibility of cytoskeletal protein degradation by calpain in aging rats (11). These findings emphasize the importance of accounting for multiple clinical variables including, but not limited to, age when evaluating the clinical utility of biomarkers of brain injury.

ADDITIONAL CYTOSKELETAL PROTEINS WITH POTENTIAL UTILITY AS BIOMARKERS

Initial research focused on proteolytic processing of cytoskeletal proteins such as lower molecular weight neurofilament 68 protein (NF-68) highlights their potential to provide useful information on activ-

ity of specific proteases such as μ-calpain and m-calpain. Importantly, 2-D gel electrophoresis studies have suggested that dephosphorylation of NF-68 may be associated with NF protein loss following TBI, a post translational modification that could have significance for biomarker development (80, 96). This important biomarker could provide important information on the pathophysiology of both dendritic and axonal damage after TBI (95). Importantly, NF-68 has been used to quantify axonal injury in closed head injury models (101). Since diffuse axonal injury (DAI) is presently considered one of the most common types of primary lesions in patients with severe closed head injury (87), a biomarker that provides information on axonal injury could potentially have clinical utility.

FUTURE DIRECTIONS

The pathology of TBI is extremely complex. As our understanding of the numerous biochemical cascades involved continues to evolve, sophisticated diagnostic tools such as biomarkers will be developed (Figure 3). Ideal biomarkers will provide information on the pathobiology of TBI and facilitate better stratification of patients by the severity of their injury, better monitoring of the progression of secondary damage, response to treatment/intervention, and prediction of outcome. Although the initial characterization of biomarkers will be mainly based on spinal fluid analysis, methods for measurement of such biomarkers in blood (plasma or serum) will be developed. The development of accessible and reliable biomarkers is likely to change the way clinical studies of head injury are conducted, resulting in more mechanism driven, optimally timed therapies.

ACKNOWLEDGMENTS

The authors acknowledge the original contributions of Dr Brian Pike, and the support from NIH R01 NS38105-01, NIH RO1 NS39091-02, DAMD 17-99-1-9565 and DAMD 17-01-1-0765. Supported in part by General Clinical Research Center grant RR00082.

REFERENCES

1. (1999) Consensus conference. Rehabilitation of persons with traumatic brain injury. NIH Consensus Development Panel on Rehabilitation of Persons With Traumatic Brain Injury. *Jama* 282: 974-983.

2. (2000) TBI State Demonstration Grants. *J Head Trauma Rehabil* 15:750-760.

3. Alexander MP (1995) Mild traumatic brain injury: pathophysiology, natural history, and clinical management. *Neurology* 45:1253-1260.

4. Anderson RE HL, Nilsson O, Dijlai-Merzoug R, Settergen G (2001) High serum S100B levels for trauma patients without head injuries. *Neurosurgery* 49:1272-1273.

5. Astudillo R, Van der Linden J, Radegran K, Hansson LO, Aberg B (1996) Elevated serum levels of S-100 after deep hypothermic arrest correlate with duration of circulatory arrest. *Eur J Cardiothorac Surg* 10:1107-1112; discussion 1113.

6. Bartus RT, Elliott PJ, Hayward NJ, Dean RL, Harbeson S, Straub JA, Li Z, Powers JC (1995) Calpain as a novel target for treating acute neurodegenerative disorders. *Neurol Res* 17:249-258.

7. Bartus RT, Hayward NJ, Elliott PJ, Sawyer SD, Baker KL, Dean RL, Akiyama A, Straub JA, Harbeson SL, Li Z (1994) Calpain inhibitor AK295 protects neurons from focal brain ischemia. Effects of postocclusion intra-arterial administration. *Stroke* 25:2265-2270.

8. Beer R, Franz G, Srinivasan A, Hayes RL, Pike BR, Newcomb JK, Zhao X, Schmutzhard E, Poewe W, Kampfl A (2000) Temporal profile and cell subtype distribution of activated caspase-3 following experimental traumatic brain injury. *J Neurochem* 75:1264-1273.

9. Behrens MM, Martinez JL, Moratilla C, Renart J (1995) Apoptosis induced by protein kinase C inhibition in a neuroblastoma cell line. *Cell Growth Differ* 6:1375-1380.

10. Bellamy R (1984) The causes of death in conventional land warfates: implications for combat casualty research. *Military Medicine* 149:55-62.

11. Bernath ED, Durham R, Duddy S, Wang KKW (In Preparation) Spontaneous cytoskeletal protein proteolysis in aged Wistar rat brains.

12. Bertrand R, Solary E, O'Connor P, Kohn KW, Pommier Y (1994) Induction of a common pathway of apoptosis by staurosporine. *Exp Cell Res* 211:314-321.

13. Bonfoco E, Krainc D, Ankarcrona M, Nicotera P, Lipton SA (1995) Apoptosis and necrosis: two distinct events induced, respectively, by mild and intense insults with N-methyl-D-aspartate or nitric oxide/superoxide in cortical cell cultures. *Proc Natl Acad Sci U S A* 92:7162-7166.

14. Buki A, Okonkwo DO, Wang KK, Povlishock JT (2000) Cytochrome c release and caspase activation in traumatic axonal injury. *J Neurosci* 20:2825-2834.

15. Chang LK, Putcha GV, Deshmukh M, Johnson EM (2002) Mitochondrial involvement in the point of no return in neuronal apoptosis. *Biochimie* 84:223-231.

16. Choi DW (1996) Ischemia-induced neuronal apoptosis. *Curr Opin Neurobiol* 6:667-672.

17. Choi SC Bullock R (2001) Design and statistical issues in multicenter trials of severe head injury. *Neurol Res* 23:190-192.

18. Clark RS, Kochanek PM, Adelson PD, Bell MJ, Carcillo JA, Chen M, Wisniewski SR, Janesko K, Whalen MJ, Graham SH (2000) Increases in bcl-2 protein in cerebrospinal fluid and evidence for programmed cell death in infants and children after severe traumatic brain injury. *J Pediatr* 137: 197-204.

19. Clark RS, Kochanek PM, Chen M, Watkins SC, Marion DW, Chen J, Hamilton RL, Loeffert JE, Graham SH (1999) Increases in Bcl-2 and cleavage of caspase-1 and caspase-3 in human brain after head injury. *Faseb J* 13:813-821.

20. Clark RS, Kochanek PM, Watkins SC, Chen M, Dixon CE, Seidberg NA, Melick J, Loeffert JE, Nathaniel PD, Jin KL, Graham SH (2000) Caspase-3 mediated neuronal death after traumatic brain injury in rats. *J Neurochem* 74:740-753.

21. Cohen GM (1997) Caspases: the executioners of apoptosis. *Biochem J* 326:1-16.

22. Colicos MA, Dash PK (1996) Apoptotic morphology of dentate gyrus granule cells following experimental cortical impact injury in rats: possible role in spatial memory deficits. *Brain Res* 739:120-131.

23. Conti AC, Raghupathi R, Trojanowski JQ, McIntosh TK (1998) Experimental brain injury induces regionally distinct apoptosis during the acute and delayed post-traumatic period. *J Neurosci* 18:5663-5672.

24. Cooper E (1994) Neuron-specific enolase. *Int J Biol Markers* 4:205-210.

25. Copin JC, Li Y, Reola L, Chan PH (1998) Trolox and 6,7-dinitroquinoxaline-2,3-dione prevent necrosis but not apoptosis in cultured neurons subjected to oxygen deprivation. *Brain Res* 784: 25-36.

26. Cunningham RT, Watt M, Winder J, McKinstry S, Lawson JT, Johnston CF, Hawkins SA, Buchanan KD (1996) Serum neurone-specific enolase as an indicator of stroke volume. *Eur J Clin Invest* 26: 298-303.

27. Cunningham RT, Young IS, Winder J, O'Kane MJ, McKinstry S, Johnston CF, Dolan OM, Hawkins SA, Buchanan KD (1991) Serum neurone specific enolase (NSE) levels as an indicator of neuronal damage in patients with cerebral infarction. *Eur J Clin Invest* 21:497-500.

28. Dauberschmidt R, Zinsmeyer J, Mrochen H, Meyer M (1991) Changes of neuron-specific enolase concentration in plasma after cardiac arrest and resuscitation. *Mol Chem Neuropathol* 14:237-245.

29. Dirnagl U, Iadecola C, Moskowitz MA (1999) Pathobiology of ischaemic stroke: an integrated view. *Trends Neurosci* 22:391-397.

30. Donato R (1999) Functional roles of S100 proteins, calcium-binding proteins of the EF-hand type. *Biochim Biophys Acta* 1450:191-231.

31. Egon MR, Doppenberg SCC, Bullock R (1997) Clinical trials in TBI, what can we learn from previous studies. *Ann NY Acad Sci* 825:305-322.

32. Eldadah BA, Yakovlev AG, Faden AI (1997) The role of CED-3-related cysteine proteases in apoptosis of cerebellar granule cells. *J Neurosci* 17:6105-6113.

33. Ellis EF, McKinney JS, Willoughby KA, Liang S, Povlishock JT (1995) A new model for rapid stretch-induced injury of cells in culture: characterization of the model using astrocytes. *J Neurotrauma* 12:325-339.

34. Fischer I, Romano-Clarke G, Grynspan F (1991) Calpain-mediated proteolysis of microtubule associated proteins MAP1B and MAP2 in developing brain. *Neurochem Res* 16:891-898.

35. Flint JP, Pike BR , Hayes RL, Moffett JR, Dave JR, X.-CM Lu, and Tortella F (2002 In Press) Accumulation of calpain and caspase-3 cleaved alpha-II spectrin breakdown products in CSF after middle cerebral artery occulsion in rats. *J Neurotrauma* (in press).

36. Fraser A, Evan G (1996) A license to kill. *Cell* 85:781-784.

37. Goodman SR, Zimmer WE, Clark MB, Zagon IS, Barker JE, Bloom ML (1995) Brain spectrin: of mice and men. *Brain Res Bull* 36:593-606.

38. Gottron FJ, Ying HS, Choi DW (1997) Caspase inhibition selectively reduces the apoptotic component of oxygen-glucose deprivation-induced cortical neuronal cell death. *Mol Cell Neurosci* 9: 159-169.

39. Gwag BJ, Lobner D, Koh JY, Wie MB, Choi DW (1995) Blockade of glutamate receptors unmasks neuronal apoptosis after oxygen-glucose deprivation in vitro. *Neuroscience* 68:615-619.

40. Haimoto H, Hosoda S, Kato K (1987) Differential distribution of immunoreactive S100-alpha and S100-beta proteins in normal nonnervous human tissues. *Lab Invest* 57:489-498.

41. Hill MD, Jackowski G, Bayer N, Lawrence M, Jaeschke R (2000) Biochemical markers in acute ischemic stroke. *Cmaj* 162:1139-1140.

42. Horn M, Seger F, Schlote W (1995) Neuron-specific enolase in gerbil brain and serum after transient cerebral ischemia. *Stroke* 26:290-296; discussion 296-297.

43. Ingebrigtsen T, Romner B (2002) Biochemical Serum Markers of TBI. The Journal of Trauma Injury, Infection, and Critical Care, 52, 798-808.

44. Ingebrigtsen T Romner B, Trumpy JH (1997) Management of minor head injury: the value of early CT and serum protein S-100 measurements. *J Clin Neurosci* 4:29-33.

45. Irazuzta JE, de Courten-Myers G, Zemlan FP, Bekkedal MY, Rossi J, 3rd (2001) Serum cleaved Tau protein and neurobehavioral battery of tests as markers of brain injury in experimental bacterial meningitis. *Brain Res* 913:95-105.

46. Jacobs A, Put E, Ingels M, Put T, Bossuyt A (1996) One-year follow-up of technetium-99m-HMPAO SPECT in mild head injury. *J Nucl Med* 37: 1605-1609.

47. Jenkins LW, Moszynski K, Lyeth BG, Lewelt W, DeWitt DS, Allen A, Dixon CE, Povlishock JT, Majewski TJ, Clifton GL, Young HF, Becker DP, Hayes RL (1989) Increased vulnerability of the mildly traumatized rat brain to cerebral ischemia: the use of controlled secondary ischemia as a research tool to identify common or different mechanisms contributing to mechanical and ischemic brain injury. *Brain Res* 477:211-224.

48. Johnson EM, Jr., Greenlund LJ, Akins PT, Hsu CY (1995) Neuronal apoptosis: current understanding of molecular mechanisms and potential role in ischemic brain injury. *J Neurotrauma* 12:843-852.

49. Johnsson P (1996) Markers of cerebral ischemia after cardiac surgery. *J Cardiothorac Vasc Anesth* 10:120-126.

50. Jonas S, Aiyagari V, Vieira D, Figueroa M (2001) The failure of neuronal protective agents versus the success of thrombolysis in the treatment of ischemic stroke. The predictive value of animal models. *Ann N Y Acad Sci* 939:257-267.

51. Jonsson H, Johnsson P, Hoglund P, Alling C, Blomquist S (2000) Elimination of S100B and renal function after cardiac surgery. *J Cardiothorac Vasc Anesth* 14:698-701.

52. Jordan J, Galindo MF, Miller RJ (1997) Role of calpain- and interleukin-1 beta converting enzyme-like proteases in the beta-amyloid-induced death of rat hippocampal neurons in culture. *J Neurochem* 68:1612-1621.

53. Kaku Y, Yonekawa Y, Tsukahara T, Ogata N, Kimura T, Taniguchi T (1993) Alterations of a 200 kDa neurofilament in the rat hippocampus after forebrain ischemia. *J Cereb Blood Flow Metab* 13: 402-408.

54. Kampfl A, Posmantur R, Nixon R, Grynspan F, Zhao X, Liu SJ, Newcomb JK, Clifton GL, Hayes RL (1996) Mu-calpain activation and calpain-mediated cytoskeletal proteolysis following traumatic brain injury. *J Neurochem* 67:1575-1583.

55. Kampfl A, Posmantur RM, Zhao X, Schmutzhard E, Clifton GL, Hayes RL (1997) Mechanisms of calpain proteolysis following traumatic brain injury: implications for pathology and therapy: implications for pathology and therapy: a review and update. *J Neurotrauma* 14:121-134.

56. Kampfl A, Whitson JS, Zhao X, Posmantur R, Clifton GL, Hayes RL (1995) Calpain inhibitors reduce depolarization induced loss of tau protein in primary septo-hippocampal cultures. *Neurosci Lett* 194:149-152.

57. Kampfl A, Zhao X, Whitson JS, Posmantur R, Dixon CE, Yang K, Clifton GL, Hayes RL (1996) Calpain inhibitors protect against depolarization-induced neurofilament protein loss of septo-hippocampal neurons in culture. *Eur J Neurosci* 8:344-352.

58. Kant R, Smith-Seemiller L, Isaac G, Duffy J (1997) Tc-HMPAO SPECT in persistent post-concussion syndrome after mild head injury: comparison with MRI/CT. *Brain Inj* 11:115-124.

59. Kaya SS, Mahmood A, Li Y, Yavuz E, Goksel M, Chopp M (1999) Apoptosis and expression of p53 response proteins and cyclin D1 after cortical impact in rat brain. *Brain Res* 818:23-33.

60. Kesler SR, Adams HF, Bigler ED (2000) SPECT, MR and quantitative MR imaging: correlates with neuropsychological and psychological outcome in traumatic brain injury. *Brain Inj* 14:851-857.

61. Kochanek PM, Clark RS, Ruppel RA, Dixon CE (2001) Cerebral resuscitation after traumatic brain injury and cardiopulmonary arrest in infants and children in the new millennium. *Pediatr Clin North Am* 48:661-681.

62. Lammie GA, Piper IR, Thomson D, Brannan F (1999) Neuropathologic characterization of a rodent model of closed head injury--addition of clinically relevant secondary insults does not significantly potentiate brain damage. *J Neurotrauma* 16:603-615.

63. Laskowitz DT, Grocott HP, Hsia A, Copeland KR (1998) Serum Markers of Cerebral Ischemia. *J Stroke Cerebro Dis* 7:234-241.

64. Levi L, Guilburd JN, Lemberger A, Soustiel JF, Feinsod M (1990) Diffuse axonal injury: analysis of 100 patients with radiological signs. *Neurosurgery* 27:429-432.

65. Leviton A, Dammann O (2002) Brain damage markers in children. Neurobiological and clinical aspects. *Acta Paediatr* 91:9-13.

66. Lyeth BG, Jenkins LW, Hamm RJ, Dixon CE, Phillips LL, Clifton GL, Young HF, Hayes RL (1990) Prolonged memory impairment in the absence of hippocampal cell death following traumatic brain injury in the rat. *Brain Res* 526:249-258.

67. Martens P (1996) Serum neuron-specific enolase as a prognostic marker for irreversible brain damage in comatose cardiac arrest surviviors. *Acad Emerg Med* 3:126-131.

68. Martens P, Raabe A, Johnsson P (1998) Serum S-100 and neuron-specific enolase for prediction of regaining consciousness after global cerebral ischemia. *Stroke* 29:2363-2366.

69. Martin SJ, O'Brien GA, Nishioka WK, McGahon AJ, Mahboubi A, Saido TC, Green DR (1995) Proteolysis of fodrin (non-erythroid spectrin) during apoptosis. *J Biol Chem* 270:6425-6428.

70. Missler U, Wiesmann M, Friedrich C, Kaps M (1997) S-100 protein and neuron-specific enolase concentrations in blood as indicators of infarction volume and prognosis in acute ischemic stroke. *Stroke* 28:1956-1960.

71. Missler U, Wiesmann M, Wittmann G, Magerkurth O, Hagenstrom H (1999) Measurement of glial fibrillary acidic protein in human blood: analytical method and preliminary clinical results. *Clin Chem* 45:138-141.

72. Mitchener A, Wyper DJ, Patterson J, Hadley DM, Wilson JT, Scott LC, Jones M, Teasdale GM (1997) SPECT, CT, and MRI in head injury: acute abnormalities followed up at six months. *J Neurol Neurosurg Psychiatry* 62:633-636.

73. Miura M, Zhu H, Rotello R, Hartwieg EA, Yuan J (1993) Induction of apoptosis in fibroblasts by IL-1 beta-converting enzyme, a mammalian homolog of the C. elegans cell death gene ced-3. *Cell* 75:653-660.

74. Moore B (1965) A soluble protein characteristic of the nervous system. *Biochem Biophys Res Commun* 19:739-744.

75. Morioka M, Fukunaga K, Yasugawa S, Nagahiro S, Ushio Y, Miyamoto E (1992) Regional and temporal alterations in Ca2+/calmodulin-dependent protein kinase II and calcineurin in the hippocampus of rat brain after transient forebrain ischemia. *J Neurochem* 58:1798-1809.

76. Narayan RK, Michel ME, Ansell B, Baethmann A, Biegon A, Bracken MB, Bullock MR, Choi SC, Clifton GL, Contant CF, Coplin WM et al (2002) Clinical trials in head injury. *J Neurotrauma* 19: 503-557.

77. Nath R, Raser KJ, McGinnis K, Nadimpalli R, Stafford D, Wang KK (1996) Effects of ICE-like protease and calpain inhibitors on neuronal apoptosis. *Neuroreport* 8:249-255.

78. Nath R, Raser KJ, Stafford D, Hajimohammadreza I, Posner A, Allen H, Talanian RV, Yuen P, Gilbertsen RB, Wang KK (1996) Non-erythroid alpha-spectrin breakdown by calpain and interleukin 1 beta-converting-enzyme-like protease(s) in apoptotic cells: contributory roles of both protease families in neuronal apoptosis. *Biochem J* 319:683-690.

79. Neumar RW, Meng FH, Mills AM, Xu YA, Zhang C, Welsh FA, Siman R (2001) Calpain activity in the rat brain after transient forebrain ischemia. *Exp Neurol* 170:27-35.

80. Newcomb JK, Kampfl A, Posmantur RM, Zhao X, Pike BR, Liu SJ, Clifton GL, Hayes RL (1997) Immunohistochemical study of calpain-mediated breakdown products to alpha-spectrin following controlled cortical impact injury in the rat. *J Neurotrauma* 14:369-83.

81. Newcomb JK, Zhao X, Pike BR, Hayes RL (1999) Temporal profile of apoptotic-like changes in neurons and astrocytes following controlled cortical impact injury in the rat. *Exp Neurol* 158: 76-88.

82. NIH (1998) Rehabilitation of persons with traumatic brain injury. *NIH Consensus Statement* 16:1-41.

83. Nishida A, Emoto K, Shimizu M, Uozumi T, Yamawaki S (1994) Brain ischemia decreases phosphatidylcholine-phospholipase D but not phosphatidylinositol-phospholipase C in rats. *Stroke* 25:1247-1251.

84. Nitatori T, Sato N, Waguri S, Karasawa Y, Araki H, Shibanai K, Kominami E, Uchiyama Y (1995) Delayed neuronal death in the CA1 pyramidal cell layer of the gerbil hippocampus following transient ischemia is apoptosis. *J Neurosci* 15: 1001-1011.

85. Nygaard O, Langbakk B, Romner B (1998) Neuron-specific enolase concentrations in serum and cerebrospinal fluid in patients with no previous history of neurological disorder. *Scand J Clin Lab Invest* 58:183-186.

86. Ogata N, Yonekawa Y, Taki W, Kannagi R, Murachi T, Hamakubo T, Kikuchi H (1989) Degradation of neurofilament protein in cerebral ischemia. *J Neurosurg* 70:103-107.

87. Paterakis K, Karantanas AH, Komnos A, Volikas Z (2000) Outcome of patients with diffuse axonal injury: the significance and prognostic value of MRI in the acute phase. *J Trauma* 49:1071-1075.

88. Perini F, Morra M, Alecci M, Galloni E, Marchi M, Toso V (2001) Temporal profile of serum anti-inflammatory and pro-inflammatory interleukins in acute ischemic stroke patients. *Neurol Sci* 22: 289-296.

89. Pike BR, Flint J, Dutta S, Johnson E, Wang KK, Hayes RL (2001) Accumulation of non-erythroid alpha II-spectrin and calpain-cleaved alpha II-spectrin breakdown products in cerebrospinal fluid after traumatic brain injury in rats. *J Neurochem* 78:1297-1306.

90. Pike BR, Zhao X, Newcomb JK, Glenn CC, Anderson DK, Hayes RL (2000) Stretch injury causes calpain and caspase-3 activation and necrotic and apoptotic cell death in septo-hippocampal cell cultures. *J Neurotrauma* 17:283-298.

91. Pike BR, Zhao X, Newcomb JK, Posmantur RM, Wang KK, Hayes RL (1998) Regional calpain and caspase-3 proteolysis of alpha-spectrin after traumatic brain injury. *Neuroreport* 9:2437-2442.

92. Pike BR, Zhao X, Newcomb JK, Wang KK, Posmantur RM, Hayes RL (1998) Temporal relationships between de novo protein synthesis, calpain and caspase 3-like protease activation, and DNA fragmentation during apoptosis in septo-hippocampal cultures. *J Neurosci Res* 52:505-520.

93. Posmantur R, Hayes RL, Dixon CE, Taft WC (1994) Neurofilament 68 and neurofilament 200 protein levels decrease after traumatic brain injury. *J Neurotrauma* 11:533-545.

94. Posmantur R, Kampfl A, Siman R, Liu J, Zhao X, Clifton GL, Hayes RL (1997) A calpain inhibitor attenuates cortical cytoskeletal protein loss after experimental traumatic brain injury in the rat. *Neuroscience* 77:875-888.

95. Posmantur RM, Newcomb JK, Kampfl A, Hayes RL (2000) Light and confocal microscopic studies of evolutionary changes in neurofilament proteins following cortical impact injury in the rat. *Exp Neurol* 161:15-26.

96. Posmantur RM, Zhao X, Kampfl A, Clifton GL, Hayes RL (1998) Immunoblot analyses of the relative contributions of cysteine and aspartic proteases to neurofilament breakdown products following experimental brain injury in rats. *Neurochem Res* 23:1265-1276.

97. Raabe A, Grolms C, Keller M, Dohnert J, Sorge O, Seifert V (1998) Correlation of computed tomography findings and serum brain damage markers following severe head injury. *Acta Neurochir (Wien)* 140:787-791; discussion 791-792.

98. Raabe A, Grolms C, Seifert V (1999) Serum markers of brain damage and outcome prediction in patients after severe head injury. *Br J Neurosurg* 13:56-59.

99. Raabe A, Menon DK, Gupta S, Czosnyka M, Pickard JD (1998) Jugular venous and arterial concentrations of serum S-100B protein in patients with severe head injury: a pilot study. *J Neurol Neurosurg Psychiatry* 65:930-932.

100. Raghupathi R, Conti AC, Graham DI, Krajewski S, Reed JC, Grady MS, Trojanowski JQ, McIntosh TK (2002) Mild traumatic brain injury induces apoptotic cell death in the cortex that is preceded by decreases in cellular Bcl-2 immunoreactivity. *Neuroscience* 110:605-616.

101. Raghupathi R, Margulies SS (2002) Traumatic axonal injury after closed head injury in the neonatal pig. *J Neurotrauma* 19:843-853.

102. Riederer BM, Zagon IS, Goodman SR (1987) Brain spectrin(240/235) and brain spectrin(240/235E): differential expression during mouse brain development. *J Neurosci* 7:864-874.

103. Ringger NC, Silver X, O'Steen B, Brabham JG, Deford SM, Pike BR, Pineda J, Hayes RL (In Preparation) CSF Calpain-induced spectrin breakdown products predict injury magnitude and chronic lesion sized in a rat model of TBI.

104. Ringleb PA, Schellinger PD, Schranz C, Hacke W (2002) Thrombolytic therapy within 3 to 6 hours after onset of ischemic stroke: useful or harmful? *Stroke* 33:1437-1441.

105. Rink A, Fung KM, Trojanowski JQ, Lee VM, Neugebauer E, McIntosh TK (1995) Evidence of apoptotic cell death after experimental traumatic brain injury in the rat. *Am J Pathol* 147: 1575-1583.

106. Roine R O, Somer H, Kaste M, Viinikka L, Karonen S L (1989) Neurological outcome after out-of-hospital cardiac arrest. Prediction by cerebrospinal fluid enzyme analysis. *Arch Neurol* 46:753-756.

107. Romner B, Ingebrigtsen T, Kongstad P, Borgesen SE (2000) Traumatic brain damage: serum S-100 protein measurements related to neuroradiological findings. *J Neurotrauma* 17: 641-647.

108. Ross SA, Cunningham RT, Johnston CF, Rowlands BJ (1996) Neuron-specific enolase as an aid to outcome prediction in head injury. *Br J Neurosurg* 10:471-476.

109. Saatman KE, Bozyczko-Coyne D, Marcy V, Siman R, McIntosh TK (1996) Prolonged calpain-mediated spectrin breakdown occurs regionally following experimental brain injury in the rat. *J Neuropathol Exp Neurol* 55:850-860.

110. Saido TC, Sorimachi H, Suzuki K (1994) Calpain: new perspectives in molecular diversity and physiological-pathological involvement. *Faseb J* 8:814-822.

111. Scheidler MG, Shultz BL, Schall L, Ford HR (2000) Risk factors and predictors of mortality in children after ejection from motor vehicle crashes. *J Trauma* 49:864-868.

112. Schwartz SM, Duffy JY, Pearl JM, Nelson DP (2001) Cellular and molecular aspects of myocardial dysfunction. *Crit Care Med* 29:S214-219.

113. Sellman M, Ivert T, Ronquist G, Caesarini K, Persson L, Semb BK (1992) Central nervous system damage during cardiac surgery assessed by 3 different biochemical markers in cerebrospinal fluid. *Scand J Thorac Cardiovasc Surg* 26:39-45.

114. Shaw GJ, Jauch EC, Zemlan FP (2002) Serum cleaved tau protein levels and clinical outcome in adult patients with closed head injury. *Ann Emerg Med* 39:254-257.

115. Singhal A, Baker AJ, Hare GM, Reinders FX, Schlichter LC, Moulton RJ (2002) Association between Cerebrospinal Fluid Interleukin-6 Concentrations and Outcome after Severe Human Traumatic Brain Injury. *J Neurotrauma* 19:929-937.

116. Sloviter RS (1996) Hippocampal pathology and pathophysiology in temporal lobe epilepsy. *Neurologia* 11 Suppl 4:29-32.

117. Squier MK, Miller AC, Malkinson AM, Cohen JJ (1994) Calpain activation in apoptosis. *J Cell Physiol* 159:229-237.

118. Suzuki K, Sorimachi H, Yoshizawa T, Kinbara K, Ishiura S (1995) Calpain: novel family members, activation, and physiologic function. *Biol Chem Hoppe Seyler* 376:523-529.

119. Thomaidou D, Mione MC, Cavanagh JF, Parnavelas JG (1997) Apoptosis and its relation to the cell cycle in the developing cerebral cortex. *J Neurosci* 17:1075-1085.

120. Usui A, Kato K, Abe T, Murase M, Tanaka M, Takeuchi E (1989) S-100ao protein in blood and urine during open-heart surgery. *Clin Chem* 35: 1942-1944.

121. van Engelen BG, Lamers KJ, Gabreels FJ, Wevers RA, van Geel WJ, Borm GF (1992) Age-related changes of neuron-specific enolase, S-100 protein, and myelin basic protein concentrations in cerebrospinal fluid. *Clin Chem* 38:813-816.

122. Vanags DM, Porn-Ares MI, Coppola S, Burgess DH, Orrenius S (1996) Protease involvement in fodrin cleavage and phosphatidylserine exposure in apoptosis. *J Biol Chem* 271:31075-31085.

123. Villa PG, Henzel WJ, Sensenbrenner M, Henderson CE, Pettmann B (1998) Calpain inhibitors, but not caspase inhibitors, prevent actin proteolysis and DNA fragmentation during apoptosis. *J Cell Sci* 111:713-722.

124. Wang KK (2000) Calpain and caspase: can you tell the difference? *Trends Neurosci* 23:20-26.

125. Wang KK, Posmantur R, Nath R, McGinnis K, Whitton M, Talanian RV, Glantz SB, Morrow JS (1998) Simultaneous degradation of alphaII- and betaII-spectrin by caspase 3 (CPP32) in apoptotic cells. *J Biol Chem* 273:22490-22497.

126. Wang KK, Villalobo A, Roufogalis BD (1989) Calmodulin-binding proteins as calpain substrates. *Biochem J* 262:693-706.

127. Wang KK, Yuen PW (1994) Calpain inhibition: an overview of its therapeutic potential. *Trends Pharmacol Sci* 15:412-419.

128. Westaby S, Johnsson P, Parry AJ, Blomqvist S, Solem JO, Alling C, Pillai R, Taggart DP, Grebenik C, Stahl E (1996) Serum S100 protein: a potential marker for cerebral events during cardiopulmonary bypass. *Ann Thorac Surg* 61:88-92.

129. Woertgen C, Rothoerl RD, Holzschuh M, Metz C, Brawanski A (1997) Comparison of serial S-100 and NSE serum measurements after severe head injury. *Acta Neurochir (Wien)* 139:1161-1164; discussion 1165.

130. Woertgen C, Rothoerl RD, Metz C, Brawanski A (1999) Comparison of clinical, radiologic, and serum marker as prognostic factors after severe head injury. *J Trauma* 47:1126-1130.

131. Yakovlev AG, Knoblach SM, Fan L, Fox GB, Goodnight R, Faden AI (1997) Activation of CPP32-like caspases contributes to neuronal apoptosis and neurological dysfunction after traumatic brain injury. *J Neurosci* 17:7415-7424.

132. Yamazaki Y, Yada K, Morii S, Kitahara T, Ohwada T (1995) Diagnostic significance of serum neuron-specific enolase and myelin basic protein assay in patients with acute head injury. *Surg Neurol* 43:267-270; discussion 270-271.

133. Yang K, Taft WC, Dixon CE, Yu RK, Hayes RL (1994) Endogenous phosphorylation of a 61,000 dalton hippocampal protein increases following traumatic brain injury. *J Neurotrauma* 11: 523-532.

134. Ytrebo LM, Nedredal GI, Korvald C, Holm Nielsen OJ, Ingebrigtsen T, Romner B, Aarbakke J, Revhaug A (2001) Renal elimination of protein S-100beta in pigs with acute encephalopathy. *Scand J Clin Lab Invest* 61:217-225.

135. Zauner A, Bullock R (1995) The role of excitatory amino acids in severe brain trauma: opportunities for therapy: a review. *J Neurotrauma* 12:547-554.

136. Zemlan FP, Jauch EC, Mulchahey JJ, Gabbita SP, Rosenberg WS, Speciale SG, Zuccarello M (2002) C-tau biomarker of neuronal damage in severe brain injured patients: association with elevated intracranial pressure and clinical outcome. *Brain Res* 947:131-139.

Journal of Neuroscience Research 52:505–520 (1998)

Temporal Relationships Between De Novo Protein Synthesis, Calpain and Caspase 3-Like Protease Activation, and DNA Fragmentation During Apoptosis in Septo-Hippocampal Cultures

Brian R. Pike,[1] Xiurong Zhao,[1] Jennifer K. Newcomb,[1] Kevin K.W. Wang,[2] Rand M. Posmantur,[2] and Ronald L. Hayes[1]*

[1]Department of Neurosurgery, Vivian L. Smith Center for Neurologic Research, The University of Texas-Houston Health Science Center, Houston

[2]Department of Neuroscience Therapeutics, Parke-Davis Pharmaceutical Research, Warner-Lambert Company, Ann Arbor, Michigan

Caspase 3-like proteases are key executioners in mammalian apoptosis, and the calpain family of cysteine proteases has also been implicated as an effector of the apoptotic cascade. However, the influence of upstream events on calpain/caspase activation and the role of calpain/caspase activation on subsequent downstream events are poorly understood. This investigation examined the temporal profile of apoptosis-related events after staurosporine-induced apoptosis in mixed glial-neuronal septo-hippocampal cell cultures. Following 3 hr exposure to staurosporine (0.5 μM), calpain and caspase 3-like proteases processed α-spectrin to their signature proteolytic fragments prior to endonuclease-mediated DNA fragmentation (not evident until 6 hr), indicating that endonuclease activation is downstream from calpain/caspase activation. Cycloheximide, a general protein synthesis inhibitor, completely prevented processing of α-spectrin by calpains and caspase 3-like proteases, DNA fragmentation and cell death, indicating that de novo protein synthesis is an upstream event necessary for activation of calpains and caspase 3-like proteases. Calpain inhibitor II and the pan-caspase inhibitor Z-D-DCB each inhibited their respective protease-specific processing of α-spectrin and attenuated endonuclease DNA fragmentation and cell death. Thus, activation of calpains and caspase 3-like proteases is an early event in staurosporine-induced apoptosis, and synthesis of, as yet, unknown protein(s) is necessary for their activation. J. Neurosci. Res. 52:505–520, 1998. © 1998 Wiley-Liss, Inc.

Key words: α-spectrin; fodrin; CPP32; cysteine proteases; brain; rat; trauma

INTRODUCTION

Apoptosis is a genetically regulated type of cell death that is fundamental to embryonic development, serving to eliminate unnecessary cells in a variety of organs and tissues. This active process of cell eradication is characterized by morphologic features that are preserved across different cell types. These morphologic alterations include cell body shrinkage and plasma membrane blebbing which are followed by nuclear chromatin condensation, segmentation and migration of nuclear fragments to the nuclear membrane and the disintegration of the nucleus into discrete membrane bound fragments (Bredeson, 1995; Wyllie, 1980). Other features of at least some forms of apoptosis include internucleosomal DNA fragmentation by endonucleases into 180 base pair inter-

Abbreviations: AEBSF, 4-(2-aminoethyl)-benzenesulfonylfluoride; Calp-Inh-II, calpain inhibitor II (N-Acetyl-Leu-Leu-methioninal); EDTA, ethylenediaminetetraacetic acid; EGTA, ethylenebis(oxyethylenenitrilo) tetraacetic acid; DMEM, Delbecco's modified Eagle's medium; DPBS, Dulbecco's phosphate buffered saline; DTT, dithiothreitol; FDA, fluorescein diacetate; GFAP, glial fibrillary acid protein; HBSS, Hanks' balanced salt solution; MAP-2, microtubule associated protein-2; PI, propidium iodide; PMSF, phenylmethylsulfonyl fluoride; SDS, sodium dedocyl sulfate; TEMED, N,N,N′,N′-tetramethylethylenediamine; Z-D-DCB, carbobenzoxy-Asp-CH_2-OC(O)-2-6dichlorobenzene.

Contract grant sponsor: NINDS; Contract grant number: RO1-NS21458; Contract grant sponsor: The Vivian L. Smith Foundation for Neurologic Research.

*Correspondence to: Ronald L. Hayes, The University of Texas-Houston, Medical School Building, Department of Neurosurgery, Suite 7.154, 6431 Fannin St., Houston, TX 77030. Fax: (713) 500-7787. E-mail: rhayes@heart.med.uth.tmc.edu

Received 6 January 1998; Revised 9 February 1998; Accepted 10 February 1998

vals (Cohen and Duke, 1984; McConkey et al., 1989; Wyllie et al., 1980) and sensitivity to protein synthesis inhibitors (Cohen and Duke, 1984; McConkey et al., 1989; Wyllie et al., 1980). Recently, investigations have focused on a potential contributory role of apoptosis in various neuropathological conditions including hypoxia-ischemia (Johnson et al., 1995; Linnik et al., 1993, 1996; Shigeno et al., 1990), neurodegenerative diseases (Forloni et al., 1993; Loo et al., 1993) and traumatic brain injury (Colicos and Dash, 1996; Conti et al., 1996; Eldadah et al., 1996; Newcomb et al., 1997; Pravdenkova et al., 1996; Rink et al., 1995; Yakovlev et al., 1997).

The majority of studies of apoptosis have involved either regional and temporal descriptions of the appearance of apoptotic morphology after various in vivo models of neuronal pathology or in vitro characterizations of the effects of initiating triggers for apoptosis (e.g., serum and/or K^+ deprivation, glucocorticoids, irradiation, staurosporine) on genetic regulators of apoptosis (e.g., Bax, Bcl-2, Ced-3, Myc, p53, Ras) or on terminal phase events that produce the hallmark apoptotic phenotype. Although apoptosis may be initiated via numerous physiological triggers, different models of apoptosis all share a final common pathway of DNA fragmentation and/or characteristic morphological alterations (Squier et al., 1994). Thus, identification of intracellular regulators common to several apoptotic model systems and cell types could provide fundamental insights into critical mechanisms of apoptotic cell death.

Calpains are calcium-activated cysteine proteases that have been implicated in a variety of neuropathological conditions (Kampfl et al., 1997; Wang and Yuen, 1994; Yuen and Wang, 1996). Intracellular substrates for activated calpain include cytoskeletal proteins, calmodulin-binding proteins, enzymes involved in signal transduction, membrane proteins, and transcription factors (for reviews see Saido et al., 1994; Suzuki et al., 1995; Wang et al., 1989). Several recent investigations have implicated calpains as candidate intracellular regulators of apoptosis (Nath et al., 1996a,b; Martin et al., 1995; Squier et al., 1994). Importantly, calpain activation has been implicated in different models of apoptosis and in different cell types, including neurons (Behrens et al., 1995; Jordan et al., 1997; Nath et al., 1996a,b; Squier et al., 1994). In addition, members of the caspase family of cysteine proteases have also been implicated as important intracellular effectors of apoptosis in various cell lines and apoptotic models (Eldadah, et al., 1997; Fraser and Evan, 1996; Miura et al., 1993; Nath et al., 1996a,b; Zhivotovsky et al., 1997). The role of caspase 1 (ICE), caspase 3 (CPP32/YAMA/apopain), and caspase 3-like (caspase 3, 6, 7, 8, 9, 10) proteases has been the focus of a number of investigations. While the contribution of caspase 1 to apoptosis in the CNS is less clear (Cohen, 1997; Zhivotovsky et al., 1997), the caspase 3 family is of particular interest. For instance, caspase 3-like proteases have been shown to cleave a variety of cytoplasmic and nuclear proteins during apoptosis including non-erythroid α-spectrin (Martin et al., 1995; Nath et al., 1996a,b; Vanags et al., 1996), poly(ADP-ribose)polymerase (PARP) (Lazebnik et al., 1994), DNA-PK_{CS} (Waterhouse et al., 1996), the 70 kD protein component of the U1 nuclear ribonucleoprotein (Casciola-Rosen et al., 1994), lamin A (Lazebnik et al., 1995), SREBP-1 and SREBP-2 (Na et al., 1996), protein kinase C δ (Ghayur et al., 1996), and gelsolin (Kothakota et al., 1997). Importantly, few studies (e.g., Nath et al., 1996) have systematically examined the role of these two major families of cysteine proteases in models of neuronal apoptosis.

Although the general protein kinase inhibitor staurosporine [which has recently been found to act by inducing cytochrome *c* release from mitochondria (Kluck et al., 1997; Yang et al., 1997)] has been shown to induce apoptosis in a wide variety of in vitro cell systems (Bertrand et al., 1994), the effects of staurosporine on primary septo-hippocampal cells have not been examined. The hippocampus is a brain region particularly vulnerable to numerous CNS insults in vivo, including ischemia (Jenkins et al., 1989), brain trauma (Lyeth et al., 1990), and epilepsy (Sloviter, 1996). In addition, mounting evidence suggests that the hippocampus may also be prone to apoptotic cell death in various brain injury models (Honkaniemi et al., 1996; Nitatori et al., 1995; Colicos and Dash, 1996; Conti et al., 1996; Rink et al., 1995; Yakovlev et al., 1997). Thus, the use of primary septo-hippocampal cultures in vitro can enhance the understanding of various biochemical processes relevant to CNS neuropathology, including apoptotic cell death.

This investigation examined calpain and caspase 3-like proteolysis of the cytoskeletal protein α-spectrin and caspase 3-like processing of PARP in mixed rat glial-neuronal septo-hippocampal cell cultures following exposure to the pro-apoptotic compound staurosporine. In neuronal cells undergoing apoptosis, α-spectrin is cleaved by calpains and caspase 3-like proteases to yield unique proteolytic fragments that are specific to each family of cysteine proteases (Nath et al., 1996a,b; Roberts-Lewis et al., 1994). This study provides the first systematic evidence that: (1) both calpain and caspase 3-like activation, inferred by proteolysis of the cytoskeletal protein α-spectrin, are downstream events from de novo protein synthesis, but upstream from endonuclease DNA fragmentation, (2) de novo protein synthesis is a requirement for activation of both calpains and caspase 3-like proteases, and (3) both calpain and caspase 3-like activation contribute to staurosporine-induced apoptosis, and co-administration of calpain and caspase inhibitors provides better protection against α-spectrin proteolysis,

DNA fragmentation and cell death than either inhibitor alone. In addition, this study provides evidence that staurosporine-induced cell death occurs primarily in neurons rather than in astroglia in mixed neuronal-glia primary septo-hippocampal co-cultures.

MATERIALS AND METHODS

Septo-Hippocampal Cultures

Eighteen-day-old rat fetuses were removed from deeply anesthetized dams. Septi and hippocampi were dissected in a dissection buffer (HBSS, with 4.2 mM bicarbonate, 1 mM pyruvate, 20 mM HEPES, 3 mg/ml BSA, pH 7.25). After rinsing in DMEM-DM, tissue was dissociated by trituration through the narrow pore of a flame-constricted Pasteur pipette. The dissociated cells were then resuspended in DMEM with 10% fetal calf serum (DMEM-10S) and plated on 24-well poly-L-lysine coated plastic culture plates or 12 mm of German glass (Erie Scientific Co.) at a density of 4.36×10^5 cells/mL. Cultures were maintained in a humidified incubator in an atmosphere of 5% CO_2 at 37°C. After 5 days of culture, the media was changed to DMEM-DM. Subsequent medium changes were carried out three times a week. By day 10 in vitro, astrocytes formed a confluent monolayer beneath morphologically mature neurons.

Pharmacological Treatment of Septo-Hippocampal Cells

Staurosporine. Ten-day-old septo-hippocampal cultures were challenged with 0.05–2.0 μM of staurosporine in DMEM-DM and cell viability was monitored at various post-injury time points. Staurosporine was added directly to the media for the entire duration of experiments. Following staurosporine challenge, cells were fixed for staining, or protein or DNA extraction was performed.

Calpain, caspase, and protein synthesis inhibitors. Sister cultures were pretreated with either 37.5 μM calpain inhibitor II (CalpInh-II) (Boehringer Mannheim, cat. no. 1-086-103), 30 μM of the pan-caspase inhibitor Z-D-DCB (Parke-Davis Warner Lambert), or 1 μg/mL of the protein synthesis inhibitor cycloheximide 1 hr prior to staurosporine challenge. The inhibitor concentrations used have been previously shown to provide optimal inhibition of calpains (Kampfl et al., 1996), caspase 3-like proteases (Nath et al., 1996a,b), and protein synthesis (Koh et al., 1995; Martin et al., 1988). As pointed out below, experimental procedures allowed independent confirmation that the concentrations of CalpInh-II and Z-D-DCB used in this study potently inhibit calpains and caspase 3-like proteases. Following each experiment, cells were fixed for staining, or protein or DNA extraction was performed.

Morphological Assessments of Cell Damage

Fluorescein diacetate and propidium iodide assay of cell viability. Fluorescein diacetate (FDA) and propidium iodide (PI) dyes were used to assess cell viability at 3 hr and 6 hr after staurosporine incubation. FDA enters normal cells where it is cleaved by esterases and emits a green fluorescence. Once cleaved, FDA can no longer permeate cell membranes. Propidium iodide is an intravital dye that is normally excluded from cells. After injury, PI penetrates cells and binds to DNA in the nucleus and emits a red fluorescence. This technique is commonly used to quantitate cell injury (Jones and Senft, 1985). Per Jones and Senft (1985), a stock solution of FDA (20 mg/ml) was dissolved in acetone. A PI stock solution was prepared by dissolving 5 mg/mL in 1 × PBS. The FDA and PI working solutions were freshly prepared by adding 10 μL of the FDA and 3 μL of PI stock to 10 mL of Dulbecco's phosphate buffered saline (DPBS). Two hundred microliters per well of FDA/PI working solution was added directly to the cells. The cells were stained for 3 min at room temperature and then put on ice. Stained cells were examined with a fluorescence microscope equipped with epi-illumination, band pass 450–490 nm exciter filter, 510 nm chromatic beam splitter, and a long pass 520 nm barrier filter. This filter combination permitted both green and red fluorescing cells to be seen simultaneously. The percent of viable cells in control cultures and following staurosporine insult (with or without protease and protein synthesis inhibitors) at different time points was determined from three separate experiments using FDA/PI. The cell viability can be determined since this procedure results in the nuclei of dead cells fluorescing red while the cytoplasm of living cells fluoresces green. Cell loss was calculated in 100× fields (five sequential 100× fields were counted and averaged per well) for three wells in each experiment as a percent of total cell number.

Hoechst staining of apoptotic nuclei. Following overnight fixation in 4% paraformaldehyde (PFA) at 4°C, cells grown on German glass were washed three times with PBS and labeled with 1 μg/mL of the adenine-thymine-base-pair-specific DNA dye Hoechst 33258 (bisbenzimide; Sigma) in PBS for 5–10 min at room temperature, using enough solution to cover the cells completely. The cells were rinsed twice with PBS and then mounted with crystal-mount medium (Biomeda). Cells were observed and photographed on a phase and fluorescence microscope with a UV2A filter.

DNA Fragmentation Assay

DNA gel electrophoresis was done as described in Gong et al. (1994). Briefly, cells were collected in the same manner as for immunoblotting. Cells in each

treatment condition were collected by centrifugation and fixed in suspension in 70% cold ethanol and stored in the fixative at −20°C (24–72 hr). Cells were then centrifuged at 800*g* for 5 min and the ethanol was thoroughly removed. The cell pellets were resuspended in 40 μL of phosphate-citrate buffer consisting of 192 parts of 0.2 M Na_2HPO_4 and 8 parts of 0.1 M citric acid (pH 7.8) at room temperature for 1 hr. After centrifugation at 1,000*g* for 5 min, the supernatant was transferred to new tubes and concentrated by vacuum in a SpeedVac concentrator for 15–30 min. Three microliters of 0.25% Nonidet NP-40 in distilled water was then added, followed by 3 μL of a solution of DNase-free RNase (1 mg/mL). After 30 min incubation at 37°C, 3 μL of a solution of proteinase K (1 mg/mL) was added and the extract was incubated for additional 30 min at 37°C. After the incubation, 1 μL of 6 × loading buffer (0.25% bromophenol blue, 0.25% xylene cyanol FF, 30% glycerol in water) was added and the entire content of the tube was transferred to a 1.5% agarose gel and electrophoresis was performed in 1 × TBE (0.1 M Tris, 0.09 M boric acid, 1 mM EDTA, pH 8.4) at 40 V for 2 hr. The DNA in the gels was visualized and photographed under UV light after staining with 5 μg/mL of ethidium bromide.

Assessment of α-Spectrin and PARP Degradation

SDS-polyacrylamide gel electrophoresis and immunoblotting. At the end of an experiment, cells were harvested from five identical culture wells and collected in 15 ml centrifuge tubes. The medium was removed and the pellet cells were rinsed with 1 × PBS. Cells were lysed in ice cold homogenization buffer [20 mM Tris-HCl (pH 7.6), 5 mM EDTA, 5 mM EGTA, 1 mM DTT, 0.5 mM PMSF, 10 μg/mL AEBSF, 5 μg/mL Leupeptin] for 30 min, and sheared through a 1.0 mL syringe 15 times with a 25 gauge needle. Protein content in the samples was assayed by the Micro BCA method (Pierce, Rockford, IL). For protein electrophoresis, equal amounts of total protein (30 μg) were prepared in twofold loading buffer containing 0.25 M Tris (pH 6.8), 0.2 M DTT, 8% SDS, 0.02% Bromophenol Blue, and 20% glycerol, and heated at 95°C for 10 min. Samples were resolved in a vertical electrophoresis chamber using a 4% stacking gel over a 7% acrylamide resolving gel for 1 hr at 200 V. For immunoblotting, separated proteins were laterally transferred to nitrocellulose membranes (0.45 μM) using a transfer buffer consisting of 0.192 M glycine and 0.025 Tris (pH 8.3) with 10% methanol at a constant voltage of 100 V for 1 hr at 4°C. Blots were blocked overnight in 5% non-fat milk in 20 mM Tris, 0.15 M NaCl, and 0.005% Tween-20 at 4°C. Comassie blue and Panceau red (Sigma, St. Louis, MO) were used to stain gels and nitrocellulose membranes (respectively) to confirm that equal amounts of protein were loaded in each lane.

Antibodies and immunolabeling. Immunoblots were probed with an anti-α-spectrin monoclonal antibody (Affiniti Research Products, UK; cat. no. FG 6090, clone AA6) that detects intact α-spectrin (240 kD) and 150, 145, and 120 kD SBDPs. The 150 kD SBDP has been reported to be a spectrin cleavage product of calpain and caspase proteases (Nath et al., 1996a,b). However, the 145 kD SBDP is a specific proteolytic fragment of calpain (Nath et al., 1996a,b). In addition, the 120 kD SBDP is reported to be a specific proteolytic fragment of caspase 3-like activation (Nath et al., 1996a,b). Following incubation with the primary antibody (1:4,000 dilution) for 2 hr at room temperature, the blots were incubated in peroxidase-conjugated sheep anti-mouse IgG for 1 hr (dilution, 1:10,000). Enhanced chemiluminescence reagents (ECL, Amersham) were used to visualize the immunolabeling on Hyperfilm (Hyperfilm ECL, Amersham). Following ECL reaction, nitrocellulose membranes were stripped of their primary and secondary antibodies by submerging membranes in 100 mM 2-mercaptoethanol, 2% SDS, 62.5 mM Tris (pH 6.7) and incubated at 60°C for 30 min. Membranes were then reprobed with an antibody (Ab38; 1:1,000) that recognizes the calpain-specific 150 kD SBDP (Roberts-Lewis et al., 1994), or with anti-poly(ADP-ribose) polymerase (PARP; 1:1,000; BioMol, Plymouth Meeting, PA, cat. no. SA-252). PARP is an enzyme involved in DNA repair and in the regulation of Ca^{2+}/Mg^{2+}-dependent endonuclease (Nelipovich et al., 1988). PARP is cleaved preferentially by caspase 3-like proteases (Rosen and Casciola-Rosen, 1997) from a 116 kD form to a 85 kD fragment (Nicholson et al., 1995), and PARP cleavage is a common occurrence in numerous apoptotic systems (Cohen, 1997). The PARP antibody also labeled a non-specific band at approximately 120 kD. Because the PARP antibody was raised against human PARP, the reactivity is a non-specific cross-species interaction. Ab38 was a generous gift of Dr. Robert Siman, Cephalon Inc., West Chester, PA. GFAP (polyclonal; Sigma) and MAP-2 (monoclonal; Sternberger) were used for immunocytochemistry.

Hoechst 33258 Staining in Glial or Neuronal Cell Types

To determine the effects of staurosporine on astroglial and neuronal cell types, cultures were labeled immunocytochemically with GFAP (for astroglia) or MAP-2 (for neurons) and counterstained with Hoechst 33258. Cultures were fixed in 4% PFA for 1 hr at 4°C and washed and stored in 1 × PBS. The cultures were permeabilized with 0.3% Triton X-100 for 30 min and blocked with 1% normal horse or goat serum at room temperature for 1 hr, followed by incubation with GFAP (1:1,000) or MAP-2 (1:1,000) antibody overnight at 4°C. The cultures were then washed three times in 1 × PBS

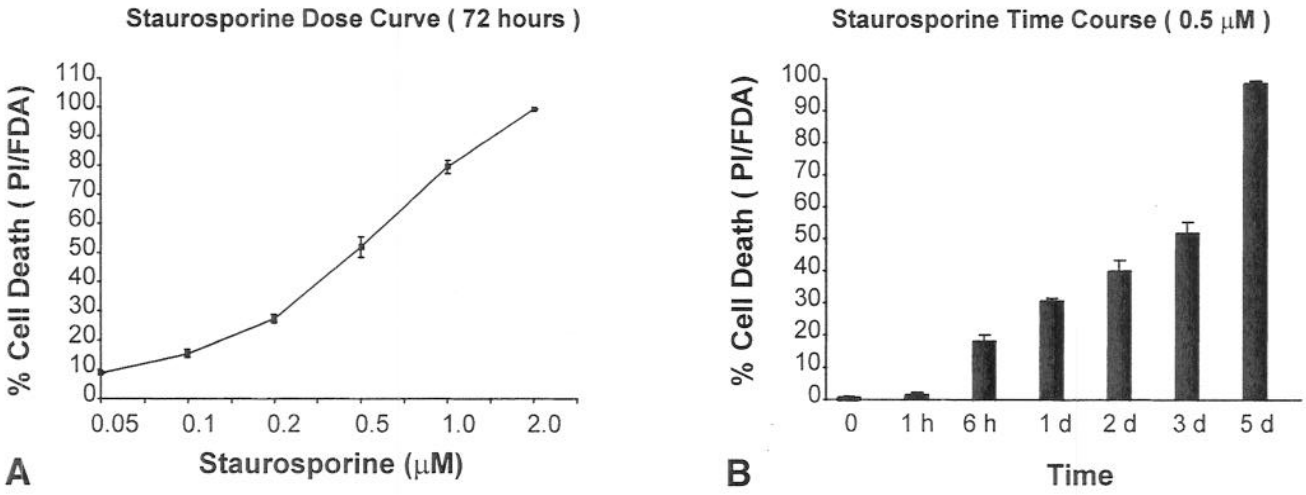

Fig. 1. Concentration and time course assays of staurosporine-induced cell death. **A:** LD_{50} for staurosporine was 0.5 μM after 72 hr of incubation. **B:** Percent cell death following exposure to 0.5 μM of staurosporine for various durations. The 0.5 μM concentration was used for all subsequent experiments.

and incubated in horseradish peroxidase conjugated goat anti-rabbit IgG (for GFAP) or sheep anti-mouse IgG (for MAP-2) (Cappel, 1;1,000) for 1 hr. Cultures were washed three times in 1 × PBS and diaminobenzidine (DAB) (Vector) was used to visualize the reaction. Following incubation in DAB, the reaction was stopped in tap water and the cultures were counterstained with Hoechst 33258 for 5 min. Following a final wash, the cells were mounted and coverslipped with Cytoseal 280 mounting medium (Stephens). Each slide was observed and photographed in the same field using light (for immunolabeled cells) and fluorescence (for Hoechst 33258 labeled cells) microscopy. A phase contrast microscope (axiovert 135) was used to distinguish glial and neuronal cell types based on immunocytochemical staining and/or phenotypical characteristics.

Statistical Analyses

Each experiment was performed three times and data were evaluated by analysis of variance (ANOVA) with a post hoc Tukey test. Values are given as mean SEM. Differences were considered significant if $P < 0.05$.

RESULTS

Effects of Staurosporine on Septo-Hippocampal Glial-Neuronal Co-Cultures

Dose- and time-dependent cell death. An initial dose-response assay was performed to determine the concentration of staurosporine to be used for all subsequent experiments. Propidium iodide and fluorescein diacetate were used to assess cell death and membrane integrity. Exposure of septo-hippocampal cultures to 0.05–2.0 μM of staurosporine induced dose-dependent cell death with an LD_{50} for 0.5 μM staurosporine at 72 hr (Fig. 1A). The 0.5 μM concentration was used for all experiments, and this concentration has been used to induce apoptosis in other cell systems (Bertrand et al., 1994; Nath et al., 1996a). The percentage of cells that stained for PI following exposure to 0.5 μM staurosporine was 3, 5, 13, 32, 42, 50, and 87% at 1 hr, 3 hr, 6 hr, 24 hr, 48 hr, 72 hr, and 120 hr (respectively) (Fig. 1B).

Morphological response to staurosporine challenge. Staurosporine-treated septo-hippocampal cultures underwent morphological alterations in cell structure that are characteristic of apoptosis (Falcieri et al., 1993). For example, at 1 hr following 0.5 μM staurosporine, blebbing of the cytoplasmic membrane was apparent with no significant nuclear uptake of PI. Following exposure to staurosporine for increasingly longer durations, the number of cells demonstrating membrane blebbing and nuclear uptake of PI increased (Fig. 2).

In order to confirm the apoptotic response of staurosporine on septo-hippocampal cultures, Hoechst 33258 was used to stain nuclear chromatin. Hoechst 33258 staining detected chromatin condensation along the periphery of the nuclear envelope, followed by fragmentation of the nucleus into dense micronuclear bodies (Fig. 3). High magnification (100× objective) fluorescence microscopy did not reveal any nuclear morphological alterations at 1 hr. After 3 hr, some nuclei demonstrated alterations in nuclear shape with slight condensation of chromatin (Fig. 3B,G). However, by 6 hr,

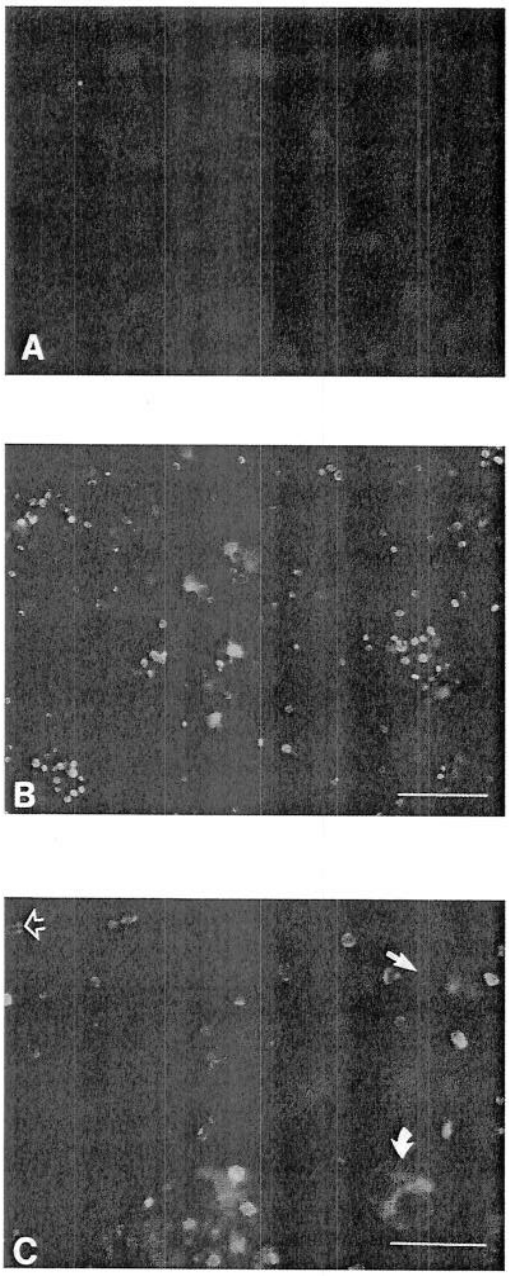

Fig. 2. Fluorescein diacetate (FDA) and propidium iodide (PI) staining of septo-hippocampal cultures undergoing apoptosis. **A:** Control cultures. Note normal somal structure in cells that take up FDA (green fluorescence) and the lack of PI uptake. **B,C:** By 24 hr of staurosporine challenge, numerous cells have lost retention of FDA and bind PI to their nucleus (red fluorescence). In addition, membrane blebbing is evident in most cells staining for FDA, indicating a preserved integrity of the plasma membrane characteristic of apoptosis. C: Curved arrow, membrane blebbing; closed arrow, nuclear uptake of PI; open arrow, apoptotic nucleus. Scale bars = 10 μm (B) and 5 μm (C).

condensation and migration of chromatin to the nuclear envelope was evident in some cells (Fig. 3C,H). By 24 hr, numerous cells were observed to be in various stages of nuclear disassembly, including nuclear condensation, migration of chromatin to the periphery of the nucleus, and the formation of dense apoptotic bodies (Fig. 3D,I). By 72 hr, there was a faded and diffuse fluorescence of Hoechst 33258, indicating digestion of the chromatin, possibly by endonucleases and/or by phagocytes (Fig. 3E,F).

DNA fragmentation. Condensation and aggregation of chromatin at the nuclear membrane may occur independent of endonuclease activation (Oberhammer et al., 1993). Thus, a DNA fragmentation assay was used to assess whether the apoptotic response to staurosporine in septo-hippocampal cultures, indicated by Hoechst 33258 staining, was associated with endonuclease activity. Figure 4A shows the characteristic pattern of nucleosomal sized DNA fragments following exposure to 0.5 μM staurosporine. Although Hoechst 33258 revealed migration of chromatin to the nuclear envelope at 3 hr, there was no DNA ladder at this time point (Fig. 4B). However, a pronounced ladder of fragmented DNA was evidenced at 6, 24, and 72 hr following staurosporine administration (Fig. 4A).

Staurosporine induces selective neuronal apoptosis in septo-hippocampal cultures. To identify the kind of cell (i.e., astroglial vs. neuronal) committed to apoptosis, cultures were stained with Hoechst 33258 and with GFAP (for astrocytes) or with MAP-2 (for neurons). The neuronal layer stained with MAP-2 (or identified morphologically in the absence of MAP-2 labeling) demonstrated a dramatic loss of MAP-2 immunolabeling. Loss of MAP-2 immunoreactivity preceded neuronal chromatin condensation revealed by Hoechst 33258 staining. This finding suggests that calpain and/or other protease activation (responsible for MAP-2 processing) is an event upstream from nuclear chromatin condensation (Fig. 5A,B). In contrast, exposure to high concentrations of staurosporine (2.0 μM; data not shown) for as long as 72 to 120 hr produced widespread, but reversible alter-

Fig. 3. Course of nuclear morphologic alterations during staurosporine-induced apoptosis. **A,F:** Hoechst 33258 nuclear stain of normal control cultures. **B,G:** Staurosporine, 3 hr: alterations in nuclear shape and slight chromatin condensation are evident. **C,H:** Staurosporine, 6 hr: increased condensation and migration of chromatin to nuclear envelope. **D,I:** Staurosporine, 24 hr: numerous cells in various stages of nuclear disassembly, including chromatin condensation, migration, and formation of dense apoptotic bodies. **E,J:** Staurosporine, 72 hr: faded and diffuse fluorescence of Hoechst 33258 indicating digestion of the chromatin by endonucleases and/or phagocytes. Scale bars = 10 μm (A,B,C,D,E) and 1 μm (F,G,H,I,J).

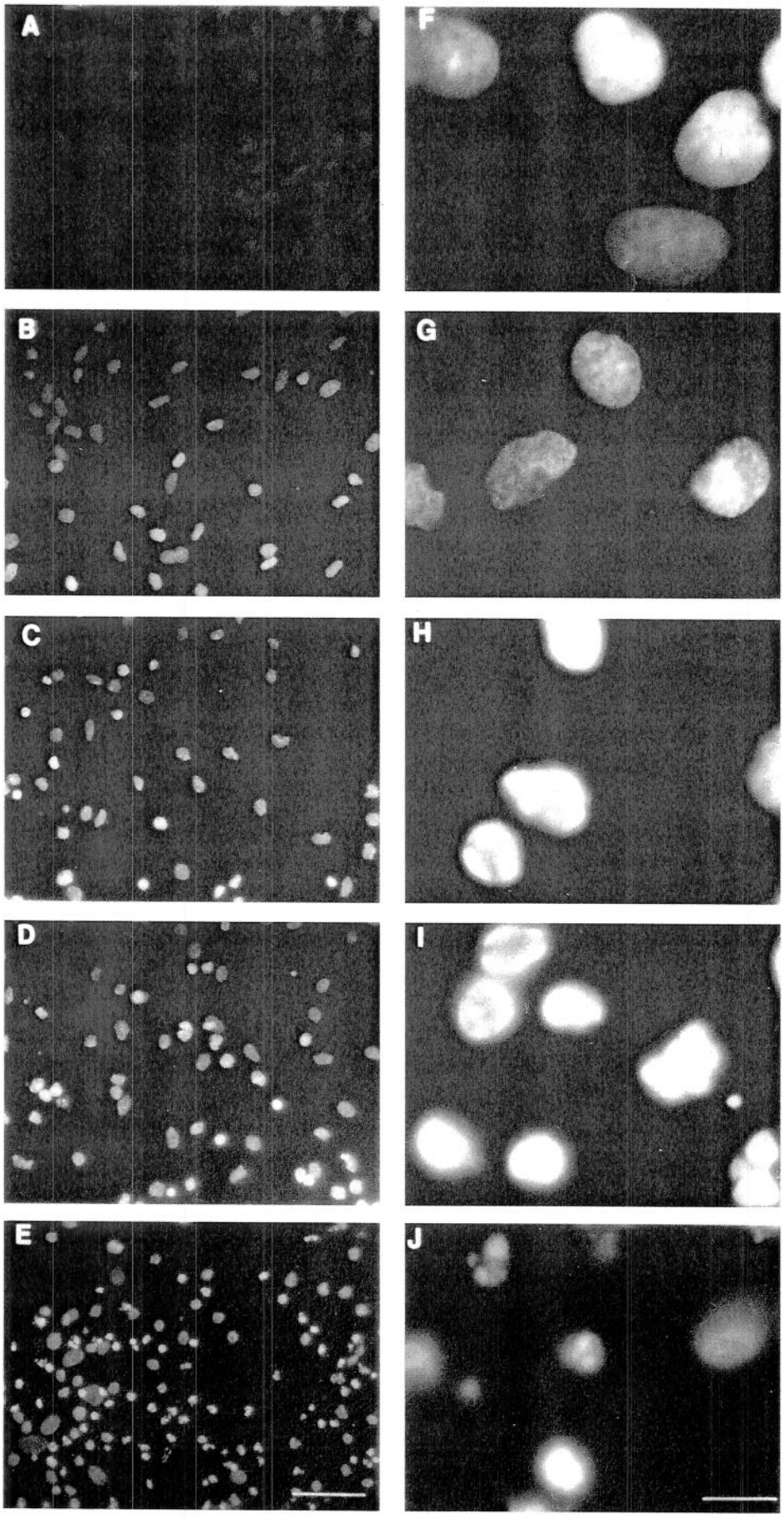

Figure 3.

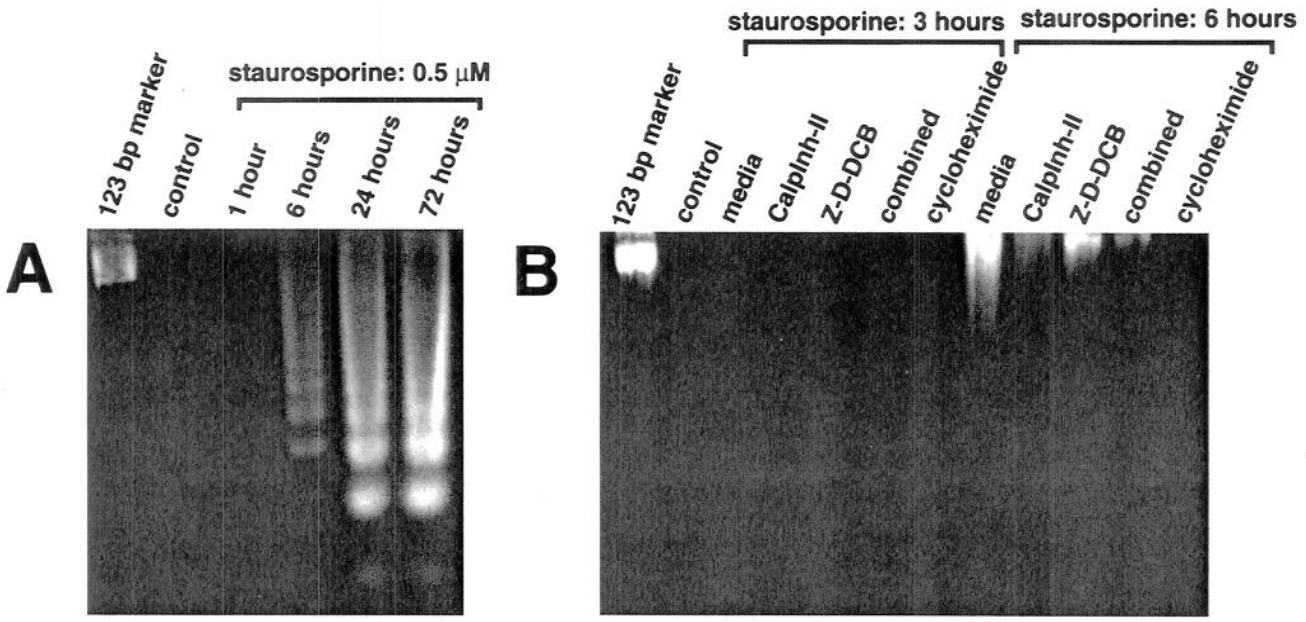

Fig. 4. Time course oligonucleosomal sized fragmentation of DNA by endonucleases and inhibition by CalpInh-II, Z-D-DCB, and cycloheximide. **A:** Staurosporine-induced apoptosis is associated with DNA laddering on agarose gels at 6, 24, and 72 hr, but not at 1 or 3 hr (A,B). **B:** Endonuclease DNA fragmentation is differentially attenuated by CalpInh-II, Z-D-DCB, CalpInh-II + Z-D-DCB, and cycloheximide with cycloheximide and the combined inhibitors producing the most marked effect.

ations in astrocyte morphology (i.e., vacuolization) and only limited astrocytic cell death (data not shown). However, concentrations of staurosporine below 2.0 μM did not kill astrocytes or alter the pattern of GFAP staining (Fig. 5C). In addition, phase contrast microscopy revealed that the astrocytic cell layer was completely void of overt chromatin condensation or segmentation at all time points following staurosporine administration (Fig. 5D).

Calpain and Caspase 3-Like Proteolysis of α-Spectrin and PARP

In addition to causing apoptosis, exposure to 0.5 μM staurosporine caused a time dependent proteolysis of neuronal α-spectrin by calpain and caspase 3-like proteases (Fig. 6A,B). At 3 hr following staurosporine administration, there was an increase in caspase 3-like specific 120 kD SBDP (Fig. 6A) and calpain-specific 150 kD SBDP (Fig. 6B). At 6 hr following staurosporine administration, the native 240 kD α-spectrin protein was undetectable on immunoblots while further processing of α-spectrin to the caspase 3-like specific 120 kD SBDP (Fig. 6A) and the calpain-specific 150 kD SBDP (Fig. 6B) was evident (Fig. 6A). Additionally, processing of PARP (116 kD) to a 85 kD fragment by caspase 3-like proteases was readily detected at 3 hr (Fig. 6C). Importantly, although proteolysis of α-spectrin by calpain and caspase 3-like proteases, and PARP by caspase 3-like protease was evident by 3 hr following staurosporine administration, DNA laddering was not evident at this time point (Fig. 4B). These results indicate that processing of α-spectrin by calpain and caspase 3-like proteases and processing of PARP by caspase 3-like protease are events initiated at some time prior to endonuclease activation and subsequent DNA fragmentation.

Effects of CalpInh-II, Z-D-DCB, or Cycloheximide on α-Spectrin and PARP Proteolysis, DNA Fragmentation, and Cell Viability

To investigate the relative contributory effects of calpain and/or caspase 3 or caspase 3-like proteases on staurosporine-induced cell viability, α-spectrin and PARP proteolysis, and on the apoptotic response in primary septo-hippocampal cultures, the effects of a calpain inhibitor (CalpInh-II), a pan-caspase inhibitor (Z-D-DCB), or a non-selective inhibitor of protein synthesis (cycloheximide) were examined. In addition, the co-administration of CalpInh-II and Z-D-DCB was also investigated.

α-Spectrin and PARP proteolysis. Three hours following staurosporine-induced apoptosis in primary septo-hippocampal cultures, 37.5 μM CalpInh-II slightly increased the level of native 240 kD α-spectrin (Fig. 6A) and almost completely blocked the formation of the calpain-specific 150 kD SBDP (Fig. 6B). CalpInh-II had

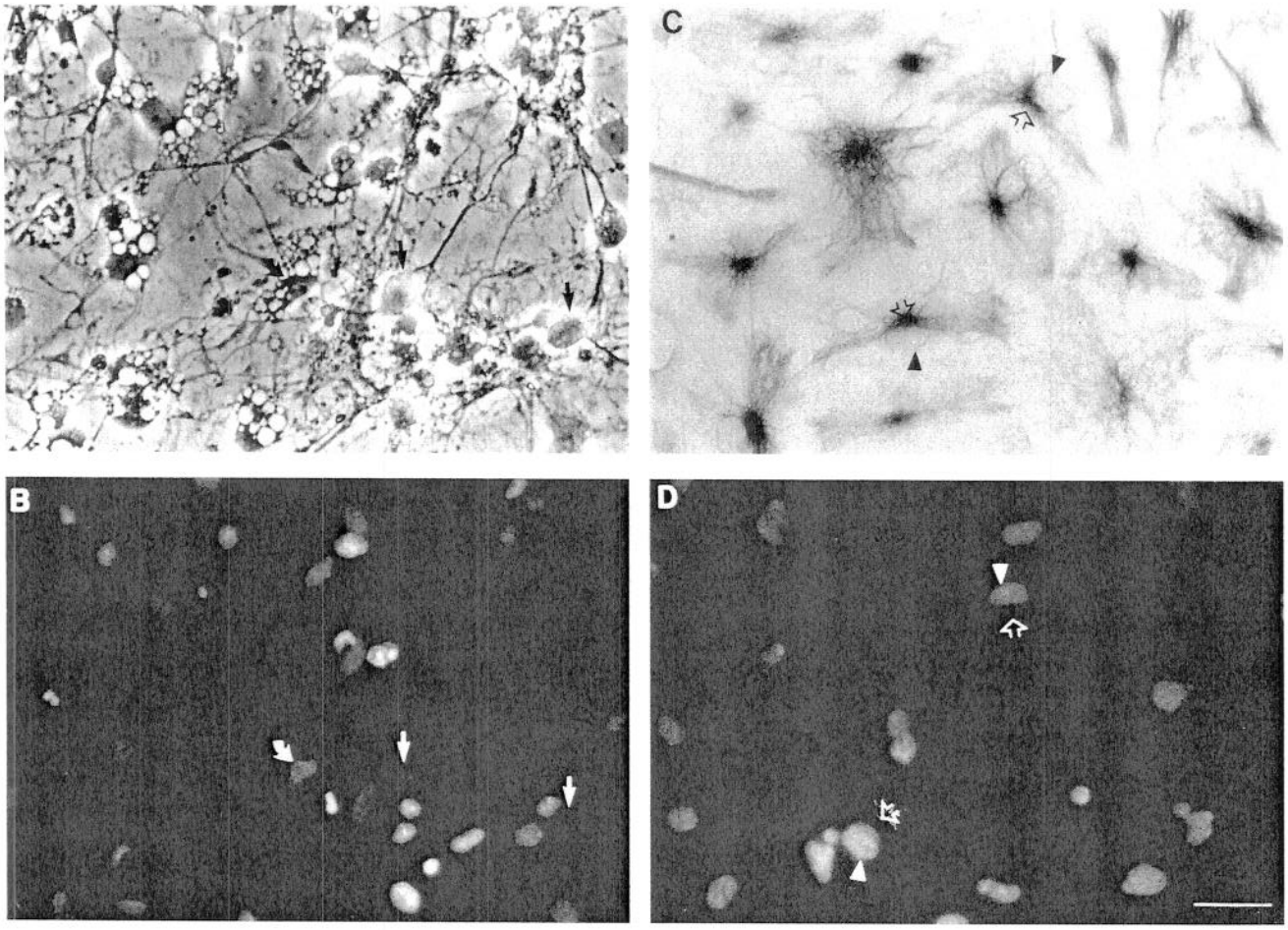

Fig. 5. Apoptosis in neuronal but not astroglial cell types in mixed glial-neuronal septo-hippocampal cultures. Phase-contrast light microscopy of double labeled neurons stained with MAP-2 (**A**) and Hoechst 33258 (**B**), or astroglial cells double labeled with GFAP (**C**) and Hoechst 33258 (**D**). Neurons underwent a dramatic loss in MAP-2 immunolabeling that preceded chromatin condensation revealed by the Hoechst stain. Neurons stained with MAP-2 (straight arrow, A) were only weakly positive for Hoechst 33258 (straight arrow, B). Apoptotic neurons that have lost MAP-2 immunoreactivity but demonstrate a neuronal phenotype (curved arrow, A) show increased Hoechst staining (curved arrow, B) and morphology characteristic of membrane blebbing. In contrast, astroglial morphology is well preserved (C) and astroglial nuclei show little or no staining for Hoechst 33258 (D). Closed arrowheads (C,D) indicate neurons that are not immunoreactive for GFAP but are Hoechst 33258 positive. Open arrowheads (C,D) indicate GFAP positive astroglia that are not positive for Hoechst 33258. Scale bar = 3 μm.

no effect on the caspase 3-like specific 120 kD SBDP. In contrast, 30 μM Z-D-DCB had no effect on the calpain-specific 150 kD SBDP. However, Z-D-DCB almost completely blocked the accumulation of the caspase 3-like specific 120 kD SBDP and resulted in an increased level of the non-specific 150 kD SBDP. The protein synthesis inhibitor, cycloheximide (1 μg/mL), completely prevented the accumulation of all SBDPs regardless of the antibody employed. In addition, accumulation of the caspase 3-like specific 85 kD fragment to PARP was blocked by Z-D-DCB and cycloheximide at 3 hr after staurosporine administration (Fig. 6C).

Six hours following staurosporine-induced apoptosis in primary septo-hippocampal cultures, CalpInh-II almost completely blocked the formation of the calpain-specific 150 kD SBDP and had no effect on the caspase 3-like specific 120 kD SBDP (Fig. 6A,B). However, CalpInh-II was unable to preserve any detectable levels of the native 240 kD α-spectrin protein (Fig. 6A). In contrast, Z-D-DCB almost completely blocked the formation of the caspase 3-like specific 120 kD SBDP and had no effect on the calpain-specific 150 kD SBDP (Fig. 6A,B). As with CalpInh-II, Z-D-DCB was unable to preserve any detectable levels of the native 240 kD α-spectrin protein (Fig. 6A). However, the combination of CalpInh-II + Z-D-DCB was able to attenuate loss of native 240 kD α-spectrin (Fig. 6D). The protein synthesis inhibitor, cycloheximide, completely prevented the accu-

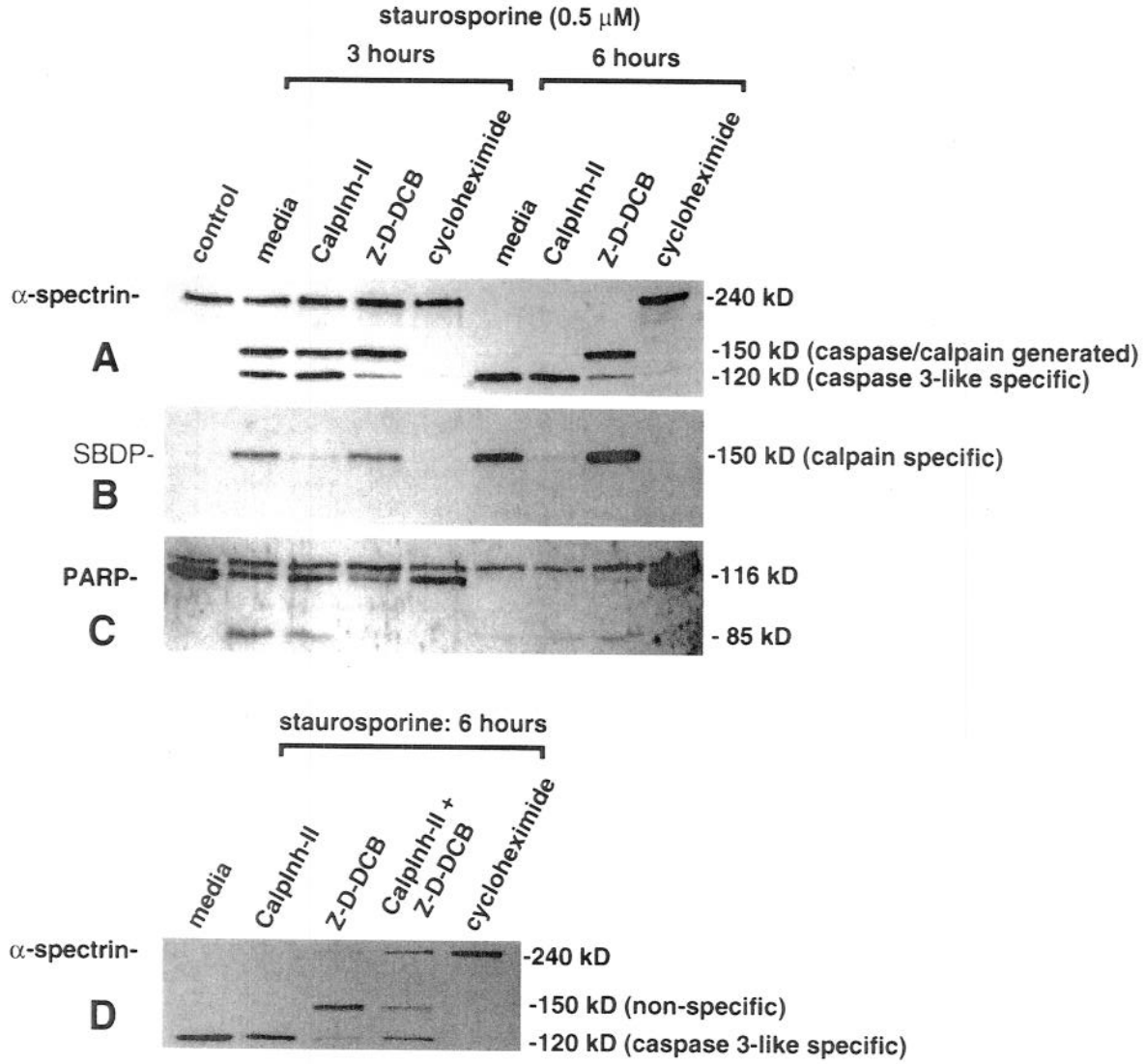

Fig. 6. Calpain and caspase 3-like protease activation occurs downstream from protein upregulation. Proteolysis of α-spectrin into caspase 3-like specific 120 kD (**A**) and calpain-specific 150 kD (**B**) SBDPs was blocked by Z-D-DCB and CalpInh-II (respectively) at both 3 and 6 hr of staurosporine exposure. Cycloheximide completely prevented accumulation of SBDPs to each protease and prevented loss of intact levels of α-spectrin, suggesting that expression of protein(s) are necessary for calpain and caspase activation (A,B). Caspase cleavage of PARP 3 hr following staurosporine treatment was also inhibited by Z-D-DCB and cycloheximide, but not by CalpInh-II (**C**). **D:** Combined administration of CalpInh-II + Z-D-DCB was more effective than either inhibitor alone, providing greater preservation of intact α-spectrin protein levels.

mulation of all SBDPs regardless of the antibody employed, and prevented the loss of the native 240 kD α-spectrin protein (Fig. 6A,B). Interestingly, by 6 hr of staurosporine administration, PARP protein (116 kD) was no longer detectable on immunoblots. In addition, the caspase 3-like specific 85 kD PARP fragment was barely detectable on Western blots, suggesting that the 85 kD fragment was further digested by one or more other proteases. However, administration of Z-D-DCB was observed to partially preserve the level of PARP and the 85 kD fragment (Fig. 6C). Cycloheximide completely prevented processing of PARP at 6 hr (Fig. 6C).

DNA fragmentation. As discussed above, there was no visualization of a DNA ladder following agarose gel electrophoresis at 3 hr of staurosporine incubation, nor was there any evidence of a DNA ladder in CalpInh-II, Z-D-DCB, or cycloheximide treated cells (Fig. 4B). By 6 hr of staurosporine incubation, DNA fragmentation into nucleosomal ladders was evident on agarose gels. The protease inhibitors CalpInh-II, Z-D-DCB, and

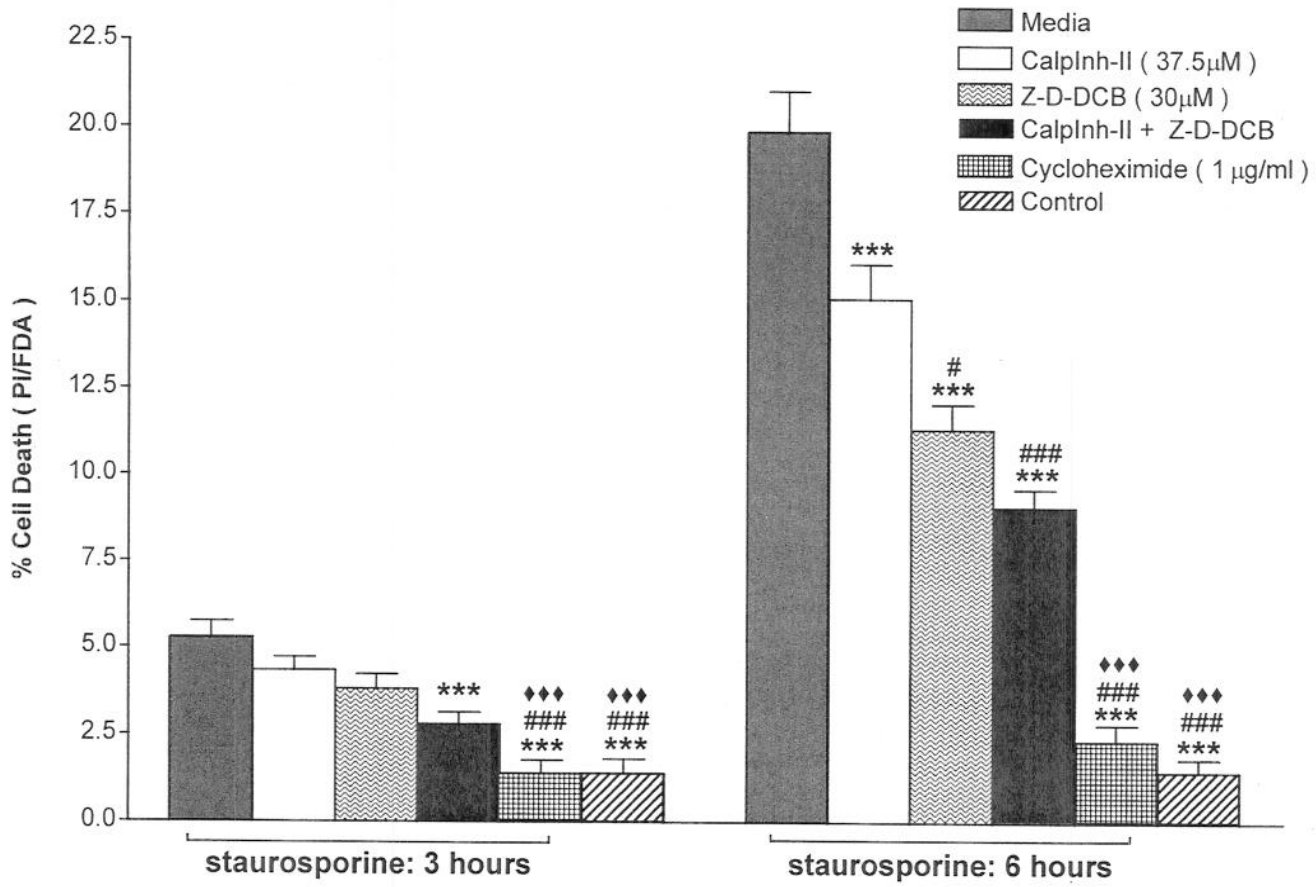

Fig. 7. Preservation of cell viability by CalpInh-II, Z-D-DCB, or cycloheximide. After 3 hr of staurosporine incubation, cycloheximide or the co-administration of CalpInh-II + Z-D-DCB attenuated PI uptake compared to staurosporine-challenged cultures treated with media. After 6 hr of staurosporine incubation, CalpInh-II, Z-D-DCB, CalpInh-II + Z-D-DCB, and cycloheximide each attenuated PI uptake with cycloheximide > CalpInh-II + Z-D-DCB > Z-D-DCB > CalpInh-II. Cycloheximide was able to completely prevent cell death after staurosporine challenge. By 6 hr, CalpInh-II + Z-D-DCB was not statistically significant from Z-D-DCB alone. $***P < 0.001$ compared to media-treated; $\#P < 0.05$ and $\#\#\#P < 0.001$ compared to CalpInh-II; $\blacklozenge\blacklozenge\blacklozenge P < 0.001$ compared to Z-D-DCB.

CalpInh-II + Z-D-DCB each attenuated the intensity of DNA fragmentation observed on agarose gels with CalpInh-II having the weakest inhibitory effect and with the combination of CalpInh-II + Z-D-DCB having the largest inhibitory effect. Only cylcoheximide was observed to completely prevent DNA fragmentation by endonucleases (Fig. 4B).

Cell viability measurements. Propidium iodide (PI) and fluorescein diacetate (FDA) were used to assess cell viability at 3 and 6 hr following staurosporine and/or administration of CalpInh-II, Z-D-DCB, CalpInh-II + Z-D-DCB, or cycloheximide (Fig. 7). Nuclear uptake of PI was almost absent from control cultures at 3 hr. In addition, fluorescein diacetate staining was uniformly distributed among cells indicating cellular membrane integrity. In contrast, a significant ($P < 0.001$) percentage (5.0%) of cells stained for PI at 3 hr in staurosporine treated cultures compared to controls. In the presence of staurosporine, neither CalpInh-II nor Z-D-DCB significantly reduced the percentage of PI stained cells compared to media treated cells (4.0% and 3.8%, respectively) (Fig. 7). In contrast, cycloheximide or the co-administration of CalpInh-II + Z-D-DCB was found to significantly attenuate PI uptake at 3 hr ($P < 0.001$). In addition, cycloheximide, but not CalpInh-II + Z-D-DCB, completely ameliorated PI uptake compared to normal, unchallenged controls.

Six hours following staurosporine administration, the percentage of cells stained for PI increased to 20%. The percentages of PI stained cells for the CalpInh-II, Z-D-DCB, CalpInh-II + Z-D-DCB, and cycloheximide conditions were 15.0, 11.5, 8.0, and 2.3%, respectively (Fig. 7). Thus, each of the inhibitors, including the combination of calpain and caspase inhibitors, significantly reduced nuclear uptake of PI ($P < 0.001$) following 6 hr of staurosporine challenge. In addition, Z-D-

DCB and CalpInh-II + Z-D-DCB provided significantly more protection than did CalpInh-II ($P < 0.05$ and $P < 0.001$). Although there was a trend toward an additive protective effect of CalpInh-II + Z-D-DCB compared to Z-D-DCB alone, this effect was not statistically significant ($P > 0.05$). Cycloheximide provided the greatest level of protection as compared to CalpInh-II or Z-D-DCB ($P < 0.001$ for each comparison).

DISCUSSION

The results of this investigation indicate that staurosporine (0.5 μM) induces selective neuronal apoptosis and eventual cell death in mixed glial-neuronal septo-hippocampal cultures. During staurosporine-induced apoptosis, the submembrane cytoskeletal protein α-spectrin was processed by both calpains and caspase 3-like proteases prior to endonuclease DNA fragmentation. Administration of a calpain inhibitor (CalpInh-II) or a pan-caspase inhibitor (Z-D-DCB) potently prevented protease specific processing of α-spectrin and attenuated endonuclease DNA fragmentation and nuclear uptake of PI. These findings are in accord with other recent papers that have implicated calpain as a potential effector of the apoptotic cascade (Behrens et al., 1995; Jordan et al., 1997; Nath et al., 1996a,b; Squier, 1994). However, no previous studies have suggested that both families of cysteine proteases could additively and independently contribute to neuronal apoptotic cell death. An additional novel finding of this investigation was that inhibition of protein synthesis (by cycloheximide) completely prevented both calpain and caspase 3-like protease activation, placing de novo protein synthesis upstream from calpain and caspase 3-like activation.

Staurosporine-Induced Apoptosis in Primary Septo-Hippocampal Cultures

Staurosporine, a non-specific protein kinase inhibitor, induces apoptosis in a wide variety of cell lines (e.g., MOLT-4, HL-60, CA46, HT-29, SUEDHL6, SH-SY5Y, Jurkat T-) and primary culture systems (cerebellar granule neurons, mixed cortical cultures) (Bertrand et al., 1994; Cagnoli et al., 1996; Falcieri et al., 1993; Koh et al., 1995; Nath et al., 1996a,b), suggesting that staurosporine activates a common biochemical pathway that may be important for elucidating critical components of the apoptotic cascade (Bertrand et al., 1994). In this investgation, we have extended the generality of staurosporine-induced apoptosis to include mixed glial-neuronal septo-hippocampal primary cell cultures. In primary septo-hippocampal cultures, staurosporine (0.5 μM) produced characteristic apoptotic morphological alterations in cell membrane and nuclear structures, endonuclease DNA fragmentation, and eventual cell death. Consistent with Koh et al. (1995), staurosporine-induced apoptotic alterations occurred primarily in neurons whereas astroglial cells were largely unaffected by staurosporine. Characterization of apoptotic responses in primary septo-hippocampal cultures is an important feature of this investigation since the hippocampus is particularly vulnerable to various CNS injuries in vivo, including cerebral ischemia (Jenkins et al., 1989) and traumatic brain injury (Lyeth et al., 1990). In addition, an increasing number of reports have demonstrated apoptotic cell death in the hippocampus following cerebral ischemia (Honkaniemi et al., 1996; MacManus et al., 1993; Nitatori et al., 1995) and traumatic brain injury (Colicos and Dash, 1996; Conti et al., 1996; Rink et al., 1995; Yakovlev et al., 1997). Thus, primary septo-hippocampal cell cultures provide an efficient in vitro tool for the investigation of biochemical alterations relevant to in vivo CNS neuropathologies.

Effects of Cycloheximide on Apoptotic Morphology and DNA Fragmentation

The protein synthesis inhibitor, cycloheximide, blunted calpain and caspase 3-like activation and apoptotic cell death. De novo expression of several mammalian gene products (e.g., bak, bax, bcl-x_S, p53) as well as the protective effect of protein synthesis administration following global ischemia suggests that death regulatory proteins play an important role in apoptotic cell death (Chopp et al., 1992; Krajewski et al., 1995; Shigeno et al., 1990; Papas et al., 1992). However, de novo synthesis of death regulatory proteins is not a requisite step for apoptosis to occur in some model systems (Bertrand et al., 1994; Raff et al., 1993; Squire et al., 1994). In the present investigation, protein synthesis inhibition completely prevented apoptosis and DNA fragmentation, suggesting that protein upregulation is a major component of staurosporine-induced apoptosis in primary septo-hippocampal cultures. This observation is consistent with the findings of Koh et al. (1995), who also demonstrated a protective effect of cycloheximide following staurosporine challenge in neuronal cortical cell cultures. An important and novel finding of this investigation is the observation that cycloheximide prevents calpain and caspase 3-like activation. This finding suggests a causal link between de novo protein synthesis and the subsequent activation of at least two families of cysteine proteases, calpains and caspases, in staurosporine-induced apoptosis. The identity of this newly synthesized protein(s) is currently unknown. However, since one recent paper has reported that neuroprotective concentrations of cycloheximide can induce expression of the antiapoptotic gene product Bcl-2 in rat hippocampal cell cultures (Furukawa et al., 1997), further studies must clarify mechanisms by which cycloheximide exerts its neuroprotective effects.

De Novo Protein Synthesis Is a Requirement for Calpain and Caspase 3-Like Protease Activation

The pattern of α-spectrin processing by calpains and caspase 3-like proteases, and the effects of cycloheximide, CalpInh-II, and Z-D-DCB reveal a temporal sequence of events that occur prior to DNA damage and significant morphological alterations. The results of this investigation indicate that protein synthesis occurs prior to, and is a requirement for, activation of both calpains and caspase 3-like cysteine proteases in staurosporine-induced apoptosis of septo-hippocampal cells. This argument is supported by the observation that: 1) calpain- and caspase 3-like specific fragments to α-spectrin, and caspase 3 processing of PARP, occur prior to any evidence of DNA fragmentation, and 2) cycloheximide completely prevents the accumulation of α-spectrin and PARP cleavage products as well as completely preventing processing of intact α-spectrin and PARP for up to 6 hr following staurosporine administration. The absence of calpain and caspase 3-like cleavage products to α-spectrin and PARP indicate that these proteases do not become active if protein synthesis is prevented from occurring. Although it could be argued that cycloheximide itself inhibits protease activity, cycloheximide does not have any inhibitory properties on proteases where protein synthesis is not a requirement for cell death (Cohen, 1991). For example, we have recently found that in septo-hippocampal cultures exposed to the Ca^{2+} channel agonist maitotoxin, which produces non-apoptotic cell death, cycloheximide was not effective in preventing α-spectrin degradation or cell death. In contrast, CalpInh-II attenuated both α-spectrin fragmentation and cell death after exposure to maitotoxin (unpublished data).

Effects of Calpain and Caspase Inhibitors During Apoptosis

The calpain inhibitor CalpInh-II and the pan-caspase inhibitor Z-D-DCB were each found to attenuate apoptotic morphological alterations (indicated by Hoechst 33258), endonuclease activation (indicated by electrophoretic DNA fragmentation), and cell death (PI staining) following staurosporine challenge. The co-administration of CalpInh-II with Z-D-DCB was found to produce the most robust inhibitory response to staurosporine regardless of the outcome measure employed. No previous studies have suggested that both calpain and caspase 3-like proteases could contribute independently to neuronal apoptosis. In addition, few reports (Nath et al., 1996a,b; Vanags et al., 1996) have investigated the relative roles of the calpain and caspase families of cysteine proteases during apoptosis. In accord with Nath et al. (1996b), CalpInh-II and Z-D-DCB were both found to significantly attenuate staurosporine-induced apoptosis and cell death. The present investigation found that Z-D-DCB was able to prevent DNA fragmentation and cell death to a greater degree than CalpInh-II (Figs. 4b, 7a,b). Importantly, this investigation provides independent confirmation that both CalpInh-II and Z-D-DCB potently inhibited calpain and caspase 3-like activation at the concentrations used in this study, further confirming that calpains and caspase 3-like proteases independently regulate cellular events that contribute to staurosporine-induced apoptosis.

Caspase 3-like proteases are known to attack numerous cytoplasmic and nuclear proteins, including α-spectrin (Nath et al., 1996a,b; Martin et al., 1995; Vanags et al., 1996) and poly(ADP-ribose) polymerase (PARP) (Lazebnik et al., 1994). Because Z-D-DCB is a pan-caspase inhibitor, use of Z-D-DCB could inhibit multiple caspase family members linked to apoptosis, including the caspase 3-like proteases, caspase 6 (Mch2), caspase 7 (Mch3/ICE-LAP3/CMH-1), and caspase 8 (MACH/FLICE/Mch5) (Cohen, 1997; Zhivotovsky et al., 1997). In addition, Z-D-DCB may also have inhibitory control over the caspase 1 family. However, recent reports indicate that caspase 1-like proteases, caspase 1 (ICE), caspase 4 (Ich-2/TX/ICE_{rel}II), and caspase 5 (ICE_{rel}III/TY) may not be involved in apoptotic responses (Cohen, 1997; Eldadah et al., 1997; Nath et al., 1996a; Zhivotovsky et al., 1997). For example, Nath et al. (1996b) found no evidence of a pro-caspase 1 (ICE) signal or any autolytic fragments to caspase 2 (ICH-1) in apoptotic rat cerebellar granule cells or human SH-SY5Y cells. In contrast, the Nath et al. study did observe fragmentation of the pro-caspase 3 (CPP32) protein (32 kD) to the active isoform (17 kD) and found the 120 kD SBDP to be preferentially produced by caspase 3-like proteases. Similarly, Eldadah et al. (1997) found that the caspase 1-like inhibitor z-YVAD-fmk was not protective against apoptosis produced by serum/K^+ deprivation in cerebellar granule cells, whereas the caspase 3-like inhibitor z-DEVD-fmk potently inhibited the apoptotic response.

Calpain activation has also been implicated in several models of apoptosis (Nath et al., 1996a,b; Squier et al., 1994; Vanags et al., 1996). However, a contributory role of calpain to apoptosis has largely been inferred from calpain inhibition studies. The general unavailability of inhibitors specific to calpain preclude determination of calpain's definite involvement in apoptosis. For example, commonly employed inhibitors of calpain, e.g., calpain inhibitor I, calpain inhibitor II, and MDL 28,170, demonstrate cross reactivity with other cysteine proteases like cathepsin B and cathepsin L. In this investigation, we examined and found no evidence that calpain inhibition had any inhibitory effects on caspase 3-like activity. However, the development of more selective and potent calpain inhibitors, such as the specific nonpeptide deriva-

tives of alpha-mercaptoacrylic acid (Wang et al., 1996), will by useful for elucidating a more definite role of calpains in apoptosis.

Calpain and Caspase 3-Like Proteolysis of α-Spectrin During Apoptosis

Identification of key substrates cleaved during apoptosis has been the focus of intensive research. It has recently been demonstrated that cleavage of α-spectrin occurs during apoptosis induced by numerous stimuli, including staurosporine (Martin et al., 1995; Vanags et al., 1996; Nath et al., 1996a,b). Cleavage of cytoskeletal proteins such as α-spectrin during apoptosis may contribute to cell shrinkage, membrane blebbing, and alter cell signalling systems (Cohen, 1997). Although α-spectrin is a preferred substrate of calpains and caspase 3-like cysteine proteases, dissociation of the relative contributions of calpain and caspase processing of α-spectrin during apoptosis has not been well characterized. This is due to the fact that both calpains and caspase 3-like proteases cleave α-spectrin to a 150 kD fragment on immunoblots. Although calpains can further cleave the 150 kD fragment to a calpain-specific 145 kD fragment (Nath et al., 1996a,b), the 145 kD band has not usually been detected on immunoblots obtained from in vitro apoptotic systems (Kluck et al., 1997; Martin et al., 1995; Vanags et al., 1996; however, see Nath et al., 1996a,b). This is probably due to preferential cleavage of the 150 kD fragment by caspase 3-like proteases to the caspase 3-like-specific 120 kD fragment. The few studies that have used α-spectrin proteolysis to examine calpain and caspase 3-like activity during apoptosis have relied on a single monoclonal antibody that is non-specific for the calpain- and caspase 3-like-mediated 150 kD fragment. Thus, dissociation of calpain or caspase contribution to α-spectrin fragmentation is not easily detected if the calpain-specific 145 kD fragment is not detected. In the present investigation, we have employed multiple antibodies to label non-specific 150 kD as well as calpain-specific 150 kD α-spectrin fragments, and the caspase 3-like 120 kD fragment, to conclusively demonstrate that α-spectrin is cleaved by both calpains and caspase 3-like proteases during staurosporine-induced apoptosis. Importantly, this investigation also demonstrates that a calpain inhibitor (CalpInh-II) and a caspase inhibitor (Z-D-DCB) potently inhibit their respective α-spectrin cleavage products and that calpain or caspase inhibition attenuates endonuclease DNA fragmentation and cell death. That calpain inhibition provided protection against α-spectrin fragmentation, endonuclease DNA fragmentation, and apoptotic cell death is further evidence that this protease may be an important effector of the apoptotic cascade.

REFERENCES

Behrens MM, Marinez JL, Moratilla C, Renart J (1995): Apoptosis induced by protein kinase-C inhibition in a neuroblastoma cell line. Cell Growth Diff 6:1375–1380.

Bertrand R, Solary E, O'Connor P, Kohn KW, Pommier Y (1994): Induction of a common pathway of apoptosis by staurosporine. Exp Cell Res 211:314–321.

Bredesen DE (1995): Neural apoptosis. Ann Neurol 38:839–851.

Cagnoli CM, Kharlamov E, Atabay C, Uz T, Manev H (1996): Apoptosis induced in neuronal cultures by either the phosphatase inhibitor okadaic acid or the kinase inhibitor staurosporine is attenuated by isoquinolinesulfonamides H-7, H-8, and H-9. J Mol Neurosci 7:65–76.

Casciola-Rosen LA, Miller DK, Anhalt GJ, Rosen A (1994): Specific cleavage of the 70-kDa protein component of the U1 small nuclear ribonucleoprotein is a characteristic biochemical feature of apoptotic cell death. J Biol Chem 269:30757–30760.

Chopp M, Li Y, Zhang ZG, Freytag SO (1992): p53 expression in brain after middle cerebral artery occlusion in the rat. Biochem Biophys Res Commun 182:1201–1207.

Cohen GM (1997): Caspases: the executioners of apoptosis. Biochem J 326:1–16.

Cohen JJ (1991): Programmed cell death in the immune system. Adv Immunol 50:55–85.

Cohen JJ, Duke RC (1984): Glucocorticoid activation of a calcium dependent endonuclease in thymocyte nuclei leads to cell death. J Immunol 132:38–42.

Colicos MA, Dash PK (1996): Apoptotic morphology of dentate gyrus granule cells following experimental cortical impact injury in rats: possible role in spatial memory deficits. Brain Res 739:120–131.

Conti AC, Raghupathi R, Becher O, Rink AD, Trojanowski JO, McIntosh TK (1996): Delayed apoptotic cell death following lateral fluid percussion brain injury in the rat: a long-term study. J Neurotrauma 13:595 [abstract].

Eldadah BA, Yakovlev AG, Faden AI (1996): A new approach for the electrophoretic detection of apoptosis. Nucleic Acids Res 24: 4092–4093.

Eldadah BA, Yakovlev AG, Faden AI (1997): The role of CED-3 related cysteine proteases in apoptosis of cerebellar granule cells. J Neurosci 17:6105–6113.

Falcieri E, Marrtelli AM, Bareggi R, Cataldi A, Cocco L (1993): The protein kinase inhibitor staurosporine induces morphological changes typical of apoptosis in MOLT-4 cells without concomitant DNA fragmentation. Biochem Biophys Res Commun 193:19–25.

Forloni G, Angeretti N, Chiesa R, Monzani E, Salmona M, Bugiani O, Tagliavini F (1993): Neurotoxicity of a prion protein fragment. Nature 352:543–546.

Fraser A, Evan G (1996): A license to kill. Cell 85:781–784.

Furukawa K, Estus S, Fu W, Mark RJ, Mattson, MP (1997): Neuroprotective action of cycloheximide involves induction of bcl-2 and anti-oxidant pathways. J Cell Biol 136:1137–1149.

Ghayur T, Hugunin M, Talanian RV, Ratnofsky S, Quinlan C, Emoto Y, Pandey P, Datta R, Huang Y, Kharbanda S, Allen H, Kamen R, Wong W, Kufe D (1996): Proteolytic activation of protein kinase C delta by an ICE/CED 3-like protease induces characteristics of apoptosis. J Exp Med 184:2399–2404.

Gong J, Traganos F, Darzynkiewicz Z (1994): A selective procedure for DNA extraction from apoptotic cells applicable for gel electrophoresis and flow cytometry. Anal Biochem 218:314–319.

Honkaniemi J, Massa SM, Breckinridge M, Sharp FR (1996): Global ischemia induces apoptosis-associated genes in hippocampus. Mol Brain Res 42:79–88.

Jenkins LW, Moszynski K, Lyeth BG, Lewelt W, DeWitt DS, Allen A, Dixon CE, Povlishock JT, Majewski TJ, Clifton GL, Young HF, Becker DP, Hayes RL (1989): Increased vulnerability of the mildly traumatized brain to cerebral ischemia: the use of controlled secondary ischemia as a research tool to identify common or different mechanisms contributing to mechanical and ischemic brain injury. Brain Injury 477:211–224.

Johnson EM, Greenlund LJS, Akins PT, Hsu CY (1995): Neuronal apoptosis: current understanding of molecular mechanisms and potential role in ischemic brain injury. J Neurotrauma 12:843–852.

Jones KH, Senft, AJ (1985): An improved method to determine cell viability by simultaneous staining with fluorescein diacetate-propidium iodide. J Histochem Cytochem 33:77–79.

Jordan J, Galindo MF, Miller RJ (1997): Role of calpain- and interleukin-1 converting enzyme-like proteases in the β-amyloid-induced death of rat hippocampal neurons in culture. J Neurochem 68:1612–1621.

Kampfl A, Posmantur RM, Zhao X, Schmutzhard E, Clifton GL, Hayes RL (1997): Mechanisms of calpain proteolysis following traumatic brain injury: implications for pathology and therapy: a review and update. J Neurotrauma 14:121–134.

Kampfl A, Zhao X, Whitson JS, Posmantur RM, Dixon CE, Yang K, Clifton GL, Hayes RL (1996): Calpain inhibitors protect against depolarization-induced neurofilament protein loss of septo-hippocampal neurons in culture. Eur J Neurosci 8:344–352.

Kluck RM, Bossy-Wetzel E, Green DR, Newmeyer DD (1997): The release of cytochrome c from mitochondria: a primary site for Bcl-2 regulation of apoptosis. Science 275:1132–1136.

Koh J, Wie MB, Gwag BJ, Sensi SL, Canzoniero MT, Demaro J, Csernansky C, Choi DW (1995): Staurosporine-induced neuronal apoptosis. Exp Neurol 135:153–159.

Kothakota S, Azuma T, Reinhard C, Klippel A, Tang J, Chu K, McGarry TJ, Kirschner MW, Koths K, Kwiatkowski DJ, Williams LT (1997): Caspase 3-generated fragment of gelsolin: effector of morphological change in apoptosis. Science 278:294–298.

Krajewski S, Krajewski M, Shabaik A, Miyashita T, Wang HG, Reed JC (1995): Upregulation of Bax protein levels in neurons following cerebral ishcemia. J Neurosci 15:6364–6376.

Lazebnik YA, Kaufmann SH, Desnoyers S, Poirer GG, Earnshaw WC (1994): Cleavage of poly(ADP-ribose) polymerase by a proteinase with properties like ICE. Nature 371:346–347.

Lazebnik YA, Takahashi A, Moir RD, Goldman RD, Poirier GG, Kaufmann SH, Earnshaw WC (1995): Studies of the lamin proteinase reveal multiple parallel biochemical pathways during apoptotic execution. Proc Natl Acad Sci USA 92:9042–9046.

Linnik MD, Zobrist RH, Hatfield MD (1993): Evidence supporting role for programmed cell death in focal cerebral ischemia in rats. Stroke 24:2002–2009.

Linnik MD, Markgraf CG, Mason PJ, Velayo N, Racke MM (1996): Calpain Inhibition attenuates apoptosis in vitro and decreases infarct size in vivo. In Krieglstein J (ed):"Pharmacology of Cerebral Ischemia." Boca Raton, FL: CRC Press, pp 33–40.

Loo DT, Copani AC, Pike CJ, Whittenmore, ER, Walencewicz AJ, Cotman CW (1993): Apoptosis is induced by β-amyloid in cultured central nervous system neurons. Proc Natl Acad Sci USA 90:7951–7955.

Lyeth BG, Jenkins LW, Hamm RJ, Dixon CE, Phillips LL, Clifton GL, Young HF, Hayes RL (1990): Prolonged memory impairment in the absence of hippocampal cell death following traumatic brain injury in the rat. Brain Res 526:249–258.

MacManus JP, Buchan AM, Hill IE, Rasquinha I, Preston E (1993): Global ischemia can cause DNA fragmentation indicative of apoptosis in rat brain. Neurosci Lett 164:89–92.

Martin DP, Schmidt RE, DiStefano PS, Lowry OH, Carter JG, Johnson EM (1988): Inhibitors of protein synthesis and RNA synthesis prevent neuronal death caused by nerve growth factor deprivation. J Cell Biol 106:829–844.

Martin SJ, O'Brien GA, Nishioka WK, McGahon AJ, Mahboubi A, Saido TC, Green DR (1995): Proteolysis of fodrin (non-erythroid spectrin) during apoptosis. J Biol Chem 270:6425–6428.

McConkey DJ, Hartzell P, Nicotera P, Orrenius S (1989): DNA fragmentation kills immature thymocytes. FASEB J 3:1843–1848.

Miura M, Zhu H, Rotello R, Hartwieg EA, Yuan J (1993): Induction of apoptosis in fibroblasts by IL-1 beta-converting enzyme, a mammalian homolog of the C. elegans cell death gene ced-3. Cell 75:653–660.

Na S, Chuang TH, Cunningham A, Turi TG, Hanke JH, Bokoch GM, Danley DE (1996): D4-GDI, a substrate of CPP32, is proteolyzed during Fas-induced apoptosis. J Biol Chem 271:11209–11213.

Nath R, McGinnis KJ, Nadimpalli R, Stafford D, Wang KKW (1996a): Effects of ICE-like proteases and calpain inhibitors on neuronal apoptosis. Neuroreport 8:249–255.

Nath R, Raser KJ, Stafford D, Hajimohammadreza I, Posner A, Allen H, Talanian RV, Yuen P, Gilbertsen RB, Wang KKW (1996b): Non-erythroid α-spectrin breakdown by calpain and interleukin 1-converting-enzyme-like protease(s) in apoptotic cells: contributory roles of both protease families in neuronal apoptosis. Biochem J 319:683–690.

Nelipovich PA, Nikonova LV, Umansky SR (1988): Inhibition of poly(ADP-ribose) polymerase as a possible reason for activation of Ca^{2+}/Mg^{2+}-dependent endonuclease in thymocytes of irradiated rats. Int J Radiat Biol 53:749–765.

Newcomb JK, Zhao X, Pike BR, Clifton GL, Hayes RL (1997): Evidence of apoptosis following controlled cortical impact injury in the rat. J Neurotrauma 14:763. [abstract]

Nicholson DW, Ali A, Thornberry NA, Vaillancourt JP, Ding CK, Gallant M, Gareau Y, Griffin PR, Labelle M, Lazebnik YA, Munday NA, Raju SM, Smulson ME, Yamin T-T, Yu VL, Miller DK (1995): Identification and inhibition of the ICE/CED-3 protease necessary for mammalian apoptosis. Nature 376: 37–43.

Nitatori T, Sato N, Waguri S, Karasawa Y, Araki H, Shibanai K, Kominami E, Uchiyama Y (1995): Delayed neuronal death in the CA1 pyramidal cell layer of the gerbil hippocampus following transient ischemia is apoptosis. J Neurosci 15:1001–1011.

Oberhammer F, Fritsch G, Schmied M, Pavelka M, Printz D, Purchio T, Lassmann H, Schulte-Hermann R (1993): Condensation of the chromatin at the membrane of an apoptotic nucleus is not associated with activation of an endonuclease. J Cell Sci 104:317–326.

Papas S, Crepel V, Hasboun D, Jorquera I, Chinestra P, Ben-Ari Y (1992): Cycloheximide reduces the effects of anoxic insult in vivo and in vitro. Eur J Neurosci 4:758–765.

Pravdenkova SV, Basnakian AG, James SJ, Anderson BJ (1996): DNA fragmentation and nuclear endonuclease activity in rat brain after sever closed head injury. Brain Res 729:151–155.

Raff MC, Barres BA, Burne JF, Coles HS, Ishizaki Y, Jacobson MD (1993): Programmed cell death and the control of cell survival: lessons from the nervous system. Science 262:695–700.

Rink A, Fung K, Trojanowski JQ, Lee VM, Neugebauer E, McIntosh TK (1995): Evidence of apoptotic cell death after experimental traumatic brain injury in the rat. Am J Pathol 147:1575–1583.

Roberts-Lewis JM, Savage MJ, Marcy VR, Pinsker LR, Siman R (1994): Immunolocalization of μ-calpain mediated spectrin degradation to vulnerable neurons in ischemic gerbil brain. J Neurosci 14:3934–3944.

Rosen A, Casciola-Rosen L (1997): Macromolecular substrates for the ICE-like proteases during apoptosis. J Cell Biochem 64:50–54.

Saido TC, Sorimachi H, Suzuki K (1994): Calpain: new perspectives in molecular diversity and physiological-pathological involvement. FASEB J 8:814–822.

Shigeno T, Yamasaki Y, Kato G, Kausaka K, Mima T, Takakura K, Graham DI, Furukawa S (1990): Reduction of delayed neuronal death by inhibition of protein synthesis. Neurosci Lett 120:117–119.

Sloviter RS (1996): Hippocampal pathology and pathophysiology in temporal lobe epilepsy. Neuroglia 11(Suppl. 4):29–32.

Squier MKT, Miller ACK, Malkinson AM, Cohen JJ (1994): Calpain activation in apoptosis. J Cell Physiol 159:229–237.

Suzuki K, Sorimachi H, Yoshizawa T, Kinbara K, Ishiura S (1995): Calpain: novel family members, activation and physiological function. Biol Chem 376:523–529.

Vanags DM, Porn-Ares MI, Coppola S, Burgess DH, Orrenius S (1996): Protease involvement in fodrin cleavage and phosphatidylserine exposure in apoptosis. J Biol Chem 271:31075–31081.

Wang KKW, Yuen P (1994): Calpain inhibition: an overview of its therapeutic potential. Trends Pharmacol Sci 15:412–419.

Wang KKW, Villalobo A, Roufogalis BD (1989): Calmodulin-binding proteins as calpain substrates. Biochem J 262:693–706.

Wang KKW, Nath R, Posner A, Rasier KJ, Buroker-Kilgore M, Hajimohammadreza I, Probert AW, Marcoux FW, Ye Q, Takano E, Hatanaka M, Maki M, Caner H, Collins JL, Fergus A, Lee KS, Lunney EA, Hays SJ, Yuen P (1996): An alpha-mercaptoacrylic acid derivative is a selective nonpeptide cell-permeable calpain inhibitor and is neuroprotective. Proc Natl Acad Sci USA 93:6687–6692.

Waterhouse N, Kumar S, SongQ, Strike P, Sparrow L, Dreyfuss G, Alnemri ES, Litwack G, Lavin M, Watters D (1996): Heteronuclear ribonucleoproteins C1 and C2, components of the spliceosome, are specific targets of interleukin 1-converting enzyme-like proteases in apoptosis. J Biol Chem 271:29335–29341.

Wyllie AH (1980): Glucocorticoid-induced thymocyte apoptosis is associated with endogenous endonuclease activation. Nature 284:555–556.

Yakovlev AG, Knoblach SM, Fan L, Fox GB, Goodnight R, Faden AI (1997): Activation of CPP32-like caspases contributes to neuronal apoptosis and neurological dysfunction after traumatic brain injury. J Neurosci 17:7415–7424.

Yang J, Xuesong L, Bhalla K, Kim CN, Ibrado AM, Cai J, Peng T, Jones DP, Wang X (1997): Prevention of apoptosis by Bcl-2: release of cytochrome c from mitochondria blocked. Science 275:1129–1132.

Yuen P, Wang KKW (1996): Therapeutic potential of calpain inhibitors in neurodegenerative disorders. Exp Opin Invest Drugs 5:1291–1304.

Zhivotovsky B, Burgess DH, Vanags DM, Orrenius S (1997): Involvement of cellular proteolytic machinery in apoptosis. Biochem Biophys Res Commun 230:481–488.

JOURNAL OF NEUROTRAUMA
Volume 17, Number 4, 2000
Mary Ann Liebert, Inc.

Stretch Injury Causes Calpain and Caspase-3 Activation and Necrotic and Apoptotic Cell Death in Septo-Hippocampal Cell Cultures

BRIAN R. PIKE,[1] XIURONG ZHAO,[2] JENNIFER K. NEWCOMB,[2] CHRISTOPHER C. GLENN,[1] DOUGLAS K. ANDERSON,[1,3] and RONALD L. HAYES[1]

ABSTRACT

Traumatic brain injury (TBI) results in numerous central and systemic responses that complicate interpretation of the effects of the primary mechanical trauma. For this reason, several *in vitro* models of mechanical cell injury have recently been developed that allow more precise control over intra- and extracellular environments than is possible *in vivo*. Although we recently reported that calpain and caspase-3 proteases are activated after TBI in rats, the role of calpain and/or caspase-3 has not been examined in any *in vitro* model of mechanical cell injury. In this investigation, varying magnitudes of rapid mechanical cell stretch were used to examine processing of the cytoskeletal protein α-spectrin (280 kDa) to a signature 145-kDa fragment by calpain and to the apoptotic-linked 120-kDa fragment by caspase-3 in septo-hippocampal cell cultures. Additionally, effects of stretch injury on cell viability and morphology were assayed. One hour after injury, maximal release of cytosolic lactate dehydrogenase and nuclear propidium iodide uptake were associated with peak accumulations of the calpain-specific 145-kDa fragment to α-spectrin at each injury level. The acute period of calpain activation (1–6 h) was associated with subpopulations of nuclear morphological alterations that appeared necrotic (hyperchromatism) or apoptotic (condensed, shrunken nuclei). In contrast, caspase-3 processing of α-spectrin to the apoptotic-linked 120-kDa fragment was only detected 24 h after moderate, but not mild or severe injury. The period of caspase-3 activation was predominantly associated with nuclear shrinkage, fragmentation, and apoptotic body formation characteristic of apoptosis. Results of this study indicate that rapid mechanical stretch injury to septo-hippocampal cell cultures replicates several important biochemical and morphological alterations commonly observed *in vivo* brain injury, although important differences were also noted.

Key words: apoptosis; calpain; caspase-3; cell culture; neuron; spectrin (fodrin); traumatic brain injury

[1]Department of Neuroscience, Center for Traumatic Brain Injury Studies, University of Florida Brain Institute, Gainesville, Florida.

[2]Department of Neurosurgery, The Vivian L. Smith Center for Neurologic Research, University of Texas Health Science Center–Houston, Houston, Texas.

[3]Department of Neurological Surgery, University of Florida College of Medicine and Malcom Randall Veterans Affairs Medical Center, Gainesville, Florida.

INTRODUCTION

TRAUMATIC BRAIN INJURY (TBI) results in numerous pathological central and systemic responses that can contribute independently or additively to neuronal cell death and dysfunction. For example, primary mechanical head injury results in a host of secondary insults such as anoxia, ischemia, hypertension, edema, inflammation, or increased cerebral perfusion pressure that complicate interpretation of the effects of the initial injury. The brain's intimate interaction with the circulatory system is an additional source of interpretive complication due to cerebral hemorrhage, metabolite removal and delivery, and as a host for neutrophil infiltration. As a result of these complications, several *in vitro* approaches to study neurotrauma have been developed that model different biomechanical or neurochemical insults associated with TBI which allow more precise control over intracellular and extracellular environments than possible *in vivo* (for reviews, see Morrison et al., 1998b; Murphy and Horrocks, 1994). The most commonly employed *in vitro* insults include glutamate toxicity (Choi et al., 1987), hypoglycemia (Monyer et al., 1989), hypoxia (Goldberg et al., 1988), ischemia (i.e., hypoglycemia + hypoxia; Nath et al., 1998), and axonal and dendritic lesions (Gross et al., 1993; Lucas et al., 1990). In addition, *in vitro* models of mechanical cell injury have been developed that replicate important biomechanical stresses commonly associated with traumatic brain injury *in vivo* (Ellis et al., 1995; LaPlaca et al., 1997; Morrison et al., 1998a; Mukhin et al., 1998; Shepard et al., 1991). For example, a major biomechanical force encountered by the brain during concussive head injury is that of rapid deformation and tensile strain, or stretch injury (Gennarelli and Thibault, 1985; Margulies et al., 1990). Several *in vitro* systems have been designed to model this sort of mechanical injury by culturing cells onto deformable substrates that are then exposed to an applied load (Cargill and Thibault, 1996; Ellis et al., 1995; Morrison et al., 1998a). Ellis and coworkers (1995) have developed and characterized a model of stretch injury and have reported a number of stretch-induced cellular alterations including mitochondrial swelling, increased plasma membrane permeability (Ellis et al., 1995), influx of extracellular Ca^{2+} (Rzigalinski et al., 1996), phospholipase C activation, arachidonic acid release (Lamb et al., 1997), and membrane depolarization (Tavalin et al., 1995, 1997). However, the effects of stretch-injury on numerous other biochemical and morphological variables related to *in vivo* brain injury are not known.

The cysteine proteolytic enzymes calpain and caspase-3 have received a great deal of attention as important mediators of cell injury/death in a variety of central nervous system (CNS) insults. The calpains have been implicated in CNS damage after traumatic brain injury (Kampfl et al., 1997; Newcomb et al., 1997; Pike et al., 1998a; Posmantur et al., 1997; Saatman et al., 1996), spinal cord injury (Banik et al., 1997; Li et al., 1995), and cerebral ischemia *in vivo* (Hong et al., 1994; Lee et al., 1991; Roberts-Lewis et al., 1994; Seubert et al., 1989). Although the calpains are generally thought to be associated with necrotic cell death, mounting evidence now indicates a role for calpains in apoptotic cell death as well (Linnik et al., 1996; Nath et al., 1996b; Pike et al., 1998b). Caspase-3 is regarded as a critical executioner of apoptosis in several *in vitro* cell culture systems (Nicholson and Thornberry, 1997) and caspase-3 activation has been observed *in vivo* after TBI (Pike et al., 1998a; Yakovlev et al., 1997) and cerebral ischemia (Chen et al., 1998; Endres et al., 1998; Kitagawa et al., 1998; Namura et al., 1998). Apoptotic cell death has also been observed in animal models of TBI (Colicos and Dash, 1996; Conti et al., 1998; Eldadah et al., 1996; Newcomb et al., 1999; Pravdenkova et al., 1996; Rink et al., 1995), spinal cord injury (Crowe et al., 1997; Kato et al., 1997; Katoh et al., 1996; Liu et al., 1997), and cerebral ischemia (Charriaut-Marlangue et al., 1998). Our laboratory has recently reported apoptotic cell death (Newcomb et al., 1999) and independent or concurrent activation of calpains and caspase-3 proteases (Pike et al., 1998a) in various brain regions following lateral cortical impact traumatic brain injury in rodents.

Although calpains or caspase-3 protease activation is widely reported after CNS injury, few investigations have assessed concurrent activation of these proteases (Nath et al., 1996a,b; Pike et al., 1998b). In addition, TBI results in calpain and caspase-3 activation and necrotic and apoptotic cell death. Because calpains are associated with necrosis and apoptotic cell death while caspase-3 is associated only with apoptotic cell death, elucidation of the relative contribution of these two protease families to cell death after CNS injury is important. For instance, we have demonstrated that both calpains and caspase-3 proteases contribute to apoptotic cell death in staurosporine-induced apoptosis (Pike et al., 1998b), whereas calpain but not caspase-3 contributes to maitotoxin-induced necrotic cell death in septo-hippocampal primary cell cultures (Zhao et al., 1999). The present investigation is the first to examine cell death phenotypes and protease activation after *in vitro* mechanical insult.

MATERIALS AND METHODS

Septo-Hippocampal Cultures

Primary glial-neuronal cultures were prepared as previously reported (Pike et al., 1998b). Briefly, septi and

hippocampi were dissected from gestational day 18 fetal Sprague-Dawley rats in Hank's balanced salt solution (HBSS) supplemented with 4.2 mM sodium bicarbonate, 1 mM pyruvate, 20 mM HEPES, and 3 mg/mL bovine serum albumin (BSA), pH 7.25. Tissue was washed in Dulbecco's modified Eagle's medium (DMEM) and triturated through the narrow pores of serial flame constricted Pasteur pipettes in DMEM. Dissociated cells were transferred to fresh DMEM with 10% fetal bovine serum (DMEM-10S) and plated onto collagen- and poly-L-lysine-coated 25-mm-diameter Flex Plate wells (Flexcell International, McKeesport, PA) at a density of 4.36×10^5 cells/mL. Cultures were maintained in a humidified incubator in an atmosphere of 5% CO_2 at 37°C and media was replenished every 2 days. After day 5 *in vitro*, medium was changed to DMEM-DM with 5% horse serum. By day 10 *in vitro*, astrocytes formed a confluent monolayer beneath morphologically mature neurons.

All protocols have been approved by the University of Florida's Animal Care and Use Committee and are consistent with National Institutes of Health (NIH) guidelines detailed in the Guide for the Care and Use of Laboratory Animals and the Animal Welfare Act. Methods of euthanasia are consistent with recommendations of the Panel on Euthanasia by the American Veterinary Medical Association.

Biomechanical Stretch Injury

Ten-day-old septo-hippocampal cultures were injured as previously described with a model 94A Cell Injury Controller (Ellis et al., 1995). Briefly, cells grown on silastic membranes of Flexcell plates were rapidly stretched (50 msec duration) by applying a positive pressure pulse of compressed nitrogen gas that allowed for a controlled deformation and rebound of the silastic membrane. Deformations of 5.7, 6.5, and 7.5 mm were used in these experiments. Following initial injury-response assays, we classified these injuries as mild, moderate, and severe, consistent with the original observations of Ellis et al. (1995).

Characterization of Cell Injury

Lactate dehydrogenase release. Assessment of cell injury was performed by measuring the release of lactate dehydrogenase (LDH) into the culture medium at various intervals after stretch injury. LDH is a stable large molecular weight cytoplasmic enzyme that is present in all cells and is rapidly released into the culture medium upon disruption of the plasma membrane (Murphy and Horrocks, 1994). LDH release into culture medium was determined spectrophotometrically using an LDH assay kit purchased from Boehringer Mannheim. One hundred microliters of cell culture medium was transferred to a 96-well microplate and diluted with an equal volume of the LDH assay reagent. A BioRad 450 microplate reader was used to measure the optical density at 490 nm.

Propidium iodide uptake and fluorescein diacetate loss. Cell injury was also qualitatively assessed by examining nuclear uptake of propidium iodide (PI) and somal loss of fluorescein diacetate (FDA) as previously described (Jones and Senft, 1985; Pike et al., 1998b). PI is an intravital dye that is excluded from cells with intact plasma membranes, but rapidly permeates cells with damaged membranes, staining nuclei with a red fluorescence. FDA readily permeates plasma membranes where esterases in the cytosol cleave the acetate from fluorescein causing a green fluorescence. Once cleaved, FDA can no longer permeate intact membranes. A stock solution of FDA (20 mg/mL) was dissolved in acetone, and a PI stock solution was dissolved in PBS (5 mg/mL). Working solutions of FDA/PI were freshly prepared by adding 10 μL of FDA and 3 μL PI stock to 10 mL of HBSS. At various time-points after injury, the culture medium was aspirated and cells were bathed in the FDA/PI solution. Cells were stained for 3 min at room temperature and examined with a Zeiss Axiovert 135 inverted fluorescence microscope equipped with epi-illumination, band pass 450–490-nm exciter filter, 510-nm chromatic beam splitter, and a long-pass 520-nm barrier filter. This filter combination permitted both red and green fluorescing cells to be seen simultaneously. Thus, cell viability can be monitored by comparing the relative magnitude of viable (green fluorescence) versus nonviable (red fluorescence) cells.

Morphological Assessment of Neuronal and Astroglial Cells

Immunocytochemistry. To determine the effects of stretch injury on neuronal and astroglial cell types, cultures were labeled immunocytochemically with antibodies against neuronal nuclear protein (NeuN; monoclonal; Chemicon) and microtubule associated protein–2 (MAP2; monoclonal Sternberger) (for neurons) or against glial fibrillary acidic protein (GFAP; polyclonal; Sigma) (for astroglia). Because MAP2 is rapidly degraded by calpain (Fischer et al., 1991), neurons were double labeled with NeuN to provide a more stable marker of neuronal cell populations after injury. At various intervals after injury, culture medium was aspirated, cells were washed 2× in PBS and fixed in 4% paraformaldehyde for 5 min at room temperature. After 2× wash in PBS cells were permeabilized with 0.5% Triton X-100 (in PBS) for 5 min and blocked with 10% goat or horse serum in PBS

for 1 h at room temperature. Cells were then incubated in appropriate primary antibodies (1:1,000) in PBS containing 1% horse or goat serum. After 2× wash in PBS/0.05% Tween-20, cells were incubated in horseradish peroxidase-conjugated goat anti-rabbit IgG (for GFAP) or sheep anti-mouse IgG (for MAP2 and NeuN; 1:1,000) for 1 h. Cells were washed 3× in PBS, and diaminobenzedine (DAB; Sigma) or SG substrate (Vector) was used to visualize the reaction. Following incubation in DAB or SG, the reaction was stopped by washing cells with distilled H_2O. To visualize stained cells with the microscope, the 2-mm-thick silastic membranes from 6 well stretch plates were gently removed and trimmed to fit on standard microscope slides.

Alterations in nuclear morphology. Nuclear alterations were examined with the adenine-thymine base-pair–specific DNA dye Hoechst 33258 (bis-benzimide; Sigma). This dye was used to identify characteristics of necrotic- or apoptotic-like morphological alterations. Nuclei of normal cells can be identified by a homogenous and diffuse fluorescent chromatin whereas apoptotic cells fluoresced intensely and were characterized by highly condensed chromatin, visibly shrunken and often eccentric shaped nuclei, and by the separation of the nucleus into discrete nuclear fragments (apoptotic bodies; Purnanam and Boustany, 1999; Schemechel, 1999). In contrast, necrotic cells fluoresce brightly with pyknotic chromatin where nuclei have maintained their basic morphology or have become rounded or swollen in appearance (Purnanam and Boustany, 1999; Schmechel, 1999). Using these criteria, the number of necrotic and apoptotic Hoechst stained nuclei were quantified in control cultures and at each time point after stretch injury.

Calpain and Caspase-3 Activation Inferred by Proteolysis of α-Spectrin Protein

SDS-polyacrylamide gel electrophoresis and immunoblotting. At various intervals after injury, cells were collected from three identically manipulated culture wells by gentle scraping in ice cold lysis buffer containing ion chelators and a protease inhibitor cocktail (20 mM HEPES, pH 7.6, 2 mM EGTA, 1 mM EDTA, 1 mM DTT, 0.5 mM PMSF, 50 μg/mL leupeptin, and 10 μg/mL each of AEBSF, aprotinin, pepstatin, TLCK, and TPCK). To facilitate cell lysis, samples were frozen (−70°C), thawed, and sheared through a 1.0-mL syringe 10 times with a 25-gauge needle. Protein content in the samples was assayed by the Micro BCA method (Pierce, Rockford, IL). For protein electrophoresis, equal amounts of total protein (20 μg) were prepared in twofold loading buffer containing 0.25 M Tris (pH6.8), 0.2 M DTT, 8% SDS, 0.02% Bromophenol Blue, and 20% glycerol, and heated at 95°C for 10 min. Samples were resolved in a vertical electrophoresis chamber using a 4% stacking gel over a 6.5% acrylamide resolving gel for 1 h at 200 V. For immunoblotting, separated proteins were laterally transferred to nitrocellulose membranes (0.45 μM) using a transfer buffer consisting of 0.192 M glycine and 0.025

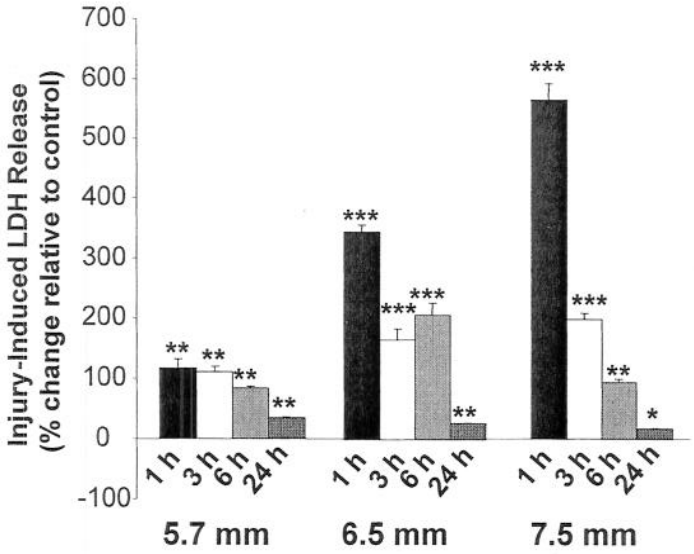

FIG. 1. Mechanical deformation of cultured septo-hippocampal cells causes graded and sustained increases in lactate dehydrogenase (LDH) release in culture medium. At all injury magnitudes (5.7, 6.5, and 7.5 mm), the largest increase in LDH release was observed at 1 h after injury. LDH levels were observed to decrease over the ensuing hours but were still significantly elevated 24 h after injury. $*p < 0.05$, $**p < 0.01$, $***p < 0.001$.

Tris (pH 8.3) with 10% methanol at a constant voltage of 100 V for 1 h at 4°C. Nitrocellulose membranes were stained with Panceau red (Sigma) to insure even transfer of all samples to the membranes and to confirm that equal amounts of protein were loaded in each lane. Blots were then blocked overnight in 5% nonfat milk in 20 mM Tris, 0.15 M NaCl, and 0.005% Tween-20 at 4°C.

Antibodies and immunolabeling. Immunoblots were probed with an anti-α-spectrin monoclonal antibody

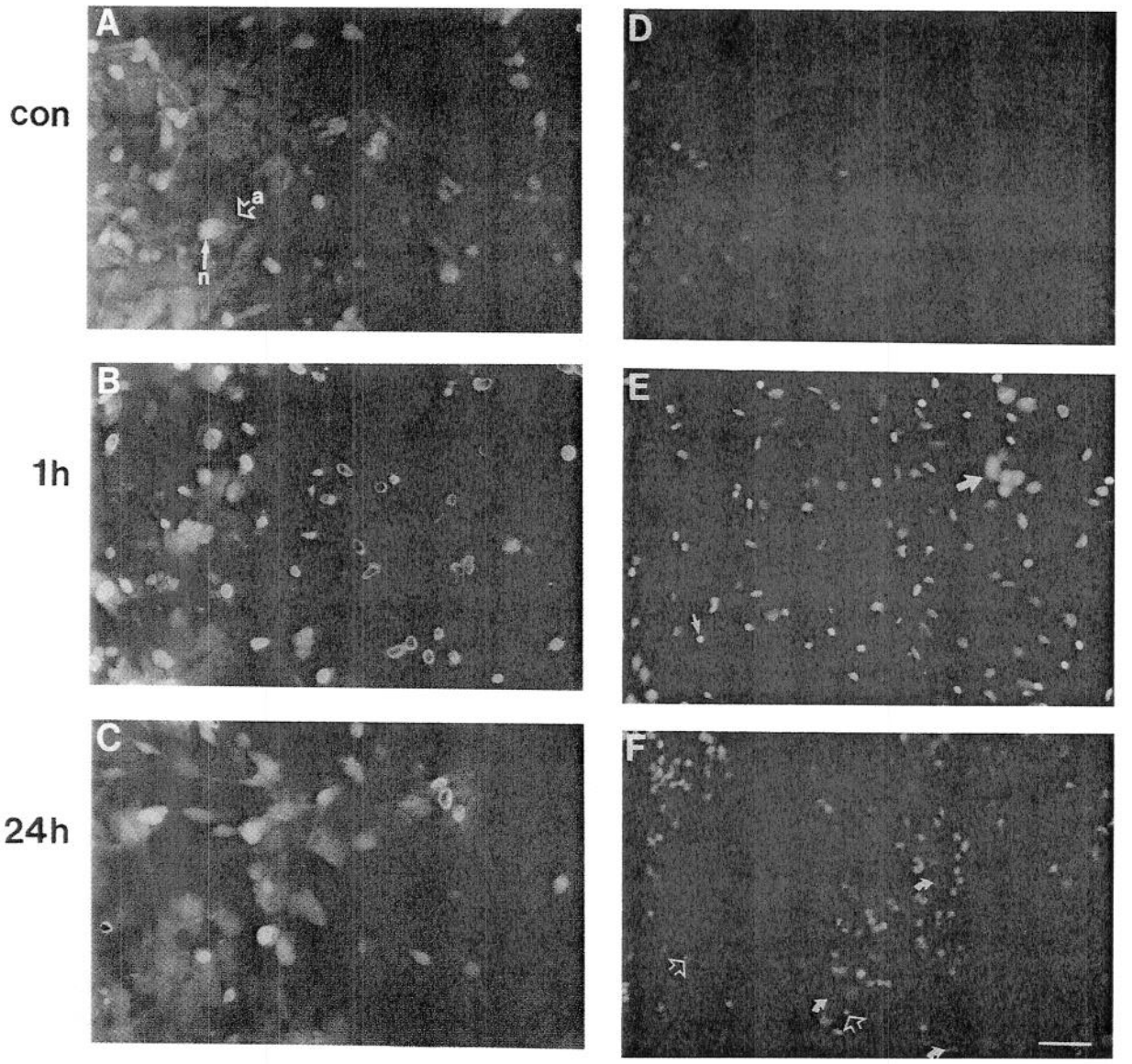

FIG. 2. FDA/PI and Hoechst 33258 staining after mechanical stretch injury (6.5 mm). (**A**) Control cultures grown on flex plates demonstrate normal somal integrity, indicated by retention of intracellular FDA (green fluorescence) and lack of nuclear PI uptake. Note confluent astroglial cell layer (open arrow, a) beneath mature neuronal cell phenotypes (closed arrow, n). (**B**) Increased PI uptake (red fluorescence) is evident 1 h after injury. (**C**) At 24 h after injury, fewer cells stained for PI, and there was a slight reduction in the number of neuronal cell phenotypes. (**D**) Hoechst 33258 staining of control cell nuclei 24 h after stretch injury to sister cells. Note homogenous, diffuse Hoechst staining in healthy unstretched cells. (**E**) At 1 h after injury, the nuclei of numerous cells appeared hyperchromatic and fluoresced brightly. Some cells maintained their normal nuclear size and shape, but had hyperchromatic nuclei that were characteristic of necrotic cell death (thick arrow). Hyperchromatic nuclei of other cells were visibly shrunken and characteristic of apoptotic cell death (thin arrow). (**F**) By 24 h after injury, all hyperchromatic nuclei appeared shrunken and in various stages of nuclear disassembly including nuclear fragmentation (open arrows) and formation of discrete apoptotic bodies (curved arrows). Bar = 50 μm.

(Affiniti Research Products, U.K.; catalogue no. FG 6090, clone AA6) that detects intact α-spectrin (280 kDa) and 150-, 145-, and 120-kDa cleavage fragments to α-spectrin. A cleavage product of 150 kDa is initially produced by calpains and caspase-3 proteases; thus, the band cannot be used to discriminate calpain versus caspase activity (Nath et al., 1996a,b; Wang et al., 1998). However, the 145-kDa SBDP is a specific proteolytic fragment of calpain (Harris et al., 1988; Nath et al., 1996a,b). In addition, the 120-kD SBDP has been identified as being a specific apoptotic-linked proteolytic fragment of caspase-3 (Nath et al., 1998; Wang et al., 1998). Following incubation with the primary antibody (1:4,000 dilution) for 2 h at room temperature, blots were incubated in peroxidase-conjugated sheep anti-mouse IgG for 1 h (dilution, 1:10,000). Enhanced chemiluminescence reagents (ECL, Amersham) were used to visualize immunolabeling on Hyperfilm (Hyperfilm ECL, Amersham).

Statistical Analyses

Each experiment was performed at least three times, and data were evaluated by ANOVA with Tukey post hoc comparisons. Values are given as mean ± SEM. Differences were considered significant if $p < 0.05$. Semiquantitative evaluation of protein levels detected by immunoblotting was performed via computer-assisted one-dimensional densitometric scanning (Alphalmager 2000 Digital Imaging System, San Leandro, CA). Data were acquired as integrated densitometric values and tranformed to percentages of the densitometric levels obtained on scans from control cultures visualized on the same blot. Transformed data was evaluated by ANOVA and post hoc comparisons as described above.

RESULTS

Effects of Stretch Injury on Septo-Hippocampal Cultures

Lactate dehydrogenase release. Initial injury-response assays were performed to determine the effects of various stretch deformations (5.7, 6.5, and 7.5 mm) on LDH release into the culture medium. Consistent with Ellis et al. (1995), increasing levels of mechanical stretch were reliably associated with significantly increased release of LDH into the culture medium as compared to nonstretched control wells ($p < 0.01$ for each injury level; Fig. 1). At all three injury magnitudes, LDH levels were highest at 1 h after injury. LDH levels were markedly elevated at each injury magnitude for the first 6 h after injury, and a lower but significant release of LDH was still detected at 24 h after stretch injury (Fig. 1).

Propidium iodide uptake and fluorescein diacetate loss. Consistent with LDH release, stretch injury resulted in a rapid increase in the number of PI stained nuclei that was positively related to increased injury magnitude. With each injury magnitude (5.7, 6.5, 7.5 mm) the number of PI-stained nuclei was greatest at 1 h after injury. All subsequent time points revealed a decreased number of PI staining compared to the 1 h time point (for profile of the 6.5 mm injury, see Fig. 2). At 24 h after injury, only a few scattered cells were observed to stain for PI. FDA staining indicated that there was a noticeable reduction in the number of neuronal cell types (based on phenotypic profile) while the number of astroglial cells appeared unaltered after 6.5-mm injury (Fig. 2). However, the 7.5-mm injury magnitude was clearly associated with both neuronal and astroglial cell loss indicated by a large loss in the number of FDA stained cells and by increased areas of cell detachment from the Silastic membranes (data not shown).

Morphological Assessment of Neuronal and Astroglial Cells

Dendritic perturbation and neuronal cell loss after stretch injury. Examination of MAP2, a structural somatodendritic protein found in neurons, and NeuN, a neuronal-nuclear protein, revealed a typical staining pattern of neuronal dendrites and nuclei in nonstretched cells. Nonstretched neurons were characterized by large nuclei, ovoid-shaped cell bodies, and by the appearance of numrous, long and smooth multipolar dendritic processes (Fig. 3A). However, after stretch injury, there was a temporally progressive decrease in the number and length of dendritic processes related to injury magnitude. For instance, within the first hour after moderate to severe injury (6.5–7.5 mm), many processes appeared fragmented with numerous punctate swellings or beads (varicousities) along distal portions of the dendrites (Fig. 3B). By 24 h after stretch injury (6.5 and 7.5 mm), most neurons had lost their multipolar dendritic arbor and extended only unipolar or bipolar processes (Fig. 3C). In addition, there was an overt reduction in the number of NeuN-stained neurons between 6 and 24 h after 6.5- and 7.5-mm stretch injury.

In contrast to the marked alterations in MAP2 immunoreactivity observed after moderate or severe levels of stretch injury, mild stretch injury (5.7 mm) resulted in transient dendritic varicousities localized along distal, but not proximal dendrites. In addition, there was no overt loss of neuronal cell phenotypes indicated by NeuN or FDA staining (data not shown).

Astroglial perturbations after stretch injury. To assess the astrocytic reaction to stretch injury, astroglial cells

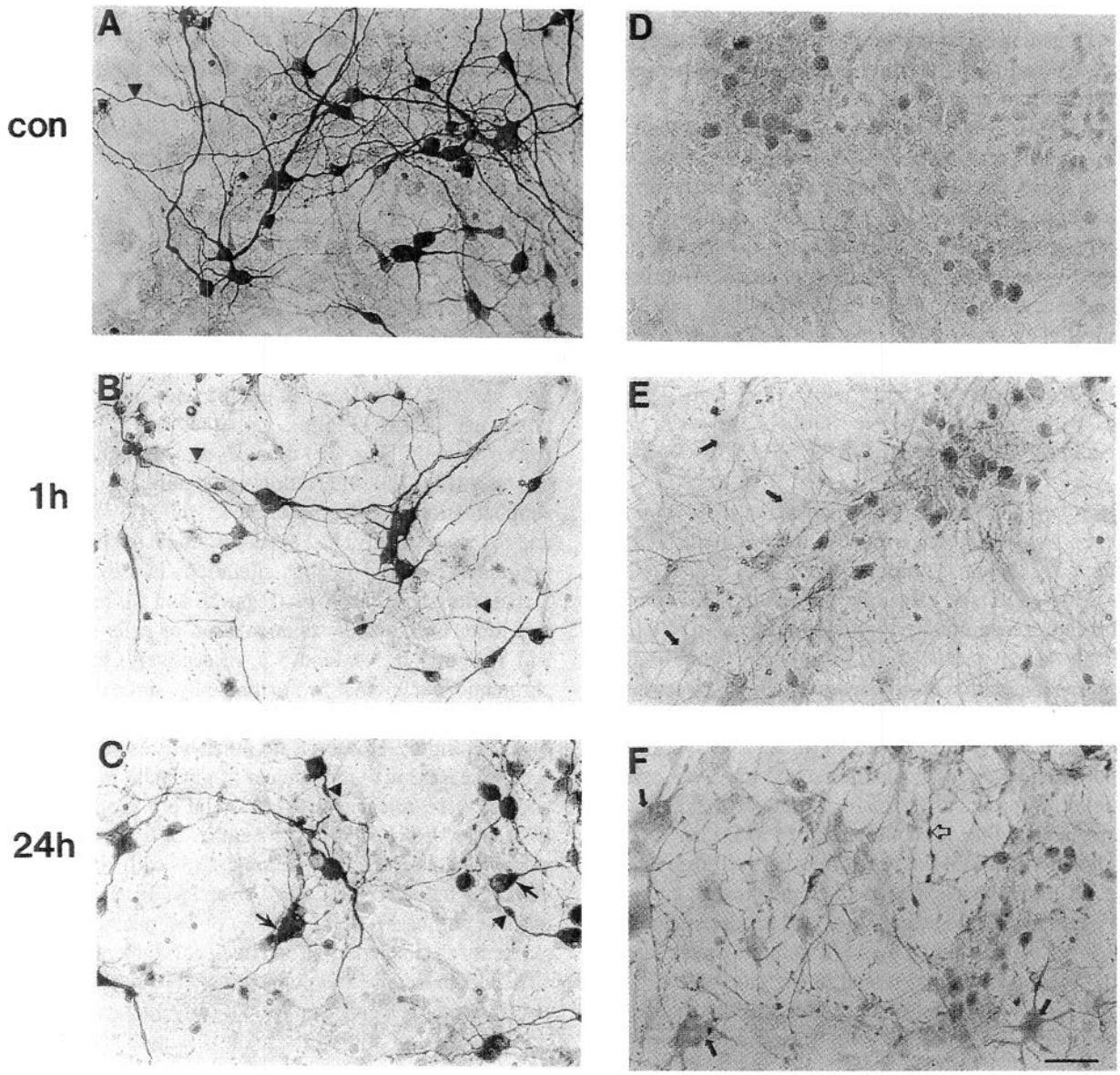

FIG. 3. Mechanical cell stretch induces alterations in neuronal and astrocyte cell morphology (representative photomicrographs from 6.5 mm injury level). *Dendritic perturbation and neuronal cell loss after stretch injury (left column)*: (**A**) Examination of MAP2 (gray-black color; in soma/dendrites) and NeuN (brown color; in nucleus) revealed a typical staining pattern of neuronal dendrites and nuclei in nonstretched cells. Note long-smooth dendrites typical of healthy cells (arrowhead). (**B**) After stretch injury, there was a temporally progressive decrease in the number and length of dendritic processes. Acutely after injury, many processes appeared fragmented with numerous punctate swellings or beads (varicousities) along distal portions of the dendrites (arrowheads). (C) By 24 h after stretch injury, MAP2 immunoreactivity was markedly reduced or was absent along distal processes and an increased number of large varicousities were detected along proximal dendrites (arrowheads). In addition, most neurons had lost their multipolar dendritic arbor and extended only unipolar or bipolar processes. Note increased somal staining of MAP2 (arrow) that may be attributable to interrupted dendritic transport of MAP. *Astroglial perturbations after stretch injury (right column)*: (D) Astrocytes (gray color) in nonstretched wells formed a confluent monolayer beneath neurons (brown color) and stained weakly with antiserum to GFAP. (E) At 1 h after stretch injury, there was an obvious increase in astrocytic hypertrophy (arrows) and GFAP immunoreactivity was increased. Hypertrophied astrocytes had enlarged irregularly shaped stellate cell bodies and extended numerous enlarged cytoplasmic processes. (**F**) At 24 h after injury, the majority of astrocytes appeared reactive and were characterized by increased GFAP immunoreactivity. Astrocyte processes revealed numerous punctate varicousities. Bar = 50 μm.

Neuronal and Astrocytic Alterations After Stretch Injury

Alterations in neuronal microtubule associated protein 2 (MAP2) and astrocyte glial fibrillary acidic protein (GFAP) are commonly observed following a variety of *in vitro* and *in vivo* CNS insults. MAP2 is a principle component of neuronal dendritic microtubules that is thought to contribute to microtubule assembly and to regulate interactions with other cytoskeletal components. Phosphorylation of MAP2 by calcium/calmodulin-dependent kinases may be an important event in neuronal neurotransmitter signaling (DeCamilli et al., 1984) and trauma-induced disruption of dendritic MAP2 organization may impair neuronal function. Several investigations have reported decreased MAP2 immunoreactivity and protein levels after traumatic brain injury in rats (Folkerts et al., 1998; Hicks et al., 1995; Lewen et al., 1996; Posmantur et al., 1996a,b; Saatman et al., 1998; Taft et al., 1992, 1993). However, the present investigation is the first to examine MAP2 immunoreactivity and dendritic morphology after mechanical stretch injury. Importantly, our investigation demonstrates the typical pattern of MAP2 loss and associated dendritic derangements commonly described after numerous neuronal insults, including excitotoxic lesions *in vitro* (Park et al., 1996) and after cerebral ischemia (Matesic and Lin, 1994) and traumatic brain injury (Folkerts et al., 1998; Lewen et al., 1996; Posmantur et al., 1996a,b) *in vivo*. These results indicate that mechanical tensile strain is sufficient to induce MAP2 cytoskeletal degradation.

MAP2 is a known substrate of calpain (Fischer et al., 1991; Johnson et al., 1991), and calcium-dependent calpain activation has been closely associated with MAP2 loss after traumatic spinal cord injury (Springer et al., 1997) and in rodent brain after excitotoxic lesions (Siman and Noszek, 1988). After mild to severe stretch injury to CNS cultures, intracellular free calcium concentrations and extracellular glutamate levels have been reported to be transiently elevated (Rzigalinski et al., 1997, 1998). Thus, stretch-induced glutamate efflux and loss of intracellular Ca^{2+} homeostasis could result in increased calpain activation and subsequent proteolysis of calpain substrates such as MAP2 and α-spectrin. In support of this hypothesis, a preliminary report from our laboratory has shown that the NMDA receptor antagonist MK-801 (50 μM) attenuated LDH release (by 26%) and calpain-mediated processing of α-spectrin after moderate stretch injury in neuronal + glial septo-hippocampal cultures (Zhao et al., 1998).

Resting astrocytes typically proliferate in response to injury and display a hypertrophied morphology characterized by enlarged, irregularly shaped cell bodies and extension of numerous processes that express increased GFAP intermediate filaments (Malhotra et al., 1990). This process of reactive gliosis is one of the most sensitive assays of neuronal injury *in vivo* (O'Callaghan, 1993) and has been frequently characterized in various models of rodent traumatic brain injury (e.g., Cortez et al., 1989; Hill et al., 1996). However, the present investigation is the first to examine GFAP immunoreactivity and reactive gliosis after mechanical stretch injury in glial-neuronal cell cultures. Stretch injury resulted in a graded response of astrocytes to various injury levels (5.7-, 6.5-, and 7.5-mm injury; data for 5.7- and 7.5-mm injury not shown). Astrocyte morphology after stretch injury was stereotypical of the classic reactive astrocyte response to injury, and these results indicate that mechanical tensile strain is sufficient to induce reactive gliosis in astrocytes.

CONCLUSION

Mechanical stretch injury to septo-hippocampal cell cultures induces a variety of pathological responses that have been observed after clinical and experimental traumatic brain injury. These alterations included increased membrane permeability, astrocyte hypertrophy and increased GFAP levels, loss of neuronal-dendritic MAP2, rapid calpain activation, caspase-3 activation, necrosis, and apoptotic cell death. However, one important difference between *in vitro* mechanical stretch injury and *in vivo* traumatic brain injury was that calpain processing of α-spectrin was confined to the period of acute injury response (1–6 h) after stretch injury, whereas calpain processing of α-spectrin after traumatic brain injury can endure for as long as 2 weeks after injury (Pike et al., 1998a). Nonetheless, mechanical stretch injury (tensile strain) is a simple and reliable method for the study of mechanically induced CNS pathology.

ACKNOWLEDGMENTS

This work was supported by NIH grant R01-NS21458 and N00014-97-1-1064 from the University of Pittsburgh and Office of Naval Research to R.L.H., and by NIH award F32-NS10584 and the State of Florida Brain and Spinal Cord Injury Rehabilitation Trust Fund (BSCIRTF) to B.R.P.

REFERENCES

BANIK, N.L., MATZELLE, D.C., GANTT-WILFORD, G., OSBORNE, A., and HOGAN, E.L. (1997). Increased calpain

content and progressive degradation of neurofilament protein in spinal cord injury. Brain Res. **752,** 301–306.

CARGILL, R.S., and THIBAULT, L.E. (1996). Acute alterations in $[Ca^{2+}]_I$ in NG108-15 cells subjected to high strain rate deformation and chemical hypoxia: an *in vitro* model for neural trauma. J. Neurotrauma **13,** 396–407.

CHARRIAUT-MARLANGUE, C., REMOLLEAU, S., AGGOUN-ZOUAOUI, D., and BEN-ARI, Y. (1998). Apoptosis and programmed cell death: a role in cerebral ischemia. Biomed. Pharmacother. **52,** 264–269.

CHEN, J., NAGAYAMA, T., JIN, K., et al. (1998). Induction of caspase-3–like protease may mediate delayed neuronal death in the hippocampus after transient cerebral ischemia. J. Neurosci. **18,** 4914–4928.

CHOI, D.W., MAULUCCI-GEDDE, M., and KRIEGSTEIN, A.R. (1987). Glutamate neurotoxicity in cortical cell culture. J. Neurosci. **7,** 357–368.

COLICOS, M.A., and DASH, P.K. (1996). Apoptotic morphology of dentate gyrus granule cells following experimental cortical impact injury in rats: possible role in spatial memory deficits. Brain Res. **739,** 120–131.

CONTI, A.C., RAGUHPATHI, R., TROJANOWSKI, J.Q., and McINTOSH, T.K. (1998). Experimental brain injury induces regionally distinct apoptosis during the acute and delayed post-traumatic period. J. Neurosci. **18,** 5663–5672.

CORTEZ, S.C., McINTOSH, T.K., and NOBLE, L.J. (1989). Experimental fluid percussion brain injury: vascular disruption and neuronal and glial alterations. Brain Res. **482,** 271–282.

CROWE, M.J., BRESNAHAN, J.C., SHUMAN, S.L., MASTERS, J.N., and BEATTIE, M.S. (1997). Apoptosis and delayed degeneration after spinal cord injury in rats and monkeys. Nat. Med. **3,** 73–76.

CRYNS, V., and YUAN, J. (1998). Proteases to die for. Genes Dev. **12,** 1551–1570.

DECAMILLI, P., MILLER, P., NAVONE, F., THEURKAUF, W., and VALLEE, R. (1984). Distribution of microtubule-associated protein 2 in the nervous system of the rat studied by immunofluorescence. Neuroscience **11,** 817–846.

ELDADAH, B.A., YAKOVLEV, A.G., and FADEN, A.I. (1996). A new approach for the electrophoretic detection of apoptosis. Nucleic Acids Res. 24, 4092–4093.

ELLIS, E.F., McKINNEY, J.S., WILLOUGHBY, K.A., LIANG, S., and POVLISHOCK, J.T. (1995). A new model for rapid stretch-induced injury of cells in culture: characterization of the model using astrocytes. J. Neurotrauma **12,** 325–339.

ENARI, M., SAKAHIRA, H., YOKOYAMA, H., OKAWA, K., IWAMATSU, A., and NAGATA, S. (1998). A caspase-activated DNase that degrades DNA during apoptosis, and its inhibitor ICAD. Nature **391,** 43–50.

ENDRES, M., NAMURA, S., SHIMIZU-SASAMATA, M., et al. (1998). Attenuation of delayed neuronal death after mild focal ischemia in mice by inhibition of the caspase family. J. Cereb. Blood Flow Metab. **18,** 238–247.

FISCHER, I., ROMANO-CLARKE, G., and GRYNSPAN, F. (1991). Calpain-mediated proteolysis of microtubule-associated proteins MAP1B and MAP2 in developing brain. Neurochem. Res. **16,** 891–898.

FOLKERTS, M.M., BERMAN, R.F., MUIZELAAR, J.P., and RAFOLS, J.A. (1998). Disruption of MAP-2 immunostaining in rat hippocampus after traumatic brain injury. J. Neurotrauma **15,** 349–363.

GENNARILLI, T.A., and THIBAULT, L.E. (1985). Biological models of head injury, in *Central Nervous System Trauma Status Report.* D.P. Becker and J.T. Povlishock (eds), National Institutes of Health: Bethesda, MD, pps. 391–404.

GOLDBERG, W.J., KADINGO, R.M., and BARRETT, J.N. (1988). Phencylidine receptor ligands attenuate cortical neuronal injury after *N*-methyl-D-aspartate exposure or hypoxia. J. Pharmacol. Exp. Ther. **245,** 1081–1087.

GROSS, G.W., LUCAS, J.H., and HIGGINS, M.L. (1993). Laser microbeam surgery: ultrastructural changes associated with neurite transection in culture. J. Neurosci. **3,** 1979–1993.

HARRIS, A.S., CROALL, D.E., and MORROW, J.S. (1988). The calmodulin-binding site in alpha-fodrin is near the calcium-dependent protease I cleavage site. J. Biol. Chem. **263,** 15754–15761.

HENKELS, K.M., and TURCHI, J.J. (1997). Induction of apoptosis in cisplatin-sensitive and -resistant human ovarian cancer cell lines. Cancer Res. **57,** 4488–4492.

HICKS, R.R., SMITH, D.H., and McINTOSH, T.K. (1995). Temporal response and effects of excitatory amino acid antagonism on microtubule-associated protein 2 immunoreactivity following experimental brain injury in rats. Brain Res. **678,** 151–160.

HILL, S.J., BARBARESE, E., and McINTOSH, T.K. (1996). Regional heterogeneity in the response of astrocytes following traumatic brain injury in the adult rat. J. Neuropathol. Exp. Neurol. **55,** 1221–1229.

HONG, S.C., GOTO, Y., LANZINO, G., SOLEAU, S., KASSELL, N.F., and LEE, K.S. (1994). Neuroprotection with a calpain inhibitor in a model of focal cerebral ischemia. Stroke. **25,** 663–669.

JANICKE, R.U., NG, P., SPRENGART, M.L., and PORTER, A.G. (1998). Caspase-3 is required for α-fodrin cleavage but dispensible for cleavage of other death substrates in apoptosis. J. Biol. Chem. **273,** 15540–15545.

JOHNSON, G.V., LITERSKY, J.M., and JOPE, R.S. (1991). Degradation of microtubule-associated protein 2 and brain spectrin by calpain: a comparative study. J. Neurochem. **56,** 1630–1638.

JONES, K.H., and SENFT, A.J. (1985). An improved method to determine cell viability by simultaneous staining with fluorescein diacetate-propidium iodide. J. Histochem. Cytochem. **33,** 77–79.

KAMPFL, A., POSPMANTUR, R.M., ZHAO, X., SCHMUTZHARD, E., CLIFTON, G.L., and HAYES, R.L. (1997). Mechanisms of calpain proteolysis following traumatic brain injury: implications for pathology and therapy: a review and update. J. Neurotrauma **14,** 121–134.

KATO, H., KANELLOPOULOS, G.K., MATSUO, S., et al. (1997). Protection of rat spinal cord from ischemia with dextrorphan and cycloheximide: effects on necrosis and apoptosis. J. Thorac. Cardiovasc. Surg. **114,** 609–618.

KATOH, K., IKATA, T., KATOH, S., et al. (1996). Induction and its spread of apoptosis in rat spinal cord after mechanical trauma. Neurosci. Lett. **216,** 9–12.

KAYA, S.S., MAHMOOD, A., LI, Y., YAVUZ, E., GOKSEL, M., and CHOPP, M. (1999). Apoptosis and expression of p53 response proteins and cyclin D1 after cortical impact in rat brain. Brain Res. **818,** 23–33.

KITAGAWA, H., HAYASHI, T., MITSUMOTO, Y., KOGA, N., ITOYAMA, Y., and ABE, K. (1998). Reduction of ischemic brain injury by topical application of glial cell line–derived neurotrophic factor after permanent middle cerebral artery occlusion in rats. Stroke. **29,** 1417–1422.

KOH, J.Y., and CHOI, D.W. (1987). Quantitative determination of glutamate-mediated cortical neuronal injury in cell culture by lactate dehydrogenase efflux assay. J. Neurosci. Methods **20,** 83–90.

KUIDA, K., ZHENG, T.S., NA, S., et al. (1996). Decreased apoptosis in the brain and premature lethality in CPP32-deficient mice. Nature **384,** 368–372.

LAMB, R.G., HARPER, C.C., McKINNEY, J.S., RZIGALINSKI, B.A., and ELLIS, E.F. (1997). Alterations in phosphatidylcholine metabolism of stretch-injured cultured rat astrocytes. J. Neurochem. **68,** 1904–1910.

LAPLACA, M.C., LEE, V.M.Y., and THIBAULT, L.E. (1997). An *in vitro* model of traumatic neuronal injury: loading rate-dependent changes in acute cytosolic calcium and lactate dehydrogenase release. J. Neurotrauma **14,** 355–368.

LEE, K., FRANK, S., VANDERKLISH, P., ARAI, A., and LYNCH, G. (1991). Inhibition of proteolysis protects hippocampal neurons from ischemia. Proc. Natl. Acad. Sci. U.S.A. **88,** 7233–7237.

LEWEN, A., LI, G.L., OLSSON, Y., and HILLERED, L. (1996). Changes in microtubule-associated protein 2 and amyloid precursor protein immunoreactivity following traumatic brain injury in rat: influence of MK-801 treatment. Brain Res. **719,** 161–171.

LI, Z., HOGAN, E.L., and BANIK, N.L. (1995). Role of calpain in spinal cord injury: increased m-calpain immunoreactivity in spinal cord after compression injury in the rat. Neurochem. Int. **27,** 425–432.

LINNIK, M.D., MARKGRAF, C.G., MASON, P.J., VELAYO, N., and RACKE, M.M. (1996). Calpain inhibition attenuates apoptosis *in vitro* and decreases infarct size *in vivo*, in: *Pharmacology of Cerebral Ischemia.* J. Krieglstein (ed), CRC Press: Boca Raton, FL, pps. 33–40.

LIU, X.Z., XU, X.M., HU, R., et al., (1997). Neuronal and glial apoptosis after traumatic spinal cord injury. J. Neurosci. **17,** 5395–5406.

LIU, X., LI, P., WIDLAK, P., et al. (1998). The 40-kDa subunit of DNA fragmentation factor induces DNA fragmentation and chromatin condensation during apoptosis. Proc. Natl. Acad. Sci. U.S.A. **95,** 8461–8466.

LUCAS, J.H., EMERY, D.G., HIGGINS, M.L., and GROSS, G.W. (1990). Neuronal survival and dynamics of ultrastructural damage after dendrotomy in low calcium. J. Neurotrauma **7,** 169–192.

MALHOTRA, S.K., SHNITKA, T.K., and ELBRINK, J. (1990). Reactive astrocytes—a review. Cytobios **61,** 133–160.

MARGULIES, S.S., THIBAULT, L.E., and GENNARELI, T.A. (1990). Physical model simulations of brain injury in the primate. J. Biomech. **23,** 823–836.

MARTIN, S.J., O'BRIEN, G.A., NISHIOKA, W.K., et al. (1995). Proteolysis of fodrin (non-erythroid spectrin) during apoptosis. J. Biol. Chem. **270,** 6425–6428.

MATESIC, D.F., and LIN, R.C. (1994). Microtubule-associated protein 2 as an early indicator of ischemia-induced neurodegeneration in the gerbil forebrain. J. Neurochem. **63,** 1012–1020.

MONYER, H., GOLDBERG, M.P., and CHOI, D.W. (1989). Glucose deprivation neuronal injury in cortical culture. Brain Res. **483,** 347–354.

MORRISON III, B., MEANEY, D.F., and McINTOSH, T.K. (1998a). Mechanical characterization of a mechanical device to quantitatively injure living brain tissue. Ann. Biomed. Eng. **26,** 381–390.

MORRISON III, B., SAATMAN, K.E., MEANEY, D.F., and McINTOSH, T.K. (1998b). *In vitro* central nervous system models of mechanically induced trauma: a review. J. Neurotrauma. **15,** 911–928.

MUKHIN, A.G., IVANOVA, S.A., ALLEN, J.W., and FADEN, A.I. (1998). Mechanical injury to neuronal/glial cultures in microplates: role of NMDA receptors and pH in secondary neuronal cell death. J. Neurotrauma **51,** 748–758.

MURPHY, E.J., and HORROCKS, L.A. (1994). Models of neurotrauma *ex vivo*, in: *The Neurobiology of Central Nervous System Trauma.* S.K. Salzman and A.I. Faden (eds), Oxford University Press: New York, pps. 28–40.

NAMURA, S., ZHU, J., FINK, K., et al. (1998). Activation and

cleavage of caspase-3 in apoptosis induced by experimental cerebral ischemia. J. Neurosci. **18,** 3659–3668.

NATH, R., McGINNIS, K.J., NADIMPALLI, R., STAFFORD, D., and WANG, K.K.W. (1996a). Effects of ICE-like proteases and calpain inhibitors on neuronal apoptosis. Neuroreport **8,** 249–255.

NATH, R., RASER, K.J., STAFFOR, D., et al. (1996b). Non-erythroid α-spectrin breakdown by calpain and interleukin 1β-converting-enzyme–like protease(s) in apoptotic cells: contributory roles of both protease families in neuronal apoptosis. Biochem. J. **319,** 683–690.

NATH, R., PROBERT, A., McGINNIS, K.M., and WANG, K.K.W. (1998). Evidence for activation of caspase-3–like protease in excitotoxin- and hypoxia/hypoglycemia-injured neurons. J. Neurochem. **71,** 186–195.

NEWCOMB, J.K., KAMPFL, A., POSMANTUR, R.M., et al. (1997). Immunohistochemical study of calpain-mediated breakdown products to α-spectrin following controlled cortical impact injury in the rat. J. Neurotrauma **14,** 369–383.

NEWCOMB, J.K., ZHAO, X., PIKE, B.R., and HAYES, R.L. (1999). Temporal profile of apoptotic-like changes in neurons and astrocytes following controlled cortical impact injury in the rat. Exp. Neurol. **158,** 76–88.

NICHOLSON, D.W., and THORNBERRY, N.A. (1997). Caspases: killer proteases. Trends Biochem. Sci. **22,** 299–306.

NORTON, W.T., AQUINO, D.A., HOZUMI, I., CHIU, F.C., and BROSNAN, C.F. (1992). Quantitative aspects of reactive gliosis: a review. Neurochem. Res. **17,** 877–885.

O'CALLAGHAN, J.P. (1993). Quantitative features of reactive gliosis following toxicant-induced damage on the CNS. Ann. N.Y. Acad. Sci. **679,** 195–210.

PARK, J.S., BATEMAN, M.C., and GOLDBERG, M.P. (1996). Rapid alterations in dendrite morphology during sublethal hypoxia or glutamate receptor activation. Neurobiol. Dis. **3,** 215–227.

PIKE, B.R., ZHAO, X., NEWCOMB, J.K., POSMANTUR, R.M., WANG, K.K.W., and HAYES, R.L. (1998a). Regional calpain and caspase-3 proteolysis of α-spectrin after traumatic brain injury. Neuroreport **9,** 2437–2442.

PIKE, B.R., ZHAO, X., NEWCOMB, J.K., WANG, K.K.W., POSMANTUR, R.M., and HAYES, R.L. (1998b). Temporal relationships between *de novo* protein synthesis, calpain and caspase 3–like protease activation, and DNA fragmentation during apoptosis in septo-hippocampal cultures. J. Neurosci. Res. **52,** 505–520.

PIWOCKA, K., ZABLOCKI, K., WIECKOWSKI, M.R., et al. (1999). A novel apoptosis-like pathway, independent of mitochondria and caspases, induced by curcumin in human lymphoblastoid T (Jurkat) cells. Exp. Cell Res. **249,** 299–307.

POSMANTUR, R.M., KAMPFL, A., LIU, S.J., et al. (1996a). Cytoskeletal derangements of cortical neuronal processes three hours after traumatic brain injury in rats: an immunofluorescence study. J. Neuropathol. Exp. Neurol. **55,** 68–80.

POSMANTUR, R.M., KAMPFL, A., TAFT, W.C., et al. (1996b). Diminished microtubule-associated protein 2 (MAP2) immunoreactivity following cortical impact brain injury. J. Neurotrauma **13,** 125–137.

POSMANTUR, R., KAMPFL, A., SIMAN, R., et al. (1997). A calpain inhibitor attenuates cortical cytoskeletal protein loss after experimental traumatic brain injury in the rat. Neuroscience **77,** 875–888.

PRAVDENKOVA, S.V., BASNAKIAN, A.G., JAMES, S.J., and ANDERSON, B.J. (1996). DNA fragmentation and nuclear endonuclease activity in rat brain after severe closed head injury. Brain Res. **729,** 151–155.

PURNANAM, K.L., and BOUSTANY, R.-M. (1999). Assessment of cell viability and histochemical methods in apoptosis, in: *Apoptosis in Neurobiology*. Y.A. Hannun and R.-M. Boustany (eds), CRC Press: Boca Raton, FL, pps. 129–152.

RINK, A., FUNG, K., TROJANOWSKI, J.Q., LEE, V.M., NEUGEBAUER, E., and McINTOSH, T.K. (1995). Evidence of apoptotic cell death after experimental traumatic brain injury in the rat. Am. J. Pathol. **147,** 1575–1583.

ROBERTS-LEWIS, J.M., SAVAGE, M.J., MARCY, V.R., PINSKER, L.R., and SIMAN, R. (1994). Immunolocalization of μ-calpain–mediated spectrin degradation to vulnerable neurons in ischemic gerbil brain. J. Neurosci. **14,** 3934–3944.

RZIGALINSKI, B.A., LIANG, S., McKINNEY, J.S., and ELLIS, E.F. (1996). The effect of calcium on astrocyte injury. F.A.S.E.B. J. **10,** A280–A281.

RZIGALINSKI, B.A., LIANG, S., McKINNEY, J.S., WILLOUGHBY, K.A., and ELLIS, E.F. (1997). Effect of Ca^{2+} on *in vitro* astrocyte injury. J. Neurochem. **68,** 289–296.

RZIGALINSKI, B.A., WEBER, J.T., WILLOUGHBY, K.A., LIANG, S., WOODWARD, J.J., and ELLIS, E.F. (1998). Glutamate release and enhanced receptor sensitivity in stretch-injured neurons [abstract]. J. Neurotrauma **15,** 894.

SAATMAN, K.E., BOZYCZKO-COYNE, D., MARCY, V., SIMAN, R., and McINTOSH, T.K. (1996). Prolonged calpain-mediated spectrin breakdown occurs regionally following experimental brain injury in the rat. J. Neuropathol. Exp. Neurol. **55,** 850–860.

SAATMAN, K.E., GRAHAM, D.I., and McINTOSH, T.K. (1998). The neuronal cytoskeleton is at risk after mild and moderate brain injury. J. Neurotrauma **15,** 1047–1058.

SCHMECHEL, D.E. (1999). Assessment of ultrastructural changes associated with apoptosis, in: *Apoptosis in Neurobiology*. Y.A. Hannun and R.-M. Boustany (eds), CRC Press: Boca Raton, FL, pps. 153–181.

SEUBERT, P., LEE K., and LYNCH, G. (1989). Ischaemia triggers NMDA receptor–linked cytoskeletal proteolysis in hippocampus. Brain Res. **492,** 366–370.

SHEPARD, S.R., GHAJAR, J.B.G, GIANNUZZI, R., KUFFERMAN, S., and HARIRI, R.J. (1991). Fluid percussion barotrauma chamber: a new *in vitro* model for traumatic brain injury. J. Surg. Res. **51,** 417–424.

SIMAN, R., and NOSZEK, J.C. (1988). Excitatory amino acids activate calpain I and induce structural protein breakdown *in vivo*. Neuron **1,** 279–287.

SPRINGER, J.E., AZBILL, R.D., KENNEDY, S.E., GEORGE, J., and GEDDES, J.W. (1997). Rapid calpain I activation and cytoskeletal protein degradation following traumatic spinal cord injury: attentuation with ribuzole pretreatment. J. Neurochem. **69,** 1592–1600.

TAFT, W.C., YANG, K., DIXON, C.E., and HAYES, R.L. (1992). Microtubule-associated protein 2 levels decrease in hippocampus following traumatic brain injury. J. Neurotrauma **9,** 281–290.

TAFT, W.C., YANG, K., DIXON, C.E., CLIFTON, G.L., and HAYES, R.L. (1993). Hypothermia attenuates the loss of hippocampal microtubule-associated protein 2 (MAP2) following traumatic brain injury. J. Cereb. Blood Flow Metab. **13,** 796–802.

TANG, D., and KIDD, V.J. (1998). Cleavage of DFF-45/ICAD by multiple caspases is essential for its function during apoptosis. J. Biol. Chem. **273,** 28549–28552.

TAVALIN, S.J., ELLIS, E.F., and SATIN, L.S. (1995). Mechanical perturbation of cultured cortical neurons reveals a stretch-induced delayed depolarization. J. Neurophysiol. **74,** 2767–2773.

TAVALIN, S.J., ELLIS, E.F., and SATIN, L.S. (1997). Inhibition of the electrogenic Na pump underlies delayed depolarization of cortical neurons after mechanical injury or glutamate. J. Neurophysiol. **77,** 632–638.

WANG, K.K.W., POSMANTUR, R.M., NATH, R., et al. (1998). Simultaneous degradation of αII and βII spectrin by caspase-3 (CPP32) in apoptotic cells. J. Biol. Chem. **273,** 22490–22497.

WILLOUGHBY, K.A., RZIGALINSKI, B.A., and ELLIS, E.F. (1998). Stretch-induced injury of cultured cells causes delayed alterations in neurons and immediate, transient alterations in astrocytes [abstract]. J. Neurotrauma. **15,** 902.

WOLF, B.B., GOLDSTEIN, J.C., STENNICKE, H.R., et al. (1999). Calpain functions in a caspase-independent manner to promote apoptosis-like events during platelet activation. Blood **94,** 1683–1692.

YAKOVLEV, A.G., KNOBLACH, S.M., FAN L., FOX, G.B., GOODNIGHT, R., and FADEN, A.I. (1997). Activation of CPP32-like caspases contributes to neuronal apoptosis and neurological dysfunction after traumatic brain injury. J. Neurosci. **17,** 7415–7424.

ZHAO, X., PIKE, B.R., NEWCOMB, J.K., WANG, K.K.W., and HAYES, R.L. (1998). Mechanisms of pharmacological protection from stretch-induced cell injury in primary cell cultures [abstract]. J. Neurotrauma **15,** 904.

ZHAO, X., PIKE, B.R., NEWCOMB, J.K., WANG, K.K.W., POSMANTUR, R.M., and HAYES, R.L. (1999). Maitotoxin induces calpain but not caspase-3 activation and necrotic cell death in primary septo-hippocampal cultures. Neurochem. Res. **24,** 371–382.

Address reprint requests to:
Brian R. Pike, Ph.D
Department of Neuroscience
University of Florida Brain Institute
100 S. Newell Dr., Box 100244
Gainesville, FL 32610

E-mail: pike@ufbi.ufl.edu

Journal of Cerebral Blood Flow and Metabolism
20:550–562 © 2000 The International Society for Cerebral Blood Flow and Metabolism
Published by Lippincott Williams & Wilkins, Inc., Philadelphia

Novel Characteristics of Glutamate-Induced Cell Death in Primary Septohippocampal Cultures: Relationship to Calpain and Caspase-3 Protease Activation

Xiurong Zhao, Jennifer K. Newcomb, *Brian R. Pike, †Kevin K. W. Wang, ‡Domenico d'Avella, and *Ronald L. Hayes

*Vivian L. Smith Center for Neurologic Research, Department of Neurosurgery, University of Texas–Houston Health Science Center, Houston, Texas, *Center for Traumatic Brain Injury Studies, Department of Neuroscience, University of Florida, Gainesville, Florida, and †Department of Neuroscience Therapeutics, Parke-Davis Pharmacological Research, Division of Warner-Lambert Company, Ann Arbor, Michigan, U.S.A.; and ‡Institute of Pharmacology, Policlinico Universitario, University of Messina, Messina, Italy*

Abstract: Studies examined the phenotypic characteristics of glutamate-induced cell death and their relationship to calpain and caspase-3 activation. Cell viability was assessed by fluorescein diacetate and propidium iodide staining and lactate dehydrogenase release. Calpain and caspase-3 activity was inferred from signature proteolytic fragmentation of α-spectrin. Characterization of cell death phenotypes was assessed by Hoechst 33258 and DNA fragmentation assays. Exposure of septohippocampal cultures to 1.0, 2.0, and 4.0 mmol/L glutamate induced a dose-dependent cell death with an LD_{50} of 2.0 mmol/L glutamate after 24 hours of incubation. Glutamate treatment induced cell death in neurons and astroglia and produced morphological alterations that differed from necrotic or apoptotic changes observed after maitotoxin or staurosporine exposure, respectively. After glutamate treatment, cell nuclei were enlarged and eccentrically shaped, and aggregated chromatin appeared in a diffusely speckled pattern. Furthermore, no dose of glutamate produced evidence of internucleosomal DNA fragmentation. Incubation with varying doses of glutamate produced calpain and caspase-3 activation. Calpain inhibitor II (*N*-acetyl-Leu-Leu-methionyl) provided protection only with a narrow dose range, whereas carbobenzoxy-Asp-CH_2-OC(*O*)-2,6-dichlorobenzene (Z-D-DCB; pan-caspase inhibitor) and MK-801 (*N*-methyl-D-aspartate receptor antagonist) were potently effective across a wider dose range. Cycloheximide did not reduce cell death or protease activation. **Key Words:** Glutamate—Calpain—Caspase-3—Proteases.

Previous studies have reported that excitotoxicity is associated primarily with necrosis (Choi et al., 1987; Siman and Card, 1988). More recent studies have maintained that both necrotic and apoptotic mechanisms are activated after excessive stimulation of various glutamate receptor subtypes (Bonfoco et al., 1995). However, the precise mode of excitotoxic neuronal cell death remains controversial. Inconsistent reports of cell death phenotypes produced specifically by glutamate toxicity *in vitro* have no doubt contributed to this controversy. For example, a number of investigators have reported glutamate-induced apoptotic-like cell death characteristics in culture (Bonfoco et al., 1995; Cebers et al., 1997; Du et al., 1997; Kure et al., 1991). In contrast, other investigators have concluded that glutamate toxicity does not produce apoptotic cell death profiles (Ikeda et al., 1996; MacManus et al., 1997). Comparison of data from these studies is complicated by the use of different culture systems, different criteria for defining apoptotic cell death phenotypes, and different glutamate dosing regimens. Equally important, and with few exceptions (Du et al., 1997; Nath et al., 1998), the possible contribution of

Received June 21, 1999; revised manuscript received November 11, 1999; accepted November 17, 1999.

Supported by National Institutes of Health grants RO1 NS21458, RO1 NS38105, and RO1 NS40182, US Army DAMD17-99-1-9565, University of Pittsburgh Navy Project N00014-99-1-0765, and an endowment from the Vivian L. Smith Center for Neurologic Research.

Address correspondence and reprint requests to Dr. Ronald L. Hayes, Center for Traumatic Brain Injury Studies, Department of Neuroscience, University of Florida, P. O. Box 100244, 100 Newell Dr., L1-100F, Gainesville, FL 32610-0244, U.S.A.

Abbreviations used: BDP, breakdown product; DMEM, Delbecco's modified Eagle's medium; FDA, fluorescein diacetate; GFAP, glial fibrillary acidic protein; LDH, lactate dehydrogenase; MAP-2, microtubule-associated protein-2; NeuN, neuronal nuclear marker; NMDA, *N*-methyl-D-aspartate; PBS, phosphate-buffered saline; PI, propidium iodide; Z-D-DCB, carbobenzoxy-Asp-CH_2-OC(*O*)-2,6-dichlorobenzene.

174

calpains and caspases as proteolytic mediators of necrotic and apoptotic cell death has not been characterized in models of glutamate toxicity.

Caspases, members of the cysteine protease family, are important intracellular effectors of apoptosis in various cell lines and apoptotic models (Nath et al., 1996*a,b*; Pike et al., 1998*b*; Zhivotovsky et al., 1997). The role of caspase-1, caspase-3, and caspase-3-like (caspase-3, -6, and -7) proteases has been the focus of numerous investigations. Although the contribution of caspase-1 to apoptosis in the central nervous system has not been well established (Nath et al., 1996*a,b*; Wang et al., 1998; Zhivotovsky et al., 1997), a number of studies have implicated caspase-3-like proteases in neuronal apoptotic cell death (Nath et al., 1996*a,b*; Pike et al., 1998*b*; Wang et al., 1998). In fact, some studies suggest that caspase-3-like proteases are activated only in apoptosis but not in necrosis (Wang et al., 1996*b*). Calpains are calcium-activated, neutral, cytosolic cysteine proteases (Nath et al., 1996*b*). Although investigators have historically assumed that calpain activation resulted in necrotic cell death, several recent investigations have suggested that calpains can also contribute to apoptosis (Nath et al., 1996*a*; Pike et al., 1998*b*; Squier et al., 1994). Importantly, calpain activation has been implicated in different models of apoptosis in different cell types including neurons (Nath et al., 1996*a*; Pike et al., 1998*b*; Squier et al., 1994). A recent study provided evidence of increased calpain and caspase-3 activity in rat cortical and cerebellar granule neurons challenged with excitotoxins *N*-methyl-D-aspartate (NMDA), 2-amino-3-hydroxy-5-methylisoxazole-4-propionic acid, and kainate, although they provided no data on cell death phenotypes (Nath et al., 1998). Similarly, Du et al. (1997) reported that activation of caspase-3-related proteases is required for glutamate-mediated apoptosis in rat cerebellar granule neurons. However, these authors did not examine calpain activity.

To address these inconsistencies in studies of excitotoxic cell death pathways, our laboratory has systematically characterized the phenotypic characteristics of apoptotic cell death produced by staurosporine (Pike et al., 1998*b*) and necrotic cell death produced by maitotoxin (Zhao et al., 1999) in primary cultures of septohippocampal neurons. We chose this culture system because the hippocampus is preferentially vulnerable to a number of acute insults including ischemia (Jenkins et al., 1989) and mechanical trauma (Lyeth et al., 1990). The present study represents the first characterization of apoptotic and necrotic cell death after glutamate toxicity in relation to activation of calpain and caspase-3 proteases. Recognizing that criteria for cell death phenotypes are subject to controversy (Portera-Cailliau et al., 1997), we incorporated a number of widely utilized morphological, biochemical, and molecular criteria to describe cell death characteristics in neurons and glia after glutamate exposure. Results of this investigation indicate that glutamate can elicit an apoptotic biochemical response not associated with apoptotic cell morphology. This result has important implications for pharmacological treatment of cell death, even in cases where apoptosis is not thought to play an important role.

MATERIALS AND METHODS

Septohippocampal cultures

Eighteen-day-old rat fetuses were removed from deeply anesthetized dams. Septi and hippocampi were dissected in a dissection buffer (Hanks' balanced salt solution, with 4.2 mmol/L bicarbonate, 1 mmol/L pyruvate, 20 mmol/L *N*-2-hydroxyethylpiperazine-*N'*-2-ethanesulfonate, 3 mg/mL bovine serum albumin, pH 7.25). After rinsing in Dulbecco's modified Eagle's medium (DMEM), tissue was dissociated by trituration through the narrow pore of a flame-constricted Pasteur pipette. Dissociated cells were resuspended in DMEM with 10% fetal calf serum and plated on 24-well poly-L-lysine-coated plastic culture plates or 12-mm German glass (Erie Scientific Co., Portsmouth, NH, U.S.A.) at a density of 4.36×10^5 cells/mL. Cultures were maintained in a humidified incubator in an atmosphere of 5% CO_2 at 37°C. After 5 days in culture, the medium was changed to DMEM with 5% horse serum. Subsequent medium changes were carried out three times a week. By day 10 *in vitro*, astrocytes formed a confluent monolayer beneath morphologically mature neurons and experiments were performed.

For neuronally enhanced cultures, hippocampi and septi were dissected and dissociated as described above. Dissociated cells were resuspended in DMEM and plated on 24-well poly-L-lysine-coated plastic culture plates at a density of 4.36×10^5 cells/mL. Cultures were maintained in a humidified incubator in an atmosphere of 5% CO_2 at 37°C. Medium was changed three times a week; however, only 50% of the medium was changed each time to enhance neuronal survival.

Pharmacological treatment of septohippocampal cells

Glutamate. Ten-day-old mixed septohippocampal cultures were challenged with 1.0, 2.0, or 4.0 mmol/L glutamate in DMEM (serum-free), and cell viability was monitored at various postinjury time points (n = 10 wells/condition). Similar glutamate concentrations have been used in mixed (Kure et al., 1991) and neuronal (Ikeda et al., 1996) studies. To assess the contribution of glia to differences in sensitivity to glutamate toxicity, neuronally enhanced septohippocampal cultures were also incubated in varying concentrations of glutamate (1 μmol/L to 2.0 mmol/L) for 24 hours (n = 3 wells/condition). Glutamate was added directly to the medium for the entire duration of experiments. Experiments were performed on day 10 *in vitro* as sensitivity of mixed septohippocampal cultures to glutamate does not differ between 10 and 15 days *in vitro* (data not shown).

N-Methyl-D-aspartate receptor antagonism, inhibition of calpain and caspase activation, and protein synthesis inhibition. Sister cultures were pretreated 1 hour before, and cotreated during, the glutamate challenge, with varying doses of the NMDA antagonist MK-801 (RBI, Natick, MA, U.S.A.; 10 to 500 μmol/L), calpain inhibitor II (*N*-acetyl-Leu-Leu-methionyl; 5 to 100 μmol/L; Boehringer Mannheim, India-

napolis, IN, U.S.A.), the pan-caspase inhibitor carbobenzoxy-Asp-CH_2-OC(*O*)-2,6-dichlorobenzene (Z-D-DCB; 30 to 300 μmol/L; Bachem, King of Prussia, PA, U.S.A.), or the protein synthesis inhibitor cycloheximide (1 μg/mL; Sigma, St. Louis, MO, U.S.A.). All inhibitors were administered in DMEM (n = 3 wells/condition). We and others have used these concentrations to provide inhibition of NMDA receptor-mediated toxicity (Carroll et al., 1996), calpain activation (Kampfl et al., 1996; Pike et al., 1998*b*), caspase-3-like protease activity (Nath et al., 1996*a,b*; Pike et al., 1998*b*), and protein synthesis (Martin et al., 1988; Pike et al., 1998*b*), respectively. As noted below, experimental procedures allowed independent assessments of whether drugs used in this study inhibited activation of calpains and caspase-3-like proteases inferred by α-spectrin proteolysis.

Chemical inducers of apoptotic or necrotic cell death phenotypes. To provide comparisons of glutamate toxicity with classic apoptotic and necrotic profiles, cultures were treated with the general protein kinase inhibitor staurosporine or maitotoxin, a potent marine toxin that activates both voltage-sensitive and receptor-operated calcium channels. Ten-day-old septohippocampal cultures were challenged with 0.5 μmol/L staurosporine for 24 hours, a dose and duration that we have previously confirmed produce apoptotic but not necrotic neuronal cell death in this *in vitro* system (Pike et al., 1998*b*). The production of apoptotic cell death by staurosporine is associated with activation of both caspase-3 and calpain proteases, and staurosporine-induced apoptosis can be attenuated by calpain or caspase inhibitors (Pike et al., 1998*b*). Cultures were also treated with maitotoxin (0.1 nmol/L for 1 hour), a dose and duration that we have previously confirmed produce an exclusively necrotic-like cell death profile in neurons and glia and are associated with calpain but not caspase-3 activation (Zhao et al., 1999).

Morphological and enzymatic assessments of cell damage

Fluorescein diacetate and propidium iodide assay of cell viability. Fluorescein diacetate (FDA) and propidium iodide (PI) dyes were used to assess cell viability at various times between 1 and 72 hours after glutamate incubation. Fluorescein diacetate enters normal cells and emits a green fluorescence when it is cleaved by esterases. Once cleaved, FDA can no longer permeate cell membranes. Propidium iodide is an intravital dye that is normally excluded from cells. After injury, PI penetrates cells, binds to DNA in the nucleus, and emits a red fluorescence. This technique is commonly used to quantitate cell injury (Jones and Senft, 1985).

A stock solution of FDA was prepared by dissolving 20 mg/mL in acetone. A PI stock solution was prepared by dissolving 5 mg/mL in 1× phosphate-buffered saline (PBS) (Jones and Senft, 1985). The FDA and PI working solutions were freshly prepared by adding 10 μL of the FDA and 3 μL of PI stock to 10 mL of Dulbecco's PBS. Two hundred microliters per well of FDA/PI working solution was added directly to the cells. Cells were stained for 3 minutes at room temperature. Stained cells were examined with a fluorescence microscope equipped with epi-illumination, bandpass 450- to 490-nm exciter filter, 510-nm chromatic beam splitter, and a long-pass 520-nm barrier filter. This filter combination permitted both green and red fluorescing cells to be seen simultaneously. Cell viability can be determined because this procedure results in the nuclei of dead cells fluorescing red and the cytoplasm of living cells fluorescing green. Cell loss was calculated in 100× fields (five sequential 100× fields were counted and averaged per well) for three wells in each experiment as a percentage of total cell number.

Hoechst staining of apoptotic nuclei. After overnight fixation in 4% paraformaldehyde at 4°C, cells grown on German glass were washed three times with PBS and labeled with 1 μg/mL of the DNA dye Hoechst 33258 (bis-benzamide; Sigma) in PBS. Cells were incubated for 5 to 10 minutes at room temperature, rinsed with PBS, and mounted with crystal-mount medium (Biomeda, Foster City, CA, U.S.A.). Cells were observed and photographed on a phase and fluorescence microscope with a UV2A filter.

Determination of lactate dehydrogenase activity Lactate dehydrogenase (LDH) activity assessed cell viability (Koh and Choi, 1987) in experiments examining the effects of NMDA receptor antagonism and inhibition of calpain and caspase proteases and protein synthesis. Lactate dehydrogenase released from damaged cells was measured by standard kinetic assay for pyruvate (Boehringer Mannheim). An increase in the amount of dead or plasma membrane-damaged cells results in an increase of the LDH enzyme activity in the culture supernatant detected by colorimetric measurements. In brief, 200 μL of culture medium was removed from each well and centrifuged at 5,000 *g* for 5 minutes. One hundred microliters of supernatant was transferred to each well of a 96-well flat bottom plate, and 100 μL of detection reagent was added. The plate was covered with foil and incubated on a shaker for 30 minutes at room temperature. The absorbance of samples was measured at 490 nm using Bio-Rad model 450 microplate reader (Hercules, CA, U.S.A.).

DNA fragmentation assay

DNA gel electrophoresis was performed as described previously (Gong et al., 1994). Cells were collected by centrifugation at 3,000 *g* for 5 minutes, fixed in suspension in 70% cold ethanol, and stored in the fixative at –20°C for 24 to 72 hours. Cells were centrifuged at 800 *g* for 5 minutes, and the ethanol was thoroughly removed. Cell pellets were resuspended in 40 μL of phosphate/citrate buffer consisting of 192 parts of 0.2 mol/L Na_2HPO_4 and 8 parts of 0.1 mol/L citric acid (pH 7.8) at room temperature for 1 hour. After centrifugation at 1,000 *g* for 5 minutes, the supernatant was transferred to new tubes and concentrated by vacuum in a SpeedVac concentrator for 15 to 30 minutes. Three microliters of 0.25% Nonidet P-40 in distilled water was added, followed by 3 μL of DNase-free RNase (1 mg/mL). After 30-minute incubation at 37°C, 3 μL of proteinase K (1 mg/mL) was added, and the extract was incubated for an additional 30 minutes at 37°C. After the incubation, 1 μL of 6× loading buffer (0.25% bromophenol blue, 0.25% xylene cyanol FF, and 30% glycerol in water) was added, the entire content of the tube was transferred to a 1.5% agarose gel, and electrophoresis was performed in 1× Tris/boric acid/ethylenediaminetetraacetate solution (0.1 mol/L Tris, 0.09 mol/L boric acid, and 1 mmol/L ethylenediaminetetraacetate, pH 8.4) at 40 V for 2 hours. The DNA was visualized and photographed under ultraviolet light after staining with 5 μg/mL ethidium bromide.

Assessment of α-spectrin degradation by calpain and caspase-3

Because the cytoskeletal protein α-spectrin contains sequence motifs preferred by both calpains and caspase-3 proteases, activation of these two protease families can be assessed concurrently by immunoblot identification of calpain and/or caspase-3 signature cleavage products. Although both calpains and caspases produce an initial fragment of nearly identical size (150 kDa), calpains further process α-spectrin into a distinctive breakdown product (BDP) of 145 kDa (Harris et al., 1988; Nath

et al., 1996*a,b*), whereas caspase-3 produces a unique 120-kDa BDP (Wang et al., 1998).

Sodium dodecyl sulfate polyacrylamide gel electrophoresis and immunoblotting. After each experiment, cells were harvested from five identical culture wells, collected in 15-mL centrifuge tubes, and centrifuged at 3,000 *g* for 5 minutes. Medium was removed, and the cells were rinsed with 1× PBS. Cells were lysed in ice-cold homogenization buffer [20 mmol/L 1,4-piperazinediethanesulfonate (pH 7.6), 1 mmol/L ethylenediaminetetraacetate, 2 mmol/L ethyleneglycol-bis-(β-aminoethyl ether)-*N,N,N′,N′*-tetraacetate, 1 mmol/L dithiothreitol, 0.5 mmol/L phenylmethylsulfonyl fluoride, 50 μg/mL leupeptin, and 10 μg/mL each of 4-(2-aminoethyl)benzenesulfonyl fluoride, aprotinin, pepstatin, *N*α-*p*-tosyl-L-lysine chloromethyl ketone, and *N*-tosyl-L-phenylalanine chloromethyl ketone] for 30 minutes and sheared through a 1.0-mL syringe 15 times with a 25-gauge needle. Protein content in the samples was assayed by the Micro bicinchroninic acid method (Pierce, Rockford, IL, U.S.A.). For protein electrophoresis, equal amounts of total protein (30 μg) were prepared in 2× loading buffer containing 0.25 mol/L Tris (pH 6.8), 0.2 mol/L dithiothreitol, 8% sodium dodecyl sulfate, 0.02% bromophenol blue, and 20% glycerol and heated at 95°C for 10 minutes. Samples were resolved in a vertical electrophoresis chamber using a 4% stacking gel over a 6.5% acrylamide resolving gel for 1 hour at 200 V. For immunoblotting, separated proteins were laterally transferred to nitrocellulose membranes (0.45 μm) using a transfer buffer consisting of 0.192 mol/L glycine and 0.025 mol/L Tris (pH 8.3) with 10% methanol at a constant voltage of 100 V for 1 hour at 4°C. Blots were blocked overnight in 5% nonfat milk in 20 mmol/L Tris, 0.15 mol/L NaCl, and 0.005% Tween 20 at 4°C. Gels and nitrocellulose membranes were stained with Coomassie Blue and Ponceau Red, respectively (Sigma) to confirm that equal amounts of protein were loaded in each lane.

Antibodies and immunolabeling. Immunoblots were probed with an anti-α-spectrin monoclonal antibody (Affiniti Research Products, Mamhead, U.K.; catalog no. FG 6090, clone AA6) that detects intact α-spectrin (M_r = 240 kDa) and 150-, 145-, and 120-kDa BDPs. After incubation with primary antibody (1:4,000) for 2 hours at room temperature, blots were incubated in peroxidase-conjugated sheep anti-mouse IgG for 1 hour (1:10,000). Enhanced chemiluminescence reagents (ECL kit; Amersham) were used to visualize the immunolabeling on Hyperfilm (Hyperfilm ECL; Amersham, Piscataway, NJ, U.S.A.).

Hoechst 33258 staining in glial or neuronal cell types

To determine the effects of glutamate on astroglial and neuronal cell types, cultures were labeled immunocytochemically with glial fibrillary acidic protein (GFAP; for astroglia) or microtubule-associated protein-2 (MAP-2) and neuronal nuclear marker (NeuN; for neurons) and counterstained with Hoechst 33258. Microtubule-associated protein-2 labels primarily dendrites, whereas NeuN is a neuronal nuclear marker. Cultures were fixed in 4% paraformaldehyde for 1 hour at 4°C and washed and stored in 1× PBS. Cultures were permeabilized with 0.3% Triton X-100 for 30 minutes and blocked with 1% normal horse or goat serum at room temperature for 1 hour, followed by incubation with GFAP (1:1,000) or MAP-2 and NeuN (1:1,000) antibody overnight at 4°C. Cultures were washed in 1× PBS and incubated in horseradish peroxidase-conjugated goat anti-rabbit IgG (for GFAP) or sheep anti-mouse IgG (for MAP-2 and NeuN) (Cappel [Durham, NC, U.S.A.]; 1:1,000) for 1 hour. Cultures were washed three times in 1× PBS, and diaminobenzidine (Vector, Burlingame, CA, U.S.A.) was used to visualize the reaction. After incubation in diaminobenzidine, the reaction was stopped in tap water, and cultures were counterstained with Hoechst 33258 for 5 minutes. After a final wash, cells were mounted and coverslipped with Cytoseal 280 mounting medium (EMS, Fort Washington, PA, U.S.A.). Each slide was observed and photographed in the same field using light (for immunolabeled cells) and fluorescence (for Hoechst 33258-labeled cells) microscopy. A phase contrast microscope (Axiovert 135) was used to distinguish the glial and neuronal cell layers.

Statistical analyses

Each experiment was performed three times, and data were evaluated by analysis of variance with a *post hoc* Tukey test. Values are given as means ± 1 SD. Differences were considered significant at $P < 0.05$.

RESULTS

Effects of glutamate on septohippocampal glial–neuronal co-cultures

Dose- and time-dependent cell death. An initial series of experiments was conducted to determine dose–response relationships between glutamate concentrations and cell viability at various times after incubation with the excitotoxin. Propidium iodide and FDA were used to assess cell death and membrane integrity. Exposure of mixed septohippocampal cultures to 1.0, 2.0, and 4.0 mmol/L glutamate induced a dose-dependent cell death with an LD_{50} of 2.0 mmol/L glutamate after 24-hour incubation (Fig. 1A). The percentages of cells that stained for PI after exposure to 2.0 mmol/L glutamate were 14.6% at 1 hour, 17.5% at 3 hours, 27.1% at 6 hours, and 51.3% at 24 hours (Fig. 1A). A one-way analysis of variance performed on these data revealed a significant effect of group ($F_{3,18} = 13.13$, $P < 0.0001$). *Post hoc* analyses showed significant increases in cell death after 1.0 mmol/L glutamate for 24 hours and at all time points using 2.0 and 4.0 mmol/L glutamate compared with control cells. Incubation with 2.0 mmol/L glutamate for 24 hours was used for most subsequent experiments, unless stated otherwise. Similar glutamate concentrations have been used to study cell death in other glial–neuronal co-culture systems (Kure et al., 1991; also see Ikeda et al., 1996). The LD_{50} for glutamate in neuronally enhanced cultures (~10 μmol/L; Fig. 1B) is similar to values reported for glutamate in other neuronally enhanced cultures (Manev et al., 1991). Univariate analysis of these data also showed a significant effect of group ($F_{7,16} = 116$, $P < 0.0001$), and *post hoc* analyses revealed significant increases in cell death at all concentrations tested.

Morphological responses to glutamate challenge. Glutamate-treated septohippocampal cultures underwent morphological alterations in cell structure that were characteristic of neither apoptosis nor necrosis (Figs. 2 and 3). For example, after 6 hours of incubation with 2.0

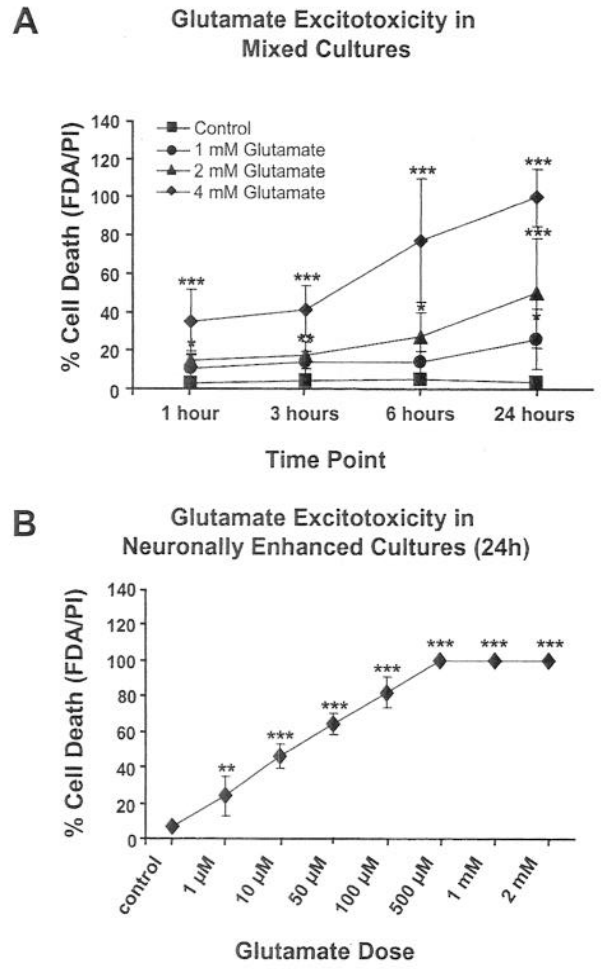

FIG. 1. Concentration and time course assays of glutamate-induced cell death. **(A)** Mixed septohippocampal cultures. Cultures were exposed to varying doses of glutamate (1.0, 2.0, 4.0 mmol/L) for 1, 3, 6, or 24 hours. Cell loss was calculated using fluorescein diacetate/propidium iodide (FDA/PI) staining and expressed as a percentage of total cell number. The LD_{50} for glutamate was 2.0 mmol/L after 24-hour incubation. **(B)** Neuronally enhanced cultures. Cultures were exposed to varying doses of glutamate (1 µmol/L to 2.0 mmol/L) for 24 hours. Cell loss was calculated using FDA/PI staining and expressed as a percentage of total cell number. All doses examined produced significant increases in the number of cells stained with PI compared with control uninjured cultures. The LD_{50} for glutamate in neuronally enhanced cultures was ~10 µmol/L. $^*P < 0.05$, $^{**}P < 0.01$, $^{***}P < 0.001$.

mmol/L glutamate (Fig. 2D), PI staining detected greater nuclear swelling than observed in maitotoxin-induced necrosis (Fig. 2B) or staurosporine-induced apoptosis (Fig. 2C). In addition, there was no evidence of apoptotic membrane blebbing or necrotic enlargement of cell bodies, as seen in cells injured with staurosporine (Fig. 2C) or maitotoxin (Fig. 2B), respectively. The FDA/PI staining of uninjured control cultures showed healthy FDA-positive cell bodies and few cells stained with PI (Fig. 2A).

Hoechst staining of nuclear chromatin further characterized cell death characteristics of glutamate toxicity in septohippocampal cultures (Fig. 3). Treatment with maitotoxin (0.1 nmol/L) for 1 hour produced necrotic cell death (Figs. 3B and 3F) that was characterized by a pyknotic but even distribution of chromatin staining. Nuclei of maitotoxin-treated cells appeared smaller, with more condensed chromatin, yielding brighter Hoechst staining. Consistent with necrotic-like cell death, Hoechst staining did not detect chromatin marginization to the nuclear envelope, formation of apoptotic bodies, or other phenotypical evidence of apoptotic-like profiles. In contrast, treatment with staurosporine (0.5 µmol/L) for 24 hours (Figs. 3C and 3G) produced increased condensation and marginization of chromatin to the nuclear envelope as well as formation of dense apoptotic bodies. Treatment with glutamate (2.0 mmol/L) for 6 hours (Figs. 3D and 3H) produced morphological alterations that differed from the classic necrotic and apoptotic changes observed after maitotoxin or staurosporine exposure. After glutamate treatment, cell nuclei were enlarged and eccentrically shaped. In addition, chromatin was aggregated in a diffusely speckled pattern throughout the entire nucleus. Chromatin clumping along nuclear margins and evidence of apoptotic body formation were not observed in glutamate-treated cells. Additional experiments examined changes in nuclear morphology after 1 hour, 24 hours, 3 days, or 5 days of incubation with 2.0 mmol/L glutamate. Hoechst staining revealed that there were no apparent changes in nuclear morphology over this 5-day period (data not shown).

DNA fragmentation. Endonuclytic DNA fragmentation can occur independently of chromatin condensation (Lin and Chou, 1992). Thus, a DNA fragmentation assay was used to determine whether DNA alterations in septohippocampal cultures assessed by Hoechst 33258 staining were associated with endonuclease activity. No dose of glutamate tested (0.5, 1.0, 2.0, or 4.0 mmol/L) produced evidence of DNA laddering after 24 hours of incubation (Fig. 4) or for any other length of incubation tested (15 minutes to 5 days; data not shown). Treatment with maitotoxin also failed to produce DNA ladders, a profile consistent with necrotic cell death. In contrast, treatment with staurosporine produced readily detectable nucleosomal-size DNA fragments characteristic of many apoptotic model systems.

Induction of cell death in both neurons and astroglia in septohippocampal cultures by glutamate. To identify the type of cell (that is, astroglial versus neuronal) injured by glutamate treatment, cells were stained with Hoechst 33258 and immunolabeled with anti-MAP-2 and anti-NeuN to identify neurons (Fig. 5) or anti-GFAP to identify astroglia (Fig. 6). After incubation with glutamate (2.0 mmol/L) for 24 hours (Figs. 5C and 5D), the number of NeuN-immunopositive neurons was markedly reduced as compared with control cultures (Figs. 5A and 5C). In addition, broken dendritic processes were appar-

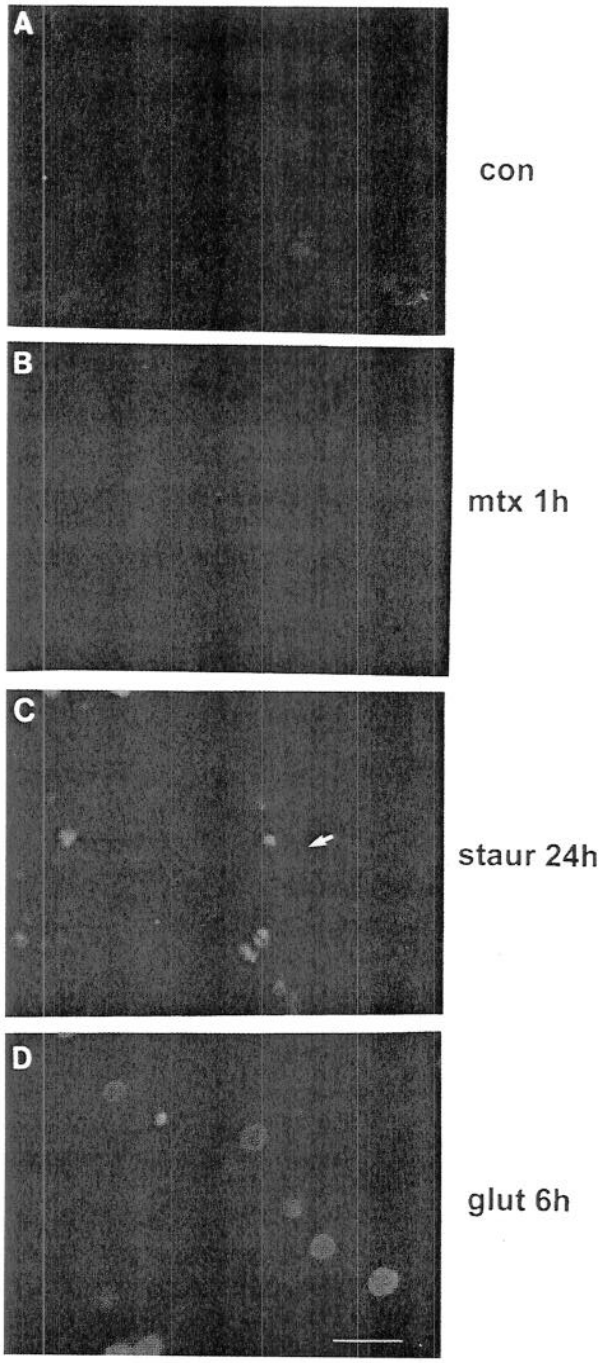

FIG. 2. Fluorescein diacetate (FDA) and propidium iodide (PI) staining of septohippocampal cultures. **(A)** Control cultures. Note normal somal structure in cells that take up FDA (green fluorescence) and the lack of PI uptake (red fluorescence). **(B)** Treatment with maitotoxin (0.1 nmol/L) for 1 hour. After maitotoxin treatment, cell bodies stained with FDA were enlarged, whereas PI-positive nuclei appeared small and uniformly rounded, features characteristic of necrotic cell death. In addition, fewer living cells were detected. **(C)** Treatment with staurosporine (0.5 μmol/L) for 24 hours. After staurosporine treatment, numerous nuclei showed positive staining for PI. Unlike maitotoxin-induced necrosis, cell bodies stained with FDA were not enlarged but did show evidence of membrane blebbing (arrow), indicating a preserved integrity of the plasma membrane characteristic of apoptosis. **(D)** Treatment with glutamate (2.0 mmol/L) for 6 hours. After glutamate treatment, PI staining detected greater nuclear swelling than observed in maitotoxin-induced necrosis (B) or staurosporine-induced apoptosis (C). In addition, there was no evidence of apoptotic membrane blebbing or necrotic enlargement of cell bodies. Bar = 5 μm.

ent as well as loss of MAP-2 immunoreactivity (Fig. 5C). The MAP-2 immunohistochemistry also detected prominent dendritic beading after glutamate treatment (Fig. 5C). Hoechst staining in injured neurons revealed chromatin aggregation in a diffusely speckled pattern with no chromatin clumping along nuclear margins (Fig. 5D). Incubation with glutamate (2.0 mmol/L) for 24 hours resulted in glial cell death (Figs. 6C and 6D) that was associated with cell shrinkage and membrane folding. These changes ultimately resulted in complete cell detachment and loss of confluence of the glial monolayer. After injury, Hoechst staining revealed DNA aggregation in a diffusely speckled pattern (Fig. 6D) in some GFAP-positive cells (Fig. 6C). Hoechst staining in injured glia revealed a similar nuclear profile to that observed in glutamate-treated neurons (Fig. 5D vs. Fig. 6D).

Calpain and caspase-3 proteolysis of α-spectrin

Proteolysis of α-spectrin into 150-kDa, calpain-specific 145-kDa, and caspase-3-specific 120-kDa BDPs was examined after incubation with varying doses of glutamate (1.0, 2.0, and 4.0 mmol/L) for 3, 6, or 24 hours (Fig. 7). Magnitudes of calpain and caspase-3 activation were dependent on concentrations of glutamate and durations of incubation. In general, every dose of glutamate tested produced prominent calpain activation. Lower glutamate concentrations (1.0 and 2.0 mmol/L) produced modest but sustained caspase-3 activation. The highest dose of glutamate (4.0 mmol/L) produced prominent caspase-3 activation after 6 hours of incubation.

Effects of *N*-methyl-D-aspartate receptor antagonism and inhibition of calpains, caspases, and protein synthesis on cell viability and α-spectrin proteolysis

Cell viability assessments. Lactate dehydrogenase release assessed cell viability 6 hours after incubation with 2.0 mmol/L glutamate alone or in combination with varying doses of the NMDA receptor antagonist MK-801 (10 to 500 μmol/L), calpain inhibitor II (5 to 100 μmol/L), and the pan-caspase inhibitor Z-D-DCB (30 to 300 μmol/L; Fig. 8). A significant effect of group was shown by a one-way analysis of variance for MK-801 ($F_{6,14} = 89.05$, $P < 0.0001$) and Z-D-DCB ($F_{6,14} = 82.77$, $P < 0.0001$) but not for calpain inhibitor II ($F_{5,12} = 3.03$, $P = 0.0535$). *Post hoc* analyses revealed significant differences in LDH release between glutamate-injured and control cells and between glutamate-injured cells and cells treated with all MK-801 doses, 25 μmol/L calpain inhibitor II, and 30 to 200 μmol/L Z-D-DCB. MK-801 provided optimal protection at 100 μmol/L concentrations, inferred by LDH release (Fig. 8A); calpain inhibitor II provided minimal protection against cell death at 25 μmol/L concentrations (Fig. 8B); and Z-D-DCB provided optimal protection at 50 to 100 μmol/L concentrations (Fig. 8C).

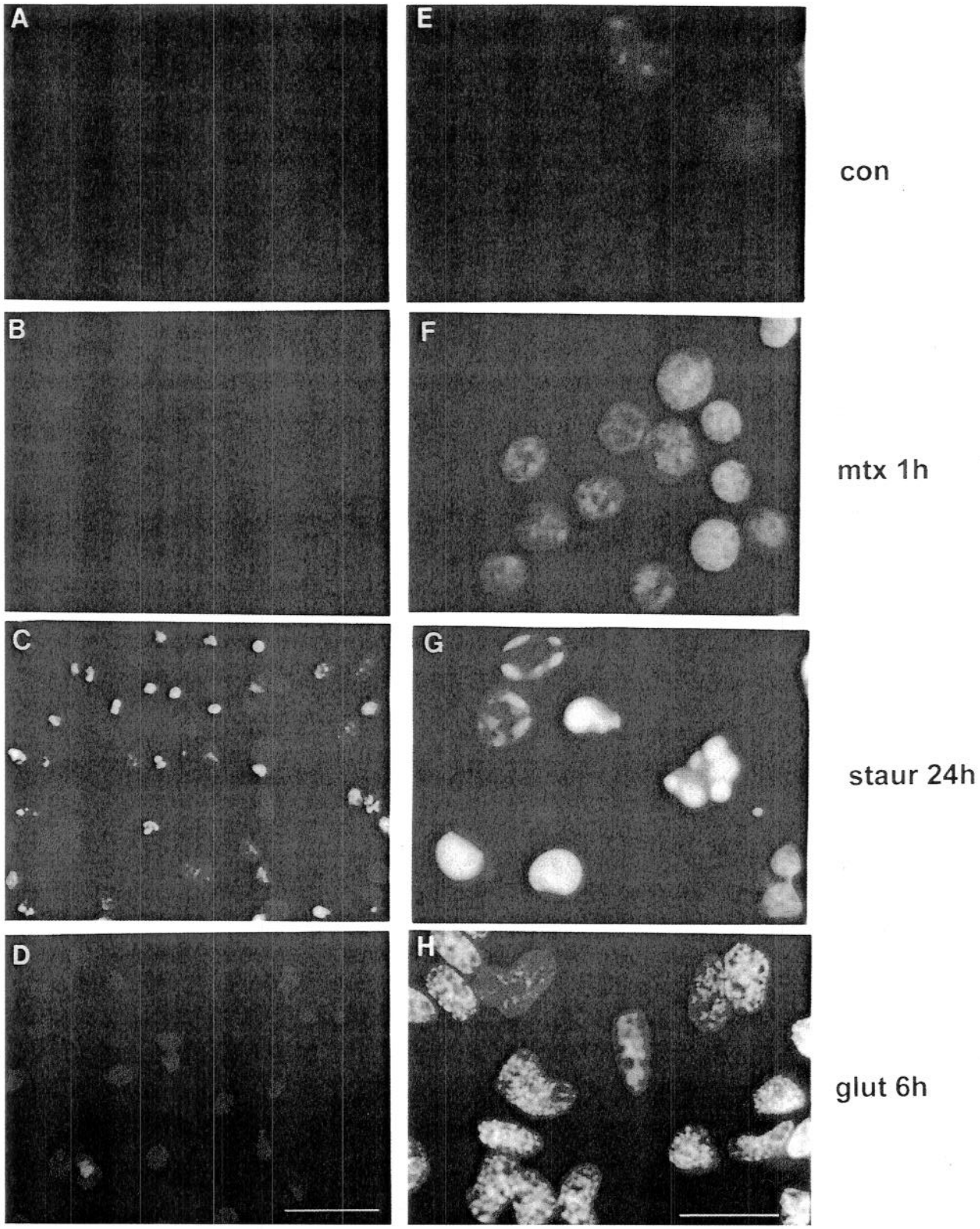

FIG. 3. Course of nuclear morphological alterations during glutamate-induced cell death detected by Hoechst 33258 staining. **(A and E)** Control cultures. Note diffuse chromatic staining. **(B and F)** Treatment with maitotoxin (0.1 nmol/L) for 1 hour. An even distribution of DNA staining in maitotoxin-treated cells is evident. Nuclei of maitotoxin-treated cells appear smaller, with more condensed chromatin yielding brighter Hoechst staining. Consistent with necrotic-like cell death, Hoechst staining did not detect nuclear chromatin margination or formation of apoptotic bodies. **(C and G)** Treatment with staurosporine (0.5 μmol/L) for 24 hours. Hoechst staining detected increased condensation and margination of chromatin to the nuclear envelope and the formation of dense apoptotic bodies. **(D and H)** Treatment with glutamate (2.0 mmol/L) for 6 hours. Glutamate treatment produced eccentric-shaped, enlarged nuclei. The DNA aggregation appeared in a diffusely speckled pattern throughout the nucleus with no chromatin clumping along nuclear margins or evidence of apoptotic body formation. Bars = 5 μm (A to D) and 2.5 μm (E to H).

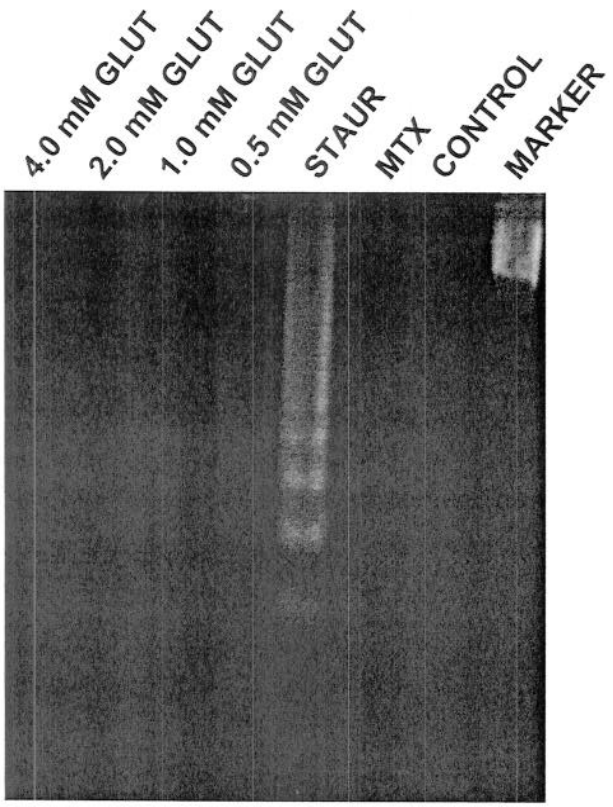

FIG. 4. Analysis of oligonucleosomal-sized fragmentation of DNA by endonucleases following treatment with glutamate, staurosporine, or maitotoxin. No dose of glutamate tested (0.5, 1.0, 2.0, 4.0 mmol/L) produced evidence of DNA ladders after 24 hours of incubation. Treatment with maitotoxin (0.1 nmol/L for 1 hour, a dose producing necrotic-like cell death at this time point) also failed to produce DNA ladders. In contrast, treatment with staurosporine (0.5 μmol/L for 24 hours, a dose producing apoptotic-like cell death at this time point) produced readily detectable nucleosomal-sized DNA fragments.

α-*Spectrin proteolysis.* Western blots examined proteolysis of α-spectrin into 150-kDa, calpain-specific 145-kDa, and caspase 3-specific 120-kDa BDPs detected after 6 hours of glutamate incubation alone (2.0 mmol/L) or in combination with optimal doses of calpain inhibitor II (25 μmol/L), MK-801 (100 μmol/L), Z-D-DCB (50 μmol/L), and cycloheximide (1 μg/ml). The effects of these drugs on α-spectrin proteolysis were compared with their effectiveness in protecting against glutamate cell death, inferred by LDH release (Fig. 9). Glutamate treatment was sometimes associated with an additional lower molecular mass band, suggesting further processing of α-spectrin not observed in control cultures. A one-way analysis of variance revealed a significant effect of group ($F_{5,12} = 193$, $P < 0.0001$). *Post hoc* analyses showed significant differences between glutamate-injured and control cells and between glutamate-injured cells and cells treated with calpain inhibitor II, Z-D-DCB, or MK-801. Although calpain inhibitor II significantly inhibited calpain activation, inhibition only minimally reduced LDH release. The pan-caspase inhibitor Z-D-DCB significantly reduced caspase-3 activation as well as LDH release. The protein synthesis inhibitor cycloheximide failed to block calpain or caspase-3 activation or to reduce LDH release. MK-801 significantly reduced calpain activation as well as LDH release.

DISCUSSION

The present study provides the first systematic examination of cell death phenotypes associated with glutamate toxicity in primary mixed neuronal cultures. The study also provides the first concurrent assessment of potential contributions of two important families of cysteine proteases, calpains and caspases, to glutamate-induced cell death in any model system. Our data suggest that activation of caspase-3 could be an important mediator of glutamate toxicity. Activation of calcium-dependent proteases also contributes to glutamate toxicity, although calpain inhibition was not as effective at providing protection against cell death as was Z-D-DCB. However, Z-D-DCB is a pan-caspase inhibitor, and thus its more robust protection may be due to inhibition of caspases other than caspase-3. Importantly, glutamate-induced cell death did not resemble apoptotic or necrotic phenotypes produced in this same cell system by chemical inducers of apoptosis or necrosis.

Glutamate toxicity in mixed primary septohippocampal cell cultures

Dose–response analyses showed that 2.0 mmol/L glutamate produced ~50% cell death in mixed neuronal–glial cultures after 24 hours of incubation. Glutamate-induced cell death in the present study was inferred by both FDA/PI staining and LDH release. In separate studies, we have confirmed that these two measures provide congruent assessments of loss of cell viability (data not shown). Researchers usually find that neuronally enhanced cultures are more sensitive to glutamate toxicity than mixed neuronal–glial cultures (Adamec et al., 1998; Manev et al., 1991), although some investigations have used millimolar concentrations to study glutamate excitotoxicity in neurons (Ikeda et al., 1996). Higher concentrations of glutamate required in mixed culture systems are largely attributable to the formation of a confluent monolayer of astrocytes on which the neurons grow. Astrocytes act as glutamate sinks, aminating this neurotransmitter to form glutamine (Murphy and Horrocks, 1994). Investigators often report that astrocytes can protect neurons from glutamate excitotoxicity (Sass et al., 1993).. We confirmed the contribution of astrocytes to reduced glutamate toxicity in our culture system by demonstrating that neuronally enhanced septohippocampal cultures have dramatically increased sensitivity to glutamate toxicity (Fig. 1B).

Major glutamate receptors studied to date are ex-

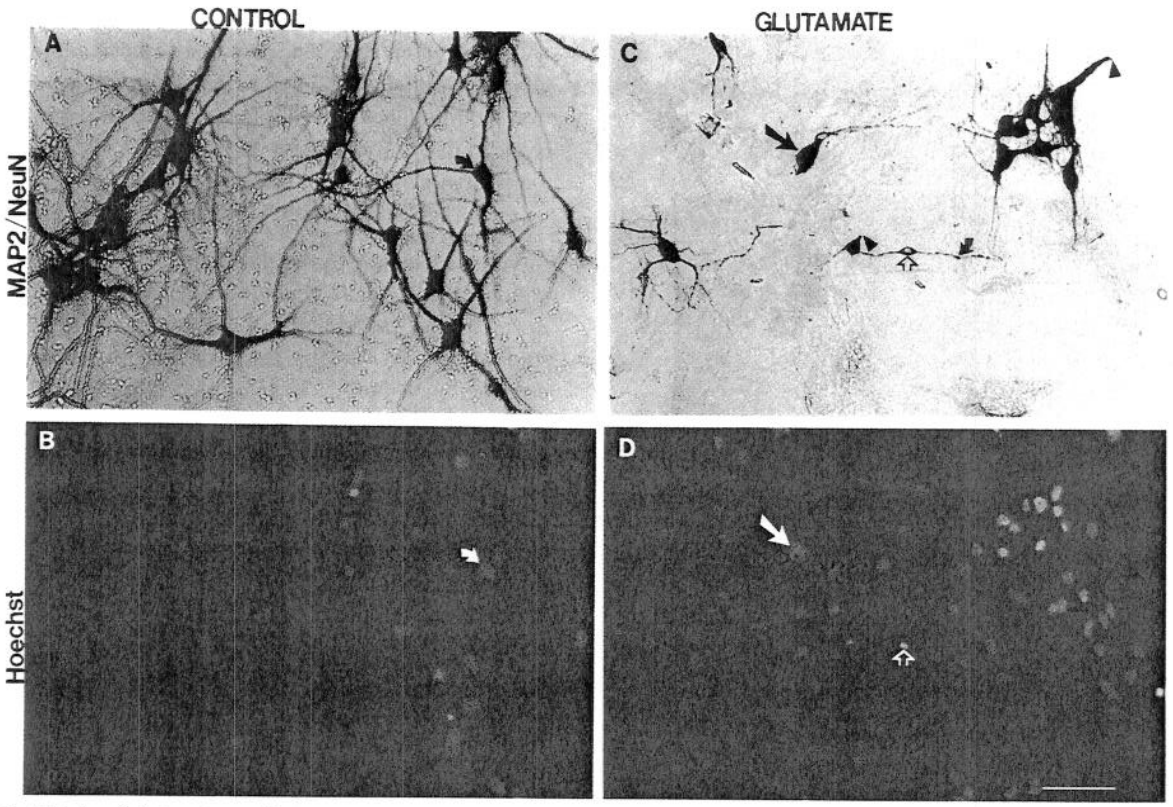

FIG. 5. Effects of glutamate toxicity on neurons in mixed septohippocampal cultures. Neurons were stained with both microtubule-associated protein-2 (MAP-2) and neuronal nuclear marker (NeuN) **(A and C)** and Hoechst 33258 **(B and D)**. Control cultures (A and B) showed normal somatic and nuclear morphology (arrows). After incubation with glutamate (2.0 mmol/L) for 24 hours (C and D), the number of immunopositive neurons was markedly reduced. Broken dendritic processes were apparent (C, arrowheads) as well as some loss of MAP-2 immunoreactivity (C, straight filled arrow). In addition, MAP-2 immunohistochemistry detected prominent dendritic beading (C, curved arrow). Hoechst staining in injured neurons revealed DNA aggregation in a diffusely speckled pattern with no chromatin clumping along nuclear margins (D, filled arrow). Occasionally, Hoechst staining detected condensed chromatin staining in the absence of formation of apoptotic bodies (D, open arrow). These changes were observed in injured neurons (C, open arrow). Bar = 5 μm.

pressed in hippocampal neurons within the first 10 days in culture, with the exception of metabotropic receptors, which constitute <1% of mature neurons (Craig et al., 1993). This observation is consistent with experiments in our laboratory showing that sensitivity of mixed septo-hippocampal cultures to glutamate excitotoxicity did not differ between 10 and 15 days *in vitro* (data not shown). However, full maturation and precise localization of glutamate receptor subtypes at synapses can evolve over >15 days (Craig et al., 1993). Future studies could more systematically examine relationships between the development of glutamate synapses in the hippocampus and mechanisms of glutamate toxicity.

In the present study, glutamate toxicity was observed both in neurons and in glia. Although investigations have assessed glutamate toxicity in neuronally enhanced (Adamec et al., 1998; Ikeda et al., 1996; Manev et al., 1991) or astrocytic (Manev et al., 1991) cultures separately, to our knowledge, no studies have compared the morphopathological changes after glutamate toxicity in neuronal and glial mixed cultures. There are reports of excitotoxic glial injury *in vivo* (Bolton and Perry, 1998; Matyja, 1986). However, other *in vivo* (Portera-Cailliau et al., 1995) and hippocampal slice (Siman and Card, 1988) studies failed to detect glial injury.

Proteolytic regulation of glutamate-induced cell death

Calpains and caspase-3 process the cytoskeletal protein α-spectrin (280 kDa) into distinctive proteolytic fragments of 145 kDa by calpains (Harris et al., 1988; Nath et al., 1996*a,b*) and 120 kDa by caspase-3 (Wang et al., 1998).. Whereas the specificity of the 145-kDa fragment for calpain is well accepted, there has been some controversy regarding the specificity of caspase-3-specific BDPs. However, the specificity of the caspase-3-generated 120-kDa α-spectrin product is well characterized. Recently, Wang and colleagues (1998) reported that when cell lysates were digested for 1 hour with recombinant caspase-1, -2, -3, -4, -6, or -7, only caspase-3 produced accumulation of the 120 kDa α-spectrin fragment. Moreover, our laboratory and others have successfully used this technique to detect independent and/or concurrent calpain/caspase-3 activation

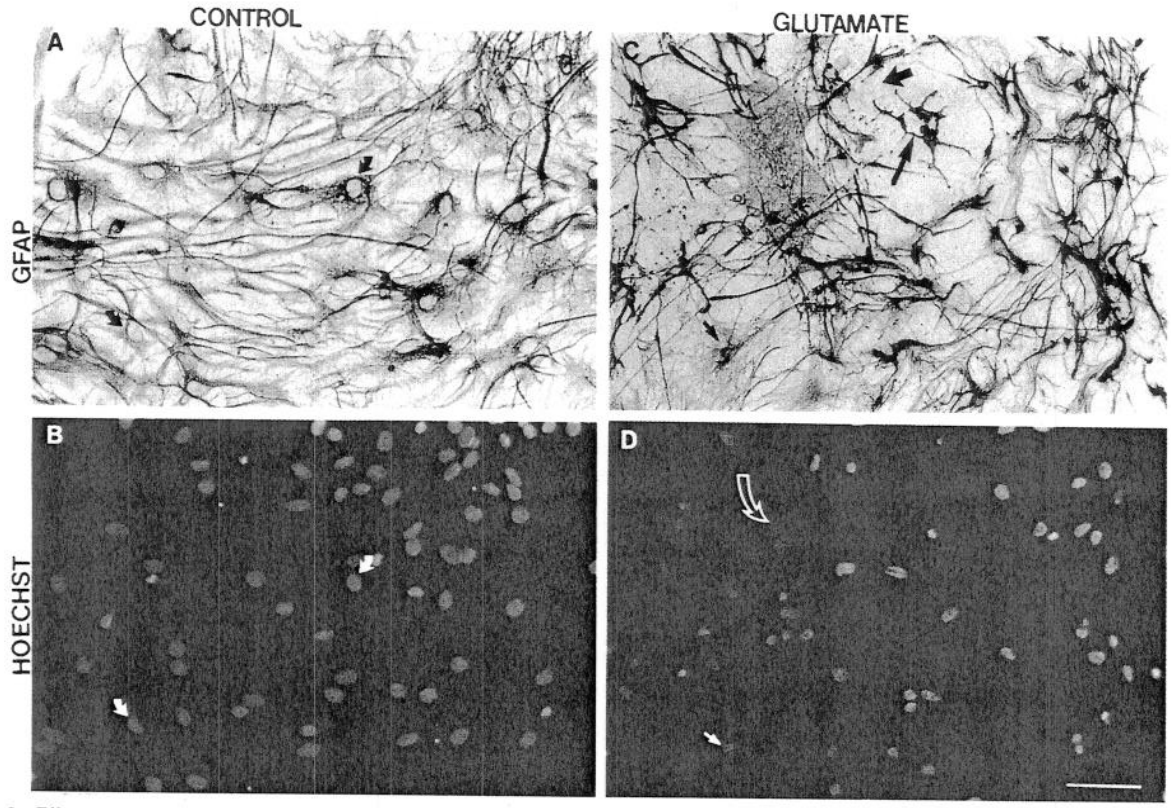

FIG. 6. Effects of glutamate toxicity on astroglia in mixed septohippocampal cultures. Astroglia were stained with glial fibrillary acidic protein (GFAP) **(A and C)** and Hoechst 33258 **(B and D).** Control cultures (A and B) showed normal somatic and nuclear morphology (arrows) in glia. Incubation with glutamate (2.0 mmol/L) for 24 hours (C and D) resulted in glial cell death associated with cell shrinkage and membrane folding (C, long arrow) and ultimately complete cell detachment and loss of confluence of the glial monolayer (C, short wide arrow). After injury, Hoechst staining revealed DNA aggregation in a diffusely speckled pattern (D, straight arrow) in some GFAP-positive cells (C, short thin arrow). In addition, some glia still underwent cell division (C and D, curved arrows). Bar = 5 μm.

in cell cultures (Nath et al., 1996*a,b*, 1998; Pike et al., 1998*b*; Wang et al., 1998) and *in vivo* after traumatic brain injury (Pike et al., 1998*a*). In addition, the caspase-3-generated 120-kDa α-spectrin fragment has been shown to be an identifying marker of apoptotic cell death in a number of cell lines and cell culture systems (Martin et al., 1995; Nath et al., 1996*b*, 1998; Pike et al., 1998*b*; Wang et al., 1998). In the present study, all three concentrations of glutamate produced robust calpain-mediated processing of α-spectrin that was especially

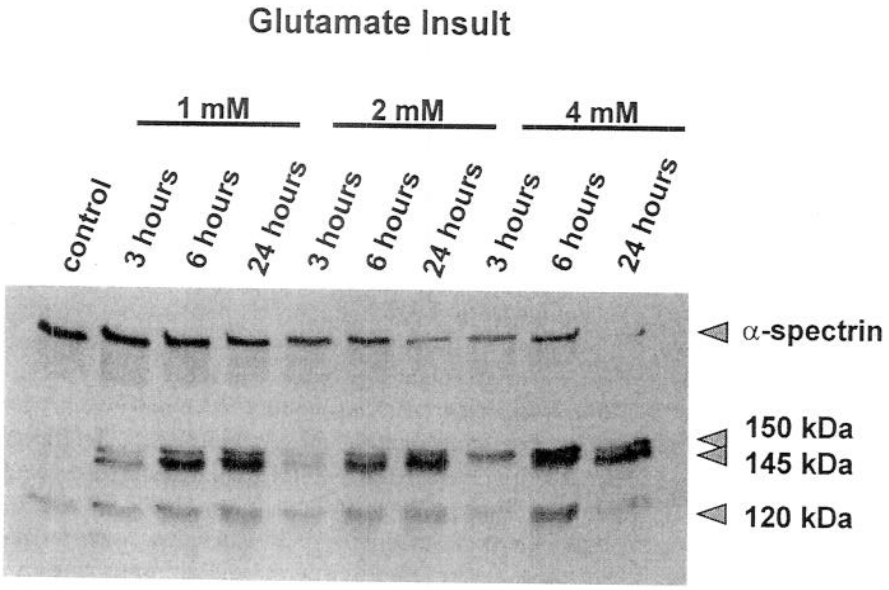

FIG. 7. Incubation with varying doses of glutamate produced calpain and caspase-3 protease activation. Proteolysis of α-spectrin into 150-kDa, calpain-specific 145-kDa, and caspase-3-specific 120-kDa breakdown products was examined after incubation with varying doses of glutamate (1.0, 2.0, and 4.0 mmol/L) for 3, 6, and 24 hours.

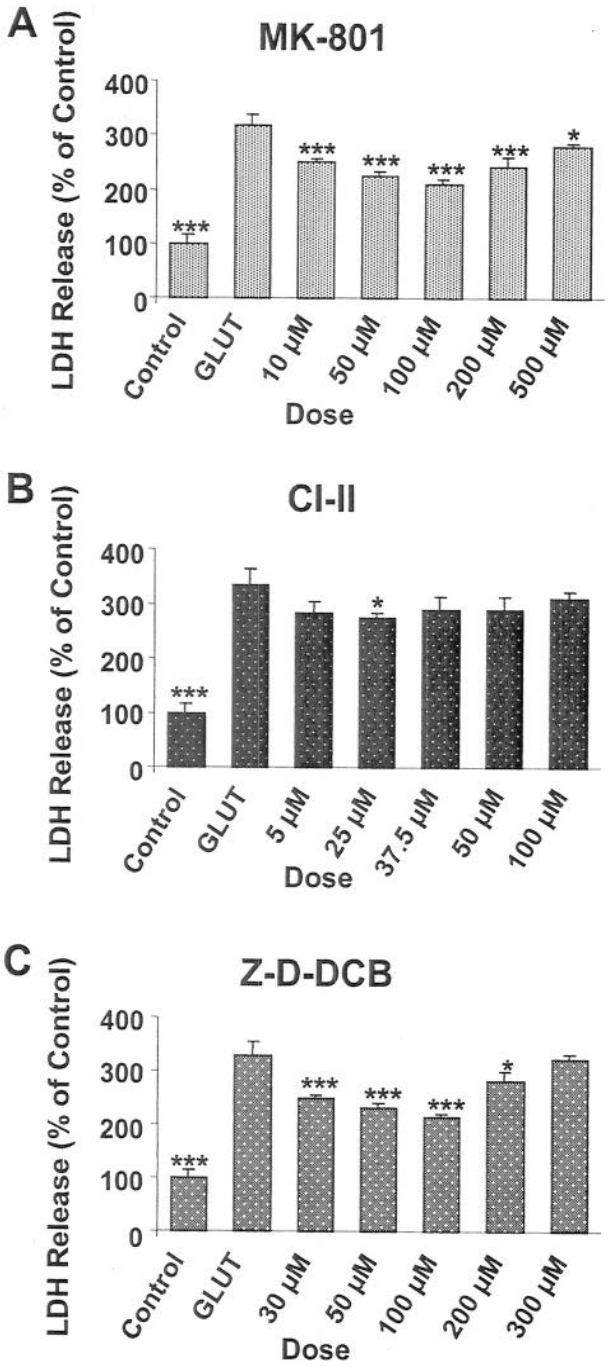

FIG. 8. Effects of preincubation with varying doses of the *N*-methyl-D-aspartate receptor antagonist MK-801 **(A)**, calpain inhibitor II (CI-II) **(B)**, and the pan-caspase inhibitor carbobenzoxy-Asp-CH_2-OC(*O*)-2,6-dichlorobenzene (Z-D-DCB) **(C)** on cell viability assessed by lactate dehydrogenase release after incubation with glutamate (2.0 mmol/L) for 6 hours. MK-801 significantly decreased cell death, compared with control, at all doses tested, with an optimal dose of 100 μmol/L ($P < 0.001$). Z-D-DCB provided significant protection against cell death with 30 to 200 μmol/L doses. The optimal dose was 50 to 100 μmol/L ($P < 0.001$). Calpain inhibitor II provided only minimal protection at 25 μmol/L ($P < 0.05$). $^*P < 0.05$, $^{***}P < 0.001$.

apparent 6 hours after injury and sustained for at least 24 hours. Caspase-3 activation was less pronounced and showed some differences associated with glutamate concentrations. Other investigators have reported calpain activation produced by glutamate in hippocampal (Adamec et al., 1998) and cerebellar (Manev et al., 1991) culture systems, and increased caspase-3 activation has been observed after glutamate treatment in cerebellar granule neurons (Du et al., 1997). The pan-caspase inhibitor Z-D-DCB produced significant reduction in caspase-3 activation and cell death, inferred by LDH release, suggesting that caspase activation importantly contributes to glutamate-mediated cell death. As Z-D-DCB is not specific for caspase-3, some protection may be attributable to inhibition of other caspases such as caspase-1. However, calpain inhibitor II, at concentrations that inhibited calpain activation, provided less robust protection against glutamate-induced cell death. Other investigators have reported that calpain inhibition does not protect against glutamate-induced cell death either in cultured hippocampal neurons (Adamec et al., 1998) or in cerebellar granule cells (Manev et al., 1991). However, other *in vitro* studies have reported protective effects of calpain inhibitors on excitotoxic cell death of cerebellar neurons employing a ligand of non-NMDA receptors (Wang et al., 1996*a*), in contrast to exogenous glutamate treatment, which was employed in the present study. The relatively modest levels of protection by calpain inhibition against excitotoxic cell death *in vitro* are surprising in view of a considerable body of evidence showing significant protective effects of calpain inhibitors in *in vivo* models of cerebral ischemia and traumatic brain injury (Kampfl et al., 1997; Posmantur et al., 1997; Wang and Yuen, 1997). It is possible that calpain inhibition provides suboptimal protection because pathological activation of calpain occurs downstream of other events that could contribute to glutamate-induced cell death, including activation of other calcium-dependent enzymes (for example, lipases and phosphatases) (Homayoun et al., 1997). There may also be important differences in pathogenic stimuli in complex *in vivo* insults versus glutamate toxicity *in vitro* that could significantly influence cell death mechanisms in ways that are currently poorly understood.

MK-801 produced significant, although incomplete, reductions in LDH release resulting from glutamate excitotoxicity at a concentration similar to those reported by others (Adamec et al., 1998). As prolonged exposure to glutamate might possibly produce toxicity by receptor-independent mechanisms such as competitive inhibition of cysteine uptake (Murphy et al., 1990), significant protection by MK-801 confirms a receptor-mediated mechanism for glutamate toxicity in hippocampal neuronal cultures. In addition, MK-801 reduced calpain activation, inferred by spectrin proteolysis, confirming pre-

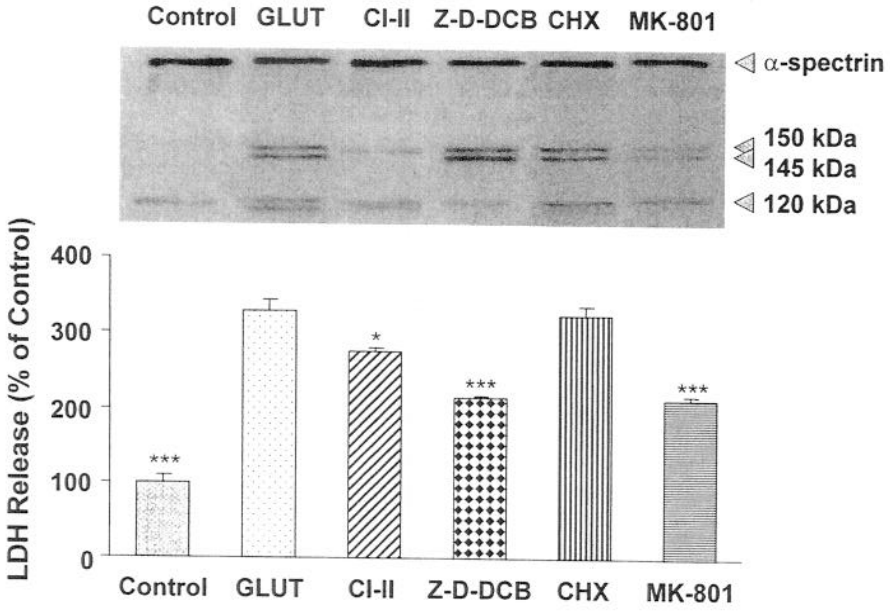

FIG. 9. (Top) Western blots examining proteolysis of α-spectrin into 150-kDa, calpain-specific 145-kDa, and caspase-3-specific 120-kDa breakdown products (BDPs) detected after 6 hours of glutamate treatment alone (2.0 mmol/L) or in combination with optimal doses of calpain inhibitor II (CI-II; 25 μmol/L), MK-801 (100 μmol/L), carbobenzoxy-Asp-CH_2-OC(*O*)-2,6-dichlorobenzene (Z-D-DCB; 50 μmol/L), and cycloheximide (CHX; 1 μg/mL). Glutamate treatment resulted in accumulation of calpain- and caspase-3-mediated BDPs. Glutamate treatment was sometimes associated with an additional lower molecular mass band, suggesting further processing of α-spectrin not observed in control cultures. Calpain (CI-II) and caspase (Z-D-DCB) inhibition reduced the accumulation of their respective BDPs, whereas cycloheximide had no effect. MK-801 reduced calpain activation but had no apparent effect on caspase-3 activation. **(Bottom)** Effects of various doses of drugs on cell viability assessed by lactate dehydrogenase (LDH) release 6 hours after incubation with glutamate alone or in combination with optimal doses of drugs. Calpain inhibitor II ($P < 0.05$), Z-D-DCB ($P < 0.001$), and MK-801 ($P < 0.001$) significantly reduced LDH release after glutamate treatment. $^*P < 0.05$, $^{***}P < 0.001$.

vious reports that activation of NMDA receptors is necessary for calpain activation (Adamec et al., 1998).

Characterization of cell death phenotypes in nervous system

Although phenotypic characterization of cell death may remain a useful adjunct strategy, ultimately cell death mechanisms must be defined by biochemical and molecular mechanisms. Activation of these biochemical and molecular mechanisms may depend on cell death signal and cell type, and different mechanisms may be activated separately or concurrently. Future studies should consider the possibility of heterogeneity in cell death mechanisms and associated cell death phenotypes.

REFERENCES

Adamec E, Beermann ML, Nixon RA (1998) Calpain I activation in rat hippocampal neurons in culture is NMDA receptor selective and not essential for excitotoxic cell death. *Mol Brain Res* 54:35–48

Bolton SJ, Perry VH (1998) Differential blood–brain barrier breakdown and leukocyte recruitment following excitotoxic lesions in juvenile and adult rats. *Exp Neurol* 154:231–240

Bonfoco E, Krainc D, Ankarcrona M, Nicotera P, Lipton S (1995) Apoptosis and necrosis: two distinct events induced, respectively, by mild and intense insults with *N*-methyl-D-aspartate or nitric oxide/superoxide in cortical cell cultures. *Proc Natl Acad Sci USA* 92:7162–7166

Carroll FY, Beart PM, Cheung NS (1996) NMDA-mediated activation of the NO/cGMP pathway: characteristics and regulation in cultured neocortical neurones. *J Neurosci Res* 43:623–631

Cebers G, Zhivotovsky B, Ankarcrona M, Liljequist S (1997) AMPA neurotoxicity in cultured cerebellar granule neurons: mode of cell death. *Brain Res Bull* 43:393–403

Choi DW, Maulucci-Gedde MA, Kriegstein AR (1987) Glutamate neurotoxicity in cortical cell cultures. *J Neurosci* 7:357–368

Craig AM, Blackstone CD, Huganir RL, Banker G (1993) The distribution of glutamate receptors in cultured rat hippocampal neurons: postsynaptic clustering of AMPA-selective subunits. *Neuron* 10: 1055–1068

Du Y, Bales KR, Dodel RC, Hamilton-Byrd E, Horn JW, Czilli DL, et al. (1997) Activation of caspase 3-related cysteine protease is required for glutamate-mediated apoptosis of cultured cerebellar granule neurons. *Proc Natl Acad Sci USA* 94:11657–11662

Gong J, Traganos F, Darzynkiewicz Z (1994) A selective procedure for DNA extraction from apoptotic cells applicable for gel electrophoresis and flow cytometry. *Anal Biochem* 218:314–319

Harris AS, Croall DE, Morrow JS (1988) The calmodulin-binding site in alpha-fodrin is near the calcium-dependent protease-1 cleavage site. *J Biol Chem* 263:15754–15761

Homayoun P, Rodriguez de Turco EB, Parkins NE, Lane DC, Soflosky J, Carey ME, Bazan NG (1997) Delayed phospholipid degradation in rat brain after traumatic brain injury. *J Neurochem* 69:199–205

Ikeda J, Terakawa S, Murota S, Hirakawa K (1996) Nuclear disintegration as a leading step of glutamate excitotoxicity in brain neurons. *J Neurosci Res* 43:613–622

Jenkins LW, Moszynski K, Lyeth BG, Lewelt N, DeWitt DS, Allen A, et al. (1989) Increased vulnerability of the mildly traumatized brain to cerebral ischemia: the use of controlled secondary ischemia as a research tool to identify common or different mechanisms contributing to mechanical and ischemic brain injury. *Brain Res* 477:211–224

Jones KH, Senft JA (1985) An improved method to determine cell viability by simultaneous staining with fluorescein diacetate-propidium iodide. *J Histochem Cytochem* 33:77–79

Kampfl A, Zhao X, Whitson JS, Posmantur R, DIxon CE, Yang K, et al. (1996) Calpain inhibitors protect against depolarization-induced neurofilament protein loss of septo-hippocampal neurons in culture. *Eur J Neurosci* 8:344–352

Kampfl A, Posmantur RM, Zhao X, Schmutzhard E, Clifton GL, Hayes RL (1997) Mechanisms of calpain proteolysis following traumatic brain injury): implications for pathology and therapy: a review and update. *J Neurotrauma* 14:121–134

Koh JY, Choi DW (1987) Quantitative determination of glutamate mediated cortical neuronal injury in cell culture by lactate dehydrogenase efflux assay. *J Neurosci Methods* 20:83–90

Kure S, Tominaga T, Yoshimoto T, Tada K, Narisawa K (1991) Glutamate triggers internucleasomal DNA cleavage in neuronal cells. *Biochem Biophys Res Commun* 179:39–45

Lin JK, Chou CK (1992) *In vitro* apoptosis in the human hematoma cell

line induced by transforming growth factor β_1. *Cancer Res* 52: 385–388

Lyeth BG, Jenkins LW, Hamm RJ, Dixon CE, Phillips LL, Clifton GL, et al. (1990) Prolonged memory impairment in the absence of hippocampal cell death following traumatic brain injury in the rat. *Brain Res* 526:249–258

MacManus JP, Rasquinha I, Black MA, Laferriere NB, Monette R, Walker T, Morley P (1997) Glutamate-treated rat cortical neuronal cultures die in a way different from classical apoptosis induced by staurosporine. *Exp Cell Res* 233:310–320

Manev H, Favaron M, Siman R, Guidotti A, Costa E (1991) Glutamate neurotoxicity is independent of calpain I inhibition in primary cultures of cerebellar granule cells. *J Neurochem* 57:1288–1295

Martin DP, Schmidt RE, DiStefano PS, Lowry OH, Carter JG, Johnson EM (1988) Inhibitors of protein synthesis and RNA synthesis prevent neuronal death caused by nerve growth factor deprivation. *J Cell Biol* 106:829–844

Martin SJ, O'Brien GA, Nishioka WK, McGahon AJ, Mahboubi A, Saido TC, et al. (1995) Proteolysis of fodrin (non-erythroid spectrin) during apoptosis. *J Biol Chem* 270:6425–6428

Matyja E (1986) Morphologic evidence of a primary response of glia to kainic acid administration into the rat neostriatum; studies *in vivo* and *in vitro*. *Exp Neurol* 92:609–623

Murphy EJ, Horrocks LA (1994) Models of neurotrauma *ex vivo*. In: *The neurobiology of central nervous system trauma* (Salzman SK, Faden AI, eds), New York: Oxford University Press, pp 28–40

Murphy TH, Schnaar RL, Coyle JT (1990) Immature cortical neurons are uniquely sensitive to glutamate toxicity by inhibition of cystine uptake. *FASEB J* 4:1624–1633

Nath R, McGinnis KM, Nadimpalli R, Stafford D, Wang KKW (1996*a*) Effects of ICE-like proteases and calpain inhibitors on neuronal apoptosis. *Neuroreport* 8:249–255

Nath R, Raser KJ, Stafford D, Hajimohammadreze I, Posner A, Allen H, et al. (1996*b*) Non-erythroid alpha-spectrin breakdown by calpain and interleukin 1 beta-converting-enzyme-like protease(s) in apoptotic cells: contributory roles of both protease families in neuronal apoptosis. *Biochem J* 319:683–690

Nath R, Probert A, McGinnis KM, Wang KKW (1998) Evidence for activation of caspase-3-like protease in excitotoxin- and hypoxia/hypoglycemia-injured neurons. *J Neurochem* 71:186–195

Pike BR, Zhao X, Newcomb JK, Posmantur RM, Wang KKW, Hayes RL (1998*a*) Regional calpain and caspase-3 proteolysis of α-spectrin after traumatic brain injury. *Neuroreport* 9:2437–2442

Pike BR, Zhao X, Newcomb JK, Wang KKW, Posmantur RM, Hayes RL (1998*b*) Temporal relationship between *de novo* protein synthesis, calpain and caspase-3 like protease activation, and DNA fragmentation during apoptosis in septo-hippocampal cultures. *J Neurosci Res* 52:505–520

Portera-Cailliau C, Hedreen JC, Price DL, Koliatsos VE (1995) Evidence for apoptotic cell death in Huntington disease and excitotoxic animal models. *J Neurosci* 15:3775–3787

Portera-Cailliau C, Price DL, Martin LJ (1997) Excitotoxic neuronal death in the immature brain is an apoptosis–necrosis morphological continuum. *J Comp Neurol* 378:70–87

Posmantur RM, Kampfl A, Siman R, Liu J, Zhao X, Clifton GL, Hayes FL, et al. (1997) A calpain inhibitor attenuates cortical cytoskeletal protein loss after experimental brain injury in the rat. *Neuroscience* 77:875–888

Sass JB, Ang LC, Juurlink BH (1993) A simple, yet versatile, coculture method for examining neuron–glia interactions. *J Neurosci Methods* 47:115–121

Siman R, Card JP (1988) Excitatory amino acid neurotoxicity in hippocampal slice preparation. *Neuroscience* 26:433–447

Squier MK, Miller AC, Malkinson AM, Cohen JJ (1994) Calpain activation in apoptosis. *J Cell Physiol* 159:229–237

Wang KKW, Yuen P (1997) Development and therapeutic potential of calpain inhibitors. *Adv Pharmacol* 37:117–152

Wang KKW, Nath R, Posner A, Raser KJ, Buroker-Kilgore M, Hajimohammadreza I, et al. (1996*a*) An alpha-mercaptoacrylic acid derivative is a selective nonpeptide cell-permeable calpain inhibitor and is neuroprotective. *Proc Natl Acad Sci USA* 93:6687–6692

Wang KKW, Nath R, Raser KJ, Hajimohammadreza I (1996*b*) Maitotoxin induces calpain activation in SH-SY5Y neuroblastoma cells and cerebrocortical cultures. *Arch Biochem Biophys* 331:208–214

Wang KKW, Posmantur RM, Nath R, McGinnis K, Whitton M, Talanian RV, et al. (1998) Simultaneous degradation of αII- and βII-spectrin by caspase 3 (CPP32) apoptotic cells. *J Biol Chem* 273: 22490–22497

Zhao X, Pike BR, Newcomb JK, Wang KKW, Posmantur RM, Hayes RL (1999) Maitotoxin induces calpain but not caspase-3 activation and necrotic cell death in primary septo-hippocampal cultures. *Neurochem Res* 24:371–382

Zhivotovsky B, Burgess DH, Vanags DM, Orrenius S (1997) Involvement of cellular proteolytic machinery in apoptosis. *Biochem Biophys Res Commun* 230:481–488

Journal of Neuroscience Research 64:121–131 (2001)

TNF-α Stimulates Caspase-3 Activation and Apoptotic Cell Death in Primary Septo-Hippocampal Cultures

Xiurong Zhao,[1] Brian Bausano,[1] Brian R. Pike,[2] Jennifer K. Newcomb-Fernandez,[1] Kevin K.W. Wang,[3] Esther Shohami,[4] N.C. Ringger,[2] S.M. DeFord,[2] Douglas K. Anderson,[5] and Ronald L. Hayes[2]*

[1]The Vivian L. Smith Center for Neurologic Research, Department of Neurosurgery, The University of Texas Health Science Center, Houston, Texas
[2]Center for Traumatic Brain Injury Studies, Department of Neuroscience, University of Florida, Gainesville, Florida
[3]Pfizer, Ann Arbor, Michigan
[4]Department of Pharmacology, The Hebrew University School of Pharmacy, Jerusalem, Israel
[5]Department of Neuroscience and Malcolm Randall VAMC, University of Florida, Gainesville, Florida

Primary septo-hippocampal cell cultures were incubated in varying concentrations of tumor necrosis factor (TNF-α; 0.3–500 ng/ml) to examine proteolysis of the cytoskeletal protein α-spectrin (240 kDa) to a signature 145 kDa fragment by calpain and to the apoptotic-linked 120-kDa fragment by caspase-3. The effects of TNF-α incubation on morphology and cell viability were assayed by fluorescein diacetate-propidium iodide (FDA-PI) staining, assays of lactate dehydrogenase (LDH) release, nuclear chromatin alterations (Hoechst 33258), and internucleosomal DNA fragmentation. Incubation with varying concentrations of TNF-α produced rapid increases in LDH release and nuclear PI uptake that were sustained over 48 hr. Incubation with 30 ng/ml TNF-α yielded maximal, 3-fold, increase in LDH release and was associated with caspase-specific 120-kDa fragment but not calpain-specific 145-kDa fragment as early as 3.5 hr after injury. Incubation with the pan-caspase inhibitor, carbobenzosy-Asp-CH_2-OC (O)-2-6-dichlorobenzene (Z-D-DCB, 50-140 μM) significantly reduced LDH release produced by TNF-α. Apoptotic-associated oligonucleosomal-sized DNA fragmentation on agarose gels was detected from 6 to 72 hr after exposure to TNF-α. Histochemical changes included chromatin condensation, nuclear fragmentation, and formation of apoptotic bodies. Results of this study suggest TNF-α may induce caspase-3 activation but not calpain activation in septo-hippocampal cultures and that this activation of caspase-3 at least partially contributes to TNF-α-induced apoptosis. J. Neurosci. Res. 64:121–131, 2001.

Key words: apoptosis; calpain; caspase; cytokine; neural injury; proteolysis

Tumor necrosis factor-α (TNF-α) is a 17-kDa pleiotrophic cytokine with both secreted and transmembrane forms, which that is known to mediate immune and inflammatory responses. TNF-α can be synthesized and released by astrocytes, microglia, and some neurons (Lieberman et al., 1989; Chung and Benveniste, 1990; Morganti-Kossmann et al., 1992). Although TNF-α was originally named for its degeneration-inducing action in some types of tumor cells, data now suggest that TNF-α has a variety of effects on different types of cells (Cheng et al., 1994). A substantial body of evidence indicates that TNF-α has a pro-inflammatory role that is acutely up-regulated in ischemic and traumatic brain injury (TBI) (Taupin et al., 1993; Shohami et al., 1994; Fan et al., 1996; Saito et al., 1996; Liu et al., 1994; Wang et al., 1994; Uno et al., 1997; Gong et al., 1999; Buttini et al., 1996). Immunocytochemical studies confirm the presence of TNF-α antigen in the brain as early as 30 min after occlusion of the middle cerebral artery in the same regions where TNF-α mRNA-positive cells were detected (Buttini et al., 1996). Increased levels of TNF-α in brain tissue, cerebral spinal fluid, and plasma have been found in several central nervous system (CNS) disorders including Alzheimer's disease (Fillet et al., 1991), Guillain-Barre Syndrome (Sharief et al., 1993), Parkinson's disease (Mogi

Contract grant numbers: R01 NS21458-15, R01 NS40182; Contract grant sponsor: U.S. Army; Contract grant number: DAMD17-99-1-9565; Contract grant sponsor: University of Pittsburgh/Navy Research; Contract grant number: N0014-97-1-1064; Contract grant sponsor:State of Florida Brain & Spinal Cord Injury Rehabilitation Trust Fund.

*Correspondence to: Ronald L. Hayes, Ph.D., Director, Center for Traumatic Brain Injury Studies, Professor of Neuroscience, Neurosurgery and Clinical & Health Psychology, University of Florida, Department of Neuroscience, 100 Newell Dr./P.O. Box 100244, Gainesville, FL 32610. E-mail: hayes@ufbi.ufl.edu

Received 15 August 2000; Revised 8 December 2000; Accepted 14 December 2000

et al, 1994, 1996), and spinal cord injury (Xu et al., 1998). Other studies have shown that TNF-α can mediate apoptotic cell death (Gelbard et al., 1993; Aggarwal et al., 1999) and can modulate Bax/BcL-2 protein levels (Pulliam et al., 1998). A variety of TNF-α antagonists or antibodies decreased TNF-α levels, improved behavioral outcome, and reduced brain damage following experimental ischemia and TBI in rats and mice (Shohami et al., 1996, 1997; Meirstrell et al., 1997; Barone et al., 1997; Dawson et al., 1996; Nawashiro et al., 1997; Leker et al., 1999; Knoblach et al., 1999).

Although the inflammatory responses evoked by TNF-α are well known, a number of investigations have posited a protective role of TNF-α against neuronal cell death. For example, it has been shown that TNF-α mediates damage to myelin and oligodendrocytes (Selmaj and Raine, 1988) but is not toxic to CNS neurons in vitro (Garcia et al., 1992). TNF-α under in vitro conditions may protect neurons against metabolic, excitotoxic, or oxidative insults by promoting maintenance of intracellular calcium homeostasis, suppression of reactive oxygen species (Cheng et al., 1994), and by activation of transcription factor NF-κB (necrosis-factor-κB; Barger et al., 1995). Mice genetically deficient in TNF-α receptor R1 or both R1 and R2, also show exacerbated neuronal damage compared to wild type controls following middle cerebral artery occlusion (Bruce et al., 1996; Gary et al., 1998) or TBI (Scherbel et al., 1999; Sullivan et al., 1999). In addition, Stahel et al. (2000) reported that in mice lacking both genes for TNF-α and lymphotoxin-α, mortality at 7 days after closed head injury was significantly higher, as compared to their matched wild type controls. Based on the literature, the concept that emerges suggests that TNF-α can have a detrimental role, in the acute postinjury phase, whereas it is protective in the delayed posinjury phase, probably by activating cellular repair mechanisms (Shohami et al., 1999). Therefore, the present study was designed to further investigate the acute mechanism(s) of TNF-α-induced cell death within 3 days of exposure of septo-hippocampal neurons to exogenous TNF-α.

In order to examine the role of TNF-α on cell viability, we investigated the effects of TNF-α stimulation on calpain and caspase-3 protease activation and on necrotic and apoptotic cell death phenotypes. Calpains are calcium-activated cysteine proteases that have been implicated in a variety of neuropathological conditions (Kampfl et al., 1997; Wang et al., 1994; Wang, 2000). Caspase-3 is a cysteine protease and a known effector of apoptosis in various cell lines (Nath et al., 1995; Pike et al., 1998; Eldadah et al., 1997; Fraser and Evan, 1996; Miura et al., 1993; Zhivotovsky et al., 1997). Caspase-3 is activated only during apoptosis and not during necrosis (Nath et al., 1998; Armstrong et al., 1996; Wang et al., 1996). In contrast, calpain activation can contribute to apoptotic as well as necrotic cell death (Pike et al., 1998; Zhao et al., 1999). The cytoskeletal protein α-spectrin is a preferred substrate of calpain and caspase-3 cysteine protease. Activated calpain and caspase-3 process α-spectrin into a signature 145-kDa fragment by calpain and to an apoptotic-linked 120-kDa fragments by caspase-3 (Pike et al., 1998; Zhao et al., 1999; Nath et al., 1995). Thus, the investigation examined calpain and caspase-3 activation, inferred by proteolysis of the cytoskeletal protein α-spectrin, in mixed rat glial-neuronal septo-hippocampal cell cultures following exposure to TNF-α. Experiments also employed morphopathological assessments and measures of DNA fragmentation to characterize necrotic and apoptotic cell death profiles in neurons and glia (Pike et al., 1998; Zhao et al., 1999). This study provides the first evidence that TNF-α produces caspase-3 but not calpain activation in mixed septo-hippocampal cell cultures. In addition, cell death in this model following TNF-α challenge manifested exclusively apoptotic-like characteristics.

MATERIALS AND METHODS

Materials

Septi and hippocampi neuronal cells were obtained from rat fetuses. Cell culture reagents were from Life Technologies, Rockville, MD, and Sigma Chemical, Inc. (St. Louis, MO). The TNF-α and actinomycin D (Act D) in which the cells were incubated were obtained from R&D Systems (Minneapolis, MN) and Sigma, respectively. Z-D-DCB was a generous gift from Pfizer, while CalpInh-II was obtained from Boehringer Mannheim (Indianapolis, IN). All other reagents used in these experiments were analytical grade quality of higher.

Septo-Hippocampal Cultures

Eighteen-day-old rat fetuses were removed from deeply anesthetized dams. Septi and hippocampi were dissected in a dissect buffer (HBSS, with 4.2 mM bicarbonate, 1 mM pyruvate, 20 mM HEPES, 3 mg/ml bovine serum albumin [BSA], pH 7.25). After rinsing in Dulbeccos'Modified Eagle Medium (DMEM)-DM, tissue was dissociated by trituration through the narrow pore of flame-constricted Pasteur pipette. Dissociated cells were resuspended in DMEM with 10% fetal calf serum (DMEM-10S) and plated onto 24-well poly-L-lysine- coated plastic culture plates or 12 mm of German glass (Erie Scientific Co., Portsmith, NH) at a density of 4.36×10^5 cells/mL. Cultures were maintained in a humidified incubator in an atmosphere of 5% CO_2 at 37°C. After 5 days of culture, the media was changed to DMEM-DM with 5% horse serum. Subsequent media changes were carried out three times a week. By day 10 in vitro, astrocytes formed a confluent monolayer beneath morphologically mature neurons.

In addition, we confirmed the presence of TNF-α receptors 1 and 2 (TNF-R1, TNF-R2) in this system by immunohistochemistry (TNFR1, sc-1070; TNFR2, sc-1074: Santa Cruz Biotechnology, Santa Cruz, CA). We found both receptor types to be condensed on the neurons as well as most glial cells (data not shown).

Pharmacological Treatment of Septo-Hippocampal Cells

TNF-α. Ten-day-old septo-hippocampal cultures were challenged with 0.3–500 ng/mL of TNF-α and 3 ng/ml of Act

D in DMEM-DM and cell viability was monitored at various postinjury time points. Cultures were exposed to TNF-α and Act D for the entire duration of each experiment. Coadministration of Act D (3 ng/ml) has been reported to enhance TNF-α induced cell death (Ruff anf Gifford, 1981), we therefore have treated parallel cultures with Act D, alone for the entire period of the experiment. Act D (3 ng/ml) alone had no effect on LDH release in septo-hippocampal cultures (data not shown). Following TNF-α challenge, cells were fixed for staining or protein was isolated and DNA extraction performed.

Calpain, caspase and protein synthesis inhibitors. Sister cultures were pretreated with either 25–50 μM calpain inhibitor-II (CalpInh-II), 30–140 μM of the pan-caspase inhibitor (Z-D-DCB), or 1 μg/mL of the protein synthesis inhibitor, cycloheximide (Sigma) 1 hr prior to TNF-α challenge. The inhibitor concentrations used have been previously shown to provide optimal inhibition of calpains (Pike et al., 1998; Kampfl et al., 1996), caspase-3 (Nath et al., 1996; Pike et al., 1998), and protein synthesis (Pike et al., 1998; Koh et al., 1995; Martin et al., 1988). In addition, other experiments in our laboratory have independently confirmed that these doses of CalpInh-II and Z-D-DCB antagonize calpain and caspase-3 activation accompanying staurosporine-induced apoptosis in septo-hippocampal cultures (Pike et al., 1998).

Morphological and Enzymatic Assessments of Cell Damage and Cell Death

Morphological assessments of cell injury and necrotic and apoptotic cell death phenotypes are controversial (Zhao et al., 1999). We have used multiple morphological criteria to examine cell injury and cell death phenotype.

Fluorescein diacetate and propidium iodide assay of cell viability. Fluorescein diacetate (FDA) and propidium iodide (PI) dyes were used to assess cell viability after TNF-α incubation. FDA enters normal cells and emits a green fluorescence when it is cleaved by esterases. Once cleaved, FDA can no longer permeate cell membranes. Propidium iodide is an intravital dye that is normally excluded from cells. After injury, PI penetrates cells and binds to DNA in the nucleus and emits a red fluorescence. This technique is commonly used to quantitate cell injury (Jones and Senft, 1985). As per Jones and Senft (1985), a stock solution of FDA (20 mg/mL) was dissolved in acetone. A PI stock solution was prepared by dissolving 5 mg/mL in phosphate-buffered saline (PBS). The FDA and PI working solutions were freshly prepared by adding 10 μL of the FDA and 3 μL of PI stock to 10 mL of PBS. Two hundred microliters per well of FDA-PI working solution were added directly to the cells, the cells were stained for 3 min at room temperature. Stained cells were observed and photographed with a fluorescence microscope equipped with epi-illumination, band pass 450–490 nm exciter filter, 510 nm chromatic beam splitter, and a long pass 520 nm barrier filter. This filter combination permitted both green and red fluorescing cells to be seen simultaneously.

Hoechst staining of apoptotic nuclei. The A-T base-pair-specific dye, Hoechst 33258 (bis-benzimide; Sigma) was used to stain cell nuclei for characterization of cell death phenotype. Following overnight fixation in 4% paraformaldyhide at 4°C, cells grown on German glass were washed three times with PBS and labeled with 1 μg/mL of the DNA dye Hoechst 33258 in PBS for 5–10 min at room temperature, using enough solution to cover the cells completely. The cells were rinsed twice with PBS and then mounted with Crystal-mount medium (Biomeda, Foster City, CA). Cells were observed and photographed on a phase contrast and fluorescence microscope with a UV2A filter.

LDH assay. This colorimetric assay quantifies cell death based on the measurement of lactate dehydrogenase (LDH) activity released from the cytosol of damaged cells into the supernatant. After TNF-α challenge, 300 μL of culture medium was collected from each well and centrifuged at 1,000 rpm for 5 min. 100 μL of supernatant was collected from each sample, and transferred to a 96-well flat bottom plate. One hundred μL of LDH (Boehringer Cat. 1 664 793) was mixed with the sample and incubated for 30 min at room temperature. A plate reader (Bio-Rad Model 450 Microplate Reader, Richmond, CA) measured the absorbance of each sample at 490 nm with a reference wavelength of 650 nm. Absorbency values were analyzed by analysis of variance (ANOVA) with Post-hoc comparisons and values were expressed as percent of control.

DNA fragmentation assay. DNA gel electrophoresis was performed as described in Gong et al. (1994). Briefly, cells were collected in the same manner as for immunoblotting. Cells in each treatment condition were collected by centrifugation and fixed in suspension in 70% cold ethanol and stored in fixative at 20°C (24–72 hrs). Cells were then centrifuged at 800 g for 5 min and ethanol was thoroughly removed. Cell pellets were resuspended in 40 μL of phosphate-citrate (PC) buffer consisting of 192 parts of 0.2 M Na_2HOP_4 and 8 parts of 0.1 M citric acid (pH 7.8) at room temperature for 1 hr. After centrifugation at 1,000 g for 5 min, the supernatant was transferred to new tubes and concentrated by vacuum in a SpeedVac concentrator for 15–30 min. Three μL of 0.25% Nonidet NP-40 in distilled water was added followed by 3 μL of DNase-free RNase (1 mg/mL). After 30 min incubation at 37°C, 3 μL of proteinase K (1 mg/mL) was added and the extract was incubated for additional 30 min at 37°C. After the incubation, 1 μL of 6× loading buffer (0.25% bromophenol blue, 0.25% xylene cyanol FF, 30% glycerol in water) was added and the entire content of the tube was transferred to a 1.5% agarose gel and electrophoresis was performed in 1× TBE (0.1 M Tris, 0.09 M boric acid, 1 mM EDTA, pH 8.4) at 40 V for 2 hr. The DNA in the gels was visualized and photographed under UV light after staining with 5 μg/mL of ethidium bromide.

Assessment of α-Spectrin Degradation by Calpains and Caspase-3

Sodium dodecylsulfate-polyacrylamide gel electrophoresis (SDS-PAGE) and immunoblotting. Because α-spectrin contains sequence motifs preferred by both calpains and caspase-3 proteases, activation of these two families of cysteine proteases can be assessed concurrently by immunoblot identification of calpain and/or caspase-3 signature cleavage products (Nath et al., 1996; Wang et al., 1998). N-terminal sequencing of the major α-spectrin fragments has confirmed specific calpain and caspase-3 target sites for the 145-kDa and 120-kDa fragments, respectively (Wang et al., 1998). Calpain has a high affinity for two sites on the native 280-kDa α-spectrin

protein. Following calpain activation, intact α-spectrin (280 kDa) is proteolyzed into distinct 150-kDa and 145-kDa fragments detected on immunoblots. The first site is rapidly attacked following calpain activation resulting in a 150-kDa spectrin breakdown product (BDP). Further calpain processing of 150-kDa BDPs at the N-terminal yields a calpain-specific 145-kDa BDP (Nath et al., 1995, 1996; Wang et al., 1998). Caspase-3 cleaves intactα-spectrin to produce 150-kDa BDPs with a different N-terminal from the calpain-generated fragments. Further processing of the caspase-3-generated 150-kDa fragment results in a unique caspase-3-specific 120-kDa BDP (Wang et al., 1998). Moreover, the 120-kDa fragment has been shown to be associated with caspase-3 activation in various in vitro systems of apoptosis (Nath al., 1995, 1996; Pike at al., 1998; Wang et al., 1998).

Cells were lysed in ice-cold homogenization buffer (20 mM PIPES, pH 7.6, 1 mM EDTA, 2 mM EGTA, 1 mM DTT, 0.5 mM PMSF, 50 μg/mL Leupeptin, and 10 μg/mL of AEBSF, apotinin, pepstatin, TLCK, and TPCK) for 30 min, then sheared through a 1.0-mL syringe with a 25-gauge needle 15 times. Protein content in the samples was assayed by the Micro BCA method (Pierce, Rockford, IL). For protein electrophoresis, equal amounts of total protein (30 μg) were prepared in two fold loading buffer containing 0.25 M Tris (pH 6.8), 0.2 M DTT, 8% SDS, 0.02% Bromophenol Blue, and 20% glycerol, and heated at 95°C for 10 min. Samples were resolved in a vertical electrophoresis chamber using a 4% stacking gel over a 7% acrylamide resolving gel for 1 hr at 200 V. For immunoblotting, separated proteins were laterally transferred to nitrocellulose membranes (0.45 μM) using a transfer buffer consisting of 0.192 M glycine and 0.025 M Tris (pH 8.3) with 10% methanol at a constant voltage (100 V) for 1 hr at 4°C Coomassie Blue and Panceau Red (Sigma) were used to stain gels and nitrocellulose membranes, respectively, to confirm that equal amounts of protein were loaded in each lane.

Immunoblots were probed with an anti-α-spectrin monoclonal antibody (Afiniti Research Products, U.K.; Cat. FG 6090, clone AA6) that detects intact α-spectrin (280 kDa) and 150-, 145-, and 120-kDa SBDPs. Following incubation with the primary antibody (1:4,000) for 2 hr at room temperature, the blots were incubated in peroxidase-conjugated sheep anti-mouse 1gG (Cappel) for 1 hr (1:10,000). Enhanced chemiluminescence reagents (ECL, Amersham, Arlington Heights, IL) were used to visualize the immunolabeling on Hyperfilm (Hyperfilm ECL, Amersham).

Statistical analyses. Each experiment was performed three times and data was evaluated by ANOVA with a post-hoc Tukey test. Values are given as mean ± S.E.M. Differences were considered significant if $P < 0.05$.

RESULTS

Effects of TNF-α on Septo-Hippocampal Glial-Neuronal Cocultures

Dose- and time-dependent cell death. An initial dose-response assay was performed to determine the best concentration of TNF-α for all subsequent experiments. LDH release was used to quantify cell death, based on the measurement of LDH activity released from the cytosol of damaged cells into the supernatant. Exposure of septo-hippocampal cultures to 0.3–500 ng/mL TNF-α alone produced minimal toxicity (data not shown); however, with the addition of Act D, toxicity was significant. TNF-α with 3 ng/ml of Act D induced dose-dependent cell death (Fig. 1A). Three ng/ml of Act D did not significantly produce cell death compared with media control at any exposure duration (data not shown). Concentrations of TNF-α between 30 and 500 ng/ml produced approximately equivalent levels of cell death. Thus, the dose of 30 ng/mL was used for all subsequent experiments. The percent of LDH release following exposure to 30 ng/mL of TNF-α compared to control was 167%, 261%, 319%, 383%, and 573% at 3.5 hr, 7 hr, 48 hr, and 72 hr, respectively (Fig. 1B).

Morphological response to TNF-α challenge. TNF-α-treated septo-hippocampal cultures underwent morphological alterations in cell structure that were characteristic of apoptosis. Within 3.5 hr after incubation with 30 ng/mL of TNF-α, PI Molecular Probes, Eugene, OR) was taken up by cells and became even more apparent at 7 hr, 24 hr, and 72 hr after injury (Fig. 2B vs. C–E). In addition, nuclei stained with PI appeared shrunken and irregularly shaped. FDA indicated appearance of membrane blebbing by 3.5 hr that became more evident at 7 hr. By 24–72 hr, the plasma membrane integrity was lost and FDA staining was lost, giving way to nuclear PI staining (Fig. 2A vs. B– E).

To further characterize cell death characteristics of TNF-α toxicity in septo-hippocampal cultures, Hoechst 33258 was used to stain nuclear chromatin (Fig. 3). Treatment with TNF-α (30 ng/ml) and Act D produced irregularly shaped nuclei (Fig. 3B,G) as early as 3.5 hr. Chromatin of TNF-α-treated cells appeared condensed with smaller and brighter Hoechst staining. Formation of apoptotic nuclei changes are evident by 7 hr (Fig. 3C,H) and became more clear by 24 hr (Fig. 3D,I). Apoptotic bodies were scattered throughout every field of view by 72 hr (Fig. 3E, J).

DNA fragmentation. Condensation and aggregation of chromatin at the nuclear membrane may occur independently of endonuclease activation (Oberhammer et al., 1993). Thus, a DNA fragmentation assay was used to determine whether DNA alterations in septo-hippocampal cultures assessed by Hoechst 33258 were associated with endonuclease activity. Figure 4 shows that TNF-α (30 ng/mL) with 3 ng/ml of Act D induced detectable DNA laddering on agarose gels, most apparent at 24 hr following treatment. However, gels showed substantial smearing even at 24 hr, indicating random DNA fragmentation characteristic of necrosis.

Caspase-3 but not Calpain Proteolysis of α-Spectrin

Exposure to 30 ng/ml of TNF-α caused a time dependent proteolysis of by caspase-3 but not calpain proteases (Fig. 5). There was a significant increase in caspase-3-specific 120- kDa breakdown products to α-spectrin as early as 3.5 hr following TNF-α administra-

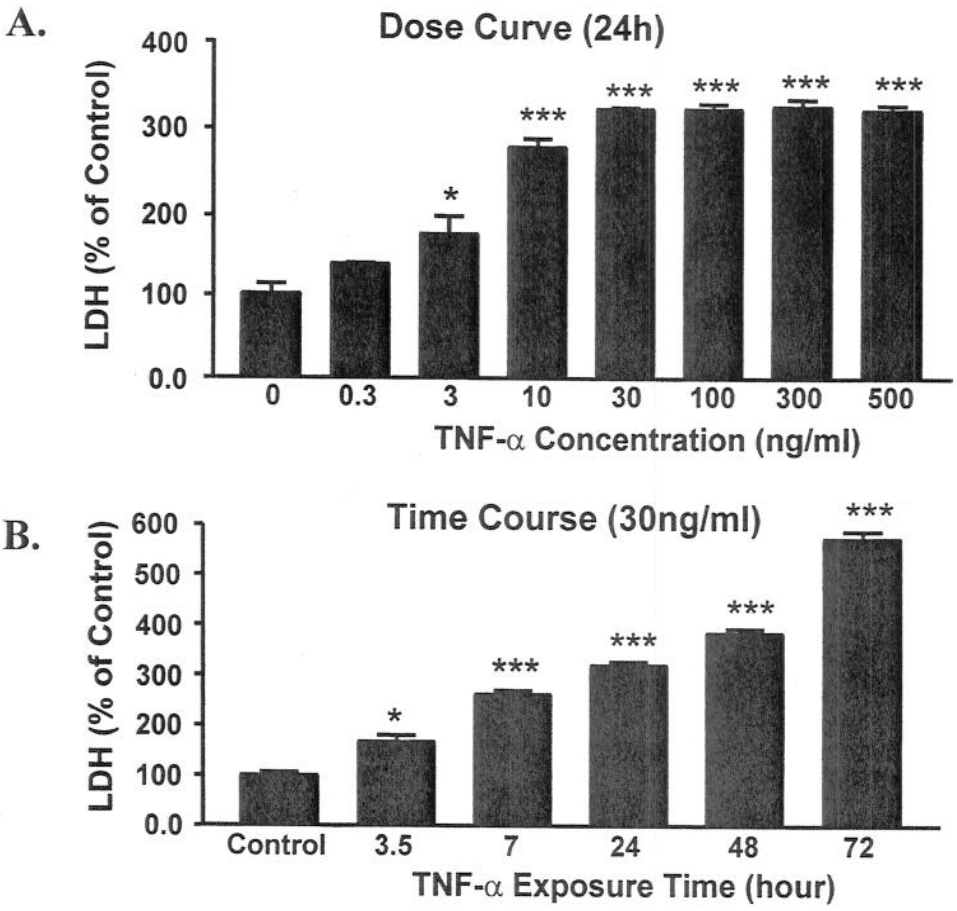

Fig. 1. Concentration and time course assays of tumor necrosis factor (TNF-α)-induced lactate dehydrogenase (LDH) release. **A:** Primary septo-hippocampal cultures were exposed to various doses of exogenous TNF-α (0.3–500 ng/ml) for 48 hr. Release of LDH was measured for each treatment condition and was expressed as mean percentages, ±S.E.M., of control. **B:** Percentage of control of LDH release to the media following addition of 30 ng/ml of TNF-α for 1 hr to 48 hr. Data are expressed as mean percentages, ± S.E.M., of control. $*P < 0.005$, $***P < 0.001$.

tion. Over the next 72 hr, a further increase in the accumulation of caspase-3-specific 120-kDa breakdown product of α-spectrin was more evident. In contrast, there was no evidence of accumulation of calpain-specific 145-kDa SBDP at any time point after TNF-α treatment.

Effects of CalpInh-II, Z-D-DCB, or Cycloheximide on TNF-α-Induced Cell Death and α-Spectrin Proteolysis

To investigate the relative contribution of calpain and/or caspase-like proteases to TNF-α-induced cell death and α-spectrin proteolysis, the effect of a calpain inhibitor (CalpInh-II) and a pan caspase inhibitor (Z-D-DCB) were examined. Since de novo protein synthesis is required for at least some forms of apoptosis and specifically for staurosporine-induced apoptosis in septo-hippocampal cultures, the effects of a nonselective inhibitor of protein synthesis (cycloheximide) were also examined.

Cell viability measurements. LDH assay was used to assess cell viability at 7 hr following TNF-α and/or administration of CalpInh-II, Z-D-DCB, or cycloheximide (Fig. 6B). Seven hrs after administration of 30 ng/ml of TNF-α with 3 ng/ml of Act D, LDH release increased to 261.4% over control. Administration of Z-D-DCB (30, 100, 140 μM) significantly reduced the percentage of LDH release to 183.1%, 175.0%, and 156.0%, respectively. CalpInh-II (37.5, 50 μM) had no protection against LDH release (268.3%, 278.3%, respectively; Fig. 6B). Cycloheximide (1 μg/ml) had the greatest effect against LDH release (137.0%) following 7 ht of TNF-α treatment.

α-spectrin proteolysis. Administration of Z-D-DCB or cycloheximide with TNF-α stimulation significantly decreased the accumulation of the 120-kDa caspase specific breakdown product of α-spectrin (Fig. 6A). In contrast, CalpInh-II did not provide any protection against proteolysis of α-spectrin. The results of these experiments confirm that caspase-3 but not calpain was activated after TNF-α stimulation in primary septo-hippocampal cultures.

DISCUSSION

Although caspases 8 and 3 were shown to mediate TNF-α-induced apoptosis in neutrophils (Yamashita et al., 1999), this study is the first demonstration that TNF-α induces activation of caspase-3 in a mixed neuro-glial culture system. Importantly, these results indicate that TNF-α may play an important role as an effector of receptor-mediated apoptotic cell death in the CNS. Characterization of apoptotic cell death responses to TNF-α in primary septo-hippocampal cultures is an important feature of this study since TNF-α protein is expressed in the

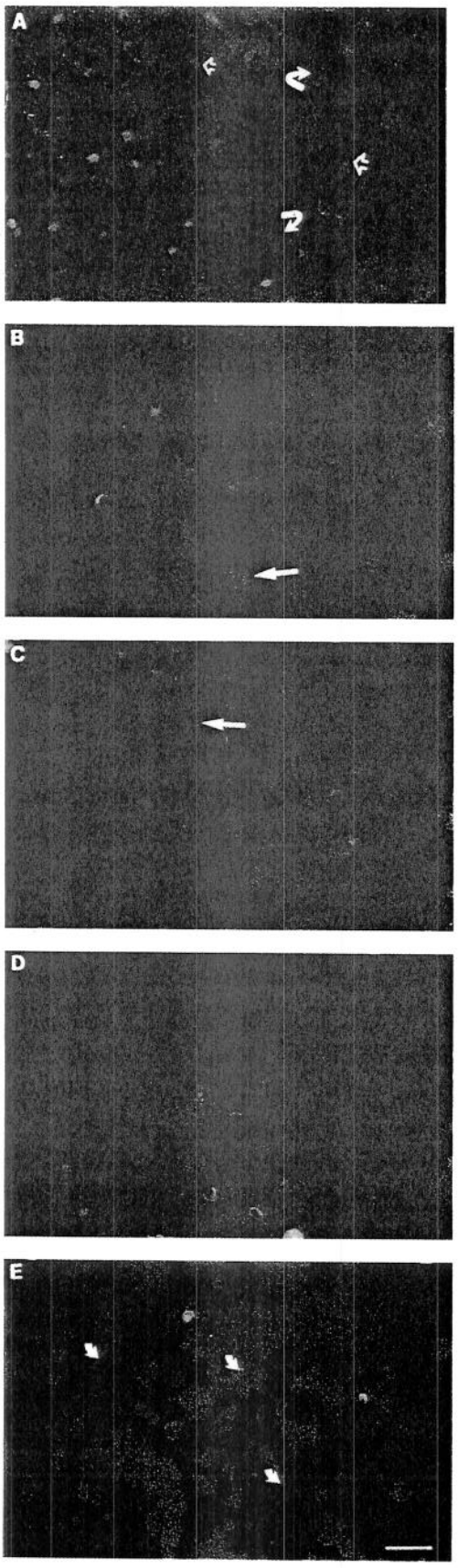

Figure 2.

hippocampus during various CNS injuries in vivo, including cerebral ischemia (Gong et al., 1998), traumatic brain injury (Shohami et al., 1997), and epilepsy (de Bock et al., 1996). Thus, primary septo-hippocampal cell cultures can provide an efficient in vitro tool for investigation of cellular and molecular mechanisms underlying apoptotic cell death relevant to in vivo CNS neuropathologies. Since Act D alone did not affect the viability of septo-hippocampal cell cultures, as assessed by LDH release, it is unlikely that Act D significantly contributed to the cell death profile observed in these studies.

Characterization of TNF-α-Induced Apoptotic Cell Death

In mixed primary septo-hippocampal cultures, TNF-α (0.3–500 ng/ml) produced apoptotic cell death characterized by the appearance of membrane blebbing, shrunken condensed nuclei, uneven distribution of DNA staining, formation of apoptotic bodies, and DNA fragmentation. These are typical phenotypic characteristics of apoptosis (Wyllie et al., 1980). Additionally, cell death was significantly prevented by the broad range protein synthesis inhibitor, cycloheximide. We have previously shown that protein synthesis is a requirement for caspase-3 activation and apoptotic cell death in this same culture system during staurosporine induced apoptosis (Pike et al., 1998). Cycloheximide is thought to protect cells from apoptosis through inhibition of de novo protein synthesis of pro-apoptotic proteins that are up-regulated during apoptosis (Koh et al., 1995; Pike et al., 1998). However, neuroprotective concentrations of cycloheximide can induce expression of the anti-apoptotic gene product Bcl-2 in hippocampal cell cultures (Furukawa et al., 1997). Further research is required to elucidate the role of transcriptional and translational regulators on apoptotic cascades. Although calpain activation can contribute to staurosporine-induced apoptotic cell death in septo-hippocampal cell cultures (Pike et al., 1998), calpain inhibition had no effect on TNF-α-induced cell death in the present model. TNF-α induced caspase-3 but not calpain proteolysis of α-spectrin during apoptotic cell death in septo-hippocampal culture.

The cytoskeletal protein α-spectrin is a preferred substrate of calpain and caspase-3 cysteine proteases. Ter-

Fig. 2. Fluorescein diacetate (FDA) and propidium iodide (PI) staining of septo-hippocampal cultures treated with TNF-α and actinomycin D. **A:** Control cultures demonstrate normal somal integrity and lack of nuclear PI uptake. Note confluent astroglial cell layer (curved arrows) beneath mature neuronal cell phenotypes (open arrows). Cells were treated with TNF-α for 3.5 (**B**), 7 (**C**), 24 (**D**), or 72 (**E**) hr. By 3.5 hr, some cells have lost retention of FDA and bind PI to their nucleus, thus indicating cell death. Membrane blebbing is observed (B, arrow), indicating a preserved integrity of the plasma membrane characteristic of apoptosis. After 7 hr of TNF-α treatment, an increase in the number of PI-stained nuclei is observed. In addition, membrane blebbing is more evident. After 24 (D) and 72 (E) hr of TNF-α treatment, the majority of cell nuclei are stained with PI and appear shrunken (curved arrows in E) compared to those observed at 3.5 hr (B). Scale bar = 10 μM.

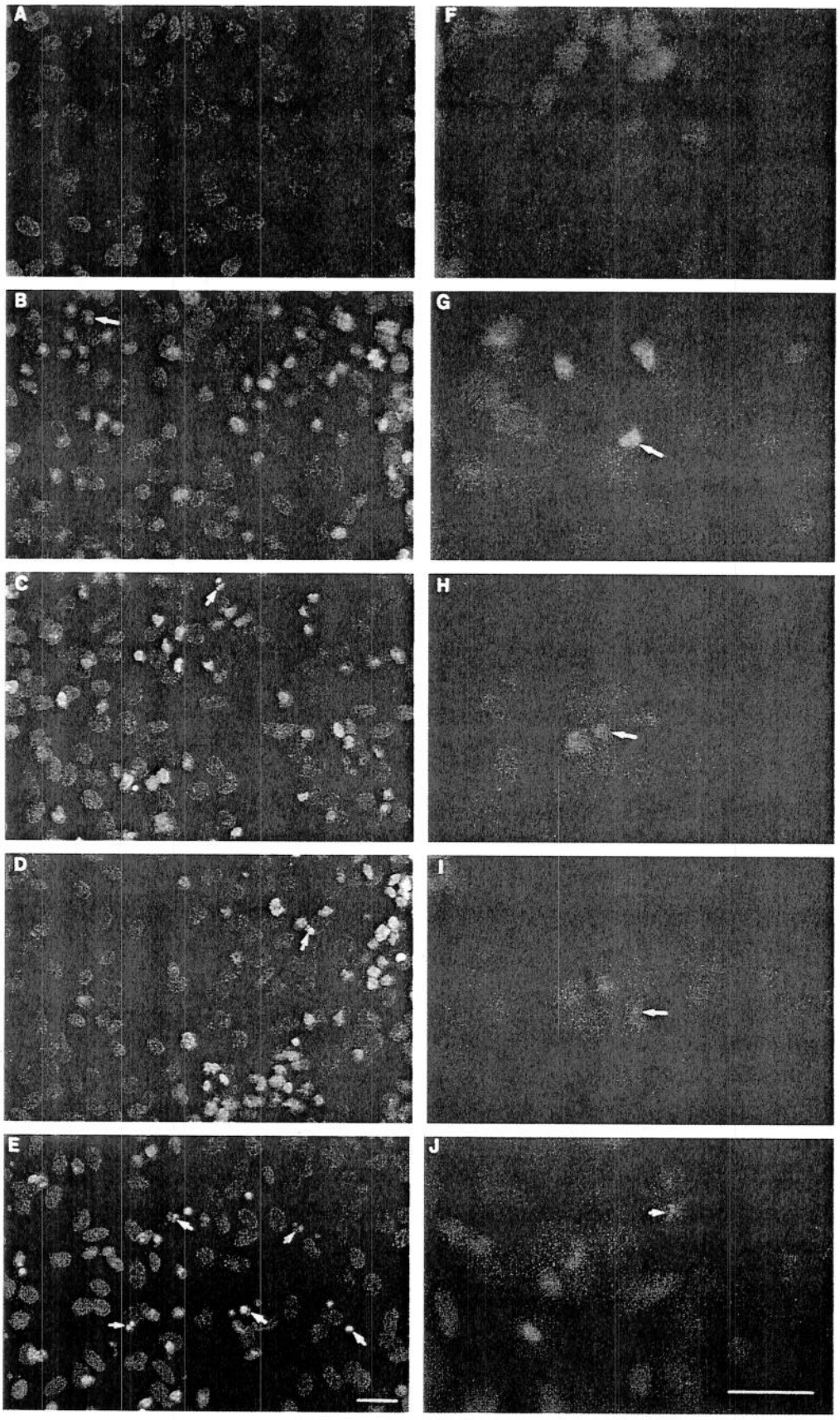

Fig. 3. Course of nuclear morphologic alterations during exogenous TNF-α-induced apoptosis detected by Hoechst 33258 staining. **A,F:** Control cultures. Cells were treated with 30 ng/ml of TNF-α and Actinomycin D for 3.5 (**B,G**), 7 (**C,H**), 24 (**D,I**), or 72 (**E,J**) hr. TNF-α-treated cells possess irregularly shaped nuclei with condensed chromatin, which are brightly stained with Hoechst (B,G–I, arrows). While some characteristic apoptotic nuclear changes such as nuclear membrane breakdown and formation of apoptotic bodies was evident as early as 7 hr (C, arrow), widespread apoptotic bodies (E, J, arrows) were not evident until 72 hr following TNF-α treatment. Scale bars = 10 μM.

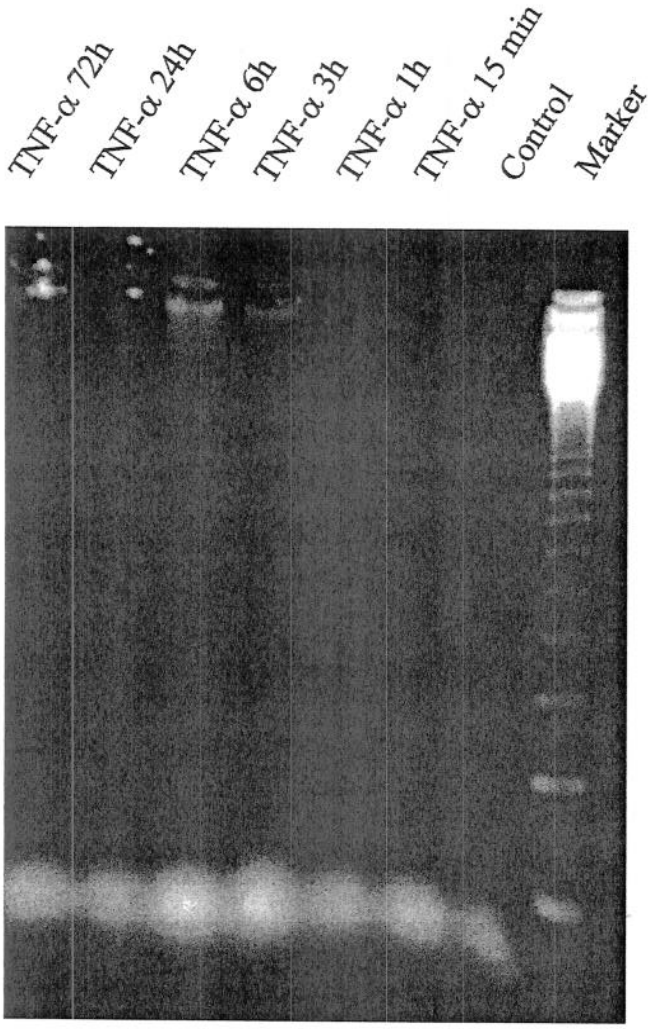

Fig. 4. Oligonucleosomal size fragmentation of DNA produced by TNF-α on septo-hippocampal cultures. TNF-α (30 ng/mL) induced readily apparent DNA laddering on agarose gels at 24 hr, and faint DNA laddering at 6 hr and 72 hr, but none at 15 min, 1 hr, or 3 hr following treatment.

minal sequencing of the major α-spectrin fragments has confirmed specific calpain and caspase-3 target sites for the 145-kDa and 120-kDa fragments, respectively (Wang et al., 1998). The distribution of calpain and caspases acting on α-spectrin to produce a calpain-specific 145-kDa fragment and an apoptotic-linked caspase-specific 120-kDa fragment during neuronal apoptosis and necrosis has been well characterized (Pike et al., 1998; Zhao et al., 1999; Nath et al., 1995). Our data did not show any 150-kDa and 145-kDa SBDPs, only the 120-kDa SBDP which appeared as early as 3.5 hr after the treatments and lasted over the 72 hr. These data supports the activation of caspase-3 and not calpain.

Effects of Calpain and Caspase Inhibitors on TNF-α-Induced Apoptosis

The pan-caspase inhibitor Z-D-DCB but not calpain inhibitor CalpInh-II attenuated cell death. Importantly, we confirmed that the dose of Z-D-DCB used in this study inhibited caspase-3 activation inferred by decreased proteolysis of α-spectrin. Reduced cell death produced by Z-D-DCB suggests that TNF-α-induced apoptosis in septo-hippocampal cultures is at least partially attributable to caspase-3 activation. In models of ischemia and status epilepticus, caspase-3 inhibitors have decreased apoptosis, loss of neurons, and ameliorated neurologic deficits (Kondratyev and Gale, 2000; Weissner et al., 2000; Endress et al., 1998; Gillardon et al., 1999). However, caspase-3 inhibition only partially reduced cell death, indicating that non-caspase-3-dependent pathways could also be activated, or that caspase-3 activation may be associated with other cellular pathways. For example, Miossec et al. (1997) demonstrated that caspase-3 (CPP32) processing could be a physiological step during T lymphocyte activation, independent of apoptosis.

A receptor-mediated pathway can trigger caspase-3 activation (for review, see Goeddel, 1999; Ksontini et al., 1998). Most cell types, including neural cells, express TNF-α receptor 1 (TNFR1; 55 kDa) which is activated by soluble TNF-α. Apoptosis through TNF-R2 appears

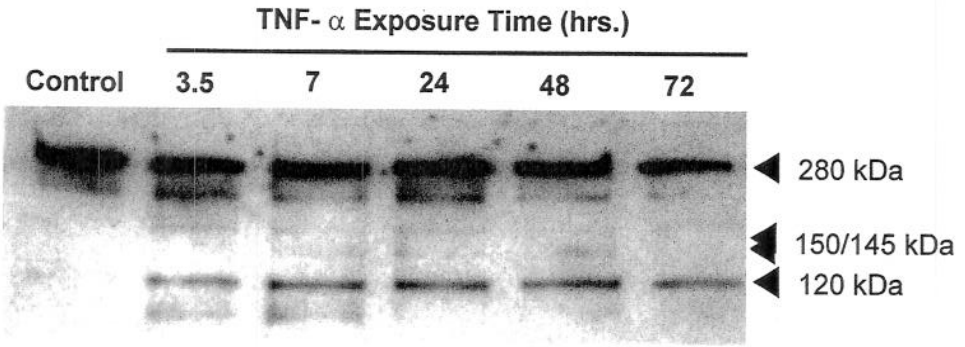

Fig. 5. TNF-α produced caspase-3-specific but not calpain-specific α-spectrin breakdown products (BDPs). Western blots examining proteolysis of α-spectrin into 150-kDa, calpain-specific 145-kDa, and caspase 3-specific 120-kDa BDPs detected after 3 hr, 7 hr, 24 hr, and 72 hr following TNF-α (30 ng/ml) with 3 ng/ml of Actinomycin D treatment. TNF-α treatment produced no increases in calpain-specific 145-kDa BDPs, but caused a marked increase in the caspase-3-specific 120-kDa BDP.

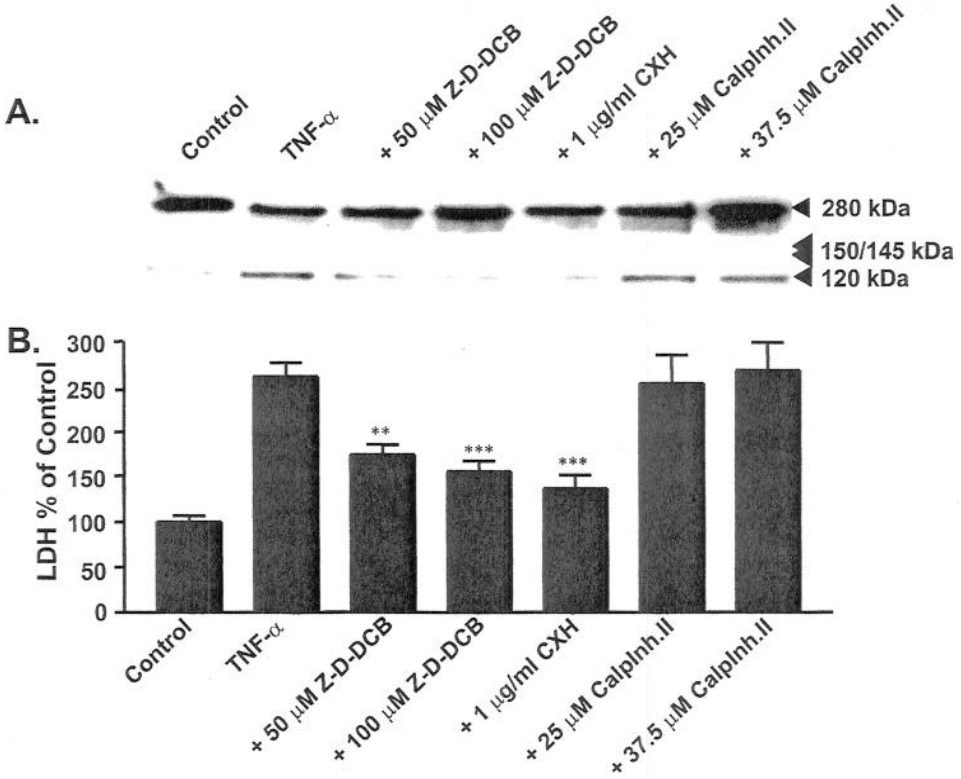

Fig. 6. TNF-α produced caspase-3 but not calpain protease activation associated with LDH release. **A:** Western blots examine proteolysis of α-spectrin into 150-kDa, calpain-specific 145-kDa, and caspase-3-specific 120-kDa breakdown products. Accumulation of 120-kDa breakdown products to α-spectrin was seen 7 hr following TNF-α treatment (30 mg/ml), as compared to untreated controls. TNF-α treatment produced no increases in 150-kDa and 145-kDa BDPs. Administration of carbobenzosy-Asp-CH_2-OC (O)-2-6-dichlorobenzene (Z-D-DCB) or cycloheximide (CHX) markedly decreased accumulation of 120-kDa breakdown products to α-spectrin. Calpain inhibitor II had no effect on α-spectrin processing. **B:** LDH release (percentage of untreated controls) was calculated 7 hr after administration of TNF-α (30 mg/ml) or coadministration of caspase inhibitor, Z-D-DCB (50 μM, 100 μM), the protein synthesis inhibitor cycloheximide (1 μg/ml), or the calpain inhibitor, calpain inhibitor II (25 μM, 37.5 μM). Z-D-DCB and cycloheximide, but not calpain inhibitor II, significantly decreased LDH release induced by TNF-α (**$P < 0.01$, ***$P < 0.001$).

to signal through a different pathway involving induction of sphingomyelinases (Grell et al., 1994). TNF-R1, when activated, recruits TRADD (TNF-associated Death Domain protein) and RIP (Receptor Interacting Protein). TRADD can interact with TRAF2 (TNF-associated factor 2) or with another adapter protein, FADD (Fas associating protein with Death Domain; Ashkenazi and Dixit, 1998; Goeddel, 1999). A TRADD-FADD-caspase-8/10 interaction has been reported to produce the autolytic activation of caspase-8/10, which in turn processes and activates the common apoptosis mediator, caspase-3 (Villa et al., 1997). In the present study, we report on the cytotoxic effect of TNF-α on septo-hippocampal cell culture, which contained both astrocytes and neurons. Taken from a brain area which is vulnerable to ischemic and traumatic injury, this mixed culture is a highly relevant model to investigate the role of TNF-α in the pathophysiology of brain injury. The question of whether this cytokine is toxic or protective in the injured brain has been raised in numerous publications in the past decade. Contradiction appears in the literature between reports on protective effects of anti- TNF-α agents, and the deleterious effects of TNF-α receptor knockouts in models of cerebral ischemia and trauma (for review, see Shohami et al., 1999). The present study sheds light on the toxic role TNF-α might play, within the first days after exposure to higher than normal physiologic levels of TNF-α, by activating apoptotic response. In contrast, Barger et al. (1995) demonstrated that TNF-α is protective against iron and amyloid-β peptide in cultured hippocampal and neocortical astrocytes 1995, and Mattson et al. (1995) showed protective effects of TNF-α under conditions of glucose deprivation and glutamate toxicity. These authors have demonstrated up-regulation of calbindin and of MnSOD in response to exposure to TNF-α. The difference between the various experimental paradigms, namely, different cell types, different insults and time of exposure, may explain the difference between the role TNF-α plays under these conditions. In conclusion, we propose that under the experimental conditions employed in the present study, TNF-α is pro-apoptotic and therefore, its inhibition in the acute postinjury phase may be beneficial.

REFERENCES

Aggarwal S, Gollapudi S, Gupta S. 1999. Increased TNF-alpha-induced apoptosis in lymphocytes from aged humans: changes in TNF-alpha receptor expression and activation of caspases. J Immunol 162:2154–2161.

Armstrong RC, Aja T, Xiang J, Gaur S, Krebs JF, Hoang K, Bai X, Korsmeyer SJ, Karanewsky DS, Fritz LC, Tomaselli KJ. 1996. Fas-induced activation of the cell death-related protease CPP32 is inhibited by Bcl-2 and by ICE family protease inhibitors. J Biol Chem 271:16850–16855.

Ashkenazi A, Dixit VM. 1998. Death receptors: signaling and modulation. Science 281:1305– 1308.

Barger SW, Hoster D, Furukawa K, Goodman Y, Krieglstein J, Mattson MP 1995. Tumor necrosis factors alpha and beta protect neurons against amyloid beta-peptide toxicity: evidence for involvement of a kappa B-binding factor and attenuation of peroxide and Ca^{2+} accumulation. Proc Natl Acad Sci USA 92:9328–9332.

Barone FC, Arvin B, White RF, Miller A, Webb CL, Willette RN, Lysko PG, Feuerstein GZ. 1997. Tumor necrosis factor-alpha: a mediator of focal ischemic brain injury. Stroke 28:1233–1244.

Bruce AJ, Boling W, Kindy MS, Peschon J, Kraemer PJ, Carpenter MK, Holtsberg FW, Mattson MP. 1996. Altered neuronal and microglial responses to excitotoxic and ischemic brain injury in mice lacking TNF-α receptors. Nature Med 2:788–795.

Buttini M, Appel K, Sauter A, Gebicke-Haerter PJ, Boddeke HM. 1996. Expression of tumor necrosis factor alpha after focal cerebral ischemia in the rat. Neuroscience 71:1–16.

Cheng B, Christakos S, Mattson MP. 1994. Tumor necrosis factors protect neurons against metabolic-excitotoxic insults and promote maintenance of calcium homeostasis. Neuron 12:139–153.

Chung IY, Benveniste EN. 1990. Tumor necrosis factor alpha production by astrocytes. Induction by lipopolysaccharide, interferon gamma and interleukin-1-beta. J Immunol 144:2999–3007.

Dawson D, Martin D, Hallenbeck JM. 1996. Inhibition of tumor necrosis factor-alpha reduces focal cerebral ischemic injury in the spontaneously hypertensive rat. Neurosci Lett 218:41–44.

de Bock F, Dornand J, Rondouin G. 1996. Release of TNF-alpha in the rat hippocampus following epileptic seizures and excitotoxic neuronal damage. Neuroreport 7:1125–1129.

Eldadah BA, Yakovlev AG, Faden AI. 1997. The role of CED-3-related cysteine proteases in apoptosis of cerebellar granule. J Neurosci 17:6105–6113.

Endres M, Namura S, Shiimizu-Sasamata M, Waeber C, Zhang L, Gomez-Isla T, Hyman BT, Moskowitz MA. 1998. Attenuation of delayed neuronal death after mild focal ischemia in mice by inhibition of the caspase family. J Cereb Blood Flow Metab 18:238–247.

Fan L, Young PR, Barone FC, Feuerstein GZ, Smith DH, McIntosh TK. 1996. Experimental brain injury induces differential expression of tumor necrosis factor-α mRNA in the CNS. Mol Brain Res 36:287–291.

Fillit H, Ding W, Buee L, Kalman J, Altstiel L, Lawlor B, Wofl-Klein G. 1991. Elevated circulating tumor necrosis factor levels in Alzheimer's disease. Neurosci Lett 131:318–320.

Fraser A, Evan G. 1996. A license to kill. Cell 85:781–784.

Furukawa K, Estus S, Fu W, Mattson MP. 1997. Neuroprotective action of cyclohexamide involves induction of Bcl-2 and anti-oxidant pathways. J Cell Biol 136:1137–1150.

Garcia JE, Nonner D, Ross D, Barrett JN. 1992. Neurotoxic components in normal serum. Exp Neurol 118:309–316.

Gary DS, Bruce-Keller AJ, Kindy MS, Mattson MP. 1998. Ischemic and excitotoxic brain injury is enhanced in mice lacking the p55 tumor necrosis factor receptor. J Cereb Blood Flow Metab 18:1283–1287.

Gelbard HA, Dzenko KA, DiLoreto D, del Cerro C, del Cerro M, Epstein LG. 1993. Neurotoxic effects of tumor necrosis factor alpha in primary human neuronal cultures are mediated by activation of the glutamate AMPA receptor subtype: implications for AIDS neuropathogenesis. Dev Neurosci 15:417–422.

Gillardon F, Kiprianova I, Sandkuhler J, Hossman KA, Spranger M. 1999. Inhibition of caspases prevents cell death of hippocampal CA1 neurons, but not impairment of hippocampal long-term potentiation following ischemia. Neuroscience 93:1219–1222.

Goeddel DV. 1999. Signal transduction by tumor necrosis factor. Chest 116:69S–73S.

Gong C, Qin, Z, Bet AL, Liu X, Yang G. 1998. Cellular localization of tumor necrosis factor-alpha following focal cerebral ischemia in mice. Brain Res 801:1–8.

Gong J, Traganos F, Dzrzynkiewicz Z. 1994. A selective procedure for DNA extraction from apoptotic cells applicable for gel electrophoresis and flow cytometry. Analyt Biochem 218:314–319.

Grell M, Zimmermann G, Husler D, Pfizenmaier K, Scheurich P. 1994. TNF receptors TR60 and TR80 can mediate apoptsis via induction of distinct signal pathways. J Immunol 153:1963–1972.

Jones KH, Senft AJ. 1985. An improved method to determine cell viability by simultaneous staining with fluorescein diacetate-propidium iodide. J Histochem Cytochem 33:77–79.

Kampfl A, Zhao X, Whitson JS, Posmantur R, Dixon CE, Yang K, Clifton GL, Hayes RL. 1996. Calpain inhibitors protect against depolarization induced neurofilament protein loss of septo-hippocampal neurons in culture. Eur J Neurosci 8:344–352.

Kampfl A, Posmantur RM, Zhao X, Schmutzhard E, Clifton GL, Hayes RL. 1997. Mechanisms of calpain proteolysis following traumatic brain injury: implications for pathology and therapy: a review and update. J Neurotrauma 14:121–134.

Knoblach SM, Fan L, Faden AI. 1999. Early neuronal expression of tumor necrosis factor-alpha after experimental brain injury contributes to neurological impairment. J Neuroimmunol 95:115–125.

Koh J, Wie MB, Gwag BJ, Sensi SL, Canzoniero MT, Demaro J, Csernansky C, Choi DW. 1995. Staurosporine-induced neuronal apoptosis. Exp Neurol 135:153–159.

Kondratyev A, Gale K. 2000. Intracerebral injection of caspase-3 inhibitor prevents neuronal apoptosis after kainic acid-evoked status epilepticus. Brain Res Mol Brain Res 75:216–224.

Ksontini R, MacKay SLD, Moldawer LL. 1998 Revisting the role of tumor necrosis factor alpha and the response to surgical injury and inflammation. Arch Surg 133:558–567.

Leker R, Shohami E, Abramsky O, Ovadia H.1999. Dexanabinol: a novel neuroprotective drug in experimental focal cerebral ischemia. J Neurol Sci 162:114–119.

Lieberman AP, Pitha PM, Shin HS, Shin MN. 1989. Production of tumor necrosis factor and other cytokines by astrocytes stimulated with lipopolysaccharide or neurotropic virus. Proc Nat Acad Sci USA 86:6348–6352.

Liu T, Clark RK, McDonnell PC, Young PR, White RF, Brone FC, Feuerstein GZ. 1994. Tumor necrosis factor alpha expression in ischemic neurons. Stroke 25:1481–1488.

Martin DP, Schmidt RE, DiStefano PS, Lowry OH, Carter JG, Johnson EM. 1988. Inhibitors of protein synthesis and RNA synthesis prevent neuronal death caused by nerve growth factor deprivation. J Cell Biol 106:829–844.

Mattson MP, Lovell MA, Furukawa K, Markesbery WR. 1995. Neurotrophic factors attenuate glutamate-induced accumulation of peroxides, elevation of Ca^{2+} and neurotoxicity, and increase antioxidant enzyme activities in hippocampal neurons. J Neurochem 65:1740–1751.

Meirstrell ME 3rd, Botchkina GI, Wang H, Di Snato E, Cockroft KM, Bloom O, Vishnubhakat JM, Ghezzi P, Tracey KJ. 1997. Tumor necrosis factor is a brain damaging cytokine in cerebral ischemia. Shock 8:341–348.

Miossec C, Dutilleul V, Rassy F, Diu-Hercend A. 1997. Evidence for CPP32 activation in the absence of apoptosis during T lymphocyte stimulation. J Biol Chem 272:13489–62.

Miura M, Zhu H, Rotello R, Hartwieg EA, Yuan J. 1993. Induction of apoptosis in fibroblasts by IL-1 beta-converting enzyme, a mammalian homolog of the C. elegans cell death gene ced-3. Cell 75:653–660.

Mogi M, Harada M, Kondo T, Reiderer P, Nagatsu T. 1994. Tumor necrosis factor-alpha increases both in the brain and in the cerebrospinal fluid from parkinsonian patients. Neurosci Lett 165:208–210.

Mogi M, Harada M, Narabayashi H, Inagaki H, Minami M, Nagatsu T. 1996. Interleukin-1 beta, interleukin-6, epidermal growth factor and transforming growth factor-alpha are elevated in ventricular cerebrospinal fluid in juvenile parkinsonian and Parkinson's disease. Neurosci Lett 211:13–16.

Morganti-Kossman MC, Kossman T, Wahl SM 1992. Cytokines and neuropathology. Trends Pharmacol 13:286–290.

Nath R, Raser KJ, Stafford D, Hajimohammadreza I, Posner A, Allen H, Talanian RV, Nitatori T, Sato N, Waguri S, Karasawa Y, Araki H, Shibanai K, Kominami E, Uchiyama Y. 1995. Delayed neuronal death in the CA1 pyramidal cell layer of the gerbil hippocampus following transient ischemia is apoptosis. J Neurosci 15:1001–1011.

Nath R, McGinnis KJ, Nadimpalli R, Stafford D, Wang KKW. 1996. Effects of ICE-like proteases and calpain inhibitors on neuronal apoptosis. Neuroreport 8:249–255.

Nath R, Robert A, McGinnis KM, Wang KKW. 1998. Evidence for activation of caspase-3-like protease in excitotoxins and hypoxia/hypoglycemia-injured cerebrocortical neurons. J Neurochem 71:186–195.

Nawashiro H, Martin D, Hallenbeck JM. 1997. Inhibition of tumor necrosis factor ameliorated brain infarction in mice. J Cereb Blood Flow Metab 17:229–232.

Oberhammer F, Fritsch G, Schmied M, Pavelka M, Printz D, Purchio T, Lassmann H, Schulte-Hermann R. 1993. Condensation of the chromatin at the membrane of an apoptotic nucleus is not associated with activation of an endonuclease. J Cell Sci 104:317–326.

Pike BR, Zhao X, Newcomb JK, Wang KKW, Posmantur RM, Hayes RL. 1998. Temporal relationships between *de novo* protein synthesis, calpain and caspase 3-like protease activation, and DNA fragmentation during apoptosis in septo-hippocampal cultures. J Neurosci Res 52:505–520.

Pulliam L, Zhou M, Stubbelbine M, Bitler CM 1998. Differential modulation of cell death proteins in human brain cells by tumor necrosis factor alpha and platelet activating factor. J Neurosci Res 54:530–538.

Ruff MR, Gifford GE. 1981. Rabbit tumor necrosis factor: mechanisms of action. Infect Immun 31:380–385.

Saito K, Suyama K, Nishida K, Sei Y Basile AS. 1996. Early increases in TNF-alpha, IL-6 and IL-1 beta levels following transient cerebral ischemia in gerbil brain. Neurosci Lett 206:149–152.

Scherbel U, Raghupathi R, Nakamura M, Saatman KE, Trojanowski JQ, Neugebauer E, Marino MW, McIntosh TK. 1999. Differential acute and chronic responses of tumor necrosis factor-deficient mice to experimental brain injury. Proc Natl Acad Sci USA 96:8721–8726.

Selmaj KW, Raine CS. 1998. Tumor necrosis factor mediates myelin and oligodendrocyte damage *in vitro*. Ann Neurol 23:339–346.

Sharief MK, McLean B, Thompson EJ. 1993. Elevated serum levels of tumor necrosis factor-alpha in Guillain-Barre syndrome. Ann Neurol 33:591–596.

Shohami E, Novikov M, Bass R, Yamin A, Galily R. 1994. Closed head injury triggers early production of TNF-alpha and IL-6 by brain tissue. J Cereb Blood Flow Metab 14:615–619.

Shohami E, Bass R, Wallach D, Yamin A, Galily R. 1996. Inhibition of tumor necrosis factor alpha (TNF-α) activity in rat brain is associated with cerebroprotection after closed head injury. J Cereb Blood Flow Metab 3:378–384.

Shohami E, Galilly R, Mechoulam R, Bass R, Ben-Hur T. 1997. Cytokine production in the brain following closed head injury: dexanabinol (HU-211) is a novel TNF-alpha inhibitor and an effective neuroprotectant J Neuroimmunol 72:169–177.

Shohami E, Ginis I, Hallenbeck JM. 1999. Dual role of tumor necrosis factor alpha in brain injury. Cytokines Growth Factors Rev 10:119–130.

Stahel PF, Shohami E, Younis FM, Kariya K, Otto VI, Lenzlinger PM, Eugster HP, Trentz O, Kossmann T, Morganti-Kossmann MC. 1999. Experimental closed head injury: analysis of neurological outcome, blood brain barrier dysfunction and intracranial polymorphnuclear leukocyte in mice deficient in genes for pro-inflammatory cytokines. J Cereb Blood Flow Metab 20:369–380.

Sullivan PG, Bruce-Keller AJ, Rabchevsky AG, Christakos S, Clair DK, Mattson MP, Scheff SW. 1999. Exacerbation of damage and altered NF-kappaB activation in mice lacking tumor necrosis factor receptors after traumatic brain injury. J Neurosci 19:6248–6256.

Taupin V, Toulmond S, Serrano A, Benavides J, Zavala F. 1993. Increase in IL-6, IL-1 and TNF-α levels in rat brain following traumatic lesion: Influence of pre- and post-traumatic treatment with Ro5 4864, a peripheral-type (p-site) benzodiazepine ligand. J Neuroimmunol 42:177–185.

Uno H, Matsuyama T, Akita H, Nishimura H, Sugita M. 1997. Induction of tumor necrosis factor-alpha in the mouse hippocampus following transient forebrain ischemia. J Cereb Blood Flow Metab 17:491–499.

Villa P, Kaufman SH, Earnshaw WD. 1997. Caspases and caspase inhibitors. Trends Biochem Sci 22:388–393.

Wang KK. 2000. Calpain and caspase: can you tell the difference? Trends Neurosci 23:59.

Wang KKW, Yuen P. 1994. Calpain inhibition: an overview of its therapeutic potential. Trends Pharmacol Sci 15:412–419.

Wang KKW, Nath R, Raser KJ, Hajimohammadreza I. 1996. Maitotoxin induces calpain activation in SH-SY5Y neuroblastoma cells and cerebrocortical cultures. Arch Biochem Biophys 331:208–214.

Wang KKW, Posmantur RM, Nath R, McGinnis K, Whitton M, Talanian RV, Glartz SB, Morrow JS. 1998. Simultaneous degradation of alpha II- and beta-II- spectrin by caspase 3 (CPP32) in apoptotic cells. J Biol Chem 273:22490–22497.

Wang XK, Yue TL, Barone FC, White RF, Gagnon RC, Feuerstein GZ. 1994. Concomitant cortical expression of TNF-α and IL-1 mRNAs follows early response gene expression in transient focal ischemia. Mol Chem Neuropathol 23:103–114.

Weissner C, Sauer D, Alaimo D, Allegrini PR. 2000. Protective effect of a caspase inhibitor in models for cerebral ischemia in vitro and in vivo. Cell Mol Biol 46:53–62.

Wyllie AH, Kerr SF, Currie AR. 1980. Cell death: the significance of apoptosis. Rev Cytol 68:251–306.

Xu IS, Grass S, Xu XJ, Wiesenfeld-Hallin Z. 1998. On the role of galanin in mediating spinal flexor reflex excitability in inflammation. Neuroscience 85:827–835.

Yamashita K, Takahashi A, Kobayashi S, Hirata H, Mesner PW, Kaufmann SH, Yonehara S, Yamamoto K, Uchiyama T, Sasada M. 1999. Caspases mediate tumor necrosis-alpha-induced neutrophil apoptosis and down-regulation of reactive oxygen production. Blood 93:674–685.

Yuen P, Gilbertsen RB, Wang KKW. 1996. Non-erythroid α-spectrin breakdown by calpain and interleukin 1-converting-enzyme-like protease(s) in apoptotic cells: contributory roles of both protease families in neuronal apoptosis. Biochem J 319:683–690.

Zhao X, Pike BR, Newcomb JK, Wang KKW, Posmantur RM, Hayes RL. 1999. Maitotoxin induces calpain but not caspase-3 activation and necrotic cell death in primary septo-hippocampal cultures. Neurochem Res 24:371–382.

Zhivotovsky B, Burgess DH, Vanags DM, Orrenius S. 1997. Involvement of cellular proteolytic machinery in apoptosis. Biochem Biophys Res Comm 230:481–488.